UNIVERSITY OF NOTTINGHAM

DEPARTMENT OF CIVIL ENGINEERING

PAVEMENT EVALUATION AND OVERLAY DESIGN

by

WING SANG TAM

B.Sc., M.Sc., D.I.C., C.ENG., M.I.C.E.

Thesis submitted to the University of Nottingham
for the degree of Doctor of Philosophy

October 1987

CONTENTS

ABSTRACT

The aim of this research was to develop analytical procedures for pavement evaluation and overlay design. Accurate site deflection measurements were recorded by a non-destructive testing device known as a Falling Weight Deflectometer (FWD).

Two computer programs, BASEM and BASEMC, have been developed to back-analyse the in-situ effective stiffnesses of bituminous and concrete pavement structures respectively. Extensive applications of these programs over a wide range of pavements have revealed a number of deficiencies and, therefore, a much improved computer program, PADAL, has been developed. Extensive tests have been performed to prove the program in deriving unique solutions for three- and four-layered structures.

Detailed theoretical studies have identified the significance of the stiffness of the subgrade layer in influencing the FWD deflection bowl. Consequently, the above pavement evaluation procedures have incorporated a well established non-linear subgrade model. Furthermore, the detailed study has enabled the development of a rational method for determining the geophone positions of a FWD for carrying out site surveys.

Detailed investigation has been carried out to validate the analytical pavement evaluation procedures. Firstly, it was established that the non-linear subgrade model correlated well with in-situ subgrade stresses and strains. Secondly, the back-analysed stiffnesses compared well with laboratory results on different pavement materials. Thirdly, comparison of back-analysed stiffnesses with a dynamic analysis program revealed very good correlation, supporting use of a static analysis computer program like PADAL, for performing back-analysis, with confidence. Fourthly, a commercially

available computer package, ELMOD, was assessed. Finally, a detailed structural evaluation of a full-scale trial was performed. Laboratory tests on bituminous beam specimens have been performed to understand the relationship between stiffness reduction and crack propagation. This has led to the proposal of a rational method for evaluating the remaining life of bituminous pavements against fatigue cracking. This method also forms an important part of an overlay design procedure for bituminous pavements.

ACKNOWLEDGEMENTS

The writer firstly wishes to acknowledge the Science and Engineering Research Council for the funding of the project.

The writer would also like to express his great gratitude to Professor Peter Pell who, not only provided all the facilities of the Department, but also nourished him with lots of stimulation.

A special thanks is due to Professor Stephen Brown who supervised this research with superb guidance and great patience amidst his own heavy workload.

Acknowledgement must go to the Transport and Road Research Laboratory for the collaboration of this project and the provision of using their Falling Weight Deflectometer (FWD) during the first year. In particular, thanks are due to Mr. Paddy Jordon and Mr.Brian Ferne for their expert advices throughout the project.

Thanks are also due to Dr. Janet Brunton and Mr. Nicholas Thom for their support and encouragement throughout the research as well as spending numerous hours to improve the draft of the thesis.

Furthermore, the excellent services provided by Cripps Computing Centre of the University of Nottingham and the permission to use various computer programs, including BISTRO, BISAR, PONOS and CHEVRON, developed by organisations such as Shell and Chevron oil companies for structural analysis, as well as a statistical computer program, BMDP, developed by the University of California, are very much appreciated.

Practical advices from Mr. Keith Cooper and Mr. Barry Brodrick and the assistance from Mr. Andy Leyko, Dennis Lockyer, Mr. Jim Moody and Mr. Jerry Barnes in the laboratory testing must be thanked.

Excellent co-operation was received from a number of outside

organisations without which this project would not have been accomplished. These include Derbyshire, Leicestershire, Essex, Nottinghamshire, and Northamptonshire, who provided staff for traffic control during FWD deflection surveys. In particular, the writer greatly appreciates the support from Derbyshire who permitted detailed structural evaluation to be carried out on an experimental road in their county.

The preparation of this thesis has involved a number of people. Merits are offered to Miss Caroline Brayley for preparing the figures and Mrs. Pam Elliot for preparing the tables.

Finally, the writer would like to thank all the academic and secretarial staff, researchers and technicians in the Department, especially those in the Pavement Research Group, for their friendship that the writer regards as a great achievement over the last three years.

NOTATIONS

A,B	Non-linear subgrade stiffness parameters.
BB	Benkelman Beam.
CBR	California bearing ratio.
CIV	Clegg impact value.
d	Surface deflection. (Numerical suffices indicate the FWD geophone position)
DCP	Dynamic cone penetrometer.
E	Elastic stiffness (equivalent to Young's modulus). (Suffices indicate the layer)
FWD	Falling weight deflectometer.
h	Thickness of layer. (Numerical suffice indicate the layer)
N_e	Fatigue life of existing pavement.
N_f	Required future traffic.
N_{ov}	Design fatigue life of overlaid pavement.
N_p	Past traffic.
N_r	Remaining life of pavement.
p	Mean effective normal stress. ($= \frac{1}{3}(\sigma_1' + 2\sigma_3')$)
q	Deviatoric stress. ($= \sigma_1' - \sigma_3'$)
r	Radial distance of measured FWD deflection from load centre.
RR	Road rater.
T	Temperature.
V_B	Volume of binder in bituminous mix.
SP_i	Initial softening point of bitumen.
σ	Total stress.
σ_1', σ_3'	Major and minor effective principal stresses.
σ_v', σ_h'	Vertical and horizontal effective stresses.
ε_t	Maximum tensile strain in bituminous material.
ε_z	Maximum vertical compressive strain in subgrade.
γ	Unit weight.

γ_w Unit weight of water.

ν Poisson's ratio.

Other symbols will be defined in the text if necessary.

CHAPTER 1

INTRODUCTION

Maintaining the structural integrity of highways is currently a major problem involving vast sums of expenditure as shown in the review submitted to the Secretary of State for Transport (1). Furthermore, the deterioration of British pavements, due to large increases in heavy commercial vehicles and to many sections of the motorway system reaching the end of their design lives, has focussed attention in this field. Therefore, procedures are required to assess and strengthen pavements well before failure occurs within the framework of a pavement management system for infrastructure. In 1973, the Transport and Road Reasearch Laboratory (TRRL) published an overlay design procedure, LR 571 (2), which is based on maximum surface deflections measured by the Benkelman Beam. This procedure was later improved in LR 833 (3) published in 1978. However, the TRRL procedures are based on empirical observations relating to standard constructions and do not allow accurate diagnosis of pavement conditions, in particular the subgrade layer, the most important layer in the pavement structure, or provide a structural basis for overlay design.

An analytical procedure which can properly evaluate the in-situ conditions of all the constituent layers and the subgrade is therefore urgently needed. The necessity for the development was emphasised by Mr. Nicholas Ridley, the former Secretary of State for Transport, who said (4),

> "We need a better scientific understanding (of road maintenance). I'd like to see the relationship between deflection and the state of the road deep down perfected, so we would only need to reconstruct the sections which were absolutely necessary."

The present research is being carried out using a non-destructive testing device known as a Falling Weight Deflectometer (FWD), as shown in Plate 1.1, to collect site performance data on existing pavements. This device is considered to have the potential for providing much more detailed information about the pavement performance than the existing Deflectograph or Benkelman Beam. These latter tools, notably the Deflectograph, are used for routine evaluation of the highway network in the United Kingdom (U.K.) and record the maximum deflection under a standard, slow moving wheel load. The capability of these devices will be described in detail in Chapter 2. In brief, the FWD is a trailer mounted apparatus which applies a load pulse to the pavement, simulating a commercial vehicle in terms of stress level and loading time. The FWD is capable of measuring surface deflections at a number of different radial distances from the centre of loading or a "deflection bowl" (refer Figure 1.1). Figure 1.2 illustrates two deflection bowls with the same maximum deflection, one produced from a weak structure and the other from a stiff structure.. Their differences in the shape of the deflection bowl are clearly observed. Furthermore, these deflection bowls enable the elastic stiffness of the underlying pavement layers, as well as the subgrade, to be assessed by theoretical back-analysis. In the U.K., a FWD was purchased by the TRRL in 1983 and used to collect site performance data on a number of pavements. Some of this data has been provided to assist with the development of the analytical work in this project undertaken at Nottingham University. During the first year of the research, arrangements were also made with the TRRL for using the FWD to survey five full-scale trial sections which were designed at Nottingham. These data form the backbone of the early development of the present analytical modelling

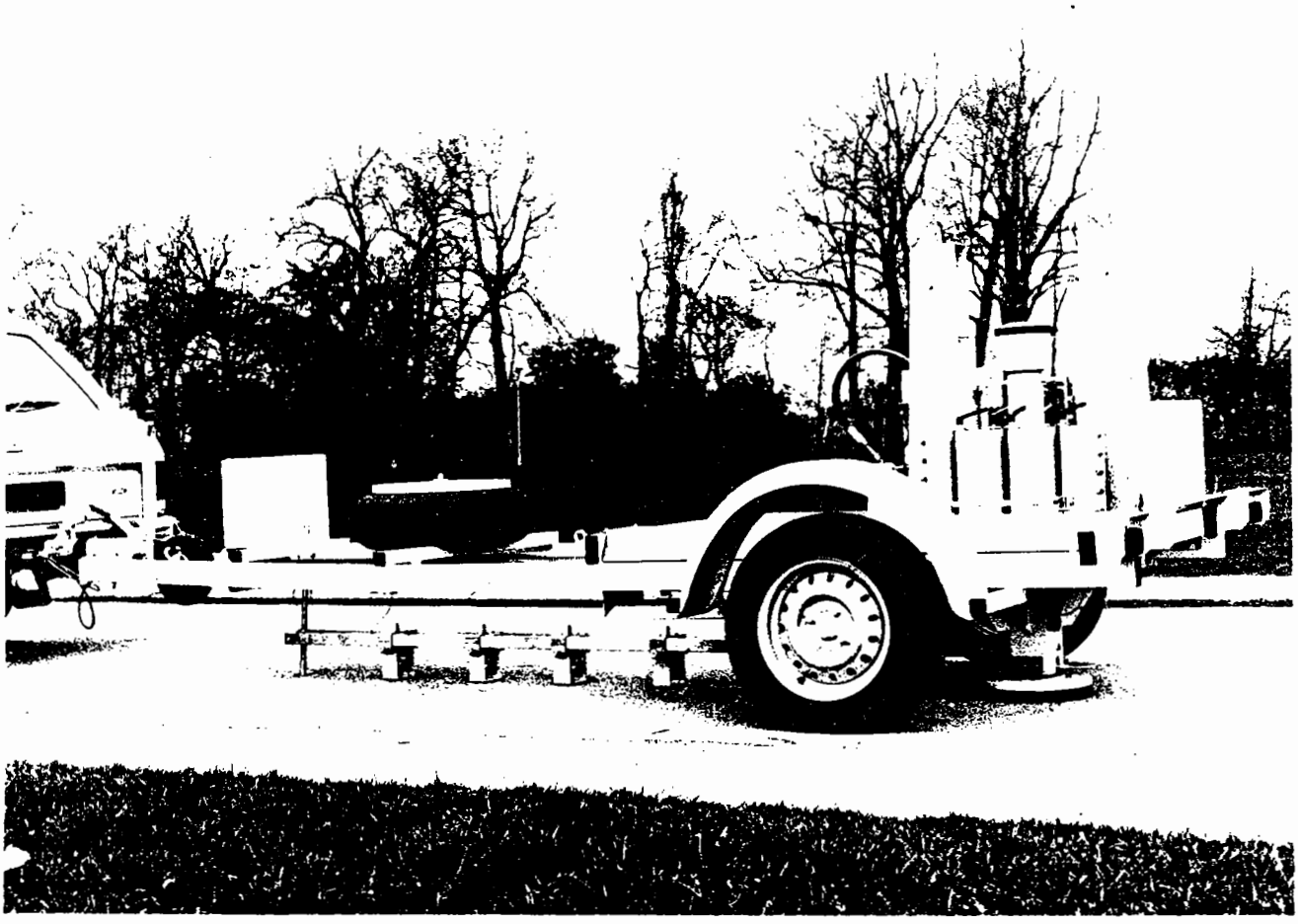

Plate 1.1 : THE DYNATEST FALLING WEIGHT DEFLECTOMETER

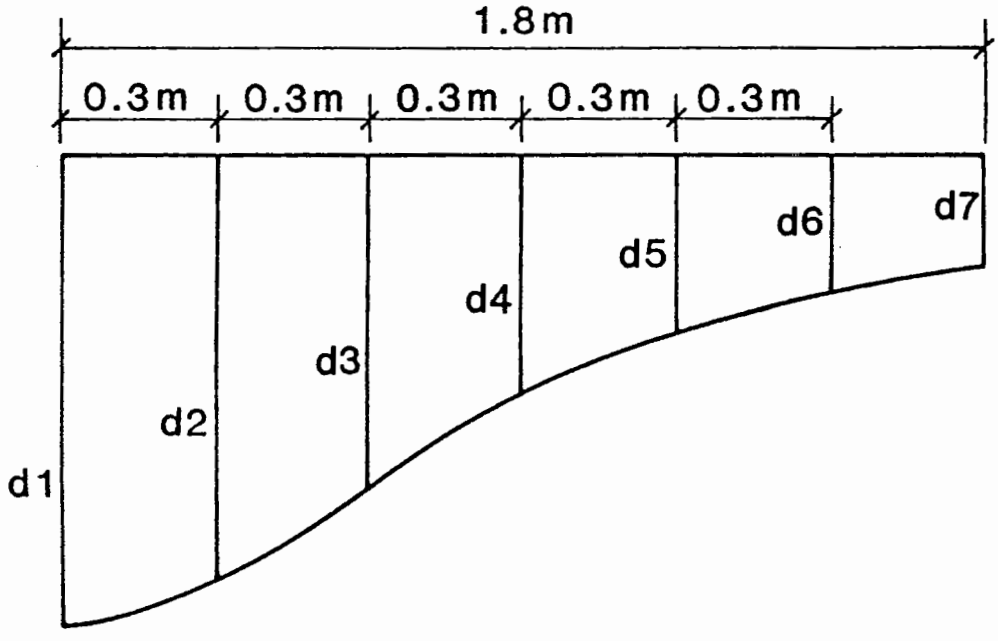

FIG. 1.1 DEFINITION OF A DEFLECTION BOWL

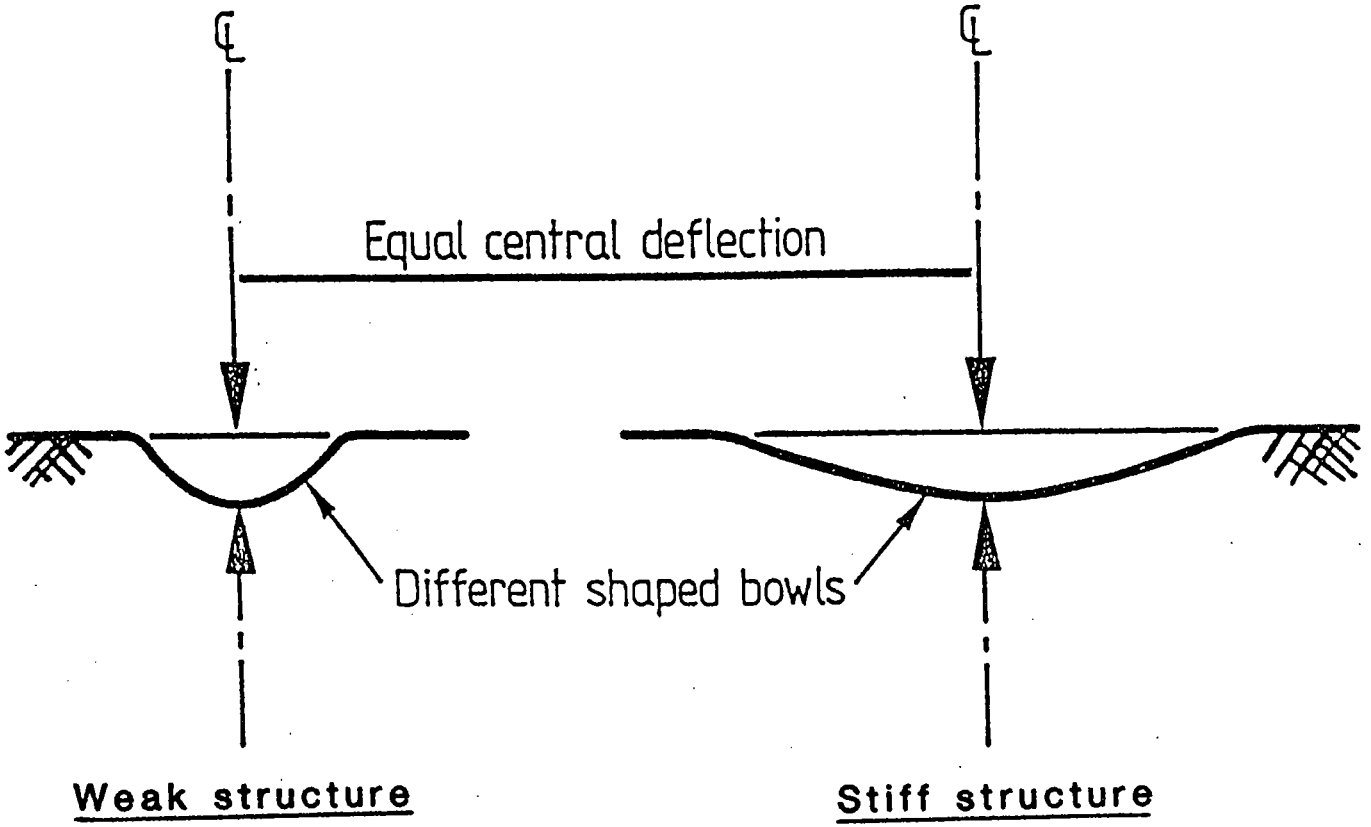

FIG. 1.2 RELATIONSHIP BETWEEN DEFLECTION BOWLS MEASURED FROM WEAK AND STIFF PAVEMENTS

for pavement evaluation.

In the second year, a FWD was purchased by the University through a Teaching Company Scheme (TCS) in conjunction with Scott Wilson Kirkpatrick and Partners, one of the largest civil engineering consultant firms in the U.K. with special expertise in highway and transportation engineering. This allowed more varied data to be obtained. With the help of the TCS, a separate company, SWK Pavement Engineering (SPE) was set up to apply the techniques, which were developed in the research, in practice. In addition to the routine testing on roads, runways and container terminals, the FWD was used to assess its potential in various special investigations. These included the identification of shrinkage or thermal cracking in lean concrete roadbases and the evaluation of load transfer at joints in concrete pavements.

1.1 ELASTIC LAYER STIFFNESSES FOR PAVEMENT EVALUATION

The structural evaluation of a pavement is basically an inverted design process. In the design process (forward analysis), if the cross-section and properties of the pavement materials and the subgrade are known, it is possible to compute the pavement responses, e.g. stresses, strains and displacements for given loading conditions. In the evaluation process (back-analysis), the response of the pavement is observed and the material properties are derived. In this Thesis, the in-situ material properties, which are derived in the back-analysis process, are the effective "elastic stiffnesses" of each layer of a pavement structure. The effective elastic stiffness is taken to be equivalent to the Young's modulus when the structure is linear and elastic. The significance of the elastic stiffness parameter is that it allows the in-situ condition of all the constituent pavement layers and the subgrade to be quantified thus enabling the probable cause of the pavement distress to be

objectively evaluated. Furthermore, with better understanding of the pavement condition, this should facilitate a more effective economic rehabilitation measure.

1.2 OBJECTIVES OF THE RESEARCH

The main objectives of the research are:

(a) To identify the factors which will influence the shape of the deflection bowls

(b) To develop and validate an analytical back-analysis procedure for evaluating the elastic stiffnesses of all the constituent layers of a pavement structure, taking into account the importance of the non-linear behaviour of the subgrade by utilising the deflection bowls measured by the FWD.

(c) To develop an analytical overlay design procedure based on experience in Nottingham in the design of pavements.

The emphasis of the research is that the analysis should be both simple and realistic; hence, the multi-layered elastic system is considered to be the best analytical tool for this research. More details on this subject will be discussed in Chapter 3.

1.3 ORGANISATION OF THE THESIS

In Chapter 2, the capability of the FWD and other non-destructive testing devices have been investigated. A theoretical study is then undertaken in Chapter 3 to examine systematically the sensitivity of the parameters of each pavement layer in influencing the deflection bowls produced by a multi-layered linear elastic system. Chapter 4 describes the formulation of non-linear subgrade stiffnesses. This formulation, together with the results of the sensitivity analysis, has led to the development of analytical procedures for pavement evaluation. This is followed by systematic validation. As part of the comprehensive validation of the analytical procedures, a detailed investigation of a full-scale trial section has been carried out and

Chapter 5 summarises the essential findings of the investigation. Chapter 6 contains findings relating to the examination of a commercial software package in terms of the accuracy of prediction and its comparison with the proposed analytical procedure.

In order to determine the remaining life against fatigue cracking of bituminous pavements, laboratory tests have been carried out using a four-point bending apparatus. The results of the tests can be found in Chapter 7. Finally, a new overlay design procedure is proposed in Chapter 8 which incorporates a rational method for the remaining life calculation.

CHAPTER 2

THE FALLING WEIGHT DEFLECTOMETER AND OTHER NON-DESTRUCTIVE TESTING DEVICES FOR PAVEMENT EVALUATION

2.1 INTRODUCTION

The Falling Weight Deflectometer (FWD), as utilised in this research project, is the latest model, Dynatest 8002 FWD, in use since 1981, and is the most sophisticated machine so far in the development, handling eight incoming signals (1 load and 7 deflections) simultaneously on a fixed datum. In 1983, TRRL purchased the latest version of the FWD and agreed to provide it for collection of site deflection data on full scale trial sections which had been designed by Nottingham University between 1978 and 1982. In 1985, a new FWD, *the* second in the United Kingdom, was purchased through *a* Teaching Company Scheme. As a result of this development, the writer was able to explore the potential of the FWD over a much wider range of applications.

This Chapter is divided into two parts. First, a wide range of non-destructive testing devices which are currently employed in the evaluation of pavement structures is reviewed. Then, some special investigations are performed, to evaluate the accuracy and capabilities of the FWD in field testing.

2.2 NON-DESTRUCTIVE TESTING DEVICES

The non-destructive testing devices currently in use to collect deflection data can be grouped into four different loading models:

(a) Static loading;

(b) Vehicular loading;

(c) Vibrating loading;

(d) Impulse loading.

Table 2.1 summarises the characteristics of the various devices to measure surface deflections.

2.2.1 Static Loading

The typical device is the plate bearing test. The load is generally applied for several minutes over a fixed point in the pavement surface. Several load increments are applied until a pre-determined cumulative settlement is reached. In Britain, the typical pre-determined cumulative settlement of the plate bearing test is 1.27 mm. Correlation charts have been produced relating California Bearing Ratio (CBR) with the maximum applied pressure for different sizes of loading plate. At a given maximum applied pressure, the CBR of the material tested can be derived. However, the large loads and static nature of the test make it unsuitable for simulating the response of the pavement under a moving wheel load.

2.2.2 Vehicular Loading

The principal devices used in this category include:

(a) Deflection Beam;

(b) Lacroix Deflectograph.

The Deflection Beam, also known as the Benkelman Beam (BB), was invented by A.C. Benkelman (5,6) to measure deflections for the WASHO Road Test in the United States. Since then, the BB has been modified by different research organisations.

The design of the version of BB used by the TRRL is illustrated in Plate 2.1. The BB is made of aluminium alloy and is very slender in order to pass between the dual rear wheels of a loaded vehicle. It is 3.66 m in length and is pivoted at a point 2.44 m from the tip giving a 1:2 length ratio. The pivot is placed on a frame made of aluminium angle supported by three adjustable feet. A dial gauge rests on the rear end to measure the movement of the free end of the beam. Figure 2.1 shows the principal dimensions of the BB.

Devices	Loading Mechanism	Maximum Peak to Peak Force	Diameter of Loading	Loading Duration or Frequency	Deflection Measuring Device	Load Measuring Device	Method of Recording Data	Remark (see footnot
1. Static Loading								
Plate Bearing Test	Static	Varied	150–500mm	few minutes	dial gauges	pressure gauge	Manual	(1)
2. Vehicular Loading								
Deflection Beam	Slow moving wheel	31 kN	Dual wheels	1 km/hr	dial gauge	N/A	Manual	(2)
La Croix Deflectograph	Slow moving wheel	31 kN	Dual wheels	1-3 km/hr	Displacement Transducers	N/A	Automatic	(3)
3. Vibratory Loading								
Dynaflect	Counter-rotating masses	4.45 kN	-	3Hz	geophones	Load cell	Automatic	(4)
Road Rater	Electrohydraulic	36 kN	-	10–40 Hz	geophones	Load cell	Automatic	(5)
4. Impulse Loading								
Falling weight Deflectometer	Falling masses	up to 105 kN	300, 450mm	25–40 msec	geophones	Load cell	Automatic	(6)

Remarks

(1) Very large load applied until deflection is less than 25 μm in three minutes.

(2) Maximum deflection measured between dual rear wheels

(3) Automatic measurements of maximum deflection between dual rear wheels at about 4 metres interval.

(4) Load applied through two 4" wide, 16" diameter rubber-coated steel wheels spaced 20" centre to centre. Maximum static preload on pavement 955 kg.

(5) Load applied through two rectangular steel pads 7" long, 4" wide, spaced at 6" apart. Maximum static preload ranging from 1000 to 2600 kg depending on type of model.

(6) Load may be varied according to drop mass and height of drop.

Table 2.1 Principle deflection measuring devices used in different loading modes.

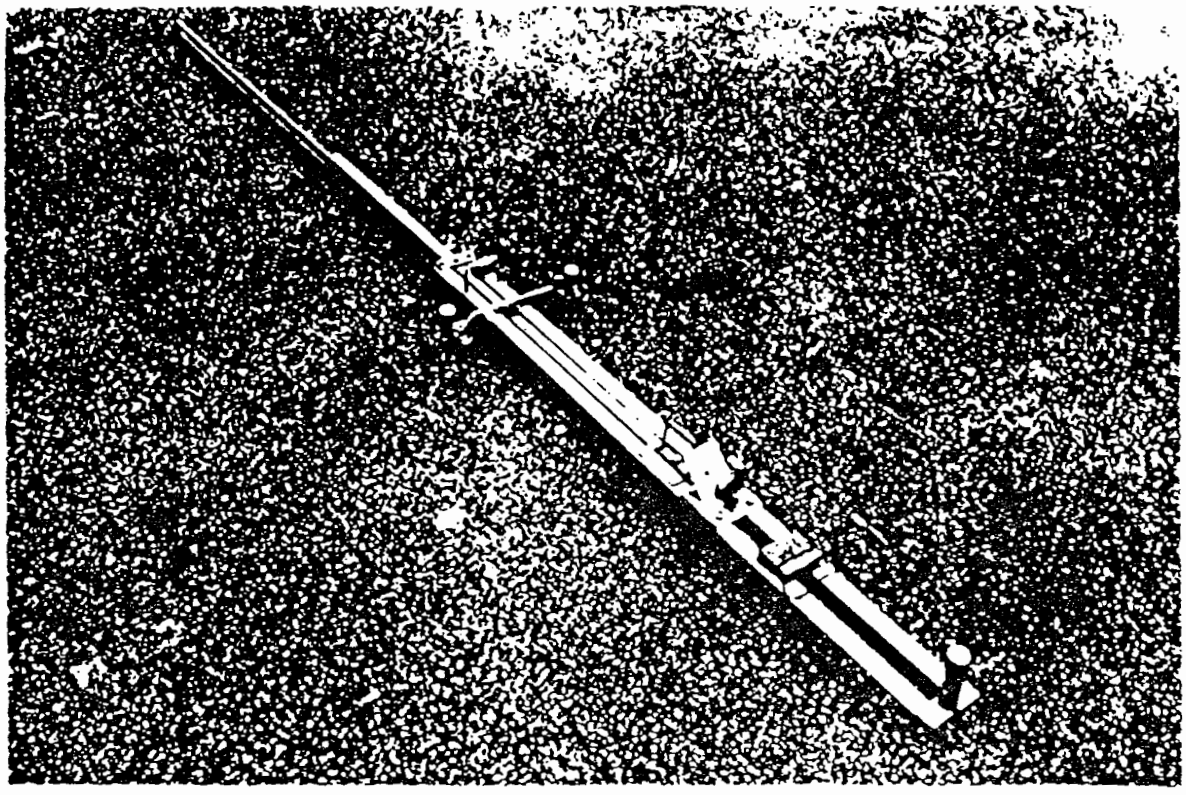

By permission of the Director of TRRL

PLATE 2.1 THE DEFLECTION BEAM

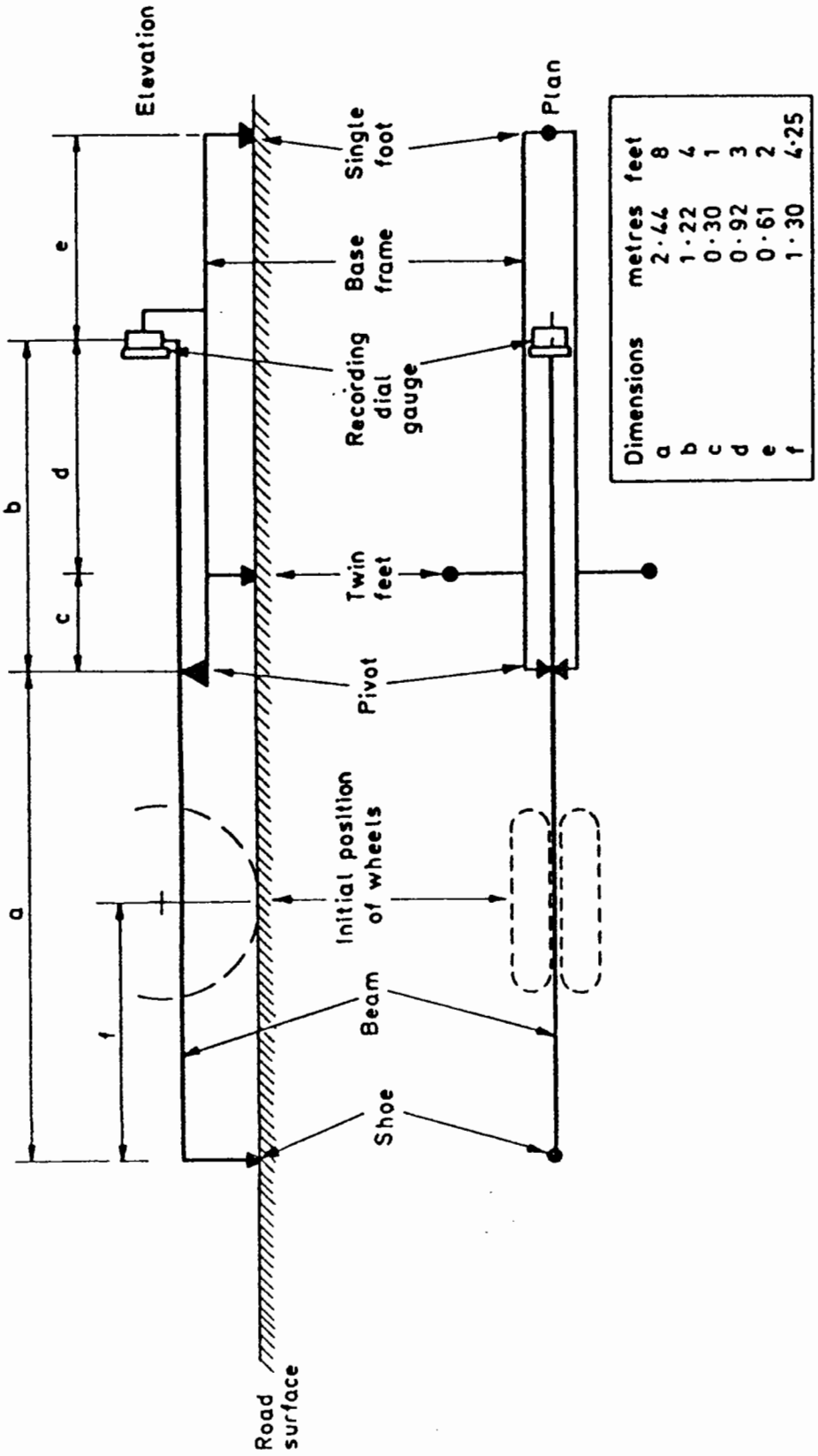

FIG. 2.1 DIAGRAMMATIC REPRESENTATION OF THE DEFLECTION BEAM

The deflection of the pavement surface is produced by a loaded vehicle with a specified rear axle load (3175kg ± 10%(2)). The device measures the maximum deflection. Since the BB was invented, it has been used by many different research organisations round the world and much of the early work in deflection-based overlay design for flexible pavements has been based on this device. In the United States, the deflection measurements are made by using one of two procedures: AASHTO T256-77, "Standard Recommended Practice for Pavement Deflection Measurements" (7); and the Asphalt Institute's rebound deflection testing procedure (8). Norman et al (2) first described the empirical method of overlay design based on the BB for U.K. conditions and the standard procedures for carrying out deflection measurements. Nowadays, the BB is already outdated and its overlay design procedure is largely superseded by the La Croix Deflectograph.

The major technical problems associated with the BB include ensuring that the front supports are not in the deflection bowl of the wheels, and the difficulty or inability in determining the shape and size of the deflection bowl accurately.

The La Croix Deflectograph, originally developed in France, is an automatic form of the BB. It has been used widely in Europe and other parts of the world but not in the United States. The California Department of Transportation has built, and used for several years, a travelling deflectometer which is similar to the La Croix Deflectograph.

The La Croix Deflectograph is a loaded vehicle with deflection beams connected to a placement frame beneath and automatic recording equipment inside a separate cab on the vehicle. Displacement transducers are fixed at each tip (one on each side) of the beam. Plate 2.2 shows the beam assembly of the Deflectograph. During the operation, the frame with both beams is placed on the road surface in front of the oncoming dual wheels. As the wheels approach the beam tip, the beam rotates about the pivot

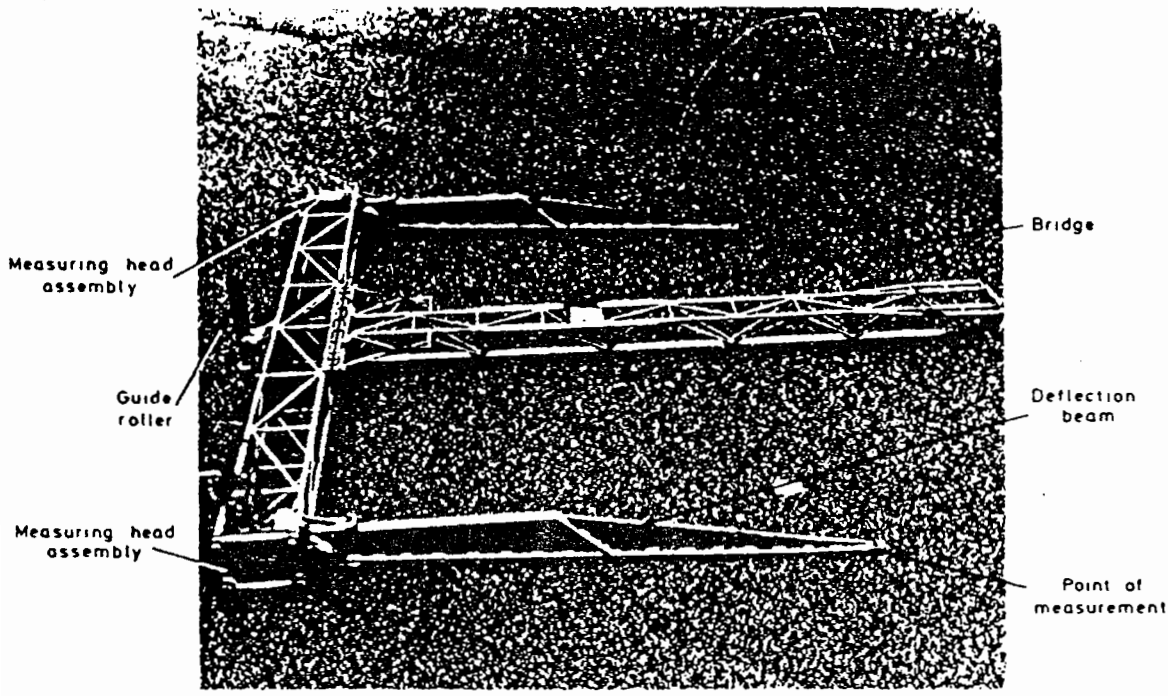

By permission of the Director of TRRL

PLATE 2.2 BEAM ASSEMBLY OF THE DEFLECTOGRAPH

and the rotation is measured by the transducers. This measurement continues until the wheels pass the beam tip. During this period, the beam remains in the same location. The beams and the frame are then drag forward, and repositioned to begin a new measuring cycle. The system was initially set up to measure maximum deflection of the road surface but recent developments allow the "deflection bowl" to be measured. Lister and Kennedy (9) describe an empirical overlay design procedure based on data collected by the La Croix Deflectograph over about twenty years.

The technical problems confronting the La Croix Deflectograph is that it is difficult to determine deflection at a given point. In addition, it cannot be used to determine load transfer across a joint or crack. Moreover, if the deflection bowl is large, the point used as reference may be within the bowl itself and, therefore, the deflections are not measured from a fixed datum. Gardiner et al (10) reveal that a 6.5m long wheel-base deflectograph has been developed in an attempt to rectify this problem.

2.2.3 Vibratory Loading

Basically, vibratory loading devices induce a steady-state harmonic vibration in the pavement with a dynamic force generator. The two common types of steady-state vibratory force generators use either counter-rotating masses or electro-hydraulic systems. The typical device utilising counter-rotating masses is the Dynaflect whereas the Road Rater (RR) incorporates the electro-hydraulic systems. The normal operating procedure for these devices is to apply a static pre-load to the pavement. A harmonic peak-to-peak load is generated at a selected driving frequency and the peak-to-peak deflection is then measured using geophones at different radial distances from the applied force. Hoffman and Thompson (11) give a detailed account of the RR and its operating

procedure. Scrivner et al (12) explain the use of Dynaflect in pavement evaluation.

The technical problem for these devices is that the magnitude of the peak-to-peak dynamic force must be less than twice the static force to ensure that the device does not bounce off the pavement surface. This places a lower limit on the amount of static force that must be applied. As the dynamic loading is increased, this preload must also be increased. It is considered that this preload changes the stress state of the existing pavement and may cause the pavement to respond differently. To overcome this, an inertial reference is used to compare any change of deflection directly with that produced by the dynamic load.

In addition, the limitations of the Dynaflect include a fixed and small peak-to-peak force (4.45 kN, refer Table 2.1), fixed driving frequency and no direct measure of the deflection under the load.

2.2.4 Impulse Loading

The Falling Weight Deflectometer (FWD) is an impulse loading device. The force impulses are generated by a mass falling down a vertical central shaft from a certain height onto a circular plate placed in contact with the pavement surface. Rubber buffers are connected beneath the falling mass to act as damping which essentially controls the duration of the load pulse. Its typical value ranges from 25 to 40 milliseconds (msec). The pulse duration has been found to be constant with depth by Bohn et al (13). The device was initially developed in France (14) during the sixties. Recently, three different makes of FWD have become available, viz, Dynatest, Kuab and Phoenix FWD manufactured in Denmark and Sweden. They all measure the maximum deflection, as well as the deflection bowl, by using several geophones at various radial distances from the load.

The Dynatest 8000 Falling Weight Deflectometer System is the most widely used device. It is trailer mounted and can be towed by an ordinary vehicle. Details of the Dynatest FWD can be found in Section 2.6.

The Kuab FWD is mounted in an enclosed trailer that can be towed by a vehicle. The falling weight system is effected by dropping two masses from different heights. The idea is to create a smoother rise of the load pulse on pavements with both stiff and soft subgrade support. During testing on normal pavements, a solid plate is recommended but on uneven surfaces, a segmented steel plate with hydraulic load distribution is used. The details of the above features are described in Tholen et al (15).

Like its counterparts, the Phoenix FWD is also trailer mounted. Its unique feature is that the mast and weight are mounted on a pivot so that they can be transported horizontally for long distances but are placed upright for testing.

In the seventies, a number of studies were carried out to investigate the FWD in simulating the stresses and strains of a moving wheel on the pavement. Figure 2.2 shows a comparison of the surface deflections produced by the FWD and the moving wheel load as reported by Larsen and Stubstad (16). In this study, Larsen tested the Dynatest FWD on Danish experimental roads. From the figure, very good correlation is clearly observed.

In another study, Ullidtz (17) compared the vertical stress and strain measurements in the subgrade between the FWD and a moving wheel load. The results are presented in Figure 2.3. Again, very good correlation is generally obtained. Examination of the data shows that when the subgrade strain exceeds 200 microstrain, the FWD tends to underestimate the actual strains produced by the moving wheel.

2.2.5 Comparison of Different Devices

Hoffman and Thompson (11,18) carried out comprehensive non-destructive testing of flexible pavements using RR, BB and FWD. They concluded that the FWD is the best device for simulating the actual pavement response under a moving wheel with respect to force, magnitude and duration. The

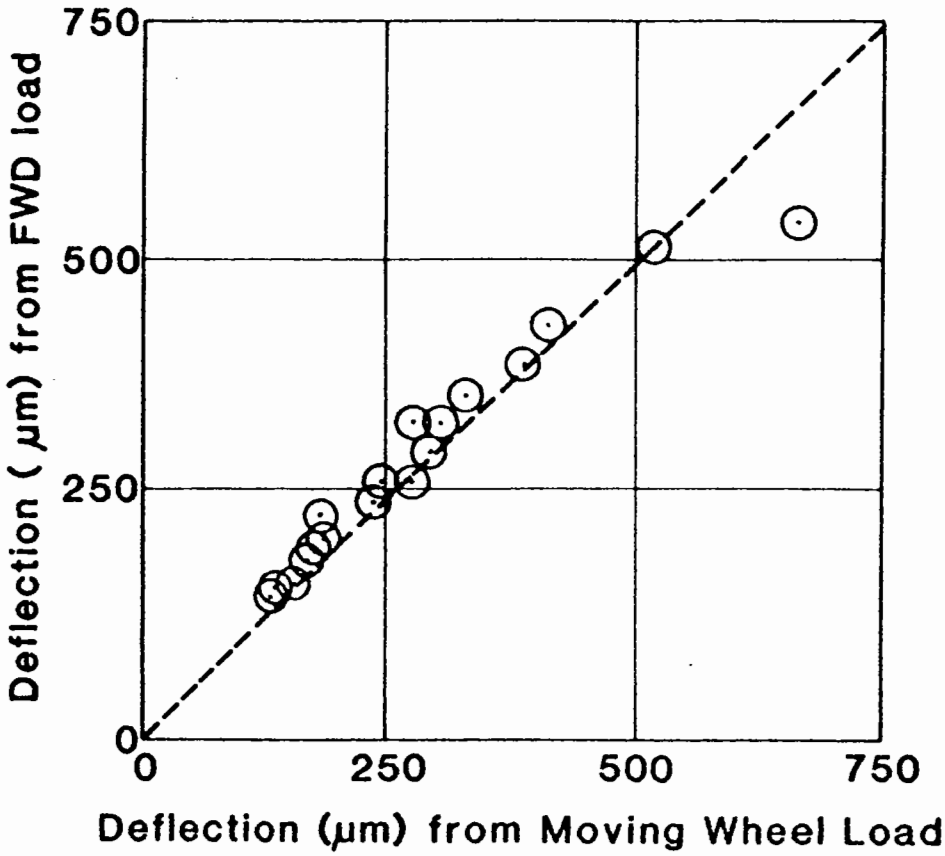

FIG. 2.2 COMPARISON OF SURFACE DEFLECTIONS PRODUCED BY FWD AND MOVING WHEEL LOAD (16)

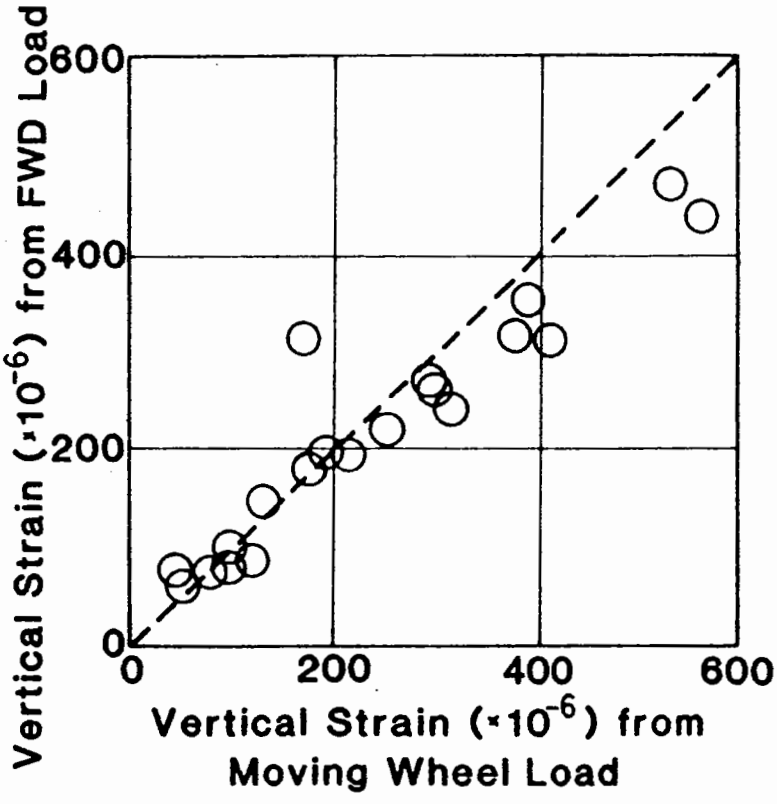

(a) Vertical Subgrade Strains

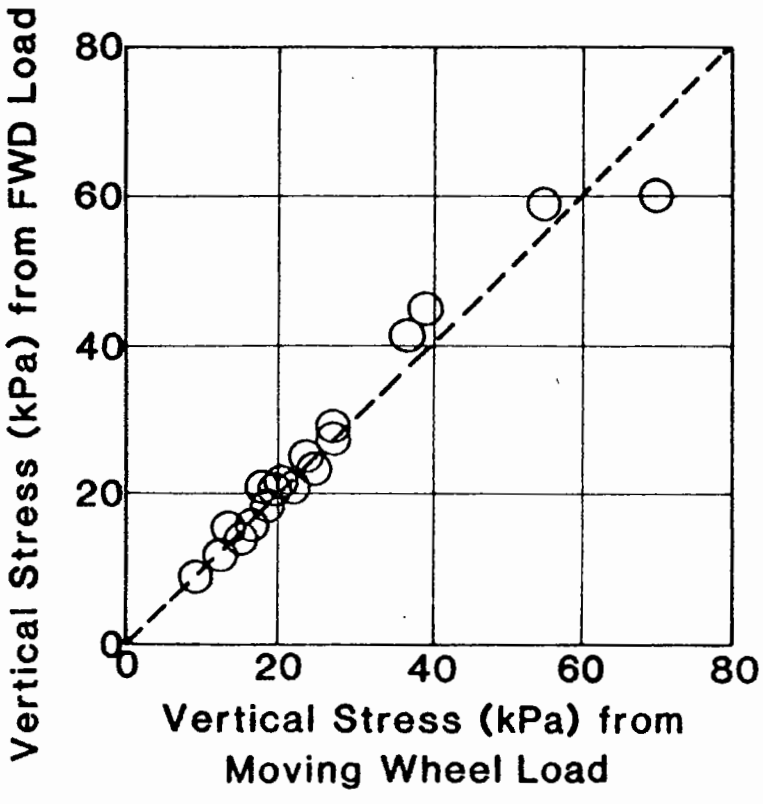

(b) Vertical Subgrade Stresses

FIG. 2.3 COMPARISON OF VERTICAL SUBGRADE STRESSES AND STRAINS PRODUCED BY FWD AND MOVING WHEEL LOAD(17)

RR induced slightly lower deflections than the FWD, indicating a stiffer pavement than is actually present under a moving wheel because of static preload, fixed force amplitude and no rest periods. On the other hand, the loading of the BB is "quasi-static", tending to overpredict deflections compared with those of a moving wheel.

Tholen et al (15) described a detailed comparison of the FWD with other deflection testing devices. The devices used for the study include FWD (Dynatest and Kuab), Dynaflect , static plate bearing, travelling deflectograph, vibrators and BB. They were used on nine different pavement structures. The results revealed a wide range of deflections depending on the magnitude and nature of the applied load, loading time, pavement thickness and in-situ conditions. Tholen concluded that the FWD is best for testing a wide range of pavements with the loading pulse simulating the actual moving wheel loads.

The conclusion from the above review on different types of deflection measuring devices shows a consensus that the FWD is the best device in measuring pavement responses. Therefore, the FWD has been widely used in the structural evaluation of pavements in countries like Denmark (Ullidtz (19)), Holland (Claessen et al (20) and Koole (21)) and the United States (Hoffman and Thompson (11) and Way, et al (22)).

2.3 REVIEW OF DEVICES AND METHODS FOR THE EVALUATION OF SURFACE CHARACTERISTICS

The devices under this category include,

(a) Portable skid resistance tester;

(b) Sideway Force Coefficient Routine Investigation Machine (SCRIM);

(c) Methods of measuring skid resistance at high speed.

The Portable Skid Resistance Tester is also called "Pendulum Tester" (23). Basically, a rubber pad is allowed to pass across a specified distance of the pavement surface having swung down from a fixed height. A proportion of its energy will be lost as it passes over the test surface.

The measure of the skid resistance is given by the arc travelled by the rubber pad in its follow through. The value obtained is the skid resistance value (SRV), which is a measure of the coefficient of friction (multiplied by 100) and assumed to be equivalent to a vehicle passing over the test surface at a speed of 48 km/hr.

The SCRIM, which developed at the TRRL, provides a rapid measurement of the skid resistance of the pavement surface. Hosking and Woodford (24,25,26) describe in detail the principles, operation and factors affecting the measurements made with SCRIM. In brief, a vehicle is driven at a specified speed (usually 50 km/hr) with a test wheel offset 20° to the line of travel, as shown in Figure 2.4. Water is constantly sprayed on the pavement surface where the test wheel is located to reduce the frictional resistance between the wheel and the pavement. The wheel has a known constant vertical force applied to it and the sideway force along the axis of rotation of the wheel is measured by means of a load cell. The ratio of these two forces gives the frictional resistance, known as Sideway Force Coefficient (SFC).

The prime purpose of the above devices is to obtain quantitative information about the ability of the surfacing to resist vehicle skidding. The skid resistance measured is simply the coefficient of friction mobilised, in the presence of water, between a wheel tyre and the pavement surface. Technical limitations are that the skid resistance varies with speed and hence any measurement of it must be at a particular speed. Also, it is noted that accumulation of various compounds on road surfaces and seasonal variations may affect the measurements. Furthermore, they are not capable of measuring skid resistance at high speeds because the effect of macro-texture of the pavement surface predominates. The macro-texture of a surface determines the ease with which water can exit between the tyre and the road surface at high speed. A simple method, known as the "sand patch

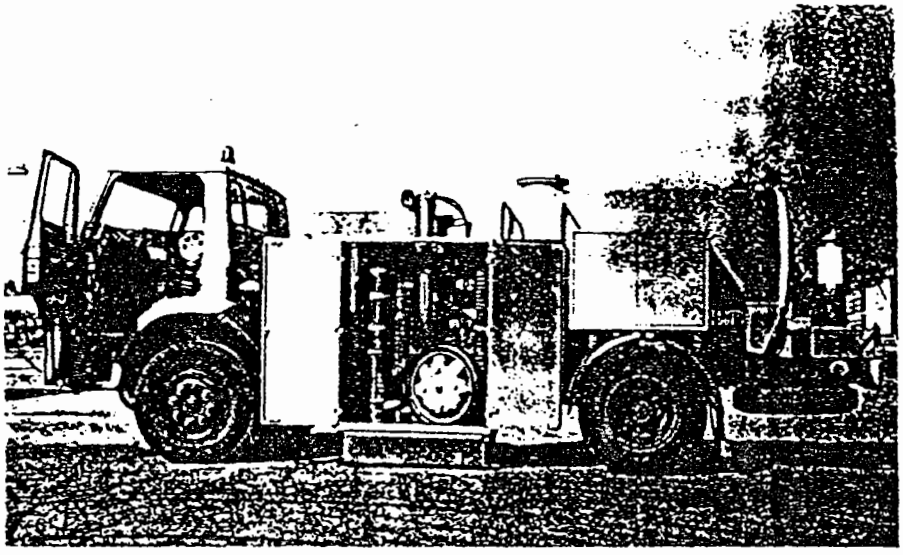

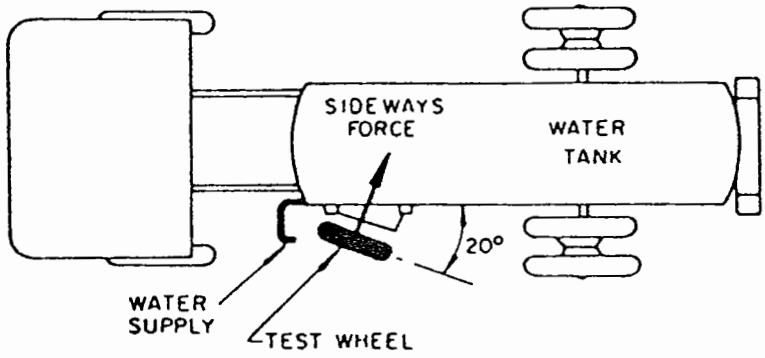

'SIDEWAYS FORCE COEFFICIENT (SFC) = $\frac{\text{SIDEWAYS FORCE}}{\text{VERTICAL REACTION AT TYRE/SURFACE INTERFACE}}$

FIG.2.4 THE SCRIM (SIDEWAYS FORCE COEFFICIENT ROUTINE INVESTIGATION MACHINE)

method", has been devised and documented in Road Note 27 (27). The depth of the macro-texture (texture depth) is measured by spreading a known amount of sand over the road surface. The area of the sand patch is inversely proportional to the texture depth. There are also other methods available. Lees and Katekhda (28) proposed the use of an outflow meter, which measures the flow of water when forced to run through the gap between a simulated tyre and the road surface. The latest development between the TRRL, the Northern Ireland Roads Service and Queen's University, Belfast involves the use of a laser device to enable continuous texture depth measurement to be made from a towed vehicle.

2.4 REVIEW OF DEVICES FOR THE EVALUATION OF SURFACE REGULARITY

The devices in this category measure the riding quality of a road. Soon after a newly constructed road is open to traffic, the plane road surface deforms in both longitudinal and transverse directions. These movements can either be traffic associated or non-traffic associated. The usual end result of surface unevenness is cracking or rutting. The devices used to measure transverse movements on the road surface are:

(a) Straight Edge

(b) Ultrasonic Rutmeter

(c) Multi-wheel Rutmeter

The devices used to measure longitudinal movements are:

(d) Bump Integrator

(e) High Speed Profilometer

To measure a transverse profile (i.e. rut profile), the simplest method is to place a straight edge across a traffic lane and then a wedge calibrated up to 40 mm is pushed manually under the edge until they touch each other. The rut depth is read off the wedge. Usually the maximum rut depth is recorded but readings of the rut profile transversely can also be taken, to indicate the integrity of the underlying layers. Lengths of straight edge are different in different

countries; while the U.K. requires its length to be 2 m, in the United States 1.2 m long straight edges are used. This variation in length results in different rut depths measured.

The Ultrasonic Rutmeter was developed in Northern Ireland. This device consists of a series of transducers placed along a reference beam parallel to the ground, which is mounted across the front of a vehicle. As the vehicle travels, ultrasonic waves are emitted onto the road surface and readings are taken for each of the transducers at regular intervals. The on-board microcomputer then processes the data to produce the rut depth on the wheelpaths.

Also along this line, the TRRL has developed an automatic Multi-wheel Rutmeter. Potter (29) described the device, mounted on a trailer, which consists of 21 wheels, each 200 mm in diameter, and spaced at 100 mm centre. Each wheel independently follows to the road surface variations. A displacement transducer is connected to each wheel. During operation, it is towed by a vehicle travelling at a speed of about 10 km/hr and an on-board computer scans each transducer at every 0.3 m distance of travel. At the end of each test section, the computer prints out the average magnitude of rut depths measured as well as their shape and standard deviation. If required, rut depths for up to 15 different locations showing the largest magnitude in the test section, are also printed.

The Bump Integrator (30) consists of a towed fifth wheel mounted via a leaf spring and shock absorber system onto a high inertia chassis. As the wheel moves (usually at a constant 30 km/hr) along a road, it will respond to any unevenness by moving vertically relative to the chassis. This vertical movement is summed and the total relative vertical movement is presented over a given distance travelled. Recently, the TRRL has improved the capability of this device by incorporating a microprocessor.

The latest advance in systems for measuring longitudinal unevenness is the High Speed Profilometer (HSP) (31). Plate 2.3 shows the HSP in which four laser-based contactless displacement transducers are mounted on the space frame of a trailer. The principle of the contactless displacement transducers is based on the optical system shown in Figure 2.5. During the survey, the trailer is connected to a towing vehicle which travels at any speed up to 80 km/hr. Data is recorded continuously and stored in the on-board microcomputer. The computer then analyses the data to produce longitudinal unevenness as well as texture depth if required. Figure 2.6 shows an example of the rut depths measured by the HSP. The High-speed Road Monitor (HRM) (32) is a further development by the TRRL with more enhanced capabilities. In routine operation, it can measure longitudinal profile, wheelpath rutting and macro-texture in a single pass at normal traffic speed.

2.5 REVIEW OF DEVICES FOR THE EVALUATION OF THE CONDITION OF INDIVIDUAL LAYERS

The device in this category consists of:

(a) Dynamic Cone Penetrometer

(b) Clegg Impact Hammer

Figure 2.7 illustrates a typical dynamic cone penetrometer (DCP). It includes a falling mass of 8 kg sliding along a shaft with a cone at its end. During operation, the mass is lifted up manually to a height 575 mm and released. The falling weight then hammers the stopper transmitting energy to the cone tip which penetrates through the pavement layer. Repeated blows are necessary with the falling mass until the desired depth has been penetrated. The relative strength of each layer is quantified by the penetration of this cone for each load repetition. Investigation with this device enables determination of the thickness of each layer and the variation of strength, in terms of CBR or Structural Number Coefficients, within each layer as well as between

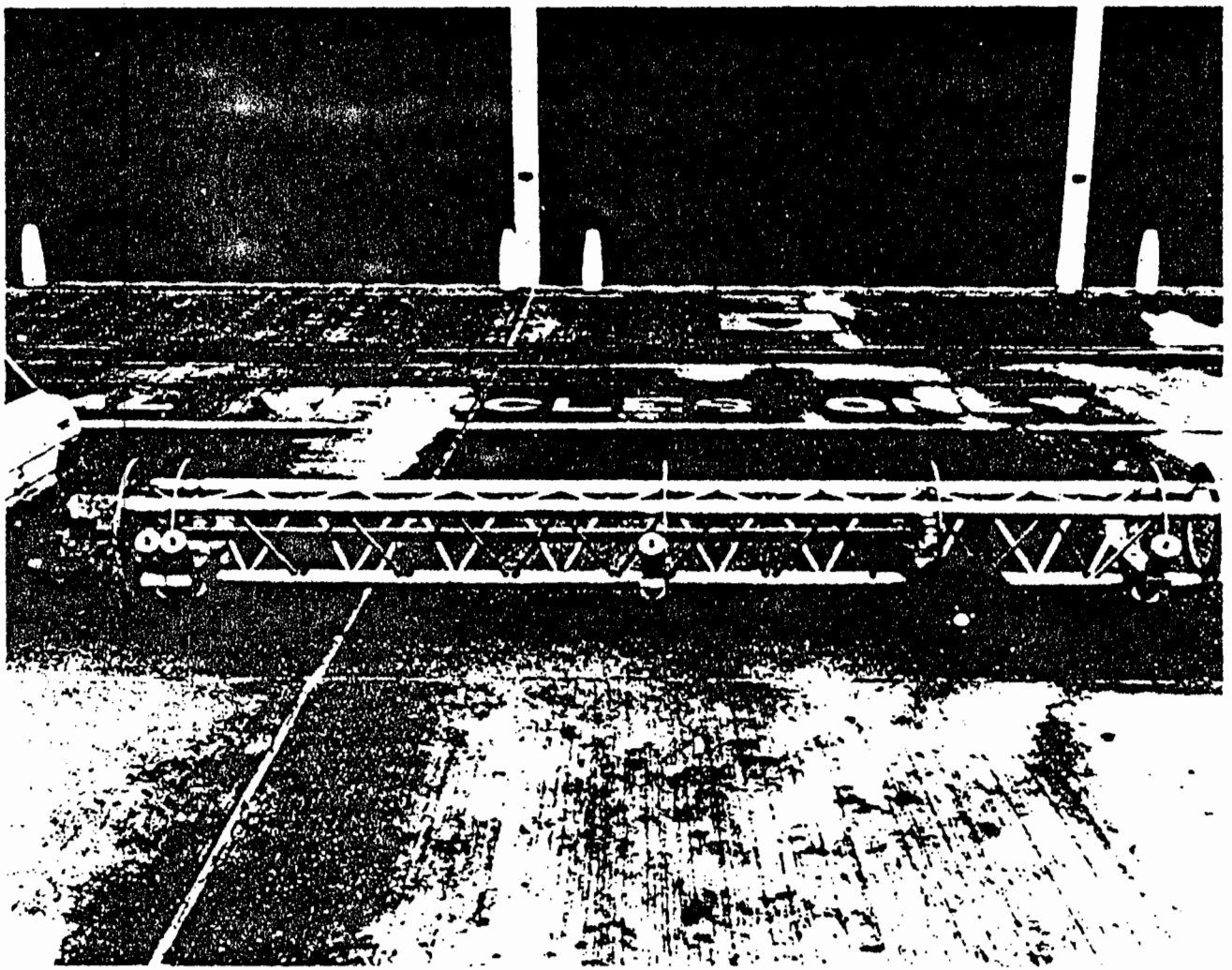

By permission of the Director of TRRL

PLATE 2.3 HIGH SPEED PROFILOMETER BEAM AND CONTACTLESS DISPLACEMENT TRANSDUCERS (31)

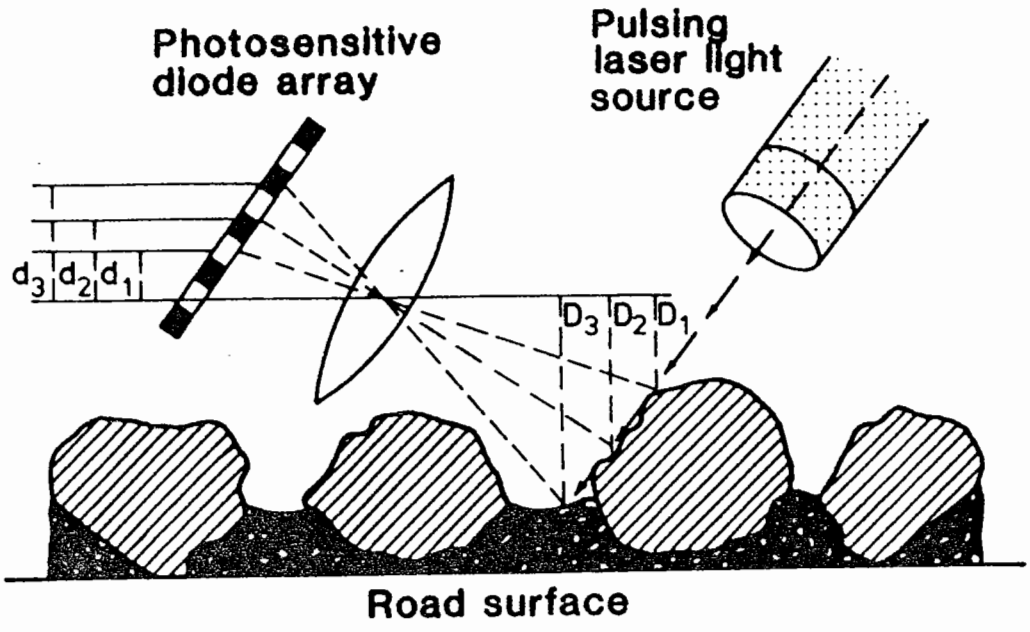

FIG.2.5 PRINCIPLE OF OPTICAL SENSOR SYSTEM

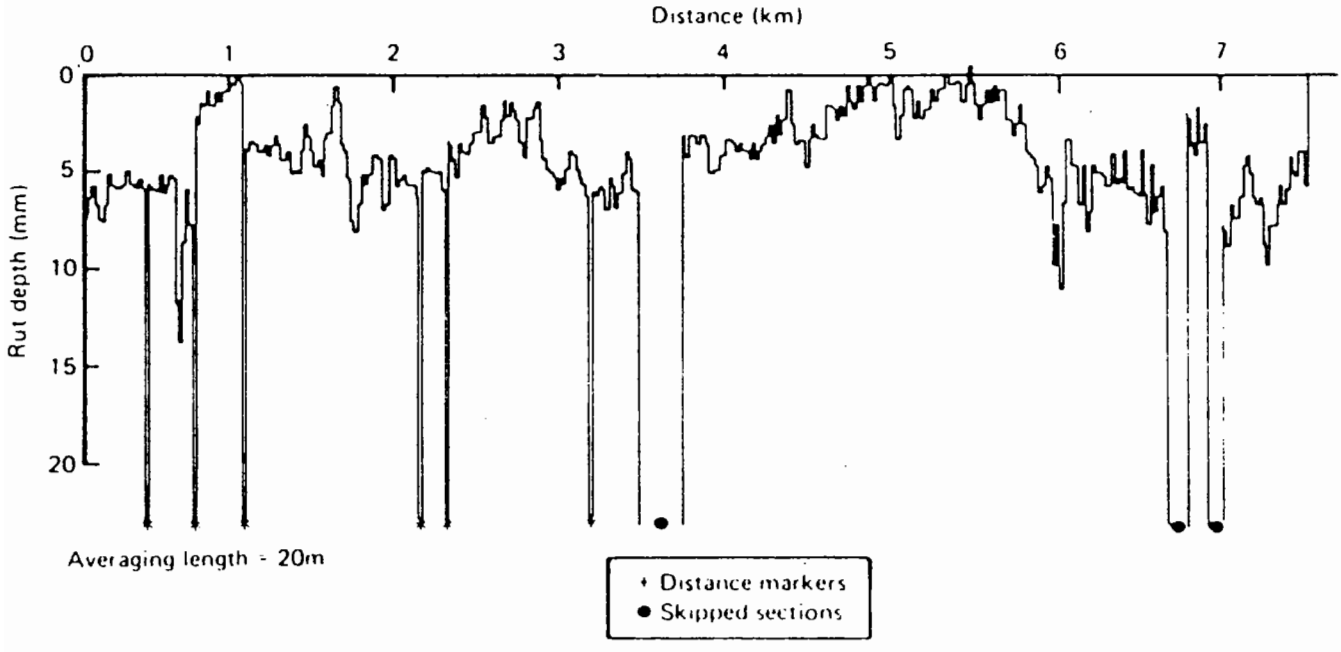

FIG. 2.6 PLOT OF RUT DEPTHS MEASURED ON A TRUNK ROAD (32)

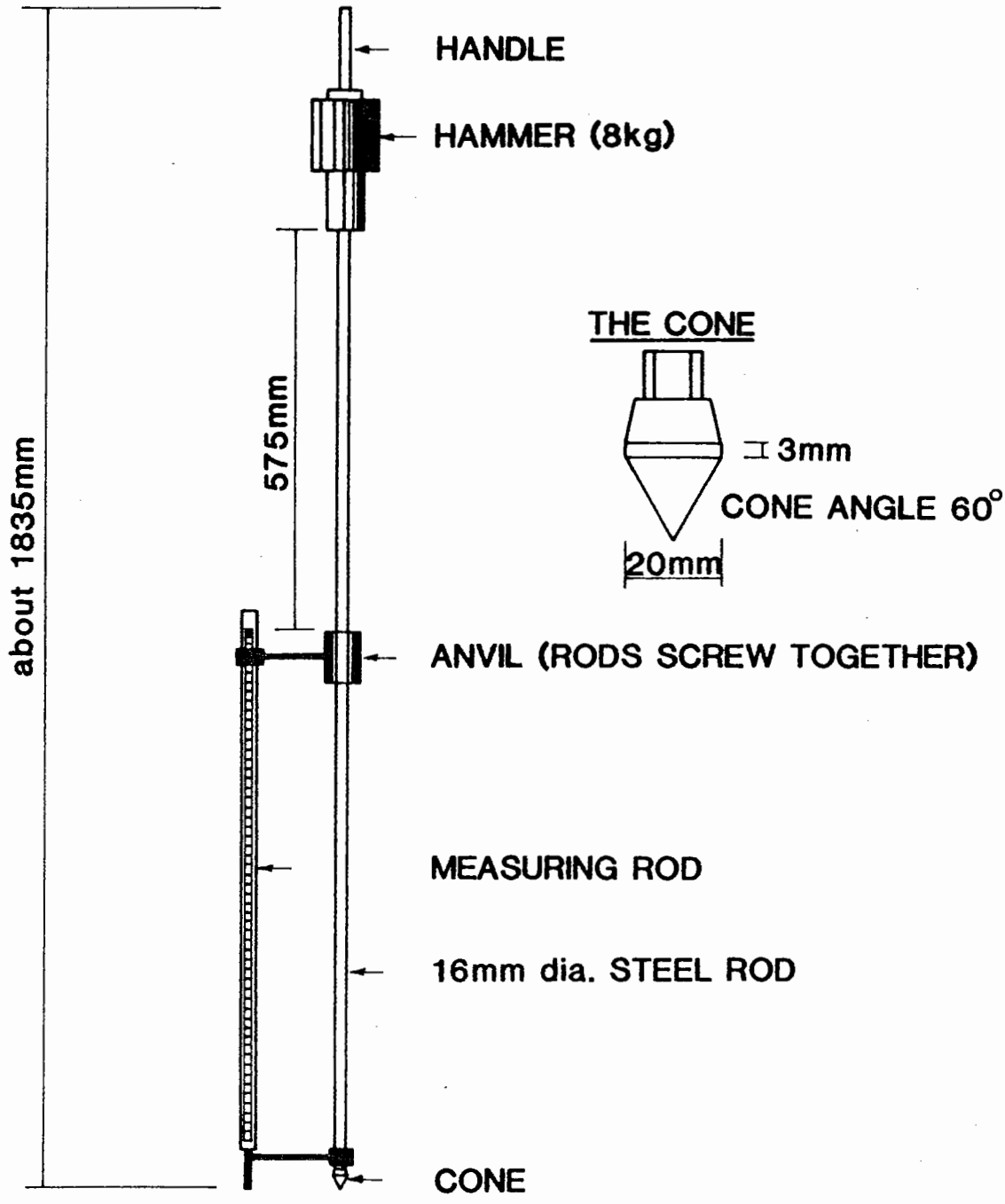

FIG. 2.7 THE DYNAMIC CONE PENETROMETER (DCP)

different layers. The DCP has been widely used in South Africa (33) and design charts have been developed based on this device. It can be used to assess the thickness of the unbound layers and the strength of the granular and clay layers. The technical limitation is it can only be used directly on pavements with unbound or thin bituminous surfacing, e.g. 50 mm or less. For pavements with thick bituminous layers, a core should first be taken before testing.

Another device in this category is called the Clegg Impact Hammer developed by Clegg (34). The device has three main components: a guide tube, a cylindrical compaction hammer of mass 4.5 kg and 50 mm diameter, and a digital readout meter. It is portable and simple to use. During testing, the hammer is raised to a specified height of 450 mm and then allowed to fall and strike the test surface. The maximum deceleration of the hammer on impact with the surface is measured by the accelerometer which is fitted in the head of the hammer. The resulting signal is processed and displayed on the meter in units of CIV (Clegg Impact Value). Each CIV unit is equivalent to 10 gravities (g) of deceleration.

Initial work was carried out by Clegg (34) to use the device for quality control of a road under construction, e.g. monitoring variation of density under compaction. Further research was carried out by Garrick and Scholer (35) to investigate its potential in evaluating the strength of unsealed gravel roads and good correlations were apparent.

Both the DCP and Clegg Impact Hammer have recently been purchased by Nottingham University. Their potentials are being assessed and some of their applications will be reported in Chapter 6.

2.6 THE FALLING WEIGHT DEFLECTOMETER AND THE EVALUATION OF ITS CHARACTERISTICS

The following sections summarise the principle of the FWD and its characteristics. Some special investigations have been carried out to

assess its potential in addition to routine testing.

2.6.1 The FWD Test System

Sorensen and Hayven (36) described the FWD Test System in detail. An attempt is made to summarise the main features of the system below. Basically, the Dynatest 8002 FWD Test System as shown in Figure 2.8 includes three principal units:

(a) A trailer-mounted FWD

(b) An 8600 System Processor

(c) A Hewlett-Packard HP-85 desktop computer

The 8002 FWD: Figure 2.9 shows a section through the Dynatest 8002 FWD. It measures 4.3 metres long and 1.3 metres high. The operation of lifting and releasing the weight is controlled by a hydraulic unit powered by a 12V DC battery. The basic principle of the FWD is that of a mass falling on a circular plate that is connected to a baseplate by a set of rubber springs (buffer). The current FWD modifies the positions of the rubber buffers by attaching them to the base of the falling mass. Figure 2.10 illustrates the operation.

The force of the falling weight can be calculated by equating the potential energy of the mass before the drop with the work done by the rubber springs after the drop. Thus, the following relationship for the peak force (F) exerted on the pavement, is obtained:

$$F = \sqrt{2Mghk} \qquad (2.1)$$

where M is mass of falling weight;

g is acceleration due to gravity;

h is drop height;

k is spring constant.

Judging from equation (2.1), there are three possible ways of changing the force amplitude by varying:

(a) The mass of the falling weight;

(b) The drop height;

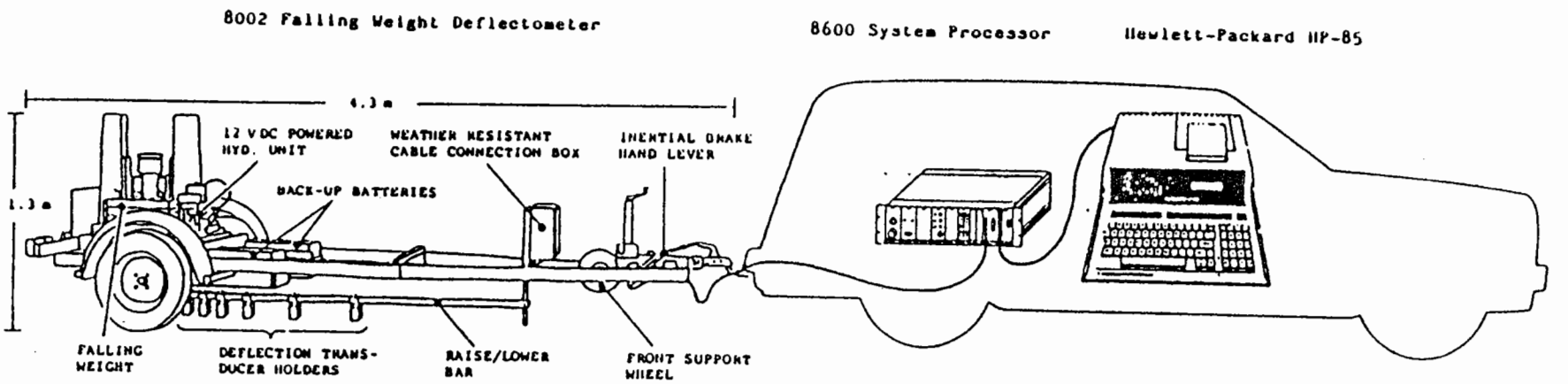

FIG. **2.8** THE DYNATEST 8002 FALLING WEIGHT DEFLECTOMETER SYSTEM

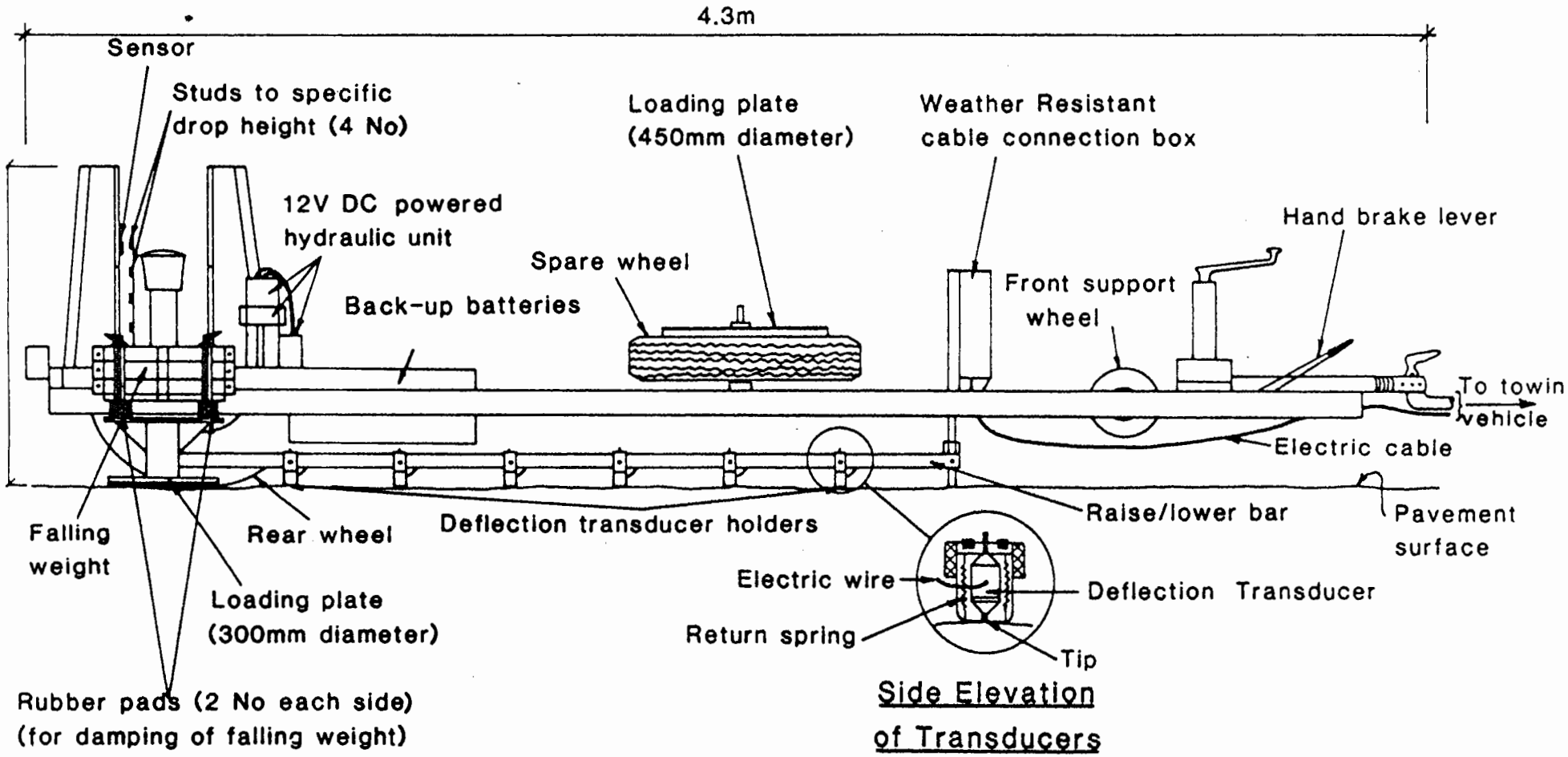

FIG. 2.9 THE DYNATEST 8002 FALLING WEIGHT DEFLECTOMETER (2)
(not to scale)

(c) The spring constant.

The current FWD is able to change alternatives (a) and (b). The mass of the falling weight can be varied from 50kg to 300kg, the intermediate weights being 100kg and 200kg. The drop height varies from 50mm to 450mm. It should be noted in equation (2.1) that a linear spring constant (k) is assumed, which is not correct for the rubber buffers used in the FWD. However, Koole (21) reported tests on the spring characteristics of rubber, showing that a linear spring constant may be assumed if the deformation of the rubber buffers is less than 30mm. The latest design removes this problem by measuring the impulse force independently with an integrated load cell which is mounted above the loading plate. The contact pressure is then calculated by dividing the load by the area of the loading plate. But, changing both the mass and rubber springs would affect the pulse duration of the applied force. The current FWD also overcomes this problem by providing four sets of rubber buffers for each load configuration.

Two different sizes, i.e. 300mm and 450mm diameter, of loading plate can also be selected according to the type of material or pavement to be tested. The 300mm diameter plate is used for routine testing work, while the 450mm diameter plate may be used on a granular layer or soil subgrade which has a low value of stiffness.

The deflections are measured by seven seismic transducers (geophones). The first one, which records the maximum deflection, is fixed and mounted at the centre of the loading plate. The other six transducers are placed in small movable brackets along a 2.45 metres raise/lower bar. This enables deflections to be measured at any distance up to 2.4 metres from the load centre.

The 8600 System Processor: This is an electronic microprocessor which controls the FWD operation from the command signals initiated by the HP-85 computer. Once initiated, it monitors the status of the FWD unit and

performs checks on the 8 incoming transducer signals (1 load + 7 deflections) for correct measurements.

The HP-85 Computer: The HP-85 computer is responsible for the overall control of the test operation as well as displaying, printing and storing on magnetic tape of the test data.

Testing Procedure: The model 8002 FWD is operated remotely from within the towing vehicle. At the start of the test, a "Field Test" program is loaded into the HP-85 computer, which activates the FWD through the 8600 System Processor, then displays, prints and stores the measured results. Since the whole measuring operation has been programmed, all one needs to do is to key in the START command to start the operation. The testing sequence is as follows:

(a) To lower the loading plate and raise/lower bar sub-assembly which supports the seismic tranducers;

(b) To raise the weight to the specified drop height;

(c) To drop the weight (with three rebounds);

(d) To record the load and deflection signals from the first drop only;

(e) To repeat (c) and (d) if more than one drop height is specified;

(f) To restore the whole sub-assembly to the original position.

The whole process is completed with an audible "BEEP". The complete testing sequence takes about one minute for three drops of the weight, excluding driving time between test points.

Figure 2.11 shows the deflection response of the pavement surface during a complete FWD load cycle, recorded by the TRRL using a displacement transducer embedded at the pavement surface.

Accuracy of FWD: Sørensen and Hayven (36) reported that the FWD transducers can measure deflections and load very accurately. Their respective accuracies are given below:

For deflection, absolute accuracy 2.0% ± 2 microns

relative accuracy 0.5% ± 1 micron

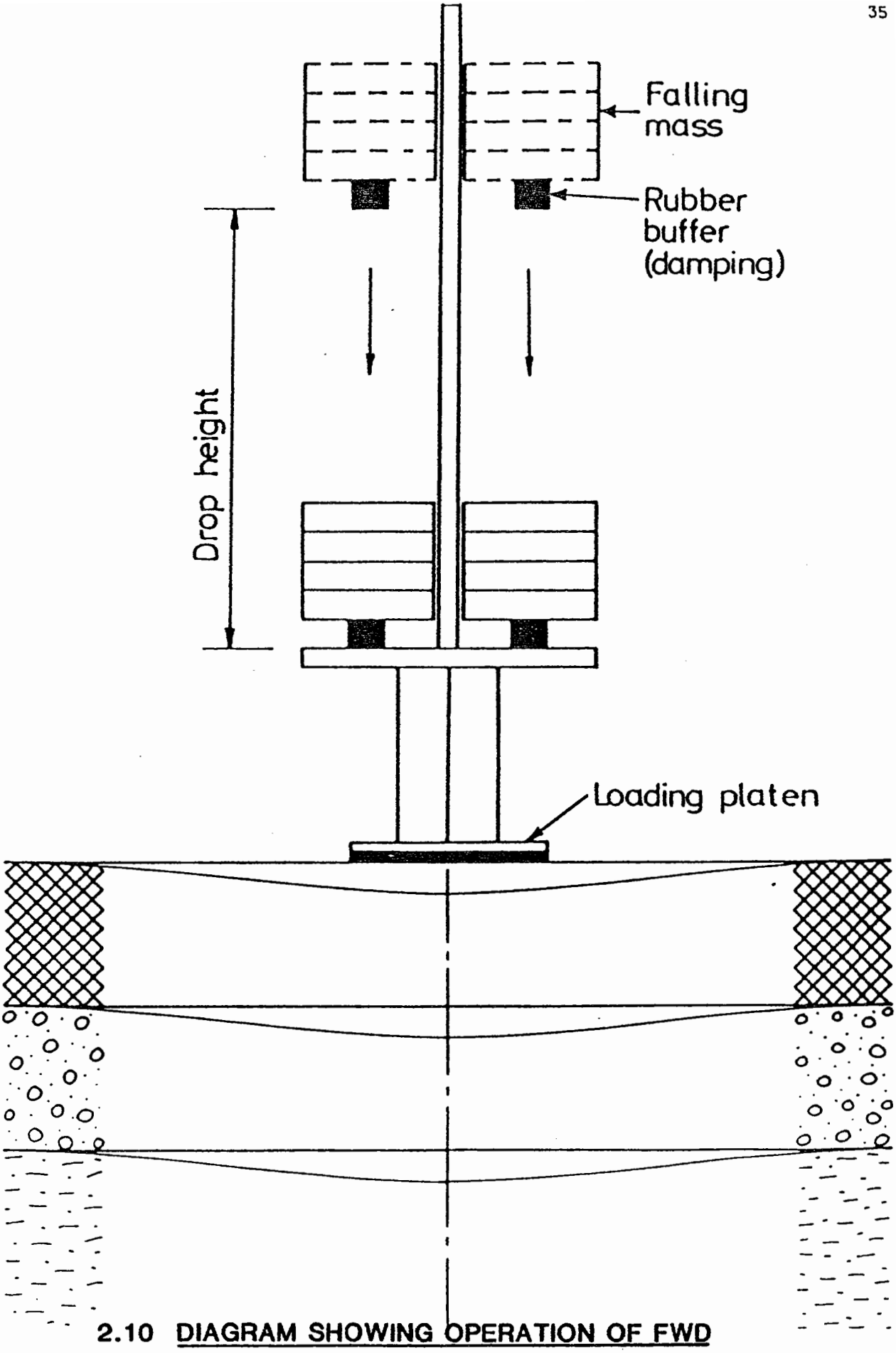

2.10 DIAGRAM SHOWING OPERATION OF FWD

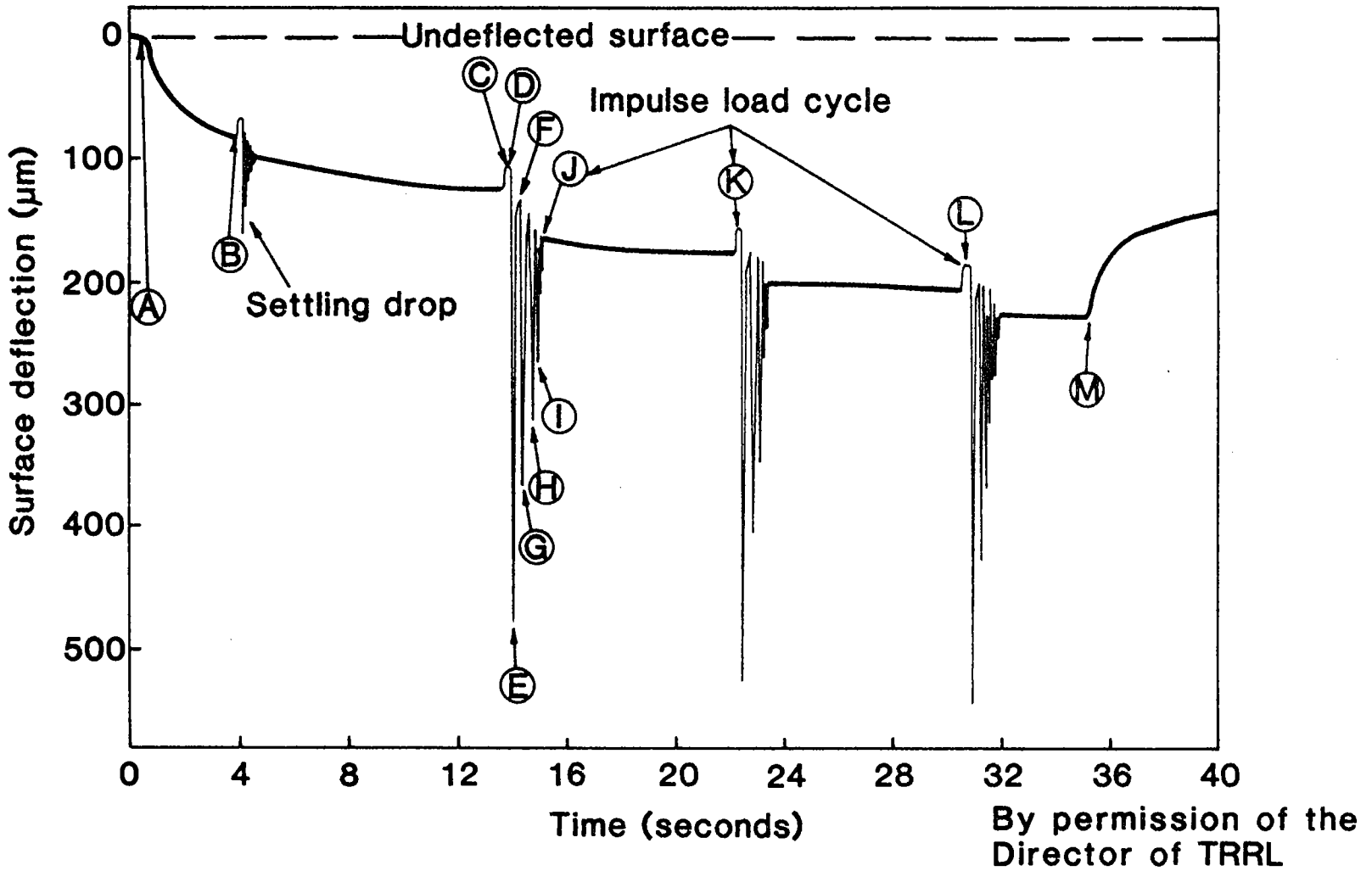

FIG. 2.11 DEFLECTION OF PAVEMENT SURFACE DURING A COMPLETE FWD LOAD CYCLE

For load, absolute accuracy 2.0% ± 0.07 kN

The resolution for deflection is 1 micron and that of the load is 0.07 kN (or 1 kPa stress over a 300mm loading plate).

2.6.2 Some Investigations of the Characteristics of the FWD

(a) Loading time

The Dynatest manufacturer reported that their FWD would produce a near half-sine stress pulse onto the pavement with a loading time of 25 to 30 msec (milliseconds). Similar results have also been reported, e.g. 26 - 33 msec from Bohn et al (13), 30 - 40 msec from Hoffman and Thompson (11).

The loading time of the FWD was recorded on two experimental sections where instruments had been installed. A loading time of 20 - 35 msec was measured which generally agrees with the results measured by the manufacturer and other researchers. It is expected that the variation of the FWD loading time is the result of testing different pavement structures. The stiffer the pavement structure, the shorter will be the measured loading time. Figure 2.12 shows a typical trace of stress pulses measured by a pressure cell buried at a depth of 138mm below the pavement surface on one of the full scale trial sections.

Bohn et al (13) studied the relationship of loading time with depth for both the FWD and a moving vehicle on a Danish test road, where stress and strain measurements were taken at different depths of a pavement. The traces from the instruments have been reported in Bohn's paper and reproduced in Figure 2.13. From the Figure, the loading time from the FWD is observed to be virtually constant with depth, i.e. 30 - 33 msec for up to 1 metre below the pavement surface. However, under the moving wheel, the corresponding durations increase progressively with depth.

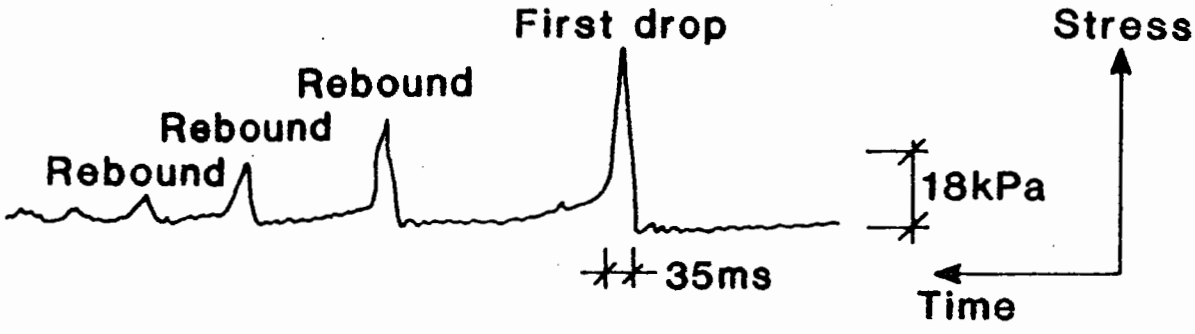

FIG. 2.12 TYPICAL FWD STRESS PULSES
(Depth = 138mm below pavement surface)

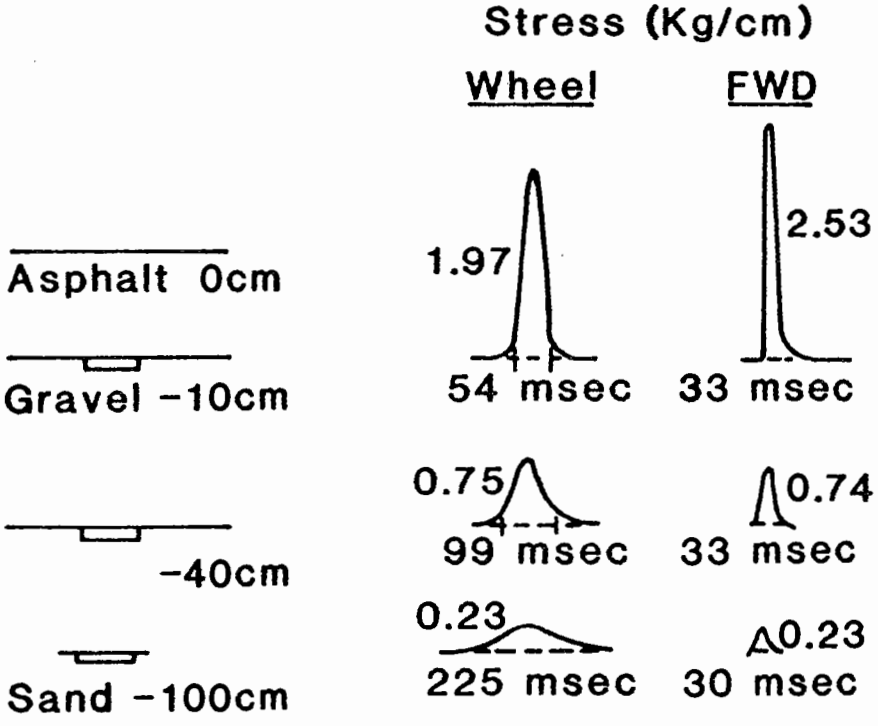

FIG. 2.13 STRESS PULSES AT DIFFERENT DEPTHS PRODUCED BY MOVING WHEEL AND FWD (13)

(b) Influence of temperature on deflection

The effect of temperature variation on the measured deflection bowl was investigated during the field work. Figure 2.14 shows the variation of FWD deflection at a specified location on a flexible pavement section which consists of bituminous surfacing and roadbase layers overlying sub-base and subgrade. During the course of the day, the pavement temperature at 40mm depth rose about 10°C (24.7 to 34.3°C). It is observed that in the first four positions (0.0, 0.3, 0.6, 0.9 m) the deflections are affected by the increase of temperature in the bituminous layers. The last three positions (1.2, 1.5, 1.8 m) are essentially unaffected by temperature rise since they reflect the properties of the unbound sub-base layers and the subgrade and their magnitudes differ by a few microns only.

(c) Repeatability of load amplitude

Tables 2.2 and 2.3 show measured contact pressures both repeatedly applied at a specific location and along whole sections. In all cases, the same loading plate of 300 mm diameter and drop height were used.

In Table 2.2, it is noticed that measured contact pressures for a specific location are quite repeatable. Closer examination reveals that the measured pressures are very consistent in a stiff structure (Derby Road) with maximum deviation of 0.4%. However, the deviation gets larger for medium stiff and weak structures, with calculated values of 1.4% and 2.3% respectively. Nonetheless, the manufacturer's claim of accuracy on load of 2% ± 0.07 kN appears to be acceptable.

Table 2.3 tabulates measured contact pressures along the whole length of a section. Again, a large range of variation, as found in Table 2.2, is observed, from 2.5% (stiff) to 7.0% (less stiff). Over a stiff structure (Derby Road), the magnitudes of contact pressure differ slightly from one location to another but appear consistent when the

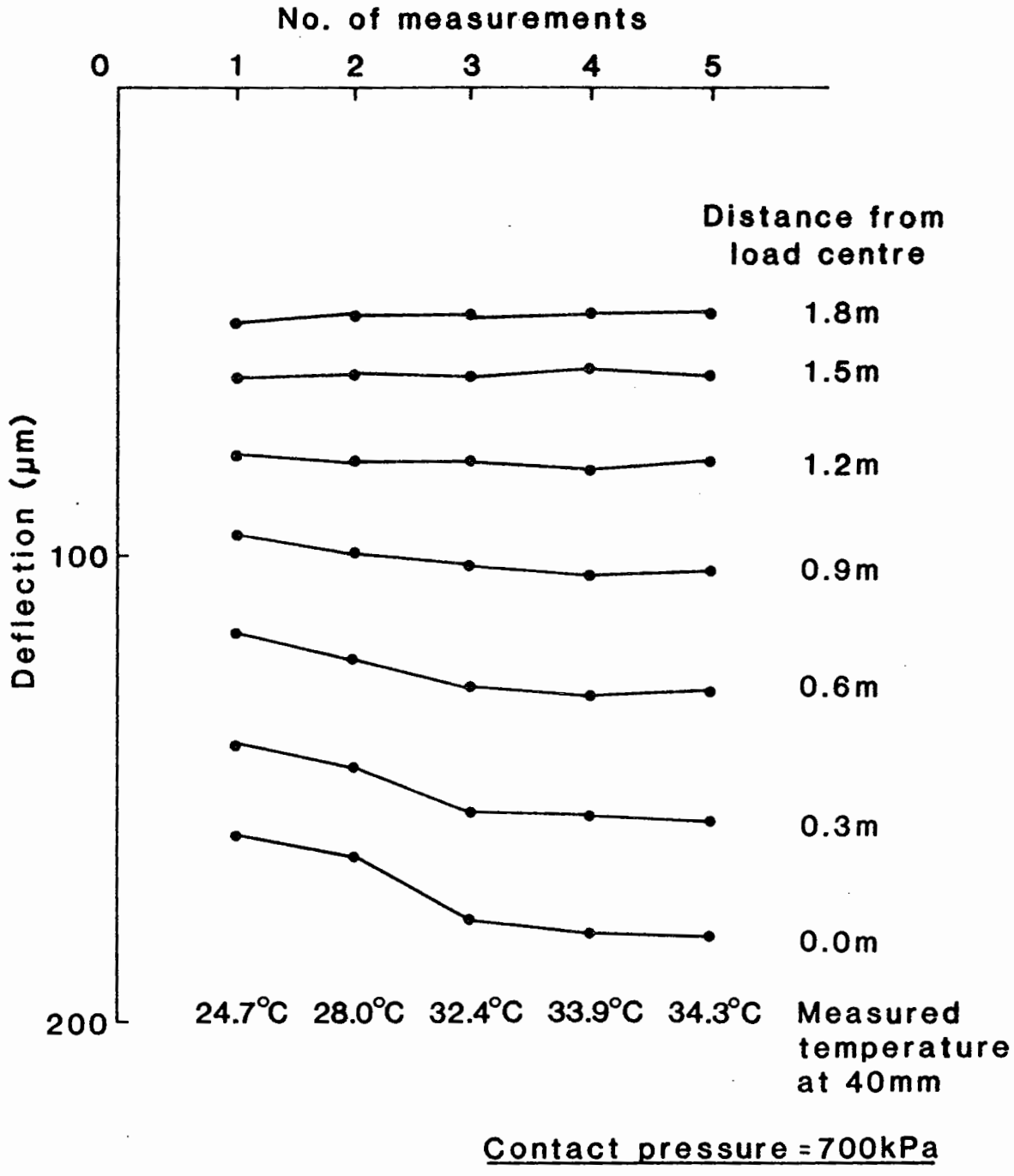

FIG. 2.14 VARIATION OF FWD MEASURED DEFLECTION ON Ch. 120m W.B. LANE CENTRE

A52 DERBY ROAD, NOTTINGHAM
(Survey on 10/8/84)

Site Location	No. of Measurements						Max. deviation from mean
	1	2	3	4	5	6	
Derby Road Ch 120 m WB	709	714	711	711	712	-	0.4%
Hasland Bypass Ch 20 m WB	664	683	-	-	-	-	1.4%
Carsington Bypass Ch 20 m WB	761	745	741	741	735	741	2.3%

Table 2.2 Repeatability of Contact Pressures (kPa) Measured at Specific Position

Derby Road		Hasland Bypass		Carsington Bypass	
Chainage (m)	Pressure (kPa)	Chainage (m)	Pressure (kPa)	Chainage (m)	Pressure (kPa)
Inner Wheel Path		Inner Wheel Path		Inner Wheel Path	
20.0	708	1.0	660	20.0	707
40.0	699	20.0	664	40.0	773
60.0	690	40.0	658	60.0	748
80.0	696	60.0	654	80.0	739
100.0	694	80.0	659	120.0	710
120.0	696	100.0	657	140.0	698
140.0	720	Lane Centre		160.0	703
160.0	696	20.0	723	Lane Centre	
Lane Centre		60.0	696	20.0	745
40.0	700	100.0	708	60.0	739
80.0	710			120.0	679
120.0	709			160.0	710
160.0	711				
Range	690-720		654-723		679-773
Mean	702.4		675.4		722.8
Max. deviation from mean	2.5%		7.0%		6.9%

Table 2.3 Repeatability of Contact Pressures along Whole Length of Section

other two structures are compared with it. Also, the variation of measured pressures is greater than that measured over a specific location, which is to be expected since the material properties are different from one location to another.

Therefore, the load amplitude of the FWD, which is applied dynamically, appears to be influenced by factors like material properties and level of compaction. Temperature, which influences the measured deflections close to the load, does not affect the load amplitude at all (see Figure 2.14 and Table 2.2).

A fact which has emerged from the data in Tables 2.2 and 2.3 is that there is a scatter of measured contact pressures instead of constant magnitude of 700 kPa as fixed at the start of the survey. Hence, the field data obtained cannot be used directly for comparing deflections over the whole section. Some work is required to convert all the deflections to the same contact pressure before analysis is carried out.

(d) Relationship between FWD deflection and applied load

Another study was to investigate the variation of measured deflection with FWD dynamic load. Figure 2.15 illustrates the relationship on three different structures. In all cases, near parabolic relationships are observed. This response deviates from the expected linear relationship as reported by Pronk and Buiter (37). From Figure 2.15, the parabolic relationship reveals a stress-hardening behaviour of the pavements, whereby increase in applied load does not produce a corresponding increase in pavement deflection. Hoffman and Thompson (11) also studied these relationships on both flexible and rigid pavements. Their results are summarised in Table 2.4 in which the values of stiffness (load/deflection) have been calculated at different load levels. From the table, it is noted that in 14 out of 17 sections there is a decrease in stiffness with inceasing load

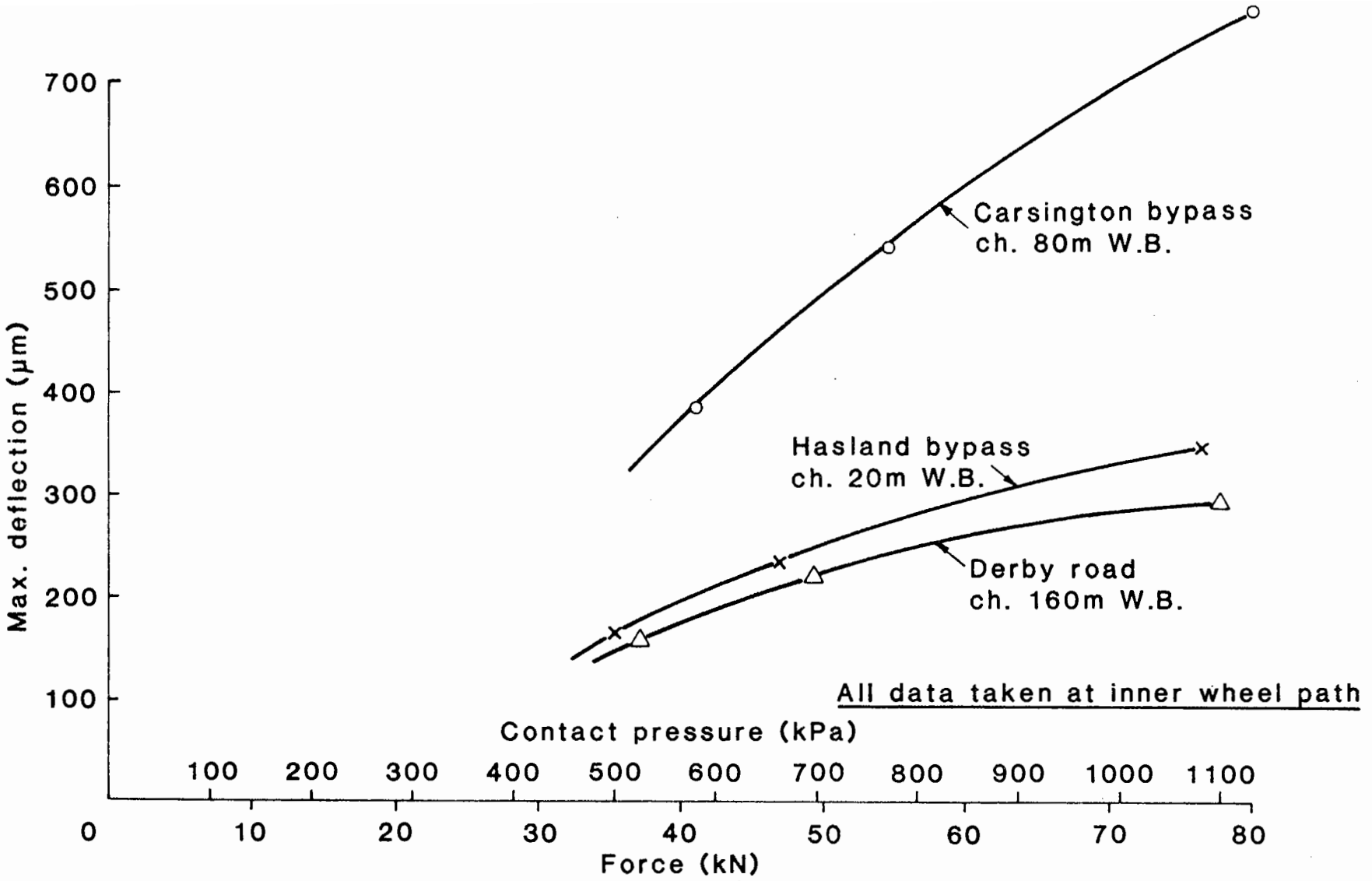

FIG. 2.15 VARIATIONS OF MAX. DEFLECTIONS WITH DIFFERENT FWD LOADS

SECTION	Stiffness at Load Shown, Kips/in				Stiffness max / Stiffness min
	3 Kips	6 Kips	8 Kips	> 8 Kips	
BEMENT*	783	779	736	711	1.10
DELAND*	175	172	170	-	1.03
MONTICELLO*	677	647	639	617	1.10
SHERRARD*	500	458	439	-	1.14
VIOLA*	316	276	261	261	1.21
AASHO-874	273	306	296	313	1.15**
AASHO-849	294	275	267	257	1.14
AASHO-872	273	273	265	257	1.06
AASHO-865	316	286	271	250	1.26
AASHO-843	120	143	143	-	1.19**
AASHO-845	100	110	110	-	1.10**
AASHO-852	111	105	105	-	1.06
RIGID 402	1905+	1935	1860	1667	1.14
RIGID 534	2162+	2143	2000	1905	1.13
RIGID 536	2222+	2105	2000	1961	1.13
RIGID 548	2963+	2857	2712	2632	1.13
RIGID 550	2424+	2500	2388	2260	1.11

* Average of three stations
** Increasing stiffness with increasing load
\+ Stiffness at 4 Kips

Units: 1 Kip = 4.45kN
1 Kip/in = 175kN/m

Table 2.4 Influence of Load Magnitude on FWD Deflections (after Hoffman and Thompson (11))

magnitude thus showing stress-softening behaviour, whereas the other three sections show a stress-hardening behaviour where the stiffness increases with the load. Reasons were sought to explain this phenomenon. The general expression relating the deflection (d) with applied stress and material properties of a layer is given by:

$$d = \frac{Ap(1-\nu^2)}{E} \qquad (2.2)$$

where d is the calculated deflection;

E, ν are Young's modulus and Poisson's ratio of the layer;

p is the applied pressure (= Load/area of loading platen);

A is a constant.

Equation. 2.2 shows that deflection, d, is proportional to p and $(1-\nu^2)$, but inversely proportional to E. Since the results obtained and presented in Figure 2.15 were over one location and within a few minutes, both the parameters E and ν should be constant during the test. Equation. 2.2 thus reduces to:

$$d = fn(p) \qquad (2.3)$$

which is a linear relationship. This is certainly not true, as the actual curves in Figure 2.15 show a non-linear relationship of the form :

$$d = fn(p^n) \qquad (2.4)$$

where n is the power index and $n \neq 1$.

It is considered that this non-linear relationship may arise from two factors ,which are the changing of the characteristics of the damping system from the rubber buffers and the characteristics of the pavement structure being tested. Of these, the former factor is considered to be less important, the reason for which has been discussed in Section 2.6.1. Therefore, the dominant factor is the non-linear behaviour of the pavement structure, in particular, the unbound granular sub-base and the subgrade

cohesive soil.

The non-linear properties of granular material can be found in Pappin (58) and that of subgrade soil in references 39, 40, 41 and 42. In recognizing this fact, the new analytical method for pavement evaluation incorporates a material model which enables non-linear subgrade stiffnesses to be calculated. The details of the formulation of this model will be described in Chapter 4.

(e) Consideration of errors in the deflection measurements from the FWD

Although the geophone of the FWD can resolve deflection measurements very accurately (to 1 micron), it is important to be aware of the accuracy of each measurement and what factors may be involved which may cause errors in the resultant deflections. After extensive applications of the FWD over a range of pavement structures, some of those factors have been realised and discussed below.

(a) Instrument error;

(b) Unstable support at the tip of the geophone;

(c) Rocking of block or slab under the applied load.

Instrument error: As seen in Section 2.6.1, the manufacturer stated that the absolute accuracy of the geophone in measuring deflections as 2% ± 2 microns. However, they do not indicate in which range the measurement should be taken to achieve such accuracy. Also, it is necessary to calibrate the geophones to ensure they achieve the required accuracy before any routine surveys. But, calibration under dynamic loading is realised to be a difficult task since special equipment is required to record the response of the geophones to a range of less than 10 microns. In order to overcome this problem, an attempt has been made by the manufacturer who supplies a calibration column which enables

up to four geophones to be stacked together. This facility thus offers a means of measuring the relative accuracy of the geophones and to identify a geophone which shows erroneous deflections. However, appropriate facilities are yet to be developed to measure the absolute accuracy of the instruments.

Unstable support: During the site survey, it is impossible to ensure that the pavement surface where measurement will be taken is absolutely clean. Therefore, it is possible that the tip of the geophone might rest over a relatively soft surface, e.g. loose mud or silt or clay sized material. During each testing cycle, the tip of the geophone is progressively moved as the result of pavement vibration due to the falling weights. In order to reduce this error to a minimum, it is important that at least three drops of the falling weight are made in each testing cycle.

Rocking of block or slab: When an edge of a block or slab, whether it be concrete or bituminous, is loaded by the FWD and the deflection is measured at the other edge of the same block or slab over a non-uniform support, it is possible that rocking of the slab could occur, causing an error in deflection measurement. Therefore, it is important that this situation should be identified, e.g. from visual inspection of surface cracks. A void in the support is another possible source which results in rocking of the slab. These problems may be identified by interpreting the effective layer stiffnesses back-analysed using the analytical procedures to be discussed in Chapter 4.

2.6.3 Some Special Applications of the FWD

In addition to routine testing with the FWD, some special tests were carried out in order to explore the extent of its application. During this period, preliminary investigation identified two areas in

which the FWD could be applied with reasonable success, which are:

(a) Locating cracks in a lean concrete layer;

(b) Evaluating the efficiency of load transfer between two adjacent concrete slabs in a concrete structure.

The following illustrates the investigation involved.

Cracks in the lean concrete layer: A FWD survey was carried out on a partly constructed pavement with a lean concrete roadbase. The purpose was to evaluate the damaging effect of trafficking by a 4-axle segment transporter, carrying unit loads of up to 105 tonnes. The structure consisted of 90 mm dense bitumen macadam basecourse, 190 mm lean concrete, 150 mm granular sub-base and 220 mm capping layer overlying a stiff subgrade. Details of the test section and analyses have been reported in Brown et al (43) and, in this section, we shall concentrate on the observation of the deflection results which reflect the condition of the lean concrete both before and after additional loading.

The pavement section was surveyed at 1 m intervals and at each test point, seven deflections (d_1 to d_7) were measured at offset distances at 300 mm centres up to 1800 mm.

Figure 2.16 presents the deflection profiles along the wheelpath of the test section. The profiles are for the central deflection (d_1), the deflection difference ($d_2 - d_4$) indicating the condition of the lean concrete and the outermost deflection (d_7). The choice of the above deflection parameters are based on results of a sensitivity analysis and will be discussed in Chapter 3.

From the profiles in Figure 2.16, spikes (sudden increases in deflection) are clearly noted at intervals of approximately 14 m, indicating evidence of thermal or shrinkage cracking. This proposition was confirmed by subsequent coring at Ch. 7.6 m. The figure also indicates that both the parameters d_1 and ($d_2 - d_4$)

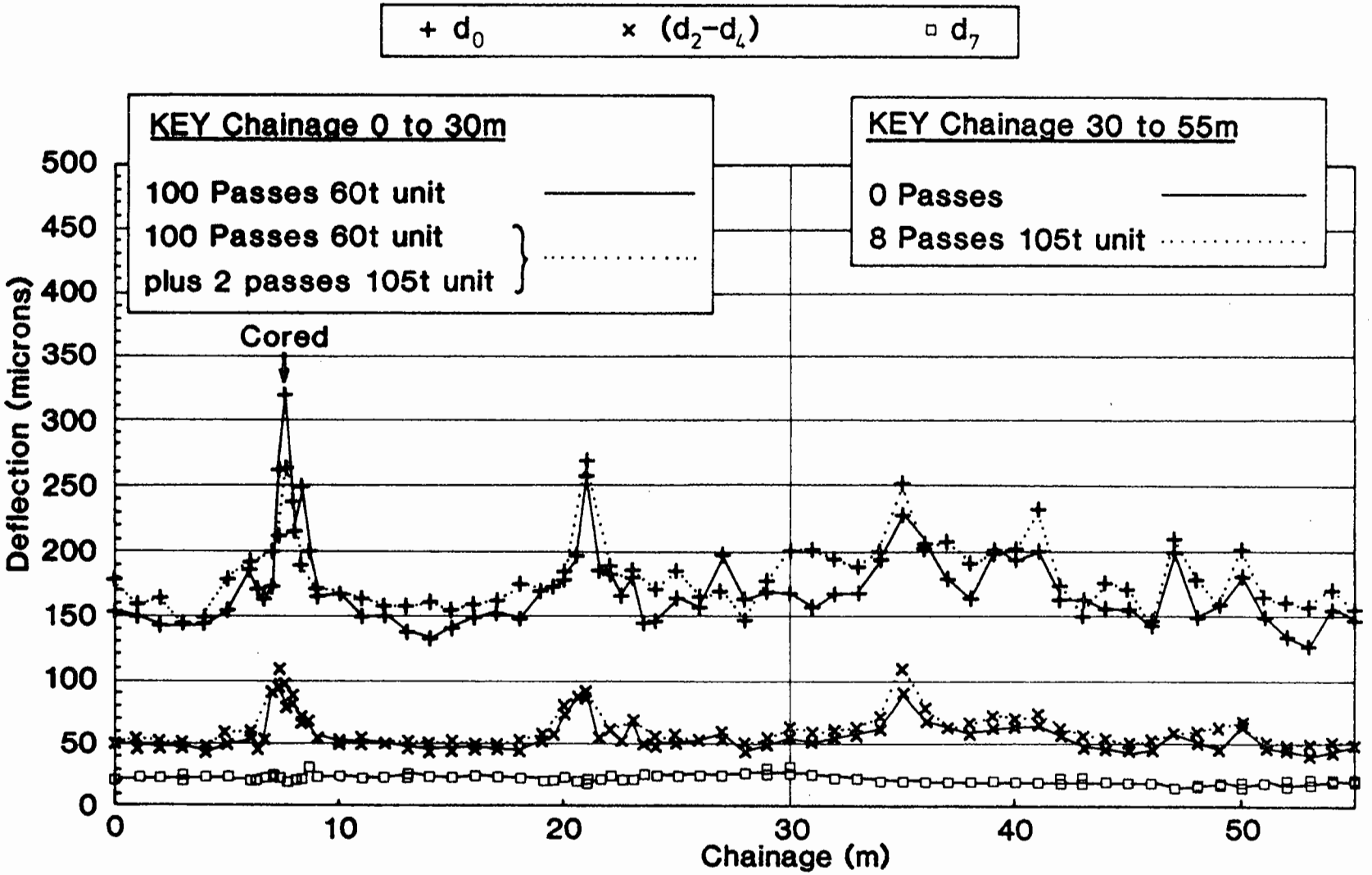

FIG. 2.16 DEFLECTION PROFILES ON A PAVEMENT SECTION WITH LEAN CONCRETE ROADBASE

increased after additional loading, whilst the d_7 values remained essentially constant. This suggests a reduction in effective elastic stiffness of the lean concrete layer as a result of load induced micro-cracking.

Therefore, it may be concluded that the FWD can be used to locate the positions of cracks in a lean concrete layer. This can be achieved by testing at 1 m interval along the pavement section. Having established the above test procedure, the FWD may be used to evaluate the condition of many heavily trafficked roads in the country, where lean concrete has been widely used as the roadbase layer.

Load transfer between concrete slabs: As well as bituminous pavements, concrete pavements have also been widely used, especially for carrying very heavy traffic, such as motorways. Since concrete is much stiffer than bituminous material, its design life is expected to be much longer. However, the durability of concrete pavements depends on a lot of factors such as workmanship, the condition of the foundation layers, the condition of joints between adjacent slabs to allow load transfer from one to another, drainage and so on. Here, the FWD has been used to identify the condition of joints by testing across them.

A newly constructed concrete pavement was tested with the FWD, where the concrete slabs were unreinforced, 5 m long with a typical thickness of 300 mm. The transfer of traffic loading was provided by a series of dowel bars placed across the joints. When a joint was tested with the FWD, a number of geophone settings were tried and the best setting was to place the second and third geophones across the joint. Figure 2.17 compares the deflection results measured across a joint with good and poor load transfer ability. From the figure, the difference in deflections between d_2 and d_3, at 0.3 m and 0.6 m respectively, is clearly shown. When a joint has good load transfer

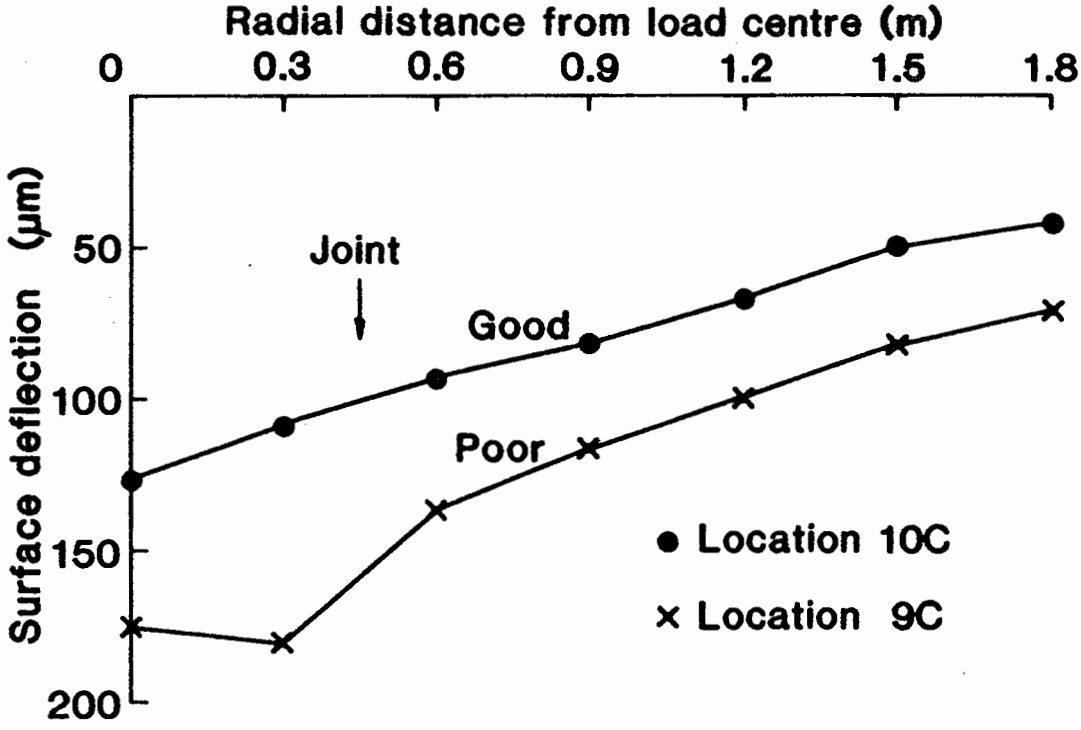

FIG. 2.17 MEASURED DEFLECTION BOWLS COMPARING DIFFERENT CONDITIONS OF LOAD TRANSFER ACROSS JOINT ON A TYPICAL CONCRETE PAVEMENT

properties, a normal deflection bowl is measured across it, with the maximum deflection occurring at the d_1. However, if the load transfer at the joint is poor, there is an increase in deflection between 0 and 0.3 m followed by a sharp reduction at 0.6 m, thus forming a kink in deflection at 0.3 m. By calculating the deflection difference between d_2 and d_3, it is possible to evaluate the efficiency of load transfer across a joint. Teller and Sutherland (44) suggested the following method for evaluating the amount of load transfer, viz,

$$LT(\%) = [(2D_u)/(D_1+D_u)] \times 100 \qquad (2.5)$$

where LT = load transfer as a percentage

D_u = deflection of unloaded slab

D_1 = deflection of loaded slab

A slightly different form of calculating joint efficiency was proposed by Gulden and Brown (45) and defined as follows:

$$LT(\%) = (D_u/D_1) \times 100 \qquad (2.6)$$

By replacing D_1 by d_2 and D_u by d_3, equation (2.5) or (2.6) may therefore be used to evaluate the joint efficiency using a FWD measurement.

2.6.4 Comparison between the Falling Weight Deflectometer and the Deflectograph in Pavement Evaluation

Since the Deflectograph has been widely used in the UK in evaluating pavement structures based on LR 833(3), it is necessary to compare the FWD with the Deflectograph in more detail. The results of the comparison are listed as follows:-

(1) The FWD can readily apply a load of variable magnitude up to 105 kN (10.5 tonnes) whereas LR 883 recommends the use of a fixed wheel loading of 31 kN on the Deflectograph. However, it is noted that the Deflectograph can be used, in other applications, with different wheel loads. Because the FWD load can be changed easily, it can be used to measure deflections quickly on a pavement section consisting of flexible, rigid and/or composite pavement structures.

(2) The loading time of the FWD, ranging from 25 to 40 msec, simulates a vehicle speed of around 30 km/hr as compared with 1 to 3 km/hr specified in LR 833 for the Deflectograph in routine operation. This feature of the FWD is very significant as the elastic stiffness of the bituminous material is time-dependent. By applying a short loading pulse to the pavement, the FWD is capable of simulating a loading condition as produced by an actual wheel load passing at normal operating speeds. Furthermore, under higher temperatures, the response of the bituminous material would still remain in an essentially elastic condition under the FWD loading in contrast with a visco-elastic behaviour for the Deflectograph under similar conditions.

(3) The FWD measures seven deflections accurately at any radial distances up to 2.4 m from the load as against one central deflection measured by the Deflectograph recommended in LR 833 even though the Deflectograph is capable of measuring a complete deflection bowl if required. Also, the FWD deflections are of absolute magnitude whereas the Deflectograph measures deflections relative to a measuring frame.

(4) In LR 833, the use of the Deflectograph is generally restricted to Spring and Autumn in comparison with the FWD which can be used virtually at any time of the year. The only difficulty that the FWD had encountered in operation, during the past two years, was when the temperature dropped to an extremely low

value around -15°C. However, this problem was solved by replacing with a lighter grade oil in the hydraulic system.

(5) As already described in Section 2.6.3, the FWD is capable of locating cracks in a lean concrete layer of a composite pavement and determining the degree of load transfer between adjacent concrete slabs of a concrete pavement. However, standard Deflectograph cannot perform these tasks.

(6) The Deflectograph has two advantages over the FWD. First, it is moving continuously during the deflection survey whereas the FWD has to be operated at a station. Hence, the cost for providing traffic control is minimised. Second, for the same reason, the Deflectograph is able to cover a long distance of around 10 km per day with measurements at 3 to 4 m intervals.

(7) The data from the FWD allows the estimation of residual life and overlay thickness design on a wide range of pavement structures using an analytical approach. However, the LR 833 Deflectograph procedure is entirely empirical. If the full deflection bowl is measured using the Deflectograph, an analytical approach may be adopted. Measurement of only the central deflection does not provide an adequate base for analytical evaluation.

The above comparison has led to a conclusion that the Deflectograph, because of its greater operational output, can be used to monitor a large network of roads in order to identify pavement sections for detailed investigation. Then, the FWD may be applied to those pavement sections to obtain more detailed information which enables analytical structural analysis to be undertaken, in order to investigate the cause of the problem as well as to provide recommendations for necessary remedial measures. An analytical structural evaluation method, utilising the FWD deflection data, will be presented in the following Chapters.

2.7 CONCLUSIONS

(1) From the review of the comparison of different non-destructive deflection-based testing devices, it can be concluded that the FWD is, on balance, the best device in simulating moving wheel loading.

(2) The FWD loading time has been found to be in the range of 25 - 40 msec and constant with depth. This is in contrast with the increase of loading time with depth due to the moving load. Nonetheless, good correlations in stresses, strains and surface deflections are observed between the FWD and a moving wheel load.

(3) The assessment of the Dynatest FWD has revealed that measured deflection was found to be repeatable on stiff pavement and repeatability reduces when used on weaker pavements.

(4) Increase of temperature affects the FWD deflections between the load and 0.9 m but the deflections from 1.2 m outward are essentially unaffected.

(5) The amplitude of the applied FWD load is influenced by different material properties and compaction level. Temperature had no noticeable effect on its amplitude. The relationship between the magnitude of contact pressures (or forces) and the corresponding surface deflection is not constant but follows a near parabolic shape.

(6) Some errors which might arise during the deflection measurements have been identified and possible steps to minimize such errors have been proposed.

(7) Special investigations on the FWD have revealed that it is capable of locating the presence of cracks in the lean concrete roadbase of a bituminous pavement as well as determining the efficiency of load transfer across the joint of a concrete pavement.

(8) Detailed comparison between the FWD and the Deflectograph has identified a number of significant differences between these two equipment. The FWD, with its more enhanced capabilities and sophistication, is able to obtain a more detailed pavement responses in order to allow detailed structural evaluation to be carried out using a versatile analytical evaluation procedure. The Deflectograph, however, can be used to monitor a large network of road system in order to identify sections of pavements for further detailed investigation.

CHAPTER 3

FACTORS INFLUENCING DEFLECTIONS

3.1 INTRODUCTION

Deflection of a pavement structure can be affected by a large number of parameters which include temperature, traffic, condition and type of subgrade, thickness and stiffness of each pavement layer, level of compaction, types of materials used, and so on. Maximum deflection has long been used as an indicator for monitoring pavement condition. In the last ten years, numerous research results have been published utilising the shape of the deflection bowl in order to assess the structural condition of the pavement layers and subgrade. As already described in Chapter 2, it is possible to measure very accurately the magnitude of the deflection bowl using the FWD. Therefore, it is very important to understand how significant some of the above parameters are in influencing the magnitude as well as the shape of the deflection bowl.

The deflection parameter described here, and in the rest of the Thesis, refers to vertical deflection on the pavement surface only. In general terms, the vertical deflection calculated at the pavement surface is the summation of all the vertical strains in each pavement layer and the subgrade, i.e.,

$$d_z = \sum (\varepsilon_z \, \delta h)_i \qquad (3.1)$$

where d_z is the vertical deflection at surface

ε_z is the vertical strain of layer i

δh is the thickness of layer i.

This Chapter attempts to identify some of the essential factors which influence the deflection of a pavement structure. The results of the analysis will lead to the development of an analytical model for the evaluation of an existing pavement, as will be described in Chapter 4. A linear, elastic multi-layered computer program BISTRO, developed by Shell in 1963 (46,47), is used for the analysis. The parameters selected for analysis are elastic stiffness, E (equivalent to Young's modulus), Poisson's ratio, ν, and thickness, h, for the pavement layers and E, ν for the subgrade.

The chapter begins with a review of developments in the use of surface deflection as an indicator in pavement evaluation. Then it is divided into two parts. Part A (Sections 3.3 to 3.6) describes a sensitivity analysis for a three-layered structure. Four-layered and five-layered structures are dealt with more briefly, looking into the effect of the layer additional to the three-layered structure only. The range of stiffnesses chosen for this analysis is only relevant to bituminous pavements.

Part B (Sections 3.7 to 3.10) examines the influence of the stiffness and thickness of each layer on the deflection bowl in much greater depth, thus leading to a proposal for a rational procedure to enable the setting of geophone positions on the FWD in a logical manner. In this part, both bituminous and concrete pavement structures have been studied.

3.2 A REVIEW OF THE USE OF SURFACE DEFLECTION IN PAVEMENT EVALUATION

In developing models for characterising the structural properties of an existing pavement, the parameters of pavement responses, e.g. stress, strain or displacement, under a particular loading condition, must be known. Among the different responses, surface deflection is the easiest to measure. More importantly, surface deflection measurements can be carried out non-destructively, quickly and at low

cost. Therefore, they have been used for many years as a universal indicator of the strength and performance of a pavement.

In 1955, results from the WASHO Road Test (5,6) enabled limiting values of allowable maximum deflection to be established under an 80 kN axle load for bituminous pavements in Spring and Autumn. Since then, limiting deflection criteria have been correlated with traffic, temperature, layer thicknesses and type of bituminous material. The results of the AASHO Road Test in 1962 established a relationship between surface deflection and Present Serviceability Index (P.S.I.), which was incorporated into a pavement design method (48,49). Also, Hoffman and Thompson (11) have presented some typical limiting deflection criteria.

Apart from the maximum deflection, there are many other performance indicators which have been suggested in the literature, utilising the shape of the deflection bowl. A fairly comprehensive review has been carried out in which eleven indicators have been found. The results are tabulated in Table 3.1. The definition of parameters associated with the deflection bowl can be found in Figures 3.1 and 3.2. The features of Table 3.1 are summarised as follows:

(1) All indicators utilise the shape of the deflection bowl in one form or another.

(2) Seven out of eleven different indicators have been suggested and used within the past ten years for evaluating pavement conditions.

(3) It is noted that some indicators are more sensitive to the condition of a particular part of the pavement or the subgrade than others.

(4) Four indicators, viz, spreadability, surface curvature index, base curvature index and deflection (subgrade), are found to be more widely used than others. On the other hand, indicators

Pavement Indicators	Reference	Formula*	Remarks
Tangent Slope	Kung (58) Stock and Yu (59)	$TS = \tan\theta = \frac{d_1 - d_t}{r_t}$	Increase of TS indicates either weaker or thinner asphalt layer.
Base Damage Index	Kilareski and Anani (57)	$BDI = d_2 - d_3$	Increase of BDI indicates weaker asphalt layer.
(C) INDICATOR FOR PAVEMENT LAYERS ONLY			
Deflection Ratio	Claessen and Ditmarsch (20)	$DR = \frac{d_r}{d_1}$	DR = 0.5 or r = 600 mm. Increase of DR indicates stiffer pavement layers.
(D) INDICATORS FOR SUBGRADE ONLY			
Base Curvature Index	Majidzadeh (54) McCullough and Taute (53)	$BCI = d_4 - d_5$	Increase of BCI indicates a weaker subgrade.
Deflection	McCullough and Taute (53) Majidzadeh (54) Way et al (22)	$D_r = d_5$	D_r normally determined at radial distance of 0.9 m or 1.2 m. Increase of D_r indicates weaker subgrade.

* See Figures 3.1 and 3.2 for definition of parameters.

Table 3.1 Summary of Indicators used for Pavement Evaluation

Pavement Indicators	Reference	Formula*	Remarks
(A) INDICATORS FOR WHOLE PAVEMENT			
Bending Index	Hveem (50)	$BI = \frac{d_1}{a}$	Increase of BI indicates weaker pavement.
Radius of Influence	Bissett and Ford (51)	$RI = \frac{R_i}{d_1}$	Increase of RI indicates stiffer pavement.
Spreadability	Vanswani (49) Rufford (52) McCullough and Taute (53) Majidzadeh (54)	$SP(\%) = \left(\frac{d_1 + d_2 + d_3 + d_4 + d_5}{5d_1}\right) \times 100$	Increase of SP indicates a stiffer pavement.
"Area"	Hoffman and Thompson (11)	$\text{"Area"} = 6\left(1 + 2\frac{d_2}{d_1} + 2\frac{d_3}{d_1} + \frac{d_4}{d_1}\right)$	Range of "Area" from 11.1 to 36 inches. Increase of "Area" indicates stiffer pavement.
(B) INDICATORS FOR ASPHALT LAYER ONLY			
Radius of curvature	Dehlen (55)	$R = \frac{r^2}{f.\delta}$	Curvature is assumed to be sine curve. F varies from 2 to 2.47.
	Leger and Autret (56)	$R = \frac{r^2}{2\delta}$	Curvature is assumed to be a parabola. Increase of R indicates stiffer asphalt layer.
Surface Curvature Index	Kilareski and Anani (57) Majidzadeh (54) McCullough and Taute (53)	$SCI = d_1 - d_2$	Increase of SCI indicates weaker asphalt layer.

Table 3.1 Summary of Indicators used for Pavement Evaluation /contd

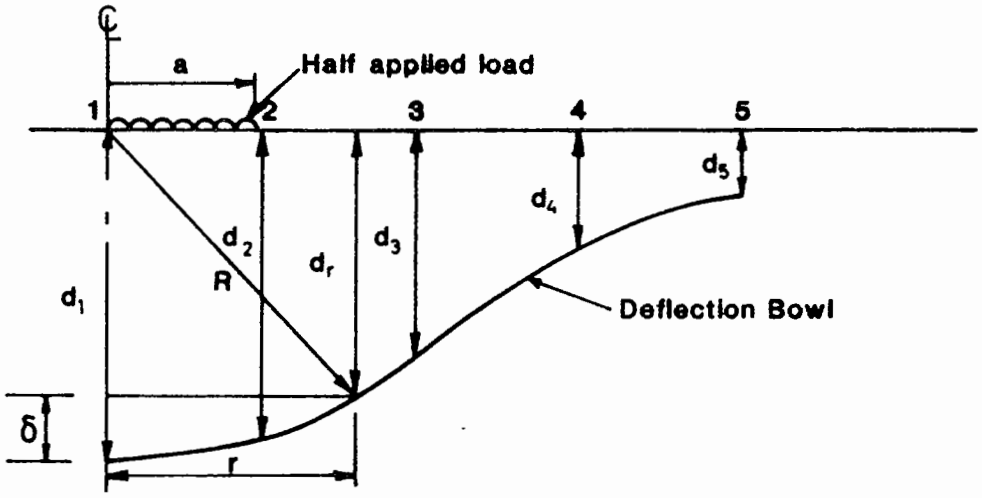

a = radius of loading

d_1, d_2, d_3, d_4 & d_5 = surface deflections at positions 1,2,3,4,5

R = radius of curvature

r = radial distance from centreline of loading

d_r = surface deflection at radial distance r

FIG. 3.1 DEFINITION OF PARAMETERS ASSOCIATED WITH SURFACE DEFLECTION BOWL

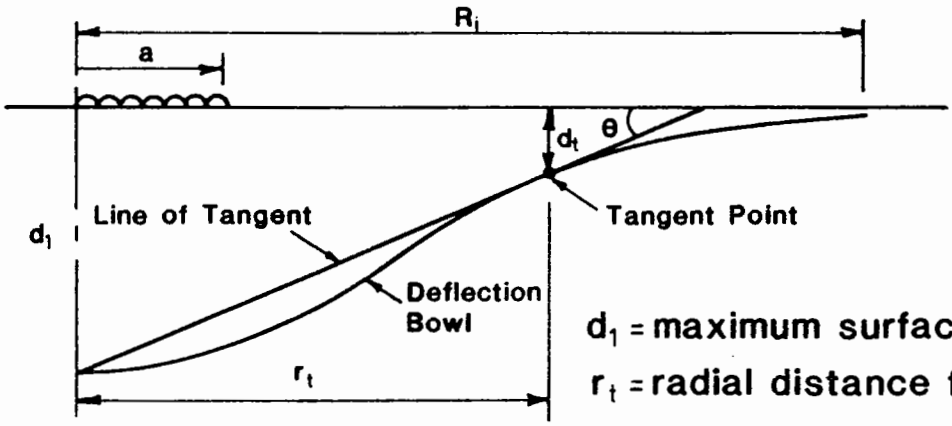

d_1 = maximum surface deflection

r_t = radial distance from load centre to tangent point

d_t = surface deflection at tangent point

a = radius of loading

FIG. 3.2 DEFINITION OF TANGENT SLOPE

like bending index, radius of influence and tangent slope are among those least used.

(5) It is possible to select a few performance indicators so that the structural properties of the pavement layers and the subgrade can be separately evaluated.

From the above survey, it is observed that there is no problem in selecting maximum deflection as an indicator for monitoring pavement conditions. However, utilising the shape of the deflection bowl gives rise to a multiplicity of alternatives. Amongst them, recent researches seem to be in favour of the use of simple deflection differences for monitoring the conditions of pavement layers (e.g. McCullough and Taute (53), Majidzadeh (54), and Kilareski and Anani (57)), and the outermost deflection value for monitoring the subgrade (e.g. McCullough and Taute (53), Majidzadeh (54) and Way et al (22)). It is along these lines that a sensitivity analysis is performed in more detail in the following section.

3.3 CHOICE OF ANALYTICAL TOOL FOR ANALYSIS

Nowadays, two computer programs, namely BISTRO (47) (or BISAR (60)) and CHEVRON (61), are widely used by research organisations throughout the world for the structural analysis of pavements. Although the computer programs use the same linear elastic multi-layered assumptions in their formulation (see Appendix A for full details of assumptions), it has been found that there are differences between them in calculating surface deflections. As surface deflections are the most important parameters in pavement evaluation, it is, therefore, necessary to choose an analytical tool which will predict realistic deflections.

A comparison between these two programs was first reported by McCullough and Taute (53) who showed that CHEVRON predicts unrealistically large deflections around the loaded area. Further

comparisons were later carried out by Brunton et al (62), in which three different structures, including both thick and thin pavements, have been analysed. A single contact pressure of 500 kPa was used. They reported similar findings to McCullough and Taute (53) but noted that the discrepancies in deflections reduce greatly from thick to thin pavements. A further three structures have been analysed by the writer in order to compare the two computer programs in more detail. The purpose of this exercise is to investigate their discrepancies in the following areas:

(a) Effect of varying applied pressures;

(b) Effect of increasing subgrade stiffness with depth;

(c) Effect of increasing stiffness of the surface layer;

(d) Effect of increasing thickness of the surface layer.

Figures 3.3, 3.4 and 3.5 compare the deflections calculated by BISTRO and CHEVRON.

Structure 1 in Figure 3.3 is a pavement structure with typical layer stiffnesses. The surface deflections have been calculated using two contact pressures, i.e. 500 kPa and 700 kPa, of which the former was analysed by Brunton et al (62). It is noted that the deflections calculated by both computer programs produce excellent agreement, both under the loaded area and from 0.4 m outward. Between the edge of the load and 0.4 m , there is a slight discrepancy in which the deflections calculated by CHEVRON are slightly less than BISTRO's values. Increase of contact pressure from 500 kPa to 700 kPa does not produce any noticeable difference from the above.

Structure 2 is shown in Figure 3.4, to observe the effect of increasing subgrade stiffness with depth. To this end, an additional layer of stiffness 100 MPa was introduced at a depth of 3.54 m below the pavement surface. It is interesting to note that the additional layer with higher stiffness in the subgrade increases the discrepancy

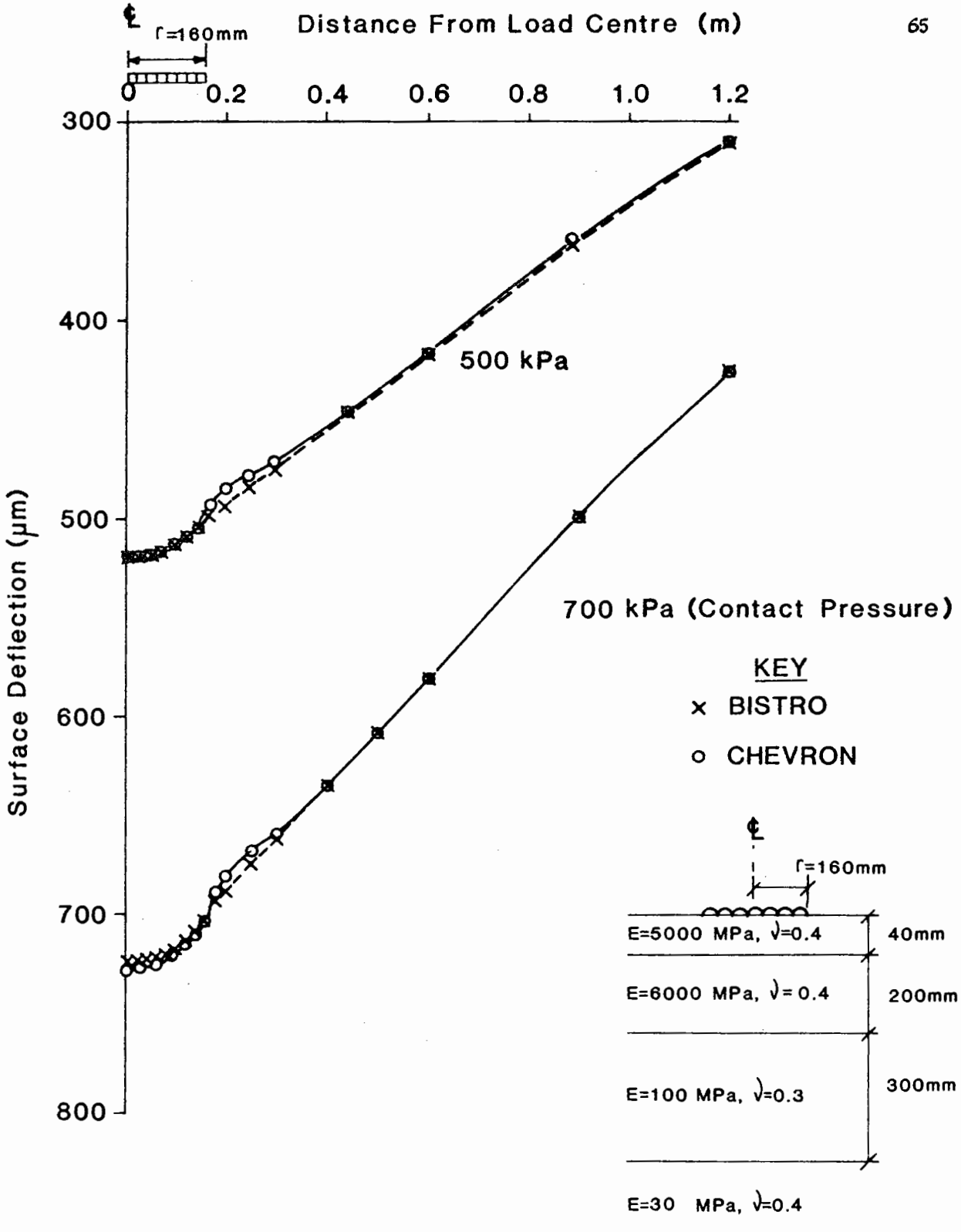

FIG 3.3 COMPARISON OF DEFLECTIONS CALCULATED BY BISTRO AND CHEVRON PROGRAMS STRUCTURE 1

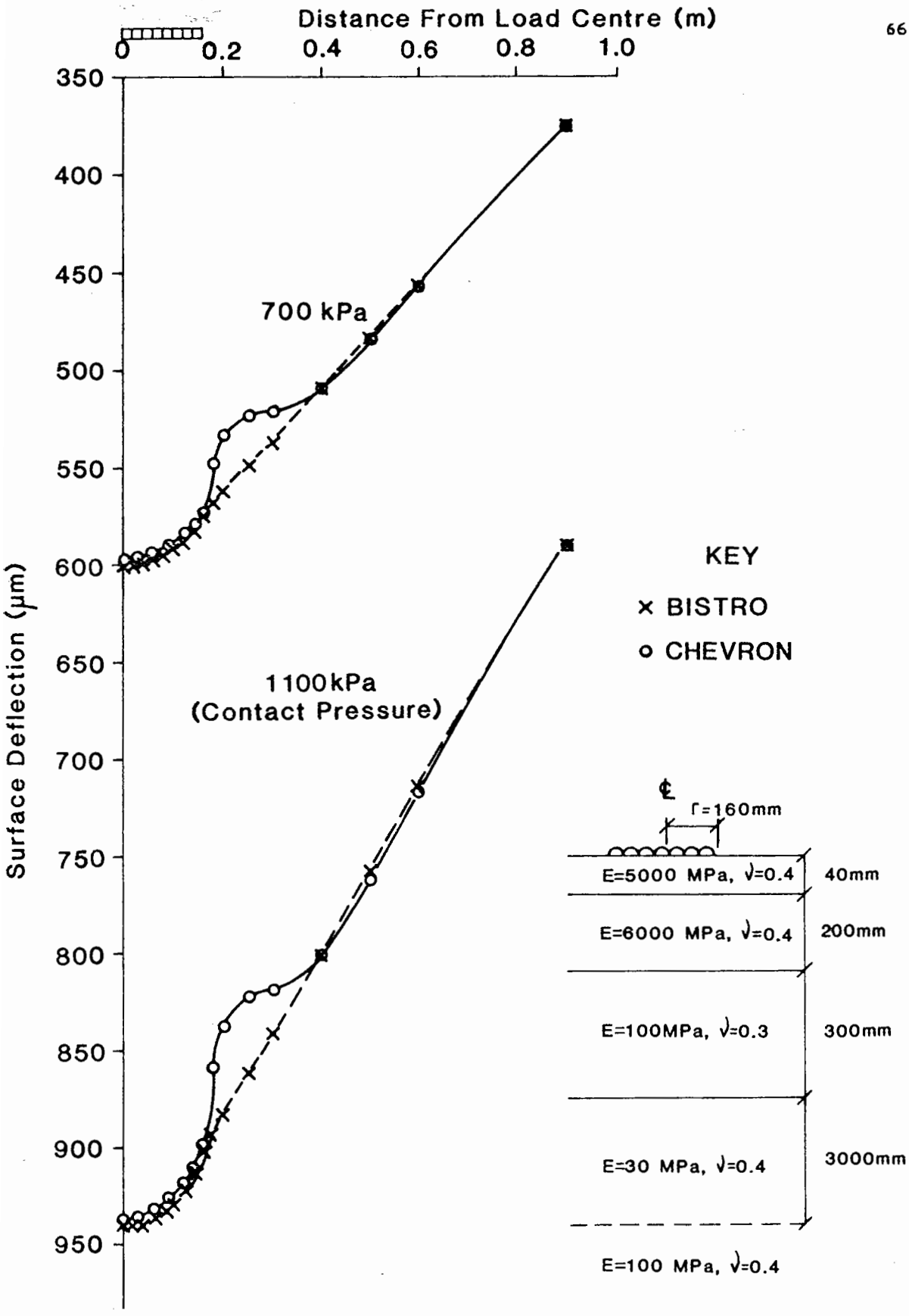

FIG 3.4 COMPARISON OF DEFLECTIONS CALCULATED BY BISTRO AND CHEVRON PROGRAMS STRUCTURE 2

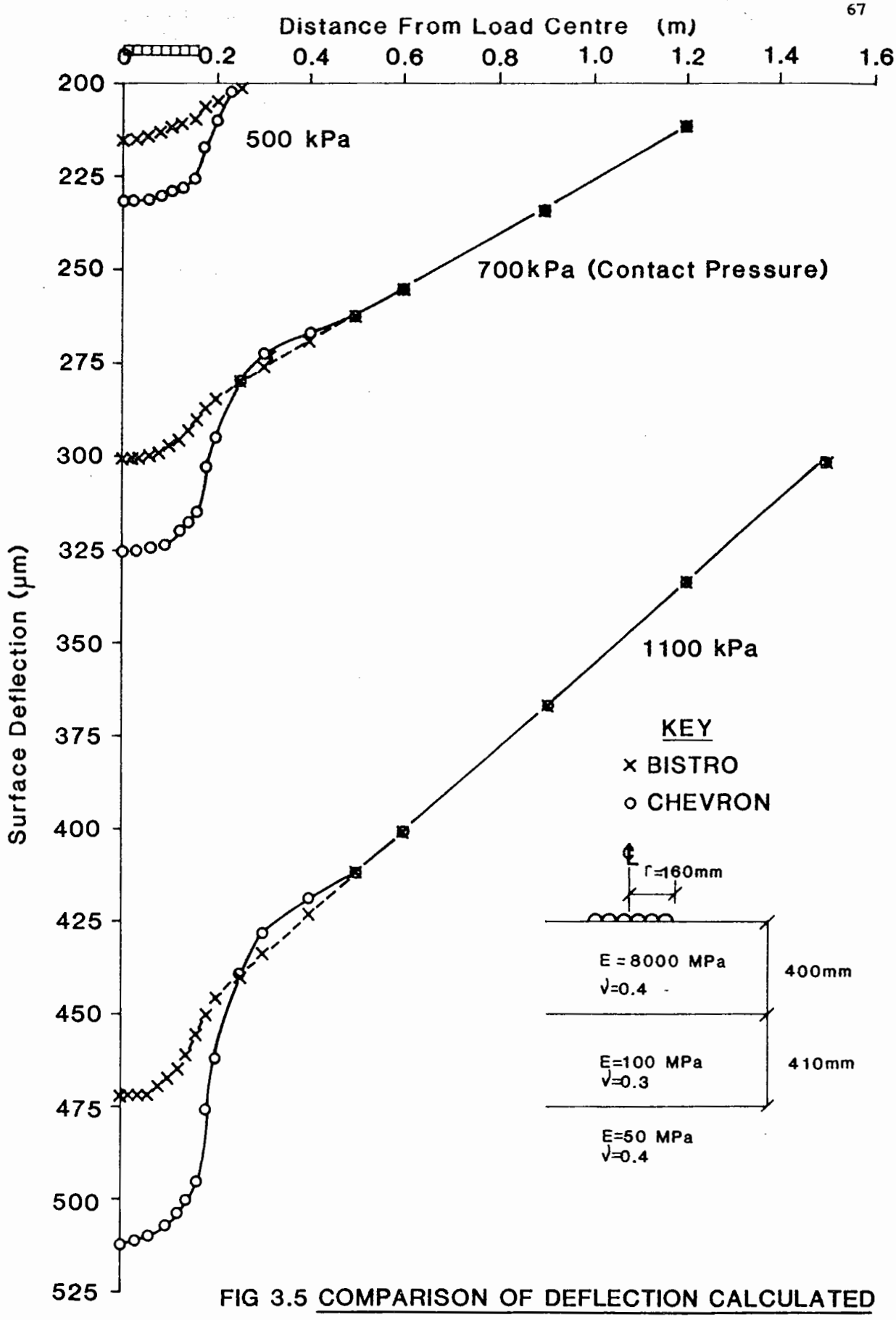

FIG 3.5 COMPARISON OF DEFLECTION CALCULATED BY BISTRO AND CHEVRON PROGRAMS STRUCTURE 3

in deflection in exactly the same position as that of Structure 1, already discussed. For example, for the deflections with 700 kPa contact pressure, the discrepancy at position 0.25 m from the load centre increases from 1.0% to 5.0%. Excellent agreement is still observed in other parts of the deflection bowl. Again, the increase of contact pressure from 700 kPa to 1100 kPa increases the magnitude of discrepancy but with the same percentage of 5%, say, at the position of 0.25 m from the load centre.

As in Brunton et al (62), Figure 3.5 shows the deflections from a thicker structure. Compared with Structure 1, Structure 3 also has a slightly higher stiffness of both the surface layer and the subgrade. The result is that CHEVRON calculates more unrealistic deflections, both beneath and near the load, than does BISTRO up to a distance of 0.5 m from the centre of loading. It is surprising to note that between the load centre and 0.25 m, CHEVRON calculates much larger deflections whereas from 0.25 m to 0.5 m, smaller deflections than BISTRO are computed. Although increase of contact pressure from 500 kPa to 1100 kPa increases the magnitude of deflections, the same percentage discrepancy between the two programs of about 7.8% is observed when central deflections are compared. Therefore, it appears that for structures with a very thick surface layer, of at least 300 mm, or with a large stiffness of surfacing layer, CHEVRON calculates unrealistically high deflections under the load. On the other hand, when subgrade stiffness is allowed to increase with depth (Figure 3.4), CHEVRON calculates unrealistically low deflections around the edge of the load. Consequently, it is concluded that BISTRO gives better predictions of deflection than the CHEVRON program. On this basis, the BISTRO computer program has been selected for use in the forthcoming analysis as well as the

development of an analytical pavement evaluation and overlay design method.

PART A : SENSITIVITY ANALYSIS

3.4 THREE-LAYERED STRUCTURE

The three-layered structure described here means a structure of full depth bituminous construction. It consists of two bituminous pavement layers, viz, a wearing course and a roadbase layer, over the subgrade as shown in Figure 3.6. This structure was chosen for sensitivity analysis because it is one of the pavement structures constructed in the U.K. and is the simplest structure in terms of number of variables for deflection analysis.

Table 3.2 shows the parameters and their magnitudes used for calculation. In all the calculations, a single vertical pressure of 700 kPa was uniformly loaded over a circular area of 300 mm diameter. The BISTRO computer program was used for the calculation, taking one structure from Table 3.2 at a time, varying systematically E_{wc}, E_{B}, E_{SG}, h_{wc}, h_{B}, ν_{wc}, ν_{B} and ν_{SG} respectively. The values as shown in the table have been selected to cover a wide range for each parameter. Vertical deflections were calculated at distances of 0.0, 0.3, 0.6, 0.9, 1.2, 1.5 and 1.8 m from the centre of the load. This layout was chosen to coincide with the normal positions of the seven geophones of the FWD. Figure 3.7 shows the layout and d_1 to d_7 are calculated surface deflection values. The results are plotted in Figures 3.8 and 3.9. Figure 3.8 illustrates the effect of varying the elastic stiffness of each layer on surface deflection. In each diagram, the stiffnesses of other layers were held constant at values 4000 MPa, 10000 MPa and 50 MPa for wearing course, roadbase and subgrade (linear subgrade) respectively. It is observed that a change of stiffness in the bituminous layers only affects the deflections close to the load, up to a distance of 0.9 m. Variation of

	Young's modulus (MPa)	Poisson's ratio	Thickness of layer (mm)
Wearing course (WC)	1000, 2000, 4000, 7000	0.3, 0.4, 0.5	20, 40, 60
Base (B)	4000, 7000, 10000, 12000, 14000	0.3, 0.4, 0.5	150, 200, 250, 300, 350
Subgrade (SG)	30, 50, 70, 90, 110	0.3, 0.4, 0.5	

Values underlined are held constant while one parameter is changed for calculation

Table 3.2 Parameters used in Deflection Calculation of Three-Layered Structure

	Young's Modulus (MPa)	Layer Thickness (mm)
Wet mix	50, 200, 300, 500, 700	100, 150, 200, 300, 500
Asphalt	4000, 7000, 10000, 15000, 20000	100, 150, 200, 300, 500
Lean Concrete	5000, 10000, 20000, 30000, 40000	100, 150, 200, 300, 500

Values underlined are held constant while one parameter is changed for calculation

Table 3.3 Parameter of Roadbase Materials used in Deflection Calculations of Five-Layered Structures

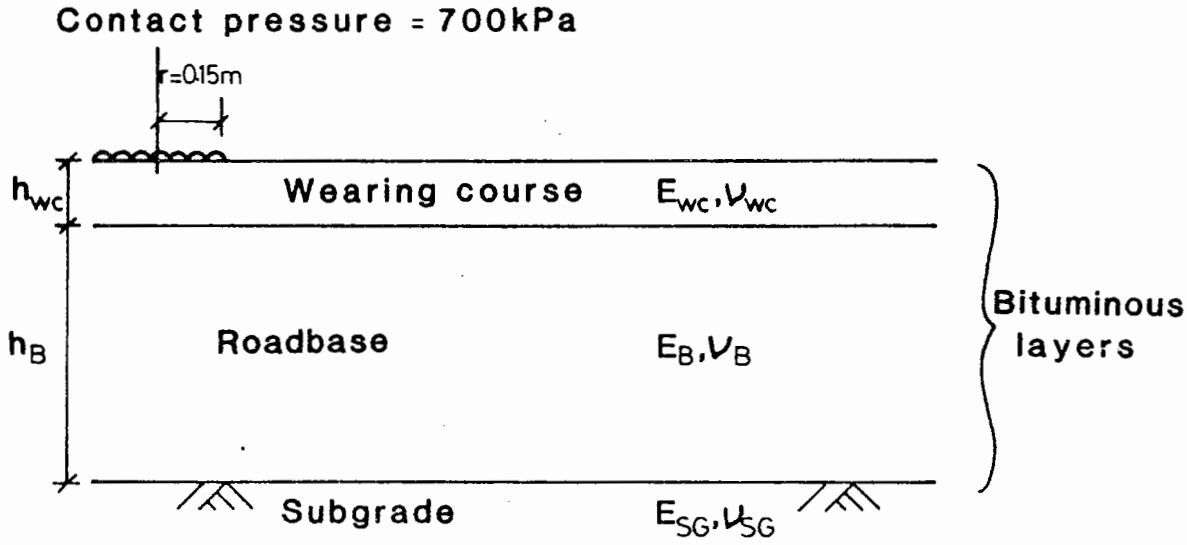

FIG. 3.6 THREE LAYERED STRUCTURE FOR PARAMETRIC STUDY

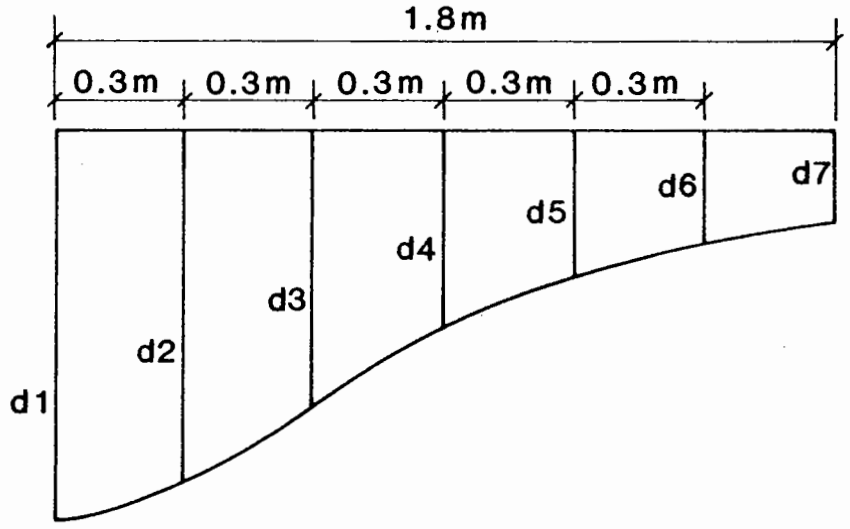

FIG. 3.7 CALCULATED DEFLECTION BOWL

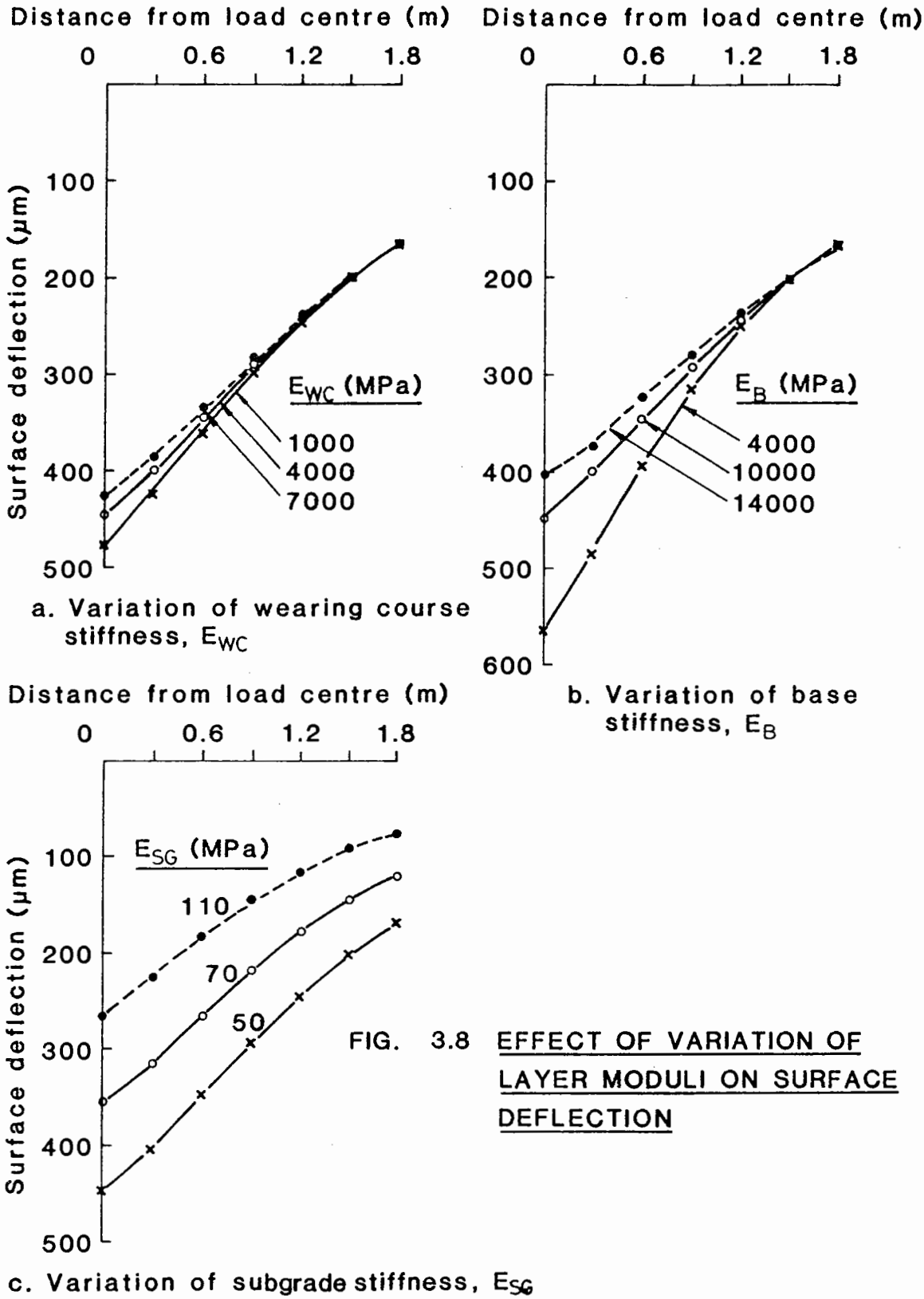

FIG. 3.8 EFFECT OF VARIATION OF LAYER MODULI ON SURFACE DEFLECTION

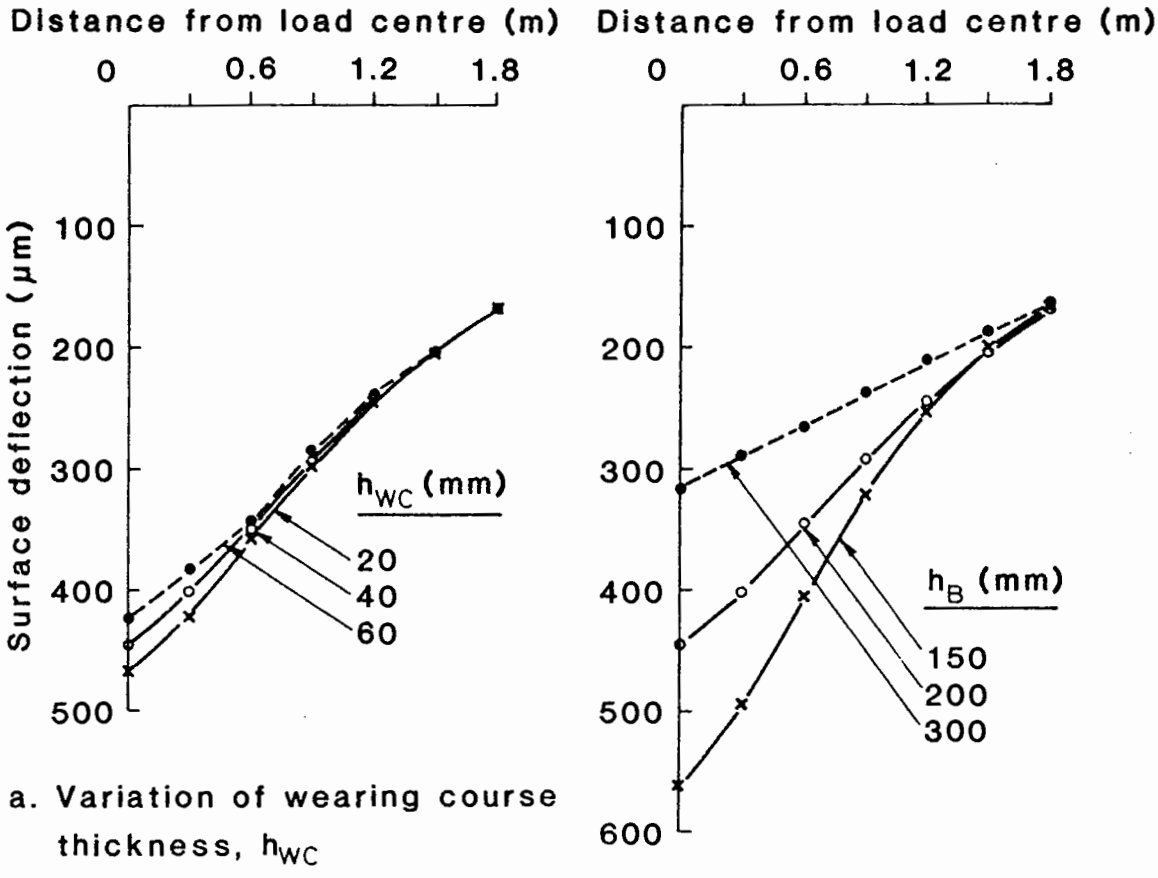

a. Variation of wearing course thickness, h_{WC}

b. Variation of Roadbase thickness, h_B

FIG. 3.9 EFFECT OF VARIATION OF LAYER THICKNESS ON SURFACE DEFLECTION

stiffness in the subgrade has the largest influence on all the deflections. It is also noted that whilst the change of stiffness of bituminous layers modifies the shape of the bowl, changes in the subgrade bring the same deflection bowl up or down the scale of the deflection axis.

Changes in thickness of pavement layers, as shown in Figure 3.9, show a similar trend to the change of stiffness discussed above. It can easily be seen that variation of roadbase thickness has a far greater influence on deflections than that of wearing course thickness. It demonstrates that the thickness of the roadbase layer should be determined as accurately as possible. This can be achieved by taking cores from the pavement. To illustrate this point, consider a structure of which the roadbase layer is 200 mm thick and of stiffness 4000 MPa, producing a deflection bowl as shown in Figure 3.8b. The same deflection bowl is plotted in Figure 3.9b, but there the deflections have been generated with a roadbase layer thickness of 150 mm and stiffness of 10000 MPa. Hence, for the same deflection bowl, a reduction of 25% in thickness (i.e. from 200 mm to 150 mm) of the roadbase layer requires a corresponding 2.5 fold increase in stiffness from 4000 MPa. Therefore, a wrong interpretation of the actual condition of the pavement will definitely occur, if the actual thickness of the roadbase layer is not recorded and used in the analytical analysis. Figure 3.10 summarises the relative importance of the effects of varying the stiffnesses of the roadbase layer and the subgrade.

The effect of varying Poisson's ratio for each pavement layer, and the subgrade, can be seen from Figures 3.11 to 3.13, from which three observations can be made. First, a change in Poisson's ratio modifies the shape of the deflection bowl close to the load for the wearing course and roadbase layers, whilst the same variation influences the whole bowl for the subgrade. Second, an increase in magnitude of Poisson's ratio reduces

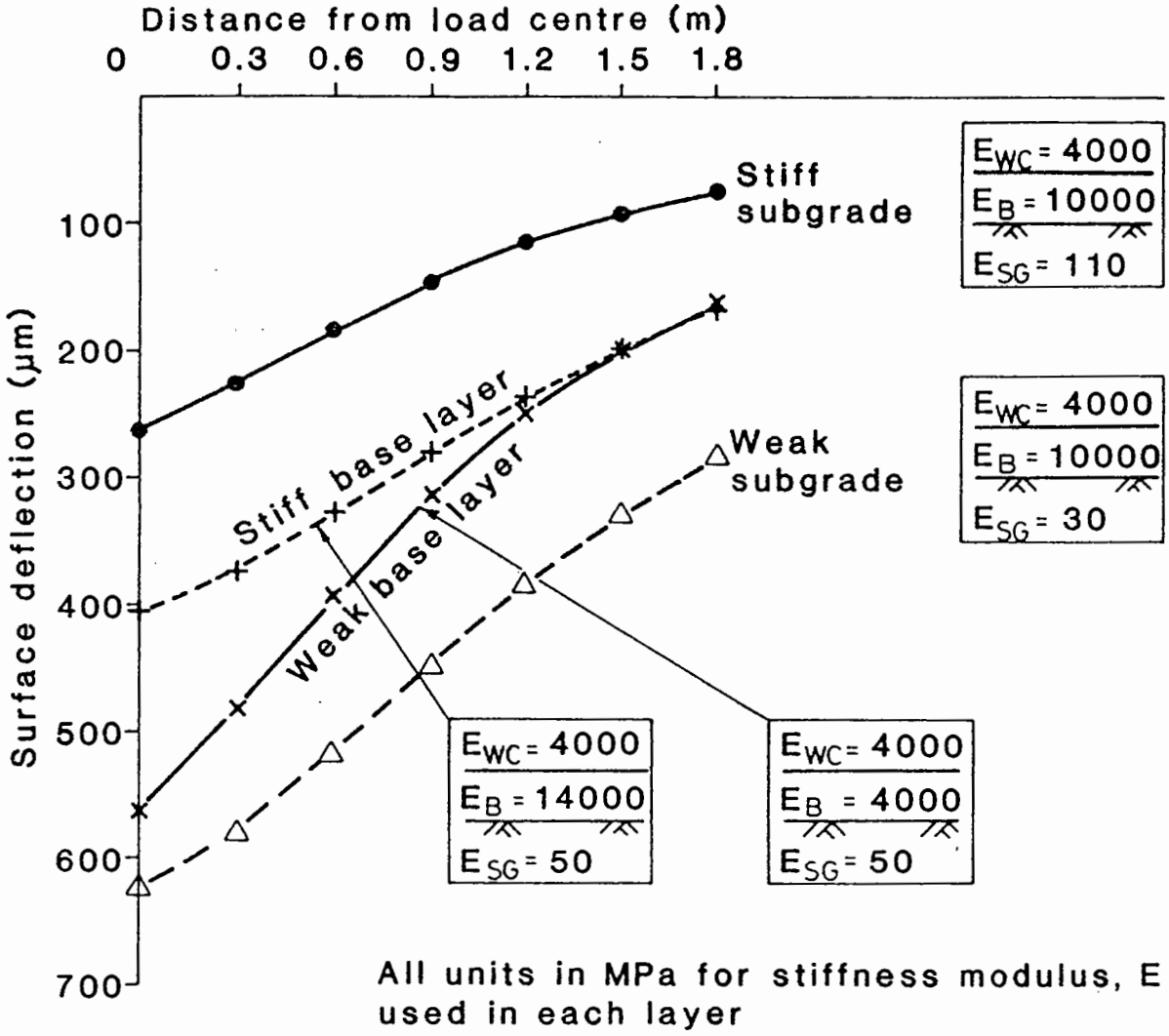

FIG. 3.10 RELATIONSHIP BETWEEN VARIATION OF STIFFNESS MODULI IN BASE LAYER AND SUBGRADE

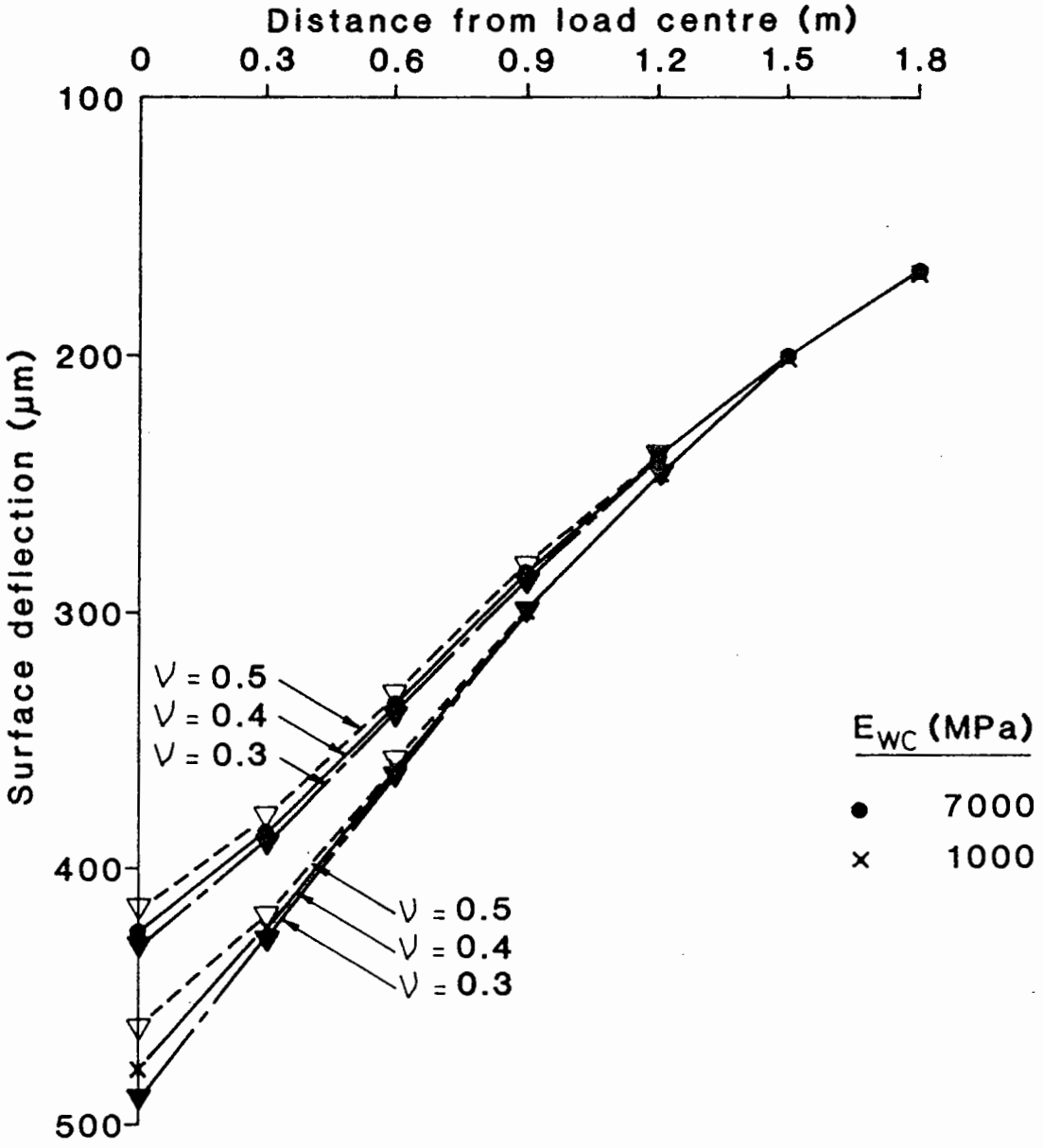

FIG. 3.11 EFFECT OF VARYING POISSON'S RATIO WEARING COURSE

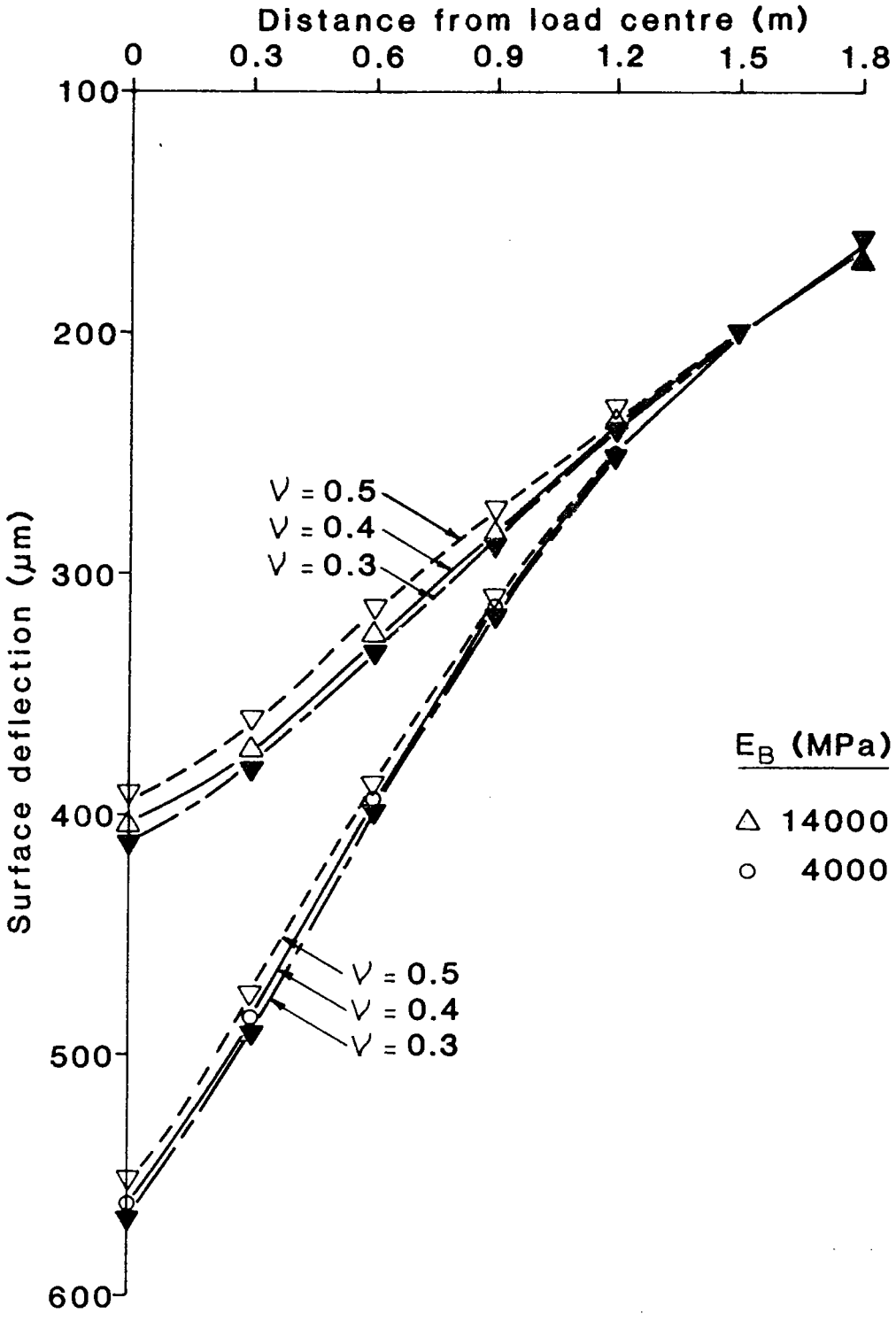

FIG. 3.12 EFFECT OF VARYING POISSON'S RATIO BASE LAYER

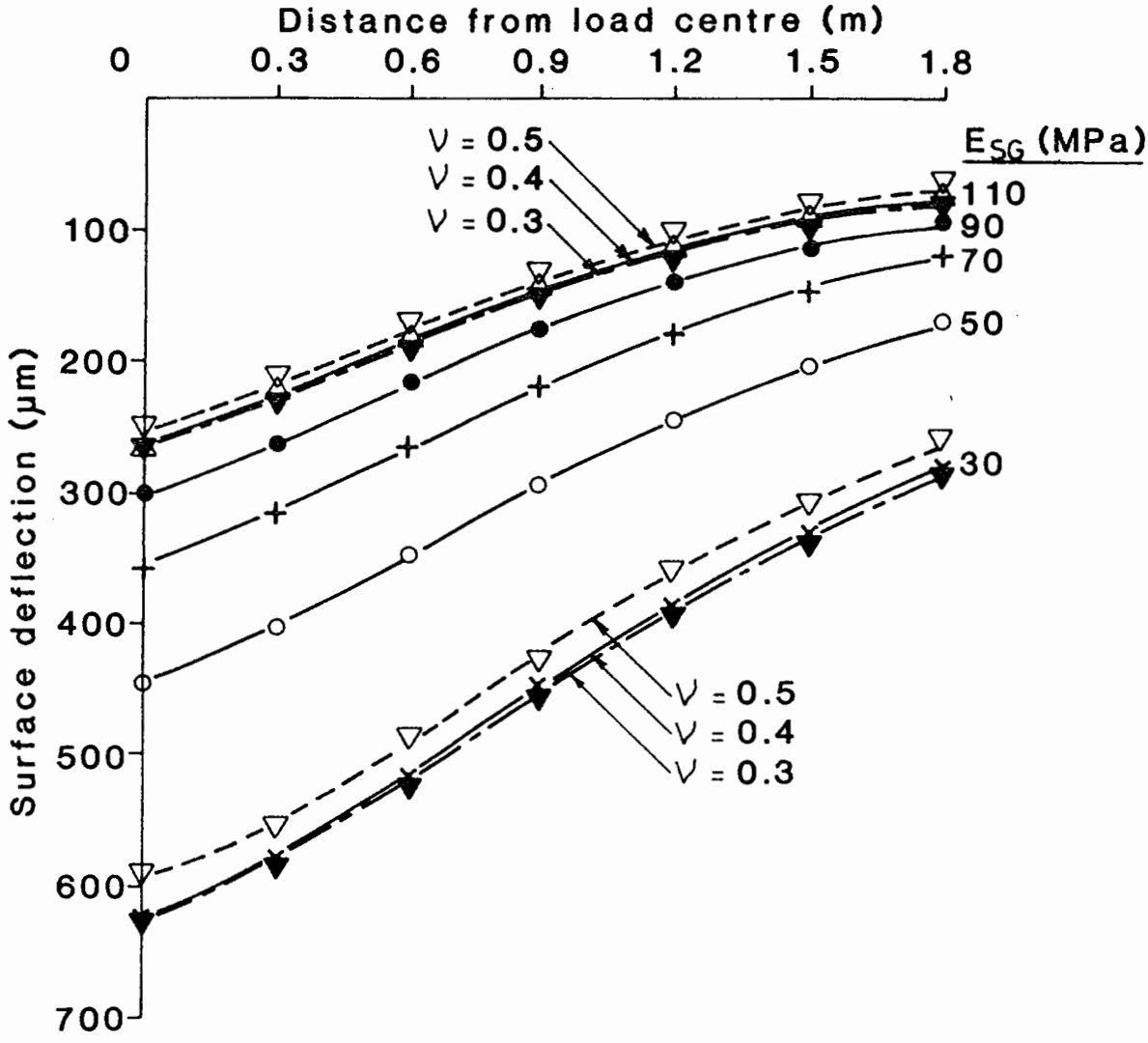

FIG. 3.13 EFFECT OF VARYING POISSON'S RATIO OF SUBGRADE LAYER

the deflections slightly, and vice versa. Third, variation of Poisson's ratio has more influence on deflections when the pavement layers are stiff and also when the value of the subgrade stiffness is low. However, the overall findings demonstrate that deflections are not sensitive to the variation of Poisson's ratio. Hence, in developing the model for back-analysis, to be described in Chapter 4, it is possible to assume that the Poisson's ratios of all the layers have a constant value without introducing significant error.

3.5 FOUR-LAYERED STRUCTURE

A typical four-layered structure is shown in Figure 3.14 which consists of two bituminous layers, (wearing course and roadbase), and a granular sub-base layer overlying the subgrade. Since the effect on deflections from variation of bituminous layers and the subgrade are very similar to those discussed previously for three-layered structures, this section only describes the influence of the sub-base layer. The parameters for other layers have been fixed and are shown in Figure 3.14.

3.5.1 Sensitivity of sub-base parameters

Within the sub-base layer, two parameters, i.e. elastic stiffness, E_{SB}, and thickness, h_{SB}, were chosen for the study. The Poisson's ratio, ν_{SB}, was fixed and equal to 0.3, a typical value (63). From the conclusion drawn in the previous section, it is considered that the deflections would also be insensitive to change in Poisson's ratio of the sub-base and hence there was no attempt to study this parameter. The sub-base stiffnesses used for deflection calculations were 50 MPa, 70 MPa, 100 MPa, 200 MPa and 300 MPa, and thicknesses used were 100 mm, 200 mm, 300 mm, 400 mm and 500 mm respectively. The reference structure had stiffnesss 100 MPa and thickness 200 mm for the sub-base. The same contact pressure of 700 kPa was used over a circular area of 300 mm diameter. Figure 3.15 illustrates the results of the calculations. It is noted that the deflection response is not sensitive to sub-base parameters at all. Close

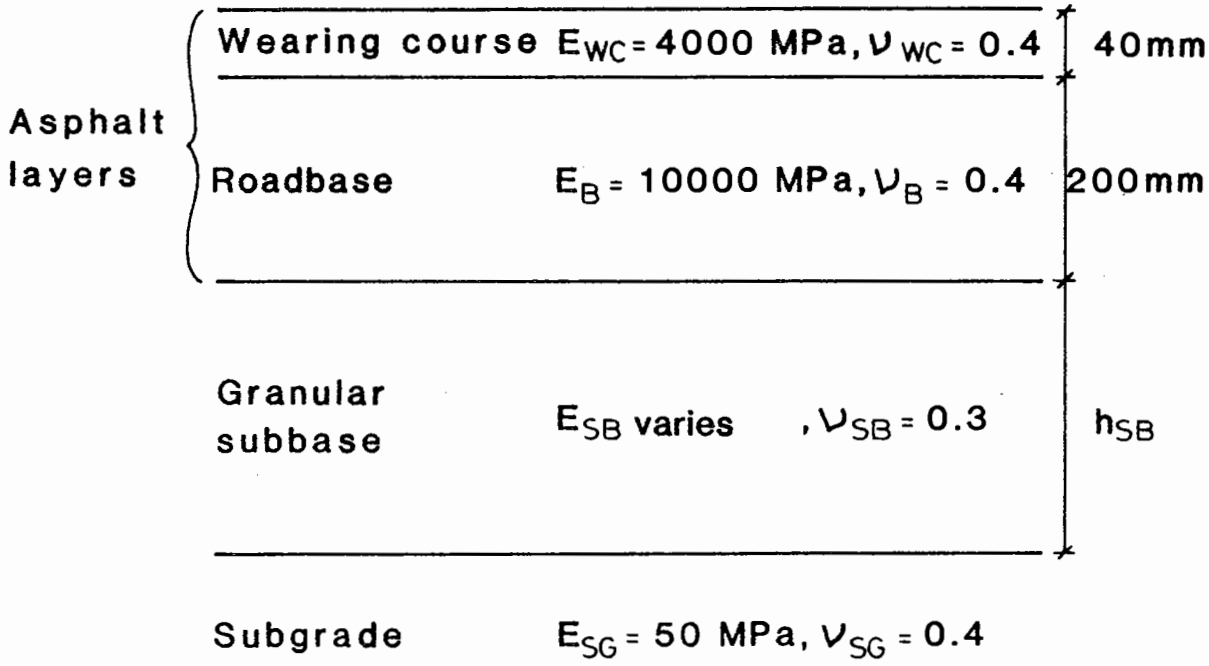

FIG. 3.14 FOUR-LAYERED STRUCTURE FOR PARAMETRIC STUDY

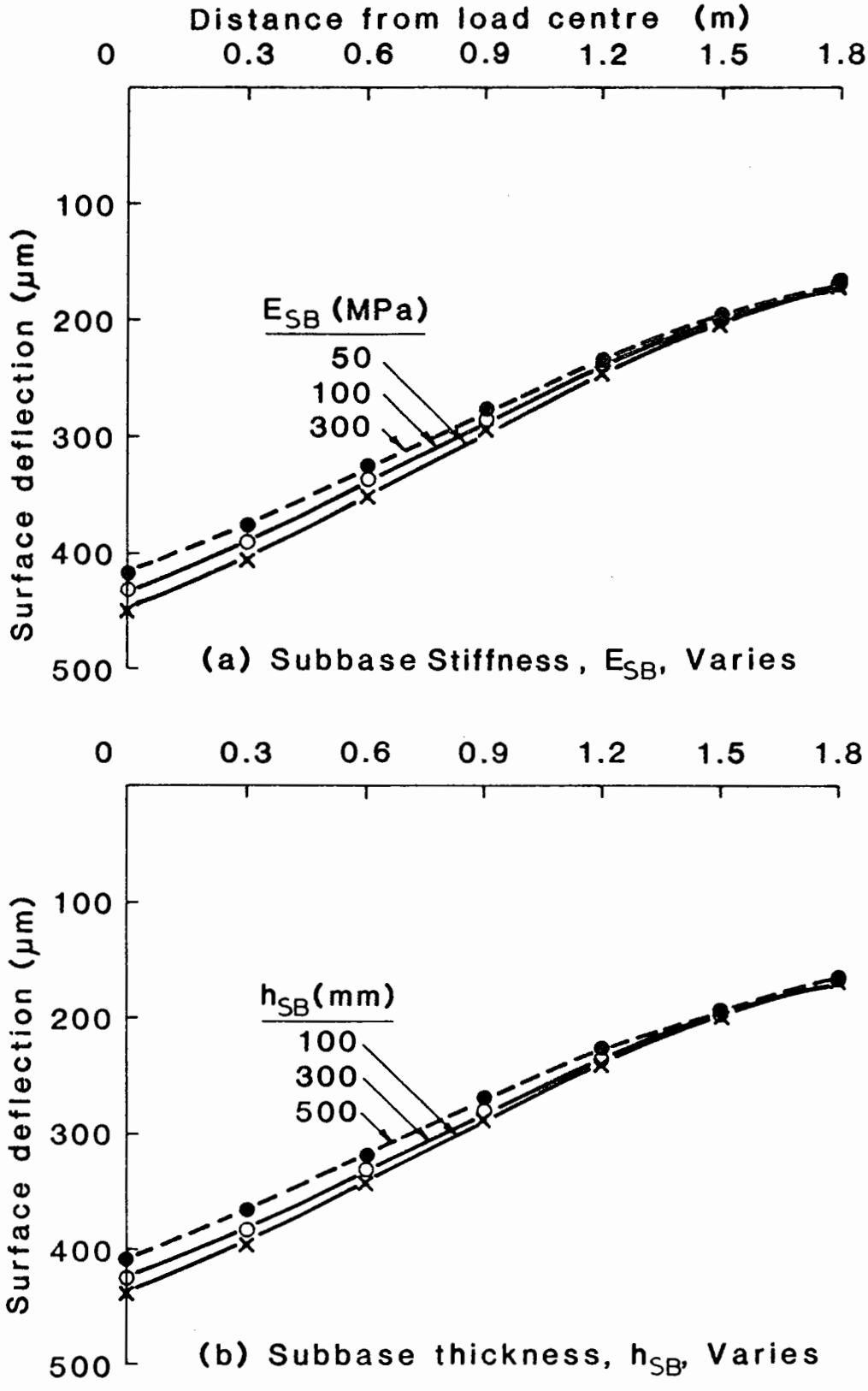

FIG. 3.15 EFFECT OF VARIATION OF SUBBASE STIFFNESS AND THICKNESS ON SURFACE DEFLECTION

examination of the results reveals the following points:

(a) A change of sub-base stiffness and thickness modifies the bowl shape, which corresponds to the findings drawn in the previous section for bituminous layers (Figures 3.8 and 3.9).

(b) Sub-base stiffness and thickness variation influence the deflections up to 1.5 m from the load.

(c) A reduction in magnitude of sub-base stiffness (e.g. from 100 MPa to 50 MPa) has greater influence than the corresponding increase in magnitude. However, the influence of thickness parameter does not produce similar effect.

This study enables two conclusions to be drawn. First, a large change in sub-base stiffness is necessary to give rise to only a small variation in deflection. In evaluating an existing pavement condition, there will therefore be difficulty in determining the actual sub-base stiffness to a high degree of accuracy. Second, any small inaccuracy in assigning a sub-base thickness will not introduce significant error in the calculated deflection.

3.6 FIVE-LAYERED STRUCTURE

In the United Kingdom, flexible pavement structures which consist of five layers, i.e. four pavement layers plus subgrade, are widely constructed to carry medium to very heavy traffic. Hence, it is necessary to study the variation of deflection for this type of structure. The pavement layers generally comprise of wearing course, basecourse, roadbase and granular sub-base. A typical five-layered structure is shown in Figure 3.16. There are three types of material currently specified for use as a roadbase layer, viz, wet mix macadam (commonly known as wet mix), bituminous and lean concrete. Since these roadbase materials are of quite different generic origin, and hence very different elastic stiffnesses, it is necessary to carry out a sensitivity study on all the parameters. The sensitivity of deflection to the stiffnesses of the other

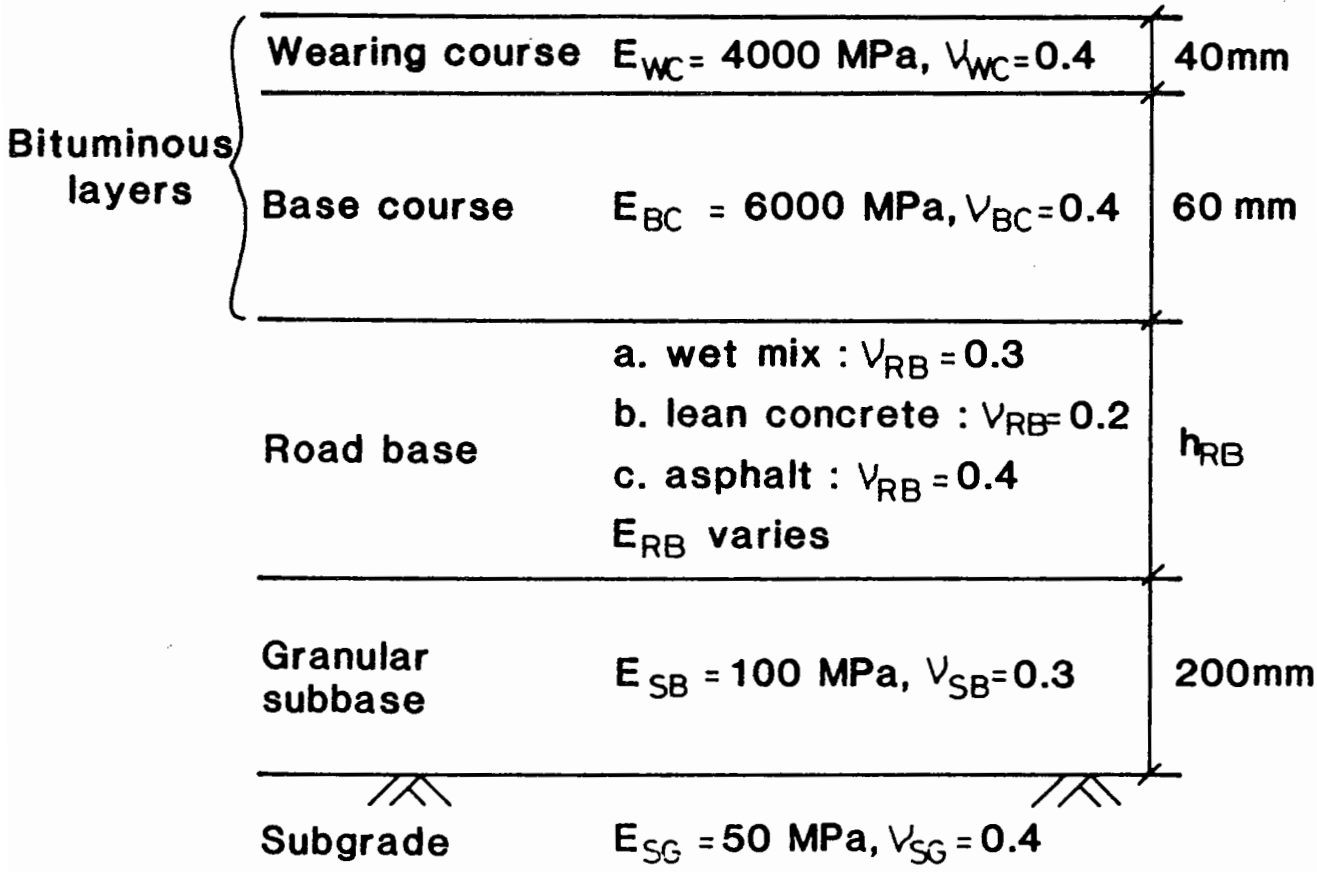

FIG. 3.16 FIVE-LAYERED STRUCTURE FOR PARAMETRIC STUDY

layers has been investigated and shown in Figure 3.17. The deflections have been calculated while the stiffnesses of the remaining layers were held constant at 4000 MPa, 6000 MPa, 100 MPa and 50 MPa for wearing course, basecourse, sub-base and subgrade respectively. The stiffness of the roadbase layer was kept constant at 10000 MPa during this exercise. From Figure 3.17, it is noted that the deflection responses for the layers are very similar to those of the bituminous layers (Figure 3.8) and the sub-base layer (Figure 3.15) described in Sections 3.4 and 3.5 respectively. Hence, no more work is attempted on varying other parameters in those layers. Work is then concentrated on the roadbase layer alone.

3.6.1 Sensitivity to parameters of the roadbase layer

Table 3.3 shows the range of values of stiffness and thickness of the roadbase layer used for deflection calculation. Typical values of 300 MPa, 10000 MPa and 30000 MPa were assigned to wet mix, bituminous and lean concrete roadbase respectively, the typical layer thickness being 200 mm for all material types. In this study, Poisson's ratios of 0.3, 0.4 and 0.2 were assigned to wet mix, bituminous and lean concrete roadbases respectively. Again, a single load of 700 kPa pressure was applied over a circular area of 300 mm diameter.

Figures 3.18 and 3.19 show the results of stiffness and layer thickness variation respectively. The observations are summarised as follows:

(a) Variation of each of the parameters of the roadbase layer modifies the bowl shape (as for the stiffness of other pavement layers, see Figure 3.17).

(b) Within the typical range of values of each parameter, the deflections are most sensitive to variation of thickness of lean concrete and bituminous roadbases.

(c) The variation in E and h of wet mix roadbase influences the deflection bowl up to 1.2 m from the load, whereas lean concrete and

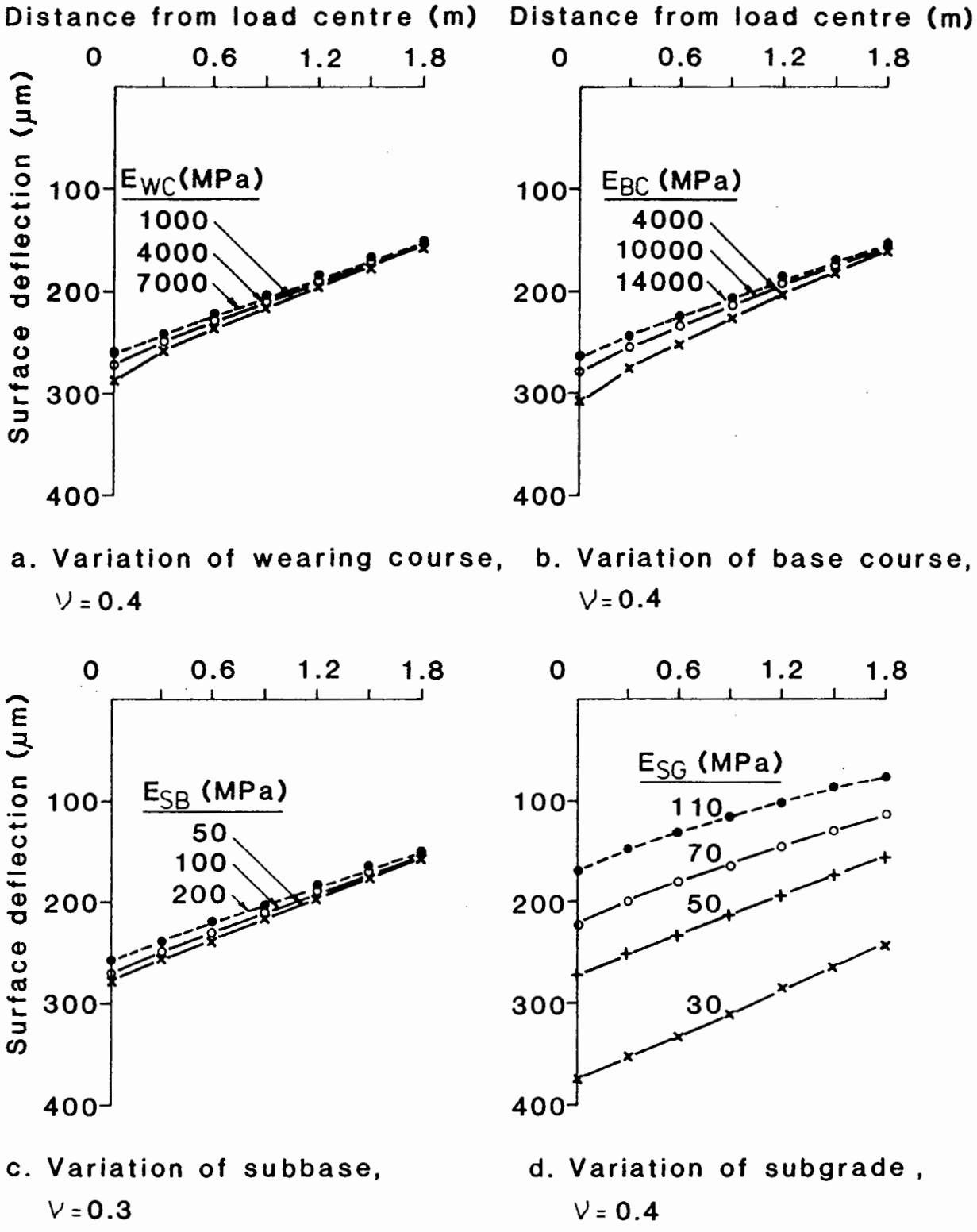

a. Variation of wearing course, $\nu = 0.4$

b. Variation of base course, $\nu = 0.4$

c. Variation of subbase, $\nu = 0.3$

d. Variation of subgrade, $\nu = 0.4$

FIG. 3.17 EFFECT OF VARIATION OF LAYER STIFFNESS ON SURFACE DEFLECTION

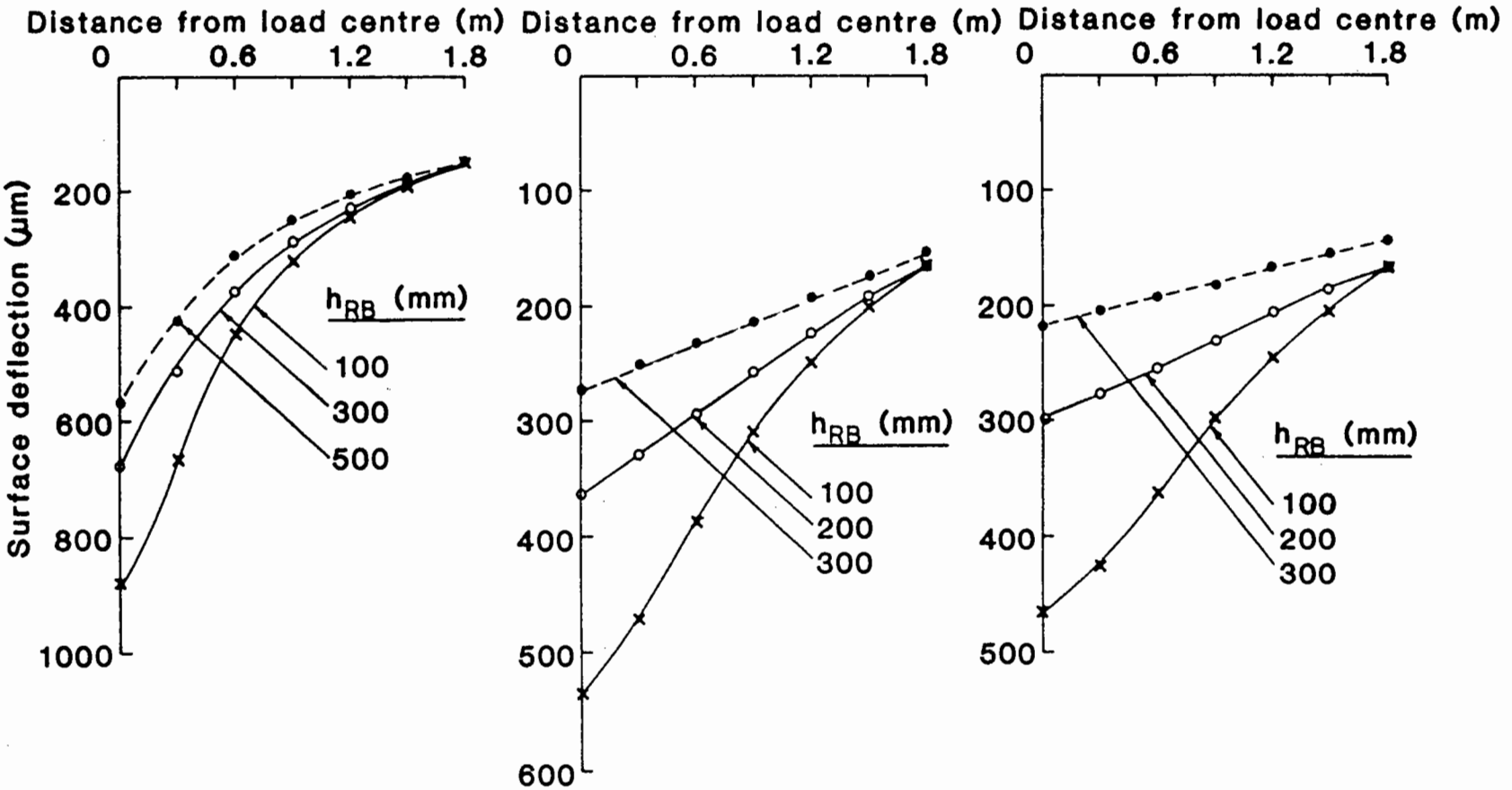

FIG. 3.18 EFFECT OF VARIATION OF LAYER THICKNESS OF DIFFERENT ROAD BASE MATERIALS ON SURFACE DEFLECTION

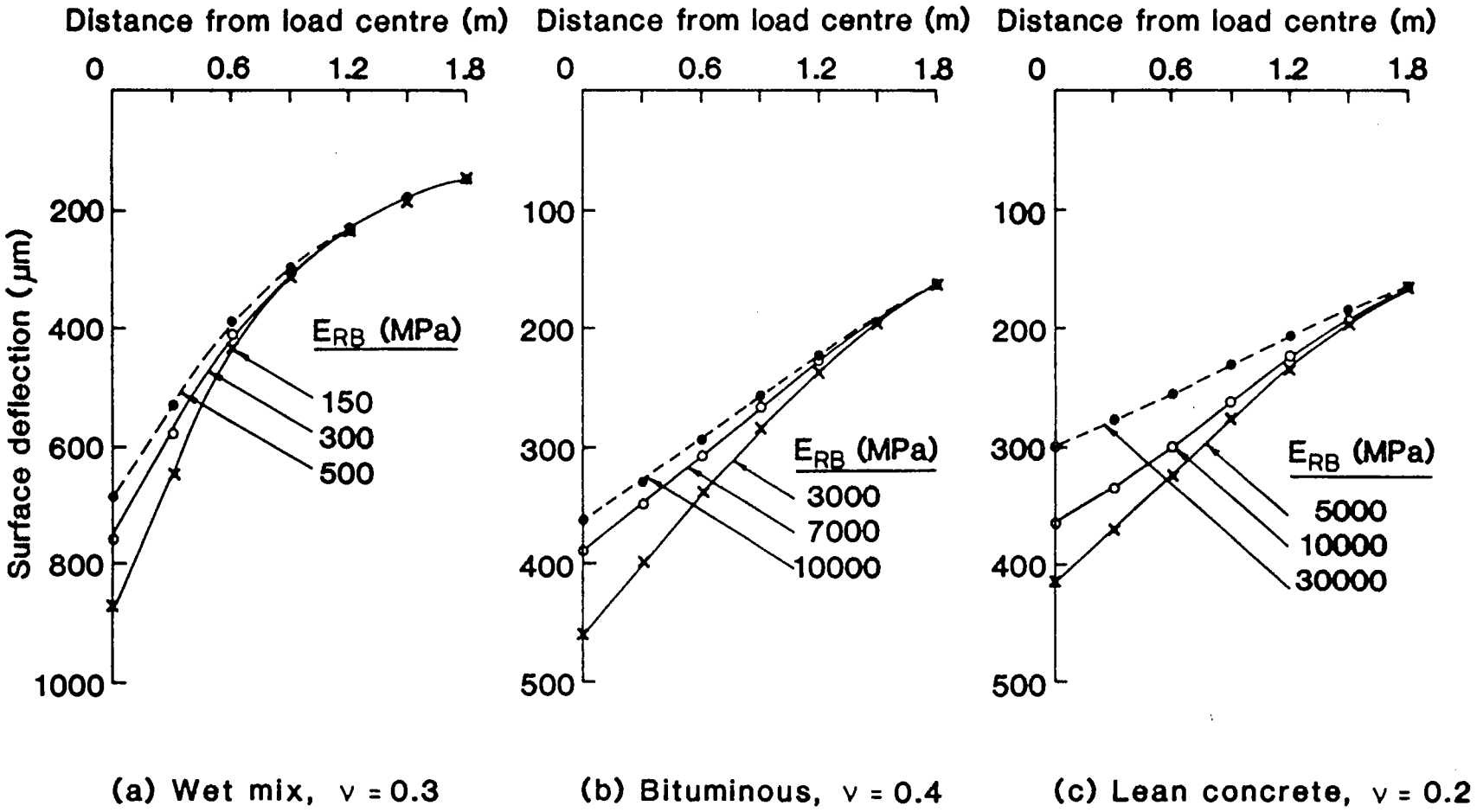

(a) Wet mix, $\nu = 0.3$ (b) Bituminous, $\nu = 0.4$ (c) Lean concrete, $\nu = 0.2$

FIG. 3.19 EFFECT OF VARIATION OF LAYER STIFFNESS OF DIFFERENT ROADBASE MATERIALS ON SURFACE DEFLECTION

bituminous material exert influence as far as 1.8 m distance.

In summary, deflections are again found to be sensitive to the variation of thickness of lean concrete and bituminous roadbases. Hence, it is important to know what the actual layer thicknesses are, to enable one to evaluate their in-situ stiffnesses with confidence.

3.7 RELATIONSHIP BETWEEN LAYER ELASTIC STIFFNESS AND DEFLECTION SLOPE

In the preceding sections, the relative sensitivity to varying parameters E, v and h of each layer has been studied. This section attempts to examine the relationship between the respective layer stiffness and deflections more closely and to identify the effect of varying the stiffness of a particular layer on the deflections. A five-layered structure, as described in Section 3.6, was used for analysis. For every deflection bowl, the difference (Δ_{ij}) between two adjacent deflection points has been computed, as shown in Figure 3.20. For seven positions (1 to 7), the deflection difference is given by:

$$\Delta_{ij} = d_i - d_j \qquad (3.2)$$

where $j = i+1$

d_i, d_j are calculated deflections at positions i and j respectively with $1 < i < 6$ and $2 < j < 7$.

These values were then made dimensionless by dividing by d_1 and termed normalised deflection difference (Δ/d_1). This parameter has been used for detailed analysis.

Figure 3.21 shows the variation of normalised deflection difference with stiffness of the wearing course layer. It is clear that while other

deflection differences are essentially constant, Δ_{12} varies to a large extent with wearing course stiffness. Figure 3.22 illustrates the effect of varying basecourse stiffness. Again, Δ_{12} is the most sensitive to the change. The variation of stiffness of roadbase

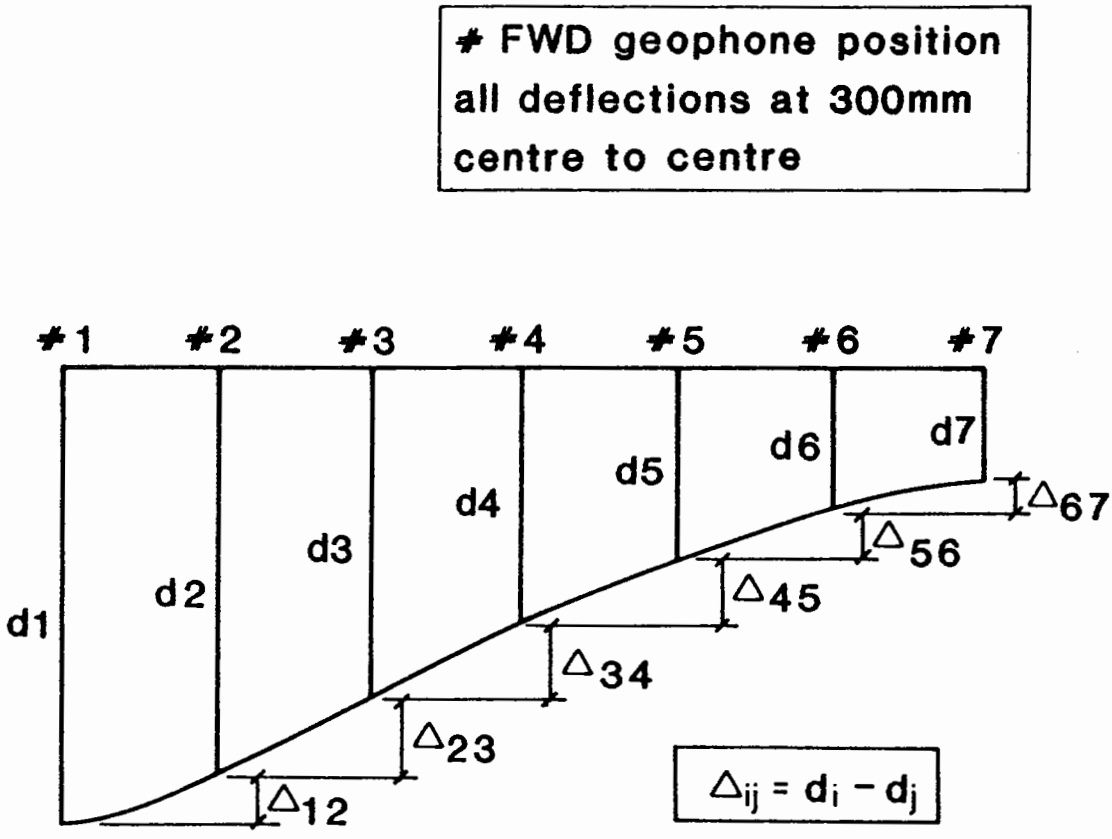

FIG 3.20 DEFLECTION BOWL AND PARAMETERS USED TO DEFINE BOWL SHAPE

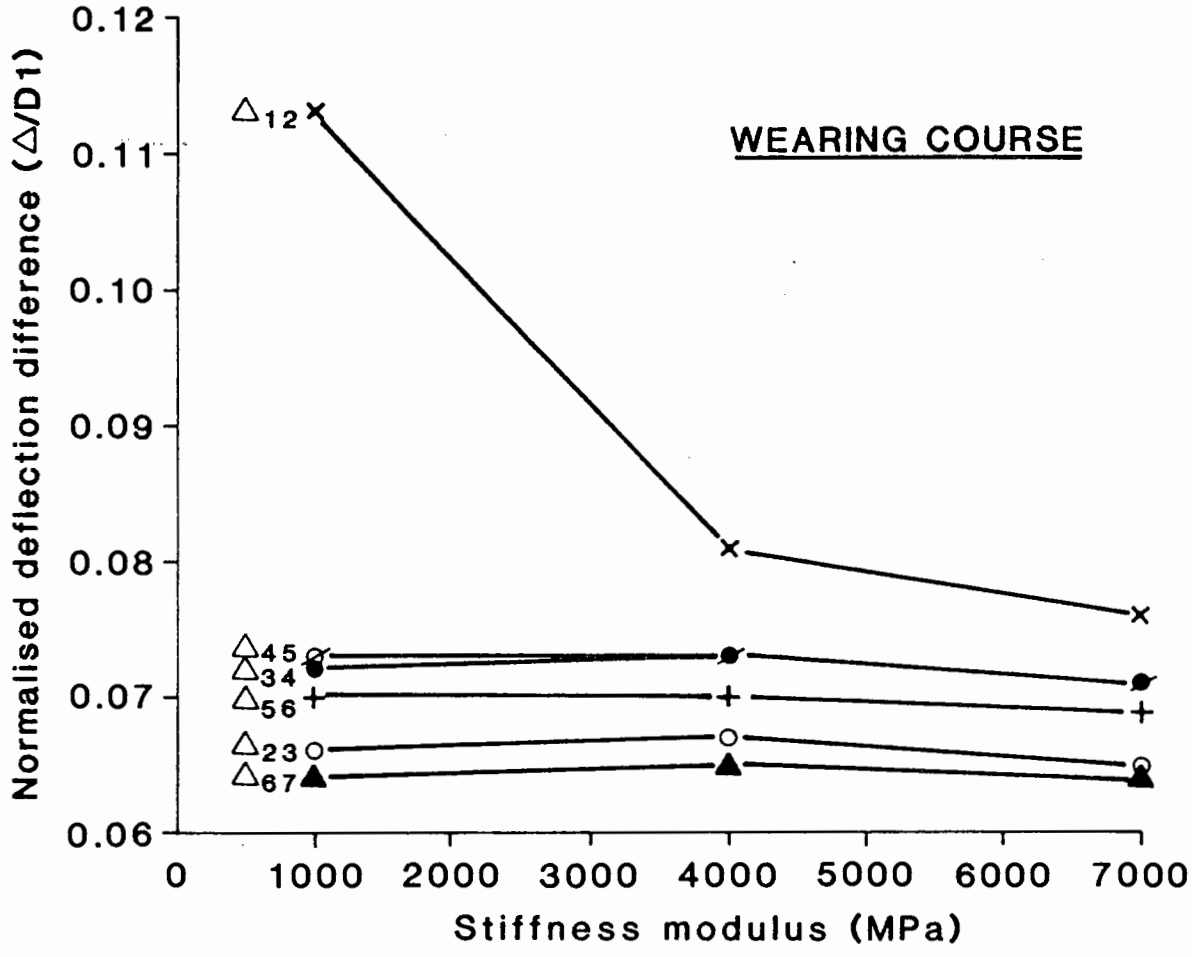

FIG. 3.21 NORMALISED DEFLECTION DIFFERENCE AND STIFFNESS MODULUS OF WEARING COURSE

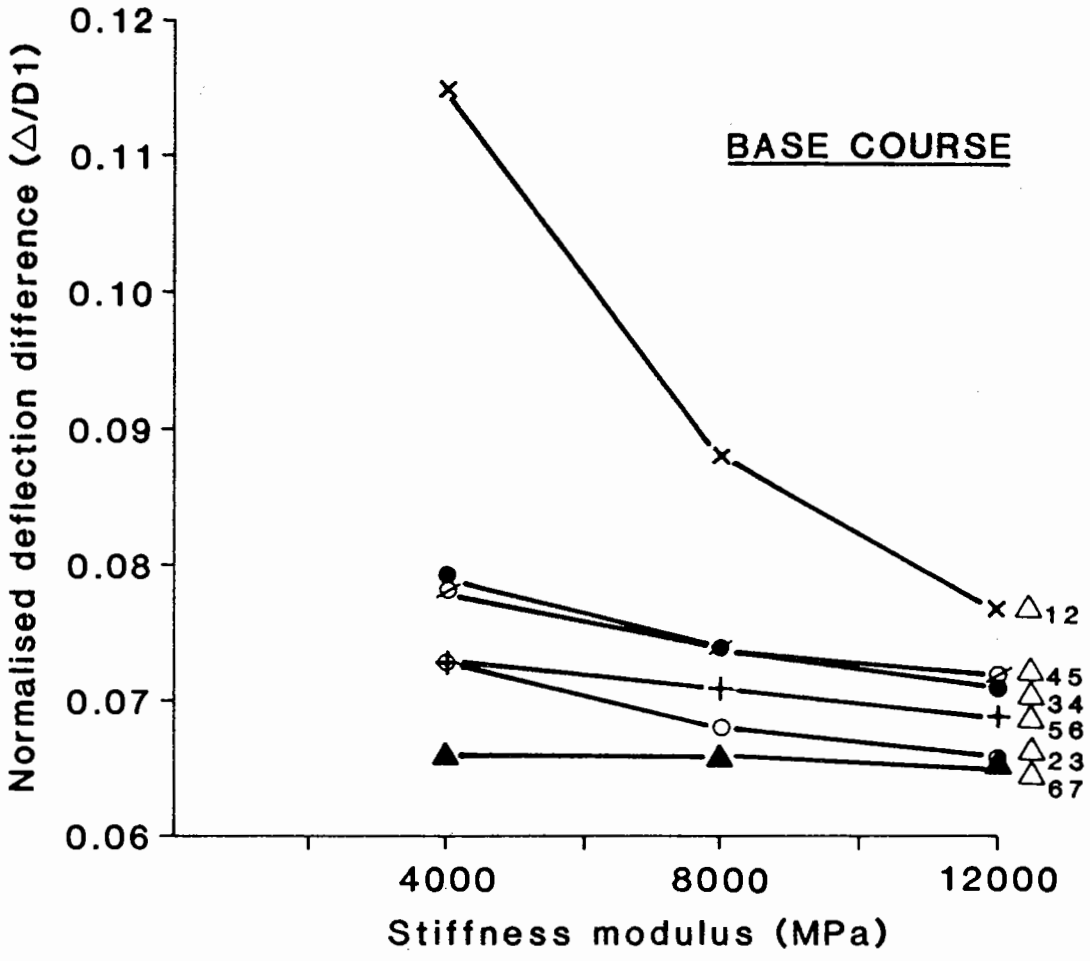

FIG. 3.22 NORMALISED DEFLECTION DIFFERENCE AND STIFFNESS MODULUS OF BASE COURSE LAYER

materials is presented in Figures 3.23, 3.24 and 3.25 for wet mix lean concrete and bituminous road- base respectively. From Figure 3.23, it is noted that Δ_{12} and Δ_{23} are influenced most significantly by wet mix stiffness. Moreover, there is no difficulty in determining that Δ_{12} and Δ_{23} in Figures 3.24 and 3.25 are greatly influenced by stiffness variation in lean concrete and bituminous roadbase layers. As far as the sub-base stiffness is concerned, its change appears not to influence any of the normalised values significantly. Amongst the various normalised deflection differences shown in Figure 3.26, one is just able to identify that the Δ_{34} and Δ_{45} are relatively more sensitive to change of sub-base stiffness.

As mentioned previously, it has been observed that variation of subgrade stiffness has the most influence on deflections. Figure 3.27 presents the results of variation in the actual deflection differences with subgrade stiffness change. Here, the actual difference is used instead of the normalised values since a much better comparison can be made. The effect of varying the subgrade stiffness is to alter the values of deflection difference only slightly near the loaded area Δ_{12} and Δ_{23}, but much more significantly for Δ_{45}, Δ_{56} and Δ_{67}, further away from the load.

So far in this section, the relative sensitivity of the deflection differences from the deflection bowl to the respective layer stiffnesses has been discussed. Table 3.4 summarises the general observations so far. It is noted that for a five-layered structure, deflections at positions 1 and 2 are more significantly influenced by the wearing course and basecourse layers; positions 1, 2 and 3 by the roadbase layer; positions 3, 4 and 5 by the sub-base layer and finally, positions 4, 5, 6 and 7 by the subgrade layer .

The general picture from the above analysis can be illustrated in Figure 3.28. For a given deflection bowl, the subgrade influences

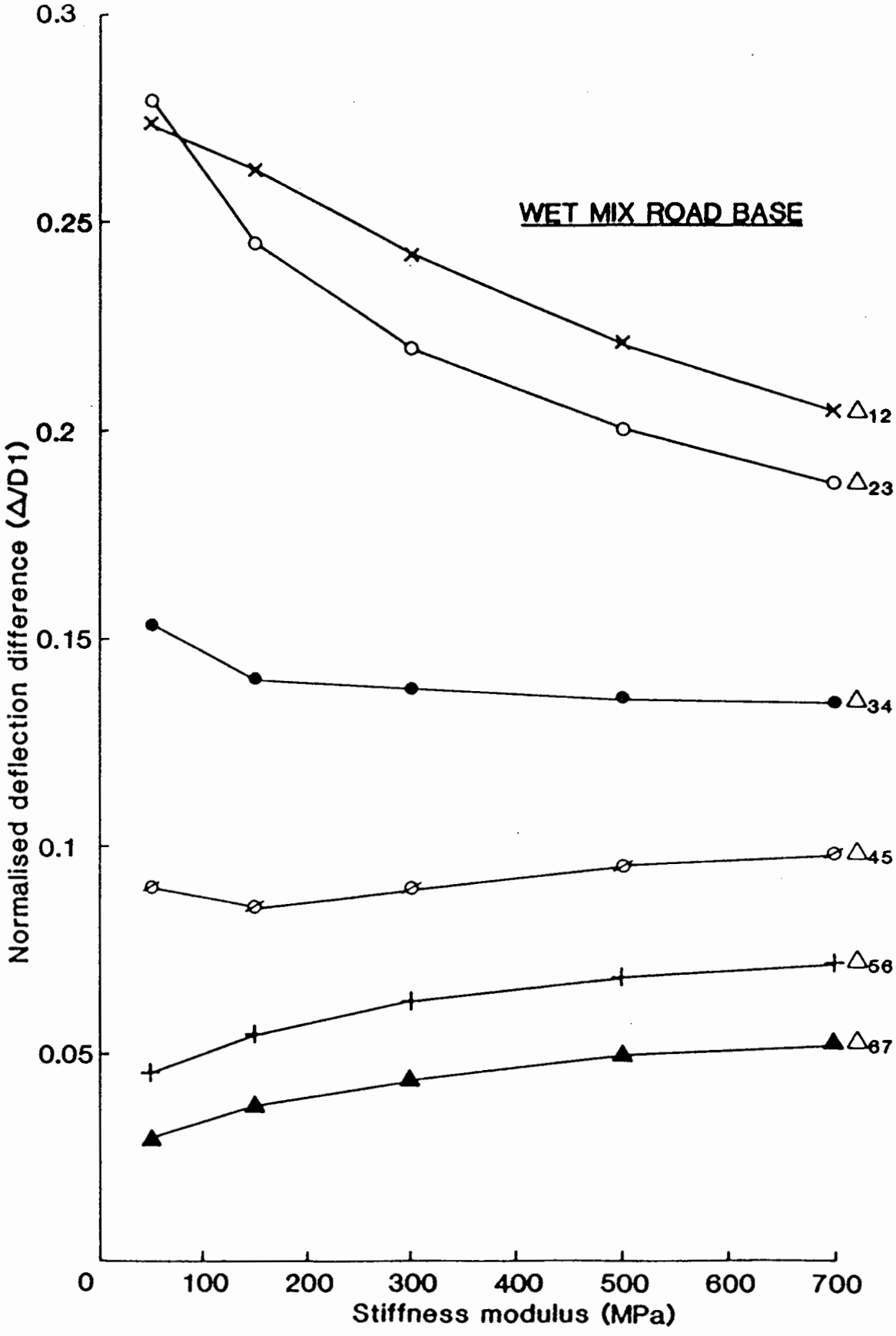

FIG. 3.23 NORMALISED DEFLECTION DIFFERENCE AND STIFFNESS MODULUS OF WET MIX ROAD BASE

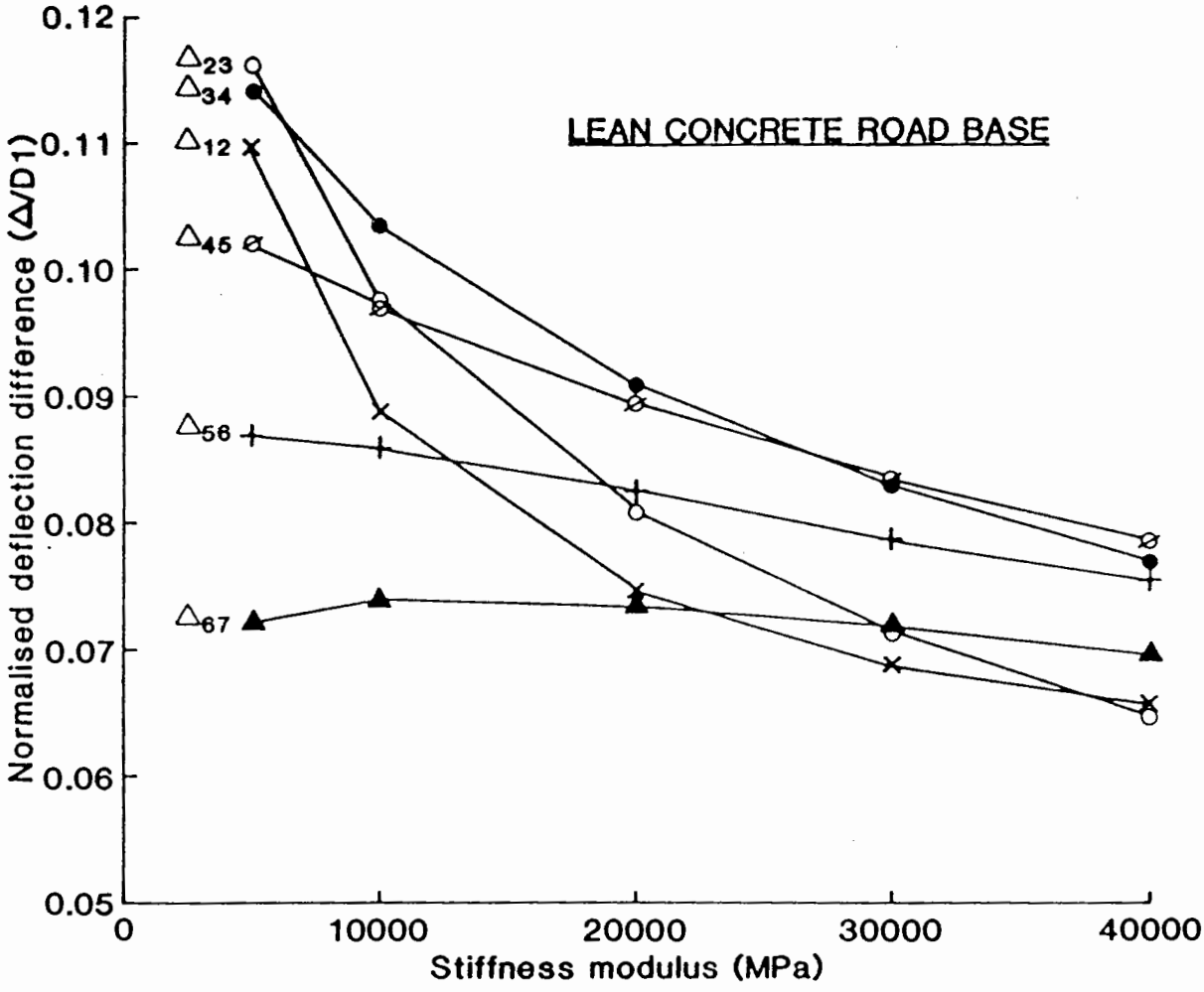

FIG. 3.24 NORMALISED DEFLECTION DIFFERENCE AND STIFFNESS MODULUS OF LEAN CONCRETE ROAD BASE

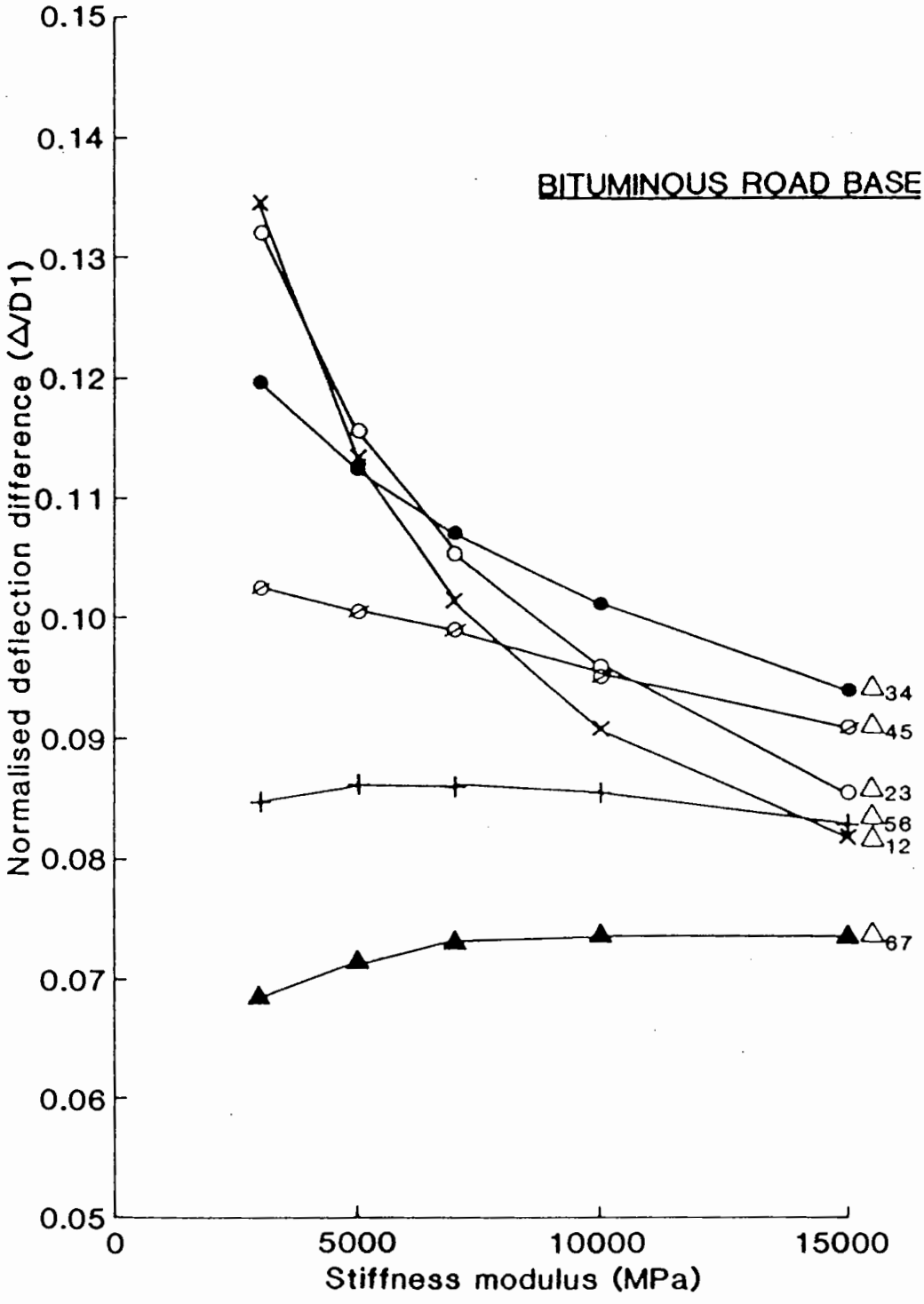

FIG. 3.25 NORMALISED DEFLECTION DIFFERENCE AND STIFFNESS MODULUS OF BITUMINOUS ROAD BASE

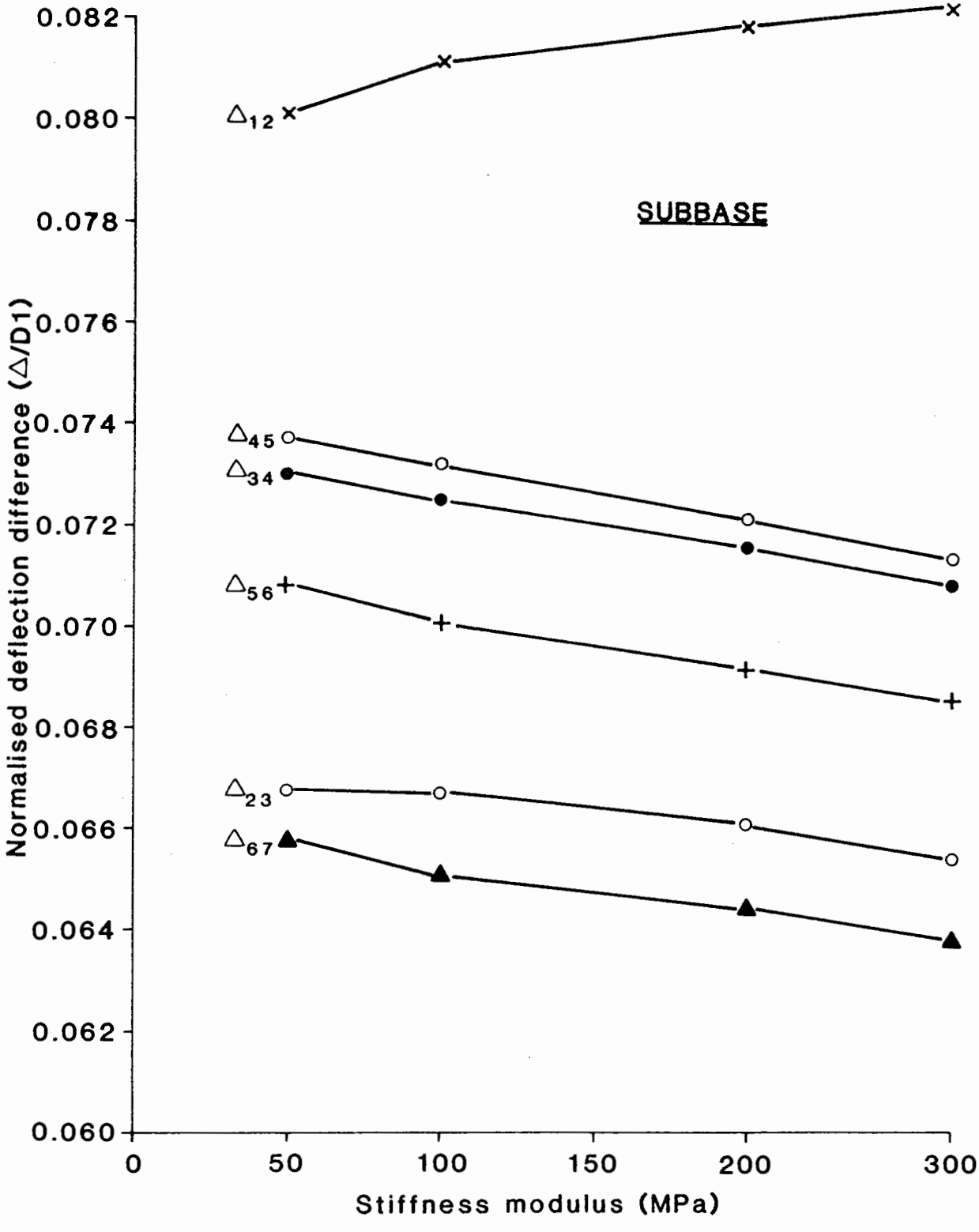

FIG. 3.26 NORMALISED DEFLECTION DIFFERENCE AND STIFFNESS MODULUS OF GRANULAR SUBBASE

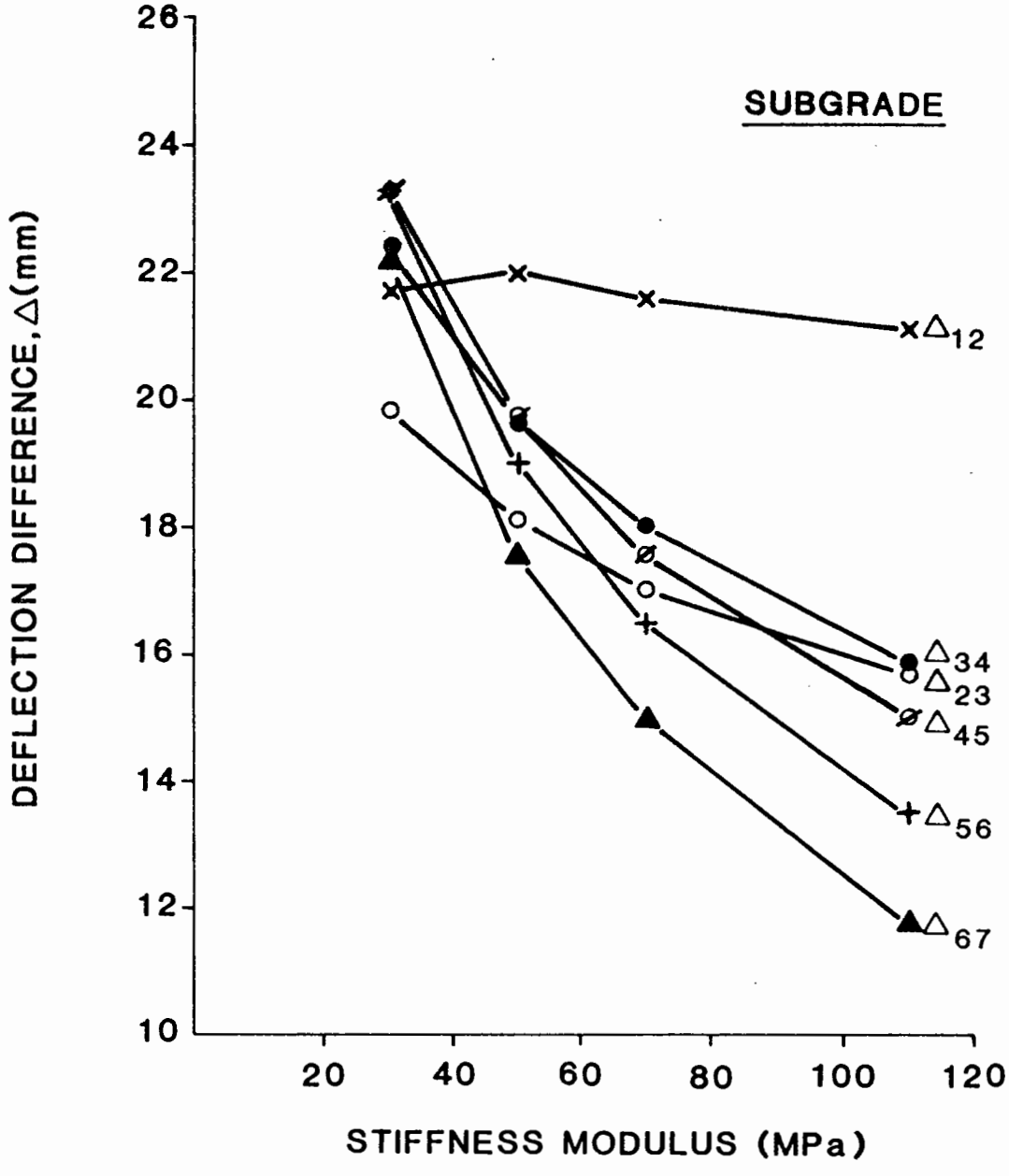

FIG. 3.27 DEFLECTION DIFFERENCE AND STIFFNESS MODULUS OF SUBGRADE

Type of Layer	Normalised Slope(s) most sensitive to layer	Corresponding Deflection Locations most sensitive to layer
Wearing Course	Δ_{12}	1, 2
Basecourse	Δ_{12}	1, 2
Roadbase	Δ_{12}, Δ_{23}	1, 2, 3
Sub-base	Δ_{34}, Δ_{45}	3, 4, 5
Subgrade	Δ_{45}, Δ_{56}, Δ_{67}	4, 5, 6, 7

Table 3.4 Sensitivity of normalised slopes and deflection locations of deflection bowl with layer type for Five-layered structure

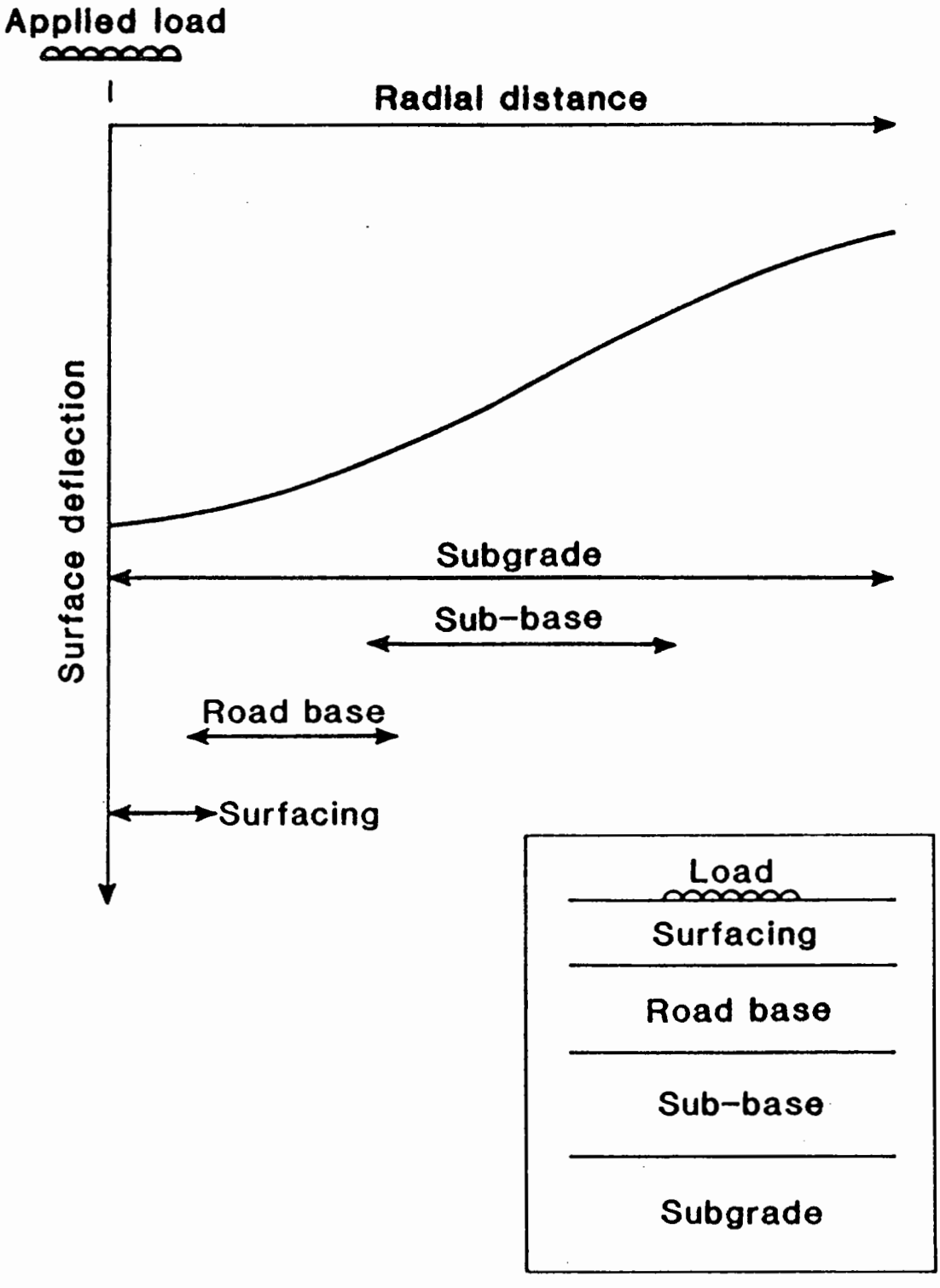

FIG. 3.28 GENERAL INFLUENCES OF ALL LAYERS ON DEFLECTION BOWL

the magnitude of the whole deflection bowl and in particular, the outermost part of the bowl. The pavement layers influence only a small part of the bowl significantly; where a layer is nearer the pavement surface, it will influence a part of the deflection bowl nearer the centre of the applied load.

The following sections examine, in greater depth, the influence of the stiffness and thickness of each pavement layer on the deflection bowl, by using a new parameter known as Influence Index.

PART B : DETAILED INVESTIGATION OF INTER-RELATIONSHIP BETWEEN LAYER STIFFNESS, THICKNESS AND RADIAL POSITION ON A DEFLECTION BOWL

3.8 DEFINITION OF INFLUENCE INDEX

Before further work is carried out, an essential parameter, called "Influence Index", is derived.

Consider a deflection bowl for any structure (termed standard structure) represented by Figure 3.29. The gradient between any two points a and b can be calculated as,

$$\text{Gradient} = \frac{\Delta d_s}{\Delta r_s} \qquad (3.3)$$

where Δd_s is the difference between deflections at a and b;

Δr_s is the difference between radial positions at a and b;

subscript s denotes standard structure.

If the stiffness (or thickness) of layer i is changed, a new deflection bowl is obtained and represented by Figure 3.29(b). Now, let points c and d on this deflection bowl be at the same radial positions as points a and b. The new gradient between c and d is then calculated as :

$$\text{Gradient} = \frac{\Delta d_i}{\Delta r_i} \qquad (3.4)$$

where Δd_i is the difference between deflections at c and d;

Δr_i is the difference between radial positions c and d;

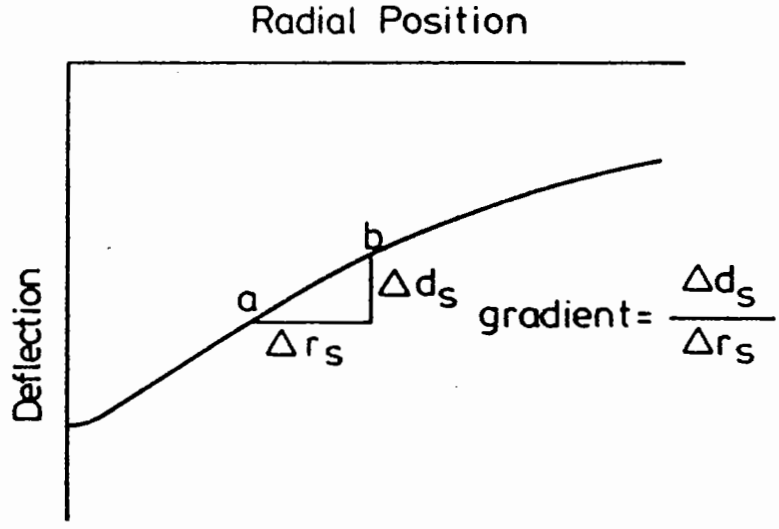

(a) Standard Structure

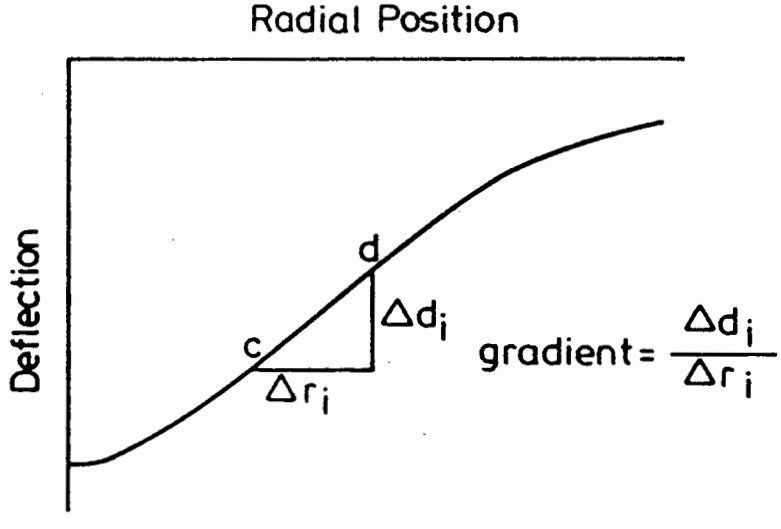

(b) Structure where Stiffness or Thickness of Layer i is changed

FIG. 3.29 DEFINITION OF PARAMETERS

subscript i denotes structure where the stiffness (or thickness) of layer i of standard structure has been altered.

Hence the rate of change of gradient due to change of stiffness (or thickness) of layer i:

$$R_{\Delta} = \frac{(\Delta d/\Delta r)_i - (\Delta d/\Delta r)_s}{(\Delta d/\Delta r)_s} \qquad (3.5)$$

Also, for layer i,

(a) rate of change of stiffness is equal to,

$$R_{\Delta E} = \frac{E_i - E_s}{E_s} \qquad (3.6)$$

(b) rate of change of thickness is equal to,

$$R_{\Delta h} = \frac{h_i - h_s}{h_s} \qquad (3.7)$$

where E_s and h_s are the stiffness and thickness respectively of layer i of the standard structure ;

E_i and h_i are the new stiffness and thickness values of layer i;

Since the effect of changing either E or h produces a similar influence on the deflection bowl, the analysis that follows therefore will not differentiate between E and h, and the same notation R_L will be used to represent a change of either parameter.

Now, let us introduce another parameter called stiffness-thickness Index. This index is defined as the change in deflection gradient at a specified radial position with respect to the corresponding rate of change of stiffness or thickness of layer i, as follows:

$$\text{Stiffness-thickness Index} = \frac{R_{\Delta}}{R_L} \qquad (3.8)$$

And finally, the "Influence Index" (II) is defined as:

$$\text{Influence Index, II} = \frac{\text{Stiffness-thickness Index at any radial position}}{\text{Maximum stiffness-thickness Index}} \qquad (3.9)$$

Hence, the "Influence Index" (II) of a deflection bowl is defined as the ratio of the stiffness-thickness index calculated at any radial position to the maximum index value of the range of radial positions studied. The II, ranging from 0 to 1, measures the sensitivity of a change in gradient on a deflection bowl to a change in stiffness or thickness of a particular layer. When II is equal to 1, the radial position which is the most sensitive to the change is located and this position is hereby known as the "best" radial position for the particular pavement layer to be studied.

3.9 USE OF INFLUENCE INDEX ON BITUMINOUS PAVEMENTS

To illustrate the use of II, twenty four-layered typical bituminous pavements were selected. Their parameters are given in Table 3.5 with the parameters explained in Figure 3.30, where the layer stiffnesses (E_1 to E_4) refer to bituminous surfacing (combined wearing course and basecourse), bituminous roadbase, granular sub-base and subgrade respectively. In Table 3.5, the selected structures are divided into four groups, each representing a thickness combination. Within each group, for instance, group A, the stiffness of each layer was doubled in turn for layers 1,3 and 4, relative to structure no. 1, while keeping other layer stiffnesses unaltered. However, the stiffness of layer 2, as shown in structure no. 3, was half that of structure no. 1. Then, for groups B, C and D, the thickness of each layer was doubled in turn relative to that of group A, while keeping other layer thicknesses unaltered. The idea of these combinations was to study the effect of varying stiffness and thickness parameters on II over a range of values. For each structure, a deflection bowl up to 2.4 m was calculated with the stiffness combination as shown in Table 3.5. Then, the stiffness of a layer was halved, e.g. 5000/2 = 2500 MPa for layer 1, and another deflection bowl,using the same

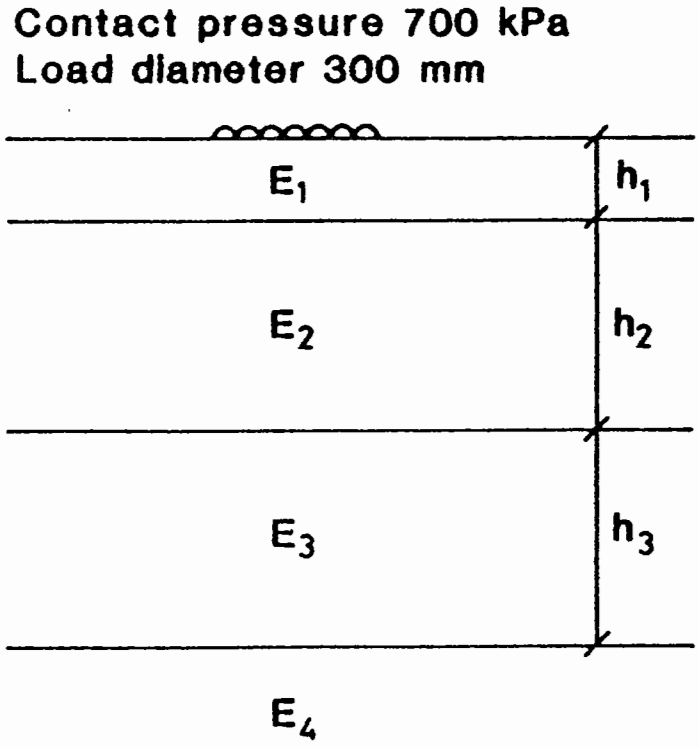

FIG. 3.30 DEFINITION OF A TYPICAL 4-LAYER STRUCTURE

Group	Structure No.	Input Parameters						
		Layer thickness(mm)			Layer stiffness(MPa)			
		h1	h2	h3	E1	E2	E3	E4
A	1	100	200	300	5000	6000	100	40
	2				10000	6000	100	40
	3				5000	3000	100	40
	4				5000	6000	200	40
	5				5000	6000	100	80
B	6	200	200	300	5000	6000	100	40
	7				10000	6000	100	40
	8				5000	3000	100	40
	9				5000	6000	200	40
	10				5000	6000	100	80
C	11	100	400	300	5000	6000	100	40
	12				10000	6000	100	40
	13				5000	3000	100	40
	14				5000	6000	200	40
	15				5000	6000	100	80
D	16	100	200	600	5000	6000	100	40
	17				10000	6000	100	40
	18				5000	3000	100	40
	19				5000	6000	200	40
	20				5000	6000	100	80

Contact pressure= 700kPa

Poisson's ratios $\nu_1 = \nu_2 = \nu_3 = 0.4$, $\nu_4 = 0.3$

Table 3.5 Input parameters used to calculate Influence Index of layer - Bituminous Pavements

radial positions as the original, was computed. Calculations using equations (3.3) to (3.8) were followed and finally, II values at each deflection position were computed using equation (3.9).

Figure 3.31 illustrates an example of a plot of the variations in influence indices against radial position for all the layers. It is noted, from the figure, that a change of stiffness in layer 1 only influences that part of the deflection bowl from the load centre to 0.2 m significantly, with the "best" radial position located at 0.15 m (i.e. II = 1). The influence of layer 2 on the deflection bowl is greater than that of layer 1, from 0 to 0.6 m, with the "best" radial position located at 0.2 m. Layer 3 is found to affect more significantly the outer part of the deflection bowl, starting from 0.25 m (where II = 0.5). This time, the "best" radial position is further out, at 1.1 m. The influence of layer 4 is greatest for the outermost part of the deflection bowl, as expected.

Table 3.6 summarises the results of the above observations for the 20 structures, where the radial positions corresponding to II = 1.0 and II = 0.5 have been calculated. These two radial positions indicate the range of the deflection bowl which is sensitive to the change of stiffness or thickness of a particular layer. This range is represented as the "spread of influence". It is noted that,

(a) Within a group (i.e. same thickness combination for the structure), the "best" radial position stays unchanged for layers 1,2 and 4. However, the "best" radial position corresponding to layer 3 is influenced by the stiffness variation of all the layers (refer II = 1.0 for layer 3). As the stiffness of other layers is varied, this position is pushed away from the load but an increase of stiffness in layer 3 pulls the position closer to the load.

(b) When the layer 1 thickness is increased, (Group B compared with Group A), the spread of influence of this layer is increased slightly from 0.18 m (II = 0.5) in Group A to 0.23 m. The "best" radial position of

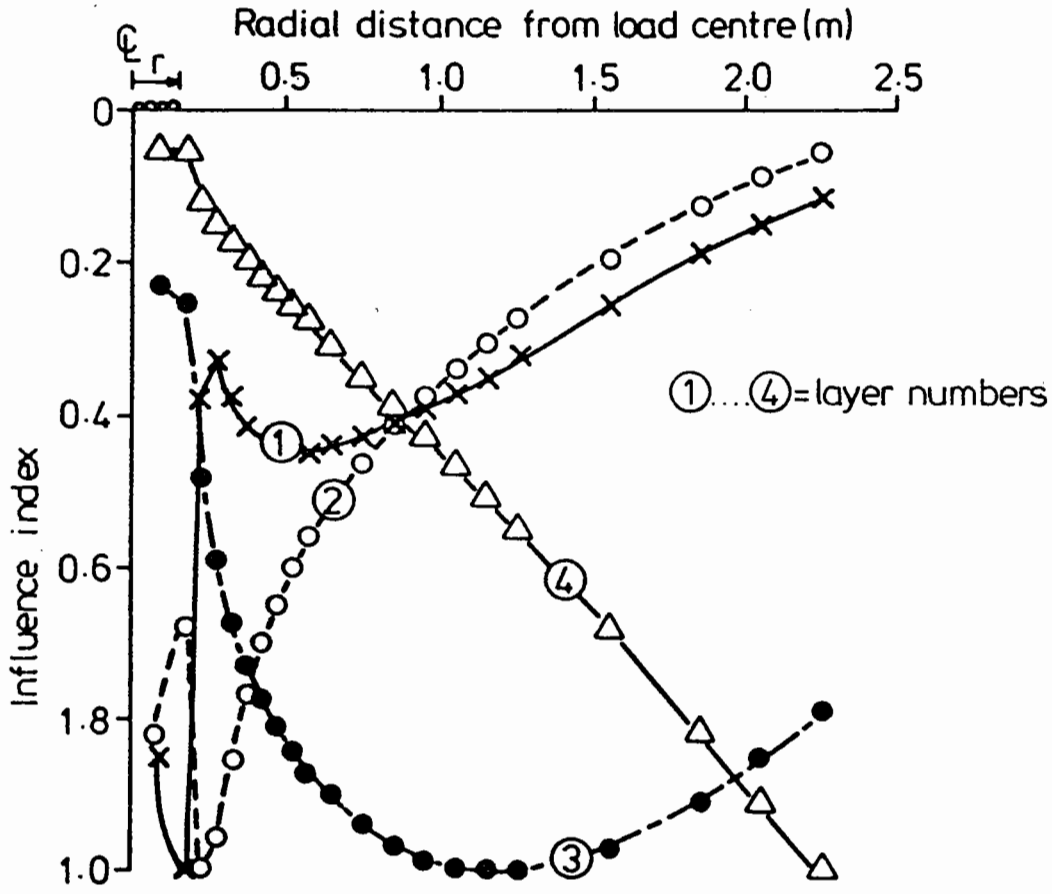

FIG. 3.31 TYPICAL DIAGRAM SHOWING VARIATION OF INFLUENCE INDICES FOR ALL LAYERS

(BITUMINOUS PAVEMENTS)

Group	Structure No.	Radial distances(m) from load centre with various Influence Indices (I I)							
	Layer No.	1		2		3		4	
	I I	1.0	0.5	1.0	0.5	1.0	0.5	1.0	0.5
A	1	0.15	0.18	0.20	0.65	1.1	0.25	2.4	1.1
	2	0.15	0.18	0.20	0.80	1.2	0.25	2.4	1.1
	3	0.15	0.18	0.20	0.70	1.3	0.20	2.4	1.1
	4	0.15	0.18	0.20	0.55	0.8	0.20	2.4	1.1
	5	0.15	0.18	0.20	0.60	1.4	0.30	2.4	1.2
B	6	0.0	0.22	0.30	1.10	1.4	0.25	2.4	1.0
	7	0.0	0.23	0.35	1.50	1.6	0.30	2.4	1.0
	8	0.0	0.24	0.30	1.10	1.9	0.25	2.4	1.0
	9	0.0	0.22	0.30	1.00	0.9	0.30	2.4	1.0
	10	0.0	0.22	0.30	1.00	1.8	0.35	2.4	1.1
C	11	0.15	0.16	0.25	0.70	1.7	0.30	2.4	1.0
	12	0.15	0.16	0.25	0.90	2.1	0.35	2.4	0.9
	13	0.15	0.16	0.25	0.90	1.8	0.35	2.4	1.0
	14	0.15	0.16	0.25	0.55	1.0	0.25	2.4	1.0
	15	0.15	0.16	0.25	0.55	2.1	0.40	2.4	1.1
D	16	0.15	0.17	0.20	0.58	1.4	0.30	2.4	1.2
	17	0.15	0.18	0.20	0.70	1.5	0.30	2.4	1.1
	18	0.15	0.18	0.20	0.65	1.6	0.30	2.4	1.1
	19	0.15	0.17	0.20	0.50	1.1	0.25	2.4	1.1
	20	0.15	0.16	0.20	0.60	1.6	0.40	2.4	1.3

Table 3.6 Summary of influence of a layer to different parts of a deflection bowl based on Influence Indices Bituminous Pavements

the layer moves from the edge to the centre of the load. However, this causes the "best" radial positions for layers 2 and 3 to be pushed away from the load.

(c) Increase in thickness of layer 2 increases its importance in the structure (Group C compared with Group A). Thus, its spread of influence is greater than in Group A. Also, its "best" radial position is shifted slightly away from the load (from 0.2 m to 0.25 m), and at the same time, the "best" radial position for layer 3 is pushed away from the load. It is interesting to note that the relative influence of layer 1 has been reduced (0.16 m compared with 0.18 m in Group A).

(d) Increase in thickness of layer 3 results in shifting its own "best" radial position away from the load slightly. (Group D compared with Group A). It is noted that the positions for layers 1 and 2 are hardly changed, except that the spread of influence of layer 2 has been reduced very slightly when compared with Group A.

(e) Variation of stiffness of layer 4 always influences the outermost deflection of the bowl significantly, with its maximum influence at 2.4m.

3.10 USE OF INFLUENCE INDEX ON CONCRETE PAVEMENTS

As for bituminous pavements, twenty typical four-layered concrete pavements have been analysed. Table 3.7 shows the input parameters, where the layers from 1 to 4 refer to pavement quality concrete, lean concrete, granular sub-base and subgrade respectively. Again, they are divided into four groups, E, F, G and H, with five structures in each group. Within each group, e.g. Group E, the stiffness of each layer was halved in turn relative to structure no. 1, while keeping other layer stiffnesses unaltered. Then, for groups F, G, and H, the thickness of each layer was doubled in turn relative to that of Group E, while keeping other layer thicknesses unaltered. For each structure, a deflection bowl was computed

Group	Structure No.	Input Parameters						
		Layer thickness(mm)			Layer stiffness(MPa)			
		h1	h2	h3	E1	E2	E3	E4
E	1	100	200	300	30000	20000	100	60
	2				15000	20000	100	60
	3				30000	10000	100	60
	4				30000	20000	50	60
	5				30000	20000	100	30
F	6	200	200	300	30000	20000	100	60
	7				15000	20000	100	60
	8				30000	10000	100	60
	9				30000	20000	50	60
	10				30000	20000	100	30
G	11	100	400	300	30000	20000	100	60
	12				15000	20000	100	60
	13				30000	10000	100	60
	14				30000	20000	50	60
	15				30000	20000	100	30
H	16	100	200	600	30000	20000	100	60
	17				15000	20000	100	60
	18				30000	10000	100	60
	19				30000	20000	50	60
	20				30000	20000	100	30

Contact pressure = 1500kPa

Poisson's ratios $\nu_1 = \nu_2 = 0.2$, $\nu_3 = 0.3$, $\nu_4 = 0.4$

Table 3.7 Input parameters used to calculate Influence Index of layer - Concrete Pavements

up to a radial distance of 3.0 m away from the load. The computation to obtain the II values follows the same procedure as for the bituminous structures already described in the previous section. Figure 3.32 shows a typical plot of variations in II for all the layers. It is noted that the maximum influence from the top two layers is again near the loaded area. However, the spread of influence for these layers is greater than for bituminous structures. As the upper layers gets stiffer, the "best" radial position for layer 3 is pushed further away from the load. The influence of layer 4, as expected, is always greatest for the outermost part of the deflection bowl.

Table 3.8 summarises the results of the calculation for all twenty structures. Again, the radial positions corresponding to II = 1.0 and 0.5 were computed to examine the spread of influence for each layer.

From the table, the following points are noted:

(a) Within a group, the "best" radial position, derived by changing layer stiffnesses, varies very slightly for layer 1 (0.15 m) and layer 2 (0.05 m). Again, the "best" position for layer 3 is influenced by the stiffness variation of all the layers (as for bituminous pavements).

(b) When the layer 1 thickness is increased (Group F compared with Group E), the spread of influence of this layer appears to be reduced, which is rather unexpected. It is considered that the main reason for such reduction is due to the presence of the "kink" on the influence index curve for layer 1 as shown in Figure 3.32. Close examination of the curves of other structures shows that where the spread of influence is less than 0.3 m, the influence index corresponding to the "kink" is usually less than 0.4; hence any increase in the influence index curve after the "kink" does not bring it to greater than 0.5. Furthermore, an increase in thickness tends to pull the "best" radial position of layer 1 towards the centre, from the loading edge, and, at the same

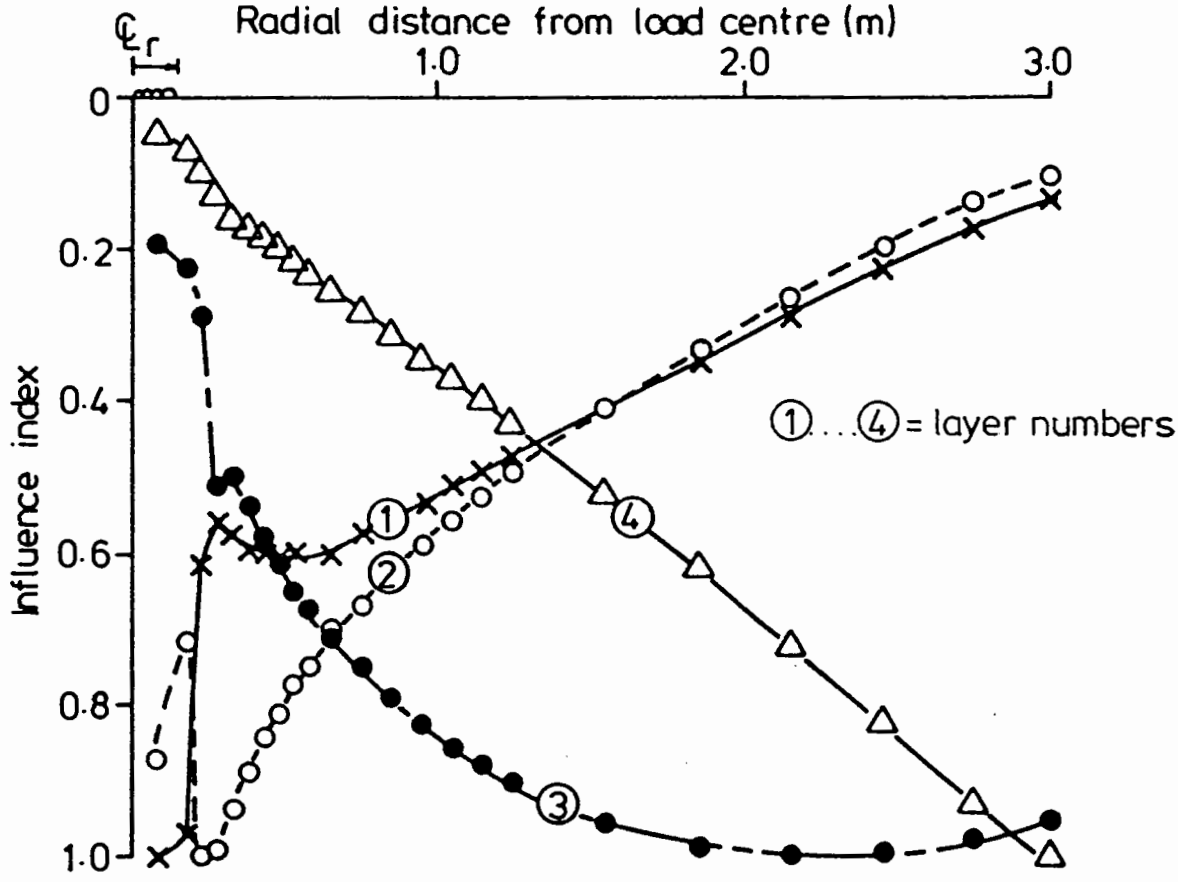

FIG. 3.32 TYPICAL DIAGRAM SHOWING VARIATION OF INFLUENCE INDICES FOR ALL LAYERS (CONCRETE PAVEMENTS)

time, push the "best" radial position of layers 2 and 3 away from the load.

(c) Unlike the top layer, the spread of influence of layer 2 is not observed to be dependent upon the increase of its layer thickness (Group G compared with Group E). The "best" radial position of this layer only moves slightly away from the load (from 0.2 m to 0.25 m distance). The increase in thickness again pushes the "best" radial position for layer 3 away from the load and at the same time, reduces the spread of influence of layer 1.

(d) Increase in thickness of layer 3 follows the same trend as for the bituminous structures. This results in the "best" radial position being shifted slightly away and a slight reduction in the spread of influence of layer 2. The "best" positions for layers 1 and 2 are unaffected.

(e) As for bituminous structures, variation of stiffness of layer 4 always influences the outermost deflections of the bowl significantly, with its "best" radial position located at 3.0 m.

3.11 A PROPOSED METHOD FOR SETTING THE RADIAL POSITIONS OF FWD GEOPHONES FOR SITE SURVEYS

The analysis described in the previous sections for bituminous and concrete pavement structures, based on the use of influence indices, has been found to provide a logical way of explaining the influences of layer thickness and stiffness variations on the deflection bowl. This is achieved by identifying the location of the "best" radial position, that which is most sensitive to the layer. Thus, it forms the basis for developing a novel method for:

(a) More effective positioning of the FWD geophones for site surveys ;

(b) Finding a better shape of the deflection bowl, providing the most essential input parameters for the PADAL back-analysis program (to be described in Chapter 4).

Since back-calculated layer stiffnesses are very sensitive to measured deflection, it is paramount that the measured deflection bowl should reflect the actual condition of the pavement being tested and to this end, the best result can only be achieved by positioning the geophones before any survey over the "best" radial positions corresponding to each layer of the structure.

The proposed method, as explained below, is based on a four-layered structure. However, the same idea can be easily adapted to a three- or five-layered structure.

3.11.1 Bituminous pavements

As observed in Figure 3.31 and Table 3.6, it is clear that layer 1 only influences that part of the deflection bowl beneath the loaded area, i.e. 0 to 0.15 m. Therefore, it is logical to select the central deflection for monitoring the behaviour of layer 1.

Section 3.9 demonstrated that the "best" radial position for layer 2 was influenced more significantly by variations in the thickness of layer 1 or layer 2 but not the stiffness of these layers. Therefore, a series of computer runs was carried out by varying the thickness of layers 1 and 2 for a given stiffness profile of 5000 MPa for layer 1, 6000 MPa for layer 2, 100 MPa for layer 3 and 40 MPa for layer 4 respectively. The "best" radial positions for layer 2 corresponding to different thicknesses of layers 1 and 2 have been plotted in Figure 3.33. It is considered that this chart can be used to locate the "best" radial position for layer 2 very easily. For instance, if h_1 = 100 mm, and h_2 = 200 mm, then the radial position for layer 2 will be 230 mm.

Due to physical constraints on the FWD, the minimum distance of the first geophone from the centre of the load is 200 mm.

It is recalled that Table 3.6 showed that the "best" radial position for layer 3 was influenced by every parameter of a pavement structure, which makes it very difficult to determine its position readily. The problem

Group	Structure No.	Radial distances(m) from load centre with various Influence Index(I I)							
	Layer No.	1		2		3		4	
	I I	1.0	0.5	1.0	0.5	1.0	0.5	1.0	0.5
E	1	0.0	1.00	0.20	1.2	2.1	0.30	3.0	1.5
	2	0.15	0.20	0.20	1.0	1.9	0.30	3.0	1.5
	3	0.15	0.70	0.25	1.2	1.7	0.30	3.0	1.5
	4	0.15	1.10	0.20	1.3	2.7	0.60	3.0	1.4
	5	0.15	1.30	0.25	1.4	1.9	0.20	3.0	1.3
F	6	0.15	0.25	0.35	2.0	3.0	0.35	3.0	1.4
	7	0.0	0.30	0.30	1.7	2.6	0.35	3.0	1.4
	8	0.0	0.25	0.35	1.9	2.3	0.30	3.0	1.4
	9	0.15	0.25	0.35	2.1	3.0	0.70	3.0	1.3
	10	0.0	0.24	0.35	2.5	2.3	0.25	3.0	1.2
G	11	0.15	0.20	0.25	1.3	1.8	0.45	3.0	1.3
	12	0.15	0.18	0.25	1.0	3.0	0.40	3.0	1.3
	13	0.15	0.18	0.30	1.2	2.1	0.45	3.0	1.3
	14	0.15	0.20	0.25	1.3	3.0	0.70	3.0	1.3
	15	0.15	0.19	0.25	1.2	2.7	0.30	3.0	1.1
H	16	0.15	0.90	0.20	1.1	2.3	0.40	3.0	1.5
	17	0.15	0.20	0.20	1.0	2.1	0.40	3.0	1.6
	18	0.15	0.80	0.25	1.0	2.0	0.40	3.0	1.6
	19	0.15	1.10	0.20	1.3	3.0	0.70	3.0	1.5
	20	0.15	1.00	0.25	1.2	1.9	0.30	3.0	1.4

Table 3.8 Summary of influence of a layer to different parts of a deflection bowl based on Influence Indices (Concrete Pavements)

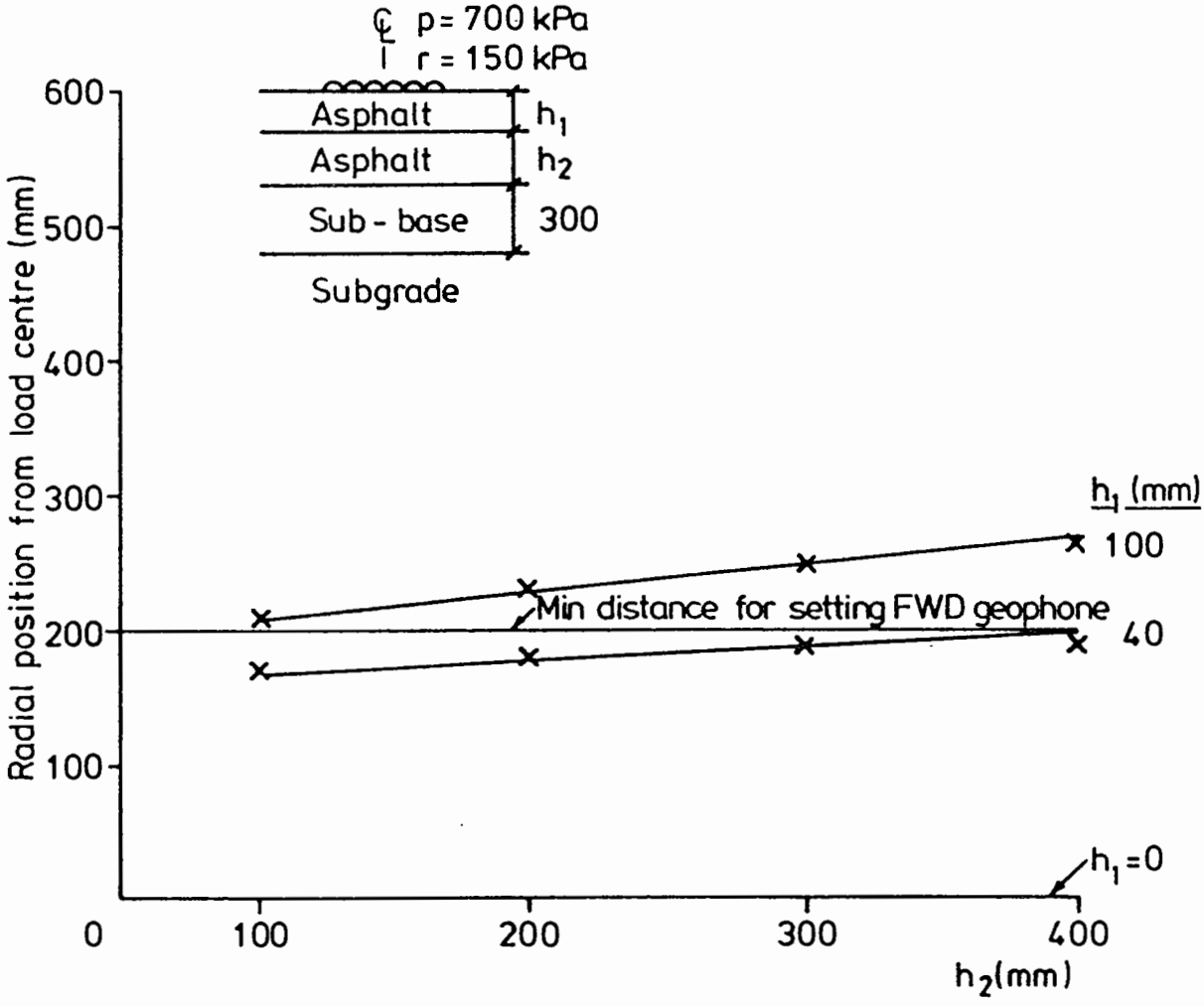

FIG. 3.33 RELATIONSHIP BETWEEN THE MOST SENSITIVE RADIAL POSITION FOR LAYER 2 AND LAYER THICKNESSES (BITUMINOUS PAVEMENTS)

has been overcome by making use of deflection ratios.

The twenty structures taken from Table 3.5 were re-analysed and the results are shown in Table 3.9. Deflection ratios were computed by dividing the deflection corresponding to the "best" radial position by the central deflection of the same deflection bowl. The ratios range from 0.4 to 0.77 with an average of 0.6. However, some of the radial positions are observed to occur at a distance more than 1.8 m from the load, e.g. structures nos. 8, 13, 15, 18 and 20 and these positions are considered to be unsuitable for two reasons:

(a) The furthermost that a geophone can be set in the FWD is 2.4 m;

(b) Reliable back-analysis results using the PADAL program can be achieved for layer 3 (the sub-base layer) if the radial position is between 0.6 m from the load centre and 1.2 m from the furthest geophones (refer Chapter 4 for more details).

Hence, another set of deflection ratios corresponding to radial positions where II = 0.9 were calculated and also summarised in Table 3.9. The ratios range from 0.61 to 0.91, with an average of 0.78, with the radial positions lying between 0.25 m to 1.2 m. After examining the radial positions carefully, it is considered appropriate to assign the radial position which is sensitive to layer 3 as the point where the deflection ratio is 0.8 or the deflection is 80% of the central deflection value

As explained in Section 3.9, layer 4 (the subgrade) always influences the outermost part of a deflection bowl. Hence, it is very straightforward to set the furthest geophone once the position for layer 3 has been located since it should be at least 1.2 m further out. In order to model non-linear subgrade behaviour with the PADAL program (refer Chapter 4), one extra deflection is required which should be placed at a distance of 0.6m from the furthest geophone.

Table 3.11(A) summarises the main steps in the selection of geophone positions for surveys on bituminous pavements using the FWD.

Group	Structure No.	Central Deflection (μm) (1)	I I=1.0 Deflection (μm) (2)	I I=1.0 Position (m)	Ratio=(2)/(1)	I I=0.9 Deflection (μm) (3)	I I=0.9 Position (m)	Ratio=(3)/(1)
A	1	447.77	286.40	1.1	0.64	359.90	0.6	0.80
	2	406.14	261.46	1.2	0.64	322.09	0.7	0.79
	3	396.27	251.30	1.3	0.63	320.78	0.7	0.81
	4	425.77	315.49	0.8	0.74	363.86	0.45	0.85
	5	298.81	133.03	1.4	0.45	182.30	0.9	0.61
B	6	352.67	223.46	1.4	0.63	283.99	0.7	0.81
	7	310.99	198.50	1.6	0.64	268.62	0.6	0.86
	8	319.45	181.68	1.9	0.57	250.13	0.9	0.78
	9	340.76	257.97	0.9	0.76	290.95	0.5	0.85
	10	236.15	103.18	1.8	0.44	144.02	1.1	0.61
C	11	287.53	182.18	1.7	0.64	232.17	0.8	0.81
	12	242.93	153.35	2.1	0.63	193.84	1.1	0.80
	13	263.13	169.59	1.8	0.64	212.27	0.9	0.81
	14	280.36	215.61	1.0	0.77	239.39	0.55	0.85
	15	192.98	87.38	2.1	0.45	122.72	1.2	0.64
D	16	419.74	234.06	1.4	0.56	321.56	0.7	0.77
	17	382.84	217.76	1.5	0.57	279.31	0.9	0.73
	18	374.85	210.65	1.6	0.56	280.41	0.9	0.75
	19	375.86	245.43	1.1	0.65	342.28	0.25	0.91
	20	293.83	116.52	1.6	0.40	240.12	0.4	0.82
				Average	0.60		Average	0.78

I I denotes Inflence Index

Table 3.9 Deflection Ratios for different Influence Indices of the Subbase layer Bituminous Pavements

3.11.2 Concrete pavements

A similar study was also carried out for concrete pavement structures. As for the bitumious structures, central deflection is selected to evaluate the behaviour of layer 1.

From Table 3.8, it is noted that thickness variation of the concrete layers has more effect on the "best" radial position of layer 2 than stiffness. Therefore, a series of computer runs was also carried out by altering thicknesses h_1 and h_2, with a layer stiffness profile of 30000 MPa, 20000 MPa, 100 MPa and 60 MPa for layers 1, 2, 3 and 4 respectively, and loaded by a vertical pressure of 1500 kPa on 300 mm diameter. Figure 3.34 shows the results. The procedure for determining the "best" radial position for layer 2 can then be followed in the same way as for the bituminous structures already described.

After the success of utilising deflection ratios to determine the "best" position for layer 3 in bituminous structures, a similar exercise was carried out for concrete structures. The results of calculations are shown in Table 3.10 based on the structures taken from Table 3.7. At the "best" radial position, the deflection ratios vary from 0.38 to 0.73 averaging at 0.55. Once again, these radial positions are found to be too far away from the load, with over 30% of them beyond the maximum length of 2.4 m of the FWD sub-frame. The results corresponding to II = 0.9 are also presented in the table which shows the deflection ratios varying between 0.5 and 0.88 with an average of 0.71. After examining the respective radial positions carefully, it is considered appropriate to assign the radial position which is sensitive to layer 3 as that where deflection ratio is 0.75 or the deflection is 75% of the central deflection. This should give a distance of about 1.2 m from the furthest geophone.

As for layer 4, Table 3.8 demonstrated that variation of its stiffness would significantly influence the outermost part of the deflection bowl.

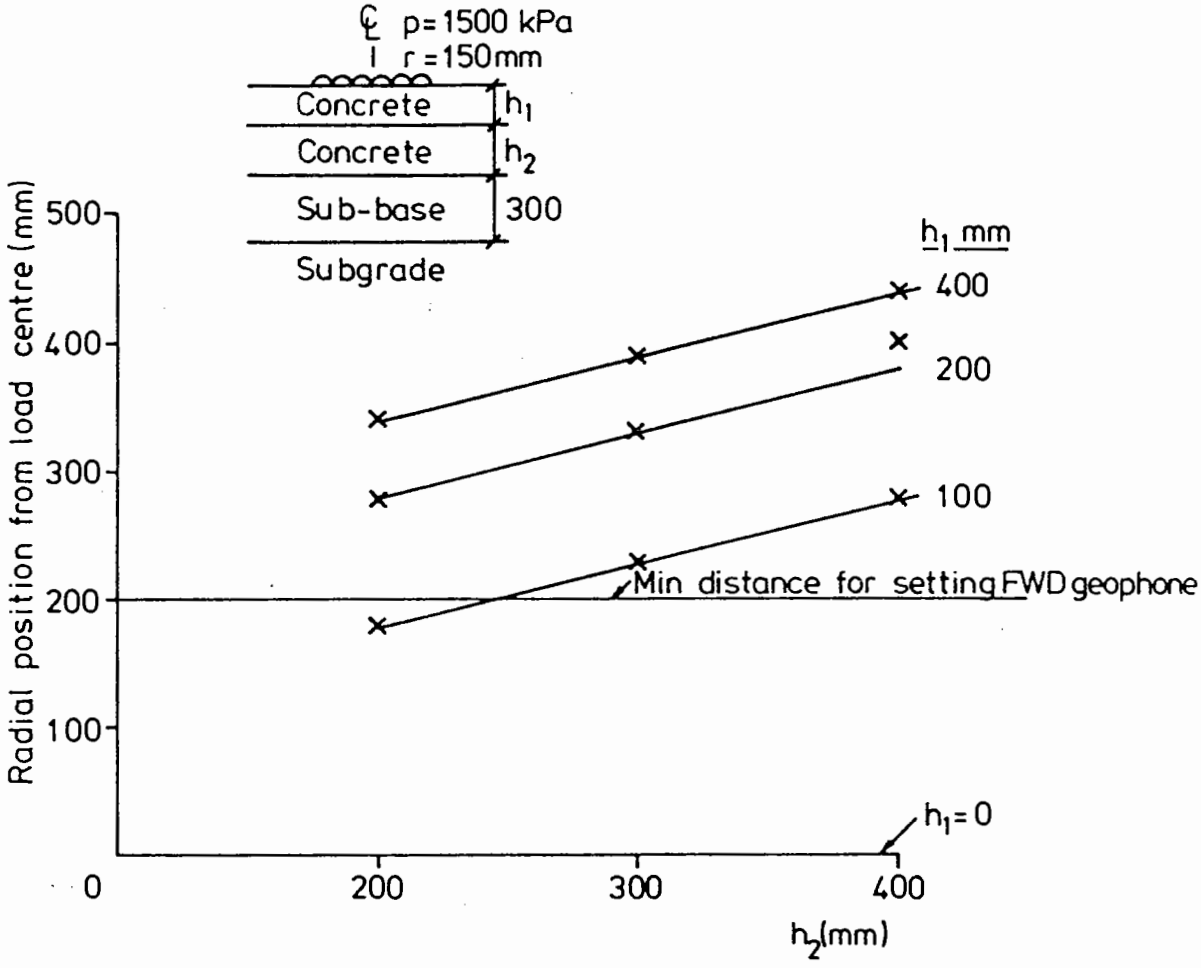

FIG. 3.34 RELATIONSHIP BETWEEN THE MOST SENSITIVE RADIAL POSITION FOR LAYER 2 AND LAYER THICKNESSES (CONCRETE PAVEMENTS)

Group	Structure	Central Deflection (μm) (1)	I I=1.0		Ratio=(2)/(1)	I I=0.9		Ratio=(3)/(1)
			Deflection (μm) (2)	Position (m)		Deflection (μm) (3)	Position (m)	
E	1	479.88	249.29	2.1	0.52	346.00	1.2	0.72
	2	536.21	275.93	1.9	0.51	381.80	1.1	0.71
	3	549.47	298.80	1.7	0.54	398.88	1.0	0.73
	4	497.10	204.63	2.7	0.41	266.64	2.0	0.54
	5	745.99	488.81	1.9	0.66	636.73	0.9	0.85
F	6	364.24	215.67	3.0	0.59	260.63	1.6	0.72
	7	415.12	203.60	2.6	0.49	294.33	1.4	0.71
	8	412.35	222.85	2.3	0.54	312.41	1.2	0.76
	9	373.78	186.27	3.0	0.50	233.57	2.1	0.62
	10	567.10	341.07	2.3	0.60	498.33	1.0	0.88
G	11	301.27	219.38	1.8	0.73	237.69	1.4	0.79
	12	332.20	177.52	3.0	0.53	231.58	1.8	0.70
	13	351.24	218.76	2.1	0.62	247.57	1.6	0.70
	14	307.44	175.86	3.0	0.57	205.70	2.2	0.67
	15	466.80	323.07	2.7	0.69	412.47	1.1	0.88
H	16	468.76	227.93	2.3	0.49	304.32	1.5	0.65
	17	522.39	249.68	2.1	0.48	330.71	1.4	0.63
	18	533.72	258.07	2.0	0.48	343.47	1.3	0.64
	19	503.79	192.87	3.0	0.38	250.99	2.2	0.50
	20	712.13	470.04	1.9	0.66	579.65	1.1	0.81
				Average	0.55		Average	0.71

I I denotes Influence Index

Table 3.10 Deflection Ratios for different Influence Indices of the Subbase layer (Concrete Pavements)

Layer	Type	Recommended 'best' radial position for layer
(A)	Asphalt pavement structures (4-layer)	
1	Bituminous	d_1
2	Bituminous	use Fig. 3.33
3	Sub-base	d_i/d_1 = 0.8
4	Subgrade	(i) Intermediate geophone at 0.6m from the specified geophone for sub-base (ii) furthest geophone at 1.2m from the specified geophone for sub-base
(B)	Concrete pavement structures (4-layer)	
1	Concrete	d_1
2	Concrete	use Fig. 3.34
3	Sub-base	d_i/d_1 = 0.75
4	Subgrade	(i) 1.8m for intermediate geophone (ii) 2.4m for furthest geophone

d_1 = central deflection
d_i = deflection within a deflection bowl

Note: Two other geophones should be set at any intermediate position so as to form a balanced deflection bowl shape

Table 3.11 Summary of recommended 'best' radial position for each layer of four-layered bituminous and concrete pavements

In order to capture the response due to subgrade behaviour, without the influence of the stiff concrete layers, the furthest geophone should always be placed at the maximum reach of the FWD sub-frame, i.e. 2.4 m. Another geophone is then placed at 1.8 m distance in order to model the non-linear behaviour of the subgrade. Table 3.11(B) summarises the main steps in selecting the geophone positions for a FWD survey of concrete pavements.

3.12 CONCLUSIONS

The relative sensitivity of surface deflection to the parameters of each layer of three-, four- and five-layered structures has been discussed, the magnitude of deflections being calculated by the linear, elastic, multi-layered program BISTRO. So far the analyses have concluded that:

(1) A comparison between two linear elastic multi-layered computer programs BISTRO and CHEVRON has established that the CHEVRON program produces unrealistic deflections around the loading area and hence the BISTRO program has been selected as an analytical tool for carrying out structural evaluation.

(2) The effect of varying the elastic stiffness of the pavement layers modifies the shape of the deflection bowl (from steep gradient to shallow gradient, for instance), while subgrade stiffness variation influences the whole deflection bowl.

(3) The thickness of the roadbase layer, especially if it is lean concrete or bituminous, should be accurately known to avoid serious errors in estimating the elastic stiffness of that layer. On the other hand, accurate thickness of sub-base layer is not required, since it does not influence the deflections significantly.

(4) Analysis of the relationship between layer stiffness and local slope of the deflection bowl indicated that the deflection bowl is influenced progressively from its extremity to the centre by the subgrade through to the total pavement structure.

(5) With the use of influence indices (II), the "best" radial position corresponding to each pavement layer has been identified for both bituminous and concrete structures. These radial positions are found to be sensitive to variation of both stiffness and thickness of the pavement layers. The study results in the proposal of a rational procedure for determining the position of the FWD geophones in a logical manner. The recommended procedure has been summarised in Table 3.11 to assist with site surveys of bituminous and concrete pavements respectively using the FWD.

CHAPTER 4

THE DEVELOPMENT OF AN ANALYTICAL METHOD FOR PAVEMENT EVALUATION

4.1 INTRODUCTION

The structural evaluation of a pavement is, to some extent, an inverted design process. In the design process (forward analysis), if the cross-section and properties of the pavement materials and subgrade are known, it is possible to compute the pavement responses, e.g. stresses, strains and displacements for given loading conditions. In the evaluation process (back-analysis), the response of the pavement is observed and the material properties are derived. In recent years, large number of research have been devoted to the rehabilitation of flexible pavements. These efforts are clearly evident in both the fourth, fifth and sixth International Conferences on the Structural Design of Asphalt Pavements. Most of the methods reported in the literature utilise the measured deflections to evaluate on existing pavement but a few of them rely on the conventional method of characterising the material properties termed as the "component analysis method" as summarised in Finn and Monismith (64). There are two main categories of evaluation method, namely, analytical methods and empirical methods. It is pointed out that the present method of pavement evaluation and overlay design in the United Kingdom, based on LR833 (3), takes an empirical approach. This Chapter firstly reviews the methods which are available for evaluating existing pavements. This is followed by a detailed description of the development of an analytical pavement evaluation method during the course of this research. The analytical method will then be validated in practical situations. In particular, a comparison is made between the analytical procedure and a dynamic

analysis program, in order to assess its accuracy of prediction in back-analysing deflections measured under the FWD dynamic loading.

4.2 A REVIEW OF EXISTING METHODS OF PAVEMENT EVALUATION

4.2.1 Analytical methods

Analytical methods are those which utilise a measured deflection bowl to back-calculate the structural properties (e.g. E and h) of the finite pavement layers and the subgrade. Table 4.1 shows some typical methods widely used for pavement evaluation at present. Observations on these analytical methods are noted as follows:

(1) The devices used are those which can measure several deflections, e.g. FWD, RR and Dynaflect.

(2) The methods use at least two deflection values in their analysis.

(3) Most of the methods use a linear elastic multi-layered model e.g. BISTRO, BISAR or CHEVRON computer program but Hoffman and Thompson (11) use ILLI-PAVE finite element program. Ullidtz (19) proposes a simplified method which is based on the Method of Equivalent Thicknesses and Boussinesq equations.

(4) Some attempts have been made by researchers (11,19,65) to incorporate non-linear subgrade stiffnesses into the analysis. But, it is not clear whether the non-linear stiffnesses are directly back-calculated, or whether matching has been carried out assuming a linear subgrade stiffness which is then corrected based on non-linear laboratory relationships.

(5) Two basic methods of analysis have been widely used, namely, computer iteration and charts or nomographs.

(6) Normally, the stiffnesses of the upper pavement layers and the subgrade are derived from a back-analysis procedure (11,19,53,57,65,66,67,68,69). A few other researchers back-analyse the effective thickness of the bituminous layer instead

Table 4.1 Summary of Analytical and Empirical Methods of Pavement Evaluation

Reference	NDT Device	Input Data	Method of Analysis	Derived Pavement Properties	Remarks
(A) ANALYTICAL METHODS					
Claessen et al (20)	Falling Weight Deflectometer	Max. deflection and deflection ratio; ν	Charts produced by three-layered linear elastic BISAR program.	E_1, E_3, $(h_1)_{eff}$ or h_2	$E_2 = 0.206\ h_2^{0.45} E_3$ used in developing charts where E_1, E_2, E_3 are layer moduli, $(h_1)_{eff}$, h_2 are layer thicknesses.
Ullidtz (19)	Falling Weight Deflectometer	Deflection ratios and h_1, ν	Charts produced by method of equivalent thicknesses and Boussinesq equations for two-layer structures. Computer solution for three-layer structures.	E_1 and E_2	Subgrade nonlinearity used is $E_2 = c(\sigma_1/\sigma')^n$ where E_2 is subgrade modulus, σ_1 is major principal stress and σ' is reference stress, c,n are constants.
Koole (21)	Falling Weight	Deflection ratios E_1, h_2 and ν	Charts produced by BISAR program for three-layer structures.	E_3 and $(h_1)_{eff}$	$E_2 = 0.2\ h_2^{0.45} E_3$ used in developing charts.
Hoffman & Thompson (11)	Falling Weight Deflectometer Road Rater	Deflection bowl	Nomographs produced by finite-element program ILLI-PAVE, for two and three-layer structures.	E_1, E_2, E_3	Use of max. deflection and deflection basin "area" in nomographs. Stress-dependent subgrade modulus has been incorporated in ILLI-PAVE program.

/contd

Table 4.1 contd

Reference	NDT Device	Input Data	Method of Analysis	Derived Pavement Properties	Remarks
Vaswani (66)	Dynaflect or Benkelman Beam	Five deflections	Nomographs derived from linear elastic method.	E of asphalt E of subgrade.	
Treybig et al (71)	Dynaflect	E, h of pavement layers; deflection bowl.	Nomographs derived from linear elastic layered method.	E of subgrade	E of pavement layers should be measured in laboratory.
Sharpe et al (70)	Road Rater	E, h of pavement layers; deflection bowl	Charts produced by CHEVRON program for two and three-layered structures.	E of subgrade or "effective" thicknesses of pavement structure.	Effective thickness is the derived layer thickness of a deteriorated pavement for constant layer moduli.
Kilareski & Anani (57)	Road Rater	E, h, ν of pavement layers; deflection bowl.	Computer program based on linear elastic layered theory.	E of pavement layers and subgrade.	Initial values of E are assumed.
Hoyinck et al (67)	Deflectograph	h,ν of pavement layers; three deflections in the deflection bowl.	Computer program based on Hogg model with infinite subgrade for two and three-layered structures.	E of pavement layers and subgrade.	Three-layered structure is converted to two-layered by using Odemark's equivalent layer thickness method.
Van der Loo (68)	Falling Weight Deflectometer	Three deflections of deflection bowl.	Charts derived from CHEVRON program and empirical equation.	E of subgrade and residual life of pavement.	

/contd

Table 4.1 contd

Reference	NDT Device	Input Data	Method of Analysis	Derived Pavement Properties	Remarks
Majidzadeh et al (69)	Dynaflect	E, h, ν of pavement layers; deflection bowl.	Computer program based on linear elastic layered theory for four-layered structures.	E of pavement layers and subgrade.	Initial values of E are assumed.
McCullough & Taute (53)	Dynaflect	E, h of pavement layers; deflection bowl.	Linear elastic layered computer program or curve fitting.	E of pavement layers and subgrade.	Initial values of E of bound layers determined from indirect tensile test and also E of unbound layers and subgrade from laboratory
Sharma & Studstad (65)	Falling Weight Deflectometer Dynaflect	E, h, ν of pavement layers; deflection bowl.	Computer program ISSEM4 based on method of equivalent thicknesses and Boussinesq equations	E of pavement layers and subgrade.	Program ISSEM4 takes into account stress-dependency of base, sub-base and subgrade layers of a four-layered structure.
(B) EMPIRICAL METHODS					
Kennedy et al (3)	Deflectograph Benkelman Beam	Max. deflection	Charts		Deflections adjusted for temperature.
Asphalt Institute (8)	Benkelman Beam	Rebound deflection	Charts		Deflections adjusted for temperature and critical season.

(20,21,70), by fixing the stiffness (E_1) of the bituminous material during the iteration process. The value of E_1 would have been determined in the laboratory.

4.2.2 Empirical methods

The empirical methods of pavement evaluation are also summarised in Table 4.1. These methods are essentially based on observations of variations of maximum surface deflection. Measured deflections are generally adjusted to a design temperature, e.g., in the TRRL method, design temperature is fixed at 20°C. The most pronounced difference between the analytical method and the empirical method is that the latter only requires one deflection - maximum deflection. However, the fundamental difference between the two methods is that of versatility. Empirical methods, which have been developed from observed performance of the pavements, have a limited range of application, in terms of types of pavement materials and environmental (e.g. temperature and seasonal variation) conditions. Analytical methods, on the other hand, are more versatile, since their use permits effective consideration of a range of different materials and treatments, variation of traffic as well as environmental conditions in a "sound" manner.

4.3 FORMULATION OF NON-LINEARITY OF SUBGRADE

In Chapter 3, the dominant effect of the subgrade on the deflection bowl was demonstrated. This influence can be explained by the vertical strain variation through a typical pavement structure in Figure 4.1. Since surface deflection is the integration of vertical strain with depth, the area under the curve (shaded) in Figure 4.1 gives the central deflection. The relatively large contribution of the subgrade is clearly observed. Moreover, Hoffman and Thompson (11) used a finite element program (ILLI-PAVE) to calculate the deflections of a three-layer, non-linear, elastic structure

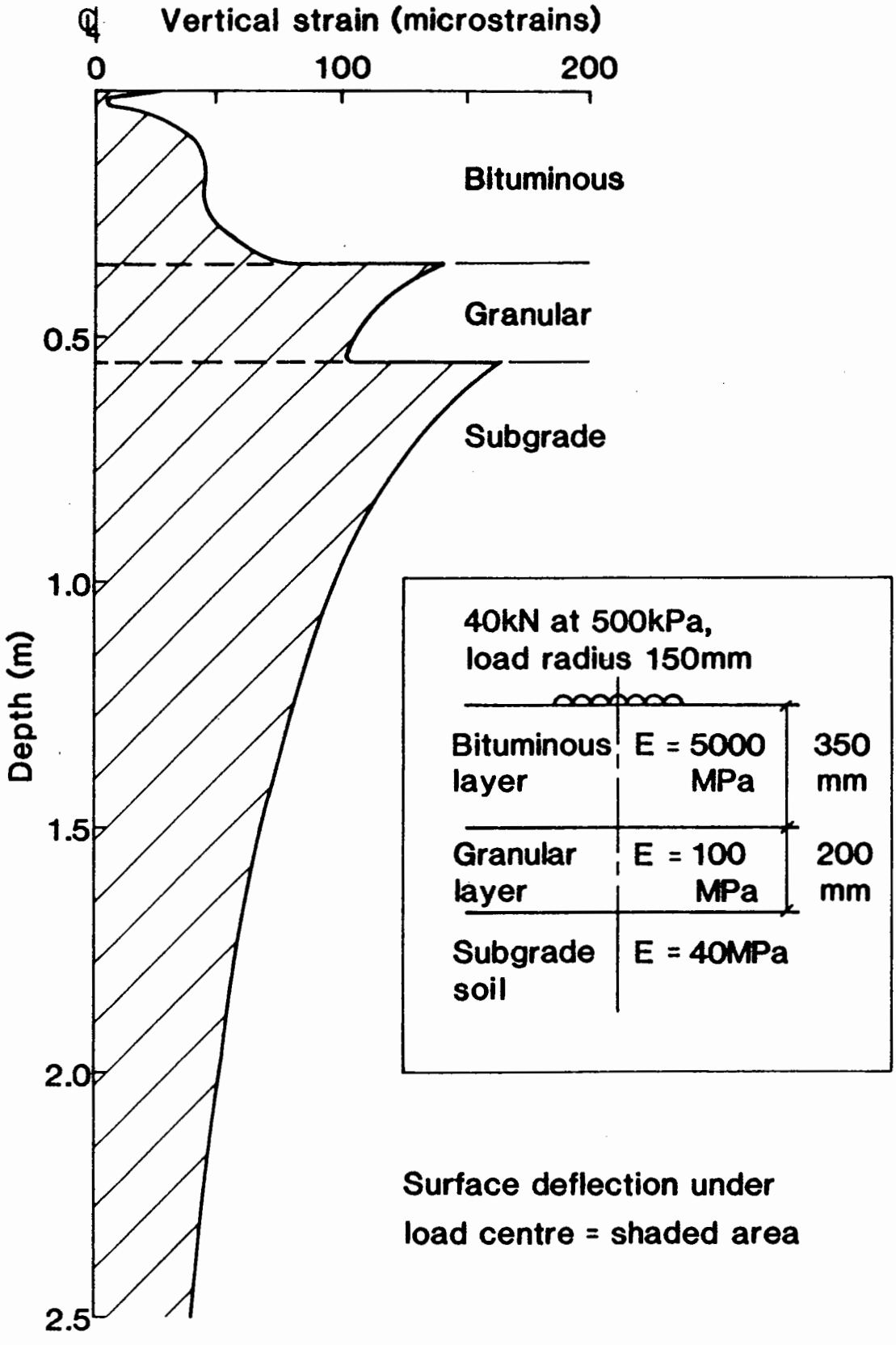

FIG. 4.1 VERTICAL STRAIN VARIATION WITH DEPTH IN A TYPICAL STRUCTURE

consisting of bituminous surfacing, granular sub-base and subgrade. They found that the deflection due to the subgrade layer was 79% of the total value. From the above results, it is very important to assess the subgrade elastic stiffness accurately in pavement evaluation. One of the approaches is to consider the non-linear stress-dependent behaviour of the subgrade rather than the current CBR approach, which is widely adopted in pavement design, in which the elastic stiffness is equal to 10 times the in-situ CBR, developed by Heukelom and Klomp (72).

Over the past thirty years, it has been found that subgrade soil tested under repeated loading in the laboratory exhibits non-linear behaviour, in which the resilient modulus (equivalent to elastic stiffness) of the soil is inversely proportional to the magnitude of the applied deviatoric stress (38,40). The following relationship is generally used in the United States, viz.,

$$E_r = k1(\sigma_d)^{k2} \qquad (4.1)$$

where E_r is the resilient modulus of the subgrade soil;

σ_d is the deviatoric stress $(\sigma_1 - \sigma_3)$

k1 and k2 are constant depending on material type and physical soil properties and k2 is negative.

From equation (4.1), it is observed that since the deviatoric stress varies with depth in the subgrade, the resilient modulus must also change with depth. The magnitude of change is strongly influenced by the magnitude of the k2 value. It is this parameter that indicates the degree of non-linearity of a subgrade soil. Ullidtz (19) also incorporates the facility to take into account non-linear behaviour when calculating the elastic stiffness of the subgrade using,

$$E = C\left(\frac{\sigma_1}{\sigma'}\right)^n \qquad (4.2)$$

where E is the elastic stiffness;

σ_1 is the major principal stress;

σ' is a reference stress (generally 1 MPa);

C and n are constants.

In the United Kingdom, Grainger and Lister (73) were amongst the first to incorporate the results of repeated loading of soils in pavement design. At Nottingham, an extensive programme of repeated load triaxial testing of soil was initiated during the late sixties and early seventies, notably the work of Lashine (41) on Keuper Marl (silty clay) and Parr (74) on London Clay. In 1975, Brown et al (42) presented detailed results of repeated load triaxial testing of Keuper Marl which was reconstituted from a slurry over a wide range of over-consolidation ratio from 2 to 20. The tests were carried out under undrained conditions with a cyclic deviatoric stress at a frequency of 10 Hz. Pore water pressure was measured in each test. They concluded that the resilient modulus of the soil was a non-linear function of the ratio of cyclic deviatoric stress and initial effective confining stress, i.e.,

$$E_r = A\left(\frac{q_r}{\sigma_3}\right)^B \qquad (4.3)$$

and

$$E_r = \left(\frac{q_r}{\varepsilon_{ar}}\right) \qquad (4.4)$$

where E_r is the resilient modulus of soil;

q_r is the cyclic deviatoric stress (= $(\sigma_1-\sigma_3)$; (4.5)

σ_3' is the initial effective confining stress;

ε_{ar} is the resilient axial strain due to q_r ;

A and B are material constants with A in units of MPa and B is negative and dimensionless.

The parameters A and B are termed as subgrade stiffness parameters. Brown (75) later generalised equation (4.3) by replacing σ_3' by p_o' which is defined as, in triaxial conditions,

$$p_o' = \frac{1}{3}(\sigma_1' + 2\sigma_3') \qquad (4.6)$$

where p_o' is the initial effective mean normal stress;

σ_1', σ_3' are initial effective major and minor principle stresses.

Equation (4.3) then becomes,

$$E_r = A\left(\frac{q_r}{p_o'}\right)^B \qquad (4.7)$$

or

$$E_r = A\left(\frac{p_o'}{q_r}\right)^B \qquad (4.8)$$

where the value of B in equation (4.8) is positive which, as with K2 in equation (4.1), determines the degree of non-linearity of the subgrade. Figure 4.2 illustrates the relationship between resilient modulus and the stress ratio (q_r/p_o') for various silty clay materials. The results for Keuper Marl were obtained over a range of over-consolidation ratios from 2 to 75, where the moisture

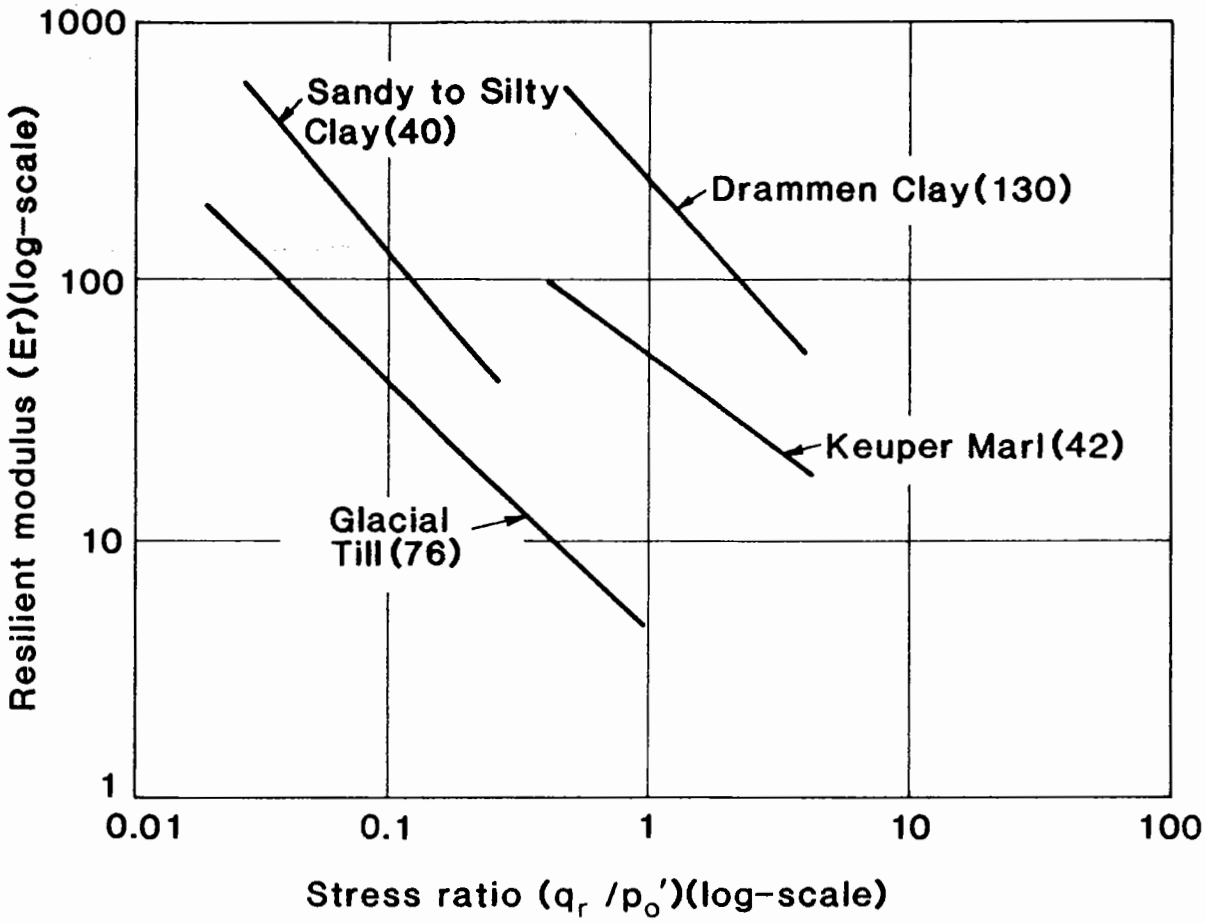

FIG. 4.2 RELATIONSHIP BETWEEN RESILIENT MODULUS AND STRESS RATIO FOR DIFFERENT SOIL TYPES (after Brown(75))

content varied between 16.5 to 23.5% and initial effective stresses between 33 to 220 kPa respectively. Repeated load tests by Dehlen (40) and Fredlund et al (76) were carried out over a range of soil suctions between 70 and 1400 kPa. The results generally demonstrate the linear relationship between the logarithms of resilient modulus and stress ratio (q_r/p_o') as proposed in equation (4.8) for modelling the non-linear behaviour of silty clays. Hence, this equation has been incorporated in the development of the analytical method which will be discussed in Section 4.4.

Further comprehensive repeated load triaxial tests on reconstituted saturated Keuper Marl were performed by Loach (77). Figure 4.3 shows results of resilient shear strain against applied repeated deviatoric stress and initial mean normal effective stress, where the stresses have been normalised by the equivalent pressure (defined in the inset of the figure). As can be seen, resilient shear strain contours radiating from the origin are obtained and the relationship can be represented by the following expression:

$$\varepsilon_{sr} = C\left(\frac{q_r}{p_o'}\right)^D \qquad (4.9)$$

where q_r is the repeated deviatoric stress;

p_o' is the initial mean normal effective stress;

ε_{sr} is the resilient shear strain;

C and D are material constants. For Keuper Marl, $C = 1.11 \times 10^{-3}$, and $D = 1.522$.

Now, since,

$$\varepsilon_{sr} = \frac{2}{3}(\varepsilon_{ar} - \varepsilon_{rr}) \qquad (4.10)$$

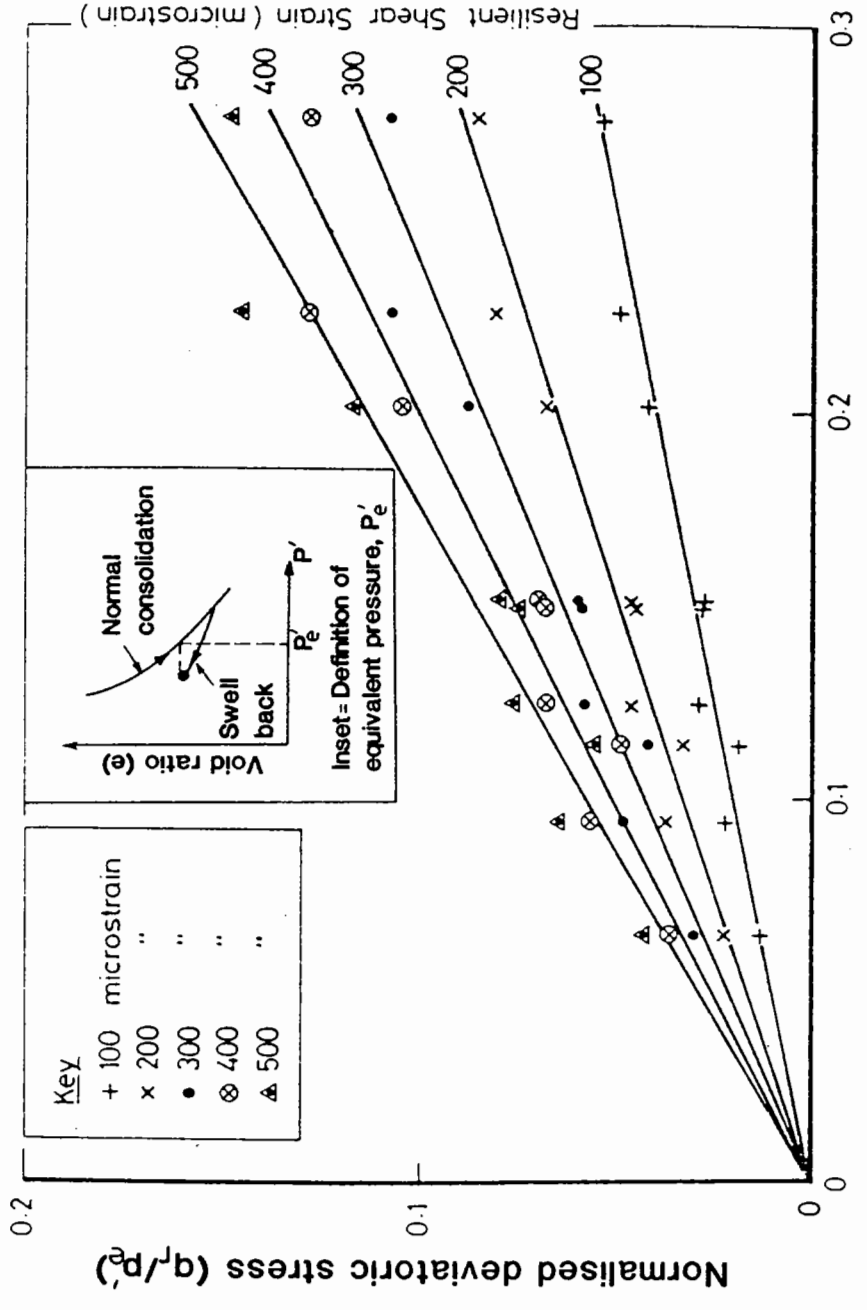

FIG. 4.3 RESILIENT SHEAR STRAIN CONTOURS FOR SATURATED KEUPER MARL (AFTER LOACH (77))

where ε_{ar} is the resilient axial strain;

ε_{rr} is the resilient radial strain.

Therefore, the resilient axial strain,

$$\varepsilon_{ar} = fn(\varepsilon_{rr}) \qquad (4.11)$$

By substituting equation (4.9) into (4.11),

$$\varepsilon_{ar} = E\left(\frac{q_r}{p_o'}\right)^F \qquad (4.12)$$

where E and F are new constants relating to C and D of equation (4.9)

From equation (4.4),

$$\varepsilon_{ar} = \left(\frac{q_r}{E_r}\right) \qquad (4.13)$$

Hence, equating equations (4.12) and (4.13) and rearranging,

$$\frac{E_r}{q_r} = E\left(\frac{p_o'}{q_r}\right)^F \qquad (4.14)$$

It can be seen that equation (4.14) has a similar form to equation (4.8) developed by Brown (75). For this reason, the analytical method, which will be described in later sections, still incorporates the previous model (equation (4.8)) for calculating non-linear subgrade stiffnesses. The new model, as described by equation (4.14), can be included in future, if required.

4.3.1 Modelling non-linear subgrade stiffnesses

Equation (4.8) can be used to model the non-linear subgrade behaviour, where the resilient modulus, E_r, is taken to be equivalent to the elastic stiffness of the subgrade layer; q_r is the deviatoric stress exerted by traffic load, and p_o' is the mean normal effective stress due to overburden above an element in the subgrade layer.

To apply equation (4.8), the value of p_o' is computed first. Assuming the soil is fully saturated, the pore pressure, u, of an element shown in Figure 4.4 is given by,

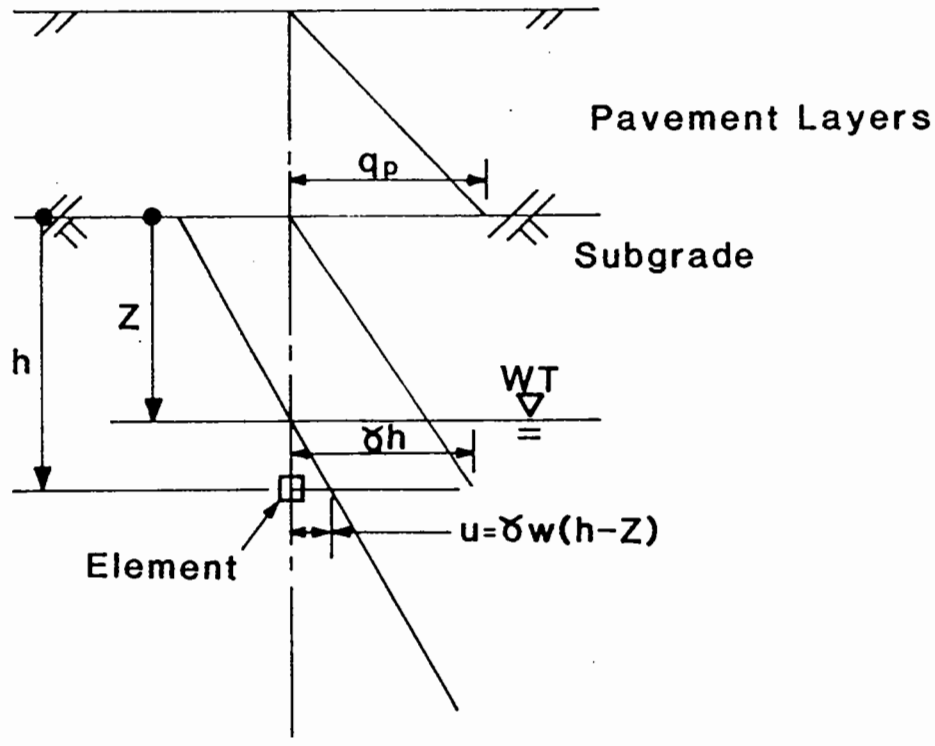

FIG 4.4 DEFINITION OF PARAMETERS FOR CALCULATION OF STRESSES IN SUBGRADE

$$u = \gamma_w (h-z) \qquad (4.15)$$

and total vertical stress, σ_z, is

$$\sigma_z = q_p + \gamma h \qquad (4.16)$$

$$q_p = \sum \gamma_i h_i \qquad (4.16a)$$

where h is the depth of the element from formation level;

z is the depth of the water table from formation level;

q_p is the overburden stress due to the pavement structure above formation level;

γ, γ_w are the total unit weights of soil and water.

γ_i, h_i are the total unit weight and thickness of the pavement layer i above the subgrade

$$\therefore \text{ effective vertical stress, } \sigma_z' = \sigma_z - u \qquad (4.17)$$

i.e. $$\sigma_z' = q_p + \gamma h - \gamma_w(h-z)$$

$$= q_p + \gamma_w z + (\gamma - \gamma_w)h \qquad (4.18)$$

and also,

$$\text{effective horizontal stress, } \sigma_h' = K_o\sigma_z' \qquad (4.19)$$

where K_o is the coefficient of earth pressure at rest.

Now, equation (4.5) can be rewritten as,

$$p_o' = \frac{1}{3} (\sigma_z' + 2\sigma_h') \qquad (4.20)$$

Substituting equation (4.19) for σ_h', we have,

$$p_o' = \frac{1}{3} (\sigma_z' + 2K_o\sigma_z') = \frac{1}{3} \sigma_z'(1 + 2K_o) \qquad (4.21)$$

The present program assumes K_o to be ,

$$K_o = \nu/(1 - \nu) \qquad (4.22)$$

where ν is the Poisson's ratio of the subgrade;

However, the program can be adapted to have a different K_o value, if required.

To calculate the non-linear elastic subgrade stiffnesses in a linear, elastic multi-layered computer program, e.g. BISTRO, the following steps are required:

(a) Sub-divide the uniform subgrade layer into 5 sub-layers as shown in Figure 4.5, where the thicknesses are 0.6, 1.0, 1.0, 2.0 m for sub-layers 1 to 4 respectively and semi-infinite for sub-layer 5. The layer thicknesses are chosen in such a way as to provide a gradual distribution of elastic stiffness with depth.

(b) Stresses at the mid-point of sub-layers 1 to 4 are then computed. The initial effective mean normal stress (p_o') at the mid-point of each sub-layer can easily be computed by following equations (4.15) to (4.22), knowing the geometry, properties of each pavement layer above the subgrade and the position of the water table. Then, BISTRO is used to calculate the major and minor principal stresses (σ_1 and σ_3) at the mid-point position of each sub-layer under the applied load. This gives the magnitude of the deviatoric stress (q_r) using equation (4.5). As for sub-layer 5, the stresses (p_{os}' and q_s) are computed at an arbitrary depth 2 m below the base of sub-layer 4, using the same procedure as already mentioned above.

(c) With assumed initial values of stiffness parameters A and B, the non-linear elastic stiffnesses in the subgrade, vertically distributed with depth, are thus obtained by substituting the stresses which have already been evaluated in step (b) into equation (4.8).

Figure 4.6 summarises the procedure of calculating the non-linear subgrade stiffnesses.

4.3.2 Effect of varying subgrade stiffness parameters

The effect of varying subgrade stiffness parameters A and B on the resultant deflection bowl was investigated. A three-layered

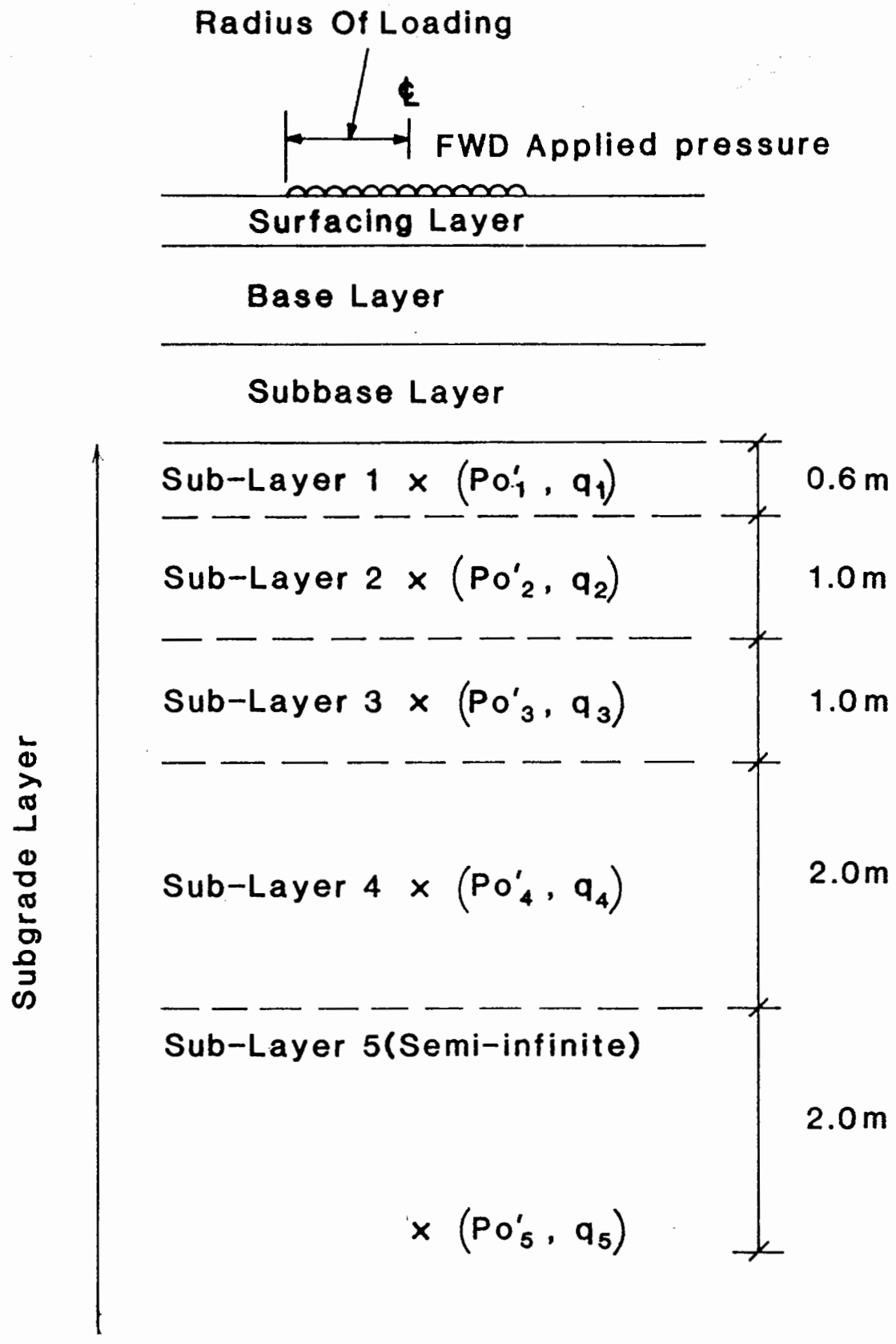

FIG 4.5 SUB-DIVISION OF SUBGRADE LAYER FOR CALCULATION OF NON LINEAR SUBGRADE MODULI

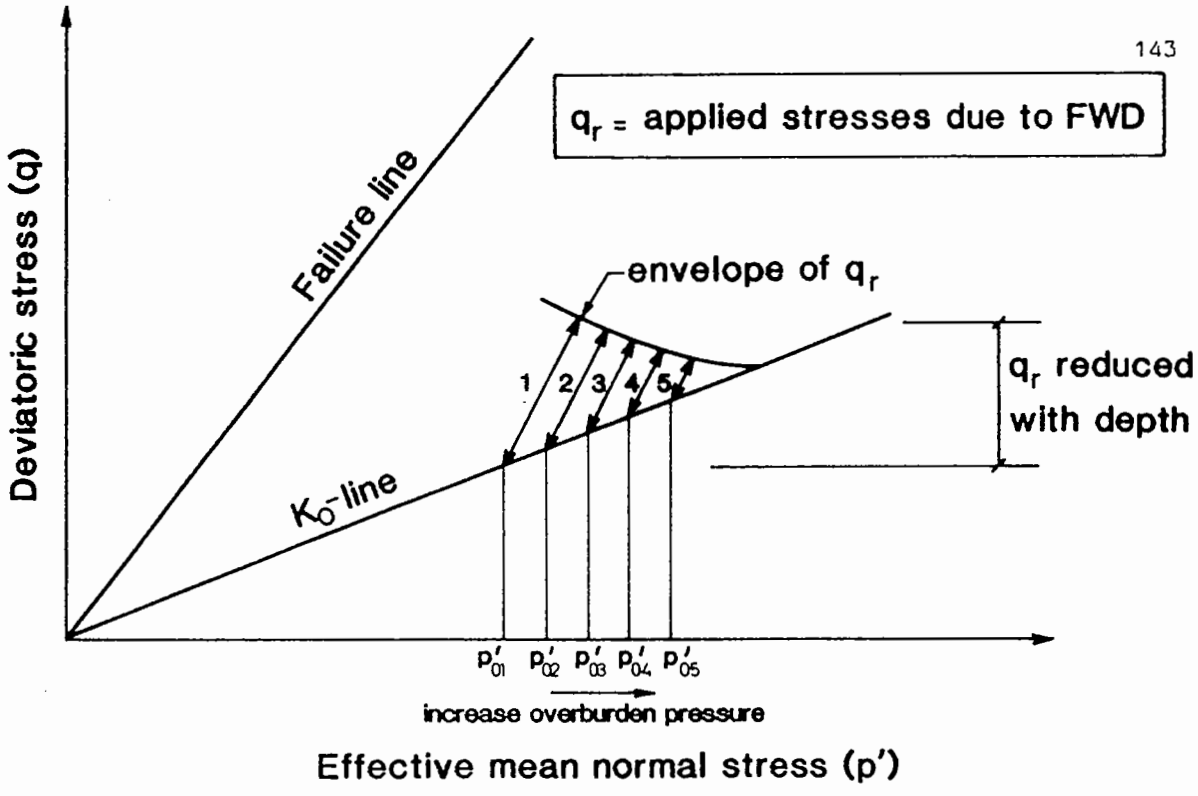

(a) Calculate Subgrade stresses with Depth

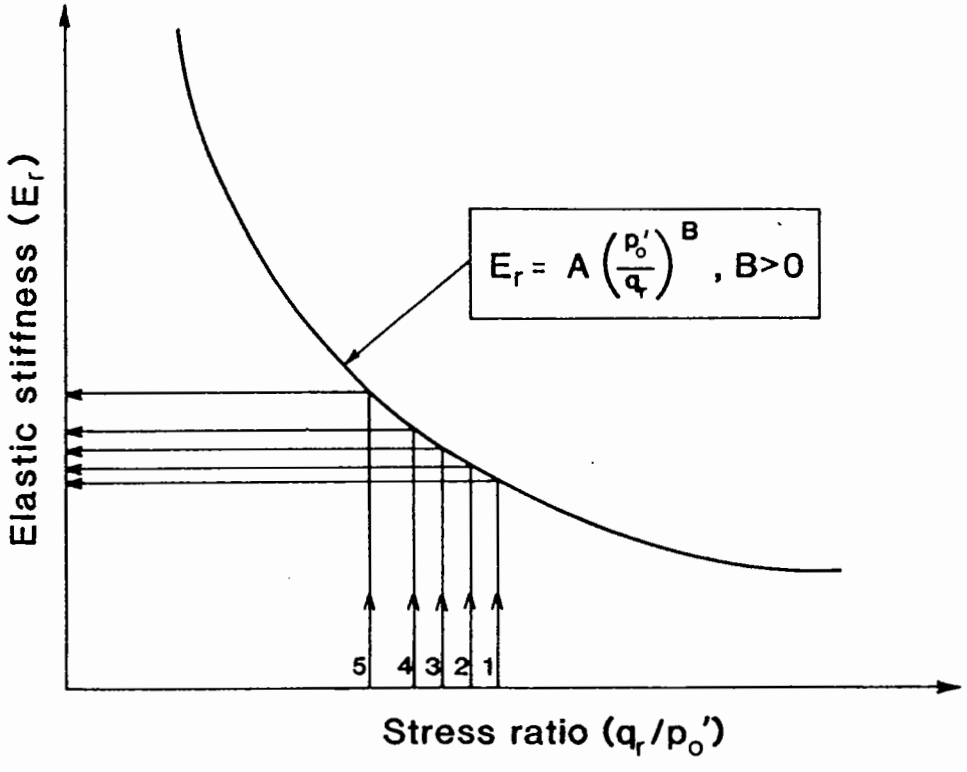

(b) Calculate Non-linear Subgrade Elastic Stiffnesses

FIG. 4.6 GENERAL PROCEDURE FOR CALCULATING NON-LINEAR SUBGRADE STIFFNESSES WITH DEPTH

structure was used, with stiffnesses of 5000 MPa and 100 MPa and thicknesses of 250 and 300 mm for the bituminous and granular sub-base layers respectively. The initial stiffness of the subgrade was taken to be 100 MPa and uniform with depth. The Poisson's ratios were 0.4, 0.3, and 0.4 respectively. The water table was assumed to be at formation level. A contact pressure of 700 kPa was applied uniformly over a 300 mm diameter loading plate, thus simulating the FWD loading condition. A series of calculations by varying the parameters A and B was performed using a simplified version of the PADAL computer program (refer Section 4.4.3 for detailed development of the program). Non-linear subgrade elastic stiffnesses were computed following the procedure proposed in Section 4.3.1. Figure 4.7 summarises the results of the calculations. As can be seen in the figure, variation of either parameter A or B affects the magnitude of the whole deflection bowl. Thus, an increase in the value of B (from 0 to 0.5 in Figure 4.7(a)) reduces all the seven deflections and brings the whole deflection bowl upward. A similar effect is observed when parameter A varies between 50 and 200 MPa (Figure 4.7(b)). The above results therefore match those based on a single subgrade stiffness in Chapter 3 (refer Figure 3.8).

However, the effect of varying parameter A is different from that for parameter B. In Figure 4.7(a), a deflection bowl calculated with A=100 MPa and B=0.2 is also included for comparison. It is noted that while this deflection bowl has a similar deflection value at the furthest radial distance (i.e. at 1.8 m) as another deflection bowl, computed with A=50 MPa and B=0.5, the slope of the former bowl is flatter. A similar observation can also be made from in Figure 4.7(b). This phenomenon is the result of different distribution of subgrade stiffness with depth, as shown in Table 4.2. The deflection bowl produced by A=100 MPa and B=0.2 has a higher stiffness value in

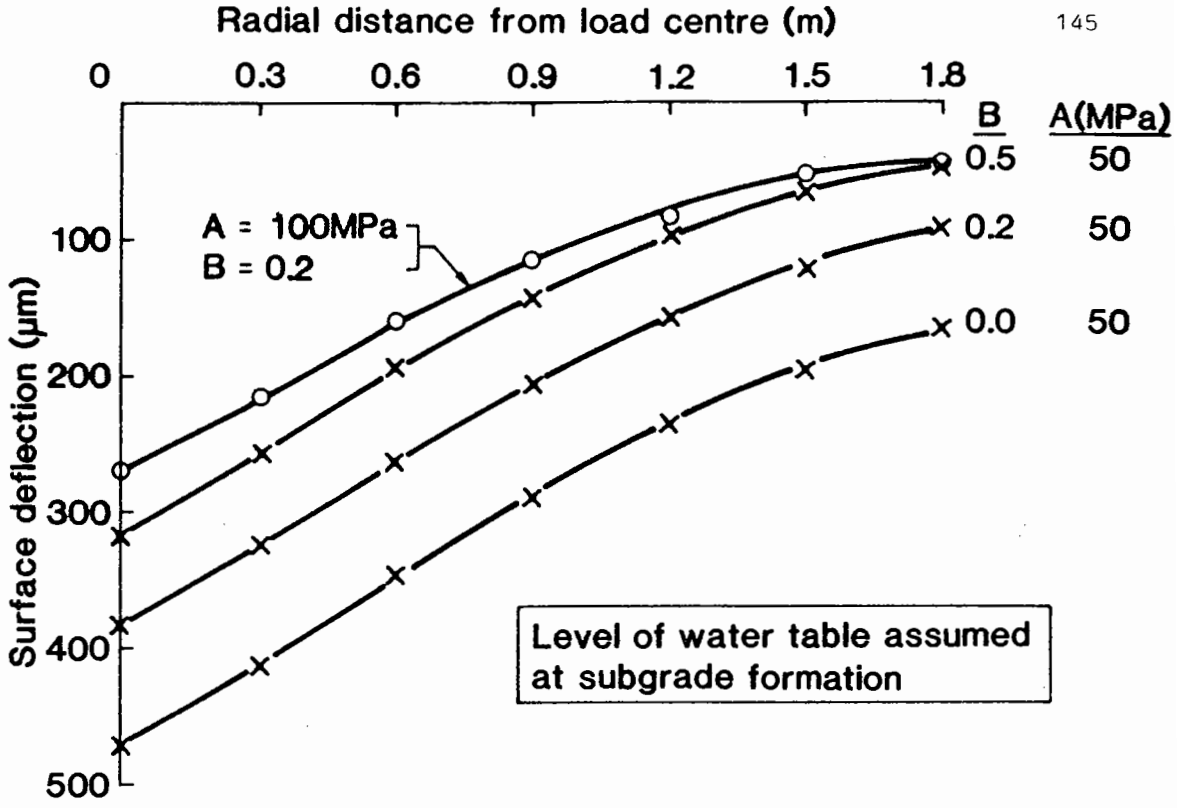

(a) Stiffness Parameter 'B' varies

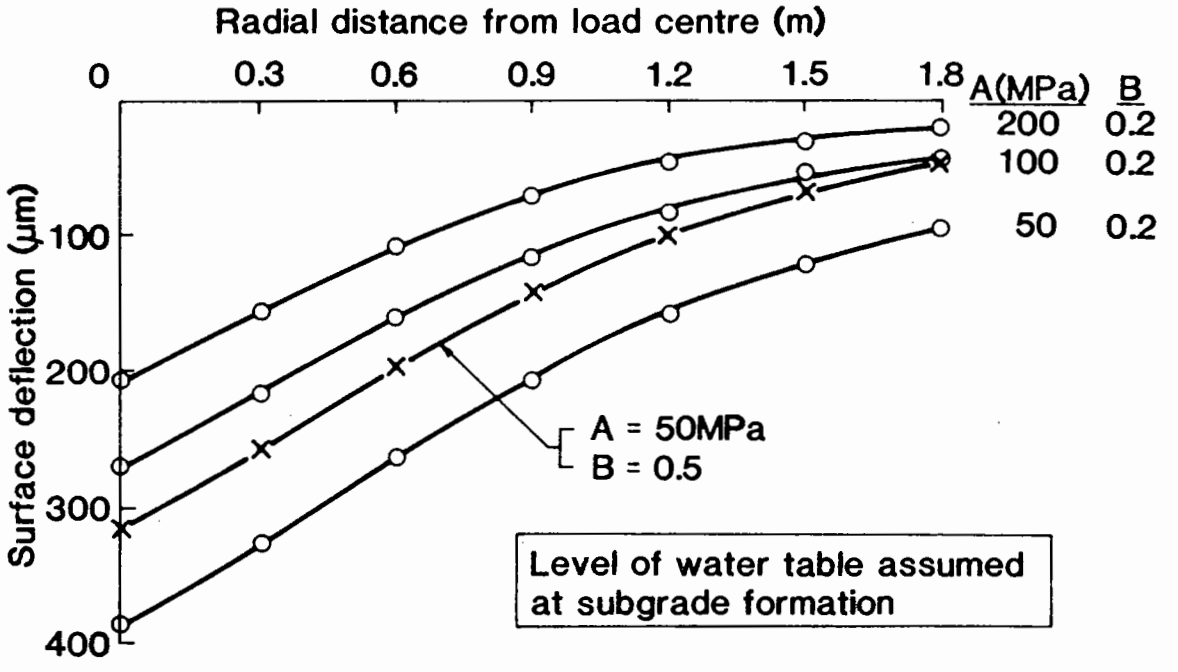

(b) Stiffness Parameter 'A' varies

FIG. 4.7 EFFECT OF VARIATION OF SUBGRADE STIFFNESS PARAMETERS ON SURFACE DEFLECTION

No.	Water table below formation (m)	Parameters		Stiffnesses in sub-layers				
		A (MPa)	B	1	2	3 (MPa)	4	5
1	0.0	50	0.0	50	50	50	50	50
2	0.0	50	0.2	50	63	79	99	134
3	0.0	50	0.5	50	90	155	276	592
4	0.0	100	0.2	105	132	162	202	271
5	0.0	200	0.2	200	253	314	396	538
6	0.0	100	0.5	100	181	310	553	1185
7	0.0	200	0.5	199	362	619	1106	2369

Table 4.2 Effect of varying parameters A and B on calculated subgrade stiffnesses with depth

sub-layer 1 than that by A=50 MPa and B=0.5 but the increase of stiffness with depth is much less rapid than for the latter. Therefore, it can be concluded that the variation of both parameters A and B affects the whole deflection bowl, but that the effect of varying the parameter B also influences the slope of the bowl.

4.3.3 Effect of varying the position of the water table

The effect of varying the position of the water table was also briefly studied. Figure 4.8 shows how the variation of subgrade stiffness with depth changes for different water table positions, as calculated by the PADAL program. Varying the water table from subgrade formation level to 5 m below formation has the effect of increasing the overall magnitude of subgrade stiffnesses. And, this increase in stiffness thus results in reduction of deflection, as shown in Figure 4.9. Another deflection bowl was calculated with stiffness parameter A=100 MPa, and the water table at formation level. In the figure, this deflection bowl matches the one computed with A=50 MPa and water table at 5 m depth very well indeed. Therefore, this comparison illustrates that varying the position of the water table influences the magnitude of non-linear subgrade stiffnesses and deflections. Its influence has been found to have an identical effect to that of varying the stiffness parameter A which has already been discussed in the previous section.

4.4 DEVELOPMENT OF ANALYTICAL METHODS

Three computer programs have been developed during the course of the research to back-analyse both bituminous and concrete pavements. They are,

(a) The computer program BASEM (Back Analysis of Stress-dependent Elastic Moduli) for bituminous pavements;

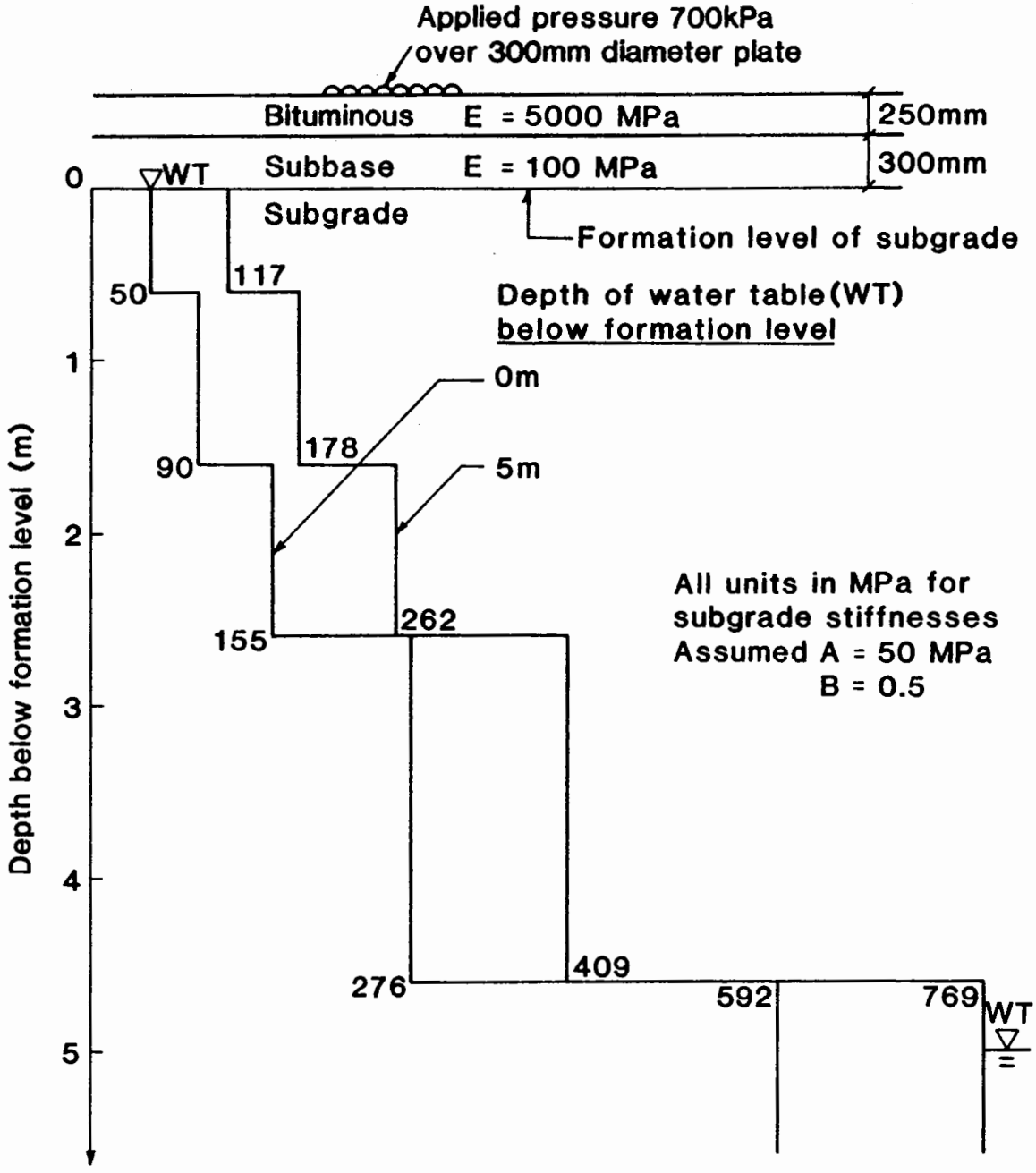

FIG. 4.8 EFFECT OF VARIATION OF LEVEL OF WATER TABLE ON THE DISTRIBUTION OF SUBGRADE STIFFNESSES WITH DEPTH

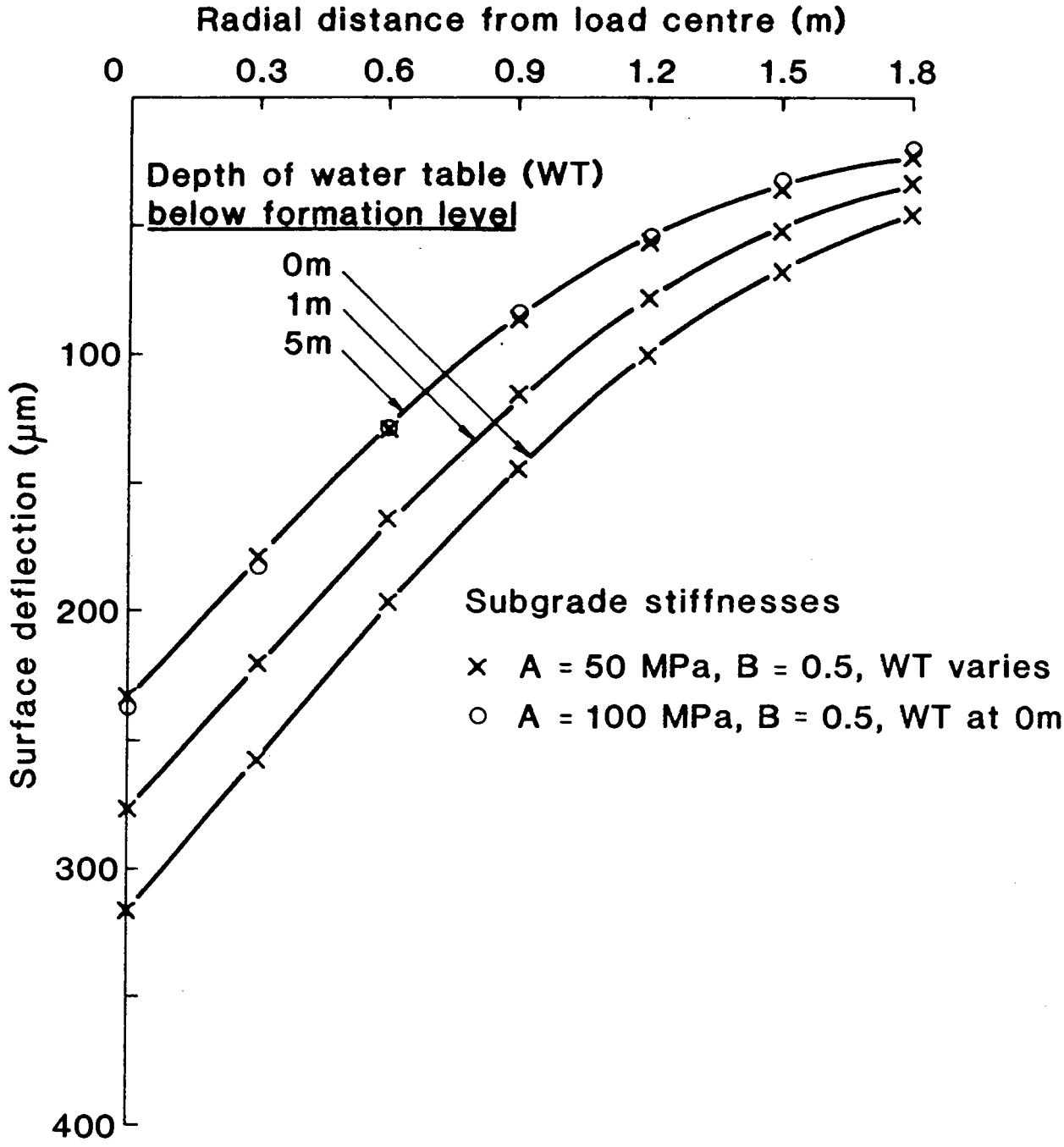

FIG. 4.9 EFFECT OF VARIATION OF WATER TABLE ON SURFACE DEFLECTION

(b) The computer program BASEMC (Back Analysis of Stress-dependent Elastic Moduli for Concrete) for concrete pavements;

(c) The computer program PADAL (PAvement Deflection AnaLysis) for both bituminous and concrete pavements.

Both the computer programs BASEM and BASEMC were developed in the first half of the research project. They were then extensively applied to evaluate the in-situ condition of a wide range of bituminous and concrete structures. Satisfactory results of back-analysed stiffnesses were generally obtained. However, it was later found that the final results were very sensitive to the initial layer stiffness values, which the user assigned as input data at the start of the calculation. Further work was followed to rectify the above problem. This has led to the development of an improved back-analysis computer program, PADAL, which supersedes the BASEM and BASEMC programs.

The following sections first describe very briefly the methodology adopted in the BASEM and BASEMC programs. The formulation and development of the PADAL program will then be described in detail in later sections.

4.4.1 The computer program BASEM

The computer program BASEM incorporates the BISTRO computer program as a subroutine to carry out the calculation of stresses and surface deflections. The reasons for choosing BISTRO have already been explained in Section 3.3. It uses a procedure which utilises the inter-relationship between the surface deflection at a particular location of the deflection bowl and the stiffness of a particular pavement layer. This inter-relationship has been fully discussed in Chapter 3. In essence, the program first back-calculates the stiffness of the subgrade using the outer portion of the deflection bowl. The subgrade stiffness is the first to be derived, because it

was found in Chapter 3 that it has greatest influence on the whole deflection bowl when compared with other layers. This is carried out by matching the measured and calculated deflections, while adjusting the subgrade stiffnesses, until a criterion on deflection is satisfied. Using the same procedure, the stiffness of the sub-base layer is next to be computed using the derived subgrade stiffnesses. This same process is repeated for the layer above the sub-base, and so on, until, lastly, the stiffness of the surfacing layer has been computed using the derived stiffness of all other layers. The above procedure is mainly based on the one already incorporated into the DEMOD computer program developed by Brunton (63). A similar methodology has also been proposed by Kilareski and Anani (57) and Uddin et al (78). Figure 4.10 shows a simplified flow diagram of the BASEM program. Full details of the program have been documented in an earlier report (Tam (79)). The following summarises the salient features of the BASEM program.

Feature of BASEM: The BASEM program has incorporated into a linear elastic multi-layered analysis a realistic soil model, which calculates non-linear subgrade stiffnesses. Details of the formulation of the non-linear soil model have been described in Section 4.3. Furthermore, in order to reduce computing time, back-analysis of layer stiffnesses is carried out with the deflection at one specified radial position for each pavement layer above the subgrade and at two specified radial positions for the subgrade layer, i.e., the total number of deflections used for back-analysis is number of layers of the pavement structure of interest plus one. For example, for a three-layered structure, total number of deflections used for back-analysis is 4.

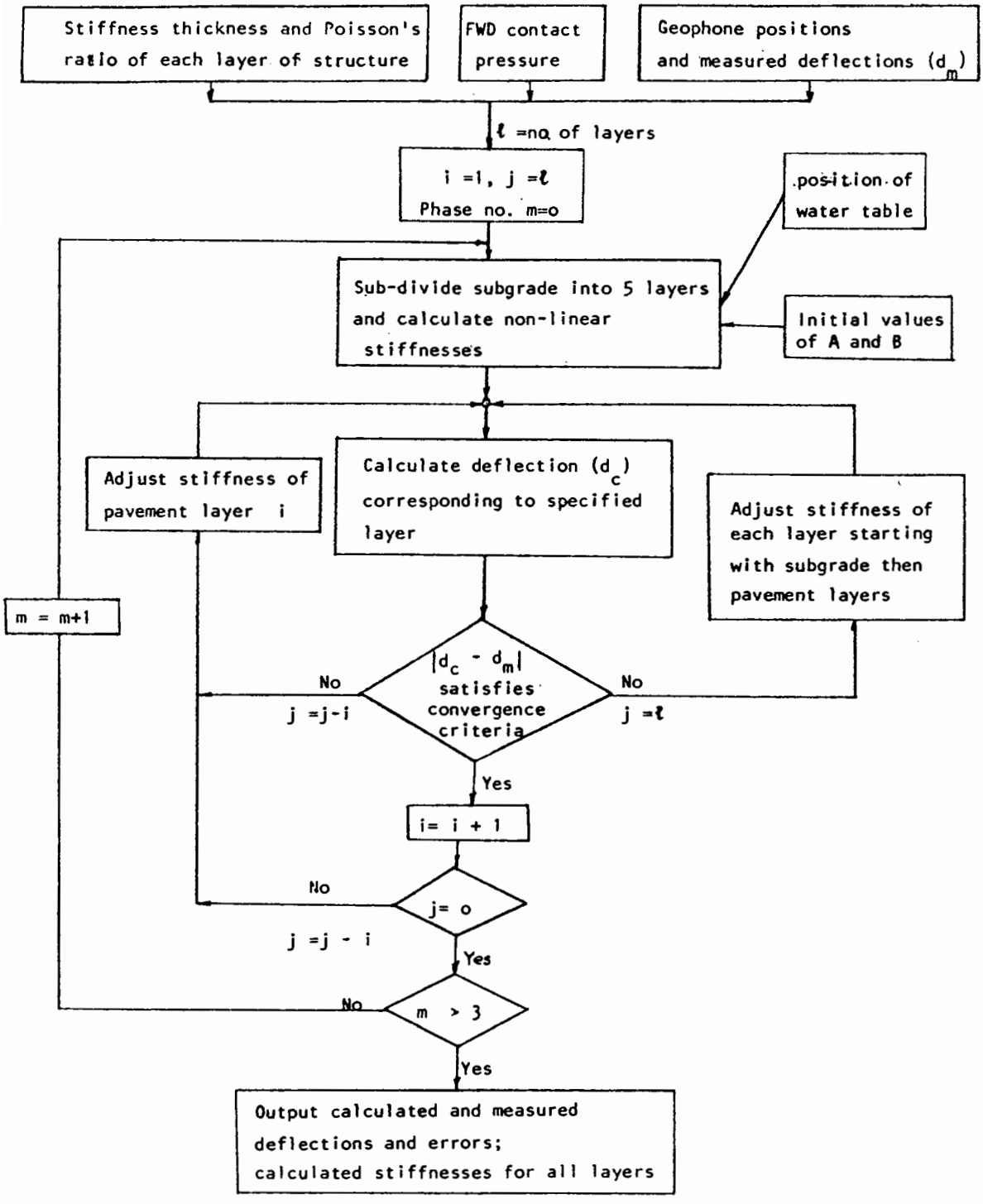

FIG. 4.10 FLOW DIAGRAM FOR 'BASEM' AND 'BASEMC' COMPUTER PROGRAMS.

Back-analysis procedure: The back-analysis of a deflection bowl is carried out in five phases (Phases 0 to 4), as indicated in Figure 4.10.

Phase 0 is the initialisation phase. It prints all the data which have been input by the user. Then, the program calculates initial estimated non-linear elastic stiffnesses for the subgrade sub-layers. In subsequent phases of iteration, the program increases the total number of layers in the structure by 4, i.e. from (y+1) to (y+5), where y is the number of layers above the subgrade.

Phases 1 to 3 back-calculate the stiffnesses of the non-linear subgrade and overlying pavement layers by matching the measured and calculated deflections, utilising different parts of the deflection bowl. These three phases of computation successively increase the accuracy of the back-analysed stiffnesses of each layer.

The final solution for the back-analysed stiffnesses of the non-linear subgrade and overlying pavement layers is then printed in Phase 4. Moreover, the errors between the measured and calculated deflection bowls at each geophone position are computed to show the goodness of fit during the matching process, thus helping the user to decide whether or not the back-analysed stiffnesses have been determined accurately.

In the back-analysis of a typical three-layered structure consisting of bituminous surfacing, granular sub-base and subgrade, deflections corresponding to four different radial positions have been selected in which deflections d_1 and d_4 are assigned for the bituminous and sub-base layers; d_5 and d_7 are used for the determination of non-linear subgrade stiffnesses. As for a typical four-layered structure with either lean concrete or bituminous as the roadbase layer, a total of five deflections are used for back-analysis. In addition to the four deflections d_1, d_4, d_5 and d_7 above, deflection d_2 is included for

the determination of the effective stiffness of the roadbase layer. The basic equation for iteration is:

$$E_{new} = E_{old} \times \frac{(d_c + d_m)}{(2 \times d_c)} \qquad (4.23)$$

Both Kilareski and Anani (57) and Brunton (63) have incorporated the above equation in their work.

Criteria for convergence: Table 4.3 summarises the criteria for convergence of the BASEM program. For pavement layers, ± 2 μm and ± 5% are employed, depending on the magnitude of the measured deflections. The criterion for the subgrade layer is specified at ± 2 μm. The choice of these criteria is primarily based on the experience that the program will converge to a solution with reasonable accuracy without taking unduly long to do so. The ± 2 μm criterion is selected for pavement layers if their deflections are 200 μm or less. If deflections are more than 200 μm, ⊕^↓ ± 5% error range will be invoked. The magnitude of 200 μm, has been selected on the basis that if the deflections fall below it, the pavement structure will be stiff *and* a lower error margin is set. Kilareski and Anani (57) used 1% as the criterion for convergence in their iterative programs for matching Dynaflect deflection bowls.

These criteria generate an envelope around the measured deflection bowl within which a solution can be obtained. Close examination reveals that even within the narrow deflection enevelope, there exists a wide range of combinations of layer stiffnesses which satisfy the criteria. A small change in deflection can produce a large change in the stiffness of a pavement layer but not the subgrade. An improved method, which is based on a new algorithm, will be described in Section 4.4.3 in an attempt to produce a more reliable set of solutions.

Type	Parameters	Convergence Criteria
Pavement layers	$d_1, d_2 .. d_\ell$	DERROR $\leq \pm$ 2μm if $d_{im} \leq$ 200μm where $i = 1,2,..\ell$ DERROR $\leq \pm$ 5% if $d_{im} >$ 200μm ℓ = no. of layers excluding subgrade
Subgrade	d_7 (BASEMC) $d_{(\ell+1)} d_7$ (BASEM)	DER $\leq \pm$ 2μm d_m = measured deflections

Table 4.3 Summary of Convergence Criteria on Deflection used in BASEM and BASEMC Computer Programs

4.4.2 The computer program BASEMC

During the second year of the research, a number of concrete pavements both in airports and highways were tested with the FWD. In order to evaluate the in-situ effective elastic stiffnesses of the concrete layers, the BASEMC computer program was developed. The procedure used in the BASEMC program is similar to that already described for the BASEM program. Therefore, the back-analysis procedure is only briefly described in the following paragraphs, full details being documented in Tam (79). The simplified flow diagram has been illustrated in Figure 4.10.

As for the BASEM program, there are five phases (Phases 0 to 4) in the calculation. Phase 0 is for generating a set of initial linear stiffnesses for the subgrade layer with the subgrade stiffness parameter B set to zero (refer equation 4.8). It is considered that this assumption is justified since the subgrade layer in a concrete pavement structure would experience very little stress variation with depth and hence very little variation in elastic stiffness. In Phases 1 to 3, the iteration starts with the subgrade layer; it is then followed by the sub-base, lean concrete and pavement quality concrete layers, each phase gradually increasing the accuracy of the back-analysed stiffnesses of each layer. The iteration stops when the deflection criteria shown in Table 4.3 have been satisfied. The solution for the back-analysed stiffnesses of all the layers of the structure is then printed in Phase 4. The errors between the measured and calculated deflection bowls are also printed to assess the goodness of fit.

In the back-analysis of concrete pavements, typically consisting of four layers, deflections corresponding to four radial positions are used. They are d_1, d_3, d_4, and d_7 which are used to determine the effective stiffnesses of pavement quality concrete layer, lean

concrete roadbase layer, granular sub-base and subgrade layer respectively. In this program, the subgrade has been taken to be linear with depth, instead of the non-linear one in the BASEM program, since it was considered that very small stress variation due to the applied load will be experienced in the subgrade. This assumption, considered appropriate for back-analysing sound pavement structures, is not applicable for situations when the structure is deteriorating, where the subgrade will experience a greater amount of stress variation. The above weakness has been corrected in the PADAL program detailed below. The BASEMC program also employs the same equation (4.23) in the iteration process.

4.4.3 The development of the computer program PADAL

Since the development of the back-analysis computer programs BASEM and BASEMC, they have been extensively applied in evaluating a wide range of pavement structures. These have included structures with bituminous layer thicknesses from around 100 mm to 500 mm ,granular layer thickness (including Type 1 sub-base and capping layer) from 150 mm to over 1000 mm, overlying a wide variety of subgrade soils. A slightly narrower range of concrete pavement structures has also been investigated.

As a result of these applications, it was found that both BASEM and BASEMC programs did not provide as accurate a method for analysing the stiffnesses of pavement structures as the writer had originally envisaged. Hence, the methodology and assumptions employed in the above programs were re-assessed to understand the cause of the problem and, if necessary, to suggest improved methods to give a more accurate solution.

A detailed assessment of the BASEM program was carried out and full details have been reported in Tam (79). It was revealed that the basic problem of accuracy of stiffness prediction was due to the fact

that the convergence criteria, which were based entirely on deflections, were not sufficient to ensure consistent answers. Thus, the final stiffnesses computed for the pavement layers were sensitive to the initial estimates of layer stiffness which were input into the program. However, reasonably good and consistent prediction for subgrade stiffnesses was observed. Moreover, other deficiencies in the iterative procedures and output format were noted. As a result of the above investigation, it was considered to be quicker to develop another computer program, with an improved methodology rather than carrying on improving the existing programs. It was also hoped that the new methodology would reduce the existing computing time.

Consequently, a new computer program PADAL was developed with a new algorithm. It is designed to provide a more dynamic iterative procedure and more stringent convergence criteria which will quickly converge to a unique solution, regardless of the initial estimates of layer stiffness. The program is also structured in a way so as to provide the user with a much clearer picture about every stage of the iterative process. Figure 4.11 shows a simplified flow diagram for the PADAL computer program.

When developing this program, it was considered that, since back-analysis of bituminous structures shares a lot of common routines with that for concrete structures, the PADAL program should be used for the analysis of both. The paragraphs that immediately follow describe in detail the analysis procedure for bituminous pavements. Application to concrete pavements will be found in the final part of this section.

Features of PADAL: The new program has three main features. These include:

(i) A material model to calculate the non-linear elastic stiffnesses in the subgrade layer (the same as in

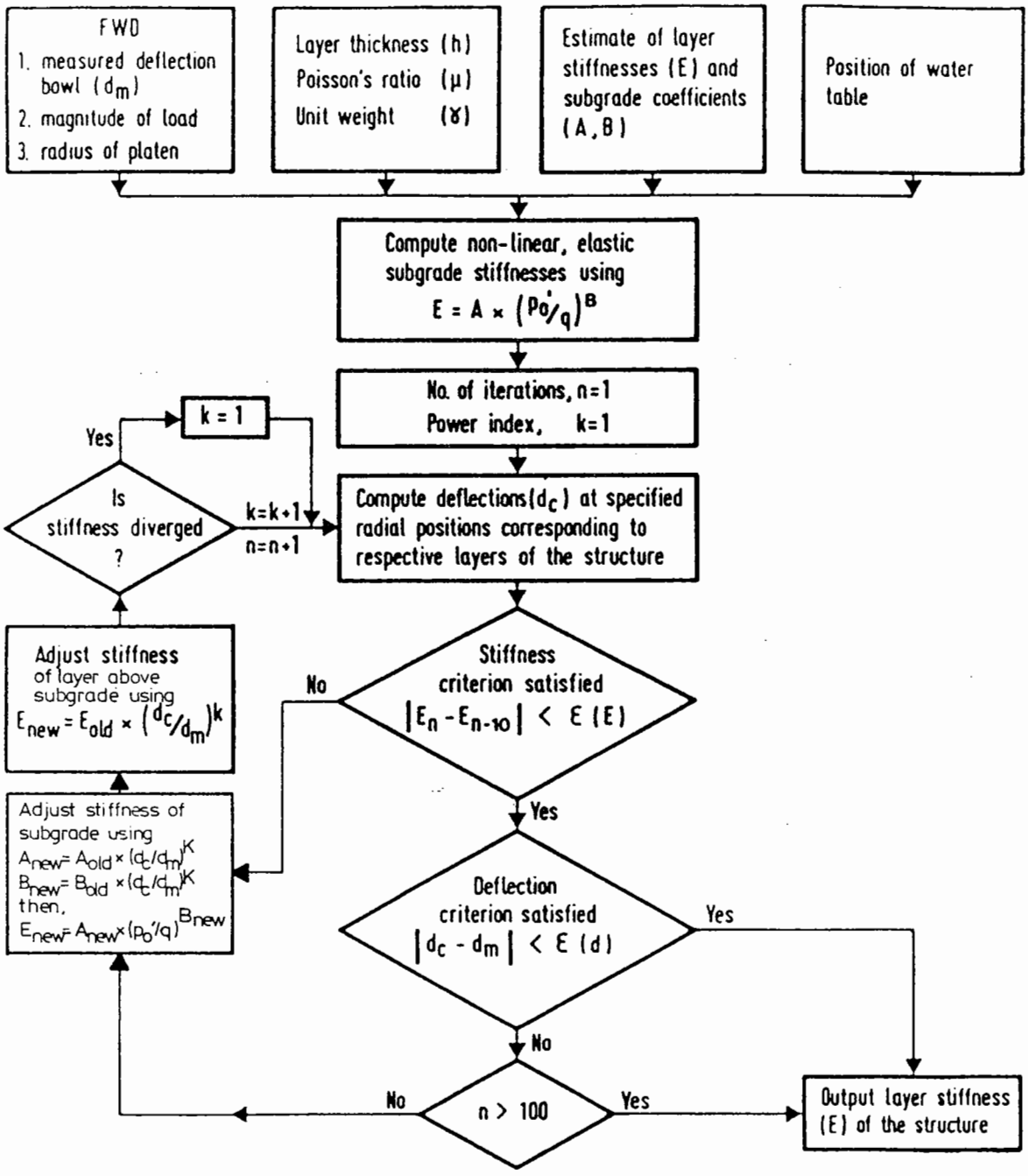

FIG. 4-11 Computer Program PADAL (PAvement Deflection AnaLysis)

the BASEM computer program);

(ii) One radial position specified for each pavement layer overlying the subgrade and two radial positions for the subgrade layer for back-analysis (the same as in the BASEM computer program);

(iii) The facility to include a rigid layer in the subgrade for back-analysis, if necessary (additional to the BASEM computer program).

The third feature is particularly useful if a rigid layer, e.g. bedrock , is known to be present close to the pavement surface. In their study of the influence of bedrock on the dynamic deflection of the FWD, Roesset and Shao (80) reported a minimum depth of 20 m from the pavement surface within which the bedrock layer has a significant effect on the FWD deflections. A similar feature has also been proposed by Uddin et al (81) in his back-analysis procedure.

New algorithm: The algorithm used in the iteration takes the form of the following expression, viz:

$$(E_{new})_i = (E_{old})_i \times \left(\frac{d_c}{d_m}\right)_j^{k1} \qquad (4.24)$$

where (E_{new}) and (E_{old}) are the new and old computed stiffnesses for layer i;

d_c and d_m are the calculated and measured deflections at radial location j;

k1 is an index number which increases as iteration progresses.

The advantage of the new algorithm, as proposed in equation (4.24) is that it improves the rate of convergence by increasing the index number k1 as iteration progresses. The higher the k1 value, the greater the ratio which can then be applied to adjust the old

stiffness value and hence, the quicker the rate of convergence to the final solution.

Convergence criteria: The new criteria are based on limiting the error in the calculated stiffnesses of each layer as well as limiting the error between the measured and calculated deflections. Table 4.4 summarises these criteria for a four-layered structure of bituminous pavement. Similar criteria have been developed for two- and three-layered structures. The error in calculated stiffness during the iteration process is computed when the number of iterations, n, is greater than 15. If the relative stiffness difference, ΔE, which is the difference between the last stiffness value and the tenth previous one (i.e. $E_{n-10} - E_n$), is less than the specified values of ± 10 MPa for bituminous layers, ± 1 MPa for the sub-base layer and ± 1 MPa for the subgrade layer simultaneously, then the error in deflections is checked to see whether or not the calculated deflections are within ± 1% of the measured values. Convergence is reached if both criteria are satisfied and iteration stops. Figure 4.12 demonstrates the principle of the use of these criteria in the program. Extensive tests on the PADAL program have been carried out to confirm the validity of using the above criteria. Detailed analysis will be discussed later.

The advantage of the improved convergence criteria is to ensure that a unique solution is reached regardless of the initial estimates of layer stiffness. A calculation shows that a change of 1% in central deflection can result in more than a 10% change in the bituminous stiffnesses. This explains why the BASEM and BASEMC programs do not always produce consistent solutions.

Since the criteria are so strict, many iterations are found to be necessary before convergence can be achieved. In general, the minimum number of iterations required is about 30 for analysis of

Layer No	Type	Convergence criteria	
		Relative Stiffness	Deflection
	(A) Bituminous structures		
1	Bituminous	$\delta E < \pm$ 10 MPa	$\frac{(d_c - d_m)}{d_m} \times 100\%$
2	Bituminous	$\delta E < \pm$ 10 MP	
3	Sub-base	$\delta E < \pm$ 1 MPa	less than
4	Subgrade	$\delta E < \pm$ 1 MPa	$\pm$ 1%
	(linear and non-linear)		
	(B) Concrete structures		
1	Concrete	$\delta E < \pm$ 30 MPa	$\frac{(d_c - d_m)}{d_m} \times 100\%$
2	Concrete	$\delta E < \pm$ 30 Mpa	
3	Sub-base	$\delta E < \pm$ 1 MPa	less than
4	Subgrade	$\delta E < \pm$ 1 MPa	$\pm$ 1%
	(linear and non-linear)		

where $\delta E = (E_{n-10} - E_n)$; n = no of iterations greater than 15
d_c = calculated deflection; d_m = measured deflection

Table 4.4 Convergence Criteria used in PADAL program for 4-layer structure

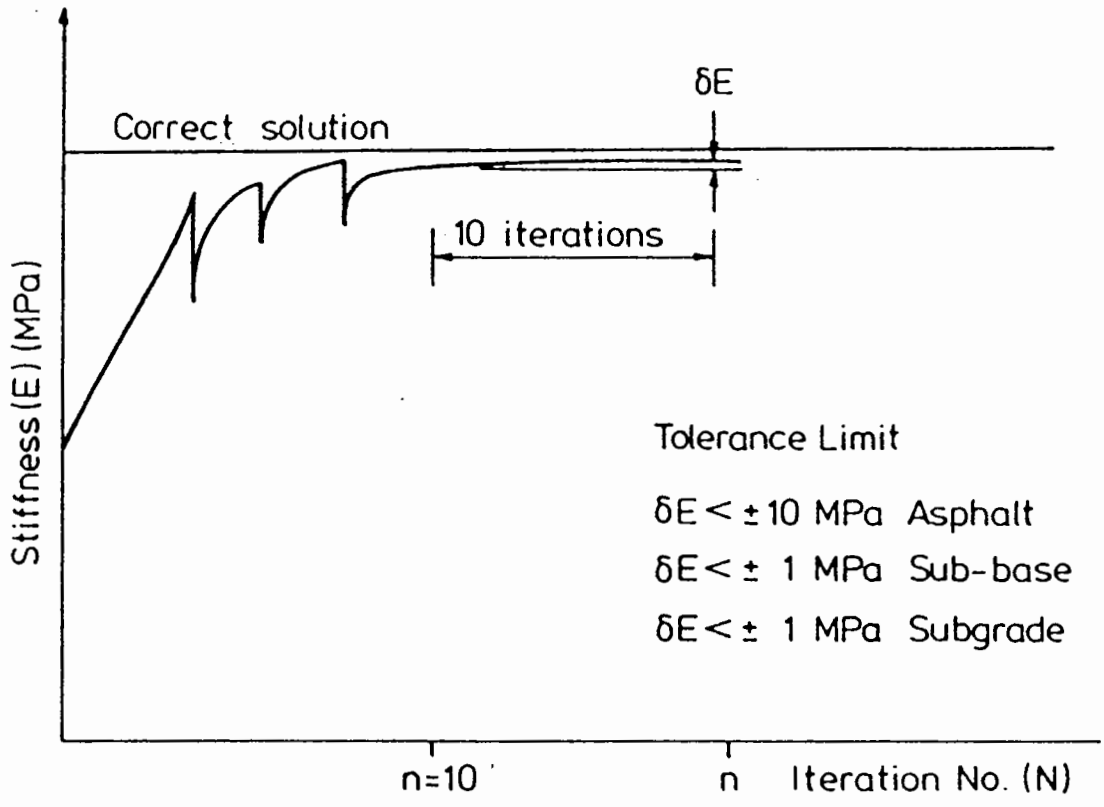

(a) Stiffness

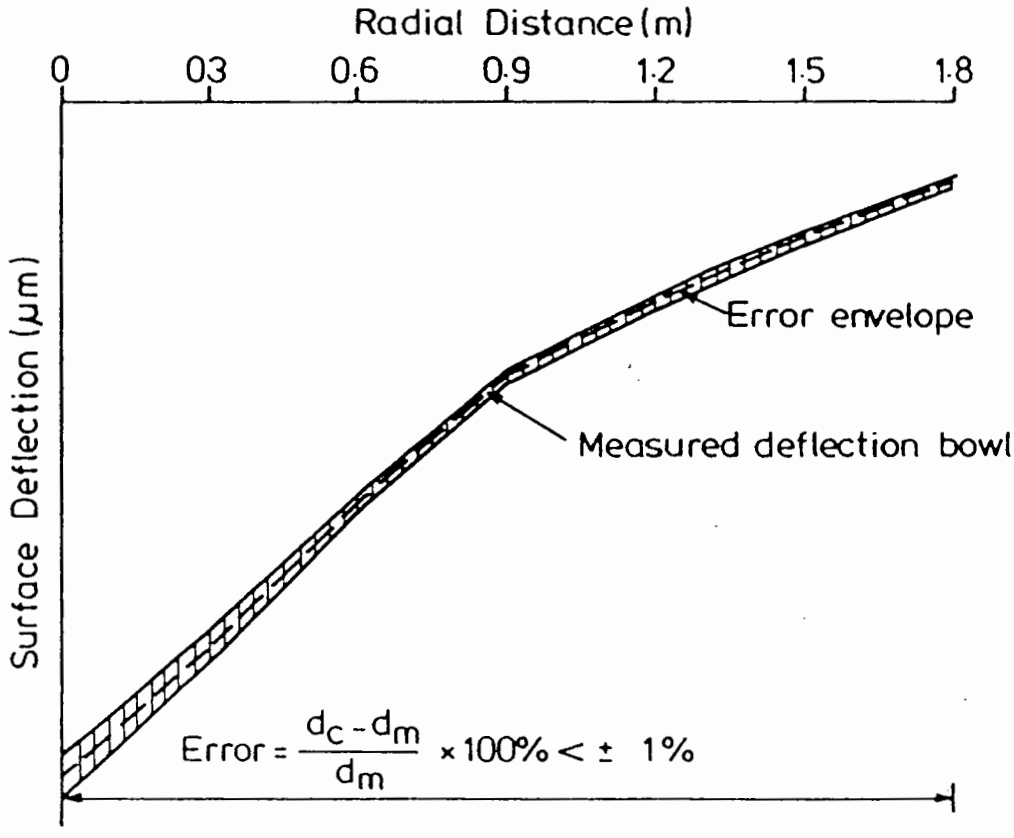

(b) Deflection

FIG. 4.12 DIAGRAMS SHOWING CONVERGENCE CRITERIA USED IN PADAL PROGRAM

structures with linear subgrade but typically 60 iterations are required for structures with non-linear subgrade. During testing of the PADAL program, a few cases have been found to require over 100 iterations to achieve convergence. Further study reveals that the calculated stiffnesses reach to within 10% of the correct answer in less than 50 iterations. Thereafter, the calculated values fluctuate above and below the correct answer but just exceeding the specified convergence criteria. Based on this finding, a decision was made to limit the maximum number of iterations to 100. If the program is terminated after 100 iterations, the solution is then obtained by averaging the calculated stiffnesses for the last 30 iterations. In order to improve the rate of convergence further, predictive equations using the multiple linear regression analysis technique have been developed in an attempt to compute a set of initial estimates of the layer stiffnesses, close to the required solutions. This work will be described in subsequent discussion.

Input data: Table 4.5 shows the required format of input data for the PADAL program, including:

(a) Option to select the procedure with or without a rigid layer within the subgrade;

(b) Initial estimate of elastic stiffnesses (equivalent to Young's modulus) of each layer;

(c) Poisson's ratio and unit weight of each layer;

(d) Layer thicknesses except subgrade;

(e) FWD applied contact pressure and load platen radius;

(f) FWD geophone positions and their corresponding measured deflections;

(g) Depth of water below subgrade formation level;

(h) Initial estimate of non-linear subgrade stiffness parameters A and B;

Table 4.5 Input Data Required for PADAL Program

Input Data	Variable	Format F = free format A = character format	Units
1. No. of structures evaluated	NSYS	F	
2. Title of Job	TEXT	20A4 (up to 80 columns)	
3. Rigid layer ø = no rigid layer 1 = rigid layer exists	IR	F	
4. No. of layers of the structure	NLAYS	F	
5. Material type to pavement layers	TYPE	A2	
6. Minimum, maximum stiffness values for material in Record 5 to ensure convergence Repeat Records 5 and 6 for all layers above subgrade (see Note (1) for detail and example)	PMIN, PMAX	F	MPa, MPa
7. E, ν, h, γ, for pavement layers E = Young's modulus of layer ν = Poisson's ratio of layer h = thickness of layer γ = unit weight of layer Repeat Record 7 for all layers above subgrade	E, NU, THICK UWP	F (all real numbers)	MPa m kN/m^3
8. E, ν, γ, for subgrade (if IR = ø) E, ν, h, γ for subgrade (if IR = 1) h = thickness of subgrade above rigid layer	E, NU, UWP) E, NU, THICK,) UWP)	F (all real numbers)	as above
9. FWD contact pressure, platen radius	LDSTRS, RADIUS	F, F	MPa, m
10. No. of surface deflections (see Note 2)	NDEF	F	
11. Geophone position, measured deflection Repeat Record 11 for all geophone positions from load centre	FWDRAD, DEFLM	F	m, μm
12. Position of water table below subgrade formation (assume ZWT = 0 if not known)	ZWT	F	m
13. Subgrade non-linear parameters (initial start A = 50, B = 0.2 for asphalt A = 100 B = 0.1 for concrete)	A, B	F	MPa, -
14. Specified geophone positions for analysis No. of required positions = NLAYS + 1 eg. 1, 2, 4, 5, 7 for a four layer structure (See Note 3 for more detail)	IPOS	F (all integers)	

Table 4-5 (Cont'd)

Notes

(1) Types of pavement materials and their recommended range of stiffnesses are:

	Min (MPa)	Max (MPa)
'AS' = Asphalt	500	20000
'CA' = Capping Layers	30	500
'LC' = Lean Concrete	5000	70000
'PC' = Pavement Quality Concrete	10000	70000
'SB' = Sub-base	30	500
'WM' = Wet Mix	30	900

Please note that the assigned stiffness range is the absolute minimum and maximum values that the stiffness of a material is allowed to vary during iteration. The iteration process might be hampered if the range is too narrow in that the stiffness fluctuates between two values only.

(2) NDEF $\geq$ NLAYS+1.

(3) During analysis, one geophone position will be assigned for each pavement layer and two geophone positions for the subgrade. Hence, the total number of geophone positions required is the total number of layers (NLAYS) plus one. The following are the recommended positions for analysis:

	Stiffness	Position
Top layer	E1	1
Second layer	E2	
(i) if E2 > E1 (not sub-base)		2
(ii) if E2 < E1 (not sub-base)		3
(iii) if sub-base - no capping		4
- with capping		3
Third layer (if present)	E3	
(i) not sub-base or capping		3
(ii) sub-base or capping		4
Subgrade	ESG	5 and 7

(i) specified geophone positions for back-analysis.

As indicated in Record 14 of the table, information is required to specify which geophone positions of the deflection bowl are to be used for back-analysis. This facility thus allows the user flexibilty in selecting the combination of geophone positions which is most appropriate in diagnosing the in-situ condition of a pavement structure. The recommended positions for each layer of a structure (up to four layers) are detailed in Note 3 of the table, beingthe results of the sensitivity analysis already discussed in Chapter 3.

Iteration procedure: As shown in Figure 4.11, the iteration procedure consists of six steps (a to f). Figure 4.13 illustrates a typical output showing the computation for a three-layered structure.

(a) This is an initialisation phase. The program begins by printing the input data to allow the user to check the accuracy of the input. It then generates initial estimates for the non-linear subgrade stiffnesses by using the initial estimates of elastic stiffness for each layer and the non-linear subgrade stiffness parameters A and B. The procedure for calculation has been discussed in section 4.4.1. In doing the computation above, the total number of layers in the structure is increased by 4, i.e. from (y+1) to (y+5) layers, where y is the number of layers above the subgrade. In subsequent iterations , the total number of layers will remain as (y+5) when the subgrade is non-linear. However, in some cases, the subgrade is found to be linear during the iteration process, i.e. when B = 0. When this situation occurs, the magnitude of stiffness for all the subgrade sub-layers will be the same and hence, subsequent iterations only require (y+1) layers.

(b) After the non-linear subgrade stiffnesses have been initialised, the program then assigns the selected radial positions for

FIG. 4.13 TYICAL 'PADAL' OUTPUT (1 of 4)

System Time:- 13: 0:18
On 6-JUL-1987

```
*****************************************
*        Computer Program PADAL         *
*     PAvement Deflection AnaLysis      *
*****************************************
```

*** INPUT DATA ***

TITLE OF JOB:
HASLAND BYPASS WB WP EXPTAL SEC., CH.20M (TP3) 02/07/86

LAYER NUMBER	MATERIAL TYPE	ELASTIC STIFFNESS (MPa)	POISSON RATIO	THICKNESS (m)	UNIT WEIGHT (kN/M3)
1	ASPHALT	3000.0	.40	.257	23.00
2	SUB-BASE	300.0	.30	.452	20.00
3	SUBGRADE	100.0	.40		20.00

FWD CONTACT PRESSURE = .700 MPa
FWD PLATEN RADIUS = .150 m

FWD MEASURED DEFLECTION BOWL DATA

	RADIUS(m)	DEFLECTION VALUES(microns)
1	.000	174.0
2	.300	131.0
3	.600	92.0
4	.900	62.0
5	1.200	43.0
6	1.500	29.0
7	1.800	22.0

DEPTH OF WATER TABLE BELOW FORMATION LEVEL = .000 m

NONLINEAR SUBGRADE BEHAVIOUR WITH E=A*((po/q)**B) WITH A=150.00MPa B= .25

FIG. 4.13 (2 of 4)

*** ANALYSIS ***

PHASE NO. 0
==========

INITIALIZE NONLINEAR SUBGRADE ELASTIC STIFFNESSES

SUBLAYER NO.	MID-DEPTH (m)	INITIAL STIFFNESS (MPa)	INITIAL EFF.NORMAL(po) STRESS(MPa)	INITIAL DEVIATORIC(q) STRESS(MPa)
1	1.009	161.374	.0140	.0105
2	1.809	219.039	.0203	.0045
3	2.809	282.971	.0283	.0022
4	4.309	370.981	.0402	.0011
5	7.309	531.373	.0639	.0004

++++ NONLINEAR SUBGRADE STIFFNESSES IN OPERATION ++++

PHASE NO. 1
==========

+++++ 3-LAYER STRUCTURE TO BE SOLVED +++++

SPECIFIED DEFLECTION OF ITER. FOR (E1) IS D1 AT .0m
SPECIFIED DEFLECTION OF ITER. FOR (E2) IS D4 AT .9m
SPECIFIED DEFLECTION OF ITER. FOR (ESG) IS D5 AT 1.2m
SPECIFIED DEFLECTION OF ITER. FOR (ESG) IS D7 AT 1.8m

ITER	PI	E1	E2	ESG(top)	E(RIGID)	A	B
1	1	3570.78	300.00	164.03		152.4652	.2500
2	2	4378.40	276.26	166.96		155.1910	.2500
3	3	4921.35	258.61	174.02		160.5215	.2762
4	4	4588.70	201.82	136.06		128.1954	.2036
5	1	5598.72	322.11	193.25		177.0585	.2994
6	1	4718.95	221.73	153.26		143.0502	.2358
7	1	5230.32	280.05	179.82		165.7180	.2793
8	1	4855.74	237.17	161.42		150.0747	.2493
9	1	5101.84	265.02	173.97		160.7858	.2696
10	1	4929.51	245.24	165.38		153.4833	.2554
11	1	5046.43	258.37	171.32		158.5531	.2649
12	1	4966.26	249.10	167.32		155.1502	.2582
13	1	5021.66	255.25	170.13		157.5583	.2626
14	1	4984.41	250.87	168.28		155.9851	.2594
15	1	5010.72	253.71	169.62		157.1390	.2614
16	1	4993.54	251.61	168.77		156.4242	.2599
17	1	5006.14	252.90	169.42		156.9877	.2608
18	1	4998.36	251.88	169.05		156.6751	.2600
19	1	5004.52	252.44	169.37		156.9606	.2604
20	1	5001.13	251.93	169.22		156.8356	.2599
21	1	5004.25	252.15	169.39		156.9901	.2601

FIG. 4.13 (3 of 4)

--- ADJUST SUBGRADE STRESSES FROM ADJUSTED STIFFNESSES IN ITERATION 21 ---

SUBLAYER NO.	MID-DEPTH (m)	STIFFNESS (MPa)	ADJUSTED EFF. NORMAL (po) STRESS (MPa)	ADJUSTED DEVIATORIC (q) STRESS (MPa)
1	1.009	169.392	.0140	.0115
2	1.809	232.766	.0203	.0056
3	2.809	303.820	.0283	.0029
4	4.309	402.680	.0402	.0014
5	7.309	585.178	.0639	.0005

22	1	5002.90	251.87	165.23	156.9522	.2598
23	1	5090.58	264.09	173.92	164.6401	.2771
24	1	4950.58	248.35	168.15	159.4742	.2676
25	1	5023.78	256.36	171.91	162.8429	.2740
26	1	4974.51	250.48	169.54	160.7298	.2697
27	1	5007.93	253.97	171.17	162.1934	.2723
28	1	4988.05	251.47	170.20	161.3345	.2704
29	1	4904.61	252.89	170.92	161.9847	.2714
30	2	4772.10	252.01	169.76	160.9738	.2687
31	3	4794.58	263.14	173.28	164.1245	.2743
32	1	4695.07	251.59	168.40	159.7560	.2664
33	1	4752.99	258.97	171.43	162.4529	.2718
34	1	4712.28	254.33	169.36	160.5947	.2686
35	1	4736.39	257.53	170.59	161.6898	.2710
36	1	4718.97	255.66	169.69	160.8758	.2697
37	1	4728.69	257.08	170.18	161.3010	.2708
38	1	4720.96	256.36	169.77	160.9256	.2703
39	1	4724.63	257.02	169.94	161.0710	.2708
40	1	4720.99	256.78	169.73	160.8807	.2707
41	1	4722.15	257.12	169.77	160.9102	.2710
42	1	4720.24	257.08	169.66	160.7989	.2711
43	1	4720.37	257.29	169.65	160.7810	.2713
44	1	4719.21	257.33	169.57	160.7042	.2714
45	1	4718.91	257.47	169.53	160.6674	.2715
46	2	4717.25	257.62	169.41	160.5457	.2717
47	3	4716.97	258.09	169.35	160.4669	.2722
48	4	4706.95	257.49	168.77	159.9259	.2720
49	5	4759.49	264.72	171.92	162.6994	.2785
50	1	4671.70	253.80	166.95	158.2763	.2698
51	1	4735.95	261.80	170.15	161.1275	.2754
52	1	4694.48	256.84	168.01	159.2096	.2719
53	1	4720.81	260.23	169.35	160.4010	.2743
54	1	4702.74	258.14	168.41	159.5637	.2729
55	1	4713.69	259.63	168.97	160.0522	.2740
56	1	4705.74	258.77	168.55	159.6764	.2734
57	1	4710.18	259.44	168.77	159.8661	.2739
58	1	4706.56	259.12	168.57	159.6877	.2737
59	1	4708.24	259.44	168.65	159.7508	.2740
60	1	4706.48	259.33	168.55	159.6573	.2739
61	1	4706.99	259.50	168.56	159.6672	.2741
62	1	4706.04	259.49	168.51	159.6105	.2741
63	1	4706.06	259.60	168.50	159.5984	.2742
64	1	4705.45	259.63	168.46	159.5582	.2743

FIG. 4.13 (4 of 4)

PHASE NO. 2

****
* 3-layer Structure successfully solved *
****

TITLE OF JOB:
HASLAND BYPASS WB WP EXPTAL SEC., CH.20M (TP3) 02/07/86

SUMMARY OF RESULTS

STIFFNESS "E1" ADJUSTED TO GIVE BETTER MATCH
BETWEEN CALCULATED AND MEASURED DEFLECTION BOWLS

RADIUS(m)	MEASURED DEFLECTION(microns)	CALCULATED	ACTUAL ERROR (%)	microns
.000	174.0	177.5	2.00	3.5
.300	131.0	128.6	-1.83	-2.4
.600	92.0	89.9	-2.25	-2.1
.900	62.0	62.0	.02	.0
1.200	43.0	43.0	-.01	.0
1.500	29.0	30.4	4.66	1.4
1.800	22.0	22.0	.03	.0

LAYER		ELASTIC STIFFNESS(MPa) ESTIMATED	CALCULATED FOR DEFLECTION	LAYER THICKNES
1	ASPHALT	3000.	4705.	.257
2	SUB-BASE	300.	260.	.452
3	SUBGRADE	161.	168.	.600
4	SUBGRADE	219.	227.	1.000
5	SUBGRADE	283.	299.	1.000
6	SUBGRADE	371.	401.	2.000
7	SUBGRADE	531.	596.	INFINITE

iteration, corresponding to each individual layer of the structure. For a three-layered structure, for example, as shown in Figure 4.13, the specified radial positions are as follows:

Specified position of iteration for (E_1) is d_1 at 0.0m

Specified position of iteration for (E_2) is d_4 at 0.9m

Specified position of iteration for (E_{SG}) is d_5 at 1.2m

Specified position of iteration for (E_{SG}) is d_7 at 1.8m

(c) The iteration begins by calling the BISTRO subroutine to calculate deflections at the above radial positions, except at 0.6 m which relates to layer 2 (sub-base). Experience has shown that divergence would occur if the sub-base stiffness E_2 were included into the iteration too soon. The stiffnesses of all the layers (except layer 2) are then adjusted simultaneously. For layers overlying the subgrade, the adjustment is carried out using equation (4.25) as shown below:

$$(E_{new})_i = (E_{old})_i \times \left(\frac{d_c}{d_m}\right)_j^{k1} \qquad (4.25)$$

where the parameters have previously been defined for equation (4.24).

For the subgrade, the stiffness parameters A and B are adjusted instead of the actual non-linear stiffnesses as follows:

$$A_{new} = A_{old} \times \left(\frac{d_c}{d_m}\right)_j^{k1} \qquad (4.26)$$

$$B_{new} = B_{old} \times \left(\frac{d_c}{d_m}\right)_j^{k1} \qquad (4.27)$$

Then, the adjusted values of A and B are substituted back into equation (4.8) to calculate a new set of non-linear stiffnesses,

taking the same stress ratio for each sub-layer as computed in the step (a). It is noted that the subgrade stresses (p_o' and q) will be updated once during each iteration until the relative stiffness ratio of the subgrade at formation level (i.e. $\Delta E_4/E_4$) is less than 0.01, indicating that a steady condition has been reached. The process in step (c) is repeated until the relative stiffness ratio of layer 1 (i.e. $\Delta E_1/E_1$) is less than 0.01.

(d) The sub-base stiffness, E_2, is now introduced into the iteration. The BISTRO sub-routine is then called to calculate deflections at all four radial positions indicated in step (b). Equations (4.25) to (4.27) are used to adjust stiffnesses of all the layers except for stiffness E_2 which is adjusted using the following expression:

$$(E_{new}) = (E_{old}) \times \left(\frac{(d_s - d_f)_c}{(d_s - d_f)_m}\right)_j^{k2} \qquad (4.28)$$

where d_{ss} and d_f are the deflections assigned for the sub-base and the furthest radial position respectively as given in input (i) of Table (4.5);

k2 is an index number which increases as iteration proceeds.

It should be noted that while the index number k1 in equations (4.25) to (4.27) is increased by 1 per iteration , the value of k2 increases by 2 each time. This is to increase the rate of convergence of the stiffness in the sub-base layer.

(e) As iteration progresses, both k1 and k2 could reach very large numbers. Divergence may then occur at one stage of the iteration when k1 and k2 values are large. A procedure has been developed to identify this behaviour and control it as soon as it starts to

occur. This is achieved by setting the indices k1 and k2 back to 1 and 2 respectively once the divergent behaviour has been identified.

(f) Steps (d) and (e) are then repeated. In each iteration, the accuracy of back-analysed layer stiffnesses is successively increased. The procedure is terminated if one of the following conditions is fulfilled:

(i) The convergence criteria for both stiffness and deflection are satisfied;

(ii) The number of iterations reaches 100.

(g) The final solution for back-analysed stiffnesses of each layer of the structure is then printed, as well as the calculated and measured deflections. Errors in the calculated deflections in comparison with the measured values are also computed, so that the degree of goodness of fit can be assessed, thus enabling the user to determine whether or not the elastic stiffnesses have been accurately back-analysed.

Uniqueness of solution: To demonstrate the applicability of the improved procedure and methodology incorporated in the PADAL program, a simple three-layered structure, with linear elastic subgrade, was tested. A theoretical deflectional bowl was calculated, with layer stiffnesses of 8000 MPa, 200 MPa, and 150 MPa respectively, and with thicknesses of 200 mm for each layer. Then, the theoretical deflection bowl was used as the input data for the PADAL program. Ten tests were made each with different initial estimates of stiffness for each layer. Table 4.6 summarises the results, in which the predicted stiffness for layer 1 is in error by less than 2%, layer 2 has a maximum error of 2% and there is a 0.7% error for layer 3. Figure 4.14 illustrates the typical iterative process of PADAL, with initial stiffnesses taken from run no. 3 of Table 4.6. Judging

Test No	Initial estimate (MPa)			Final solution (MPa)			Number of Iterations
	E_1	E_2	E_3	E_1	E_2	E_3	
1	1000	150	100	8141	196	149	38
2	6000	150	100	8129	197	149	15
3	10000	150	100	8125	197	149	36
4	10000	50	50	8078	198	149	47
5	8000	150	300	8132	196	149	28
6	8000	150	50	8125	197	149	36
7	1000	150	300	8134	197	149	30
8	1000	150	50	8137	196	149	34
9	5000	300	300	8133	197	149	30
10	5000	150	50	8127	197	149	18
		Correct values		8000	200	150	

Table 4.6 Test on Uniqueness of Solution using PADAL program

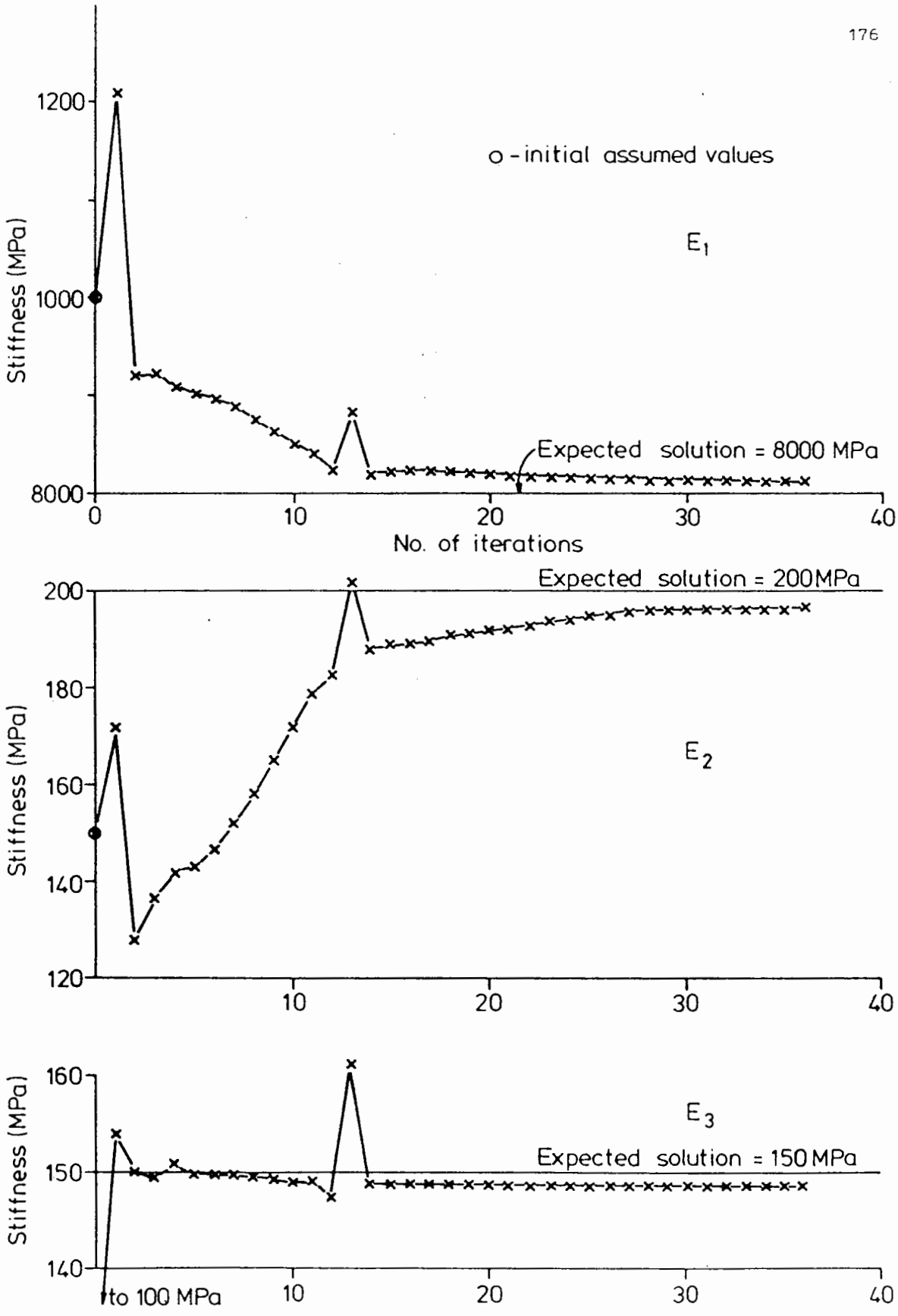

FIG 4.14 TYPICAL EXAMPLE OF ITERATIVE PROCESS IN PADAL PROGRAM (3-layer structure)

from the consistency of the results, it is clear that the PADAL program can be used with confidence for the evaluation of pavement structures, with linear elastic subgrade, regardless of the initial estimates of layer stiffness with linear elastic subgrades.

To investigate the suitability of PADAL for pavement structures with non-linear subgrade, 15 different four-layered bituminous structures were analysed, representing a wide range of combinations of both stiffness and thickness. Table 4.7 summarises the results of the calculations. It is noted that, except for those structures with thin top layers (e.g. 40 mm of layer 1 for structure nos. 4, 8, and 12), very good results are generally achieved. Maximum errors of less than 6.0% are recorded for all layers other than the stiffness of layer 3 (E_3), for which a maximum of 16% error is noted in structure no. 3. From this analysis, it is considered that the PADAL program can again be used very satisfactorily for the analysis of any structure of up to four layers, with the thickness of the surfacing layer greater than 50 mm. However, if the program is used to predict the stiffness of a surfacing layer of thickness less than 50 mm, an error of up to 50% from the correct value may be expected.

Procedure for improved estimate of initial stiffnesses: During the development of the PADAL program, it was realised that the rate of computation of the PADAL program had not been improved as a result of the new proposed algorithm described earlier on. And, in some cases, computing time was much longer than in the BASEM program. The problem was mainly caused by the much stricter convergence criteria proposed. As a result, a lot more iterations, compared with the BASEM program, are required for convergence. For example, the time required to analyse a three-layered structure with the PADAL program is up to 30 minutes on an IBM PC/AT micro-computer, as compared with 10 minutes for the BASEM program. Therefore, it was necessary to

TABLE 4.7 BACK-CALCULATED LAYER STIFFNESSES USING "PAOAL" PROGRAM

Structure No.	Layer thickness (mm)	Initial estimated stiffness (MPa)					Final calculated stiffness (MPa)				Error (%) from correct value			
	$h_1 + h_2 + h_3$	E_1	E_2	E_3	(non-linear subgrade) A	B	E_1	E_2	E_3	E_f	E_1	E_2	E_3	E_f
		Correct Stiffnesses →					(1000)	(1500)	(50)	varies				
1	100+200+300	800	1800	100	50.5	0.1	994	1499	50	50 [50]	-0.6	-0.1	0.0	0.0
2	100+300+300	800	1800	100	50.5	0.1	1013	1487	55	25 [26]	1.3	-0.9	10.0	-3.8
3	200+200+300	800	1800	100	50.5	0.1	1007	1448	58	47 [50]	0.7	-3.5	16.0	-6.0
		Correct Stiffnesses →					(1000)	(3000)	(100)	varies				
4	40+150+200	800	3100	120	50.5	0.1	1010	2965	107	47 [46]	1.0	-1.1	7.0	2.0
5	100+200+300	1242	3604	82.5	52.3	0.09	986	3066	95	52 [51]	-1.4	2.2	-5.0	2.0
6	100+300+300	1172	4130	93	50.9	0.1	1001	3014	98	54 [54]	0.1	0.5	-2.0	0.0
7	200+200+300	821	3330	111	50.5	0.1	1001	2960	105	52 [53]	0.1	-1.3	5.0	-1.8
		Correct Stiffnesses →					(5000)	(6000)	(150)	varies				
8	40+150+200	4000	4000	131	50.5	0.1	4563	5900	170	68 [69]	-8.7	-1.7	13.3	-1.4
9	100+200+300	4000	4000	131	50.5	0.1	4960	6030	147	72 [72]	-0.8	0.5	-2.0	0.0
10	100+300+300	4000	4000	131	50.5	0.1	5050	5900	152	74 [74]	1.0	1.7	1.3	0.0
11	200+200+300	4000	4000	131	50.5	0.1	4994	6021	148	74 [74]	-0.1	0.4	1.3	0.0
		Correct Stiffnesses →					(8000)	(10000)	(200)	50				
12	40+150+200	9067	4884	96	47.0	0.0	11301	9234	139	50	41.3	-7.7	-30.5	0.0
13	100+200+300	8410	8900	135	56.0	0.0	8045	9970	200	50	0.6	-0.3	0.0	0.0
14	100+300+300	9460	9410	133	50.0	0.0	8010	9980	198	50	0.1	-0.2	-1.0	0.0
15	200+200+300	8120	12360	138	47.0	0.0	8002	10003	200	50	0.0	0.0	0.0	0.0

E_f = Non-linear subgrade stiffness at formation level; No. in [ ] is magnitude of the correct non-linear subgrade stiffness at formation level

improve the program efficiency.

It was considered that program efficiency could be improved if the initial estimates of stiffness were close to the final solution. One possible way to achieve this is to produce predictive equations relating layer stiffnesses of the structure with layer thicknesses, as well as measured deflections. It has been noted in the literature that the regression technique has been widely used to obtain predictive equations, especially in the United States e.g. Uddin (82).

Therefore, stiffness predictive equations were developed, based on 6561 (3^8) theoretical deflection bowls for various combinations of stiffness and thickness for four-layered bituminous structures. The predictive equations are expressed in the following form:

$$\log(E_i) = f(\log(d_j), d_j^2, d_j^3, d_j d_k, h_1, h_1^2, h_1^3, \log(h_1), h_1 h_m, h_1 d_j, h_1^2 d_j, h_1 d_j^2) \quad (4.29)$$

where E_i is the stiffness of layer i (MPa);

d is the deflection (microns);

h is the layer thickness (m);

j & k are deflection subscripts from 1 to 7;

l & m are pavement layer subscripts from 1 to 3.

For each deflection bowl, seven deflections have been calculated at radial positions of 0, 300, 600, 900, 1200, 1500, and 1800 mm from the load centre respectively.

In order to improve the correlation further, two sets of stiffness equations have been developed corresponding to 'thin' and 'thick' structures, the ranges of all the parameters being presented in Tables 4.8 and 4.9. The differences between 'thin' and 'thick' structures were solely based on the differences in thicknesses that

Layer	Material	Parameters	Range of values
1	Asphalt	E_1 (MPa)	1000, 3000, 10000
		h_1 (mm)	30, 70, 120
		ν_1	0.4
2	Asphalt	E_2 (MPa)	1000, 3000, 10000
		h_2 (mm)	60, 120, 200
		ν_2	0.4
3	Sub-base	E_3 (MPa)	50, 100, 300
		h_3 (mm)	100, 300, 600
		ν_3	0.3
4	Subgrade	E_4 (MPa)	50,
	non linear	A (MPa)	50, 100, 200
	coefficients	B	0.0, 0.1, 0.3
		ν_4	0.4

Contact pressure = 700 kPa; Load radius = 150mm

Total no. of structures = 3^8 = 6561

Table 4.8 Parameters and their range of values used for the development of Stiffness Predictive Equations for 'THIN' asphalt pavements

Layer	Material	Parameters	Range of values
1	Asphalt	E_1 (MPa)	1000, 3000, 10000
		h_1 (mm)	100, 200, 300
		ν_1	0.4
2	Asphalt	E_2 (MPa)	1000, 3000, 10000
		h_2 (mm)	100, 200, 300
		ν_2	0.4
3	Sub-base	E_3 (MPa)	50, 100, 300
		h_3 (mm)	100, 300, 600
		ν_3	0.3
4	Subgrade	E_4 (MPa)	50,
	non-linear	A (MPa)	50, 100, 200
	coefficients	B	0.0, 0.1, 0.3
		ν_4	0.4

Contact pressure = 700 kPa; Load radius = 150mm

Total no. of structures = 3^8 = 6561

Table 4.9 Parameters and their range of values used for the development of Stiffness Predictive Equations for 'THICK' asphalt pavements.

were assigned for layers 1 and 2 (bituminous layers) only, while other parameters remained the same throughout the calculation. In deriving the equations, non-linear subgrade stiffness parameters A and B were varied in order that both linear and non-linear subgrade stiffnesses could be included.

As a result, six stiffness predictive equations were formed for E_1, E_2, E_3, E_f, A and B respectively for both the 'thin' and 'thick' structures, where E_1, and E_2 were the stiffnesses of the bituminous surfacing and roadbase layers, E_3 was the stiffness of the sub-base layer, E_f was the stiffness of the subgrade at formation level and A and B were non-linear subgrade stiffness parameters. A multiple regression analysis technique (83) was used to develop the above equations, where the coefficient of correlation, R^2, ranged from 0.473 to 0.956. Appendix B contains details of the predictive equations for both 'thin' and 'thick' structures. The reasons for obtaining predictive equations for parameters A and B was to enable the variation with depth of the non-linear subgrade stiffnesses to be estimated.

The next step is to check the accuracy of prediction of the equations by calculating the elastic stiffnesses from all the theoretical deflections from which the equations have been derived. The errors in stiffness prediction from each stiffness equation are plotted in Figures 4.15 and 4.16 for both 'thin' and 'thick' bituminous pavement structures. As may be seen in Figure 4.15 for 'thin' structures, the stiffness equation for E_f gives the best correlation with $R^2 = 0.956$, whilst E_1 shows the poorest correlation with $R^2 = 0.494$. The stiffness equations for E_f, A and B are observed to be able to predict the corresponding layer stiffnesses within 50% error for over 90% of the total number of structures, while the equivalent predictions for E_2, and E_3 are for about 80% of the total. This

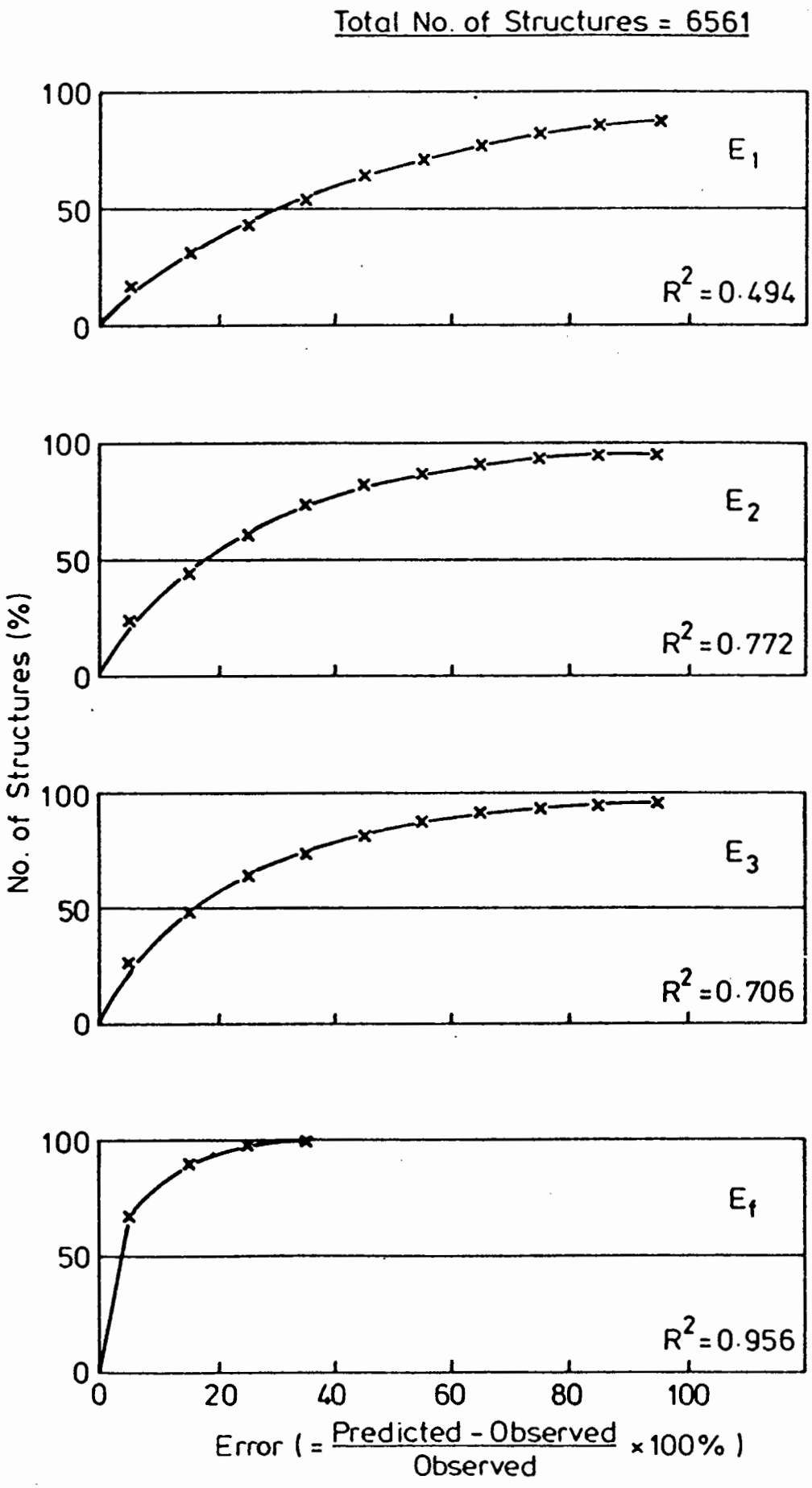

FIG. 4.15a CUMULATIVE FREQUENCY SHOWING ACCURACY OF PREDICTIVE EQUATIONS FOR 'THIN' ASPHALT STRUCTURES

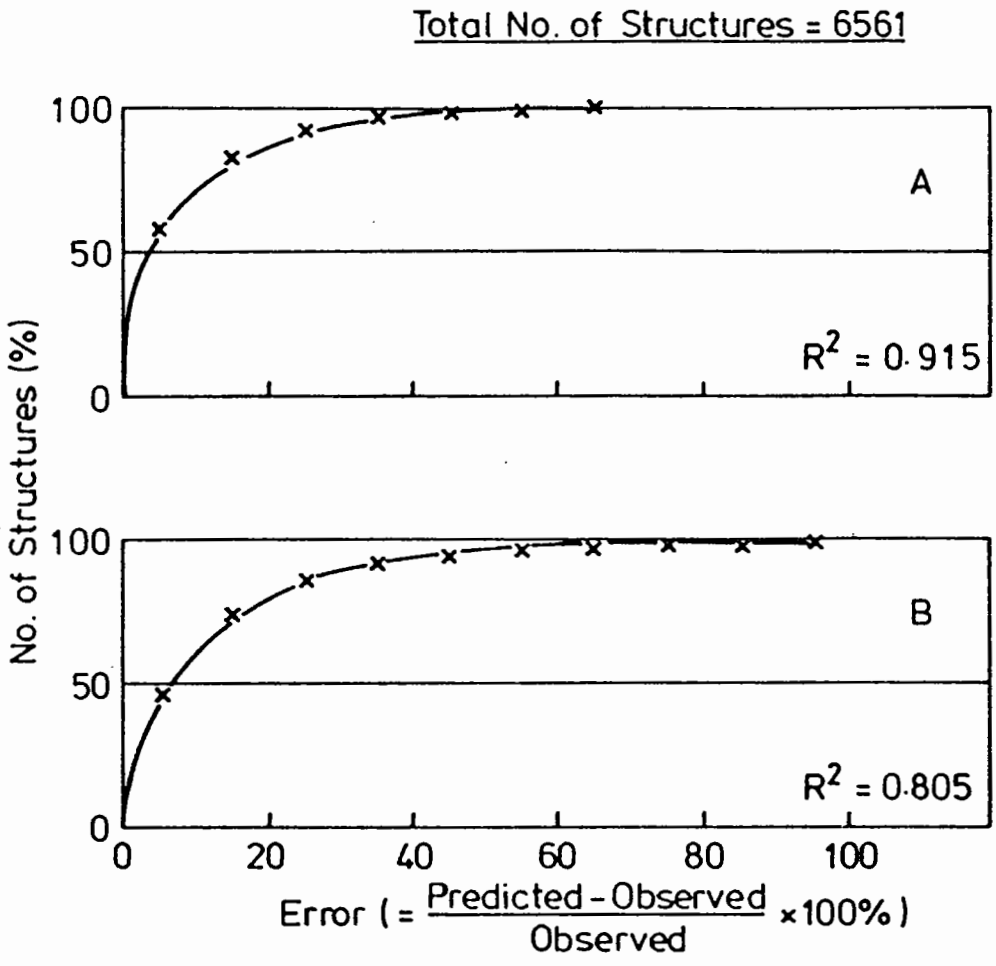

FIG. 4.15b CUMULATIVE FREQUENCY SHOWING ACCURACY OF PREDICTIVE EQUATIONS FOR 'THIN' ASPHALT STRUCTURES

compares with just over 65% of the total number of structures for E_1. The main cause for the poor correlation of the E_1 stiffness is the small thickness of layer 1, and hence the deflection bowls are not sensitive to variation of the E_1 stiffness.

Figure 4.16 shows the error in the calculated stiffness of each layer for the 'thick' structures. It is noted that the stiffness prediction for E_3 is the poorest with R^2 = 0.473. The best correlation is for the stiffness, E_1, with R^2 = 0.952 and, at the same time, the accuracy of prediction for the stiffness, E_f, is found to be reduced slightly with R^2 = 0.894 (refer Figure 4.15(a)). It is also observed that the stiffness equations for E_1, E_f, A and B are able to predict within 50% error for over 90% of the total number of structures, while the prediction for E_2 is slightly less good at 85% of the total. However, the stiffness equation for E_3 manages to predict within 50% error for only 70% of the total number of structures.

Close examination shows that errors of prediction larger than 50% always occur when parameters at the lower limit of the range are combined together for deflection computation, e.g. deflections calculated from the lowest layer stiffnesses and smallest layer thicknesses. Hence, from the analysis above, it is considered that the predictive equations may be used to estimate the elastic stiffnesses of a four-layered structure, with reasonable accuracy, if the magnitudes of the in-situ stiffnesses and thicknesses lie within the middle third of the range shown in Tables 4.8 and 4.9. Two computer programs have been written, for the 'thin' and 'thick structures, on the Hewlett Packard HP-85 micro-computer, with a view to estimating the elastic stiffnesses from the measured FWD deflections before more detailed back-analysis is carried out using the PADAL program. The programs have been extended to include the

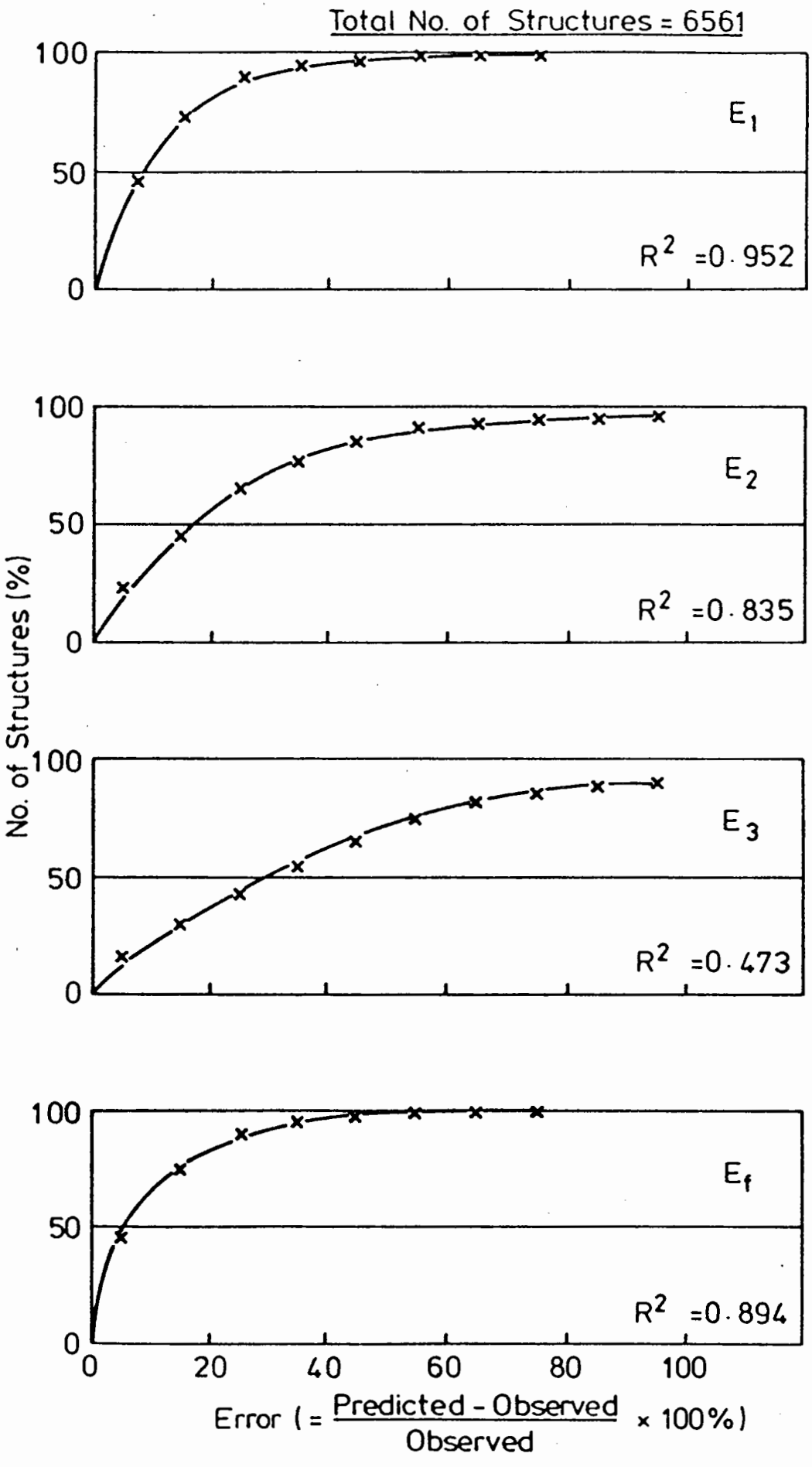

FIG. 4.16a CUMULATIVE FREQUENCY SHOWING ACCURACY OF PREDICTIVE EQUATIONS FOR 'THICK' ASPHALT STRUCTURES

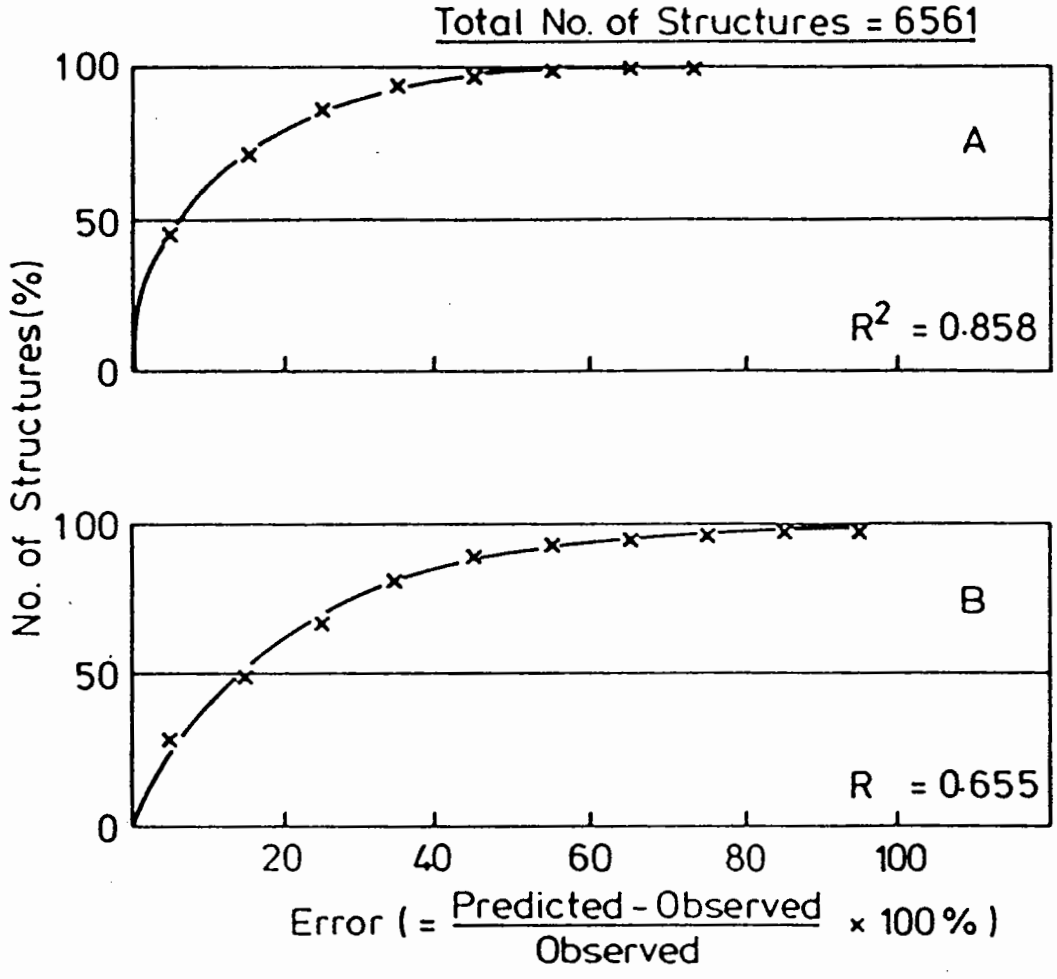

FIG. 4.16b CUMULATIVE FREQUENCY SHOWING ACCURACY OF PREDICTIVE EQUATIONS FOR 'THICK' ASPHALT STRUCTURES

stiffness prediction of three-layered structures. Similar developments have also been made separately for concrete pavements, as will be described in the forthcoming section.

As a further check, the theoretical deflection bowls of a number of four-layered structures were produced and the initial layer stiffnesses were computed using the predictive equations; it was then found that the estimated layer stiffnesses were able to improve the efficiency of the PADAL program. However, when the predictive equations were applied to some measured FWD deflection bowls for back-analysis, no significant improvement was observed on the efficiency of the PADAL program. A possible reason for this result is that the measured deflection bowls are not exactly the same as the theoretical bowls produced by the BISTRO program. As a result, these equations have not been incorporated into the PADAL program for routine analysis.

4.4.4 Applicability of PADAL program for concrete pavements: While developing the PADAL program for bituminous pavements, it was considered that similar iterative procedures and algorithm could also be applied for concrete pavement structures. Detailed descriptions of the iterative procedures and a similar algorithm have been given in Section 4.4.3. This section therefore summarises the salient features applicable only to concrete structures.

Convergence: The convergence criteria applicable to concrete structures are also summarised in Table 4.4. To ensure that unique solutions are derived, two criteria, similar to those for bituminous structures, one on stiffness and the other on deflection, are necessary. For the relative stiffness criterion, the difference between the last calculated stiffness value and the tenth previous value is limited to ± 30 MPa for lean concrete and pavement quality concrete layers; and ± 1 MPa for the sub-base and subgrade layers.

The deflection criterion limits the difference between the measured and calculated deflections to be less than ± 1% of the measured value. Convergence is said to be achieved if both criteria have been satisfied simultaneously. In order to avoid unduly long computing time, the execution is terminated after 100 iterations. The solution is then obtained by averaging the calculated stiffnesses over the last 30 iterations.

Determination of improved estimates of initial stiffnesses: As for bituminous structures, predictive stiffness equations for four-layered structures were developed for concrete pavements. Table 4.10 tabulates the parameters and range of values used to generate 2187(3^7) deflection bowls for analysis. The range of values was selected to cover the complete range for each parameter encountered in practical situations. For each combination, eight deflections between the load centre and a radial distance of 2100 mm, at spacings of 300 mm were calculated. It should be noted that only a linear subgrade was considered in developing the stiffness equations.

Four predictive stiffness equations were formed for the pavement quality concrete layer (E_1), lean concrete layer (E_2), granular sub-base layer (E_3), and the subgrade (E_4) respectively, using the multiple linear regression analysis technique (83). The general form of the equation is the same as that shown in equation (4.28) and details of the equations are given in Appendix B. The coefficients of correlation, R^2, are found to range from 0.429 to 0.998.

Figure 4.17 summarises the accuracy of prediction of the stiffness equations by substituting the original 2187 deflection bowls into the equations. It is clear that the equation for E_4 performs best, whilst E_3 is the poorest with E_1 and E_2 lying in between. Furthermore, the predictive equations for E_1, E_2, and E_4 are able to predict the corresponding layer stiffnesses within 50% error for over

Layer	Material	Parameters	Range of values
1	Pavement quality concrete	E_1 (MPa)	10000, 20000, 40000
		h_1 (mm)	100, 200, 400
		ν_1	0.2
2	Lean Concrete	E_2 (MPa)	5000, 10000, 30000
		h_2 (mm)	100, 200, 400
		ν_2	0.2
3	Sub-base	E_3 (MPa)	100, 200, 300
		h_3 (mm)	100, 300, 600
		ν_3	0.3
4	Sub-grade	E_4 (MPa)	50, 100, 300
		ν_4	0.4

Contact pressure = 1500 MPa; Load radius = 150mm

Total no. of structures = 3^7 = 2187

Table 4.10 Parameters and their range of values used for the development of Stiffness Predictive Equations for concrete pavements

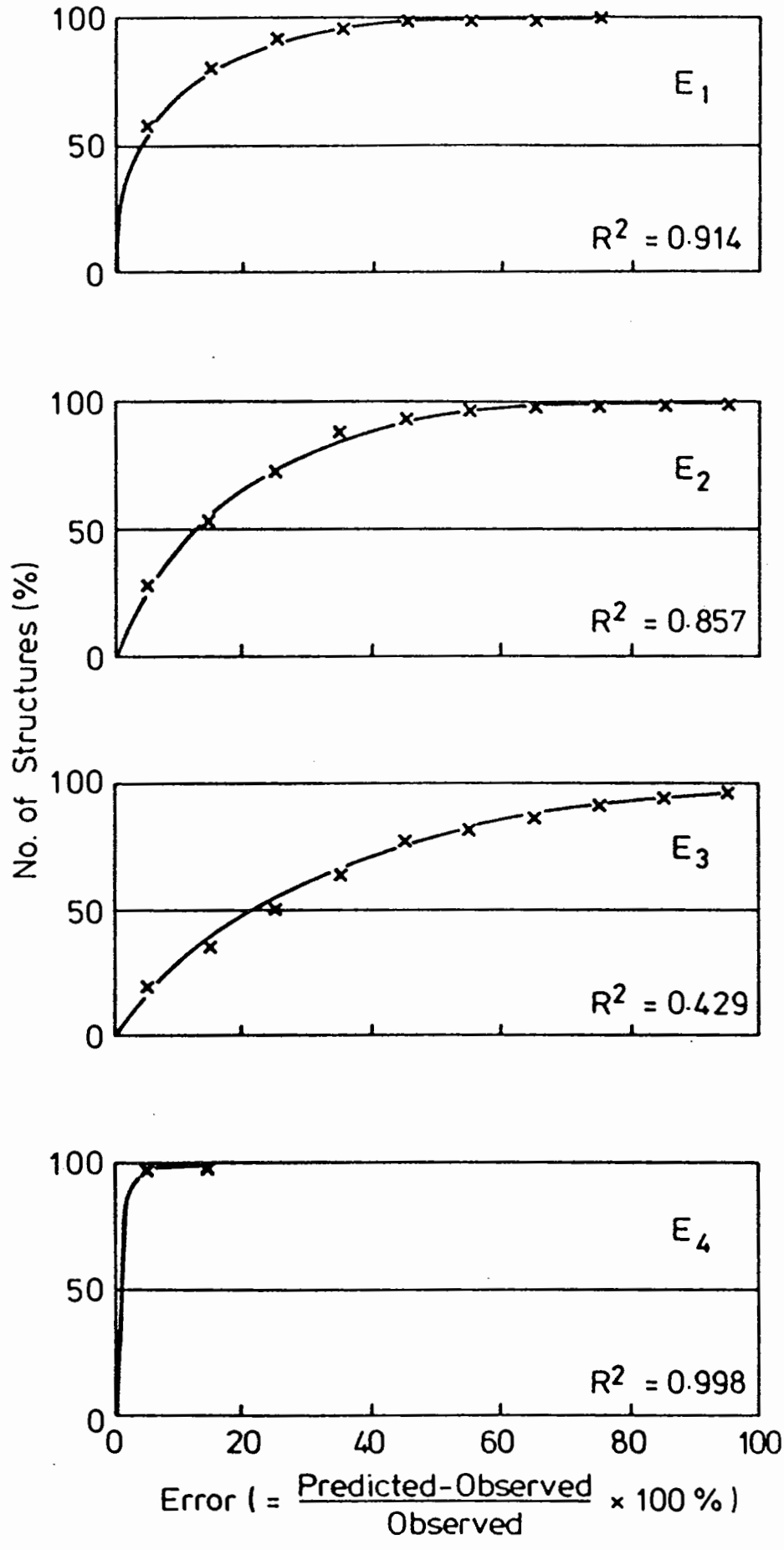

FIG. 4.17 CUMULATIVE FREQUENCY SHOWING ACCURACY OF PREDICTIVE EQUATIONS FOR CONCRETE STRUCTURES

90% of the total number of structures, whereas the stiffness equation for E_3 it manages for about 75% of the total.

The above predictive stiffness equations were then programmed into the Hewlett Packard HP-85 computer to estimate the elastic stiffnesses of four-layered structures. The program was later modified to include stiffness predictions for three-layered structures.

Uniqueness of solution: In order to investigate the accuracy of prediction of the PADAL program, 25 four-layered structures were selected, covering a wide range of stiffnesses and thicknesses. Theoretical deflection bowls for these structures were first computed. These deflections and layer thicknesses were entered into the predictive stiffness equations to estimate the stiffnesses of each layer as shown in Table 4.11. The PADAL program then back-analysed the stiffnesses of each layer for all the structures. Iteration was terminated when the specified convergence criteria were satisfied. Table 4.12 summarises the results of the calculation and error of prediction from the correct stiffnesses. As may be seen in the table, the stiffnesses of the concrete layers (including layeres 1 and 2) have errors of between 3.2% and -2.5%. The errors for the sub-base stiffness range from 0 to 18.6%. The stiffness of the subgrade layer was found to be the best predicted of all the layers, with errors ranging from 0.3% to -1.0%. From this analysis, it may be concluded that the PADAL program can be also used to predict the elastic stiffnesses of concrete structures with confidence.

4.5 VALIDATION OF ANALYTICAL METHODS

Both the BASEM and PADAL programs have been validated by comparing calculated stresses and strains with in-situ measured values, as well as by comparing back-analysed effective stiffnesses with stiffnesses determined in the laboratory.

Structure No.	Layer thicknesses (mm)	Layer Stiffness (MPa)				Error (%) from correct value			
		E1	E2	E3	E4	E1	E2	E3	E4
	Correct	40000	10000	300	300				
1	100+100+600	32006	12147	322	299	-20.0	21.5	7.3	-0.3
2	100+300+300	32012	12513	244	310	-20.0	25.1	-18.7	3.3
3	300+100+600	38326	13539	212	306	- 4.2	35.4	-29.3	2.0
4	300+300+300	41286	8478	187	307	3.2	-15.2	-37.7	2.3
5	200+200+300	41948	10678	217	310	4.9	6.8	-27.7	3.3
	Correct	40000	30000	300	300				
6	100+100+600	44656	25745	262	307	11.6	-14.2	-12.7	2.3
7	100+300+300	40087	32187	201	305	0.2	7.3	-33.0	1.7
8	300+100+600	35702	22420	207	303	-10.7	-25.3	-31.0	1.0
9	300+300+300	38420	25429	183	304	- 4.0	-15.3	-39.0	1.3
10	200+200+300	36913	25860	196	305	- 7.7	-13.8	-34.6	1.7
	Correct	30000	10000	200	300				
11	100+100+600	26906	11252	329	297	-10.3	12.5	9.7	-1.0
12	100+300+300	25656	12449	232	310	-14.5	24.5	-22.7	3.3
13	300+100+600	28833	12116	221	307	- 3.9	21.2	-26.3	2.3
14	300+300+300	30470	8287	196	307	1.6	17.1	-34.6	2.3
15	200+200+300	31189	10388	218	310	4.0	3.9	-27.3	3.3
	Correct	30000	30000	200	200				
16	100+100+600	35568	22554	193	204	18.6	-24.8	- 3.5	2.0
17	100+300+300	31647	29768	195	200	5.5	- 0.8	- 2.5	0.0
18	300+100+600	27788	19902	215	199	- 7.4	-33.7	7.5	0.5
19	300+300+300	28543	25290	204	200	- 4.9	-15.7	2.0	0.0
20	200+200+300	26686	24338	199	200	-11.0	-18.9	0.5	0.0
	Correct	10000	5000	150	100				
21	100+100+600	10663	5002	131	99	6.6	0.0	-12.7	-1.0
22	100+300+300	7045	8884	142	101	0.30	77.8	- 5.3	1.0
23	300+100+600	10224	7128	172	101	2.2	42.9	14.7	1.0
24	300+300+300	10931	4088	170	100	9.3	-18.2	13.3	0.0
25	200+200+300	10585	5689	167	101	5.9	13.8	18.0	1.0

Table 4.11 **Initial estimated stiffness from predictive equations - concrete pavements**

Structure No.	Layer thicknesses (mm)	Back-calculated layer stiffnesses (MPa)				Error (%)				No. of iterations
		E1	E2	E3	E4	E1	E2	E3	E4	
	Correct	40000	10000	300	300					
1	100+100+600	40030	9994	300	300	0.08	-0.06	0.0	0.0	26
2	100+300+300	41279	9843	301	300	3.2	-1.6	0.3	0.0	32
3	300+100+600	39926	10166	298	300	-0.2	1.7	-0.7	0.0	49
4	300+300+300	39998	10002	300	300	-0.0	0.0	0.0	0.0	55
5	200+200+300	39922	10022	300	300	-0.2	0.2	0.0	0.0	33
	Correct	40000	30000	300	300					
6	100+100+600	40580	29621	300	300	1.5	-1.3	0.0	0.0	37
7	100+300+300	40094	29967	299	300	0.2	-0.1	-0.3	0.0	46
8	300+100+600	39999	30027	300	300	0.0	0.1	0.0	0.0	56
9	300+300+300	40023	29990	299	300	0.0	0.0	0.3	0.0	76
10	200+200+300	39818	30152	299	300	-0.5	0.5	-0.3	0.0	39
	Correct	30000	10000	300	300					
11	100+100+600	30409	9896	300	300	1.4	1.0	0.0	0.0	42
12	100+300+300	30060	10000	299	300	0.2	0.0	-0.3	0.0	100
13	300+100+600	29911	10146	299	300	-0.3	1.5	-0.3	0.0	41
14	300+300+300	29989	9999	300	300	-0.0	0.0	0.0	0.0	57
15	200+200+300	29976	10001	300	300	-0.08	0.0	0.0	0.0	26
	Correct	30000	30000	200	200					
16	100+100+600	30418	29592	200	200	1.4	-1.4	0.0	0.0	87
17	100+300+300	30044	29981	200	200	0.1	-0.06	0.0	0.0	34
18	300+100+600	30016	29940	200	200	0.0	-0.2	0.0	0.0	82
19	300+300+300	30001	29990	201	200	0.0	-0.0	0.5	0.0	73
20	200+200+300	29963	30012	201	200	-0.1	0.04	0.5	0.0	35
	Correct	10000	5000	150	100					
21	100+100+600	9762	5095	150	100	-2.3	1.9	0.0	0.0	80
22	100+300+300	9749	5069	151	100	-2.5	1.4	0.7	0.0	53
23	300+100+600	9996	5014	150	100	-0.04	0.3	0.0	0.0	32
24	300+300+300	10156	4943	153	100	1.6	-1.1	2.0	0.0	40
25	200+200+300	9994	4981	152	100	-0.06	0.4	1.3	0.0	17

Table 4.12 Back-calculated layer stiffnesses using PADAL program - concrete pavements

4.5.1 Comparison of stresses and strains in the A617 Hasland Bypass

In-situ vertical stresses and strains in the subgrade were measured during a FWD survey in August,1984 on the A617 Hasland Bypass, westbound carriageway. Full details of the instrumentation were documented in a report by Brown et al (84). Figure 4.18 shows a typical design section through the experimental pavement, in which two sets of pressure cells and strain coils have been installed at 0.5 m intervals in the nearside wheelpath, 100 mm below the formation level of the subgrade.

Stress and strain measurements were taken beneath both the Benkelman Beam (BB) and the FWD by experienced staff. Table 4.13 summarises the results of the measurements. During the site measurement, one of the pressure cells at Chainage 62.5 m was noted to be malfunctioning. The effective elastic stiffnesses of the structure in Figure 4.19 were evaluated manually, since the BASEM program was not yet ready for automatic back-analysis at that time. Table 4.14 shows the results of the calculation. The maximum deflection from the BB was modelled by assuming the subgrade to be linear. During the process of computing the deflection at Chainage 62.0 m, a judgment has been made to assign the appropriate stiffnesses for each layer. Since only one deflection was measured at Chainage 62.0 m, this value was assumed to be the same in the other locations. The deflection bowls obtained from the FWD were modelled assuming the subgrade to be linear and non-linear respectively. The idea is to assess the merit of introducing subgrade non-linearity into the calculation. From the table, it is observed that, by assuming the subgrade to be non-linear (case(iii)), the deflection bowls can be modelled to a much higher degree of accuracy than with a linear subgrade (case(ii)). The non-linear subgrade stiffnesses were computed to vary from 79 MPa (at formation level) to about 200 MPa (bottom sub-layer) (refer Figure

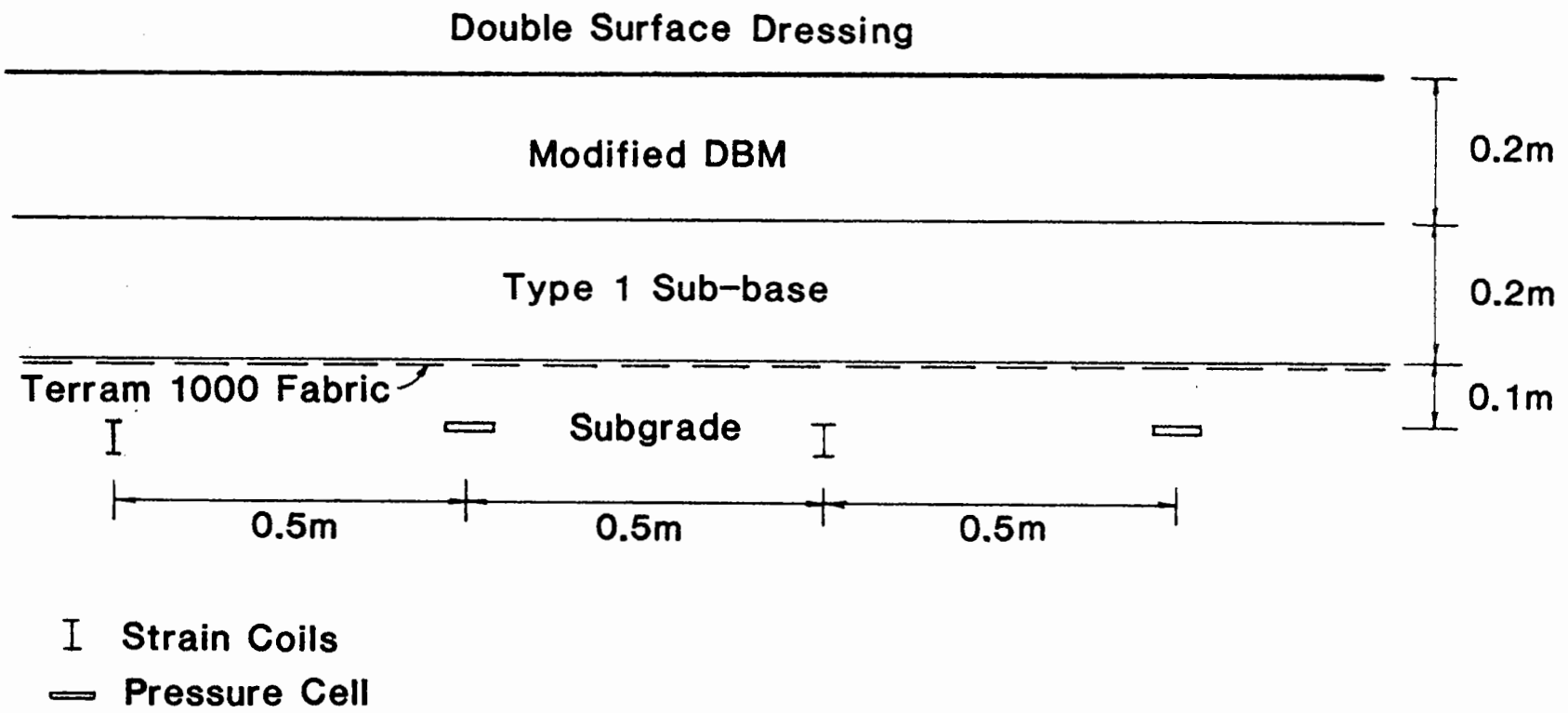

FIG. 4.18 EXPERIMENTAL SECTION STRUCTURE FOR A617 HASLAND BYPASS SHOWING LOCATION OF INSTRUMENTS

Chainage (m)	Applied Pressure (kPa)	Vert. subgrade stress[2] (kPa)		Vert. subgrade strain[3] (μm)	
		Location of instruments from load			
		Centre	0.5 m	Centre	0.5 m
(i) BB					
62.0	285[1]	-	-	493	-
63.0	285[1]	-	-	748	-
63.5	285[1]	32.3	-	-	-
(ii) FWD					
62.0	1023	-	-	378	-
62.5	1020	-	-	-	242
63.0	1019	-	22.7	789	-
63.5	1019	55.7	-	-	353

[1] Dual wheel load.

[2] Values shown have been corrected by a factor of 0.92 for dynamic effect (85).

[3] Values shown have been corrected for dynamic effect by a factor of 1.32 for BB and 1.36 for FWD.

Table 4.13 Measured Vertical Stresses and Strains in Subgrade with BB and FWD (8.8.84)

Table 4.14 Backcalculated Layer Moduli using Deflections from BB and FWD

Chainage (m)	Applied Pressure (MPa)	Subgrade Assumption		Calc. Layer Moduli (MPa)			Calculated Surface Deflection (μm)							Error[a] (%)						
				Base	Sub-base	Subgrade (top)	D1	D2	D3	D4	D5	D6	D7[b]	D1	D2	D3	D4	D5	D6	D7
(i) BB																				
62.0	285	linear		1300	90	45	498							-0.4						
63.0	285	linear		1300	90	45	498							-0.4						
63.5	285	linear		1300	90	45	498							-0.4						
			Ave	1300	90	45														
(ii) FWD																				
62.0	1023	linear		3300	100	105	640	486	337	235	170	130	104	3.4	-4.0	-0.9	9.3	21.4	32.7	48.6
62.5	1020	linear		2800	100	103	681	506	345	237	171	131	106	4.1	-1.6	0.6	9.2	24.8	37.4	51.4
63.0	1019	linear		2700	100	103	689	510	345	237	170	130	105	4.9	-4.3	-0.9	9.7	25.9	36.8	38.2
63.5	1019	linear		2700	100	103	689	510	345	237	170	130	105	1.0	-4.3	0.9	13.4	25.0	38.3	45.8
			Ave	2875	100	103.5														
(iii) FWD																				
62.0	1023	nonlinear		3200	100	80 (B=0.17)	647	486	326	214	142	98	72	4.5	-4.1	-4.1	-0.5	0.7	0	2.8
62.5	1020	nonlinear		2800	100	79 (B=0.17)	681	503	331	214	141	97	71	4.1	-2.1	-4.6	-1.4	1.4	3.2	1.4
63.0	1019	nonlinear		2700	100	81 (B=0.15)	689	506	334	216	144	101	75	4.9	-5.0	-4.0	0	6.6	6.3	1.3
63.5	1019	nonlinear		2400	100	83 (B=0.15)	709	510	329	209	138	96	72	4.0	-4.3	-3.8	0	1.5	2.1	0
			Ave	2775	100	81.75														

a error = ((Calculated-measured)/measured) x 100%

b deflections obtained at 300 mm intervals.

4.19). Therefore, it is clear that the calculation with a linear subgrade assumption underpredicts the stiffnesses of the subgrade at depth but overpredicts at formation level and, hence, it is reflected by a slightly higher derived elastic stiffness for the bituminous layer. When comparing the effective stiffnesses for the bituminous layer between the BB and FWD, it is considered loading time is the main cause for the difference. Since the BB travelled at a speed of about 2 km/hr as compared with about 30 km/hr effectively for the FWD, it is logical to expect that the effective stiffness of the bituminous layer from the BB would be lower than that from the FWD.

The next step is to compare the measured and calculated stresses and strains. Figure 4.19 shows the structures used for the case with a non-linear subgrade assumption. For BB loading, dual loads, each of contact pressure 285 kPa, are used, whereas the contact pressure for the FWD is shown in Table 4.14 applying over a loading platen of 300 mm diameter. The vertical stresses and strains at a depth of 0.5 m beneath the load centre and at 0.5 m distance have been computed and are shown in Table 4.15. It is interesting to observe that the vertical stresses computed for cases (ii) and (iii) (linear and non-linear subgrades) are about the same whereas the vertical strains calculated for case (iii) are higher than the corresponding ones in cases (ii). Table 4.16 compares the measured and calculated vertical stresses and strains in the subgrade.. The following observations can be made.

(a) For BB loading, as in case (i), the calculated values compare poorly with the measured ones, with average error of 80% for vertical stress and 61% for vertical strain. This indicates that the method assuming linear elastic response of the pavement structure under the BB loading is not appropriate. Another method, e.g. a visco-elastic anlaysis is preferable.

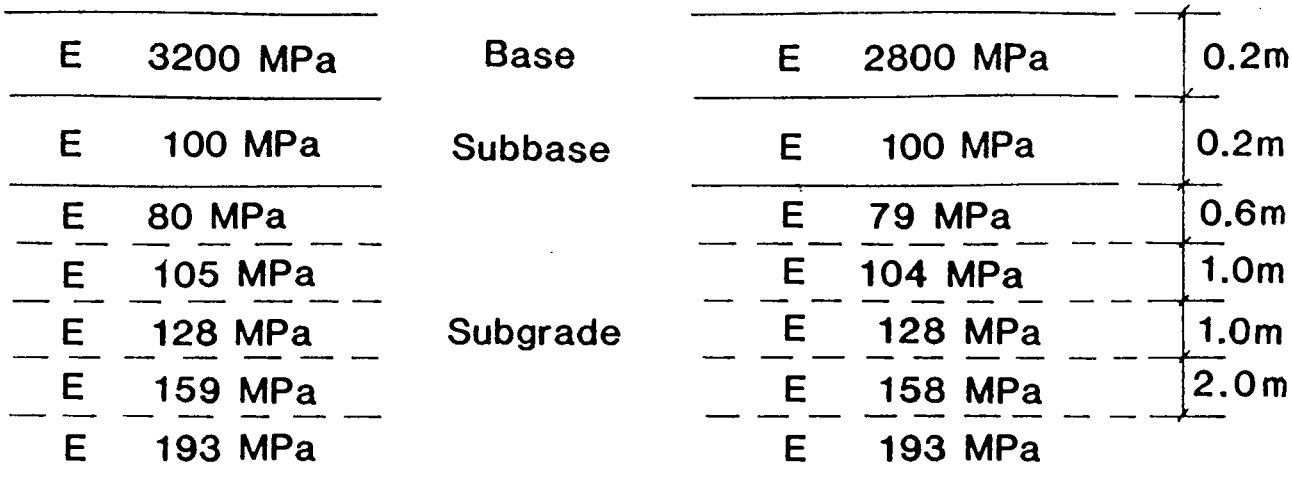

(a) Ch. 62.0m

(b) Ch. 62.5m

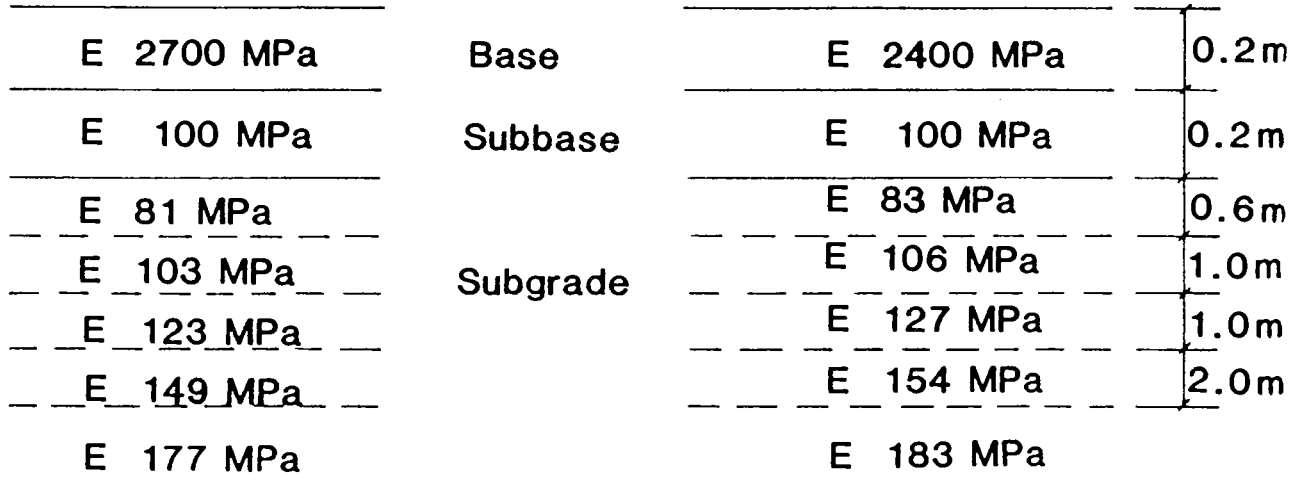

(c) Ch. 63.0m

(d) Ch. 63.5m

FIG. 4.19 STRUCTURES FOR CALCULATION OF STRESSES AND STRAINS

Chainage (m)	Applied Pressure (kPa)	Vertical subgrade stress (kPa)		Vertical subgrade strain (με)	
		Location of Instruments from Load			
		Centre	0.5 m	Centre	0.5 m
(i) BB					
62.0	285	17.88	-	386	-
63.0	285	17.88	-	386	-
63.5	285	17.88	-	386	-
	Ave	17.88		386	
(ii) FWD (linear subgrade)					
62.0	1023	-	-	415	-
62.5	1020	-	-	-	192
63.0	1019	-	24.6	459	-
63.5	1019	50.5	-	-	192
	Ave	50.5	24.6	437	192
(iii) FWD (nonlinear subgrade)					
62.0	1023	-	-	514	-
62.5	1020	-	-	-	244
63.0	1019	-	24.3	546	-
63.5	1019	51.0	-	-	241
	Ave	51.0	24.3	530	242.5

Table 4.15 Calculated Vertical Subgrade Stresses and Strains

Chainage (m)	Meas./calc. ratio for vert. subgrade stress		Meas./calc. ratio for vert. subgrade strain	
	Location of Instruments from Load			
	Centre	0.5 m	Centre	0.5 m
(i) BB				
62.0	-	-	1.28	-
63.0	-	-	1.94	-
63.5	1.80	-	-	-
Ave	1.80		1.61	
(ii) FWD (linear subgrade)				
62.0	-	-	0.91	-
62.5	-	-	-	1.26
63.0	-	0.92	1.72	-
63.5	1.10	-	-	1.84
Ave	1.10	0.92	1.32	1.55
(iii) FWD (nonlinear subgrade)				
62.0	-	-	0.74	-
62.5	-	-	-	0.99
63.0	-	0.93	1.45	-
63.5	1.09	-	-	1.46
Ave	1.09	0.93	1.10	1.23

Table 4.16 Comparison of Measured and Calculated Vertical Subgrade Stresses and Strains

(b) The calculated vertical stresses in cases (ii) and (iii) come within 10% of the measured values at the load centre whereas, at 0.5 m distance, a slightly better correlation, with an error of 7 - 8%, is obtained.

(c) Correlation of the vertical strains in case (iii) (non-linear subgrade) with measured values is much better than for case (ii) (linear subgrade), e.g., 10% error for case (iii) at the load centre as compared with 32% error for case (ii). Also, in both cases, the errors computed at the load centre compare favourably with those at 0.5 m distance.

From the observations in (b) and (c) above, it is clear that the method of taking consideration of subgrade non-linearity is the most realistic method for evaluating pavement structures. This analysis thus confirms the procedures for incorporating non-linear subgrade behaviour proposed in the BASEM and PADAL programs.

4.5.2 Comparison of elastic stiffnesses

As part of the detailed structural evaluation of the A617 Hasland Bypass in 1986, a large number of samples were taken from the site for analysis. Full details of the evaluation will be discussed in Chapter 6. The main objective here is to compare the elastic stiffnesses back-analysed by the PADAL program with the laboratory results.

The results of the comparison for the bituminous materials are given in Table 4.17. Seven 102 mm diameter cores were obtained from the existing pavement, of which two cores at Ch. 30 m on the eastbound carriageway were fully bonded at the interface, whilst the interface of the other five cores were found to be debonded. Push-pull tests were performed to determine the elastic stiffnesses of the fully bonded cores whilst indirect tensile tests (ITT) were applied to the debonded samples since their lengths were too short for push-pull

tests. The tests were carried out with a frequency of 4 Hz and over a range of temperature up to 35°C. The resulting measured elastic stiffnesses are given in column (1) of Table 4.17. Back-analysis was carried out using the PADAL program on the structures at the positions where cores were taken. In all calculations, the interfaces between the layers were assumed to be fully bonded. The results of the PADAL calculation are shown in column (2) of the table. When comparing with the measured results in column (1), the stiffnesses derived from the debonded bituminous layers are found to be consistently lower than the measured results whereas this is not observed for the cases with the fully bonded layers determined at Ch. 30 m. Hence, it can be deduced that debonding must be the cause of the reduction of the effective back-analysed stiffnesses. For fully bounded bituminous layers, the comparison with the measured values appears satisfactory. with the mean ratio of 1.0, even though the ratios vary by up to 24%.

A separate computation was performed using the BISAR(60) computer program which considers the influence of the debonded layer within the bituminous material. The calculation was performed manually by adjusting the stiffness of the bituminous layer until the calculated and measured deflection bowls were accurately matched whilst keeping the back-analysed stiffnesses of both the sub-base and subgrade unchanged. The degree of smoothness at the interface has been assumed to be 0.7 in all caculations. Column (3) of the table shows the results of elastic stiffnesses including the effect of debonding. Comparison with the measured values in column (1) gives ratios ranging from 0.87 to 1.64, giving an overall mean of 1.39.

As for the bituminous material, a series of triaxial tests was undertaken on the unbound granular sub-base and clay subgrade material taken from the trial pits. The sizes of specimen used for

Location		Elastic stiffness (MPa)				
		Measured (1)	PADAL* (2)	BISAR+ (3)	(2)/(1)	(3)/(1)
Eastbound						
Ch. 20m LC	D	6700	4690	11000	-	1.64
Ch.100m LC	D	7500	2100	6500	-	0.87
Ch.180m LC	D	5900	2790	9000	-	1.53
Ch. 30m WP	F	11200	8470	-	0.76	-
Ch. 30m LC	F	5000	6180	-	1.23	-
Westbound						
Ch.125m WP	D	3350	1810	5000	-	1.49
Ch.140m LC	D	3200	1490	4500	-	1.41
				Mean	1.00	1.39
				Overall Mean	1.19	

Notes: Stiffnesses measured in laboratory using push-pull or I.T.T. tests.
* - stiffnesses inclusive of the effect of debonding
+ - stiffnesses without the effect of debonding
D - Cores with debonding interface
F - Cores with full bond

Table 4.17 Comparison of back-analysed elastic stiffnesses of bituminous cores using PADAL program with laboratory results

Location	Elastic stiffness (MPa)					
	Granular sub-base			Clay subgrade		
	Measured (1)	PADAL (2)	(2)/(1)	Measured (3)	PADAL (4)	(4)/(3)
Ch. 125m WB (TP1)	62	31	0.50	80	175	2.18
Ch. 100m EB (TP2)	85	48	0.56	390	201	0.52
Ch. 20m EB (TP3)	390	262	0.67	-	-	-
		Mean	0.58		Mean	1.35

Note: stiffnesses measured in the triaxial apparatus under repeated loading.

Table 4.18 Comparison of back-analysed elastic stiffnesses of unbound layers using PADAL program with laboratory results

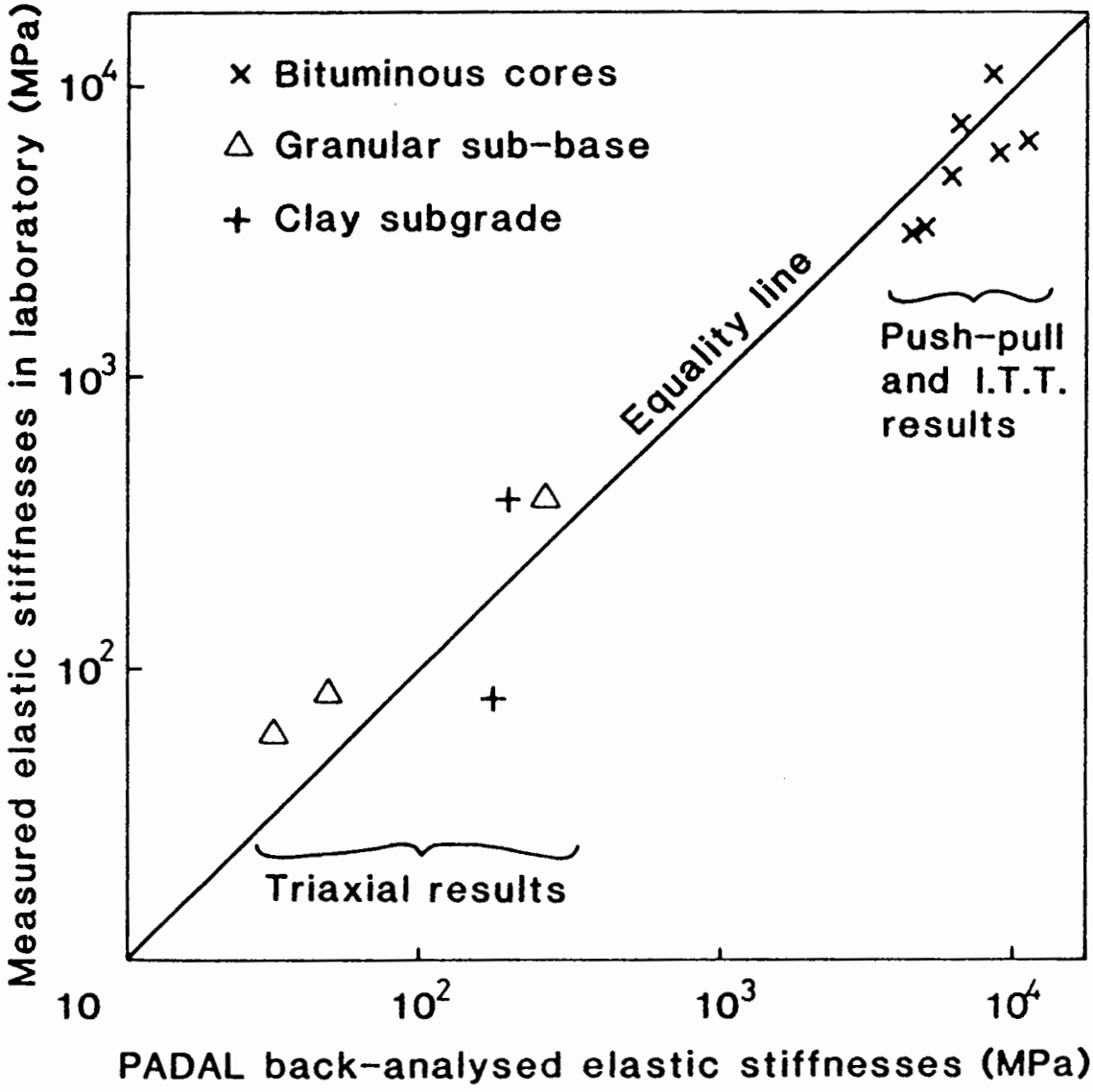

Fig. 4.20 COMPARISON OF ELASTIC STIFFNESSES BACK-ANALYSED USING PADAL AND LABORATORY RESULTS

the triaxial tests were 150 mm diameter and 300 mm height for the granular material and 102 mm diameter and 150 mm height for the clay material. The tests were carried out over a range of stress paths simulating the traffic loading, at 1 Hz frequency, at room temperature. The measured stiffnesses are presented in Table 4.18, appropriate to the in-situ stress conditions, together with the values back-analysed using the PADAL program. As seen in the table, the back-analysed stiffnesses for the granular sub-base material are consistently lower than the measured values with a mean ratio of 0.58. The results for the clay subgrade, however, vary more widely, ratios ranging from 0.52 to 2.18 with a mean of 1.35.

In summary, the results of the comparison of back-analysed elastic stiffnesses with laboratory results are reasonably good. The best comparison is observed for bituminous material, where the prediction is about 20% from the measured values. The correlation for the granular sub-base and the clay subgrade is found to be less good but within a factor of two, their mean ratios being 0.58 and 1.35 respectively. However, it is considered that the comparison for the unbound materials is not as conclusive as for the bound bituminous materials and, therefore, more results are necessary to clearly establish the relationship. Figure 4.20 shows the results of the comparsion between the back-analysed stiffnesses determined by the PADAL program and the corresponding laboratory results.

4.6 COMPARISON WITH DYNAMIC ANALYSIS

4.6.1 A Review of recent developments in dynamic analysis

Judging from the above comparisons, the PADAL computer program, based on static loading for back-analysis, is found to be both realistic and efficient. However, some concern has been raised about the accuracy of its stiffness prediction using the deflection bowls produced by the FWD dynamic loading, in particular the inertial

effect of the pavement on the measured deflections. Furthermore, the significance of the effect of dynamic loading was observed by Hoffman and Thompson (11), who used non-destructive testing equipment, including the FWD and the Road Rater, for their study. Figure 4.21 is included to illustrate the response of the maximum deflection, measured by a Road Rater, at different driving frequencies at six different sites. It may be clearly seen for all six sites that the trend of the deflections is generally to rise to a peak and then decrease. At this peak deflection, the pavement is said to have resonated at its natural frequency.

In 1984, Mamlouk and Davies (86) proposed the formulation of a dynamic analysis, simulating a dynamic loading on a pavement structure. A similar analysis was also proposed by Roesset and Shao (80) in 1985. A brief summary of the method is attempted below.

Consider a flexible pavement structure idealized as a layered visco-elastic continuum overlying bedrock at a finite depth as shown in Figure 4.22. Five parameters are required in each layer, namely, Young's modulus (E), Poisson's ratio (v), material damping (β), density (ρ), and layer thickness (h). Each layer is assumed to be linear, elastic and isotropic. Rough interfaces are also assumed between layers.

Mamlouk and Davies (86) proposed to solve the response of the structure to applied dynamic loads by using wave propagation theory. The formulation starts by considering steady-state harmonic forces and displacements at a given frequency. In the case of a harmonic excitation caused by a vibrating machine, rotating at a specified velocity (e.g. Road Rater), a direct solution can be obtained. For an arbitrary transient excitation (e.g. FWD), the time history of the specified forces are first decomposed into different frequency components using Fourier Transforms. Results obtained for each

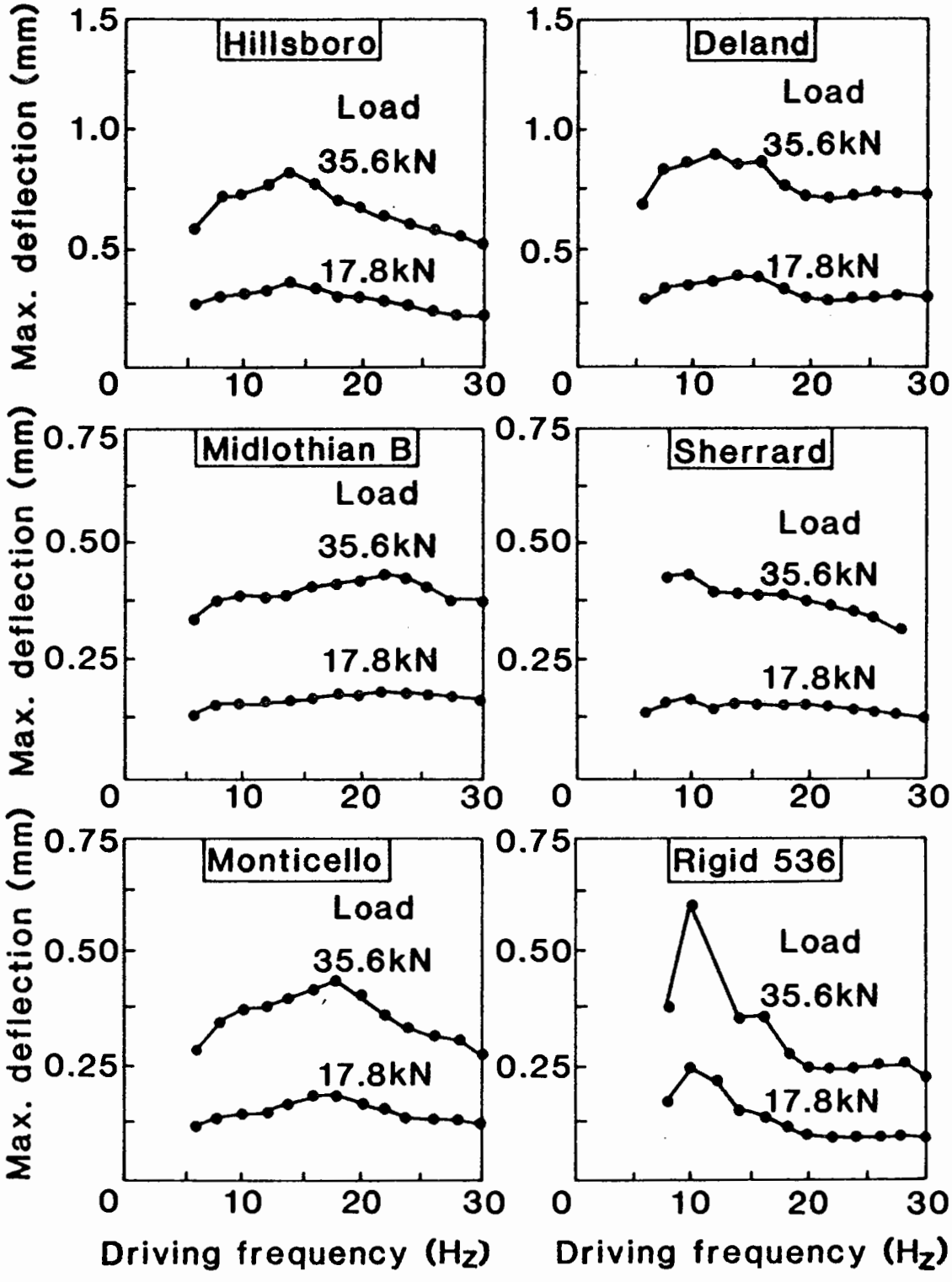

Fig. 4.21 TYPICAL ROAD RATER LOAD AND FREQUENCY SWEEP TEST RESULTS (after HOFFMAN AND THOMPSON (11))

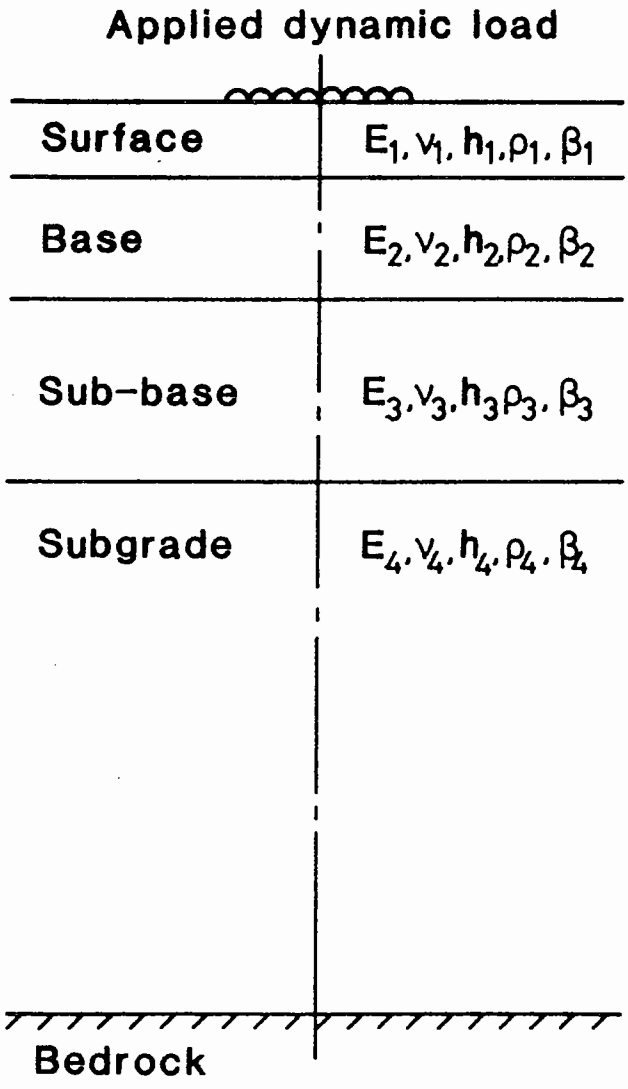

Fig. 4.22 FLEXIBLE PAVEMENT CHARACTERISATION FOR DYNAMIC ANALYSIS

frequency are then combined to form a time history of displacements by inverse Fourier Transforms. Thereafter, the numerical solution of Kausel and Peek (87) is applied, which involves the sub-division of the given layered system into thin artificial sub-layers. For each sub-layer, a stiffness matrix in the so-called frequency-wave number domain, relating forces and displacements, may be found. Stiffness matrices for each layer can then be assembled to form a global stiffness matrix, in a similar way to finite element formulation. The displacements are computed by solving the global stiffness matrix.

Based on the above method, Davies and Mamlouk (88) studied the effect of frequency on the surface deflections for different combinations of stiffnesses and thicknesses. They noted that:

(a) For the same frequency, the stiffer the pavement, the closer to unity was the ratio of dynamic and static deflections. When the pavement was weak, the deflection ratio decreased.

(b) The deflection ratios tended to increase with increasing subgrade stiffness and decreasing pavement stiffness, but tended to decrease at frequencies above the resonant frequency. The latter was caused by inertial forces increasing rapidly with increasing frequency.

(c) Static back-analysis of dynamic deflections might yield misleading results if the driving frequency of the loading device was close to the resonant frequency of the pavement structure or was so high that inertial forces became dominant.

(d) Resonance in the subgrade was pronounced if the rock layer was found to be at shallow depth.

Using the same method as mentioned above, Sebaaly et al (89) studied the dynamics of the FWD. They reported that deflections produced by the FWD loading lagged behind the loading pulse due to the inertia

effect of a pavement structure. Based on their theoretical analysis, they concluded that static back-analyses of FWD results could over-estimate the stiffness of a pavement by approximately 25-30%.

Roesset and Shao (80) investigated the effect of depth to bedrock on the dynamic response of a pavement. Both the FWD and Dynaflect were examined. They reported that:

(a) The effect of bedrock was insignificant if its depth was more than 20 metres.

(b) Dynamic effects were much less pronounced for the FWD because a broad range of frequencies was excited instead of a single one, as in the case of the Dynaflect.

4.6.2 Comparison with dynamic analysis results

As already noted in the literature, Sebaaly et al (89) suggested that the static back-analysis of FWD deflections could over-estimate fairly significantly the stiffness of the pavement layers. Since the back-analysis computer program PADAL (refer Chapter 4) was developed based on a static load assumption, it was therefore important to compare the predicted stiffnesses with the dynamic analysis method proposed by Mamlouk and others based on deflections produced by the FWD.

In this comparison, deflection bowls over three different sites were selected. Table 4.19 tabulates the details of each pavement structure, the measured deflections and loading conditions. It is noted that structure$^{nos.}$ 1, 2 and 3 correspond to two-, three- and four-layered bituminous structures respectively. These three deflection bowls were back-analysed using the PADAL computer program and the results of the elastic stiffnesses are summarised in Table 4.20. The information given in Tables 4.19 and 4.20 was then sent to Mamlouk at the University of Arizona, U.S.A. in 1986 for carrying out dynamic calculations.

Structure 1 : Aetheric Road

Layer 1 =	Asphalt Surfacing and Roadbase	330mm thick
2 =	Subgrade	CBR about 6% (sub-divide into 5 layers) (thicknesses to be 0.6m, 1.0m, 1.0m, 2.0m, ∞)
FWD radial position of geophones (7)(m)		= 0, 0.3, 0.6, 0.9, 1.2, 1.5, 1.8
measured deflections (μm)		= 183, 140, 103, 68, 49, 30, 23
platen radius		= 150mm
contact pressure		= 642 kPa
Back-calculated elastic stiffnesses		= see Table 4.20

Structure 2 : Hasland Bypass

Layer 1 =	Asphalt Base	220mm thick
2 =	Granular sub-base	220mm thick
3 =	Subgrade	CBR about 4.5% (sub-divide into 5 layers) (thickness as Structure 1)
FWD radial position of geophones		= as Structure 1
measured deflections (μm)		= 528, 390, 225, 125, 75, 54, 39
platen radius		= 150mm
contact pressure		= 700 kPa
Back calculated elastic stiffnesses		= see Table 4.20

Structure 3 : Bideford Bypass

Layer 1 =	Asphalt Surfacing	90mm thick
2 =	Lean concrete	200mm thick
3 =	Sub-base and capping layer	370mm thick
4 =	Subgrade	(sub-divide into 5 layers) (thickness as Structure 1)
FWD radial position of geophones		= as Structure 1
measured deflections (μm)		= 154 115, 88, 63, 46, 32, 24
platen radius		= 150mm
contact pressure		= 1100kPa
Back-calculated elastic stiffnesses		= see Table 4.20

Table 4.9 Details of pavement structures for dynamic analysis

Structure No.			1	2	3
Material	Poisson's ratio	Unit Weight (kg/m³)	Layer stiffnesses (MPa)		
Asphalt	0.4	23)	3813	1809	2450
Asphalt	0.4	23)			
Lean concrete	0.2	24	-	-	27450
Sub-base	0.3	20	-	31	200
Subgrade	0.4	20	119	175	340
			181	176	410
			261	178	500
			387	180	630
			651	182	840

Table 4.20 **Details of back-analysed layer stiffnesses**

Since his program was only capable of carrying out forward analysis, Mamlouk therefore computed the resultant surface deflection response by inputting the material properties of each layer, including the non-linear elastic stiffnesses of the subgrade and the corresponding FWD loading. In the calculation, a rigid layer at a depth of 18 m was assumed and a typical damping ratio of 5% was also assumed for each layer. The dynamic loading pulse was taken as harmonic with a pulse time of 40 msec, occurring over a total period of 220 msec. Calculation was performed at 4 msec intervals in order to capture the peak deflection value. Figure 4.23 illustrates the variation of deflection with time for the three structures. Two points are clearly observed from the figure. Firstly, the deflection rises sharply as the load is being applied and then rapidly reduces, followed by small oscillations. Secondly, the time corresponding to the peak deflection at each radial position is not the same. The further the radial position (e.g. a geophone of the FWD) is away from the load, the longer the time that is taken to reach the peak value. Also, the difference in arrival time at the geophones is influenced by the stiffnesses of the structure. It is seen that the difference in arrival time between d_1 and d_7 is smallest for Bideford Bypass, where the structure is the stiffest, whereas the greatest difference can be observed on the weaker structure of Hasland Bypass. The structure of Aetheric Road lies in between the two.

Figures 4.24a and b compare the computed deflection bowls, using the dynamic analysis, and the measured values. Very good agreements are clearly observed. It is interesting to note that the deflections computed by the dynamic analysis program are generally slightly lower than the measured values near the loaded area but slightly higher at radial distances between 900 and 1800mm. However, it is considered that a comparison of the deflection bowls alone is not sufficient to

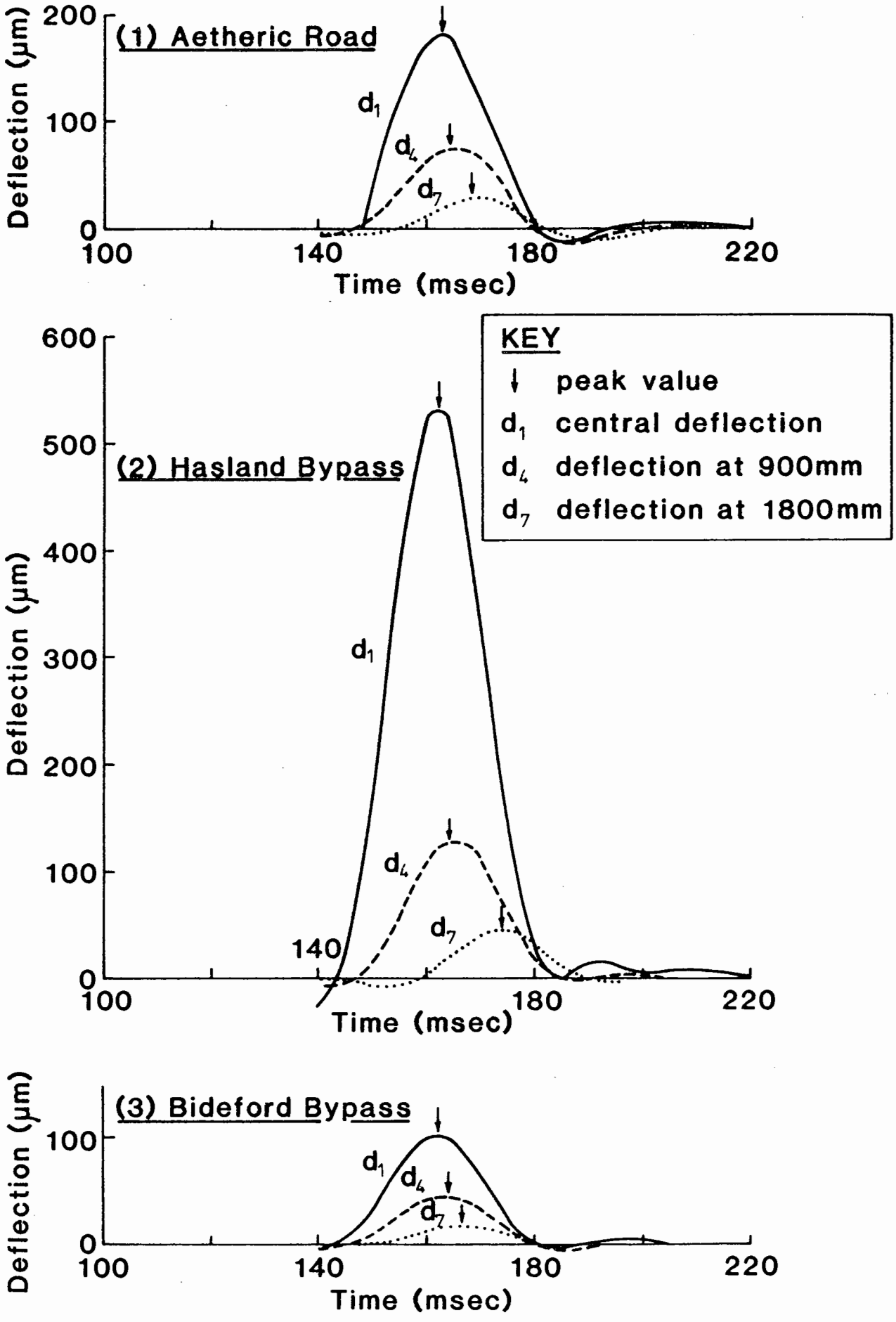

Fig. 4.23 VARIATION OF DEFLECTION WITH TIME COMPUTED BY DYNAMIC ANALYSIS WITH F.W.D. LOADING

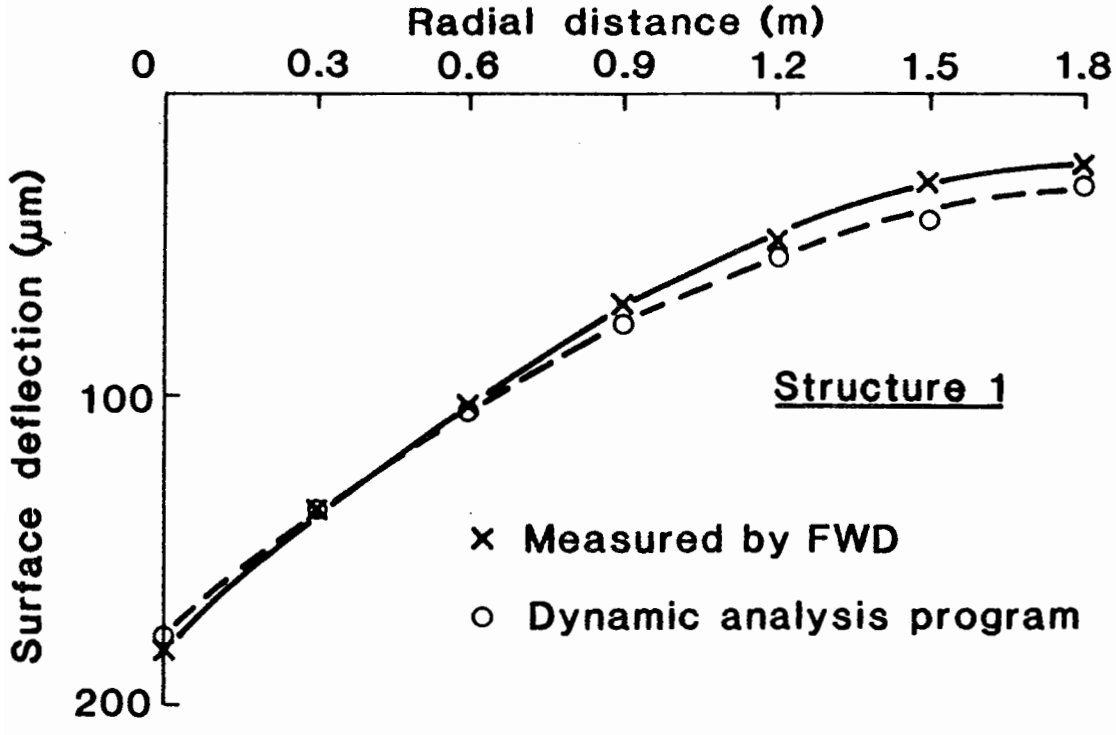

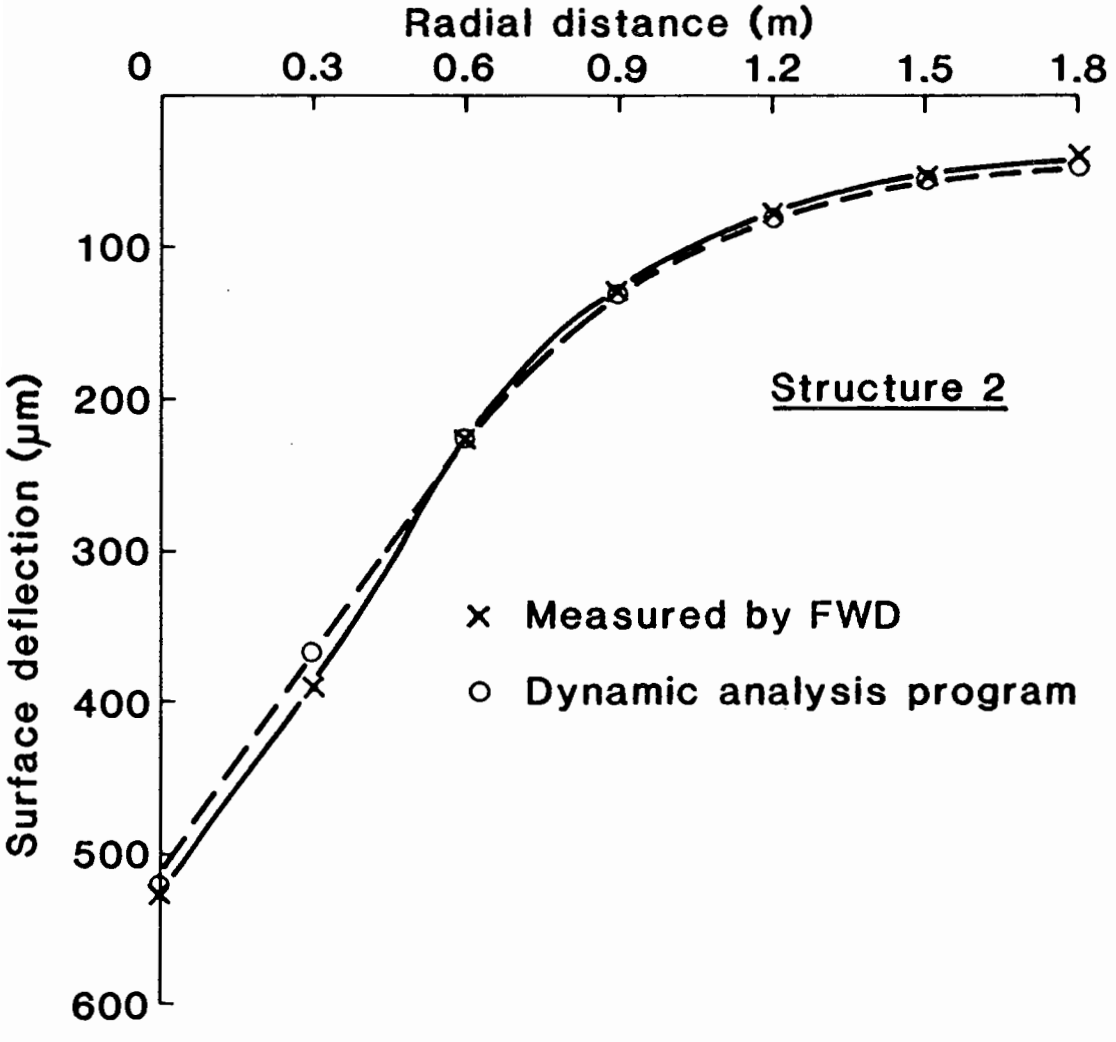

Fig4.24a COMPARISON OF DEFLECTION BOWLS MEASURED BY FWD AND DYNAMIC ANALYSIS COMPUTATION

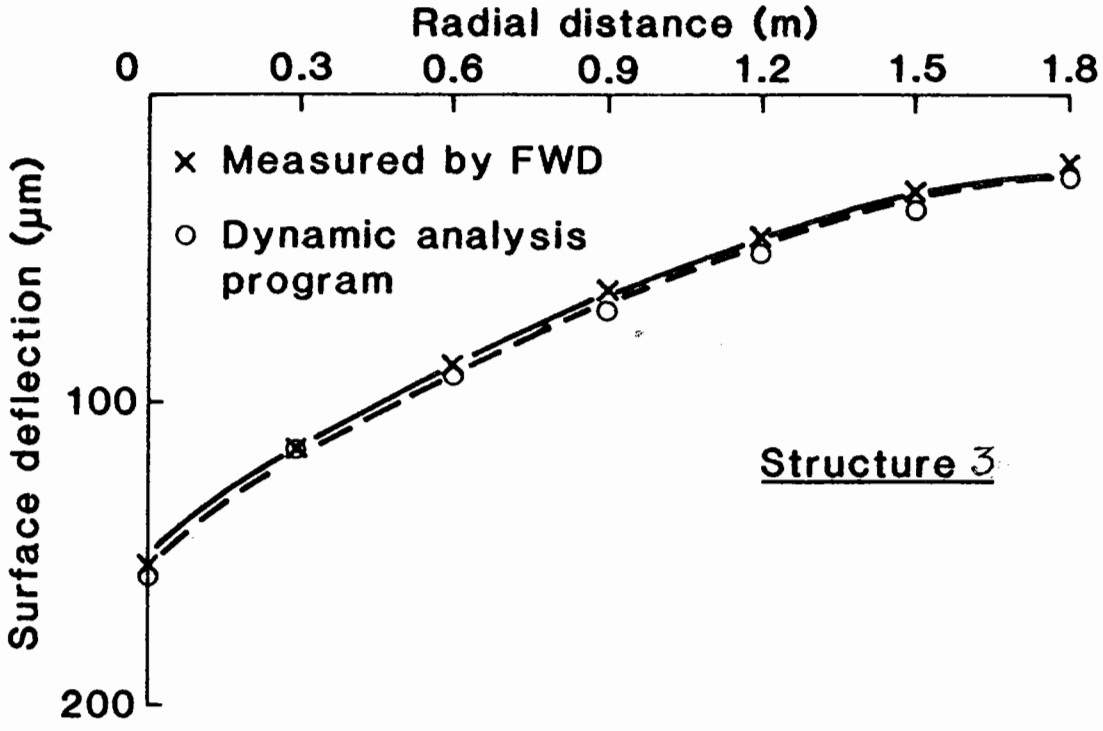

Fig4.24b COMPARISON OF DEFLECTION BOWLS MEASURED BY FWD AND DYMAMIC ANALYSIS COMPUTATION

understand the influence of dynamic loading on "static loading" type analysis, since the real objective is to investigate the differences between static and dynamic analysis in back-analysing the layer stiffnesses.

To resolve this problem, the deflection bowls computed by the dynamic analysis program were fed back into the PADAL computer program for back-analysis. Table 4.21 gives the results of those calculations compared with the original back-analysed elastic stiffnesses of each layer. It is noted that the error in elastic stiffness for the bituminous layer ranges from -0.2 to 13.6% with a mean of 4.9%, whereas the error for the lean concrete layer is 4.4%; the error for the granular sub-base ranges from 0.0 to 16.1% averaging 8.0% and that for the top of subgrade layer ranges from -7.4 to 13.4% with a mean of -0.1%. However, different distributions of subgrade stiffness are observed with an average error of less than 10%.

Therefore, based on the above comparison, which shows very good correlation both on deflections and elastic stiffnesses, it may be concluded that, as far as the dynamic loading produced by the FWD is concerned, the effect of the inertia of the pavement structure on deflection response, as strongly advocated by Sebaaly et al (89), is found to be insignificant. Also, pavement structures tested under the FWD would not be expected to resonate, since the FWD exerts a broad range of driving frequencies, instead of a single value, onto the pavement and, hence, the possibility of measuring erroneous deflections resulting from the resonant driving frequency is avoided. Finally, it is considered that a static analysis method, such as the PADAL computer program, can be used with confidence to back-analyse elastic stiffnesses from deflection bowls measured by the FWD, rather than resorting to a more sophisticated method based on dynamic analysis.

Table 4.21 **Variation of back-calculated elastic stiffnesses based on "dynamic analysis" deflection bowls from correct stiffnesses**

Material	Back-calculated elastic stiffnesses (MPa)									Mean difference (%)
	1 (a)	2 (b)	3 difference (%)	1 (a)	2 (b)	3 difference (%)	1 (a)	2 (b)	3 difference (%)	
	Structure 1			Structure 2			Structure 3			
Bituminous	3813	4331	13.6	1809	1806	-0.2	2450	2416	1.4	} 5.9
Lean concrete	-	-	-	-	-	-	27450	28656	4.4	
Sub-base	-	-	-	31	36	16.1	200	200	0.0	
Subgrade (1)	119	135	13.4	175	164	-6.3	340	315	-7.4	-0.1
Sub layers (2)	187	177	-2.2	176	164	-6.4	410	384	-6.3	
(3)	261	223	-14.6	178	164	-7.9	500	461	-7.8	
(4)	387	284	-26.6	180	164	-8.9	630	566	-10.2	
(5)	651	392	-39.8	182	165	-9.3	840	752	-10.5	

Note: 1. Back-calculated stiffnesses based on original measured deflection bowl.
2. Back-calculated stiffnesses based on deflection bowl from dynamic analysis.

3. $$\text{difference} = \frac{(b) - (a)}{(a)} \times 100\%$$

4.7 CONCLUSIONS

(1) A rational method of formulating non-linear (or stress-dependent) stiffnesses in the subgrade, the most important layer of a pavement structure, has been developed. The method takes into account the overburden of the pavement layers and the applied stresses, as well as the position of the water table in the subgrade.

(2) A sensitivity analysis on the subgrade stiffness parameters A and B has revealed that both parameters affects the whole deflection bowl but that the effect of varying parameter B is to influence the slope of the bowl relatively more than by varying parameter A. Variation of the position of the water table influences the magnitude of the non-linear subgrade stiffnesses and the resultant deflections. Its influence has been found to be identical to parameter A.

(3) Two computer programs, BASEM and BASEMC, have been developed for evaluating the in-situ conditions of bituminous and concrete structures respectively. After extensive application, they were found to be sensitive to the initial estimates of layer stiffnesses which were input into the program. As a result of an investigation, the programs were superseded by a new program known as PADAL (PAvement Deflection AnaLysis).

(4) The PADAL program has incorporated the same method for calculating the non-linear elastic stiffnesses of the subgrade and an additional facility to include a rigid layer in the subgrade for back-analysis. Also, it has incorporated improved convergence criteria on limiting the errors of both stiffnesses and deflections, to ensure unique solutions, regardless of initial estimates of layer stiffnesses. Furthermore, a new algorithm has been proposed to improve the rate of convergence.

The program has been formulated to solve both bituminous and concrete pavement structures up to four layers including three pavement layers and the subgrade.

(5) The uniqueness of back-analysed stiffnesses determined from the PADAL program has been extensively evaluated using theoretical deflection bowls produced for three- and four-layered bituminous structures. Very good correlations have been obtained in all cases except for those structures with thin top layers (e.g. 40 mm). It was observed in the analysis that maximum errors of 2% for all the layer stiffnesses of three-layered structures and 6% for the four-layered structures (except the sub-base layer which showed 16%) were obtained. Similar tests have also been carried out on four-layered concrete structures and results similar to those for bituminous structures were also found.

(6) A set of predictive stiffness equations corresponding to bituminous and concrete structures has been developed using the multiple regression analysis technique. The R^2 values range from 0.473 to 0.956 for equations corresponding to bituminous structures and, for concrete structures, they rang from 0.429 to 0.998. However, these equations have not yet been incorporated into the PADAL program for routine analysis since preliminary checks show that there is no significant improvement on programming efficiency.

(7) The capabilities of the proposed analytical procedures in practical application have been evaluated. In the first case, where vertical stresses and strains in the subgrade were measured, evaluation has established that the best agreement with the measured values was obtained when a non-linear subgrade was considered in the analysis. In the second case, where elastic stiffnesses were compared, the back-analysed stiffnesses from the

PADAL program generally agreed well with laboratory values. The best comparison was observed for the bituminous material, where the error in prediction was about 20%. The correlations for unbound granular sub-base and clay subgrade were less good, with mean ratios of 0.58 and 1.35 respectively. From the above analysis, it was established that the PADAL program could be used with sufficient confidence for back-analysing elastic stiffnesses in practical situations.

(8) From the literature review, dynamic loading produced by the FWD is unlikely to cause resonance in pavement structures, since it exerts a broad band of frequencies onto the pavement, instead of a single frequency, as produced by the Road Rater. The effect of dynamic loading on the elastic stiffnesses back-analysed by a static analysis program like PADAL has been found to give errors between 4 to 10%, which is considered to be acceptable for practical applications. The comparison also indicates that the effect of the inertia of pavement structures on deflection responses is not significant. Therefore, these findings have led to the conclusion that static analysis can be used with confidence to back-analyse the elastic stiffnesses of pavement structures, using deflection bowls measured by the FWD.

CHAPTER 5

COMPARISON WITH ANOTHER ANALYTICAL METHOD OF PAVEMENT EVALUATION

5.1 INTRODUCTION

During the development of the PADAL computer program, it was considered necessary to compare its solutions with other analytical back-analysis methods for completeness. A copy of the computer program ELMOD (Evaluation of Layer Moduli and Overlay Design) and user's manual (90) were acquired in the first year of research, on loan from the TRRL as part of the research collaboration. This was to enable a detailed evaluation to be performed, studying the accuracy of the program in predicting elastic stiffnesses for a range of pavement structures, both with linear and non-linear subgrades. Accuracy of prediction of the ELMOD program is evaluated in this Chapter, followed by a comprehensive comparison with the PADAL program.

5.2 EVALUATION OF THE COMPUTER PROGRAM 'ELMOD'

The ELMOD program was originally developed by Ullidtz (19) . It is widely used all over the world, since it is supplied by Dynatest as part of the package offered to customers who purchase their FWDs. The following sections detail the investigation.

5.2.1 A review of the ELMOD program system

The ELMOD program system is comprised of a number of computer programs written in the BASIC language for the Hewlett Packard HP-85 micro-computer. In the third release of the program system, there are four main analysis programs, of which the ELMOD program is one, together with an assortment of small programs to edit, print and transfer the FWD field data. Operation of the ELMOD program is divided into four parts, viz,

(a) Evaluation of layer stiffnesses;

(b) Adjustment of stiffnesses to design conditions;

(c) Evaluation of remaining life;

(d) Overlay thickness design.

The following paragraphs briefly review the ELMOD program .

Evaluation of layer stiffnesses: The ELMOD program was developed by Ullidtz (19) in 1977 to back-analyse the elastic stiffnesses of pavement structures from FWD deflection bowls. The analysis was based on the use of the Method of Equivalent Thicknesses (MET), originally developed by Odemark (91), in order to convert pavement layers with distinctly different elastic stiffnesses into a single layer of the same stiffness as the subgrade. This is achieved by adjusting the thicknesses of each pavement layer using the following conversion equation:

$$h_e = f \times \sum h_i \times \sqrt[3]{\frac{E_i}{E_n}} \qquad (5.1)$$

where h_e is the equivalent thickness of layer i with original thickness h_i and stiffness E_i;

E_n is the stiffness of the bottom layer of an n-layered structure;

f is a conversion factor; f=0.8 except at the first interface where f=1.0.

Once the conversion is completed, Boussinesq equations are applied to calculate stresses, strains and deflections at various specified positions. Together with the above analysis method, an iterative procedure has been developed in the ELMOD program for the back-analysis of layer stiffnesses by matching measured deflections. Nonlinearity of the subgrade is modelled using equation (5.2) below:

$$E_o = C_o \times \left(\frac{\sigma_1}{\sigma'}\right)^n \qquad (5.2)$$

where E_o is the subgrade stiffness;

σ_1 is the major principle stress;

σ' is the reference stress;

C_o and n are constants and $n<0$.

All pavement layers are assumed to be homogeneous, isotropic and linear elastic. A Poisson's ratio of 0.35 is assumed for all layers including the subgrade.

Ullidtz and Peattie (92) attempted to demonstrate the usefulness of the MET by carrying out a series of comparisons with the multi-layered programs CHEVRON and BISTRO. They reported good agreement with the multi-layered programs provided certain conditions were met:

(a) Stiffnesses should be decreasing with depth; stiffness ratio (E_i/E_{i+1}) should be greater than 2;

(b) The structure should contain only one stiff layer with $(E_1/E_{subgrade})>5$. If the structure contains more than one stiff layer, e.g. wearing course, basecourse and roadbase layers, they should be combined into one layer for the purpose of structural evaluation;

(c) The thickness of the top (stiff) layer (h_1) should be greater than half the radius of the FWD loading platen, e.g. at least 75mm for a typical 300mm diameter loading platen. The thickness of the top layer of a three-layered structure should be less than the diameter of the loading platen and also less than the thickness of layer 2.

It is noted from the user's manual that the ELMOD program is capable of back-analysing two-, three- and four-layered stuctures. However,

in the analysis of a four-layered structure, the stiffness of layer 2 is not calculated independently but related to the stiffness of layer 3 using the relationship proposed by Dorman and Metcalf (93):

$$E_g/E_s = 0.2 \times h_g^{0.45} \qquad (5.3)$$

where E_g (kPa) is the stiffness of the granular layer with thickness h_g (mm);

E_s (kPa) is the stiffness of the subgrade.

The user's manual does not explain how the stiffness of layer 2 (E_2) is calculated, except to state that "this relationship is used in conjunction with the Method of Equivalent Thicknesses to calculate the ratio E_2/E_3".

It is possible that equation (5.3) is modified as equation (5.4) in order to calculate stiffness, E_2, once the stiffness of layer 3 (E_3) has been evaluated during the iterative process:

$$E_2/E_3 = 0.2 \times h_2^{0.45} \qquad (5.4)$$

where E_2, E_3 are stiffnesses of the layers 2 and 3 (kPa);

h_2 is thickness of layer 2 (mm).

If the above assumption is correct, three points emerge. First, the ELMOD program can only back-analyse two- and three-layered structures since for four-layered structures, the stiffness of layer 2 is assumed to be dependent on the stiffness of layer 3. Second, the stiffness of layer 2 has an order of magnitude similar to that of granular material and is always greater than the stiffness of layer 3. Third, the assumption prevents proper evaluation of the in-situ elastic stiffness of layer 2.

Adjustment of stiffnesses to design conditions: The back-analysed stiffnesses are adjusted according to design conditions for each season (up to a maximum of 12). The adjustment of bituminous material given in equation (5.5) is based on the work of Ullidtz and Peattie (92) who derived that:

$$E_T/E_C = A - B \times \log_{10}(T/C) \qquad (5.5)$$

where E_T, E_C are the stiffnesses at temperature T and reference temperature C (25°C) respectively;

A,B are constants (typical values are 1 and 2).

A sinusoidal relationship is assumed for temperature variation and stiffnesses of the bituminous material are adjusted for each season, according to temperature variation. In the program, seasonal variation of stiffness in the unbound granular material and clay subgrade can be included, if required, for frost and spring thaw conditions, using an exponential expression.

Evaluation of remaining life: Damage in each season is then computed using the adjusted stiffnesses and specified loading conditions and summed using Miner's rule (94). The remaining life calculation is based on two different pavement conditions, namely, structural and functional. The structural condition relates to the bearing capacity and the functional conditon to the riding quality. The estimation of structural deterioration in the ELMOD program comes from the following general empirical expression,

$$N = K \times S^a \qquad (5.6)$$

where N is the number of load applications;

S is the stress or strain level;

K and a are user-dependent constants.

It is assumed that structural deterioration is mainly caused by fatigue cracking of the bituminous or cement bound layers. Functional deterioration is governed by the change in Present Serviceability Rating (PSR), which has been derived from the AASHO Road Test field data. The pavement is said to have reached functional failure if the calculated PSR is less than the minimum permissible PSR and to have reached structural failure if fatigue cracking in the bound layers is observed.

Overlay thickness design: An overlay is required if the structural condition is poor and an overlay would increase the in-situ PSR by two. However, no reference has been given as to how the overlay thickness has been computed.

Figure 5.1 illustrates a typical set of output from the ELMOD program.

In summary, the review has led to the following observations:

(a) Although the ELMOD program, which is based on the MET is very simple and efficient to run on the computer, there are a number of questions to be answered before the results can be used with confidence. These are,

(i) How is the iterative procedure formulated?

(ii) How is a non-linear subgrade incorporated in the procedure?

(iii) What are the convergence criteria for terminating the iterations ?

Furthermore, since no information is given on how good the match between measured and calculated deflection bowls, crucial to any back-analysis method, the accuracy of prediction of back-analysed elastic stiffnesses must be questionable.

(b) The ELMOD program is found to be only capable of analysing two- and three-layered structures, although it has been stated that it can also analyse four-layered structures. The reason is that the

FILE ST .1 TO 1 2 ON 83/9/18

FOAD No. 208 /OUTERWHEEL

LAYER NO. 1 CONSISTS OF
4.5 IN ASPHALT
LAYER NO. 2 IS 9 IN THICK

ΔPSR= .5

EQUIVALENT GEARS/LANE/SEASON

SEASON	ESGL
1	25000
2	25000
3	25000
4	25000

E-VALUES, ksi 83/9/18

ST.	E1	E2	EM	C0	M
.10	817	19	9	9	-0.09
.20	113	8	5	5	-0.23
.30	899	25	8	6	-0.20
.40	293	25	8	8	-0.15
.50	469	29	9	8	-0.10
.60	414	31	12	11	-0.13
.70	761	20	8	7	-0.20
.00	268	13	8	8	-0.11
.90	778	20	9	9	-0.05
1.00	276	15	11	11	-0.11
1.10	464	33	5	3	-0.36
1.20	642	9	7	6	-0.21

MODULI FOR EACH SEASON, ksi

$	ST.	E1	E2	EM
1	.10	1438	15	7
2	.10	1096	16	8
3	.10	721	19	9
4	.10	928	18	9
$	ST.	E1	E2	EM
1	.20	195	6	4
2	.20	152	6	4
3	.20	106	7	5
4	.20	120	7	5
$	ST.	E1	E2	EM
1	.30	1582	20	6
2	.30	1205	21	6
3	.30	793	25	8
4	.30	1020	24	7
$	ST.	E1	E2	EM
1	.40	516	19	6
2	.40	394	20	7
3	.40	259	24	8
4	.40	333	23	8
$	ST.	E1	E2	EM
1	.50	825	22	7
2	.50	629	24	7
3	.50	414	28	9
4	.50	533	27	8
$	ST.	E1	E2	EM
1	.60	729	24	9
2	.60	556	28	10
3	.60	365	31	12
4	.60	470	29	11

REMAINING LIFE ΔPSR= 5

ST	LIFE YEARS	CRITICAL LAYER	FAILURE MODE
0.10	2.9	2	FUNCTIONAL
0.20	0.0	1	STRUCTURAL
0.30	2.5	2	FUNCTIONAL
0.40	0.8	2	FUNCTIONAL
0.50	1.7	2	FUNCTIONAL
0.60	2.1	2	FUNCTIONAL
0.70	2.0	2	FUNCTIONAL
0.80	0.4	2	FUNCTIONAL
0.90	2.5	2	FUNCTIONAL
1.00	0.6	2	FUNCTIONAL
1.10	0.7	2	FUNCTIONAL
1.20	0.5	2	FUNCTIONAL

NEEDED OVERLAY THICKNESS, IN

ST	OVERLAY IN
0.10	1.14
0.20	7.28
0.30	1.26
0.40	3.11
0.50	1.89
0.60	1.92
0.70	1.65
0.80	4.06
0.90	1.22
1.00	2.83
1.10	3.70
1.20	3.62

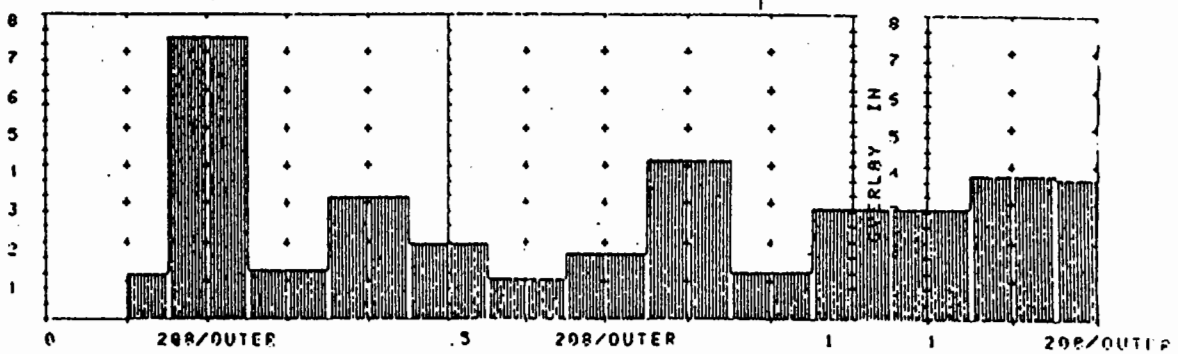

Figure 5. Sample ELMOD output - overlay design based on FWD test data, traffic layer thicknesses, and fatigue &performance equations.

stiffness of layer 2 is assumed to depend on the stiffness of layer 3, instead of being back-analysed independently through an iterative procedure. As a result, the back-analysed elastic stiffness of layer 2 has an order of magnitude similar to granular material and is always greater than that of layer 3.

(c) It is noted that the ELMOD program cannot analyse structures with a lean concrete roadbase layer, a common type of structure for heavily trafficked roads in the United Kingdom. This is because of the inherent assumption in the Method of Equivalent Thicknesses that the stiffnesses of a pavement structure have to decrease with depth.

(d) It is not clear how the ELMOD program calculates remaining pavement life without a knowledge of the original life of the pavement. Furthermore, the use of PSR to determine the riding quality of the pavement is very subjective.

(e) On the aspect of overlay design, no indication is given on how the computation has been performed, which raises doubts on the validity of prediction of overlay thicknesses.

As a result of the above review, a series of analyses, to be described later, has been performed, in order to study the accuracy of the ELMOD program in predicting elastic stiffnesses over a range of pavement structures, with both linear and non-linear subgrades.

5.2.2 Evaluation of accuracy of prediction of the ELMOD program

In order to ascertain the accuracy of prediction of the ELMOD program, a series of analyses has been performed in the following areas:

(a) Two-layered structures;

(b) Three-layered structures;

(c) Comparison of back-analysed elastic stiffnesses based on field data.

(A) Two-layered structures

A number of theoretical deflection bowls were calculated, taking the subgrade to be both linear and non-linear. The input data for the calculations are given in two tables (Tables 5.1 and 5.2). In each calculation, a vertical pressure of 700 kPa was applied over a loading platen of 300 mm diameter. Deflections were computed at distances of 0, 300, 600, 900, 1200, 1500 and 1800 mm from the load centre. In all, 48 deflection bowls were computed, half of which were for linear subgrade and half for non-linear subgrade. The BISTRO program was used to calculate deflections for those structures with linear subgrades, whereas in the case of nonlinear subgrades, a simplified version of PADAL was employed. These theoretical deflection bowls and the data on loading conditions were input into the ELMOD program manually for back-analysis. Back-analysed elastic stiffesses were compared with the original stiffnesses and the results of the comparison are shown in Figure 5.2 and 5.3, for linear and non-linear subgrades respectively.

In Figure 5.2, for linear subgrade, it is clearly noted that ELMOD generally over-predicts the correct stiffness of the bituminous layer (E_1) but under-predicts the stiffness of the subgrade layer (E_2). As layer thickness increases, both the mean stiffness ratio reduces and gets closer to unity and at the same time, standard deviation also reduces. A general observation is that the ELMOD prediction of E_2 is relatively better than that of E_1. Maximum error is noted when the thickness of the bituminous layer is smallest.

When the subgrade is non-linear, the ELMOD prediction, as shown in Figure 5.3, is much worse than with the linear subgrade and generally over-predicts the correct values. Studying the results

Layer	Material type	Parameters	Range of values
1	Bituminous	E_1 (MPa) h_1 (mm) ν_1	1000, 3000, 10,000 90, 150, 250, 350 0.4
2	Subgrade	E_2 (MPa) ν_2	50, 200 0.4

Table 5.1 Parameters used for calculation of deflection bowls for linear subgrade (two-layered structures)

Layer	Material type	Parameters	Range of values
1	Bituminous	E_1 (MPa) h_1 (mm) ν_1	1000, 3000, 10,000 90, 150, 250, 350 0.4
2	Subgrade	E_2 (MPa) A^2 (MPa) B ν_2	100 100 0.1, 0.3 0.4

Table 5.2 Parameters used for calculation of deflection bowls for non-linear subgrade (two-layered structures)

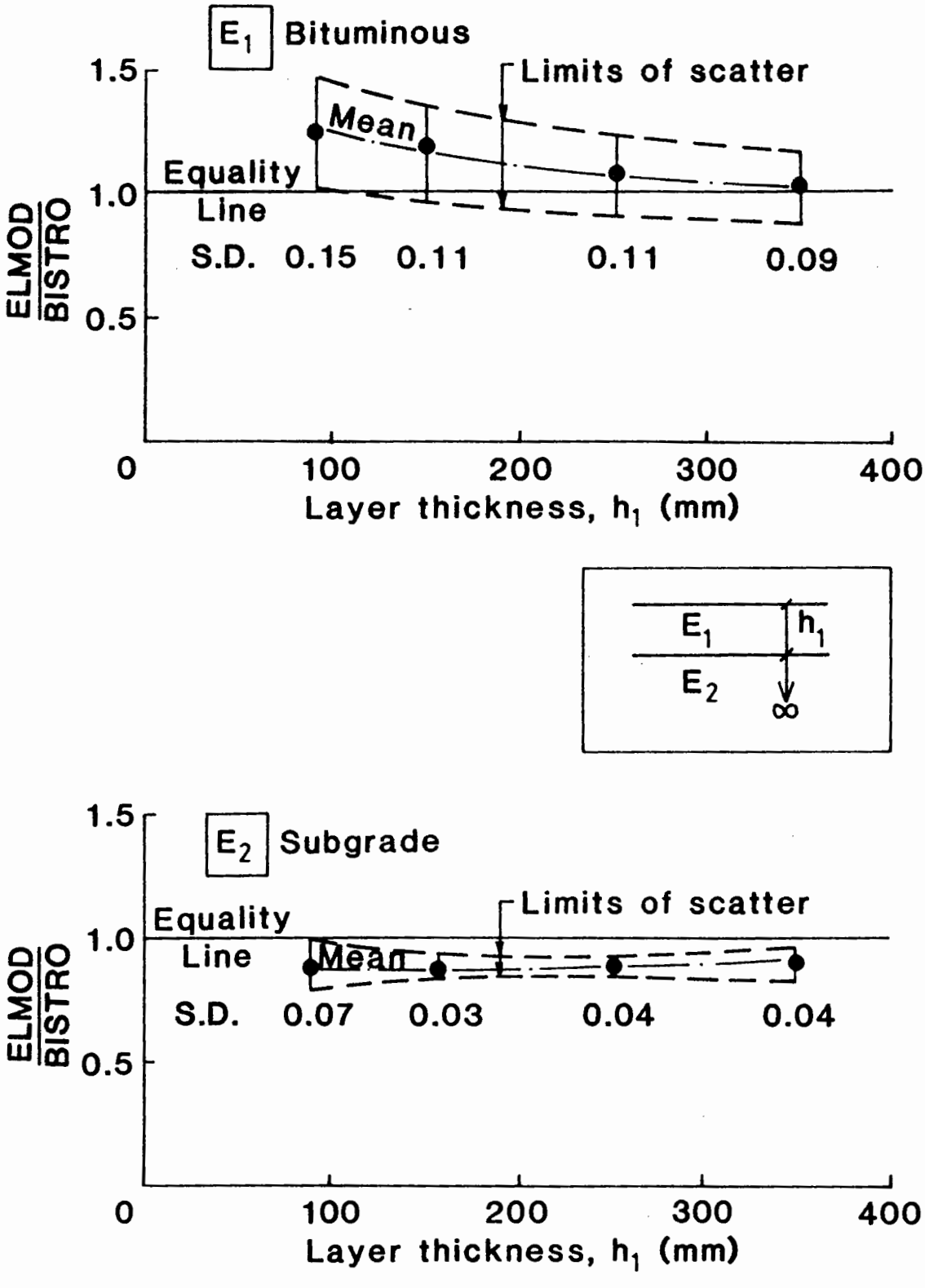

Fig. 5.2 COMPARISON OF ELMOD AND BISTRO PROGRAM FOR TWO-LAYER STRUCTURES (LINEAR SUBGRADE)

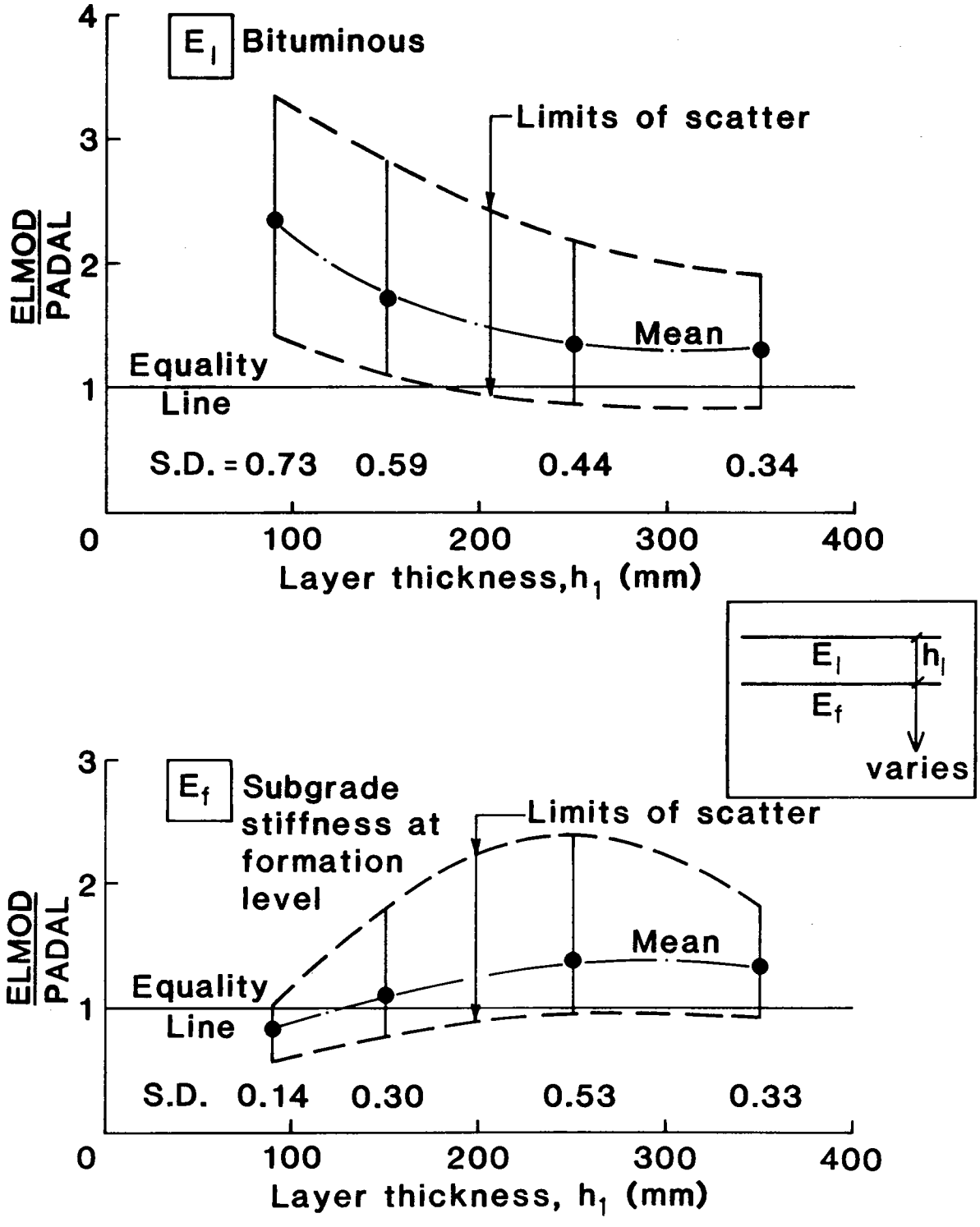

Fig. 5.3 COMPARISON OF ELMOD AND PADAL PROGRAM FOR TWO-LAYER STRUCTURES (NON LINEAR SUBGRADE)

for E_1, the highest mean stiffness ratio is noted at h_1=90mm with value of 2.35 and standard deviation of 0.73. As the layer thickness increases, the ratio and standard deviation gradually improves to a value of 1.62 and 0.34 respectively corresponding to h_1=350mm. When compared with stiffness ratios for a linear subgrade, these results are found to be more scattered.

In the printout from the ELMOD program, only one non-linear subgrade stiffness is listed, together with corresponding non-linear coefficients(i.e. C_o and n, refer equation (5.2)). In order to facilitate a comparison, this stiffness value was made to compare with the subgrade stiffness at formation level (E_f) from the PADAL program. As seen in Figure 5.3, the results are clearly more scattered than for linear subgrade (refer Figure 5.2) and generally over-predict the correct values. The mean stiffness ratios vary from 0.83 to 1.65 and corresponding standard deviation between 0.14 and 0.53 over a range of layer thicknesses (h_1).

Table 5.3 summarises all the results of the comparison for two-layered structures. Examination of the results reveals that the ELMOD program gives best overall agreement for elastic stiffnesses in a linear subgrade. As for the E_1 values, the ELMOD prediction for structures with the non-linear subgrade is about 50% worse than for cases with linear subgrade.

(B) Three-layered structures

As for two-layered structures, a number of theoretical deflection bowls for three-layered structures were also computed, in order to determine the accuracy of stiffness prediction of the ELMOD program . The range of input data is presented in Tables 5.4 and 5.5 for linear and non-linear subgrades respectively. In all, 144 deflection bowls were computed, half of which were for the

	ELMOD/BISTRO Linear subgrade		ELMOD/PADAL Non-linear subgrade	
Ratio of stiffness	E_1	E_2	E_1	E_f
Minimum	0.89	0.79	0.85	0.57
Maximum	1.46	0.99	3.33	2.46
Mean	1.14	0.89	1.70	1.16
S.D.	0.12	0.05	0.55	0.35

Note: E_f denotes layer 2 subgrade stiffness at formation level of PADAL program.
E_1 denotes bituminous stiffness
E_2 denotes linear subgrade stiffness

Table 5.3 Overall summary of deviation of ELMOD prediction of layer stiffnesses from BISTRO and PADAL programs for two-layered structures

Layer	Material type	Parameters	Range of values
1	Bituminous	E_1 (MPa) h_1 (mm) ν_1	1000, 3000, 10,000 90, 200, 400 0.4
2	Sub-base	E_2 (MPa) h_2 (mm) ν_2	100, 300 300 0.3
3	Subgrade	E_3 (MPa) ν_3	50, 200 0.4

Table 5.4 Parameters used for calculation of deflection bowls of three-layered structures (linear subgrade)

Layer	Material type	Parameters	Range of values
1	Bituminous	E_1 (MPa) h_1 (mm) ν_1	1000, 3000, 10,000 90, 200, 400 0.4
2	Sub-base	E_2 (MPa) h_2 (mm) ν_2	100, 300 300 0.3
3	Subgrade	E_3 (MPa) A B ν_3	50, 200 100 0.1, 0.3 0.4

Table 5.5 Parameters used for calculation of deflection bowls of three-layered structures (non-linear subgrade)

case of linear subgrade and the other half for non-linear subgrade. In all calculations, the thickness of the sub-base layer was fixed at 300 mm, since its variation was not considered to be so significant as other parameters. Again, these deflection bowls were entered into the ELMOD program for back-analysis. Calculated stiffnesses were then compared with the original values and the results are shown in Figures 5.4 and 5.5, for linear and non-linear subgrades respectively.

As shown in Figure 5.4 for a linear subgrade, the ELMOD predictions are much more scattered than in the case of the two-layered structures (refer Figure 5.2). It is observed that while the ELMOD program generally over-predicts the stiffness of the bituminous (E_1) and sub-base (E_2) layers, it under-predicts the subgrade stiffness (E_3). Best agreement is observed for E_3 with a constant mean ratio and standard deviation of 0.9 and 0.1 respectively, the prediction for E_1 is second with 1.2 and 0.52; and the poorest is E_2 with 2.0 and 1.62. The ELMOD prediction for the subgrade is also the most consistent with very little scatter and the sub-base results are the most scattered.

Increase of layer thickness h_1 does not have any influence on the subgrade stiffness but the stiffnesses of the bituminous and sub-base layers are greatly influenced by its variation, especially the sub-base stiffness. This is reflected in a large range of sub-base stiffness ratios between 0.6 and 7.2 being computed at h_1=400mm.

Figure 5.5 presents results of the comparison for non-linear subgrade. It is interesting to note that the E_1 stiffnesses predicted by the ELMOD program are much improved over the corresponding cases for linear subgrade. The subgrade stiffness at formation level, E_f, however, is more variable. Once again,

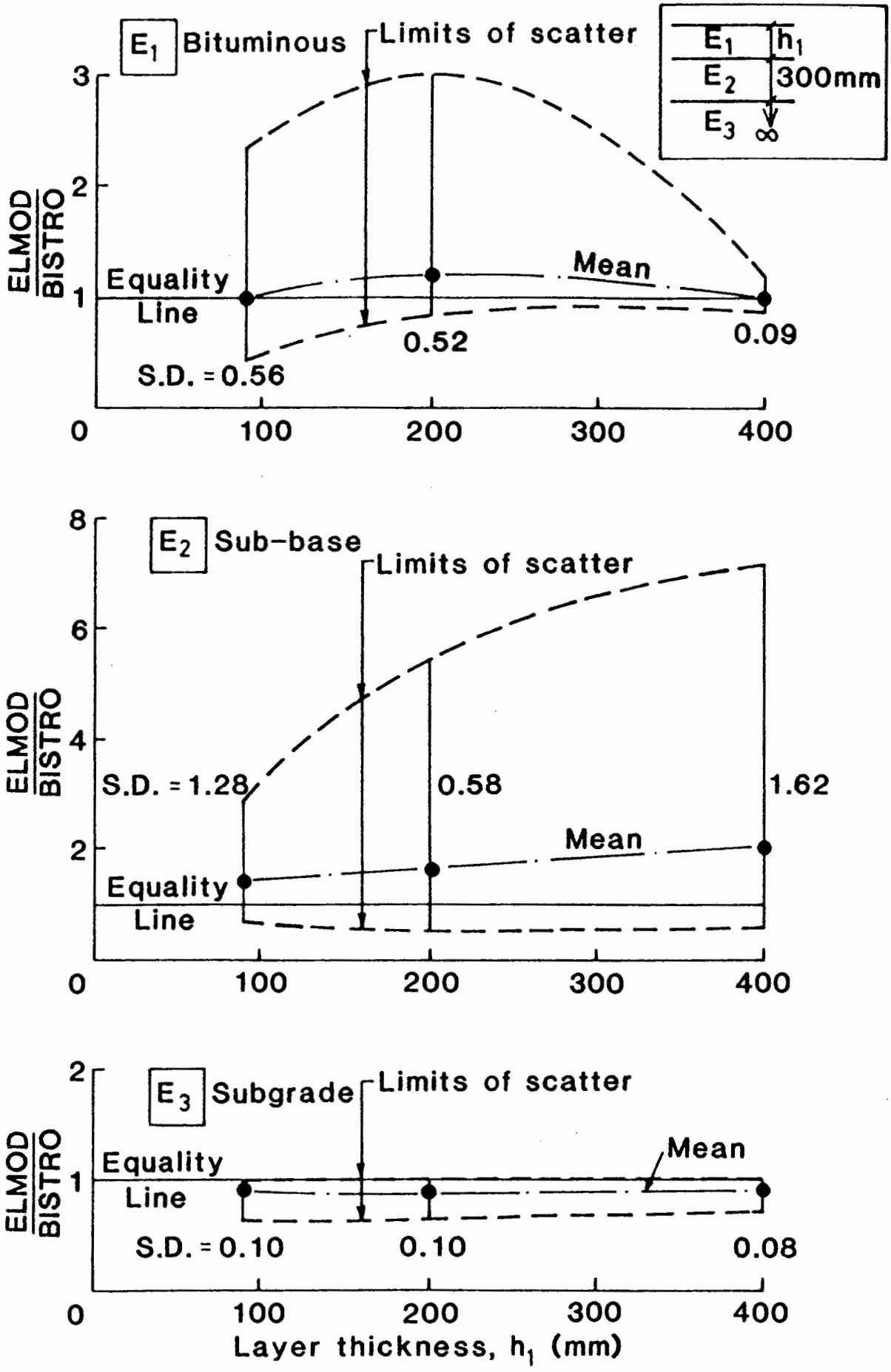

Fig. 5.4 COMPARISON OF ELMOD AND BISTRO PROGRAMS FOR THREE-LAYER STRUCTURES (LINEAR SUBGRADE)

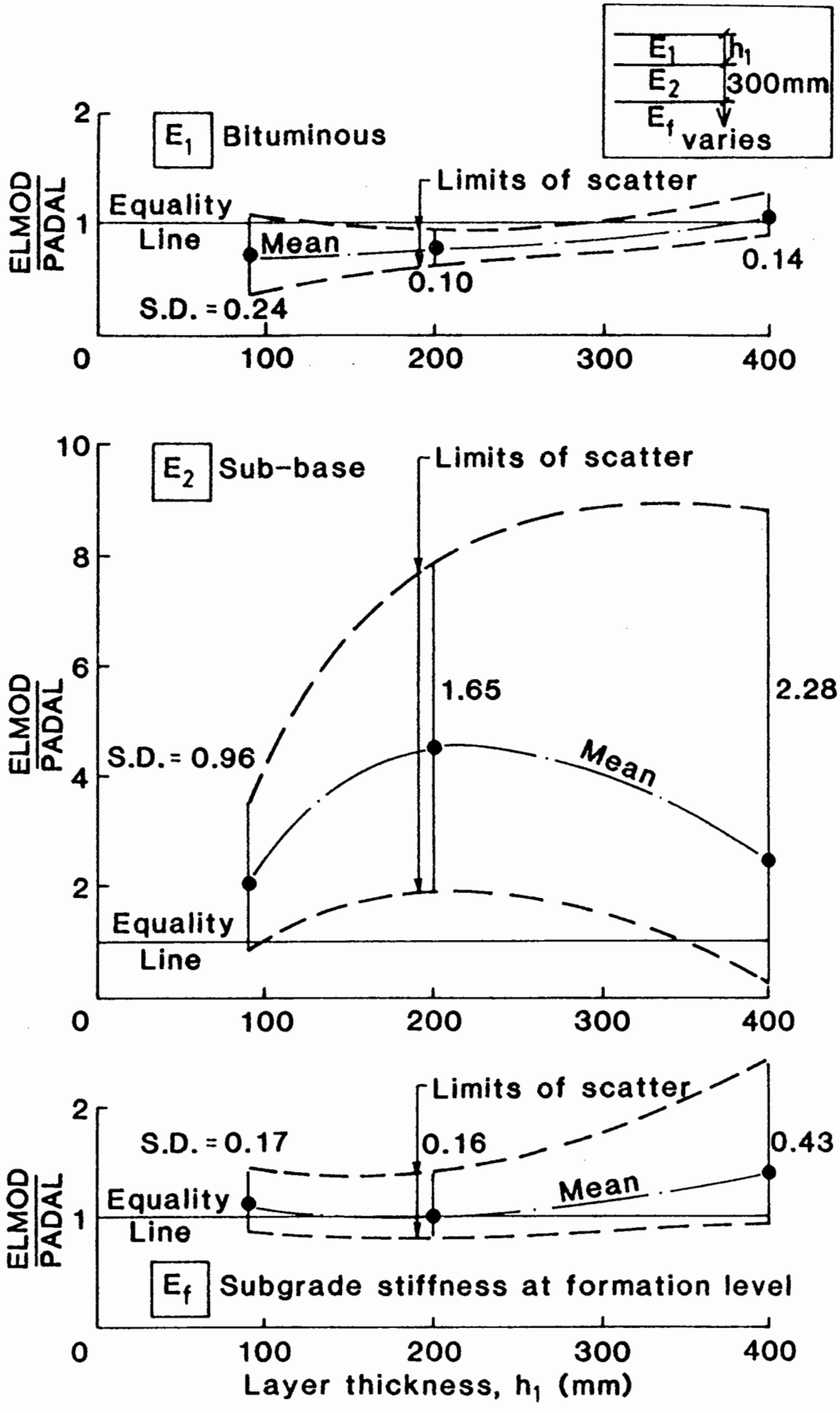

Fig. 5.5 COMPARISON OF ELMOD AND PADAL PROGRAMS FOR THREE-LAYER STRUCTURES (NON LINEAR SUBGRADE)

Ratio of stiffness	ELMOD/BISTRO Linear subgrade			ELMOD/PADAL Non-linear subgrade		
	E_1	E_2	E_3	E_1	E_2	E_f
Minimum	0.42	0.55	0.64	0.34	0.30	0.84
Maximum	3.02	7.13	1.03	1.25	8.84	2.39
Mean	1.08	1.67	0.91	0.85	2.94	1.19
S.D.	0.44	1.53	0.09	0.17	1.65	0.27

Note: E_f denotes subgrade stiffness at formation level of PADAL program.
E_1 denotes bituminous stiffness
E_2 denotes granular sub-base stiffness
E_3 denotes linear subgrade stiffness

Table 5.6 Overall summary of deviation of ELMOD prediction of layer stiffnesses from BISTRO and PADAL programs for three-layered structures

the predicted stiffnesses for the sub-base layer are the poorest with results up to about 9 times the original value. Mean stiffness ratios for the bituminous layer vary from 0.7 to 1.06; the sub-base layer varies from 2.0 to 4.57; and the subgrade layer from 1.0 to 1.4 respectively, with the corresponding range of standard deviation between 0.24 and 0.14 for the bituminous layer; between 0.96 and 2.28 for the sub-base as well as between 0.17 and 0.43 for the subgrade. The variation of layer thickness, h_1, is seen to affect the stiffnesses of all layers, being a dominant influence on the sub-base layer. It can be seen that the greater the value of h_1, the more variable is the predicted stiffness of the sub-base, resulting in a large range of stiffness ratios from 0.3 to 8.8 corresponding to the h_1=400mm. Table 5.6 summarises all the results of the comparison for three-layered structures. Based on the range of parameters studied, the overall impression is that, in general, better agreement is observed for structures with linear subgrade than non-linear ones, e.g. about 8 to 9% of error for linear subgrade as against above 15% for the non-linear subgrade. It is worth noting that while the ELMOD program, on average, over-predicts E_1 and under-predicts E_2 in the case of linear subgrade, the reverse is observed for non-linear subgrade. However, the ELMOD program consistently over-predicts the sub-base stiffness, E_2, with large variation. Structures with a non-linear subgrade reduce the accuracy of prediction even further.

(C) Comparison of back-analysed elastic stiffnesses based on field data: The previous investigation enables one to observe the accuracy of prediction of the ELMOD program, using theoretical deflection bowls derived from the computer programs BISTRO and PADAL. To gain more insight into how the ELMOD and PADAL

programs compare in practical situations, they were used to back-analyse a common set of field deflection bowls measured by the FWD. The field results were selected from data provided by the TRRL. In 1984, the TRRL carried out a series of regular deflection measurements on test sections of their small roads system using the FWD. In all, fourteen sets of test results were provided by the TRRL for research purposes. After examining the data, the structures at two locations, S1.4 and S2.4 were selected for this analysis, approximately representing the 85-percentile deflection value of sections 1 and 2 respectively. The structure of Section 1 consisted of an HRA wearing course, DBM basecourse and Dense Tarmacadam with total thickness of 172mm overlying a Type 1 sub-base of thickness 148 mm. The structure in Section 2 included HRA wearing course and DBM basecourse overlying wet mix and Type 1 sub-base layers. The thickness of the bituminous surfacing was 102 mm whereas the wet mix and sub-base layers were 318 mm and 210 mm respectively. The subgrade was a stiff clay and was the same for both sections. The choice of these two structures was made to compare the elastic stiffnesses back-analysed by the ELMOD and PADAL programs under different thickness combinations.

The analysis was carried out by treating both pavements as three-layered structures, the limit of the ELMOD program. This was achieved by combining all the bituminous layers of structure S1.4 into one layer. In Section 2, apart from combining the bituminous layers, the wet mix and sub-base layers of structure S2.4 were also combined into one layer. Thirteen deflection bowls on each structure were fed into the ELMOD and PADAL programs separately for back-analysis. Figures 5.6 and 5.7 plot

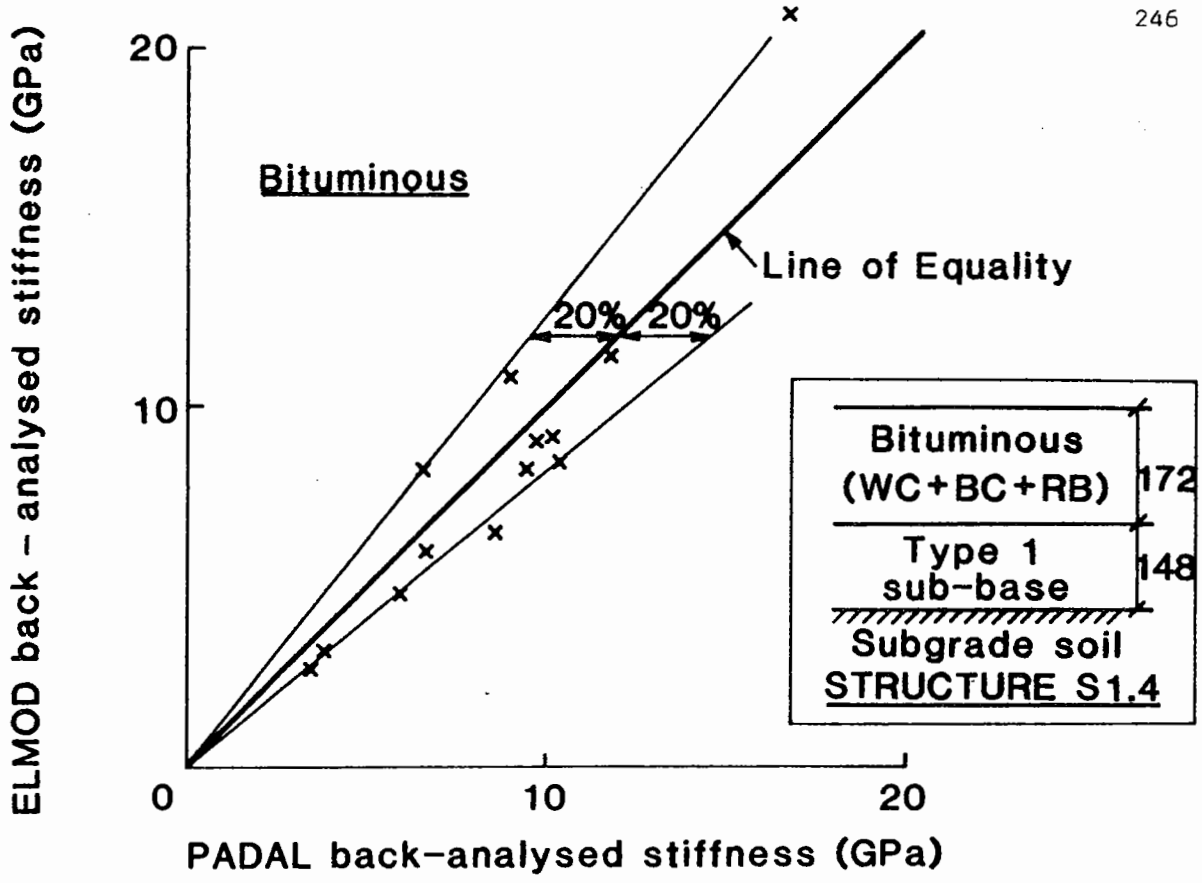

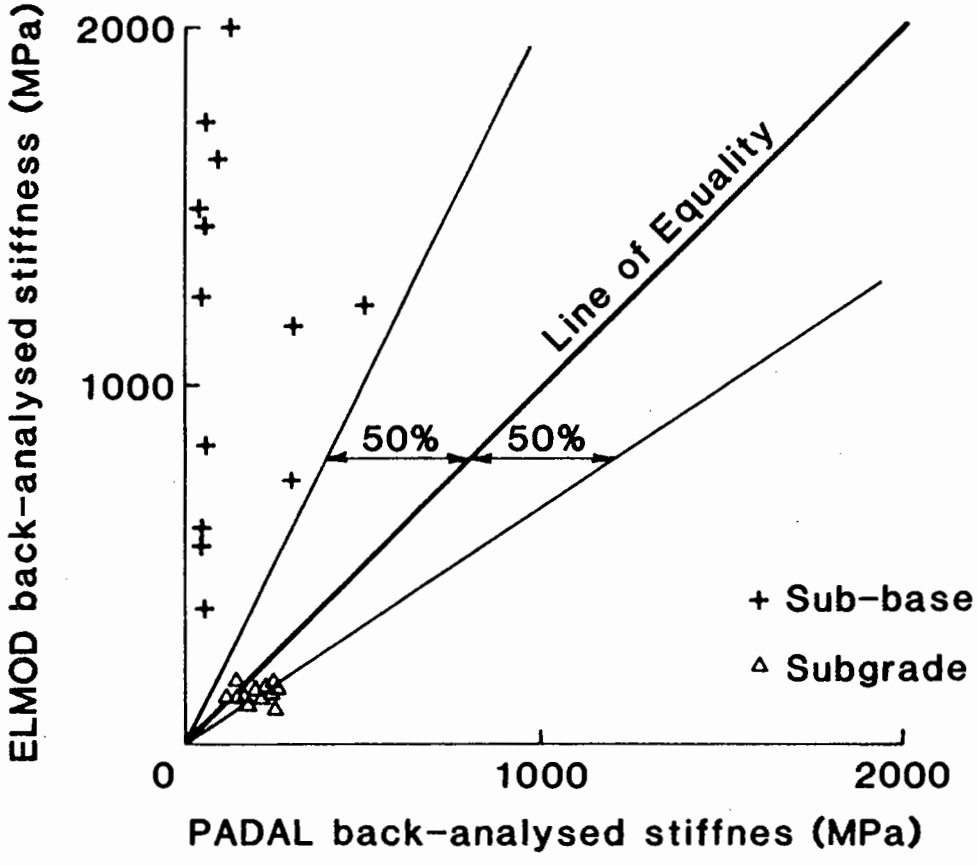

Fig. 5.6 COMPARISON OF ELASTIC STIFFNESSES BACK-ANALYSED USING ELMOD AND PADAL (TEST SECTION 1)

the results of the comparison of back-analysed elastic stiffnesses.

As seen in Figure 5.6, elastic stiffnesses for the combined bituminous layer of Section 1, back-analysed by the ELMOD and PADAL programs, achieved reasonably good agreement. The majority of the results lie within 20% either side of the equality line. The comparison of subgrade stiffnesses are less good, the ELMOD back-analysed stiffnesses being generally smaller than those produced by PADAL. Over 50% of the results are found to lie within 50% of the PADAL back-analysed stiffnesses. However, very poor agreement is noted for sub-base stiffnesses. Very high stiffnesses have been back-analysed by ELMOD with 8 out of 13 results exceeding 1000 MPa. These large stiffnesses are considered too high to be achieved in British pavements. Since this finding is consistent with observations already described in the previous section of three-layered structures, in which the sub-base stiffnesses have been grossly over-predicted (refer Figures 5.4 and 5.5), it further reinforces the view that the ELMOD program cannot be used to evaluate the condition of the sub-base accurately.

As for Section 2, comparison of the elastic stiffnesses for the combined bituminous layer, as shown in Figure 5.7, reveals good agreement with PADAL, the results generally lying within 20% of the equality line, with the exception of one test point where the ELMOD program gives an unrealistically large stiffness value of 68.7 GPa. — *for* pavement quality concrete! A comparison of subgrade stiffnesses shows that the prediction of the ELMOD program is generally smaller than that from PADAL. The majority of the results are found within 50%. In contrast, the elastic stiffnesses for the combined granular

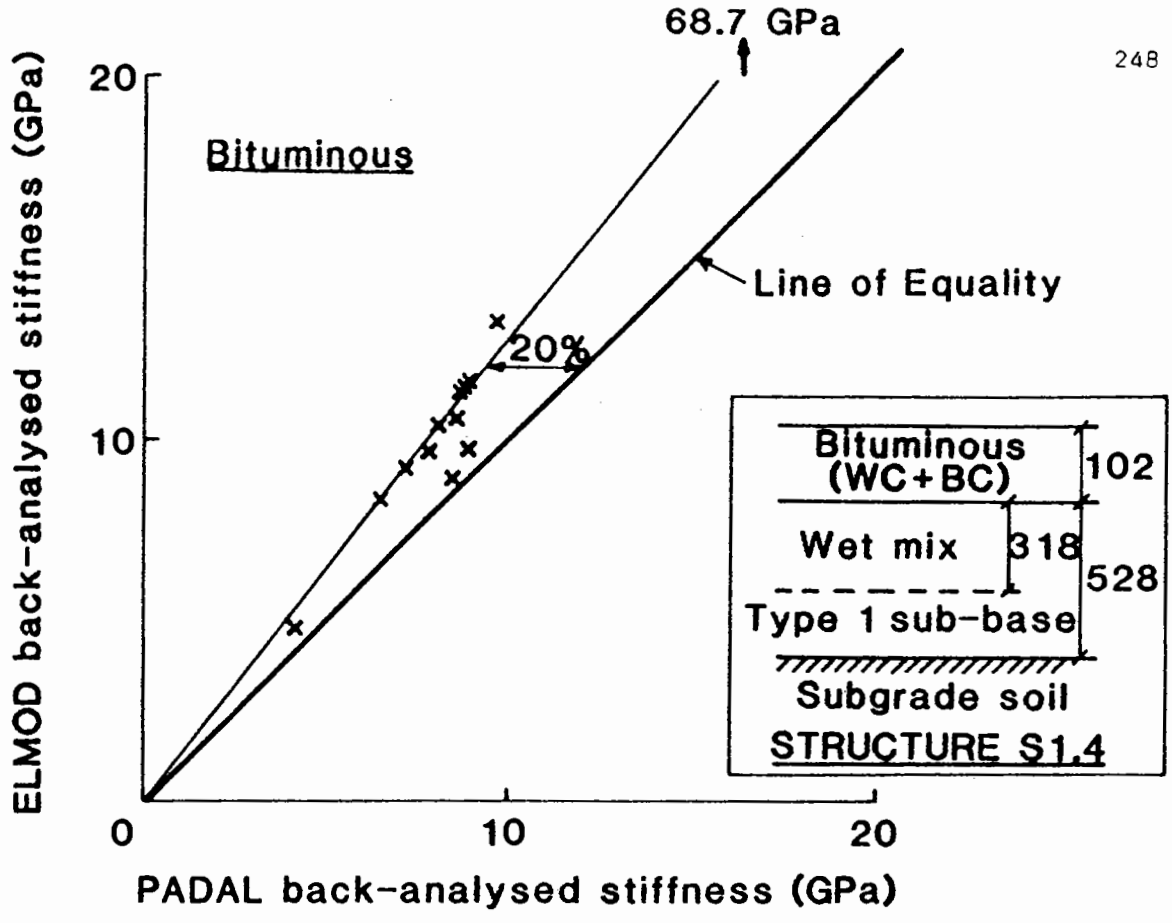

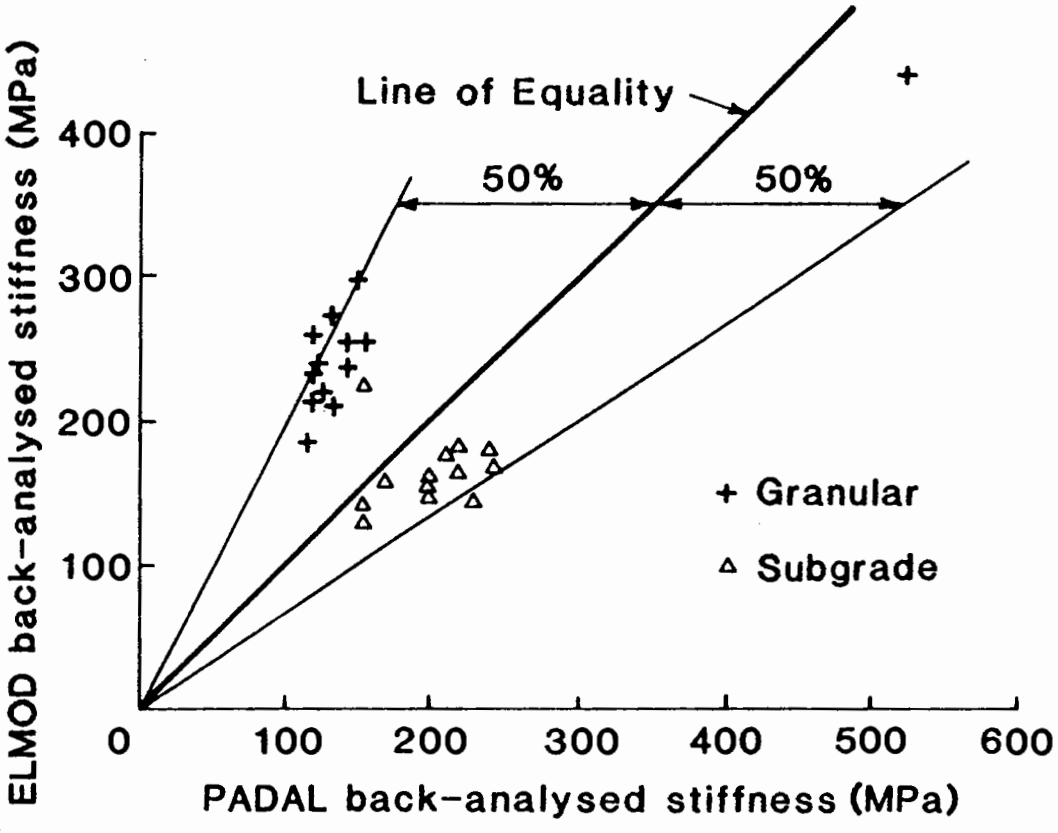

Fig. 5.7 COMPARISON OF ELASTIC STIFFNESS BACK-ANALYSED USING ELMOD AND PADAL (TEST SECTION 2)

layer (wet mix and Type 1 sub-base) computed by the ELMOD program are higher than those from PADAL. As for subgrade stiffnesses, the majority of the results also lie within 50% of equality. When these results are compared to Figure 5.6, the elastic stiffnesses computed in Section 2 are much more realistic than in Section 1. The difference is believed to be the result of a combination of having a greater thickness of granular layer underlying a thinner bituminous layer. Consequently, the contribution of the granular layer is increased which, in turn, influences the ELMOD computation.

5.3 CONCLUSIONS

(1) The review of the ELMOD program gives rise to four observations. First, it is not clear how the ELMOD program formulates its iterative procedure, nor what the convergence criteria are, nor how non-linear subgrade is incorporated into the iterations. Second, there is uncertainty about the accuracy of the back-analysed elastic stiffnesses, since no information is given on the goodness of fit with measured deflection bowls. Third, the ELMOD program treats a four-layered structure as three-layered for back-analysis since layer 2 is assumed to vary with the stiffness of layer 3, the granular sub-base layer, according to a fixed relationship. Fourth, the ELMOD program cannot analyse structures with a lean concrete roadbase layer.

(2) The evaluation of the ELMOD program reveals that, for linear subgrade, the ELMOD program can predict the elastic stiffness of the subgrade layer with good accuracy, whereas the stiffness prediction for the bituminous layer is less good and the sub-base layer is worst. A similar finding is also recorded for the non-linear subgrade formulation. In general, prediction of layer stiffnesses for structures with non-linear subgrade is worse than

with linear. One reason may be that the formulation of non-linear subgrade stiffnesses in the ELMOD program is different from that of PADAL. However, no literature is so far available to determine how exactly the ELMOD program calculates non-linear subgrade stiffnesses. As far as the sub-base layer is concerned, the study has clearly demonstrated that the ELMOD program is unable to accurately predict the stiffness of this layer. The results are extremely variable and grossly over-predict the correct value by as much as 9 times. Even the mean stiffnesses are consistently around 2 to 3 times the correct values.

(3) The overall finding from the comparison based on field data is that there is general agreement between the ELMOD and PADAL programs in predicting the elastic stiffnesses of a combined bituminous layer, with differences less than 20%. However, the ELMOD prediction on subgrade stiffness is consistently smaller than the PADAL calculation, by up to 50%. These low predicted stiffnesses in the subgrade layer may then cause over-prediction of sub-base stiffnesses. In cases where the thickness of sub-base is relatively small as for the Section 1 structure, the ELMOD prediction becomes unrealistically large (refer Figure 5.6).

(4) From the above analysis, it may be concluded that the ELMOD program, in its present form, may only be used for the structural evaluation of a two-layered structure (i.e. a bituminous layer overlying the subgrade), with reasonable confidence.

CHAPTER 6

STRUCTURAL EVALUATION OF A FULL SCALE TRIAL SECTION

6.1 INTRODUCTION

Since 1978, a number of experimental pavements and overlays have been designed by Nottingham University. Amongst them, five structures have been selected for monitoring of performance, as well as to provide a database for the development of analytical work on pavement evaluation and overlay design. These five structures, whose material properties and details of construction are known, consist of four new pavements and an overlaid pavement. Table 6.1 summarises the full scale trials. Full details can be obtained in Brunton (63).

During the past three years, altogether four surveys have been carried out on each trial section, undertaken with the tremendous support and assistance of all the Local Authorities concerned, who provided excellent traffic control and some additional core information. Some of the results of the surveys have been described in the first year report (93).

During the FWD survey in September, 1985, structural failure at Ch.90m in the left hand lane of the eastbound carriageway of the trial section at Hasland Bypass was noted. In the subsequent survey in May, 1986, another failure was also noted at Ch.75m in the same carriageway. The above matter was discussed in a meeting with Derbyshire County Council (D.C.C.) It was agreed that a full structural evaluation should be carried out to ascertain the cause of failure.

Consequently, a comprehensive site investigation was carried out with co-operation of D.C.C. over three days between 2nd and 4th of July,1986. The survey involved deflection measurements taken by both the FWD and Benkelman Beam, coring, pitting and numerous in-situ

Name of Full Scale Trials	Year of Construct'n	Location	Type	C'way Type	Length of Section		Instruments
					Total	Experiment	
A617 Hasland Bypass, Derbyshire	1978	Western end of A617 near Chesterfield	New	Dual	∿ 6000 m	180 m	Yes
B5035 Carsington Bypass, Derbyshire	1981	Whitehouse Corner, between Ashbourne and Wirksworth	New	Single	350 m	150 m	No
Aetheric Road, Braintree, Essex	1979	Between A120 and A130 in Braintree	Reconstruct	Single	240 m	240 m	Yes
A52 Derby Road, Nottingham	1982	Between Sandy Lane and Cow Lane	Reconstruct	Dual	1100 m	190 m	Yes
A427 Theddingworth, Leicestershire	1981	At Theddingworth, South Leicestershire	Overlay	Single	575 m	280 m	No

Table 6.1 Summary of Full Scale Trials

tests in each trial pit to determine the condition of the sub-base and subgrade layers. A large number of samples was also taken and tested at the University. The following sections describe the structual evaluation of Hasland Bypass in detail.

6.2 THE SITE

6.2.1 Background

The full scale trial section of Hasland Bypass is situated on the A617 between Chesterfield and Junction 29 of the M1 motorway in Derbyshire. Figure 6.1 shows the location of the site. The experimental section, which consisted of about 190 m length of dual carriageway, was constructed in 1978 as part of the A617 Hasland Bypass. The exercise was a joint venture between the County Surveyor's staff from D.C.C., the suppliers of the bituminous material (Hoveringham Stone Ltd (now Tarmac Roadstone Ltd)) and the Pavement Research Group at the University of Nottingham.

The chosen design is fundamentally different from conventional practice carried out in accordance with Road Note 29 (94). Brown (95) detailed the design philosophy used in the analytical approach, material testing and pavement construction. A summary of this novel design will be given in the next section.

Instruments to measure transient stresses and strains due to traffic loading were installed during construction. They were located just below the formation level of the subgrade and at the bottom of the bituminous layer. The type of instrumentation has been described elsewhere (85) and details of the installation were reported in Brown et al (84). These in-situ measurements, together with surface deflections from the Benkelman Beam, have already formed a part of the development of the analytical pavement design procedure proposed by Brunton (63). They also formed a basis for the development of the computer programs BASEM and PADAL, as already described in Chapter 4.

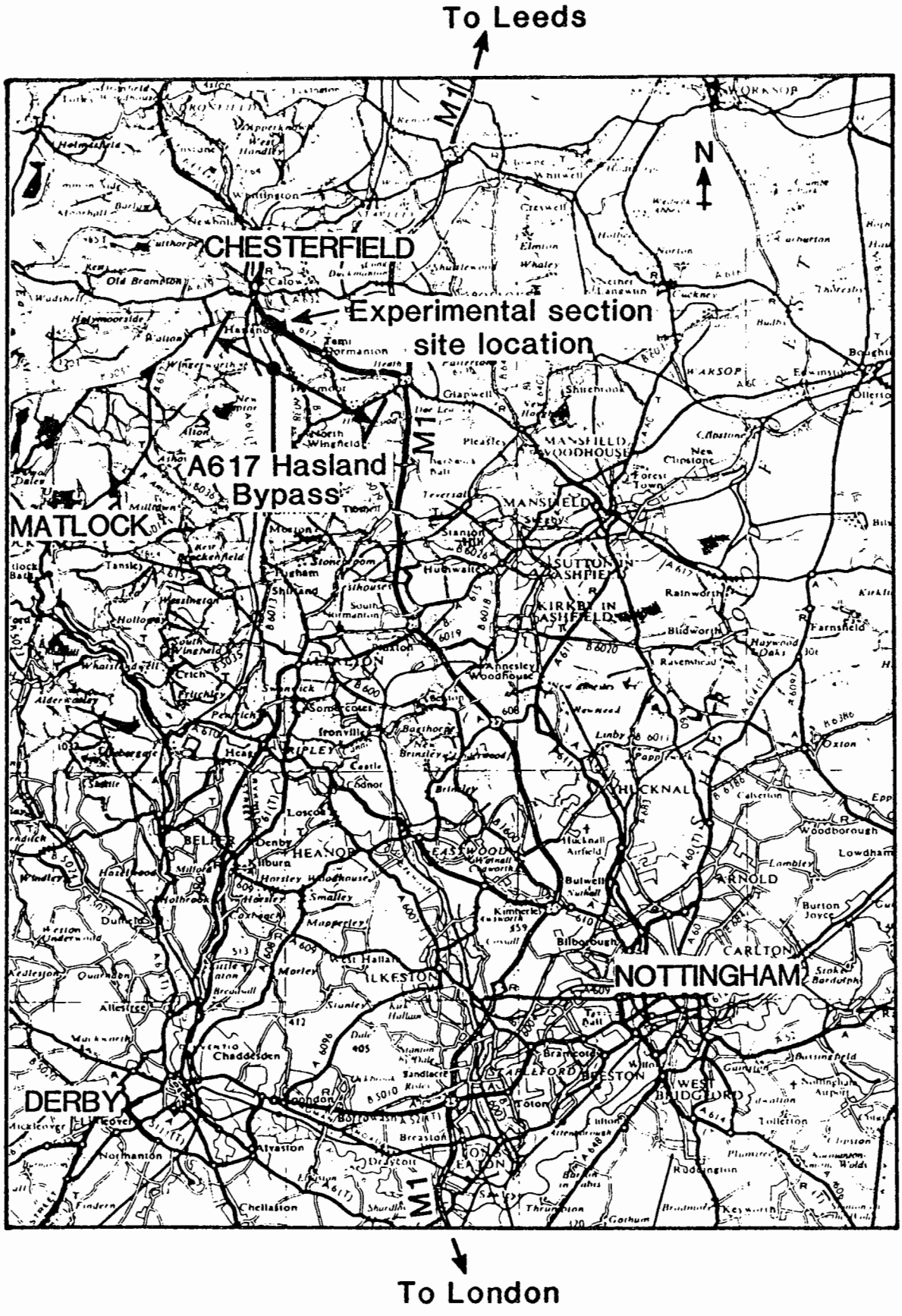

FIG. 6.1 SITE LOCATION OF A617 HASLAND BYPASS EXPERIMENTAL SECTION

The Bypass was open to traffic in September, 1978. Since then, the experimental section has been continuously monitored. Table 6.2 summarises all the site surveys since 1978.

6.2.2 Carriageway design

The original design parameters for the carriageway, provided by D.C.C., were as follows :

Traffic volume : 13 msa (million standard axles) over 20 years

Soil strength : 3% CBR

(a) Conventional section : Based on Road Note 29, the chosen design is as follows :

40 mm rolled asphalt wearing course

60 mm dense bitumen macadam basecourse

150 mm dense bitumen macadam roadbase

410 mm Type 1 granular sub-base

(b) Experimental section : The final design is summarised as follows:

200 mm modified dense bitumen macadam (DBM) roadbase

200 mm type 1 granular sub-base

The skid resistance was provided by a surface dressing layer. A layer of Terram 1000 fabric was specified at the interface between the sub-base and subgrade layers in order to avoid intrusions of clay soil from the subgrade layer.

The modified DBM roadbase material was produced from a standard BS 4987 40 mm DBM grading but with a binder content and type of 4% and 50 pen respectively as against 3.5% and 100 pen for a conventional material. In addition, it was intended that the void content should not exceed 7%. The idea was to increase the elastic stiffness of the material from 9000 MPa to 12000 MPa. The design

Date of Survey	Types of Survey
1978 24-28 July	Benkelman Beam deflection survey.
1979 October	Benkelman Beam deflection survey.
1980 10 December	Surface irregularity using Bumpometer and rolling straight edge.
1981 April	Benkelman Beam deflection survey; High-speed profilometer survey.
1982 18 May	Benkelman Beam deflection survey.
1984 5 April	FWD deflection survey.
8 August	FWD and Benkelman Beam deflection surveys.
1985 30 September	FWD deflection survey.
1986 2 July	FWD and Benkelman Beam deflection surveys.

Table 6.2 Summary of site surveys to date.

pavement temperature and speed of commercial vehicles were taken as 12.5°C and 80 km/hr respectively.

Figure 6.2 compares the conventional and experimental structures.

6.3 FIELDWORK

6.3.1 Falling Weight Deflectometer survey

The FWD survey was carried out at 10 m intervals in the nearside wheelpath and lane centre of both eastbound and westbound carriageways. In each carriageway, both the conventional and experimental sections of the left hand lane were surveyed. The test length which totalled 400 m, was sub-divided as follows :

190 m experimental section

100 m conventional section, east of experimental

110 m conventional section, west of experimental

Figure 6.3 shows the layout of the test area.

The idea was to compare the performance of the experimental section with the conventional one on either side of it. Additional deflection measurements were made over the locations where structural failure had occurred in the eastbound carriageway.

Throughout the survey, temperature readings at depths of 20, 40, 100 and 160 mm in the bituminous material were recorded. Table 6.3 shows the results of temperature variation. This information is required to enable back-analysed stiffnesses of the bituminous material to be adjusted to design conditions.

6.3.2 Benkelman Beam survey

The Benkelman Beam deflection survey was carried out by County Laboratory personnel at the same time as the FWD survey. The deflections along the wheelpath were measured at the same FWD chainage locations. Detailed results of this survey have been reported elsewhere (96).

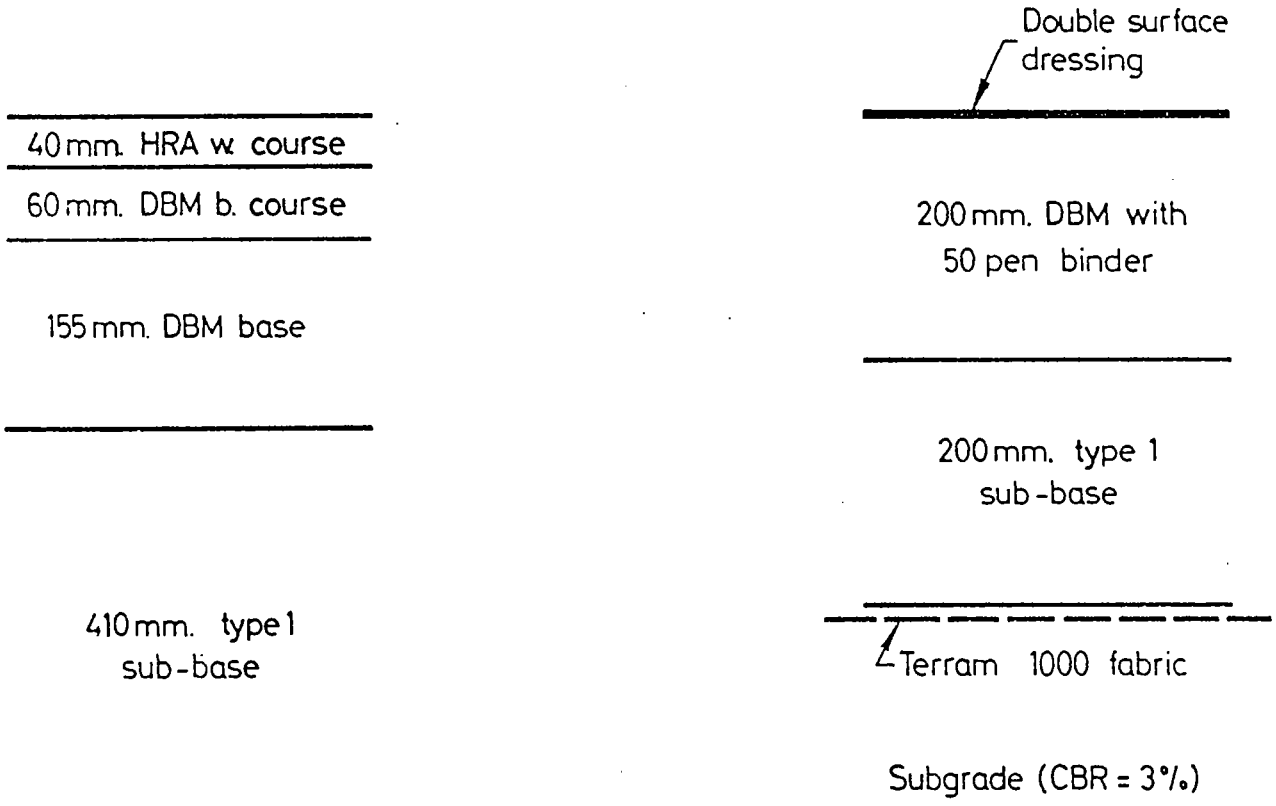

FIG. 6·2 COMPARISON OF STRUCTURAL DESIGNS FOR THE CONVENTIONAL PAVEMENT (ON THE LEFT) AND THE EXPERIMENTAL SECTION

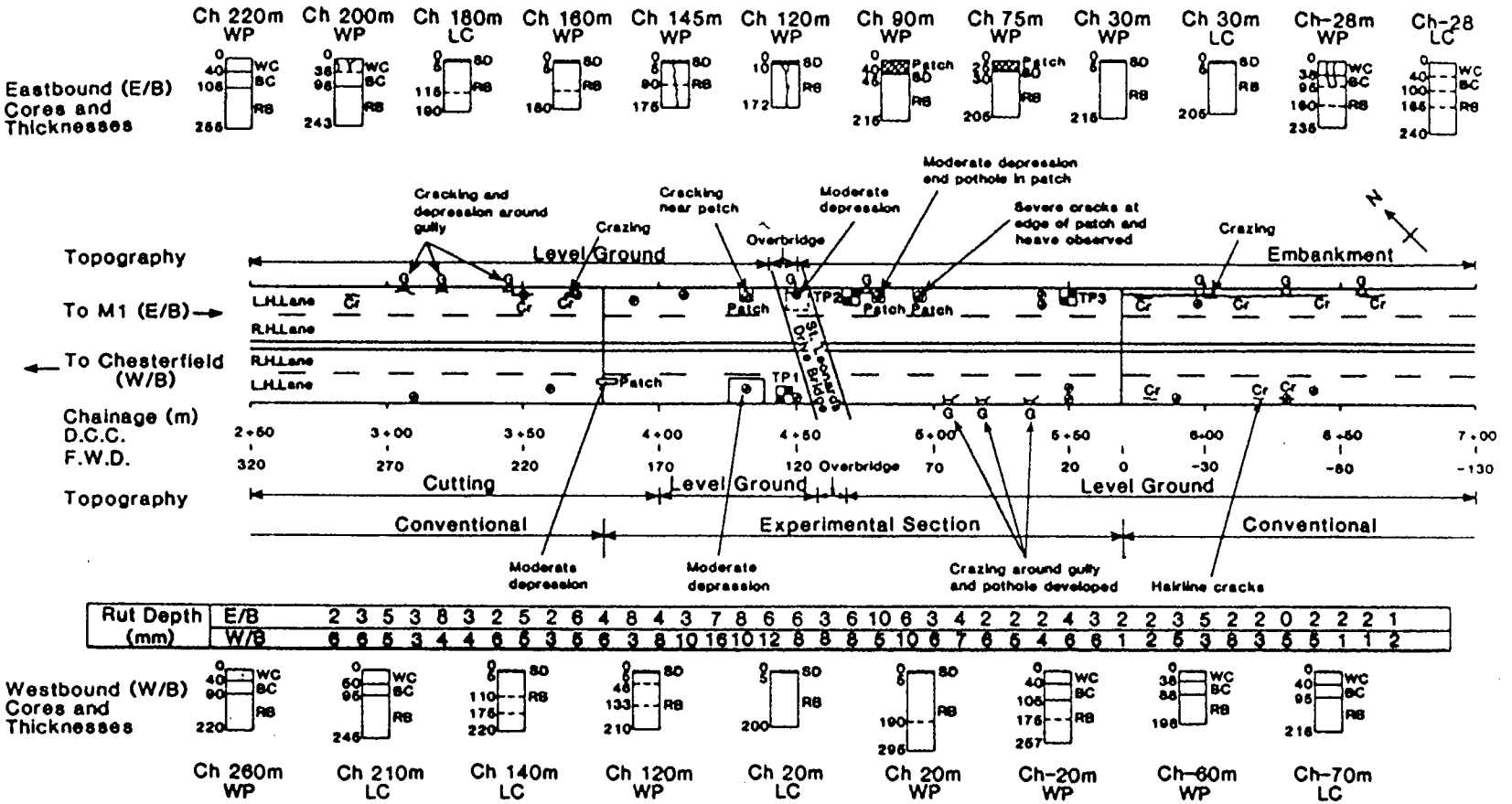

Notation : G – Gully, C – Crack
WP – Wheel path/nearside), LC – Lane Centre
WC – Wearing Course
BC – Basecourse
RB – Roadbase
SD – Surface Dressing
--- Debonding at interface of cores
• Core Location
Trial Pit

FIG. 6.3 PLAN SHOWING DETAILED LAYOUT AND STRUCTURAL CONDITIONS OF TEST SECTIONS, A617 HASLAND BYPASS, DERBYSHIRE

Time of day (hrs)	Air temperature (°C)	Pavement temperature at depths (°C)				Remarks
		20mm	40mm	100mm	160mm	
1010	24.8	31.7	28.4	24.9	24.3	Sunny
1050	23.1	33.9	30.2	25.8	24.2	"
1130	25.0	37.7	33.9	28.0	25.4	"
1210	26.9	37.5	34.6	28.4	25.6	"
1430	25.9	41.9	39.6	33.4	28.1	"
1510	27.1	38.1	37.1	32.9	28.7	Cloudy
1600	25.0	38.5	36.9	32.3	28.4	Sunny

Table 6.3 Measured air and pavement temperatures during FWD survey (02/07/86)

6.3.3 Visual condition survey

A condition of the pavement surface was inspected within the test section. Detailed results of the survey can be found in Section 6.4.1.

6.3.4 Coring survey

The coring operation was carried out by a team of three University personnel at the same time as the FWD survey. A total of 21 cores were recovered, 12 of which were taken from the experimental section and 9 from the conventional section. Figure 6.3 shows a plan of the core locations. These cores were taken with the following objectives :

(a) To obtain actual thicknesses for the back-analysis of layer stiffnesses;

(b) To determine the refusal density;

(c) To determine the aggregate type and grading, voids content, binder type and content.

Of the 12 cores taken from the experimental section, two were taken from the failed area at Ch. 75 m and Ch. 90 m of the eastbound carriageway in order to determine the cause of structural failure.

6.3.5 Trial pitting survey

Three trial pits were excavated in the experimental section. Figure 6.3 shows the exact locations of the trial pits. Both pits TP1 and TP2 were chosen based on 85 percentile deflections measured by the FWD in 1985. For comparison, pit TP3 was excavated in a good area, in which low deflections were measured.

The excavation of each pit was carried out by the County. It was agreed that the general procedure followed advice note HA 30/85 from the Department of Transport (97). In each pit, measuring 1.5m x 1.0m, the bituminous material was first sawn into small sized beams and slabs by using a mechanical saw and carefully removed. The

condition of the unbound sub-base and subgrade layers was recorded. A series of in-situ tests were then carried out on each layer which included,

(a) Density and moisture content, recorded using two nuclear density meters, one from the County Laboratory and one from the University;

(b) Density measurement determined by sand replacement;

(c) Clegg Impact Hammer (CH) tests;

(d) Dynamic cone penetrometer (DCP) tests.

In addition, bulk samples of the material in each pavement layer were taken to the University for detailed analysis. Cylindrical specimens of the subgrade were taken by a 102 mm core cutter at the formation for stiffness measurement in the triaxial apparatus.

Bulk excavation of the granular material was carried out using a mechanical excavator which was then followed by hand digging to expose the layer of Terram fabric at the sub-base/subgrade interface. The Terram layer was carefully torn off and taken for further analysis. It was surprising to discover that Terram was not present in pit TP3 although it was in the required design (refer to Section 6.2.1 and Figure 6.2).

6.4 RESULTS OF FIELDWORK

6.4.1 Visual condition

The results of the visual condition survey of the left hand lane for both carriageways are summarised in Figure 6.3. The general impression from the test sections was that the predominant mode of distress in the experimental section was in the form of rutting, whereas in the conventional sections it was surface cracking. Furthermore, surface cracking was observed around a number of gullies, some of which had developed into crazing and potholes.

In the eastbound carriageway of the experimental section, patching

was observed in three areas at chainages 140m, 90m and 75m respectively. However, the patches were noted to be poorly compacted as cracking was visible around their edges. The general condition of the surface dressing was quite poor with a lot of chippings stripped off at the lane centre. In contrast, chippings in the wheelpath were well compacted into the layer resulting in a shiny surface. A lot of loose chippings were also noted along the drainage channel. Rut depth varied from 2 to 10 mm.

The westbound carriageway was generally observed to be in a better condition but a moderate depression was located at Ch 140 m with a maximum rut depth of approximately 16 mm. As with the eastbound carriageway, the condition of the surface dressing layer was generally poor.

The conventional section had less permanent deformation than the experimental one, with a maximum rut depth of 8 mm, but with more visible distress on the pavement surface. Longitudinal cracking was found to be the major mode of structural distress.

During the survey, it was particularly noted that a lot of water was retained in the holes after coring. A return visit a few hours later confirmed that very little drainage had occurred. This finding suggested that the permeability of the sub-base layer could be very low.

Furthermore, it was noted that plants had grown on the verge in the westbound carriageway and, in particular, over the french drains. Also, a lot of water was retained in the gully pots. These signs suggested that the drainage system was not working effectively.

6.4.2 F.W.D. measurements

The deflection profiles are shown in Figures 6.4 and 6.5 for the eastbound and westbound carriageways respectively. The deflections shown are the central deflection, d_1, the fifth deflection, d_5 and

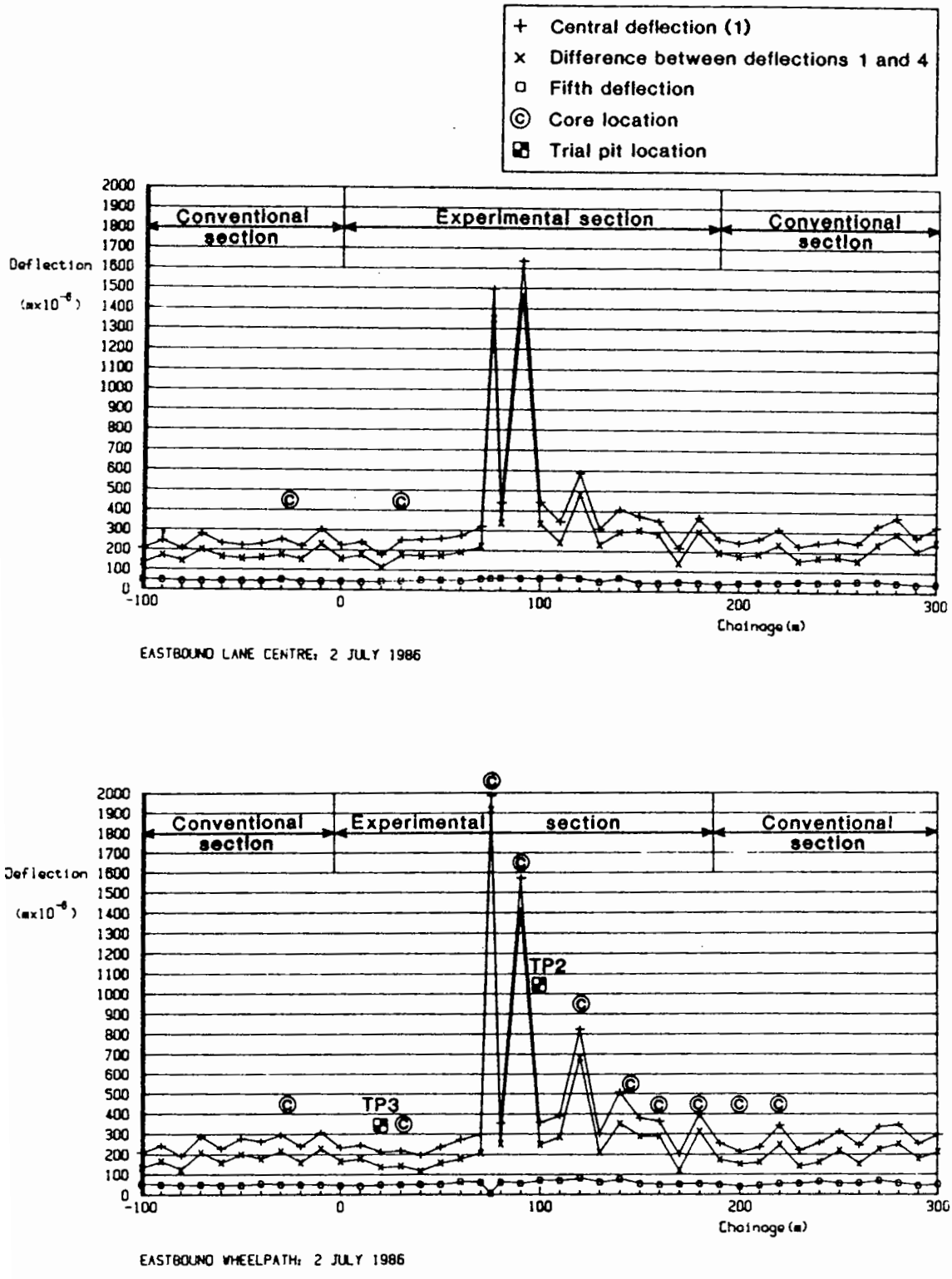

Fig. 6.4 F.W.D. DEFLECTION PROFILES OF EASTBOUND CARRIAGEWAY

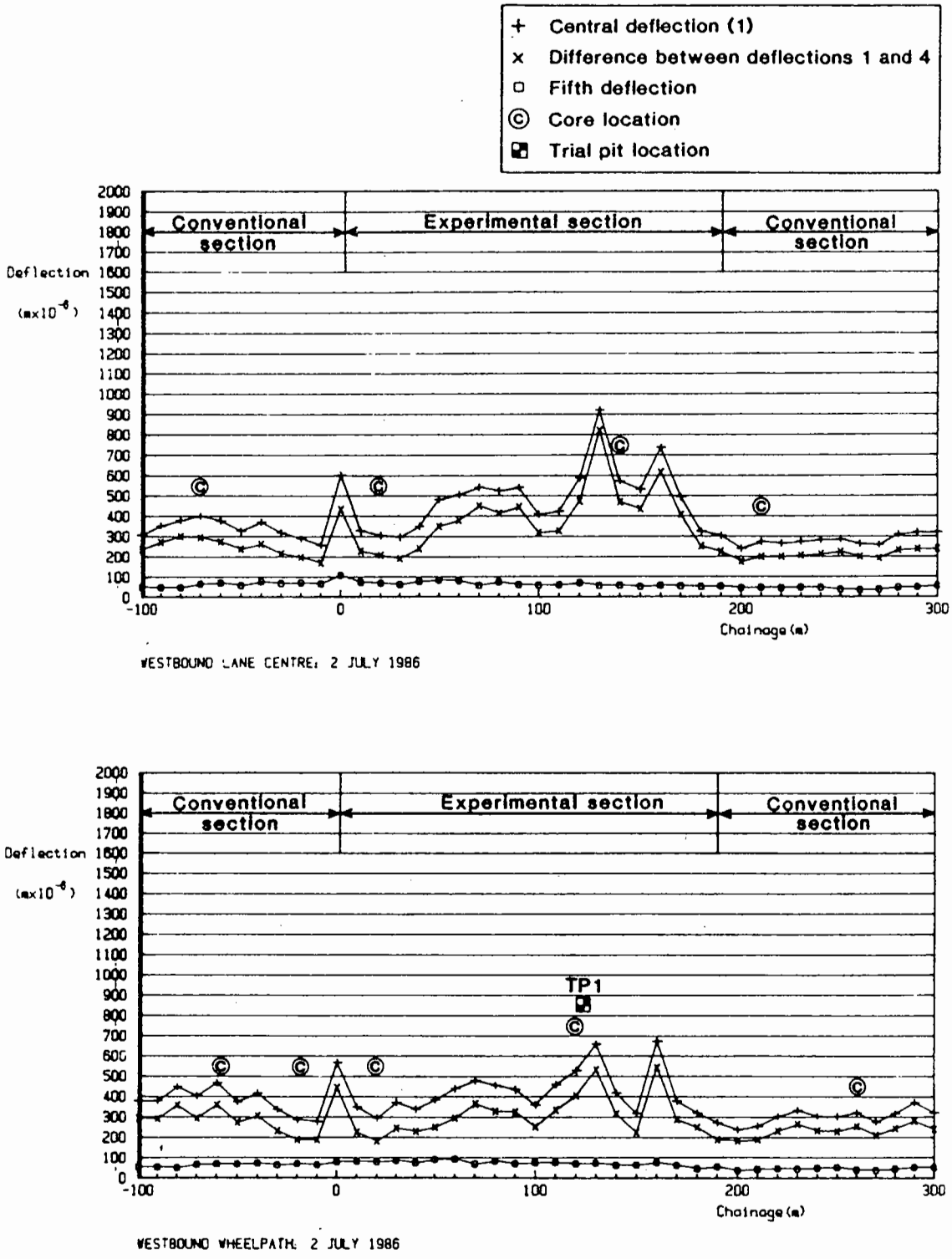

Fig. 6.5 F.W.D. DEFLECTION PROFILES OF WESTBOUND CARRIAGEWAY

the deflection difference d_1-d_4. These parameters are indicators of the response of the whole pavement structure, the subgrade and the upper pavement layers respectively and the data have been normalised to a standard contact pressure of 700 kPa. In this investigation, the deflection d_5 instead of the usual d_7 in monitoring the subgrade response because it is found to be more sensitive to subgrade variation.

(a) Eastbound carriageway

In the experimental section, the deflections in the nearside wheelpath were variable and of large magnitude in the area between Ch.75 m and Ch. 160 m whereas those in the area between Ch.0 m and Ch.70 m were found to be reasonably uniform and of much lower magnitude. This indicates that the pavement structure in the former case is relatively weak, thus supporting the visual distress observed on the pavement surface, where areas at Ch.75 m and Ch.90 m have failed and temporary patching has been carried out. Longitudinal cracks were observed at Ch.120 m, and in the case of Ch.140 m, patching was noted close to the test point again, indicating the possibility of a weak and deteriorating structure. Large values of (d_1-d_4) indicate that the pavement layers are likely to be weak. Moreover, the slightly larger d_5 values observed between Ch.80 m and Ch.140 m indicate a relatively soft subgrade in that area. In contrast, the lower d_5 values in the area from Ch.0 m and Ch.70 m show a stiff subgrade. (It is pointed out that the exceptionally small magnitude of d_5 measured at Ch.75 m is the result of testing over a very weak surface layer, i.e. the patching material, is to be ignored in the analysis). When comparing the profile at the lane centre, a similar pattern of deflections is generally observed but the magnitude of deflections at Ch.120 m and Ch.140 m in the wheelpath were found to be slightly larger than in the lane centre

positions, indicating that some damage had occurred at these locations under the action of traffic.

Deflections for the two areas of conventional section were more uniform and of similar magnitude, though the area between Ch.200 m and Ch.300 m was slightly more variable than the area starting from Ch.0 m. When compared with the experimental section, it is noted that it has a similar level of deflection from Ch.0 m to Ch.70 m but much lower than the rest of the experimental section. The subgrade is generally stiffer in this section as the lower values of d_5 indicate.

(b) Westbound carriageway

The profile of the experimental section in Figure 6.5 was much less variable than in the eastbound carriageway but the general level of deflection was slightly higher than in the conventional one. The highest deflections occur at Ch.130 m and Ch.160 m and, in view of the corresponding high (d_1-d_4) values, the bituminous roadbase and/or sub-base layer were considered to be the main cause of the weakening of the structure. A study of the profile of the d_5 parameter revealed higher values between Ch.0 m and Ch.160 m, indicating that the subgrade in the area is softer than in other areas of the carriageway. This observation was noted to be consistent with the pattern of rut depths measured along the whole carriageway. Further discussion on the possible cause of rut depth development will be made in Section 6. For the conventional section, the deflection profiles were again observed to be uniform. Measured deflections in the area from Ch.0 m to Ch.-10 m were slightly higher than in the area between Ch.200 m and Ch.300 m, which is considered to be the result of softer subgrade in this area.

6.4.3 Trial pits

Details of each pavement layer are presented in Tables 6.4, 6.5 and 6.6 for trial pits TP1, TP2 and TP3 respectively.

TABLE 6.4

UNIVERSITY OF NOTTINGHAM

Trial Pit Record

Project title : A617 Hasland Bypass
Location : Chainage 125m, westbound - Experimental Section
Trial pit no. : TP1 Date : 3 July 1986 Logged by : AT

Depth (m)	In-situ tests	Water	Samples	Description
0			B	Bituminous layer. Debond at depth 120mm within layer. Free water at interface with sub-base.
			B	
0.225				
	ND DCP SR CH	w	B	Granular sub-base. Medium dense yellowish brown sand and gravel. Crushed Limestone.
			B	
0.445			B	Terram fabric
	ND DCP SR CH CP		D	Subgrade soil. Very stiff olive brown silty clay with occasional cobble sized rocks
0.645				End of pit

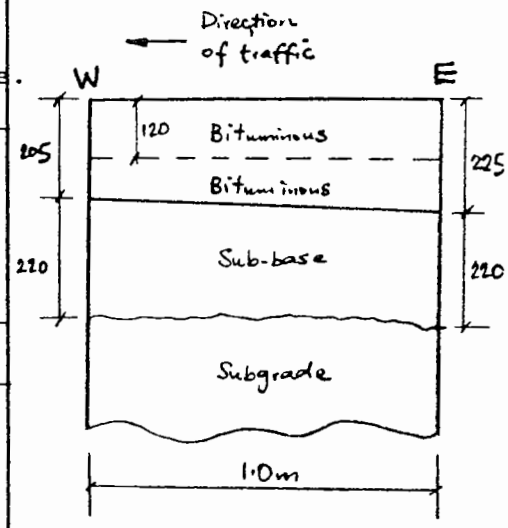

NB : East and west faces similar.

Notes

1. see Table 6.6 for detail of in-situ test results and Fig. 6.8 for DCP results.
2. Bituminous layer sawn into small beams and slabs and then broken up with jack hammer.
3. Granular material dug up by a small excavator.
4. Size of pit 1.5 m x 1.0 m
5. All layer thicknesses in mm.

B - Bulk ; J - Jar ; D - Disturbed ; U - Undisturbed
w - Free water encountered
CH - Clegg hammer
DCP - Dynamic cone penetrometer
CBR - California bearing ratio
SR - Sand replacement method
ND - Nuclear density gauge

TABLE 6.5

UNIVERSITY OF NOTTINGHAM

Trial Pit Record

Project title : A617 Hasland Bypass
Location : Chainage 100m, eastbound - Experimental Section
Trial pit no. : TP2 **Date :** 3 July 1986 **Logged by :** AT

Depth (m)	In-situ tests	Water	Samples	Description
0			B	Bituminous layer. Debond at depth 118mm within layer. Very voidy at bottom of upper layer.
			B	Lower layer very friable and voidy. Water at interface with sub-base.
0.22	ND PCP SR CH	W	B	Granular sub-base. Medium dense yellowish brown sand and gravel crushed Limestone.
			B	
0.50			B	Terram fabric
	ND DCP SR CH CP		D B	Subgrade soil. Very stiff olive brown silty clay with occasional cobble sized rocks.
0.75				End of pit

Notes

Please refer to notes in trial pit TP1.

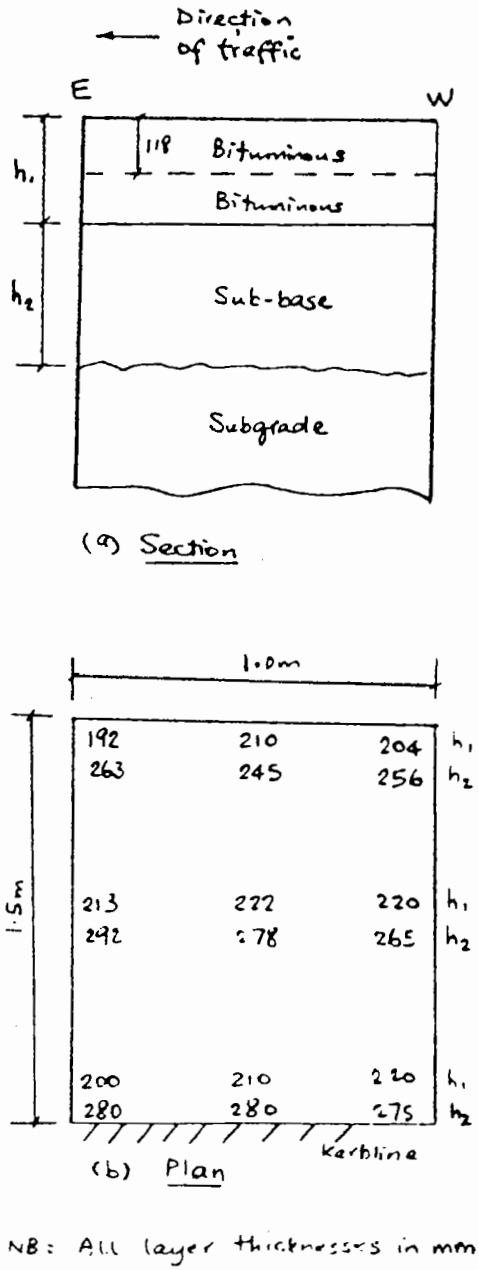

B - Bulk , J - Jar , D - Disturbed ; U - Undisturbed

w	- Free water encountered	CBR	- California bearing ratio
CH	- Clegg hammer	SR	- Sand replacement method
DCP	- Dynamic cone penetrometer	ND	- Nuclear density gauge

TABLE 6.6

UNIVERSITY OF NOTTINGHAM

Trial Pit Record

Project title : A617 Hasland Bypass
Location : Chainage 20m, eastbound - Experimental Section
Trial pit no. : TP3 Date : 4 July 1986 Logged by : AT

Depth (m)	In-situ tests	Water	Samples	Description
0			B	Bituminous layer constructed in three lifts. Debond at depth 185mm within layer.
0.26	ND DCP SR CH		B	Granular sub-base. Dense yellowish brown sand and gravel crushed Limestone. No free water at top of layer.
0.70	HD DCP SR CH CH		D B	Subgrade soil. Very stiff Olive brown silty clay with occasional cobble sized rocks
0.95				End of pit

Notes

Please refer notes in trial pit TP1

Cross-section

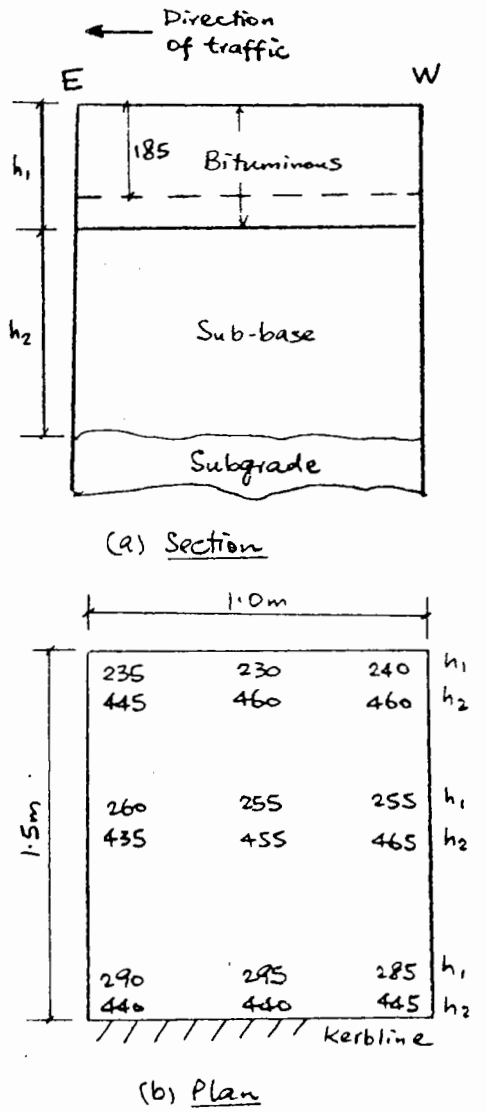

NB: All layer thicknesses in mm

B - Bulk ; J - Jar ; D - Disturbed ; U - Undisturbed
w - Free water encountered
CH - Clegg hammer
DCP - Dynamic cone penetrometer
CBR - California bearing ratio
SR - Sand replacement method
ND - Nuclear density gauge

Trial pit TP1 shows that the bituminous layer varied from 205 mm to 225 mm but was found to have debonded at a depth of 120 mm; the interface between two lifts. The granular sub-base was 220 mm thick medium dense yellowish brown sand and gravel (crushed Limestone). Water was observed at the interface between the bituminous and sub-base layers. The Terram fabric at the sub-base/subgrade interface was found to be in good condition and no clay intrusion was observed. The fabric was later left to dry naturally in the laboratory and a moisture content of 23.8% was recorded.

The thickness of the bituminous layer in trial pit TP2 varied from 192 mm to 220 mm and, as with TP1, debonding was noted at a depth of 118 mm. At this level, the bottom of the upper layer was observed to be very voidy indicating under-compaction. Again, water was noted at the interface with the sub-base layer. The sub-base material was exactly the same as TP1 but slightly thicker from 245 mm to 292 mm. The Terram material which was laid at the sub-base/subgrade interface was also in good condition with no clay intrusion. Moisture content had not been measured for this material; however, it is not expected to be different from that in TP1.

In trial pit TP3, the bituminous layers had been constructed in three lifts with a total average thickness of 265 mm. As with the other trial pits, debonding at a level of 185 mm was noted. In contrast, water had not been found at the interface with the sub-base layer. The sub-base material in this pit was again the same as other pits and well compacted. Much greater thicknesses (between 435 mm and 465 mm were recorded). This unusually large thickness was later found to be a part of a drain trench mentioned in the previous report (84). No Terram fabric was found at the sub-base/subgrade interface, perhaps because of the presence of the trench.

The subgrade soil in all the trial pits was an olive brown stiff

silty clay with occasional cobble and gravel sized rocks. Measurements recorded by a portable static cone penetrometer indicated a uniform subgrade with in-situ CBR of 4.0% to 4.8%, as shown in Table 6.7.

Table 6.7 also includes the results of bulk densities measured by the sand replacement method and nuclear density meter. For the sub-base layer the densities measured by sand replacement, ranging from 2129 kg/m^3 to 2280 kg/m^3, are, on average, slightly higher than the corresponding ones recorded by nuclear density meter, which were 2021 kg/m^3 to 2208 kg/m^3. These densities are generally consistent with results recorded during construction in 1978, which were low, resulting in high air voids. More details of laboratory results for the sub-base material will be discussed in the next section. The bulk densities measured by sand replacement on the subgrade were variable, ranging from 1684 kg/m^3 to 2125 kg/m^3 but more consistent results were observed with the nuclear density meter (1883 kg/m^3 to 2002 kg/m^3).

The results from the Clegg Hammer are also presented in Table 6.7. It was used as part of the investigation in order to evaluate its potential in field testing. The Clegg Hammer was found to be portable and easy to use. From the table, the CIVs of the sub-base range from 25.4 to 51.6 for trial pits TP1 to TP3, whereas the corresponding values for the subgrade lie between 6.0 and 9.4. Judging from the limited results above, the Clegg Hammer tends to give a measure of the bearing capacity of the unbound material, since the stronger sub-base material gives greater CIV, but the above assessment will be modified in the light of a more detailed study currently being carried out in another research project (98).

The variation of shear strength with depth of the unbound layers was investigated using a dynamic cone penetrometer (DCP). Since limited

Trial pits	TP1		TP2		TP3	
In-situ tests	sub-base	subgrade	sub-base	subgrade	sub-base	subgrade
	Bulk density (kg/m^3)					
Sand replacement	2129	1765	2283	1684	2199	2125
Nuclear density by						
(a) DCC+	2021	1945	2097	1809	2208	2002
(b) NU*	2095	1883	2152	1904	2189	1982
Clegg impact value (CIV)	25.4	6.0	34	6.4	51.6	9.4
Cone penetrometer (% CBR)	N/A	4.0	N/A	4.4	N/A	4.8

\+ DCC denotes Derbyshire County Council
* NU denotes Nottingham University

Table 6.7 In-situ test results for sub-base and subgrade layers in the trial pits

knowledge was available about the equipment before this investigation, the results are analysed qualitatively by cross comparison amongst the trial pits only. The test results in each trial pit are shown in Figure 6.6 in which the term "blows/cm" means the number of blows of the DCP in order to penetrate 10mm of the test material, averaged over a thickness of 50 mm. The averaging procedure is preferred to the actual recorded results to avoid anomalies which might arise if it were tested over large particles in the sub-base layer. The results are considered to reflect the variation of shear strength; the lower the shear strength, the less is the number of blows recorded and vice versa. The test was carried out up to a depth of 500 mm from the surface of the sub-base layer. The following conclusions can be made from the figure:

(a) The shear strength of the sub-base material in all the trial pits increases to a maximum value at a depth 100 mm from the surface but reduces towards the base of the layer. It is considered that the reduced strength measured for the top 100 mm could be due to a combination of increase in moisture and reduction in confining pressure on the aggregate. In contrast, the gradual increase of strength from the base may be the result of increasing interlock amongst the particles under compaction, which is expected when compacting over a subgrade of lower shear strength. Comparing the sub-base materials, the highest blowcount was recorded in trial pit TP2 with 5.4 blows/cm, whereas TP3 and TP1 have respectively, 4.1 and 2.6 blows/cm, suggesting that the shear strength in TP2 is highest and that TP1 is lowest. Recent research on granular material reported by Thom (100) has shown that increase in the shear strength of a material will result in the reduction of permanent deformation, hence, rutting in the pavement surface. Hence, considering the granular material

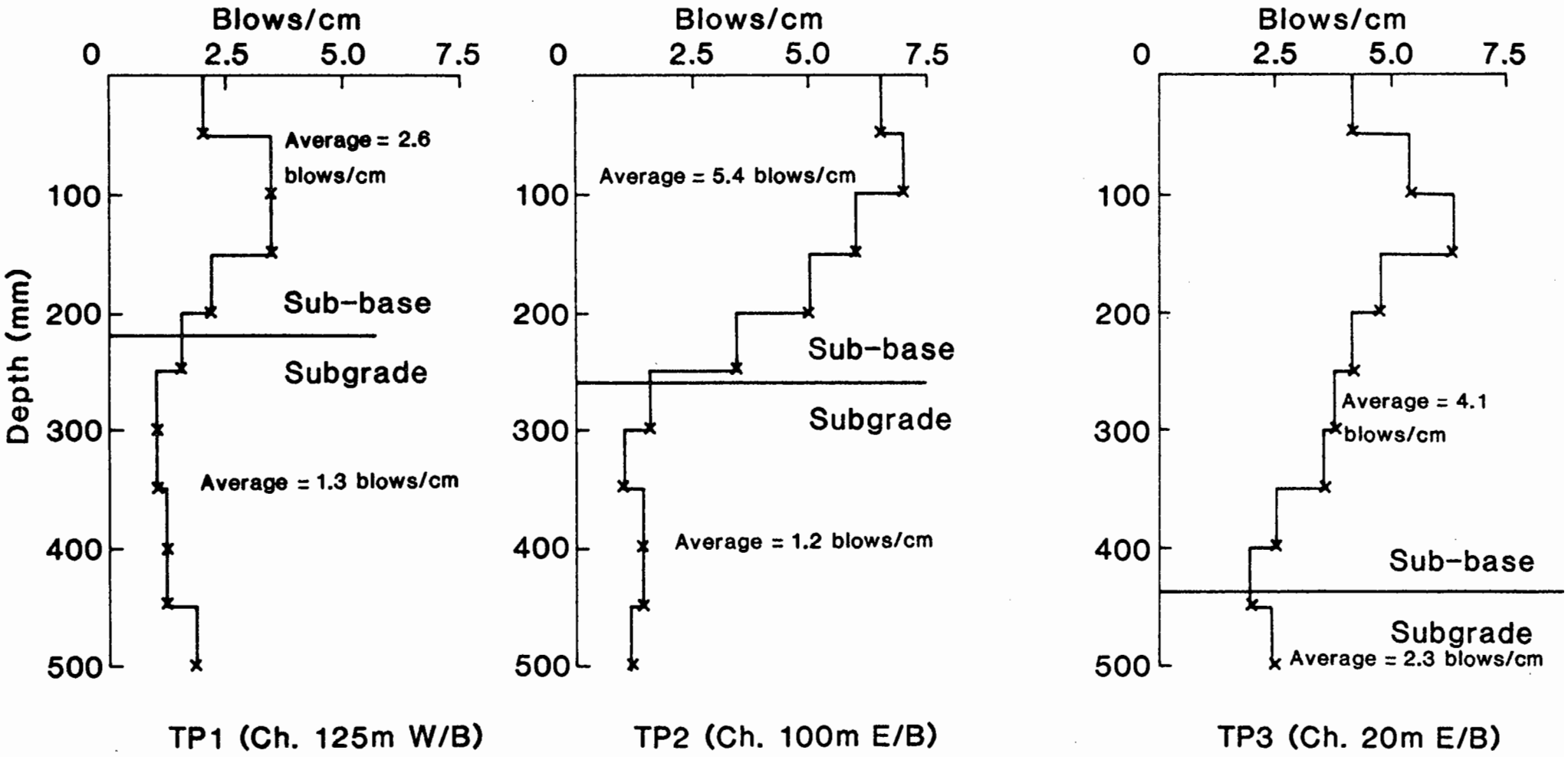

FIG. 6.6 STRENGTH PROFILE WITH DEPTH OF THE UNBOUND MATERIALS IN TRIAL PITS USING DYNAMIC CONE PENETROMETER

alone, the structure of trial pit TP1 will be the most susceptible to permanent deformation and TP2 the least.

(b) The DCP also penetrated into the subgrade, though only by 60mm in trial pit TP3. The results recorded were 1.3 blows/cm for TP1 and TP2 and 2.3 blows/cm for TP3. Interpreting the DCP results, the shear strength of this layer is quite uniform with depth (refer TP1 and TP2) but much weaker than the sub-base material.

(c) The interface between sub-base and subgrade layers has been drawn in the figure from the measured thicknesses and is found to agree well with the marked change in strength profile. Therefore, it is considered that the DCP is able to determine the thickness of layers if their shear strengths are distinctly different.

6.5 DETAILED ANALYSIS OF LABORATORY RESULTS

As stated in Section 6.3, a large number of samples was taken to the University laboratory for detailed analysis. These included 21 core specimens and materials from various pavement layers in three trial pits. Table 6.8 summarises all the tests which have been performed for each material, and the results are analysed in the following sections.

6.5.1 Clay subgrade

The results of laboratory tests on the clay subgrade are summarised in Table 6.9. It can be seen that the moisture contents measured in trial pits TP1, TP2 and TP3 were 19.0%, 19.6% and 12.9% respectively. The measured value in TP3 is too low, and was the result of a cobble sized piece of rock embedded in the cylindrical sample. Results obtained in 1978 during the construction of the bypass are also shown in brackets, where the moisture contents were 12.6% and 16.3% at the locations corresponding to TP1 and TP2. Hence, there had been an increase of moisture in the subgrade since 1978. Nonetheless, the subgrade is still regarded as stiff since the existing moisture

Test type	Core specimens	Trial Pits		
		Bituminous	Granular	Clay subgrade
Density	46	3	3	3
P.R.D.	3	3	-	-
Elastic stiffness	13	6	3	3
Binder content, M_B	10	3	-	-
Void content, V_V	10	3	-	-
Grading	4	3	-	-
Binder rec. pen.	5	-	-	-
Moisture content	-	-	3	3

Table 6.8 Number of measurements performed in the laboratory for various pavement materials.

Trial pits	TP1 Ch 125m WB	TP2 Ch 100m EB	TP3 Ch 20m EB
Dry density (kg/m^3)	1730	1750	2000
Moisture content (%)	19.0 (12.6)	19.6 (16.3)	12.9
Elastic stiffness (MPa)			
1. Triaxial apparatus	80	390	Cobble in specimen
2. PADAL program	175	201	167
In situ CBR (%)	4.0 (12.5)	4.4 (10.5)	4.8

Silty clay with LL = 34%, PL = 17.6%. PI = 16.4%

Note: number in bracket denotes measured result in 1978.

Table 6.9 Summary of laboratory test results for clay subgrade in trial pits

content is close to the plastic limit (about 2% over).

Using the triaxial apparatus, two clay specimens were tested under cyclic loading with stresses simulating the traffic load. The elastic stiffness results shown in Table 6.9 are variable but with an average of 235 MPa, confirming the generally stiff nature of the material. Back-analysis was carried out using the PADAL computer program at these locations. The back-analysed stiffnesses obtained are between 167 MPa and 201 MPa, giving an overall average stiffness of 181 MPa, which is slightly lower than the triaxial test results, but still indicates that the subgrade is stiff.

The in-situ CBR values are also compared. The results show a reduction of CBR from over 10% in 1978, to around 4% in the latest test. The results from the static cone penetrometer are considered to be too low since the measurement was carried out on the top 30 mm of clay subgrade, which was generally weaker than the material beneath. An alternative and more realistic set of results was deduced from Loach (77) who studied the effect of the stress dependency of a clay soil (Keuper Marl) under cyclic loading. Keuper Marl was found to have similar plasticity properties to the clay subgrade on this site. Figure 6.7 the relationship between the elastic stiffnesses and CBR of the material. For elastic stiffnesses ranging from 167 MPa to 201 MPa as determined from back-analysis, with corresponding applied deviatoric stresses (q_r) between 17.8 kPa and 27.8 kPa a CBR in the range of 4 to 8% is obtained. This result indicates that there is a reduction in the CBR of the subgrade as a result of the increase in moisture content, as the subgrade layer approaches an equilibrium condition.

6.5.2 Bituminous materials

It was noted that the majority of the core specimens of the bituminous material from the experimental section were generally in

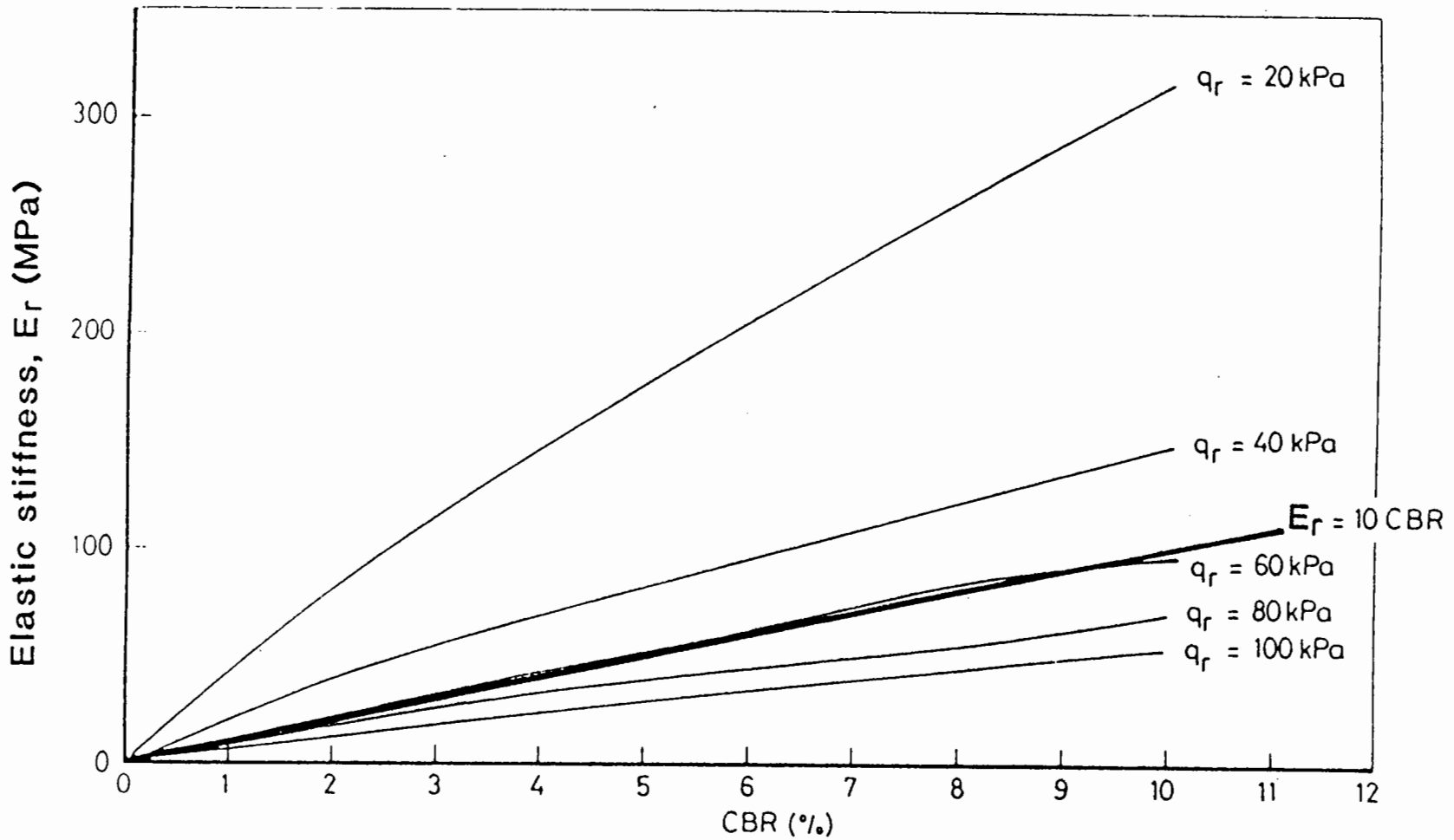

Fig. 6.7 THE RELATIONSHIP BETWEEN STIFFNESS AND CBR FOR KEUPER MARL FOR A RANGE OF STRESS PULSE AMPLITUDES (q_r)

good condition with few voids. However, large voids were noted at the interface between the two lifts indicating inadequate compaction. The visual condition of some of the specimens has been illustrated in Plates 6.1 and 6.2. The following observations are noted:

(A) Experimental section

(a) In the eastbound carriageway, cores taken over a surface crack at Ch.120 m and Ch.145 m revealed that the crack had propagated through the whole layer. However, cores taken from the failed areas (i.e. Ch.75 m and Ch.90 m) did not indicate any sign of cracking, which means that the failure was mainly caused by rutting. Looking at the sides of these cores, they appeared to be darker in colour and had aggregate sizes smaller than the other specimens. The patching material was found to be friable, loose and poorly mixed. Thus, this material was unable to withstand heavy traffic, resulting in rutting in the wheelpath and cracking at the edge of the patches as already reported in the visual survey.

(b) Debonding at the interface between lifts was recorded in six cores, amounting to 50% of the total.

(c) With the exception of Ch.30 m, all the cores in the eastbound carriageway had thicknesses ranging between 170 mm and 185 mm, 15 to 30 mm less than the design thickness of 200 mm specified for the layer. The thickness of the cores from the westbound side were found generally to exceed the specification, ranging from 195 mm to 290 mm.

(B) Conventional section

(d) The general impression from the cores was that they were in good condition with few voids in all the layers. However, the interface between the basecourse and roadbase layers was voidy.

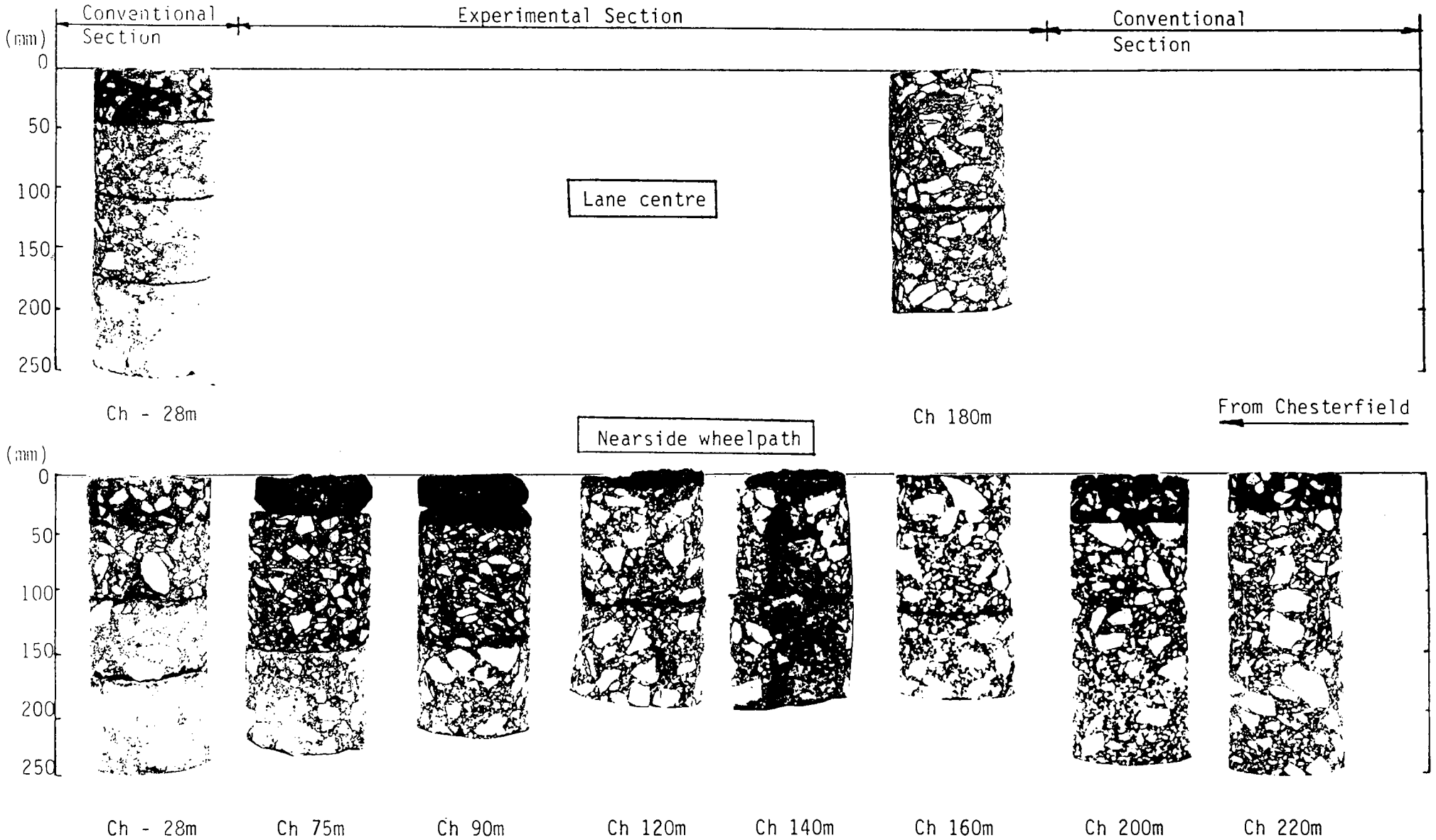

PLATE 6.1 CORE SPECIMENS OF EASTBOUND, A617 HASLAND BYPASS

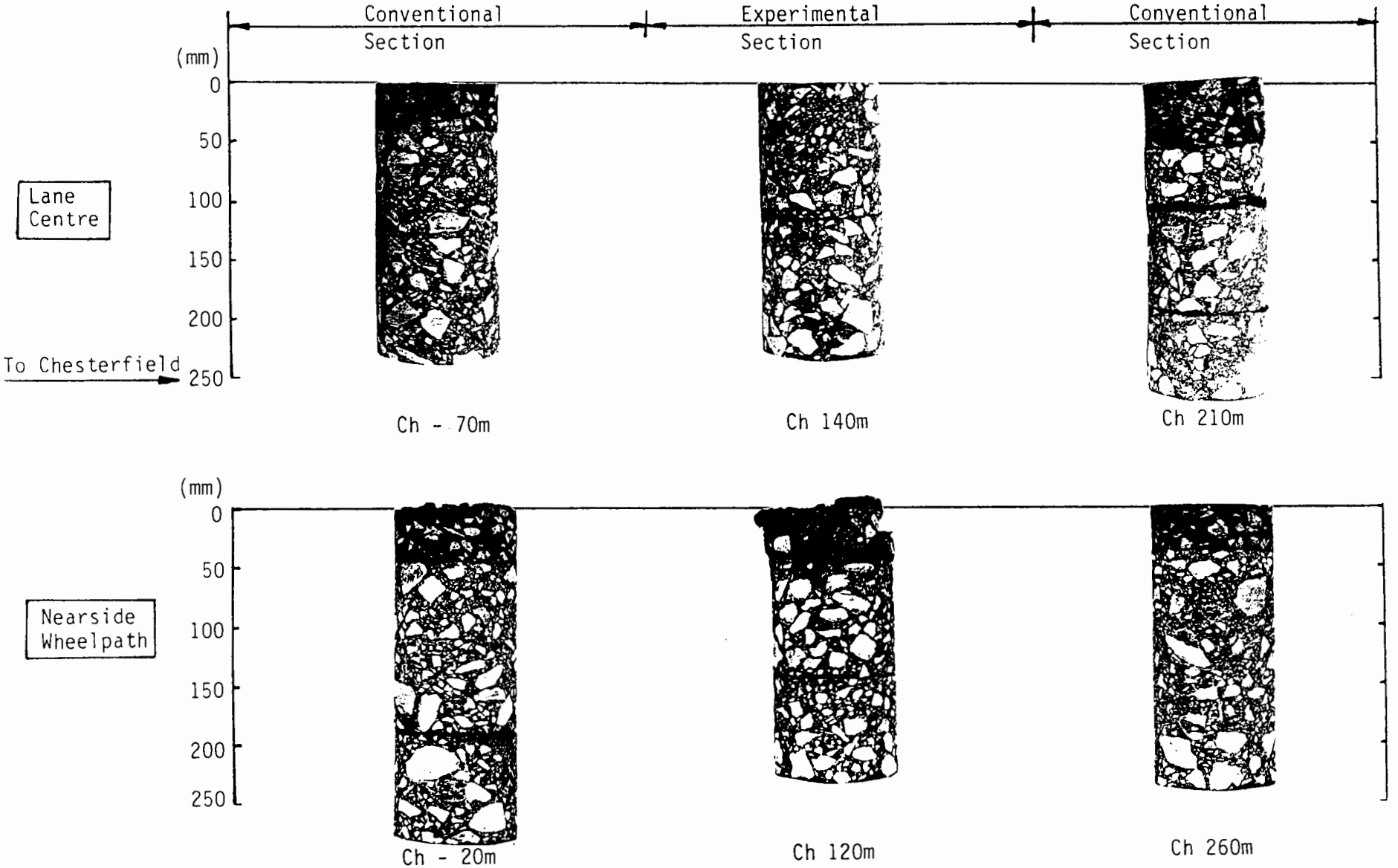

PLATE 6.2 CORE SPECIMENS OF WESTBOUND, A617 HASLAND BYPASS

(e) Two cores had been taken over surface cracks in the eastbound carriageway at Ch.-28 m and Ch.200 m. The crack was noted to have propagated downwards from the pavement surface. In the case of the core at Ch.-28 m, the crack had propagated through both the wearing course and basecourse layers but there was no sign of cracking in the roadbase. At Ch.200 m, however, only the wearing course layer was badly affected.

(f) Debonding was also noted in four out of nine cores. It was found at the interfaces between the bituminous layers.

(g) Thicknesses ranging between 198 mm and 255 mm were up to about 50 mm less than the required total design thickness of 255 mm, the shortest core being located at Ch.-60 m of the westbound carriageway.

The frequency of debonding, occurring in about 50% of the core specimens, gives cause for concern since its presence effectively reduces the load spreading ability of the bituminous layers and, hence, reduces the life of the pavement. The influence of debonding will be included in the pavement life calculation in Section 6.6.2.

A series of tests was performed in the laboratory in order to assess the structural conditions of the cores, under the following headings:

(a) Densities

(b) Refusal density tests

(c) Composition analysis

(d) Elastic stiffness

Densities: The results are summarised in Table 6.10, which shows that the average densities of the bituminous material in both carriageways of the experimental section are almost identical at about 2400 kg/m^3 and are greater than for the conventional section where they are in the range of 2310 - 2380 kg/m^3. This finding reflects the higher compactive effort which was applied to the modified bituminous

EASTBOUND		WESTBOUND	
Location	Density (kg/m^3)	Location	Density (kg/m^3)
	Experimental Section		
Ch 20m WP (TP3)	2386	Ch 20m WP	2228
		Ch 120m WP (U)	2404
Ch 75m WP (U)	2421	(L)	2438
(L)	2369		
		Ch 125m WP (TP1)	2448
Ch 90m WP (U)	2376		
(L)	2403		
		Ch 140m WP (U)	2477
Ch 100m WP (TP2)	2412	(L)	2411
Ch 120m WP	2377		
Ch 160m WP (U)	2401		
(L)	2364		
Ch 180m LC (U)	2417		
(L)	2418		
Average	2395		2401
	Conventional Section		
Ch -28m WP WC, BC	2344	Ch - 20m WP WC	2373
		BC	2300
RB(U)	2332	RB(U)	2336
RB(L)	2297	RB(L)	2343
Ch -28m LC WC	2409	Ch - 70m LC WC	2348
BC	2344	BC	2278
RB(U)	2353	RB(U)	2240
RB(L)	2335	RB(L)	2376
Ch 200m WP WC	2392	Ch 210m LC WC	2369
BC	2424	BC	2404
RB(U)	2305	RB(U)	2318
RB(L)	2308	RB(L)	2319
Ch 220m WP WC	2373	Ch 260m WP WC	2354
BC	2335	BC	2260
RB	2304	RB(U)	2325
		RB(L)	2249
Average WC	2380		2361
BC	2361		2310
RB	2319		2313

Note:
(U) - upper portion
(L) - lower portion
WP - rearside wheelpath
LC = lane centre
WC = wearing course
BC = basecourse
RB = roadbase
TP1, TP2, TP3 = trial pits

Table 6.10 Densities of bituminous material in experimental and conventional sections

material in the experimental section.

Refusal density tests: A series of tests was performed to determined the PRD(percentage refusal density) of the material. Sample preparation and testing followed the TRRL procedure as outlined in SR717(101). Table 6.11 gives the results, where 5 no. tests were performed on the experimental section and 1 no. on the conventional section. The core specimen at Ch.90 m was selected because it was inside a failed area. As may be seen in the table, the PRD ranges from 96.8% to 100% for the modified material and a slightly lower value of 93.7% for the conventional material. This clearly demonstrates that the materials in both carriageways are well compacted, satisfying the 94% PRD condition suggested by the TRRL. This set of results is consistent with the density measurements as described above. In particular, it is significant to note that the failure at Ch.90 m is not caused by under-compaction.

Composition analysis: Eight core specimens were analysed to determine the composition of the materials. The results of binder content and air void measurements are presented in Table 6.12. The binder content of the modified material varied from 3.5% to 4.5% giving an average of 4.1% which satisfies the required design value of 4.0%(refer Section 6.2.1). The air void contents averaged at 5.3%, which is well within the maximum requirement of 7%. The results from the conventional material are also found to satisfy the required design values for binder content and air voids.

The gradings of the modified material are plotted in Figure 6.8. The shaded area between curves represents the grading of all the specimens except for Ch.75(U) and Ch.90(U) (U stands for upper roadbase layer), whose gradings are given separately. The limits given by BS4987(102) are also included for comparison. From the figure, it is clear that the gradings of the modified material comply

Core location	Original density$_3$(1) (kg/m^3)	Compacted density$_3$(2) (kg/m^3)	PRD = $\frac{(1)}{(2)}$x100
(a) Experimental			
Ch 125m WB WP (TP1)	2448	2430	100
Ch 100m EB WP (TP2)	2412	2446	98.6
Ch 20m EB WP (TP3)	2386	2437	97.9
Ch 90m EB WP (U)	2376	2430	97.8
(L)	2403	2482	96.8
(b) Conventional			
Ch 220m EB WP (RB)	2304	2459	93.7

U = Upper layer; L = Lower layer, RB = Road base

PRD = percentage refusal density (%)

Table 6.11 PRD tests on core specimens

Core location	Binder content (%)	Air void (%)	Recovered penetration of binder (pen)
(a) Experimental			
Ch 125m WB WP (TP1)	4.5	3.6	
Ch 100m EB WP (TP2)	4.2	5.0	
Ch 20m EB WP (TP3)	4.5	5.1	
Ch 75m EB WP (U)	4.5	3.7	>300
(L)	3.5	7.2	35-38
Ch 90m EB WP (U)	3.8	6.5	>300
(L)	4.2	4.8	32-35
Ch 120m EB WP	4.3	5.7	35-40
Ch 120m WB W	3.5	5.8	
Average	4.1 (4)	5.3 (7 max)	
(b) Conventional			
Ch 220m EB WP			
WC	7.8 (7.9)	0.3	
BC	5.1 (5.0)	6.3	
RB	3.7 (3.5)	9.5	

Numbers in brackets are design criteria

Table 6.12 Composition analysis of core specimens

UNIVERSITY OF NOTTINGHAM

Aggregate grading analysis report sheet

Origin of Aggregate ...Limestone.....

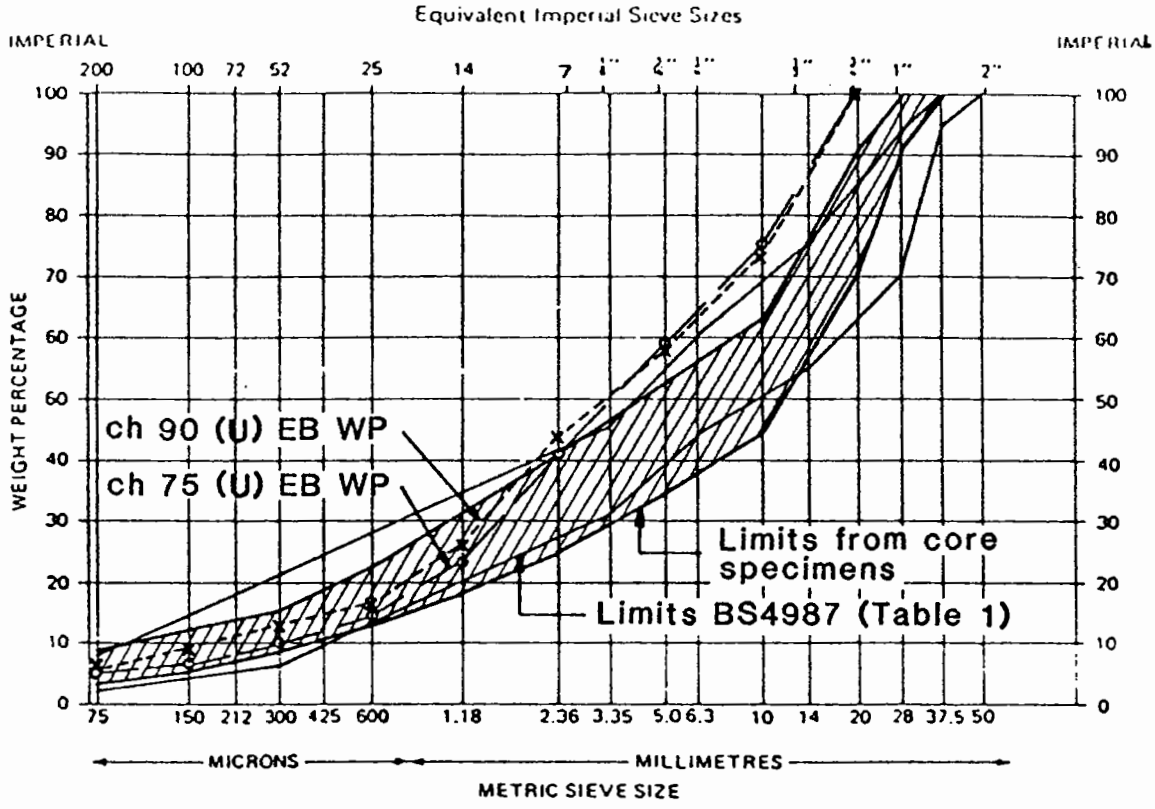

Fig. 6.8 SUMMARY OF PARTICLE SIZE DISTRIBUTION OF BITUMINOUS CORE SPECIMENS IN EXPERIMENTAL SECTION

with the requirement; however, the cores at Ch.75(U) and Ch.90(U) are found to have different gradings with a maximum aggregate size of 20 mm.

Further analysis was also performed to determine the recovered penetration of bitumen used in these cores. The bitumen, which was extracted from five specimens, was taken from Ch.75(U), Ch.75(L), Ch.90(U), Ch.90(L) and Ch.120 m of the eastbound carriageway (L stands for lower roadbase layer). The tests were performed using a sliding plate micro-viscometer. The results of the investigation are again recorded in Table 6.12. It is clearly seen that the recovered penetrations of the bitumen at locations of Ch.75(L), Ch.90(L) and Ch.120m are similar ranging from 32 to 40 pen, confirming the original design penetration of 50 pen, whereas over 300 pen was recorded at Ch.75(U) and Ch.90(U) respectively. Moreover, a strong tar-like smell was detected from these bitumen samples, as distinct from the typical "near odourless" bitumen, suggesting that a fluxing agent could have been added to the mix.

Therefore, the conclusion from the composition analysis is that the modified material in the experimental section (excluding the upper layer of the failed area) is found to comply with all the design requirements. Analysis of the material taken from the upper layer at Ch.75 m and Ch.90 m complies only with the requirement of binder and air void contents. However, this material has an aggregate grading which is very different from the specification and a very soft bitumen. This evidence, therefore indicates, quite conclusively, that the material has been manufactured to a totally different specification.

Determination of elastic stiffness: A series of tests was performed to determine the elastic stiffness of core specimens using two different methods, namely, the uniaxial tension-compression test and

Core location	Measured elastic stiffness (MPa)				
	using I.T.T.			using uniaxial test	
	18°C	25°C	35°C	18°C	28°C
(a) Experimental section, eastbound					
Ch 20m WP (U)	14181	7761	3409		
(TP3) (L)	9245	5228	2052		
Ch 30m WP	-	-	-	14900	10500
Ch 30m LC	-	-	-	9500	5000
Ch 75m WP* (U)	700	459	broken up by hand		
(L)	10730	8255	4058		
Ch 100m WP (U)	14895	8200	3230		
(TP2) (L)	11030	7916	2615		
Ch 180m LC (U)	-	7146	4070		
(L)	-	6355	3099		
(b) Experimental section, westbound					
Ch 20m WP	-	-	-	13500	5100
Ch 20m LC	-	-	-	16200	6400
Ch 120m WP (U)	10123	5376	2361		
(L)	9308	4817	1703		
Ch 125m WP (U)	9183	4836	1755		
(TP2) (L)	9775	5295	2101		
Ch 140m LC (U)	-	4996	1907		
(L)	-	5526	2670		
(c) Conventional section, eastbound					
Ch 220m WP (BC)	4571	2582	1119		
(RB)	12313	9002	2819		
(RB)	8897	6905	2305		

* Failed area; All tests at frequency 4Hz

Table 6.13 Summary of stiffness measurements on core specimens

the indirect tensile test(I.T.T.). This was to enable tests to be performed on core specimens of different lengths. All the core specimens were tested at a frequency of 4 Hz and over a range of temperature from 18°C to 35°C. Results are given in Table 6.13. At 18°C, very high stiffness values were measured, typically from 9000 MPa to 15500 MPa for the experimental section, excluding the failed areas. This demonstrates the good condition of the modified material. The test results taken from the failed area at Ch.75 m are also shown and, at 18°C, while the lower portion has an elastic stiffness of 10730 MPa, a very low stiffness value of 700 MPa was recorded for the upper portion. Raising the temperature to 35°C, this upper portion of the core was easily broken up by hand, thus indicating the very weak nature of the mix. This is in agreement with the very high recovered penetration determined (Table 6.12).

As for the conventional section, only one core specimen (at Ch.220 m eastbound) was tested; the elastic stiffnesses at 18°C for the basecourse and roadbase layers are found to be typical for these materials.

6.5.3 Granular sub-base

Detailed analysis was carried out on the granular sub-base material taken from the trial pits. Table 6.14 shows the test results for dry density and moisture content. The moisture content was determined using BS1377(103). It can be seen that the dry density ranges from 1900 kg/m^3 to 2000 kg/m^3 and moisture content from 8.8% to 10.5%. The 1978 results at locations corresponding to trial pits TP1 and TP2 show similar dry density results but the moisture content has since increased by 3 to 5% .

Figure 6.9 illustrates the relationship between the dry density and moisture content of the sub-base material. The compaction curve, determined in accordance with the Vibrating Hammer Method in

Trial pits	TP1 Ch. 125m WB	TP2 Ch. 100m EB	TP3 Ch 20m EB
Dry density (kg/m^3)	1913 (1920)	1973 (1973)	2010
Moisture content (%)	8.8 (6.1)	10.4 (5.6)	9.4
Elastic stiffness (MPa)			
1. triaxial apparatus	62	85	390
2. PADAL program	31	48	262

Note: Number in brackets denotes measured results in 1978.

Table 6.14 Summary of laboratory test results for granular sub-base in trial pits.

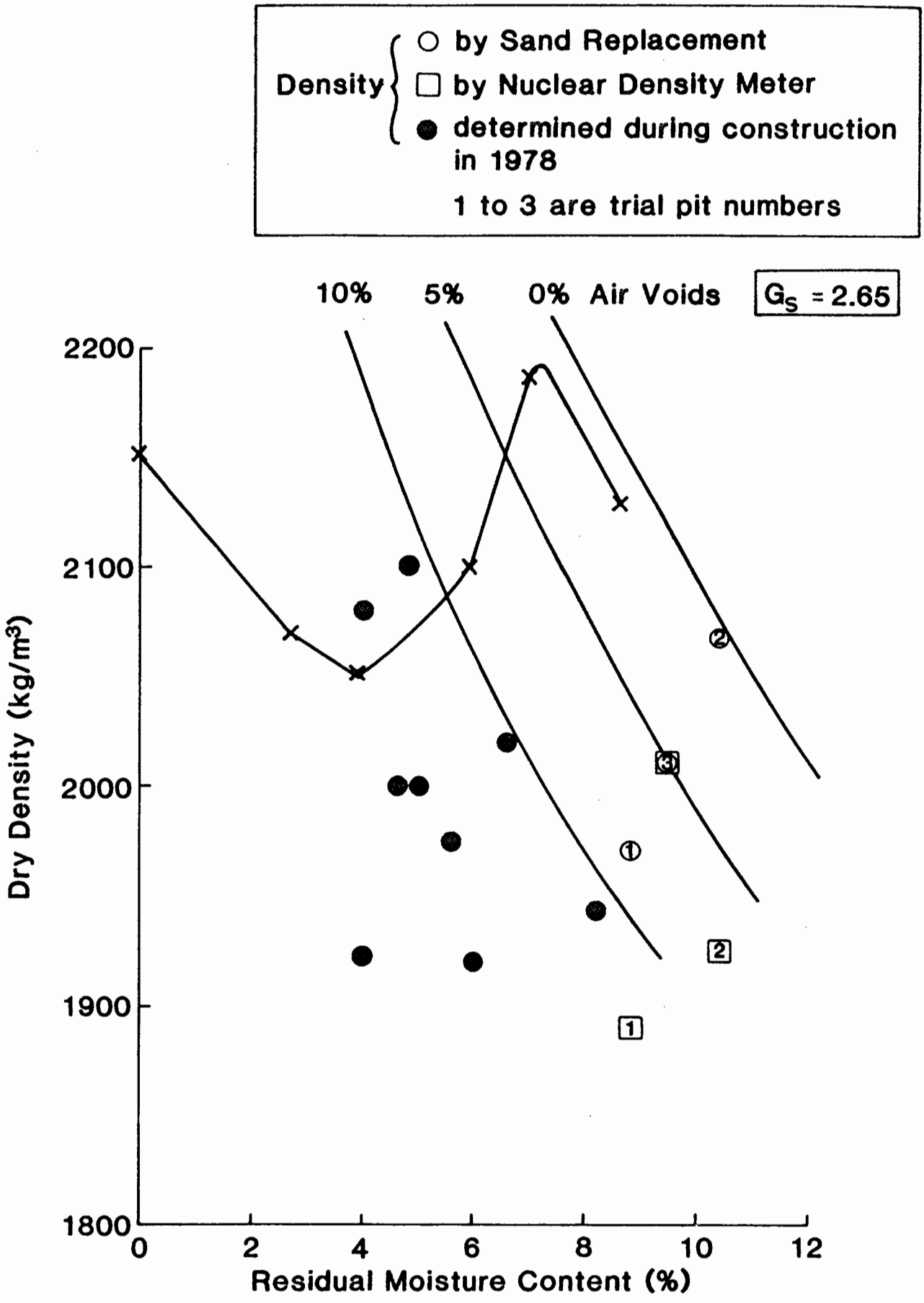

Fig. 6.9 RELATIONSHIP BETWEEN DRY DENSITY AND MOISTURE CONTENT OF GRANULAR SUB-BASE

BS5835(104), clearly indicates that the material has pessimum and optimum moisture contents of 4% and 7.2%, corresponding to minimum and maximum dry densities of 2050 kg/m^3 and 2190 kg/m^3 respectively. When the results recorded in 1978 are compared, the dry densities of the sub-base are found to be very low, and the moisture contents are at or around the pessimum value, resulting in the air voids greater than 10%. All these results suggest that the sub-base was very weak initially. The results of the recent investigation have also been plotted for comparison. While the densities are consistent with the original in-situ values, the increase in moisture content of the material effectively shifts the 1978 points horizontally to the right, passing the optimum moisture content. The consequence of this change is that the material has becomed more saturated, which, when combined with a low initial density, means that the material is very susceptible to permanent deformation and leading to rutting of the pavement surface under the action of the traffic.

It is considered that the increase of moisture in the sub-base layer is due to two factors: low permeability and ineffective drainage. Evidence of low permeability of the material was recorded during the survey; e.g. free water on the sub-base layer in the trial pits and a lot of water retained in some of the cored holes for a long time, especially in the experimental section. Hence, the grading of the material was investigated and the results are shown in Figure 6.10. The material in all trial pits was found to be outside the required specification for Type 1 material, with a greater percentage passing the 6 mm mesh. The percentage passing 75 microns is 11% to 16%, which is 6 to 11% higher than the average 5% for Type 1 material. Judging from the gradings, therefore, the permeability of the sub-base material is likely to be low. Furthermore, it is possible for the sub-base in a pavement structure to attain a very low

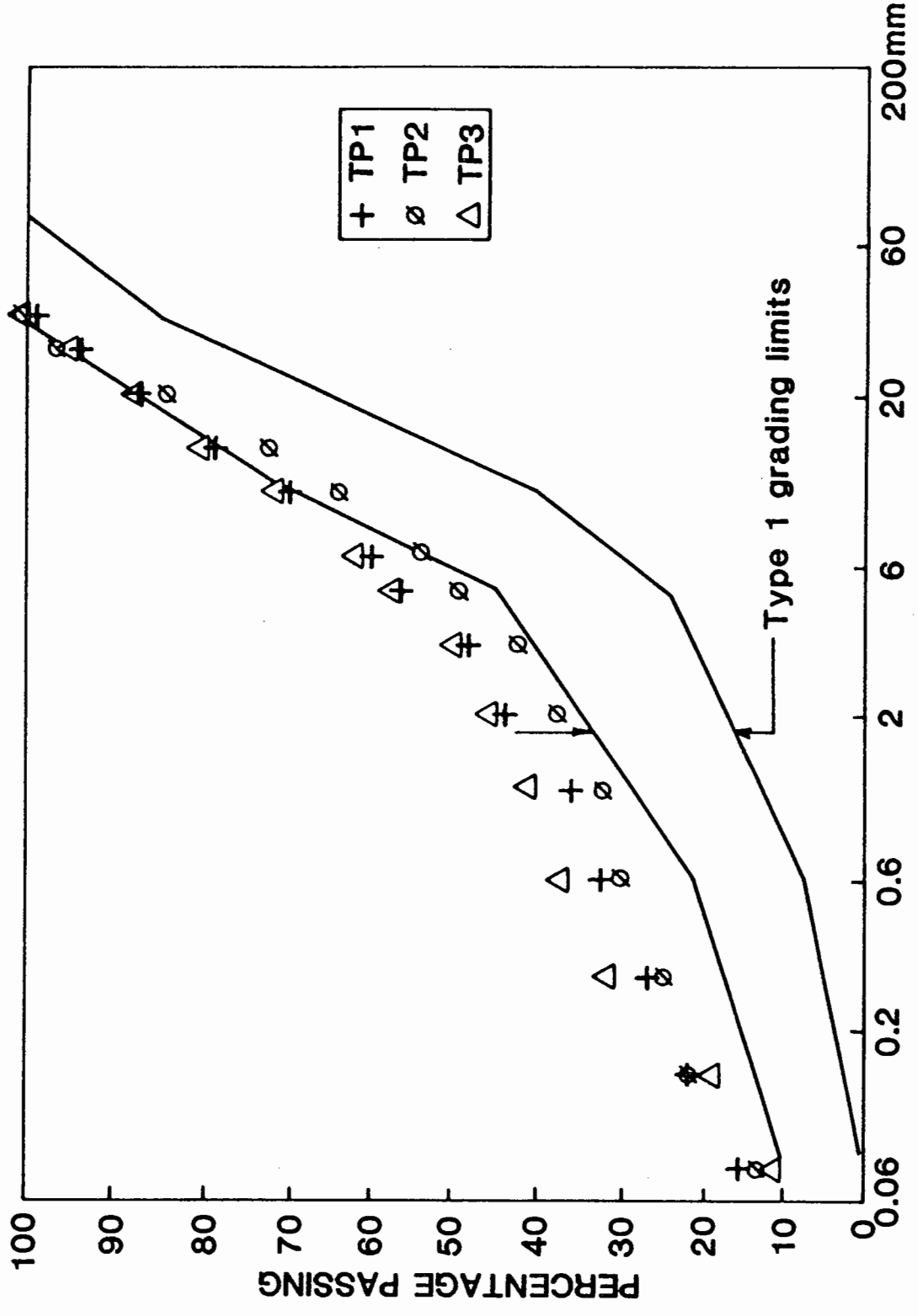

Fig. 6.10 PARTICLE SIZE DISTRIBUTION OF GRANULAR MATERIAL IN TRIAL PITS

permeability across the top surface, as a result of degradation of the material directly underneath the compacting roller. Under this condition, once water manages to percolate through the bituminous layers, it is likely to lead to free water standing in the sub-base layer for some time, since the vertical permeability is low. As this mechanism appears to agree very well with visual observations on site, it confirms that the vertical permeabilty of the sub-base layer is indeed very low.

Figure 6.11 shows a typical section of the drainage system designed for draining sub-surface water out of the pavement structure, in which a step-down of layer thickness to about 80 mm from full thickness is noted linking the sub-base to the french drain. The french drain generally runs in the central reserve area and an additional run is made in the verge in a cutting or on an embankment. After examination, the existing drainage system is considered to be ineffective since no consideration has been given to the existence of a near impervious layer at the surface of the sub-base. By stepping down the sub-base thickness, free water migrating laterally has effectively been stopped at the edge of the carriageway. When coupled with low vertical permeability, this results in standing water in the pavement structure and thus, under the action of traffic, water is unable to escape and positive pore pressure develops. This, in turn, reduces the shear strength of the granular material and causes permanent deformation to occur. By comparing the various test results, the sub-base at TP1, on balance, is considered to be the most susceptible to permanent deformation since its in-situ shear strength (from DCP results) and density are the lowest and moisture content is high. The material in TP2 is slightly better since its shear strength and density are higher than that in TP1, but the excess moisture in the layer causes a reduction in its ability to

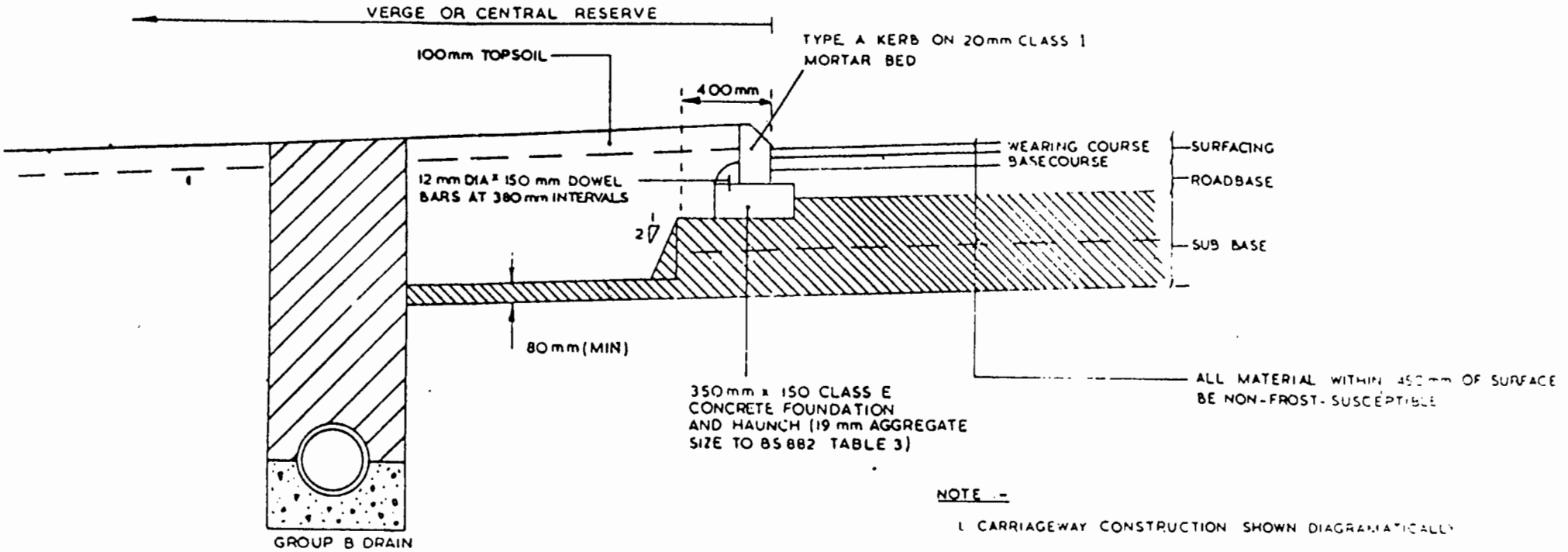

Fig. 6.11 TYPICAL DRAINAGE SYSTEM CONSTRUCTED FOR THE BYPASS (D.C.C. Drg. No. D5001/35/1A)

resist permanent deformation. The highest density and elastic stiffness, as well as a relatively high shear strength, are recorded in TP3 and they make it the least susceptible for permanent deformation.

6.6 ANALYSIS OF DEFLECTION DATA AND EVALUATION OF PAVEMENT LIFE

6.6.1 Analysis of FWD results

Eight cases were selected for detailed analysis using the PADAL program. They are given as follows:

Eastbound carriageway

(i) Ch.140 m, nearside wheelpath, experimental section

(ii) Ch.140 m, lane centre, experimental section

(iii) Ch.220 m, nearside wheelpath, conventional section

(iv) Ch.220 m, lane centre, conventional section

Westbound carriageway

(v) Ch.120 m, nearside wheelpath, experimental section

(vi) Ch.120 m, lane centre, experimental section

(vii) Ch.-40 m, nearside wheelpath, conventional section

(viii) Ch.-40 m, lane centre, conventional section

Details of the layer thicknesses and conditions at points (i),(iii) and (v) have been shown in Figure 6.3, whilst the layer thickness at point (vii) was interpolated between those cores obtained at Ch.-20 m and Ch-60 m. The analysis of those cases corresponding to lane centre locations assumed equal layer thicknesses to those in the nearside wheelpath at the same chainage. All the cases in the nearside wheelpaths were chosen such that the measured deflections closely corresponded to the 85th percentile value for d_1,d_1-d_4, and d_6 of the section considered, the 85th percentile value being that

with 85% of the measured deflections less than or equal to it. These deflection bowls were then analysed using the PADAL program which determined in-situ effective elastic stiffnesses of the pavement layers. The back-analysed elastic stiffnesses of the bituminous layers were then adjusted for temperature (see Table 6.3) and speed of loading to design conditions. The impulse loading produced by the FWD is taken as being equivalent to a vehicle speed of 30km/hr. Table 6.15 presents results of the back-analysed elastic stiffnesses. It is noted that the elastic stiffnesses for the modified bituminous material in the experimental section are reasonably high, ranging from 7500 MPa to 12100 MPa, indicating that good compaction had been achieved. Moreover, those magnitudes confirm the elastic stiffnesses measured in the laboratory (refer Section 6.5.2).

However, the sub-base layer is weak, with elastic stiffnesses of less than 50 MPa being determined for all cases. These low stiffnesses were found to be the result of a combination of factors, notably low density, and excess moisture of the material as discussed in Section 6.5.3.

For the conventional section, the bituminous layers are generally in a sound condition, with the exception of case (iii) at eastbound Ch.220 m, which show values slightly lower than expected, indicating that some damage might have occurred. This is generally confirmed by the visual condition shown in Figure 6.3. The condition of the sub-base is just below average with back-analysed elastic stiffnesses ranging from 71 MPa to 98 MPa as compared with an expected value of 100 - 150 MPa for the material in good condition. However, these stiffnesses compare favourably with the sub-base material in the experimental section. It is considered that the greater thickness, i.e. 410 mm against around 220 mm in the experimental section, could have helped to redistribute the moisture within the layer.

Point	Location	Description	Elastic stiffness of layers (MPa)			
			Bituminous surfacing	Bituminous road base	Granular sub-base	Subgrade formation
(a) Experimental section						
1	Ch 140m E/B NSWP	85%	-	11200 (D) 9000 (F)	30	125
2	Ch 140m E/B, LC		-	19200 (D) 15500 (F)	30	219
3	Ch 120m W/B, NSWP	85%	-	11800 (D) 8400 (F)	32	172
4	Ch 120m W/B, LC		-	11400 (D) 9250 (F)	45	160
(b) Conventional section						
5	Ch 220m E/B, NSWP	85%	6700 (D) 5400 (F)		71	245
6	Ch 220m E/B, LC		7300 (D) 5900 (F)		97	278
7	Ch -40m W/B, NSWP	85%	9050 (D) 7300 (F)		91	134
8	Ch -40m W/B, LC		11300 (D) 9200 (F)		98	123

NSWP = nearside wheelpath; LC = Lane centre; (D) = Deformation critical; (F) = Fatigue critical

Table 6.15 Back-analysed stiffnesses of pavement layers under FWD loading at design conditions

In contrast, judging from the reasonably high elastic stiffnesses determined for the subgrade layer, its condition is considered to be good (from 123 MPa to 278 MPa).

6.6.2 Calculation of pavement life

After elastic stiffnesses of the pavement structures had been determined, the induced elastic strains under a standard 40kN dual wheel loading (i.e. 80kN axle) were computed. Extensive work has shown that the vertical compressive subgrade strain and horizontal tensile strain at the bottom of the bituminous roadbase (63) are the most significant parameters in determining pavement life; the former relates to permanent deformation and the latter to a fatigue cracking failure mechanism. In the calculation, pavement lives corresponding to both critical and failure conditions are estimated.* Critical condition is defined by a 10 mm rut (105) or the first appearance of fatigue cracking, while failure is represented by a 20 mm rut or extensive fatigue cracking (96). During the site survey, debonding of bituminous layers was recorded on core specimens and in trial pits. Brown and Brunton (106) indicated that the life of a pavement structure would be substantially reduced as a result of debonding. Since the modified material in the experimental section was frequently debonded, the computation assumed debonding at an interface at a depth of 100 mm within the bituminous layer. The structure in the conventional section was assumed to be fully bonded. The BISAR program was used for the strain computation, which enabled debonding to be included in the structural analysis. In the analysis, the degree of smoothness of the debonded interface was taken as 0.7. Table 6.16 summarises results of the pavement life calculations. It can be seen that the predicted failure life of the experimental section calculated at the lane centre locations (undamaged section) are 40 msa and 21 msa for the eastbound and

* For pavement life calculation at critical conditions, use equations (8.18) and (8.16).
For pavement life calculation at failure conditions, use equations (8.17) and (8.15).

Point	Location	Calculated life (msa)	
		critical	failure
(a) Experimental section			
1	Ch 140m E/B, NSWP	9.1	52.0
2	Ch 140m E/B, LC		
3	Ch 120m W/B, NSWP	25.0	144.0
4	Ch 120m W/B, LC		
(b) Conventional section			
5	Ch 220m E/B, NSWP	3.4	19.4
6	Ch 220m E/B, LC		
7	Ch -40m W/B, NSWP	5.8	33.6
8	Ch -40m W/B, LC		

NSWP = nearside wheel path; LC = lane centre
E/B = eastbound; W/B = westbound

Note: All calculated lives are fatigue cracking critical.

Design life = 13 msa
Traffic to date (1986) = 2.4msa

Table 6.16 Calculated pavement lives

westbound carriageways respectively. In both cases, fatigue cracking is the controlling mechanism. Moreover, they are 3.0 and 1.6 times greater than the design failure life of 13 msa. Since the actual traffic to-date of 2.4 msa is quite low, this suggests that the overall performance of the experimental section is still good. The calculated lives for the wheelpaths show some slight damage to the eastbound carraigeway resulting in a slightly lower life, although an almost unchanged life, is noted for the westbound carriageway. Judging from the relatively large magnitude of predicted lives computed for the wheelpaths, the experimental section, in general, should be expected to last to the end of the design life, requiring minimum maintenance. It should be noted that the above analysis is based on the assumption that the condition of the sub-base layer will not deteriorate in the future, which means that the necessary steps are taken to improve the existing drainage in the sub-base layer.

The analysis performed on the conventional section shows that the predicted lives are similar to the experimental section with the original pavement lives calculated at the lane centre locations giving 29 msa and 57 msa which are 2.2 and 4.4 times of the design life. The pavement lives calculated for the wheelpaths indicate a similar life in the eastbound but a shorter one for the westbound carriageway suggesting that some damage has occurred to the eastbound carriageway. As a whole, the conventional section, nonetheless, should achieve the required design life adequately.

6.7 INVESTIGATION OF PREMATURE FAILURE

It was noted in the visual survey that premature failure had been observed at two locations, i.e. Ch.75 m and Ch.90 m in the eastbound carriageway of the experimental section. Therefore, attempts are made here to explain the cause of this premature failure.

A calculation was carried out to determine the original life of the

failed areas. Four structures were used in the calculation as follows:

(a) Existing pavement structure with actual layer thicknesses and in-situ and laboratory stiffnesses;

(b) As (a) but thickness of lower bituminous layer increased by 30 mm;

(c) As (a) but the upper bituminous layer replaced by a good layer having the same stiffness as the lower layer;

(d) The pavement structure assumed in the design but the elastic stiffness of the bituminous layer the same as (a).

Results of the pavement life calculations are summarised in Figure 6.12. The predicted original life of the existing pavement is computed as 2.8 msa, which is found to match the actual traffic of 2.4 msa reasonably well, indicating that failure is expected to occur imminently. This is equivalent to only 22% of the required design life. By increasing the thickness of the lower bituminous layer, it is noted that another 30% of the design life can be gained. But the real gain in pavement life is to replace the existing weak upper layer by a good material; the calculation shows a tenfold improvement on the design life! Even the predicted life using the original design parameters gives about twice the design life of the pavement. Hence, the above calculation reveals that the main cause of the failure is that the upper bituminous layer was too weak to sustain the traffic load. This resulted in the development of severe rutting. Other factors, such as low elastic stiffness of the sub-base layer and reduced thickness of the bituminous layers, also have an effect in reducing the life of the structure, though their influences are not as significant as the weak bituminous layer.

It is interesting to speculate how such a different material could be able to slip through the quality control process undetected. It is

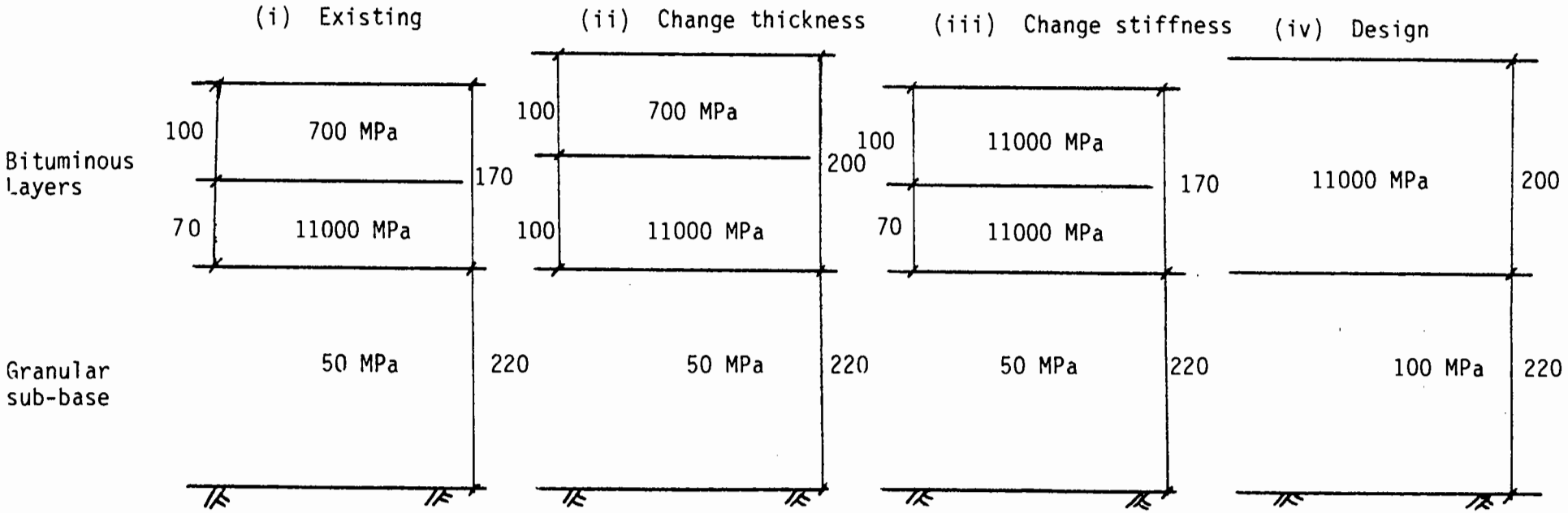

	(i) Existing	(ii) Change thickness	(iii) Change stiffness	(iv) Design
Subgrade	200 MPa	200 MPa	200 MPa	50 MPa
Predicted Life (failure)	2.8 msa	6.8 msa	153 msa	27 msa
Proportion of design life	0.22	0.52	11.8	2.1

Traffic to-date = 2.4 msa ← good agreement

Note: all layer thickness in mm.

Design Life = 13 msa

FIG. 6.12 SUMMARY OF PAVEMENT LIFE CALCULATION OF FAILED AREA

considered that during the production of the modified material a mistake could have happened, probably due to human error. This is possible since the required material is a mix which is different from typical rolled asphalt or dense macadam mixes. In order to overcome this technical difficulty, it is probable that the quarry decided to use the dense macadam plant to produce the modified material, since the only difference is in the use of 50 pen bitumen instead of the usual 100 pen or 200 pen bitumen as the grading of the modified material is similar to the typical dense macadam. On the day when the modified material was required, it was amongst a number of other different mixes to be produced, the blending of which required manual switching by the operator for the particular recipe. It is considered that mistakes could have happened in the change-over stage after the production of the modified material was stopped for a relatively long break. During this time, the same plant was switched to produce other mixes. When the break was over, it is probable that the operator forgot to change the setting for the modified material or changed to a totally different mix by mistake. Consequently , the first lorry, immediately after the break, was loaded with a different mix.

The above hypothesis thus initiated further investigation into the production and delivery of the modified material from the plant to the site.

In the report submitted to the D.C.C.(84), comprehensive site records were included and these were examined in detail. Figure 6.13 shows the plan of the location of the individual lorry loads and the order in which they were laid. It is noted that the failed areas lie within area no. 18, which covers an approximate distance of 27m between Ch.68 m and Ch.95 m. The lorry which laid this area was then traced back through records supplied by the quarry and it was found

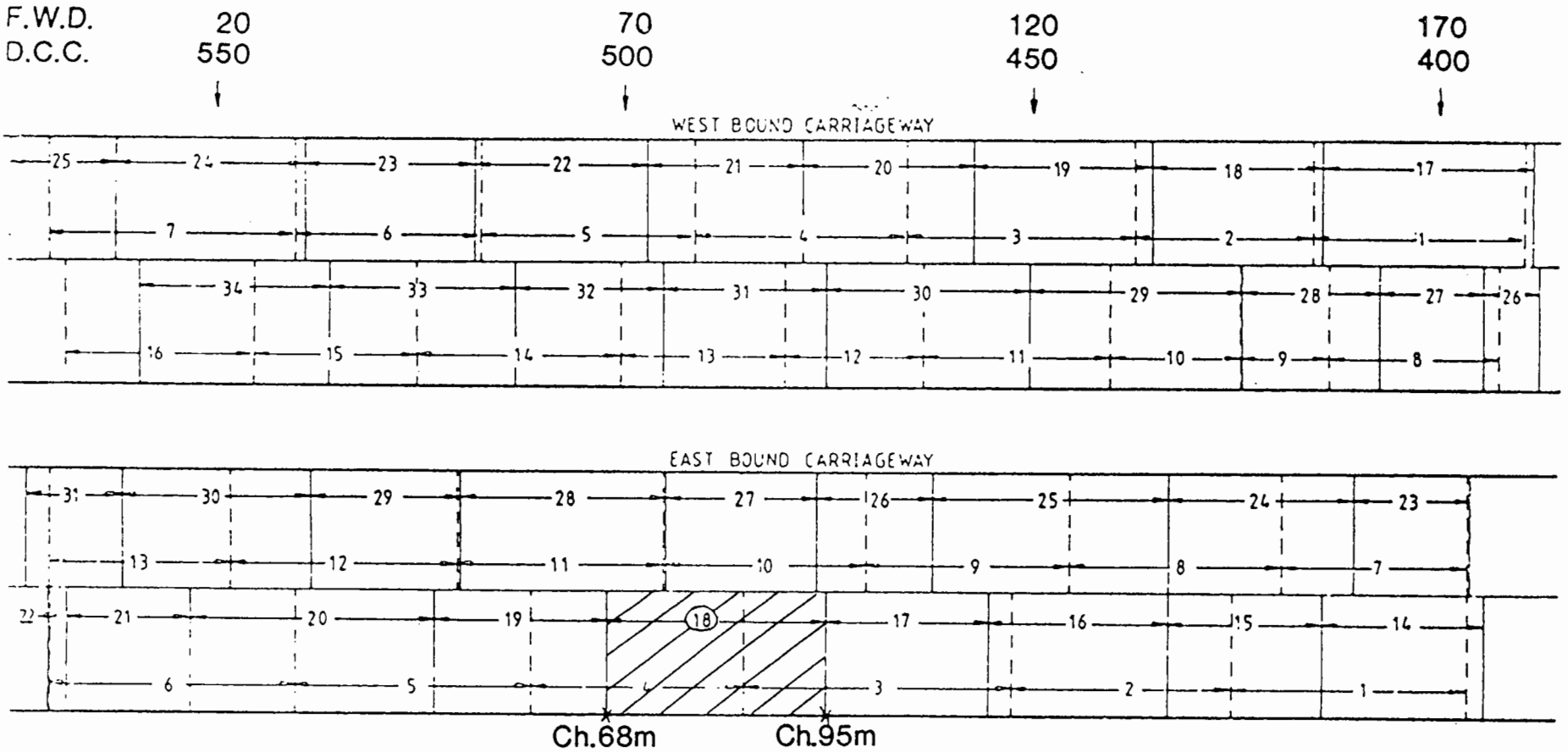

Fig.**6.13** PLAN OF EXPERIMENTAL SECTION OF HASLAND BYPASS SHOWING LOCATION OF INDIVIDUAL LORRIES AND THE ORDER IN WHICH THEY WERE LAID IN 1978 **(84)**

Upper layer ————
Lower layer – – – – –

to be loaded at 1125hrs on 20 July 1978, as shown in Table 6.17. These records are transposed onto Figure 6.14, showing the relationship between the time each lorry was loaded and the total number of lorries leaving the quarry. It is significant to note that the lorry which covered area no. 18 was indeed the first one loaded after a relatively long break of 55 minutes, and it matches the above hypothesis exactly!

6.8 DISCUSSION AND RECOMMENDATION

The analysis has shown that , for the experimental section, if the failed area is excluded, the modified bituminous material is in good condition with high stiffnesses. This confirms the original philosophy of reducing air void content, thus increasing the overall stiffness of the material. However, debonding between lifts has reduced the ability of the layer to spread the traffic load thus reducing the anticipated pavement life. Furthermore, the poor condition of the surface dressing makes the whole experimental section appear to be in a worse state than it actually is. The bituminous material in the conventional section is also in reasonably good condition, but with stiffnesses lower than in the experimental section. The cracks are found to have originated from the surface. Judging from the position of the cracks in the wheelpaths, it is possible that they were caused by the high horizontal tensile stresses at the edge of a fully laden wheel.

The subgrade material is reasonably stiff as noted from the laboratory and back-analysed elastic stiffnesses. The CBR values vary from 4% to 8%, representing a slight reduction since construction. Moisture content has also increased, which is possible as the subgrade approaches its equilibrium condition.

In contrast, the granular sub-base material in the experimental section is generally very weak. Low density, low permeability, and

HOVERINGHAM STONE LTD. **RECORD OF LABORATORY TESTS (COATED MACADAM)** YEAR 1978 CODE No. 359 (J)

ORDER OF LAYING	Test No.	Works Sample Advice No.	Date Taken	Time	Site of Work	Constituent Binder	Constituent Water	Grading of Aggregate % 50	37.5	28	14	6.3	3.35	300	75	Type	Category	Temperature Readings Front	Middle	Rear	Time
						3.4%	50 Pen	%													
						4.6%	Blt.	Specification 100	95/100	70/94	56/76	44/60	32/46	7/21	2/8						
1	764	SRR 676L	20/7	06	30	D.C.C. Haaland By-Pass St. Leonard's Drive Access	3.7		100	100	90	64	54	46	13	5.4		A	160°	150°	164°	3:
2	765	SAE 163	20/7	06	35	" "	3.9		100	100	84	63	53	46	9	3.9		A	160°	150°	158°	3:
3	766	LNN 422P	20/7	06	45	" "	4.2		100	100	94	[illegible]	56	41	14	4.5		A	165°	155°	170°	3:
4	767	SRR 675L	20/7	07	10	" "	4.0		100	100	88	65	52	37	16	4.4		A	158°	160°	160°	3:
5	768	SRR 674L	20/7	07	20	" "	4.0		100	100	91	65	52	39	11	4.8		A	165°	165°	170°	3:
6	769	URA 51P	20/7	07	35	" "	4.0		100	100	91	67	56	39	11	4.8		A	156°	165°	160°	3:
9	770	YRR 755M	20/7	09	10	" "	4.2		100	100	91	62	48	36	10	4.2		A	151°	155°	158°	3:
8	771	YRR 754M	20/7	08	50	" "	4.3		100	100	90	71	48	34	14	4.2		A	156°	156°	154°	3
10	772	WRR 88M	20/7	09	20	" "	4.2		100	100	89	63	46	36	19	4.5		A	162°	164°	166°	3:
11	773	SAE 138	20/7	09	30	" "	3.5		100	100	82	58	51	40	13	4.3		A	168°	165°	176°	3
12	774	SRR 676L	20/7	09	40	" "	3.9		100	100	84	57	44	34	9	3.9		A	163°	161°	163°	3
13	775	SAE 165	20/7	09	50	" "	4.2		100	100	88	57	48	39	12	4.8		A	166°	166°	163°	3
14	776	LNN 422P	20/7	10	15	" "	4.4		100	100	90	63	52	40	13	6.2		A	162°	170°	159°	3
15	777	SRR 674L	20/7	10	30	" "	4.3		100	100	87	65	52	41	12	4.5		A	165°	173°	168°	3
18	778	VRC 270S	20/7	11	25	" "	4.0		100	100	94	70	58	46	16	6.8		A	165°	167°	169°	3
19	779	SRR 675L	20/7	11	50	" "	4.5		100	100	92	56	52	40	11	5.0		A	157°	157°	162°	3
17	780	LNN 421P	20/7	11	30	" "	4.4		100	100	94	56	49	42	11	4.7		A	159°	155°	159°	3:
20	781	YRR 754M	20/7	12	20	" "	4.3		100	100	94	59	50	39	12	5.5		A	159°	156°	154°	3
21	782	YRR 755M	20/7	12	30	" "	4.2		100	100	92	64	52	40	12	4.3		A	157°	159°	155°	3
22-23	783	SRR 675L	20/7	12	45	" "	4.2		100	100	90	67	51	34	10	4.6		A	157°	158°	161°	3:
24	784	SAE 163	20/7	13	00	" "	4.3		100	100	94	63	51	43	14	5.1		A	158°	156°	155°	3:
25	785	JRC 813R	20/7	13	20	" "	4.2		100	100	91	62	45	31	12	6.0		A	169°	175°	157°	3
26	786	KRR 461S	20/7	13	40	" "	4.0		100	100	93	62	46	35	11	4.5		A	167°	171°	164°	3:
27	787	NOU 870R	20/7	14	10	" "	4.0		100	100	84	66	56	37	11	4.6		A	179°	178°	177°	3:
	788	NVO 978M	20/7	14	40	" "	3.8		100	95	85	63	49	40	13	5.9		A	164°	169°	155°	JP
30	789	SRR 674L	20/7	14	50	" "	3.4		100	100	92	58	50	42	12	4.3		A	171°	175°	169°	JP
31	790	LRR 421P	20/7	15	05	" "	4.1		100	100	90	61	54	44	12	4.9		A	171°	175°	167°	JP

TABLE 6.17 RECORDS OF TIME OF LORRIES LEAVING QUARRY WHEN LAYING UPPER BITUMINOUS LAYER IN THE EXPERIMENTAL SECTION ON 20/7/1978 (4)

(refer FIG.6.14 for order of laying)

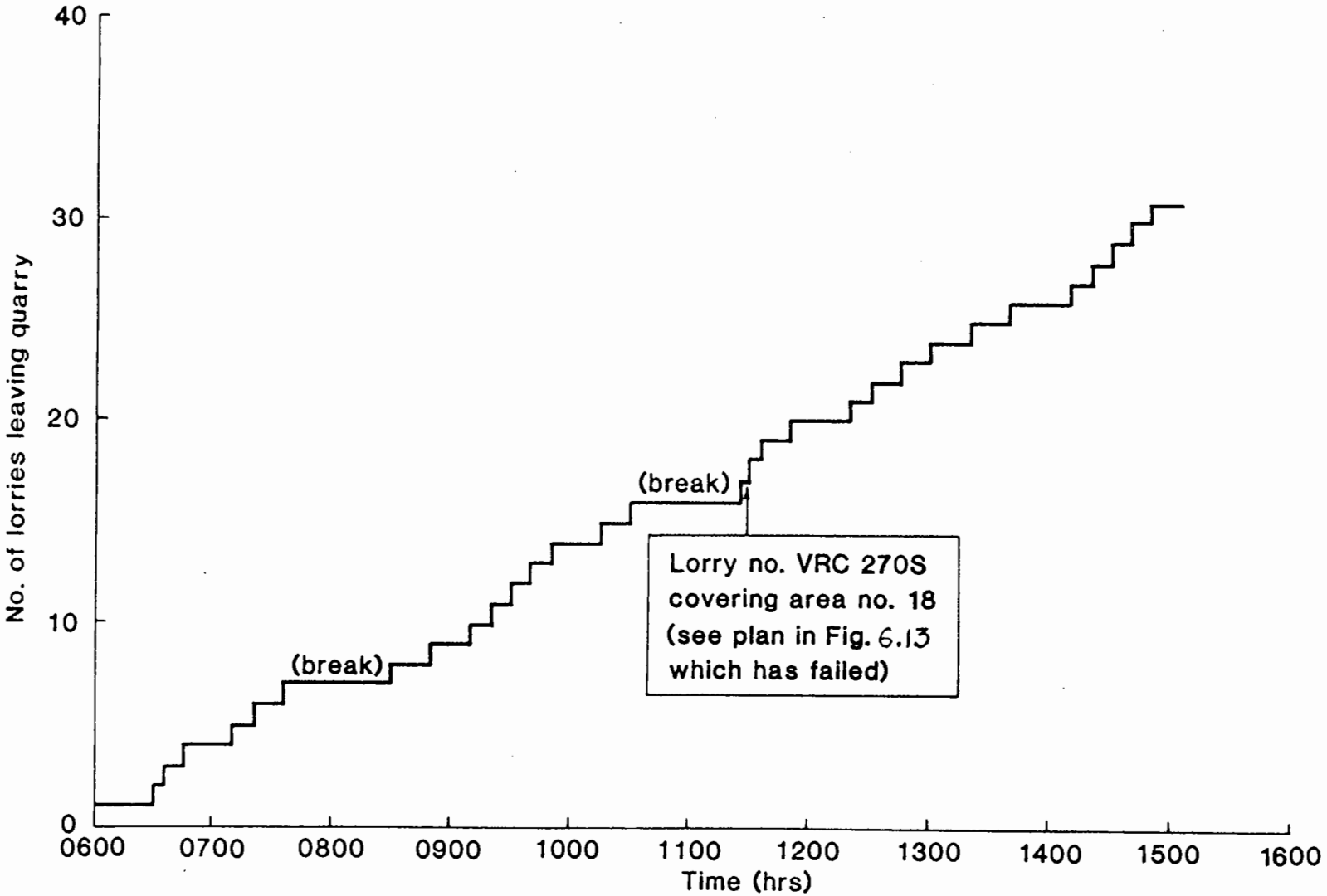

Fig. 6.14 DIAGRAM SHOWING THE TIME OF LORRIES LEAVING QUARRY WHEN LAYING UPPER BITUMINOUS LAYER IN THE EXPERIMENTAL SECTION ON 20/7/1978

high moisture content have been identified as the causes of the problem. Moreover, the grading of the material does not comply with the specification for Type 1 material. As a result, water which has percolated through the bituminous layers is trapped within the sub-base layer. Further investigation reveals a design fault in the sub-surface drainage system, in which a step-down layer has been designed linking the sub-base in the main carriageway and the french drain at the verge(see Figure 6.11). In its design, the sub-base material was assumed to be quite permeable in both vertical and horizontal directions. Any sub-surface water should flow to the bottom of the layer and drain away laterally through the link to the french drain. Unfortunately, the real situation is that the permeability of the top surface is very low and hence water is left standing there. This excess water thus causes a reduction in shear strength of the sub-base and increases the permanent deformation of the layer. Coupled with low density, this results in significant permanent deformation which is reflected as rut depth on the pavement surface. It is believed this mechanism is operating in the whole of the test section and that the two areas of the experimental section, namely Ch.120 m - Ch.150 m eastbound and Ch.100 m - Ch.170 m westbound, demonstrate the significant effect of it. It is considered, therefore, that improvement to the existing sub-surface drainage should be carried out quickly in order to halt further deterioration of the sub-base and, subsequently, the subgrade layer. If the existing system is allowed to continue, the modified bituminous layer will suffer as a result of increasing permanent deformation in the sub-base.

The calculation of pavement life has shown that the overall life of the experimental section is similar to that of the conventional section. This is achieved with a layer thickness 20% less than the conventional section(200 mm compared with 255 mm). This result

generally confirms the basis of the experiment that, by increasing the stiffness of the bituminous material, greater life can be achieved or, given the same pavement life, reduced layer thicknesses can be used. The increase of stiffness has been successfully effected through the use of a harder bitumen, i.e. 50 pen instead of 100 pen, and by the reduction of air voids.

For the area between Ch.68 m and Ch.95 m in the eastbound carriageway, which failed prematurely, detailed analysis confirms that it was primarily caused by a soft bituminous material which was laid in the upper 110 mm. Laboratory results demonstrate conclusively that it is a totally different mix consisting of a soft bitumen (probably 200-300 pen) and a different grading. As a result, this material is of very low stiffness, which leads to very low pavement life. Calculation of original pavement life gives good agreement with the actual traffic figure, thus reinforcing the findings of the above analysis. Further investigation reveals that human error is most likely to be the cause of the delivery of a wrong mix to site.

A number of recommendations have been made to D.C.C. which include:

(a) The existing sub-surface drainage system should be improved by increasing to the full thickness the granular material in the link between the main carriageway and the french drain.

(b) The surface cracks in the conventional section should be sealed as soon as possible to minimise further deterioration to the bituminous layers.

(c) Immediate work should be carried out to remove the upper 110 mm of bituminous material in the left hand lane, between Ch.68 m and Ch.95 m of the eastbound carriageway, and to replace this by a modified material consisting of 50 pen bitumen and a 40 mm DBM grading in accordance with BS 4987. This material is to be compacted so as to achieve a maximum air void content of 7%.

6.9 ASSESSMENT OF BACK-ANALYSIS PROCEDURE

An attempt has been made to validate the back-analysis procedure in the PADAL computer program. In general, it is considered difficult to compare the back-analysed stiffnesses with the stiffnesses measured in the laboratory from bituminous cores and from the triaxial apparatus for unbound granular and clay subgrade. This is because the number of cores and samples of unbound material taken from a test section is generally too small to enable a comprehensive statistical comparison. Nevertheless, experience in applying the PADAL computer program in pavement evaluation during the period of the research has highlighted the limits of its application. They are listed in the following area:-

6.9.1 Limitation of Application

(1) The PADAL computer program has been formulated based on a linear elastic theory. However, the real material behaviour is often non-linear, non-homogenous and anisotropic. An attempt has been made to model the subgrade layer in a non-linear manner. Other pavement layers are assumed to be linear. Although the granular material is known to be stress-dependent (refer 58,100), this linear assumption is considered to be adequate if the material is overlaid by a stiffer bound layer (eg. bituminous base or concrete) and its layer thickness is not greater than three times the thickness of the bound layer, since the variation of stresses within the granular material is relatively small. The PADAL program, in its present form, should not be used to analyse pavement structures with a thick granular layer (eg. 900mm) underlying a thin surfacing (eg. 40mm) since the non-linear stress-dependent behaviour of the granular material should be considered in the back-

analysis. However, the program could be modified to accommodate a non-linear granular layer.

(2) The PADAL program has been found to apply satisfactorily for both bituminous and concrete pavement structures under the following limits of layer thicknesses for different types of pavement material.

Material Type	Limit of Thickness
Bituminous	$\geq$ 100 mm
Granular	200 mm to 600 mm
Pavement Quality Concrete	$\geq$ 100 mm
Lean Concrete	$\geq$ 100 mm
Cement stabilised material	$\geq$ 100 mm.

6.9.2 Range of Stiffnesses

The following summarises the range of stiffnesses evaluated for materials in sound and poor conditions:-

Material Type	Range of Stiffnesses (MPa)	
	Sound Condition	Poor Condition
Bituminous (depending on temperature)	4,000 - 7,000	< 1,000
Pavement Quality Concrete	40,000 - 50,000	< 10,000
Lean Concrete	30,000 - 40,000	< 5,000
Granular Base	300 - 1,000	< 150
Granular Sub-base	100 - 300	< 100
Subgrade Soil (depending on soil type)	$\geq$ 100	< 50

6.9.3 Correlation With In-situ Testing Devices

Only limited experience has been acquired in the use of in-

situ testing devices such as the DCP and the Clegg Hammer (CH) during this project although results are reported in Table 6.7. The results which were obtained are insufficient to provide a comprehensive correlation with back-analysed stiffnesses for the granular material.

Clegg Hammer Results:

The comparison of the back-analysed stiffness as illustrated in Table 6.14 and CIV using CH summarised in Table 6.7 on the granular material appears to have a reasonably good correlation (refer following Table).

		Back-Analysed Stiffnesses (MPa)	CIV
Granular Sub-base	TP1	31	25.4
	TP2	48	34
	TP3	262	51.6
Clay Subgrade	TP1	175	6.0
	TP2	201	6.4
	TP3	167	9.4

It can be observed that increase of back-analysed stiffnesses (of the granular sub-base) produces an increase of CIV from the Clegg Hammer.

In contrast, there is no correlation between the back-analysed stiffnesses of the clay subgrade and the CIV (refer Table above). The real reason for non-correlation on the clay subgrade is unclear and more work is required to explain the discrepancy. One possible reason is that the CH measures both the combined transient and permanent response of the unbound material. For the granular material, having a larger shear strength than the clay soil, the CH predominantly measures the transient response

and, hence, the elastic stiffness of the material. However, if the shear strength or the CBR of the material is low, the CH will correlate more closely with strength. Consequently, correlation is observed between the back-analysed elastic stiffnesses and the CIV for granular material but not for the clay subgrade.

Dynamic Cone Penetrometer Results:

The results of the back-analysed stiffnesses on the trial pits and the DCP data are summarised as follows taken from Fig. 6.6, Tables 6.9 and 6.14.

		Back-Analysed Stiffnesses (MPa)	DCP (blows/cm)
Granular Sub-base	TP1	31	2.6
	TP2	48	5.4
	TP3	262	4.1
Clay Subgrade	TP1	175	1.3
	TP2	201	1.2
	TP3	167	2.3

Judging from the above results, no correlation between the back-analysed stiffnesses and DCP results is apparent. One possible reason for the above apparent discrepancy may be that the DCP only measures the strength of both the granular sub-base and the clay subgrade and not the elastic stiffnesses of the material. This idea is supported by related work at Nottingham on pavement foundations conducted by Thom (100).

6.10 CONCLUSIONS

A detailed structural evaluation of a full scale trial section has been carried out. The site investigation included deflection surveys using the Falling Weight Deflectometer and Benkelman Beam, coring and pitting. Specimens taken from site were carefully tested in the laboratory. Their analysis has led to the following conclusions:

(1) All the analysis indicates that the modified bituminous material used in the experimental section is in good condition, demonstrating the successful use of this novel mix in a full scale situation.

(2) The pavement lives of the experimental and conventional sections were shown to be similar , both being at least 1.5 times greater than the design life of 13 msa. This confirms the basis of the experiment that, given the same pavement life, increasing the stiffness of the bituminous material can allow a reduction in layer thickness. In this experiment, about 20% saving in layer thickness has been achieved. The increase in stiffness has been derived from the use of a harder grade bitumen and by reduction of air voids.

(3) The subgrade in the test sections is in a reasonably stiff condition. The trial pit results show in-situ CBR values from 4% to 8%, which represents a slight reduction since construction and a slight increase in moisture content, which is to be expected as the subgrade approaches the equilibrium condition.

(4) The condition of the granular sub-base layer in the experimental section is found to be poor, with very low elastic stiffnesses being measured. This poor condition is caused by low density, low permeability and high moisture content. Furthermore, analysis reveals that the grading does not comply with the

specification for Type 1 material. When combined with ineffective sub-surface drainage, the result is an accumulation of free water on the top surface of the sub-base layer, as observed in trial pits TP1 and TP2. This condition thus results in significant permanent deformation of the material and the large rut depths recorded in two areas of the experimental section, namely, between Ch.120 m - Ch.150 m eastbound and Ch.100 m - Ch.170 m westbound are partly the result of the weak sub-base.

(5) Detailed analysis reveals that the observed premature failure in one area was mainly caused by the presence of a mix consisting of a soft bitumen (probably 200-300 pen) and a different grading, forming the upper 110mm of the bituminous layer. The failed area has been located between Ch.68 m and Ch.95 m of the left hand lane in the eastbound carriageway. Further investigation has concluded that human error is most likely to be the cause of the problem.

(6) The whole structural evaluation has demonstrated that the PADAL program can be used satisfactorily in evaluating in-situ elastic stiffnesses of pavement structures. However, further validation is considered necessary.

CHAPTER 7

LABORATORY INVESTIGATION INTO THE INFLUENCE OF CRACK PROPAGATION ON REDUCTION OF ELASTIC STIFFNESS IN BITUMINOUS MATERIAL

7.1 INTRODUCTION

In developing the overlay design procedure, to be discussed in Chapter 8, it is important to estimate the remaining life of the pavement structure to enable decisions to be made on whether an overlay is necessary. It was noticed in the literature that the majority of the evaluation methods estimated the remaining life against fatigue cracking by computing the horizontal tensile strain at the bottom of the bituminous layers.

The above procedure is adequate for a sound, uncracked bituminous material but it would be wrong, in principle, to apply the same procedure to an in-service pavement in which the bituminous material has been partially cracked. Therefore, a new procedure is necessary to determine the remaining life against fatigue cracking in a logical manner.

In this Chapter, a laboratory experiment will be described to study the relationship between reduction in the effective stiffness of a bituminous beam specimen and crack propagation, as the beam is cyclically loaded. The results then lead to the proposal of a new procedure for determining the remaining life of a partially cracked pavement structure against fatigue cracking.

7.2 REVIEW OF PREVIOUS WORK ON CRACK PROPAGATION

Van Dijk (107) was the first to study the effect of crack propagation logically using a wheel tracking machine on a bituminous slab. The slab, of dimensions 950 x 440 x 40 mm, rested over a rubber base and was tracked by a rolling wheel. Strain guages were installed at the bottom of the slab to measure the variation in tensile strain as the

crack propagated through the slab. To monitor the crack initiation and propagation, both sides of the slab were photographed periodically, enabling comparison between development of strain and number of wheel passes. Three different mixes were investigated, being a typical Dutch grade mix, a Californian medium grade and a British hot rolled asphalt. Figure 7.1 summarises his findings. It is noted that four distinct stages were identified:

(a) Up to point N1, hairline cracks were observed and strains started to increase;

(b) Between points N1 and N2, the hairline cracks widened and strains continued to increase until point N2;

(c) Between N2 and N3, real cracks were formed and strains started to decrease until point N3, where total failure was imminent.

(d) At and after N3, total failure was reached and no further change of strain occurred since the slab was completely cracked through.

This last stage usually corresponded to pavement failure observed on site. Based on the above results, Brunton (63) derived a factor of 20 to be applied to the laboratory fatigue life from crack initiation to allow for the effect of crack propagation through the bituminous layer after cracks were initiated.

A different approach, based on the theory of fracture mechanics, was considered by Ramsamooj, Majidzadeh and Kauffman (108) . Laboratory results on fatigue cracking were obtained by testing slabs and beams under a controlled stress condition with a cyclic 1 Hz half-sine load at 25°C. The specimens rested on an elastic support. They concluded that the crack propagation behaviour of bituminous material could be modelled by the crack propagation law proposed by Paris and Erdogan (109) given below:

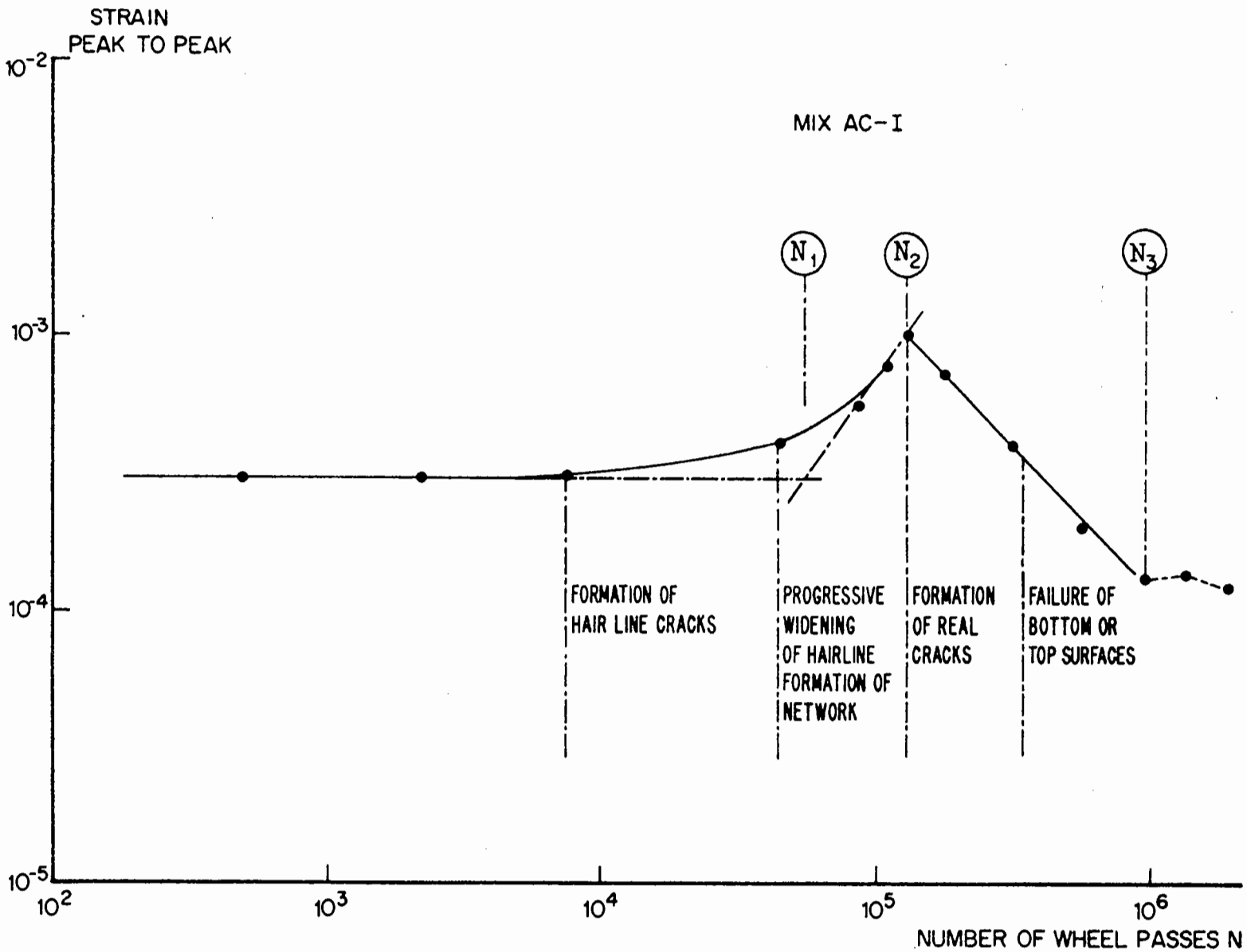

Figure 7.1 RELATIONSHIP BETWEEN MEASURED STRAINS, CRACK DEVELOPMENT AND NUMBER OF WHEEL PASSES (105)

(109) given below:

$$\delta c/\delta N = AK^n \qquad (7.1)$$

where $\delta c/\delta N$ is increase in crack length per load cycle

K is stress intensity factor

A and n are material constants

Similar work was also carried out by Molenaar (110) who arrived at similar conclusions.

Freeme and Marais (111) studied the fatigue behaviour on trapezoidal specimens, with half-sine cyclic loading applied at a frequency of 5 Hz over a range of temperatures between -10°C and 40°C. Two different types of material were studied, namely, a British hot rolled asphalt and a continuously graded asphaltic concrete. Figure 7.2 shows a typical relationship between reduction in peak stiffness and number of load applications, under controlled strain conditions. Three distinct zones were clearly observed; rapid stiffness reduction, crack initiation and crack propagation. They also concluded that, while the rate of crack initiation R_i was unchanged, the rate of crack propagation reduced with increase of temperature, as Figure 7.3 indicates. A fatigue prediction program, mainly based on the work of Kasiuchuk (112), was developed with additional features. The program not only predicted the onset of crack initiation, but also the rate of reduction of stiffness with time. Both controlled stress and controlled strain conditions were incorporated. Figure 7.4 is a typical representation of the computer prediction for gap-graded and asphaltic concrete material. More discussion will be presented on the reduction of stiffnesses in the later sections.

From the literature review, it is observed that the area of crack propagation and its effect has not been studied in detail and, in particular, no relationship is recorded between crack growth and the

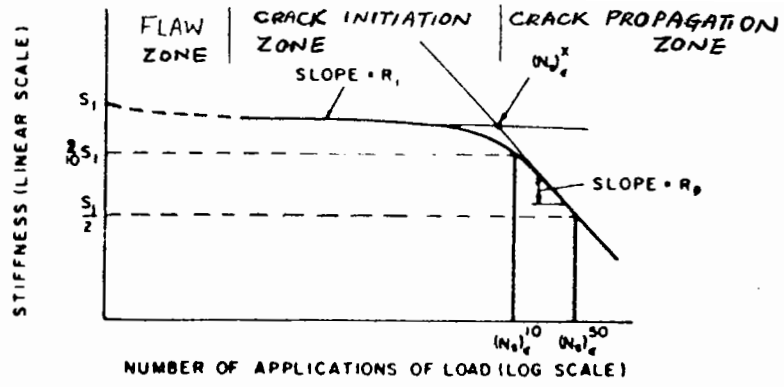

FIG. 7.2 REDUCTION OF PEAK STIFFNESS WITH INCREASE OF LOAD APPLICATIONS (109)

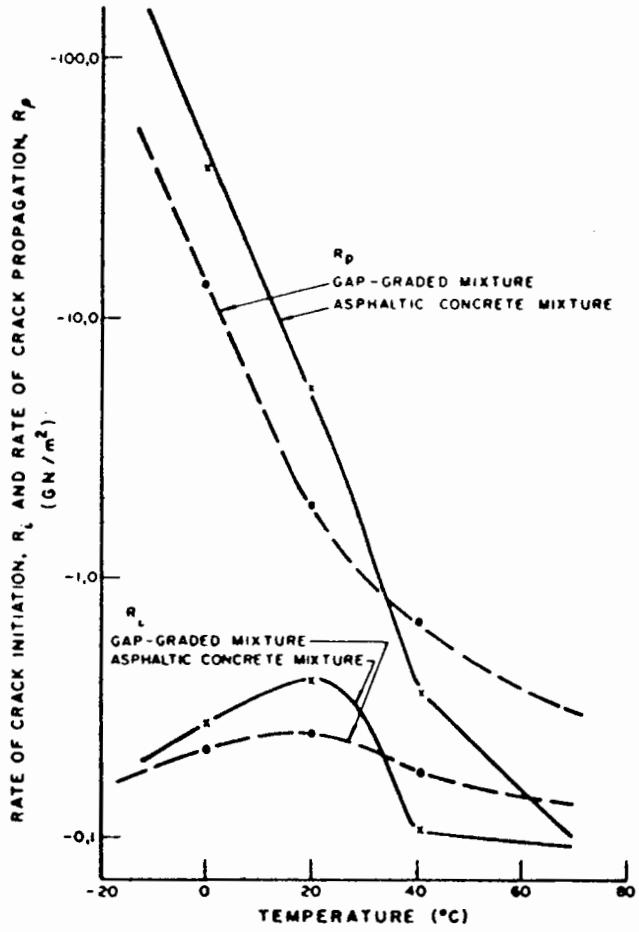

FIG. 7.3 VARIATION OF RATES OF CRACK INITIATION AND PROPAGATION WITH TEMPERATURE (109)

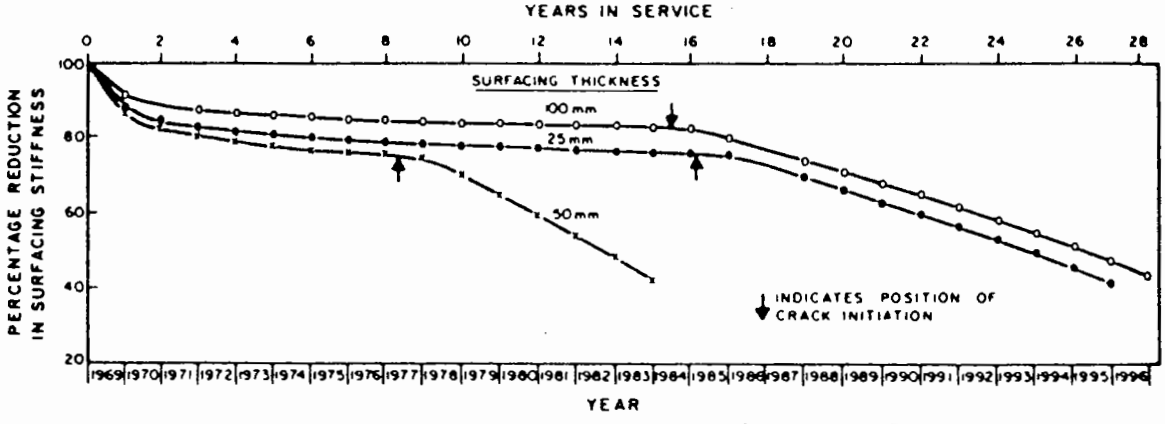

FIG. 7.4 REDUCTION OF GAP-GRADED SURFACE STIFFNESS WITH TIME (109)

corresponding reduction in stiffness, though the work of Freeme and Marais (111) threw some light on this area indirectly. With the advent of the FWD, which can measure deflection bowls very accurately, and the development of the back-analysis computer program already described in Chapter 4, it is possible to monitor the reduction of stiffness of a bituminous layer in a pavement structure. If procedures can be developed to convert stiffness reduction into the length of crack present within the material, this will enable the residual life against fatigue cracking of the pavement structure to be calculated in a logical manner by using the analytical pavement design method already developed at the University of Nottingham. The following sections explain the development behind the present study.

7.3 EXPERIMENTAL WORK

A test programme was initiated to study the relationship between crack growth and reduction of the stiffness in a bituminous material. Three different types of test were considered for the study, namely, the axial "push-pull" fatigue test, the " beam on elastic support" test and the "four-point bending" test. The first test was considered inappropriate since it did not simulate the actual traffic loading and propagation of the crack could not be easily controlled. The second one was best in simulating the in-situ condition but it was also rejected since the equipment setup did not allow variation in the stiffness to be readily calculated. Hence, it was decided to use the four-point bending test for this experiment based on the fact that the rate and position of crack propagation through the material could be controlled and that stiffness reduction could be readily calculated by using a simple bending equation. The test was displacement controlled instead of stress or strain controlled. As the crack lengthened during the test, the bending displacement of the beam tended to increase. Constant displacement was achieved by

reducing the applied load appropriately.

7.3.1 Sample Preparation

Beam specimens of typical dimension 710 x 150 x 90 mm were made in a steel mould. Compaction of the mix was carried out using a vibrating hammer. Attempts were made to ensure uniform density of the mix during compaction. To start with, the mix was spread evenly inside the mould. It was then compacted, first gently all round the mould, and later with more sustained vibration from one end to the other. A level surface was achieved by applying further vibration via a long piece of plywood placed over the mix. After the beam was cooled sufficiently, it was taken out of the mould and two notches of depth 3 to 4 mm acting as crack initiators were made in the top and bottom at the central section of the beam using a mechanical saw. Both the front and back faces of each beam were then painted white to reflect the crack growth during the test. Altogether eight beams were made from two different mixes, where Beam nos 1 to 4 were DBM wearing course and Beam nos 5 to 8 were HRA wearing course, the gradings being given in Table 7.1 (a) and (b). The former was designed to have 5.0% of 100 pen bitumen and a target void content of 8% while the latter had 7.9% of 50 pen bitumen and a target void content of 5%. However, as will be explained in Section 7.4, only four specimens were successfully tested.

7.3.2 Four-Point Bending Apparatus

Figure 7.5 shows the apparatus which consists of four clamps, two fixed and two movable. The outer clamps are fixed to the pedestal supports at each end, while the inner ones are mounted on the hydraulic actuator, which applies cyclic loading to the beam specimen. In the original design of the apparatus, the specimen was clamped in place between semi-circular cross bars. The semi-circular surface was lubricated, which reduced the friction between the clamps and the

Constituent component	% by mass of beam	Sieve size (mm)	% passing by mass
Coarse aggregate (Limestone)	30%	14 10 5	19.5% 8.7% 1.8%
Sand (Bardon Hill)	53.2%	-	-
Filler (Limestone)	8.9%	-	-
Binder (50 pen)	7.9%	-	-

Target void content = 5%

Table 7.1(a) Mix proportion specified for HRA wearing course beam specimens

Sieve size (mm)	% passing by mass
14	100
10	80
5	47
2.36	32
1.18	23
0.6	17
0.3	13
0.15	8.5
0.075	5
dust	0

Total percentage by mass of aggregate = 95%
Total percentage by mass of 100 pen bitumen = 5%
Target void content = 8%

Table 7.1(b) Mix proportion specified for DBM wearing course beam specimens

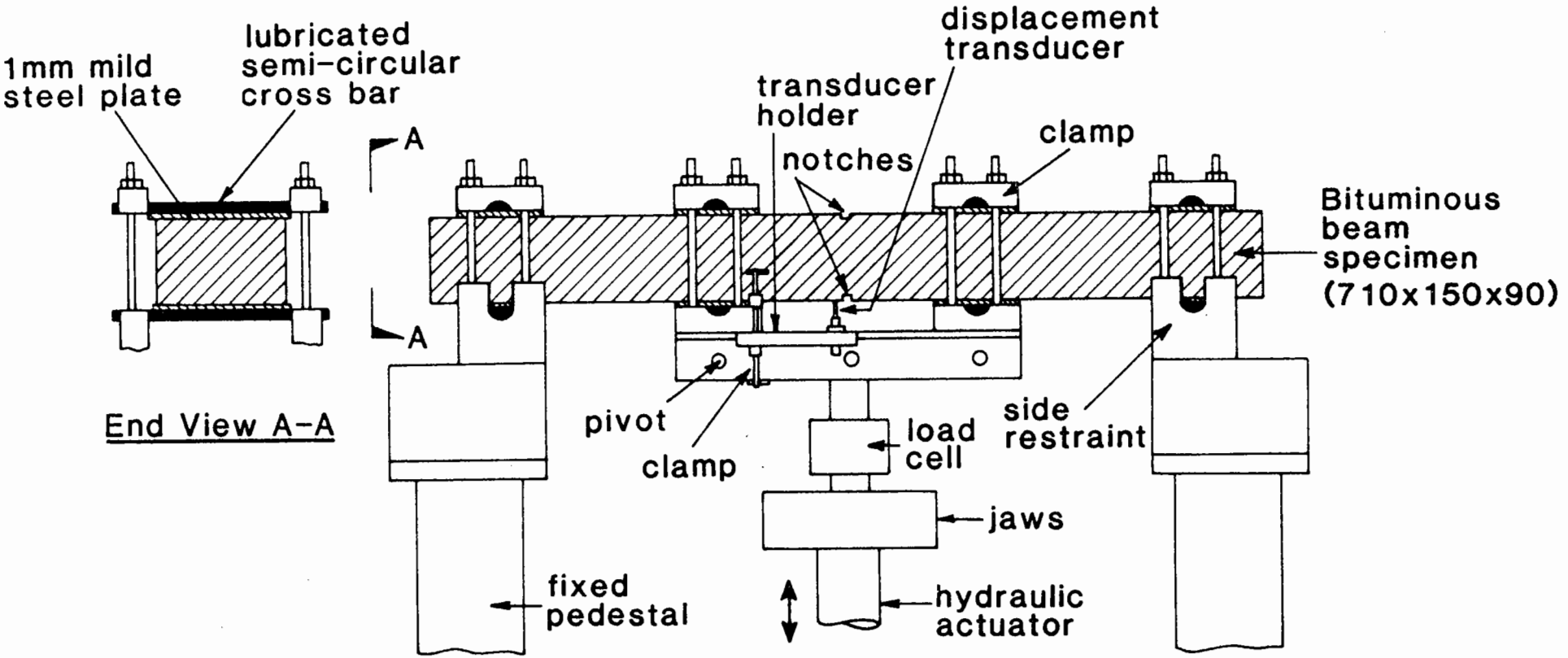

Fig. 7.5 FOUR POINT BEAM BENDING APPARATUS (NOT TO SCALE)

specimen. However, during a preliminary test, it was realized that the specimen in the area of the clamps had cracked pre-maturely as a result of very high stress concentration. To overcome this problem, 4 pairs of 1 mm thick mild steel plates were inserted between the cross bars and the specimen. This modification was found to be successful in minimizing the occurrence of pre-mature cracks at the clamps throughout the rest of the test programme.

The variation in applied load was measured by a load cell mounted beneath the movable clamps. Displacement was recorded by an LVDT (linear voltage displacement transducer) on the underside of the specimen, with the transducer holder fixed to the lower end of the movable clamps, as shown in Figure 7.5. Plates 7.1 and 7.2 illustrate the whole arrangement of the apparatus for testing.

7.3.3 Testing Procedure

Beam specimens were tested under full sine wave loading at a frequency of 5 Hz. The temperatures used were $\sim$23 °C, 8°C, 15°C and 20°C for Beam nos 3, 5, 7 and 8 respectively. The initial peak-to-peak displacement was set at 0.5 mm, 0.2 mm, 0.2 mm and 0.05 mm respectively. At the start, the applied load was slowly increased until the above peak-to-peak displacement was reached by monitoring the display on an oscilloscope. A careful check was made at intervals to monitor crack growth at the notches and also the magnitude of the displacement. The peak-to-peak applied load and number of cycles were also recorded. When the crack lengthened, the displacement of the specimen increased. The displacement was brought back to the set magnitude by reducing the level of applied load. As the crack progressively lengthened, it reached a stage where no further noticeable crack growth was observed at the specified peak to peak displacement. The displacement was then doubled by increasing the applied load appropriately. Again, the magnitude of crack growth,

Plate 5.1 : FOUR-POINT BENDING APPARATUS SET-UP

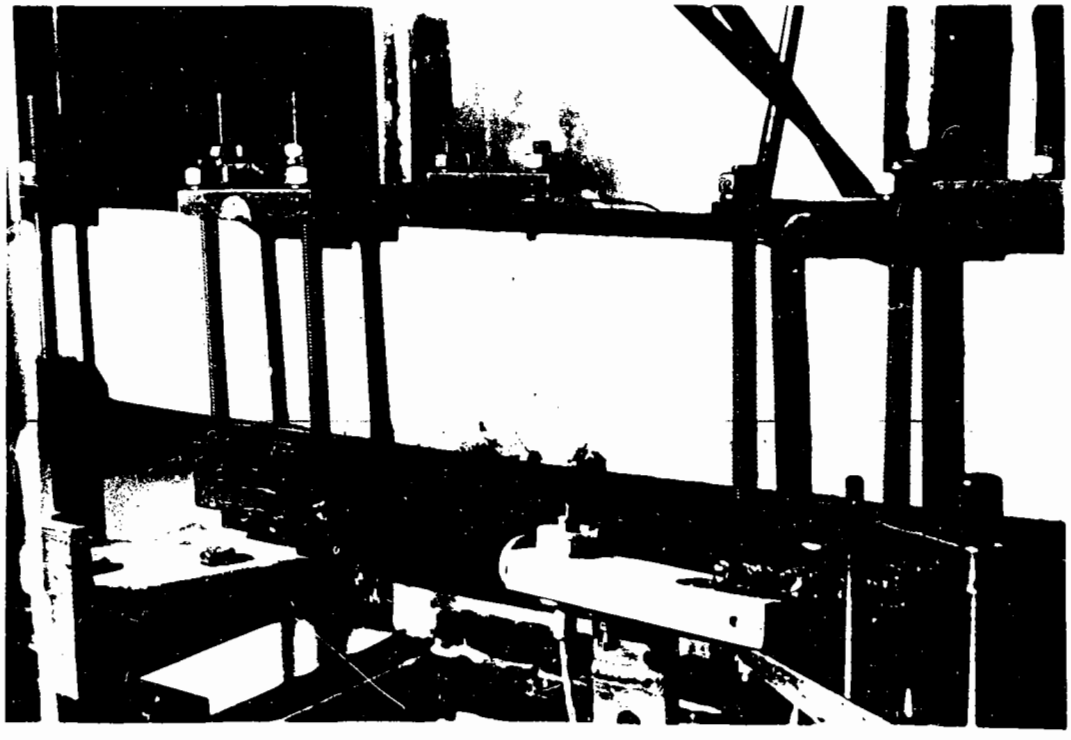

Plate 5.2 : [illegible] LOADING THE [illegible] ON THE
[illegible] TRANSDUCER

applied load and number of cycles were monitored. This process was continued until the cracks had propagated through the whole specimen. During the test, it was noted that the cracks did not propagate evenly from the top and bottom notches. Therefore, the lengths of all four cracks on both faces were measured.

7.4 DISCUSSION OF RESULTS

Out of eight beams, only four (nos 3, 5, 7 and 8) yielded results useful for analysis. this was because Beam nos 1 and 2 were used for preliminary testing and Beam nos 4 and 6 were broken pre-maturely during the set-up stage. The results of the four beams are presented

Figures 7.6 to 7.9. The variation in effective stiffness of the partially cracked beam has been presented as a proportion of initial uncracked stiffness. The calculaton of stiffness of a beam specimen is based on the simple bending equation as follows:

$$E = \frac{MR}{I} \qquad (7.2)$$

where E is the Young's modulus (taken as elastic stiffness) of the specimen;

M is the bending moment exerted by the applied load;

I is the second moment of inertia of the rectangular beam section;

R is the radius of curvature resulted from the applied bending moment.

also,

$$M = \frac{P}{4} \times r_c \qquad (7.3)$$

$$I = \frac{bh^3}{12} \qquad (7.4)$$

$$E = \frac{L^2}{8\delta} \qquad (7.5)$$

where (P/4) is the reaction at each clamp;

r_c is the distance between the movable clamps (= 255 mm);

b is the breadth of the beam (= 150 mm);

h is the thickness of the beam;

L is the length of the beam (= 710 mm);

δ is half the peak-to-peak displacement.

Since all the parameters in equations (7.3) to (7.5) are known, the stiffness of the beam can be computed using equation (7.2).

As can be seen in the figures, the maximum ratio (c/h) of crack length to total uncracked thickness is only 0.5, even though the cracks have fully propagated through the beam. This is because the load was applied as a full sine waveform and hence, in each load cycle, the same force was applied to both the top and bottom of the beam, causing the cracks to propagate from the top and bottom towards the middle section where they eventually met.

From the figures, the following findings have been observed:

(a) Crack propagation is very variable which is to be expected as the cracks propagate round the sides of the aggregate particles. Also, propagation from the bottom notch is always faster than from the top notch.

(b) As the cracks lengthen, the effective stiffness of the beam reduces very rapidly up to about 50% of the uncracked stiffness and, thereafter, the rate of reduction decreases. Also, a crack length of 10 to 15% of the total uncracked thickness results in a 50% reduction in the effective stiffness of the beam.

This finding is very significant since, in a pavement structure, the reduction of effective stiffness would in turn

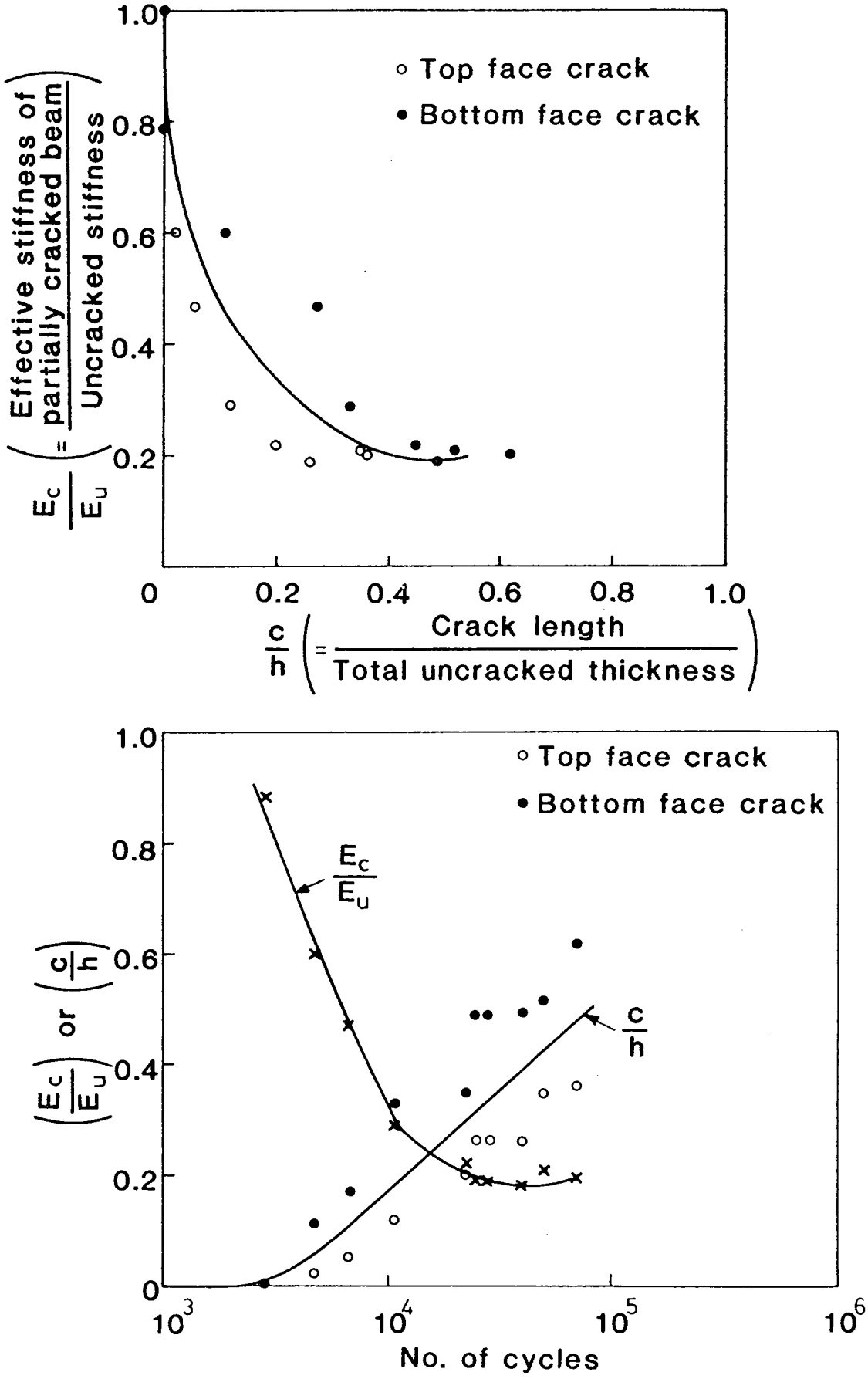

Fig. 7.6 RESULTS OF CRACK PROPAGATION TEST FOR BEAM NO. 3 (DBM BASECOURSE) AT 22-24°C

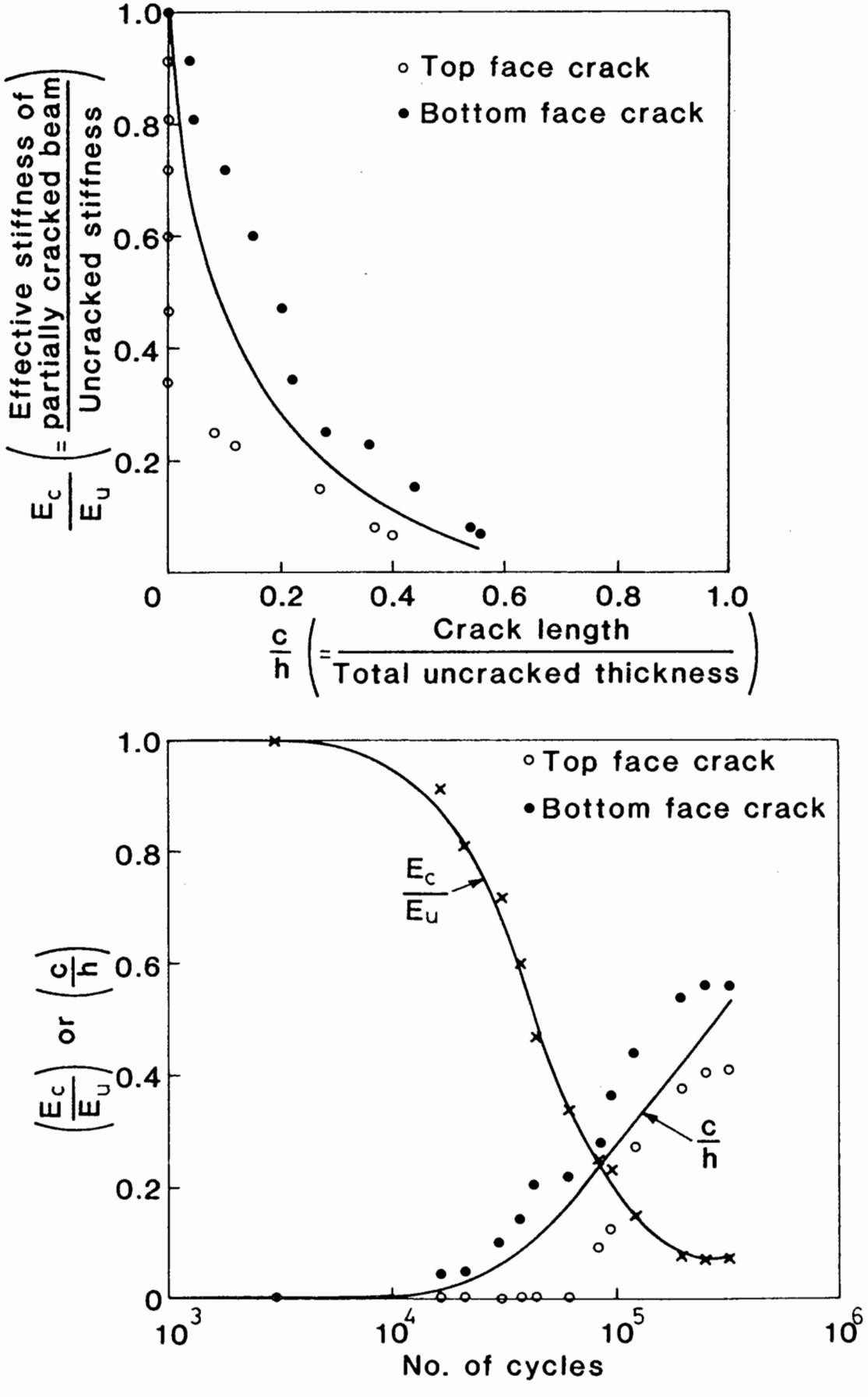

Fig. 7.7 RESULTS OF CRACK PROPAGATION TEST FOR BEAM NO.5 (HRA WEARING COURSE) AT 15°C

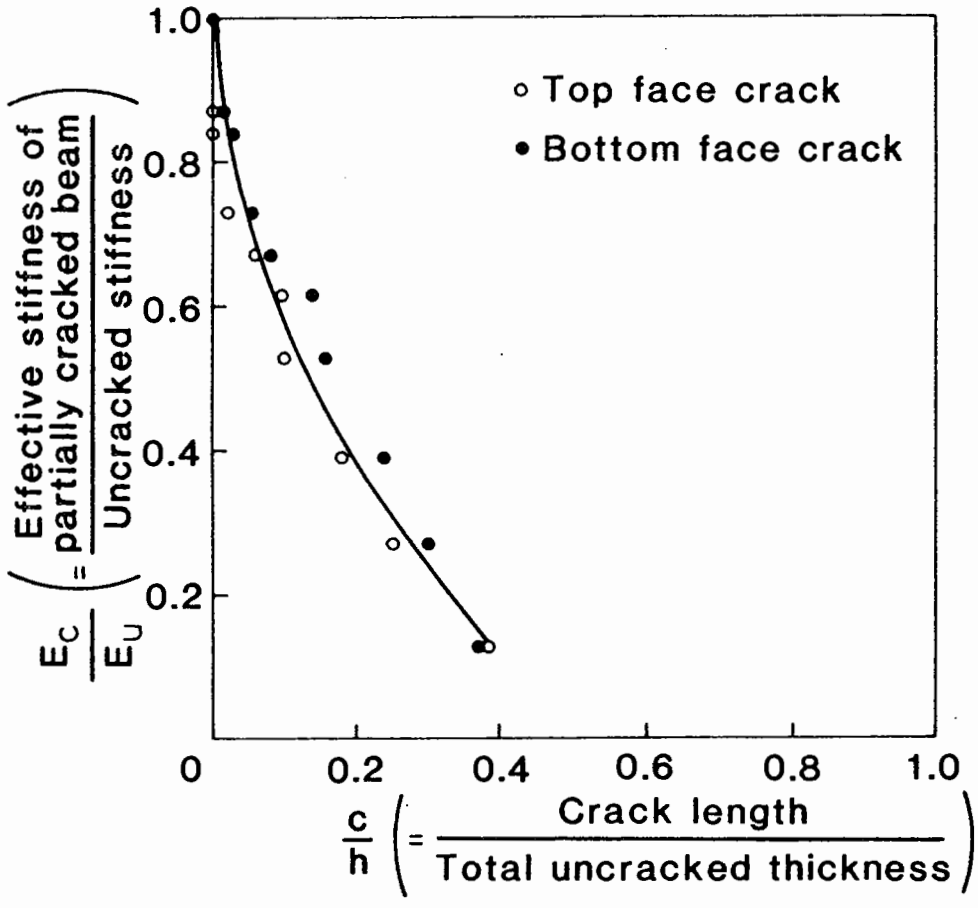

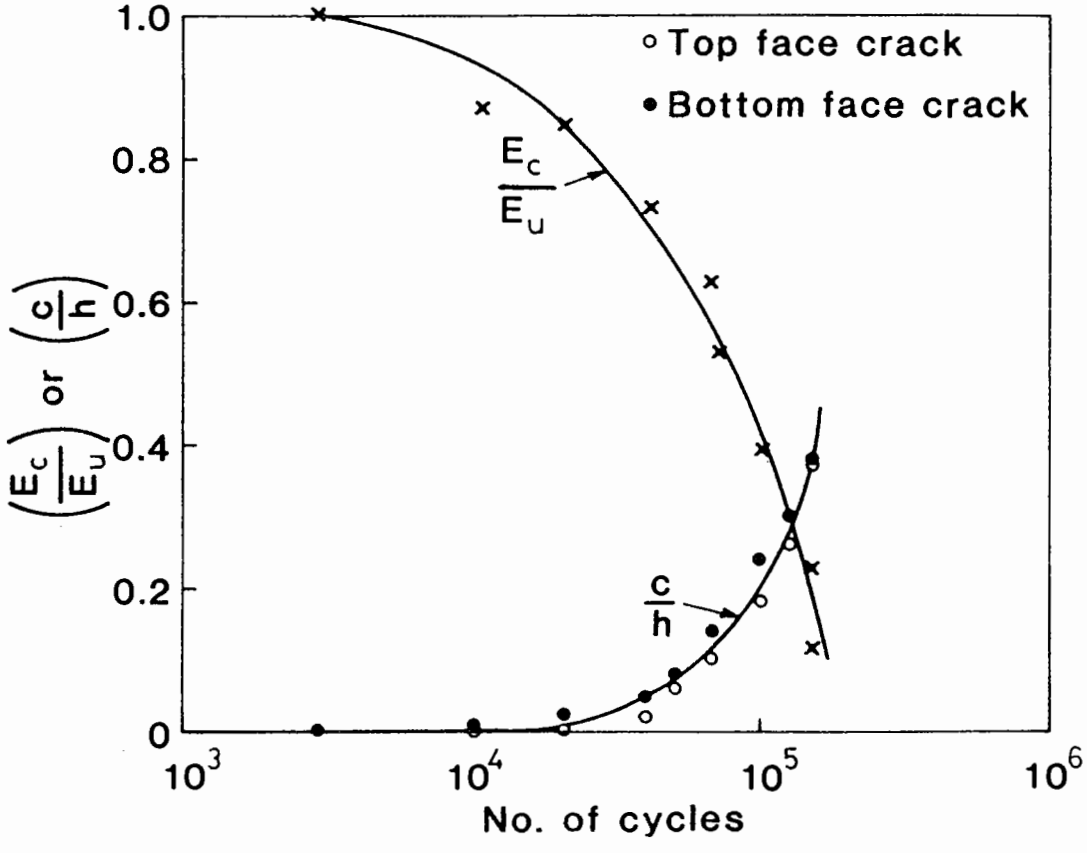

Fig. 7.8 RESULTS OF CRACK PROPAGATION TEST FOR BEAM No. 7 (HRA WEARING COURSE) AT 20°C

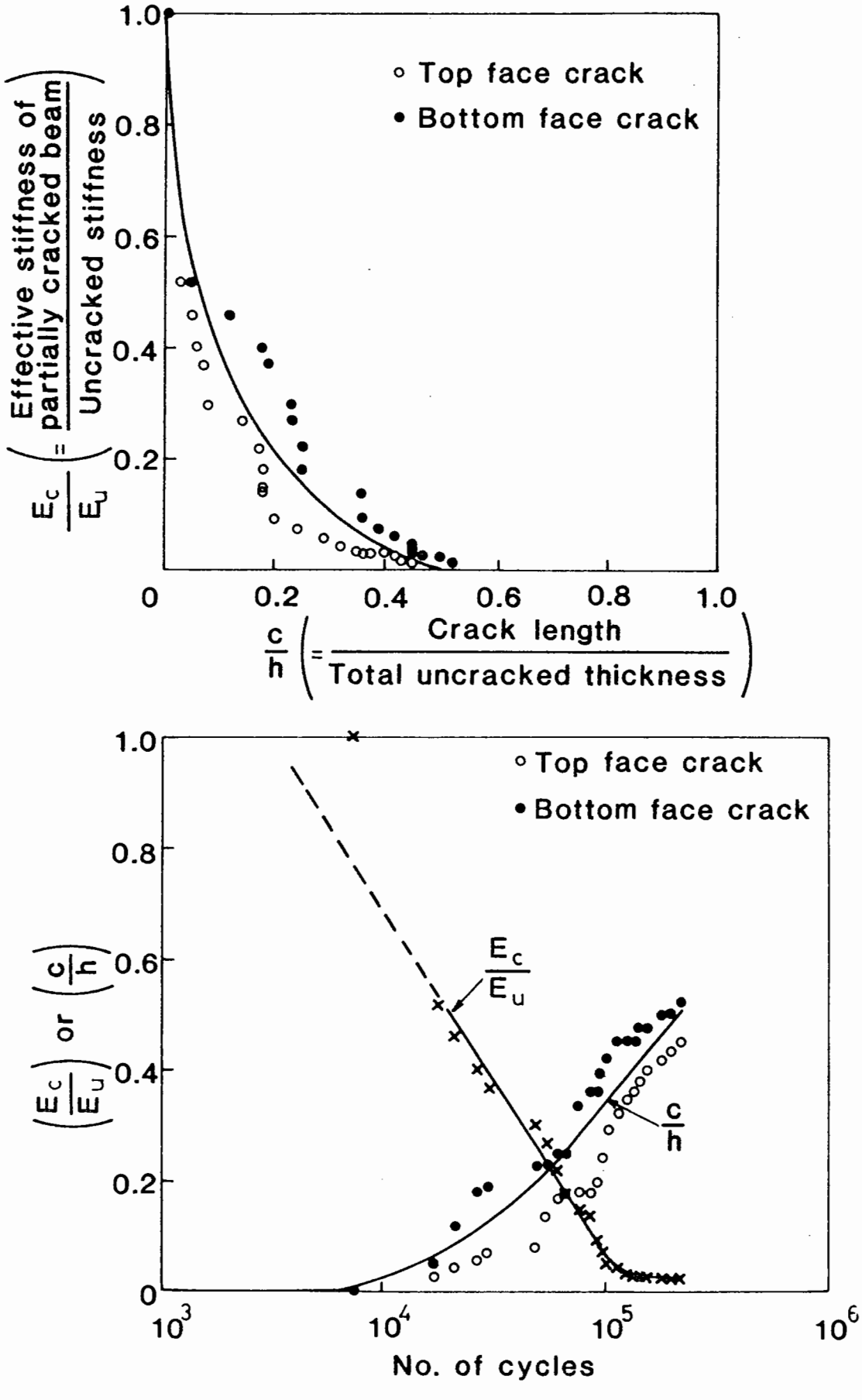

Fig. 7.9 RESULTS OF CRACK PROPAGATION TEST FOR BEAM NO. 8 (HRA WEARING COURSE) AT 9°C

reduce the flexural rigidity and thus the load spreading of the bituminous layer.

(c) The stiffness reduction responses due to crack propagation on two different mixes are similar (see Figures 7.6 and 7.7).

(d) It is encouraging to note that the effect of stiffness reduction on fatigue behaviour is similar to that obtained by Freeme and Marais (111) (see Figure 7.4), even though different testing methods have been used.

Broadly speaking, there exists a linear relationship between stiffness reduction and log (no. of cycles) as the crack propagates through the beam.

(e) Variation in temperature is observed to influence the rate of stiffness reduction of the HRA wearing course specimens. Figure 7.10 shows that, for the same crack length, the lower the test temperature, the higher is the rate of stiffness reduction and vice versa. The results for a gap-graded material obtained by Freeme and Marais (111) are also plotted. As can be seen in the figure, similar trends in the temperature dependence of rate of stiffness reduction are noted. The difference in the slopes is considered to be caused by the use of different testing methods.

Table 7.2 summarises the main results of the crack propagation tests. After the tests were completed, each beam specimen was sawn into small portions and their mean void contents were recorded as 2.5%, 5.8%, 5.0% and 5.7% for Beam Nos. 3, 5, 7 and 8 respectively.

7.5 PROPOSED PROCEDURE FOR EVALUATING CRACK LENGTH

It has been acknowledged that the study of the crack propagation behaviour of bituminous material in the laboratory is very laborious and time-consuming. Therefore, it would be advantageous if the problem could be solved by analytical techniques using computers. As a result, a procedure is proposed below.

Beam No.	Type	Mean Temperature (°C)	Initial peak-to-peak deflection (mm)	Calculated stiffness (MPa)		No of cycles
				uncracked	fully cracked	
3	DBM basecourse	23	0.5	1630	310	70 000
5	HRA wearing course	15	0.2	3100	200	319 400
7	HRA wearing course	20	0.2	2620	300	125 900
8	HRA wearing course	9	0.05	29880	670	210 000

Table 7.2 Summary of crack propagation testing results

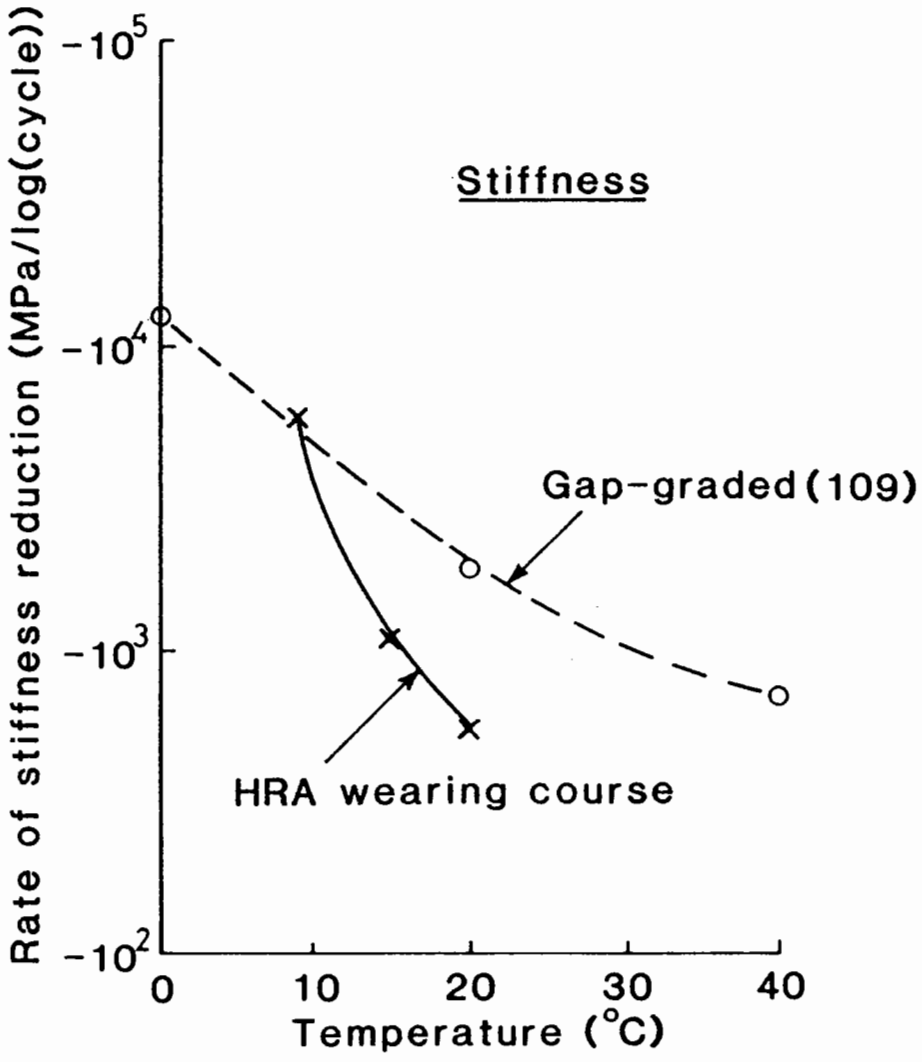

Fig.7.10 EFFECT OF TEMPERATURE VARIATION ON STIFFNESS REDUCTION

7.5.1 Procedure for Calculating Proportion of Stiffness Reduction

A computer program has been developed for the calculation of the proportion of stiffness reduction when the bituminous layer is partially cracked with a specified value of crack length. The purpose is to investigate the accuracy of prediction of the computed stiffness reduction with the four-point bending test results. In the following computation, a two-layer structure with a bituminous layer overlying a supporting layer is used. Figure 7.11 illustrates the general procedure. The BISTRO computer program is used for deflection calculation. The required input data are:

(a) Measured uncracked stiffness of bituminous layer, (E_u) (layer 1);

(b) Assumed stiffness of supporting layer (E_2) (layer 2);

(c) Poisson's ratios of 0.4 assigned to layers 1 and 2 respectively;

(d) Thickness of layer 1 (h);

(e) Applied load (P);

(f) Radius of load of 150 mm;

(g) Measured maximum deflection (d_m);

(h) Assigned crack ratio in layer 1.

The problem is then solved in three stages.

Stage 1 : The stiffness of the supporting layer (E_2) is calculated for given values of uncracked stiffness (E_u), measured maximum deflection (d_m) and applied load (P) which can be obtained from four-point bending tests before crack has initiated. The reason for calculating the E_2 value is to obtain an equilibrium of the structure under the load (P) and deflection (d_m), thus simulating the initial four-point bending condition. The iteration is to compare the calculated deflection (d_c) with the measured value (d_m). If the difference exceeds a limit of 0.01 micron, adjust the layer 2 stiffness (E_2) until the condition is

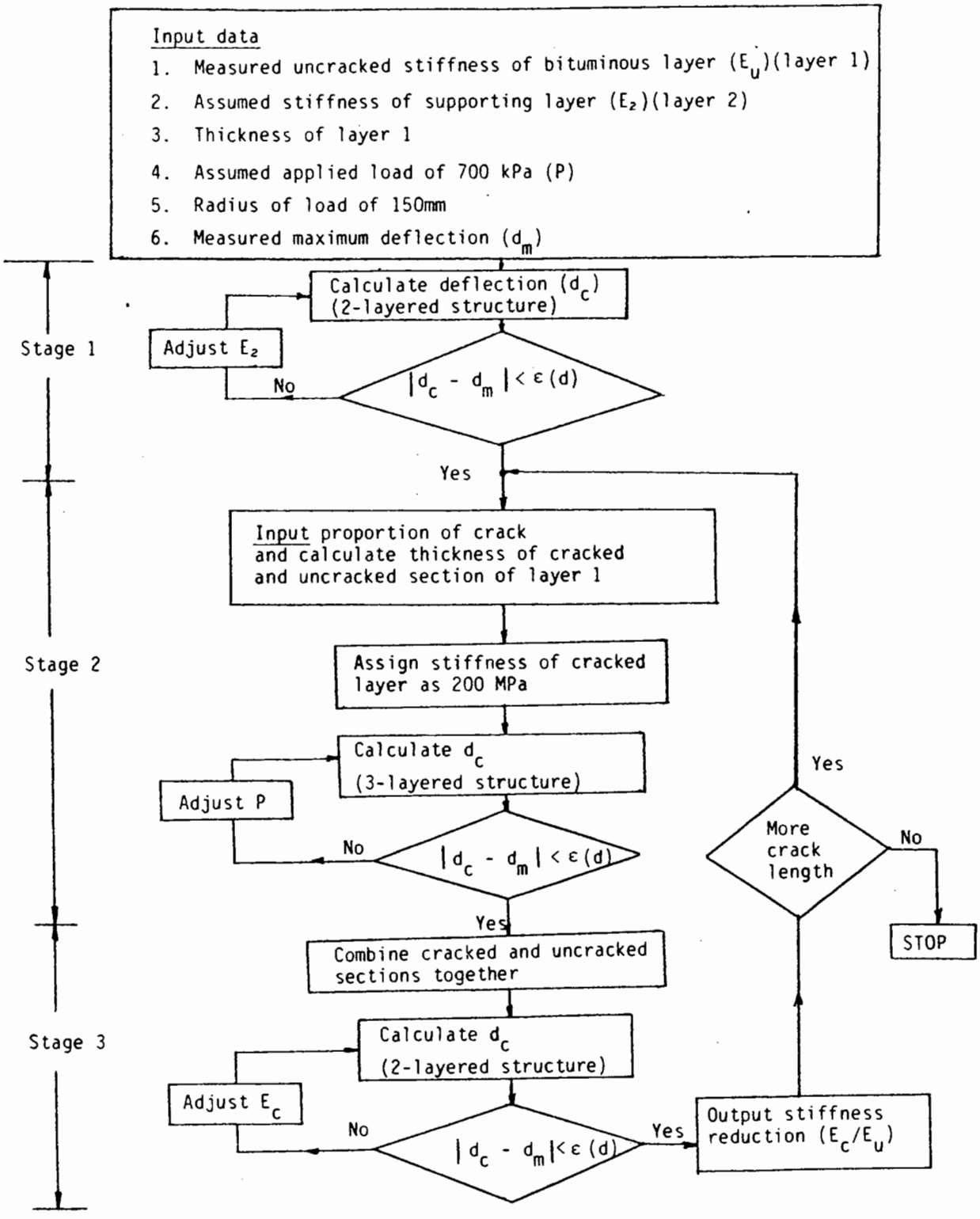

Fig. **7.11** PROCEDURE FOR CALCULATION OF STIFFNESS REDUCTION

satisfied.

Stage 2 : Crack is then initiated at the bottom of layer 1 by introducing a given crack ratio into the calculation. The thickness of the cracked and uncracked sections of layer 1 is then computed. Now, in the following calculation with BISTRO, the original two-layered structure is increased to three-layered where the stiffness of the cracked layer is assigned as 200 MPa, a value obtained from the experiment (refer Section 7.4). To simulate the four-point bending test condition, the applied load should be reduced accordingly in order to keep to the same peak to peak deflection (d_m). Keeping the same stiffness for layer 2 (E_2) calculated in Stage 1 and (E_u) for the stiffness of the uncracked section, the applied load (P) is adjusted until the calculated and measured deflections are matched within the acceptable limit.

Stage 3 : Effective stiffness of partially cracked layer and corresponding stiffness reduction for a given crack ratio are then evaluated. First of all, both the cracked and uncracked sections are combined into one layer to form back into the two-layered structure. Then an arbitrary stiffness value of 1000 MPa is assigned to this partially cracked layer to start the calculation. Deflection is calculated under the adjusted load obtained in Stage 2 and the E_2 value obtained in Stage 1. The calculated deflection is compared with the measured deflection d_m. If the difference exceeds the limit, adjust the stiffness of layer 1. The process is continued until the condition is satisfied. The effective stiffness of the partially cracked layer 1 is found. Proportion of stiffness

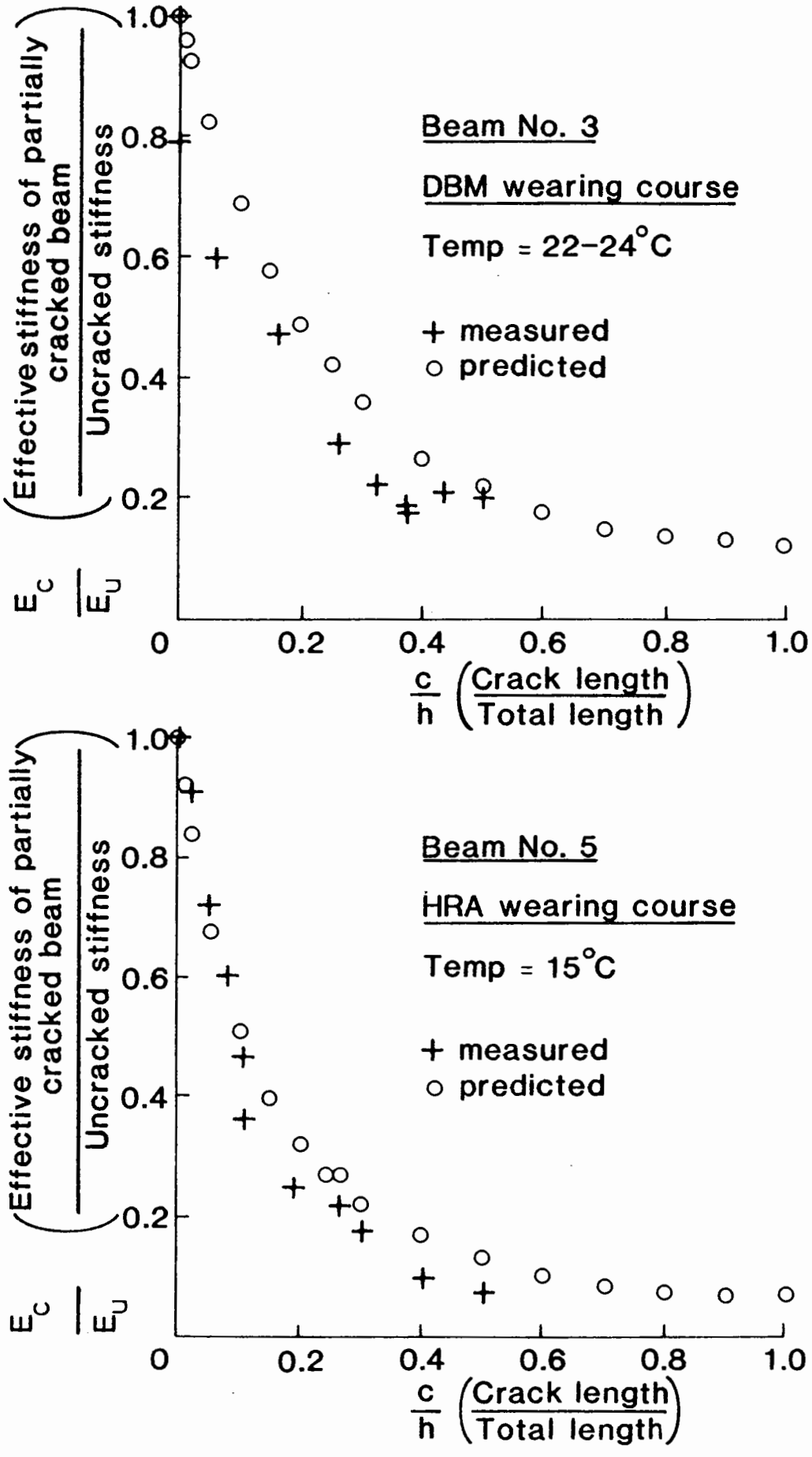

Fig.7.12(a) COMPARISON OF MEASURED AND PREDICTED RESULTS OF CRACK PROPAGATION TEST

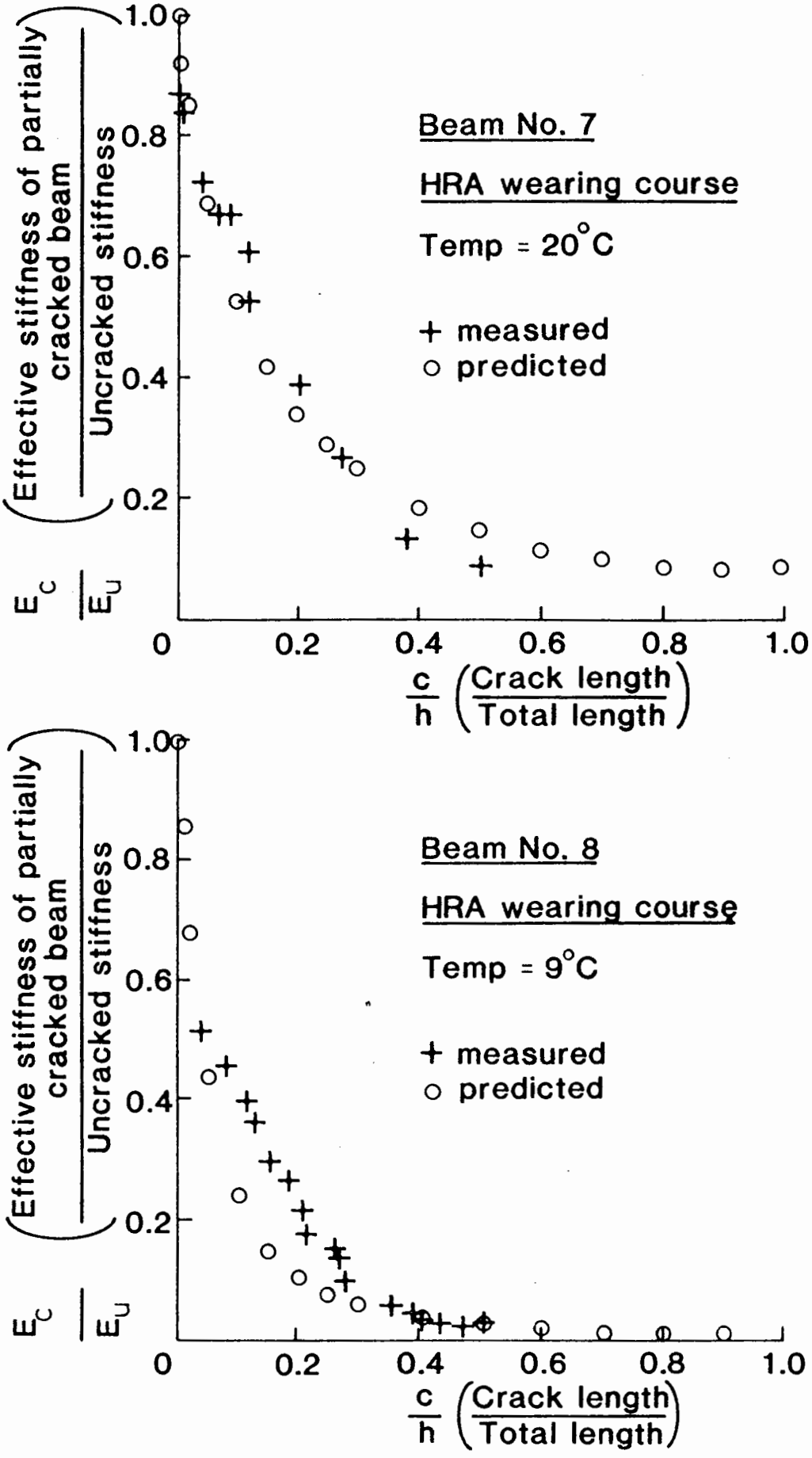

Fig. 7.12(b) COMPARISON OF MEASURED AND PREDICTED RESULTS OF CRACK PROPAGATION TEST

reduction is obtained by taking the ratio of the effective stiffness and the uncracked stiffness, E_u. Repeat Stages 2 and 3 for different values of crack length within the bituminous layer.

7.5.2 Comparison with Experimental Results

The results obtained from the previous section were used to compare with measured results taken from the beam specimens. The input data for the uncracked stiffness of layer 1 was the same as the uncracked stiffness of the beam specimens given in Table 7.2 . The input for the measured maximum deflections varied in accordance with the laboratory results. The initial stiffness of the supporting layer was assumed to be 100 MPa. Figure 7.12 (a) and (b) show the results of the comparison. The measured values, as shown in the figures for crack growth, are the mean values of crack length measured from the top and bottom faces. It is noted that the results for Beam No. 7 give the best agreement. However, the predicted results for Beam Nos. 3 and 5 are higher than the measured values, giving an over-prediction of about 10% on the estimation of crack length for a given stiffness ratio. Under relatively low test temperature, as shown by Beam No. 8, under-prediction of up to about 10% is observed. However, the prediction for DBM basecourse is slightly less accurate than for HRA wearing course at an equivalent temperature.

From the above comparison, it may be seen that, for a given length of crack in a bituminous layer, the proposed analytical procedure is able to predict stiffness reduction with reasonable confidence, and vice versa. This development is useful in evaluating the remaining life of a pavement structure against fatigue cracking as will be discussed in Chapter 8.

7.6 CONCLUSION

A series of laboratory tests has been performed to investigate the influence of crack growth on the reduction of effective stiffness of a bituminous material, using a four-point bending apparatus.

It was found that the rate of stiffness reduction is very rapid if the length of the crack is less than 10 to 15% of the total thickness. Thereafter, the rate of change is much reduced. The effect of temperature variation is found to influence the rate of stiffness reduction in its absolute magnitude. The lower the temperature, the greater is the rate of reduction and vice versa. An analytical procedure relating stiffness reduction to crack growth has been proposed. In general, reasonably good agreement is observed though the prediction for DBM basecourse is not as good as for HRA wearing course. The development of this procedure will be useful in determining the remaining life against fatigue cracking of a bituminous layer, as will be described in Chapter 8.

CHAPTER 8

DEVELOPMENT OF ANALYTICAL OVERLAY DESIGN PROCEDURE

8.1 INTRODUCTION

The present method for designing overlays in the United Kingdom, as documented in LR 833 (3), is based on an empirical approach. However, this approach has its shortcomings. Firstly, the remaining life of an existing pavement and required thickness of overlay can only be calculated for typical roadbase materials, viz, hot rolled asphalt, dense bitumen macadam, wet mix and lean concrete. Secondly, there is no allowance for new materials to be used even if detailed information is known. Thirdly, the present charts given in LR 833 are for bituminous pavements with design lives up to 40 msa and overlaid pavements up to 80 msa only. However, pavements which carry very heavy traffic always have design lives of a much higher magnitude. It is therefore logical to develop an analytical procedure for overlay design which can overcome the above shortcomings.

This chapter begins with describing the different categories of existing overlay design procedures, then discusses the development of a new analytical procedure and, lastly, illustrates an example of pavement evaluation and strengthening of an in-service pavement structure.

8.2 REVIEW OF EXISTING OVERLAY DESIGN PROCEDURES

Over the past two decades, numerous procedures for overlay design of bituminous pavements have been developed. They have mainly been designed to rehabilitate pavement structures with conventional distress mechanisms, e.g. fatigue cracking or permanent deformation. Recently, new methods have been proposed to solve distress problems as a result of reflection cracking in bituminous overlays.

The review therefore commences with a description of the conventional

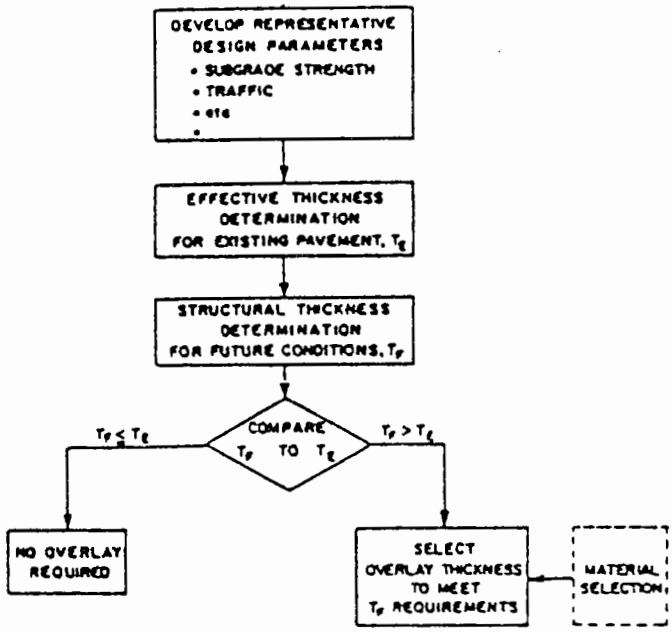

FIG.8.1 OVERLAY DESIGN BY COMPONENT ANALYSIS (64)

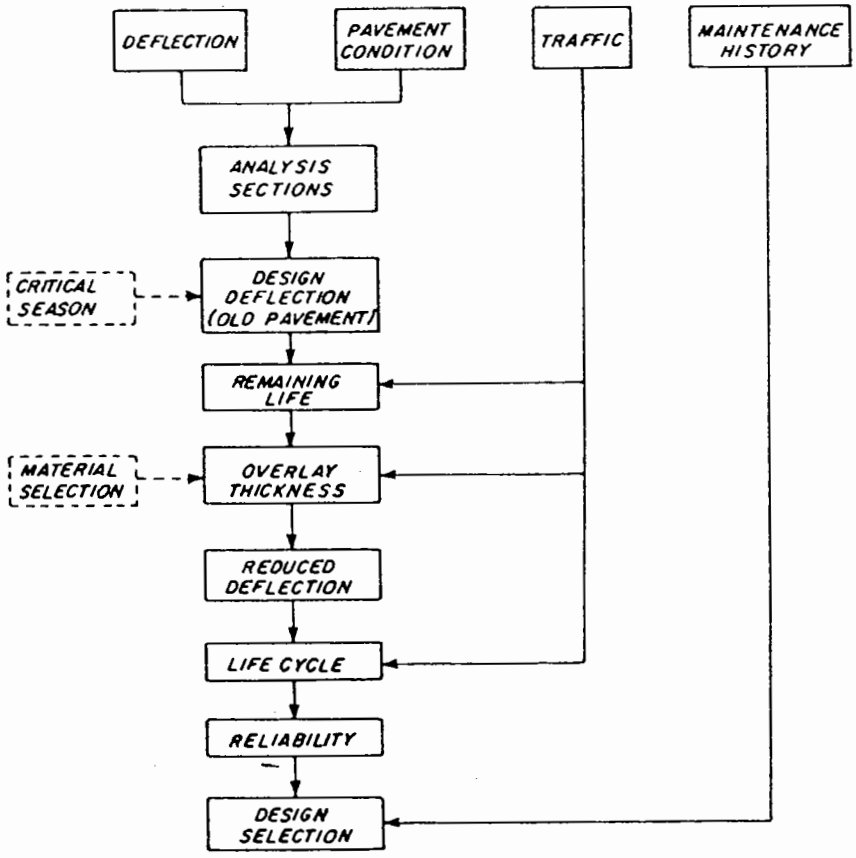

FIG.8.2 GENERAL PROCEDURE OF OVERLAY DESIGN USING DEFLECTION MEASUREMENTS (64)

methods. A brief summary is then followed showing some of the techniques to minimize reflection cracking.

8.2.1 Overlay design procedures against conventional distress mechanisms

In general, there are three main types of procedure under this category:

(A) Empirical procedures based on composition analysis ;

(B) Empirical procedures based on measured deflections;

(C) Analytical overlay design procedures.

(A) Empirical procedures based on composition analysis

The Asphalt Institute Method (MS-17) (8) is one such procedure. The following briefly summarises the essence of the procedure.

The principle of the component analysis procedure is illustrated in Figure 8.1. To apply the procedure, samples of materials from the existing pavement are required as well as in-situ density and moisture content profiles in the subgrade. Standard laboratory tests are then performed simulating the in-situ conditions on each pavement component material, including the subgrade soils, to develop design parameters. The parameters generally include (a) strength of the subgrade; (b) characteristics of pavement materials (e.g. treated and untreated materials); (c) traffic in terms of equivalent 80 kN (18 kips) single-axle loads and possibly (d) regional factors signifying the variation of rainfalls or frost penetration.

Once the design parameters are obtained, the life of the existing pavement structure is evaluated. One of the procedures is to use the AASHTO Interim Design Guide (113) where the pavement layers are converted into an equivalent structural number using the following relationship:

$$SN = a_1h_1 + a_2h_2 + a_3h_3 \qquad (8.1)$$

where a_1, a_2, a_3 are layer coefficients representing the surface, base and sub-base layers respectively;

h_1, h_2, h_3 are thickness of surface, base, and sub-base layers respectively.

A major disadvantage of the AASHTO system lies in the selection of layer coefficients for in-service pavements, since a considerable amount of judgment and experience is required to assign the values of the coefficients realistically. An alternative approach is that of the Asphalt Institute, which provides recommended conversion factors for converting the thickness of existing pavement component layers to an effective thickness of bituminous material. Conversion values ranging from 0.9 to 1.0 are assigned to uncracked bituminous material. For bituminous material which exhibits some distress, coefficients in the range of 0.5 to 0.8 are assigned. Other layers are assigned lesser values depending on their condition, e.g. granular sub-base or base 0.2 to 0.5 depending on grading, plasticity, and general compliance with standards for the respective materials. Together with information on traffic analysis, and regional factors, it is possible to determine thickness requirements for the new construction. If the existing pavement is equivalent to or exceeds the limits for new construction, overlay is required to restore the pavement to its original condition. In the case of the Asphalt Institute procedure, the difference between the full-depth bituminous material requirement and the effective equivalent thickness of the existing pavement is the thickness recommended for overlay. A similar procedure is also proposed by the U.S. Corps of Engineers (114).

The main advantages of this procedure are:

(a) It evaluates individual pavement layers using established testing methods;

(b) It explores potential groundwater and drainage problems;

(c) It records actual thicknesses of the pavement layers.

The main disadvantages of this procedure are:

(a) Laborious testing of samples in the laboratory;

(b) Limited coverage within the test program;

(c) Uncertainty about the applicability of the laboratory test results to long term field conditions;

(d) Subjective selection of layer coefficients for each pavement component layer.

(B) Empirical procedures based on measured deflections

During the 1960s, a lot of research effort was devoted to developing empirical overlay design procedures based on pavement deflection measurements. Leading research centres responsible for such development include the Califoria Department of Transportation (50), the Kentucky Department of Transportation (115), the U.S. Corps of Engineers (116), The Asphalt Institute (117), the Transportation Research Board (6) and the Canadian Good Roads Association (118) and, in the early seventies, the TRRL (2). This resulted in considerable literature regarding deflection measurements and their correlation with performance and use for overlay design. The devices used for measuring deflections consisted of Benkelman Beam, Dynaflect, Road Rater, and Deflectograph.

Figure 8.2 summarises the general approach to overlay design procedure which basically required three common design elements, namely, deflections, pavement condition and the estimation of traffic. Table 8.1, taken from Finn and Monismith (64), summarises the essential features of overlay design procedure proposed by some

Method	Deflection Measurement	Condition Survey	Establishment of Analysis Sections	Design Deflection	Provision for Remaining Life Estimate	Overlay Thickness Determination
Asphalt Institute	Benkelman beam rebound deflection	Yes	Yes	$\delta + 2S$ adjusted for temperature and critical season	Yes	Based on response of overlayed pavement as two-layer elastic system and relationship between allowable deflection and repetitions of 18-kip EAL.
California Department of Transp.	Dynaflect; Traveling deflectometer	Yes	Yes	$\delta + 0.845$	No	Based on relation between permissible deflection as a function of asphalt layer thickness and repetitions of 18-kip EAL and reduction in deflection achieved by different thicknesses of overlay materials.
Transport and Road Research Laboratory	LaCroix deflectograph	Yes	Yes	85th percentile	Yes[a]	Observed damping effect on deflection under 18-kip EAL for various overlay thicknesses used to develop design charts as a function of repetitions of 18-kip EAL.
Roads and Transp. Association of Canada	Benkelman beam rebound deflection	Yes	Yes	$\delta + 2S$	Yes	Overlay thickness selection procedure similar in format to Asphalt Institute procedure.
U.S. Army[b] Corps of Engineers Waterways Experiment Station	WES heavy[c] (16-kip) vibrator	Yes	Yes	Mean DSM	Yes	With parameters developed from nondestructive testing, the CBR of the subgrade is ascertained. Using the ESWL procedure, a pavement thickness is selected according to the current CE procedure. Overlay thickness is the difference between existing pavement thickness and the new thickness.

[a] A series of relationships developed between deflection change and traffic, depending on type of base course. Includes provision for different probabilities of achieving desired design life. Overlay material is hot-rolled asphalt.

[b] For airfield pavements; all others for highways.

[c] A dynamic stiffness module (DSM), defined as force/displacement, is used as the measure of pavement response rather than deflection.

Table 8.1 Summary of empirical deflection-based overlay design procedures (64)

of the major research centres. To demonstrate how the method works, the procedure proposed by the TRRL is described in more detail in the following paragraphs.

TRRL overlay design procedure: The procedure was first published in LR 571 in 1973 (2) which related the maximum surface deflection measured using a BB to the strength of the road. The relationships were developed after systematic measurements had been made with the BB over a 20-year period on TRRL full scale road experiments (117,9). In 1978, the design procedure was further extended in TRRL report LR 833 by Kennedy and Lister (3). However, it is noted that although LR 833 was mainly developed from Defectograph measurements, its principle was basically similar to LR 571. The salient features of the overlay design procedure described in LR 833 are summarised below.

(1) Estimation of traffic: The first problem in overlay design is the estimation of past traffic (since construction) and future traffic (after overlay) carried by the road. Two nomographs (120), shown in Figure 8.3, are available for the estimation of traffic in terms of numbers of commercial vehicles. Damage factors are applied to convert the number of commercial vehicles to an equivalent number of standard axles. The factors in Table 2 of Road Note 29 (96) may be used for past and for future traffic, revised damage factors issued by the Department of Transport (121) and TRRL (122) may be applied.

(2) Deflections: Deflection measurements using the BB are carried out at intervals of 12 to 25 m depending on the condition of the existing pavement. One kilometre of pavement may be surveyed in a working day. The Deflectograph, however, measures deflections automatically at about 4.0 m intervals, travelling at a creep speed of 1 - 3 km/hr. Normally, about 10 - 12 km of pavement can

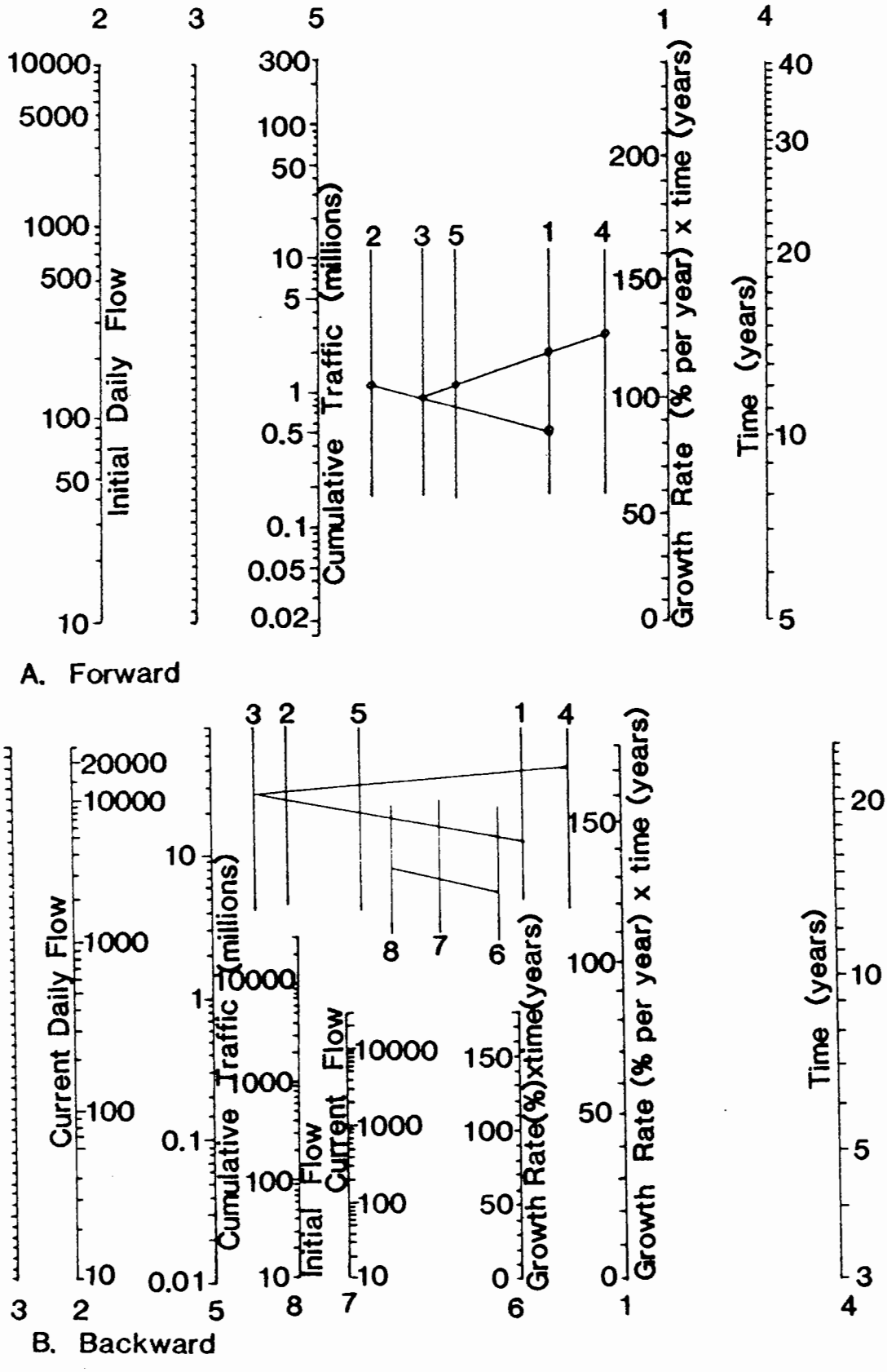

FIG. 8.3 NOMOGRAMS FOR ESTIMATION OF CUMULATIVE ONE-WAY TRAFFIC IN THE LEFT HAND LANE (AFTER THROWER & CASTLEDINE(118))

be surveyed in a working day.

Measured deflections are adjusted to correct for the influence of temperature. The standard deflection corresponds to that measured by the BB when the pavement temperature is 20°C at a depth of 40 mm below the surface. A number of charts with different thicknesses of bituminous layer have been prepared for temperature correction and Figure 8.4 shows a typical one. If the Deflectograph is used, these deflections are first corrected to the equivalent BB deflections, using the relationship in Figure 8.5, and then, using Figure 8.4, they are corrected to equivalent deflections at the standard temperature of 20°C.

(3) Design deflection: The measured uncorrected deflection profile of the pavement is divided into different lengths for which reasonably constant deflections can be identified. The design deflections are at those locations within each length of the section which are likely to reach a critical condition at the earliest time. The 85th percentile deflection is chosen in the analysis. Then, the design deflections are corrected to standard conditions as already described above.

(4) Evaluation of pavement performance: During the deflection survey, a visual assessment of the quality of the pavement and rut depth measurements in the wheelpaths (using a 2 m straight edge) have to be made. The condition of the existing pavement is then classified using Table 8.2. Assessment of remaining life is obtained from four performance charts for pavements with different roadbases. Figure 8.6 shows an example for bituminous roadbases. In order to use these charts, a design deflection and an estimate of past traffic (in msa) are required. From the figure, following the deflection trend line, the deflection of a pavement is fairly constant during its life until the critical

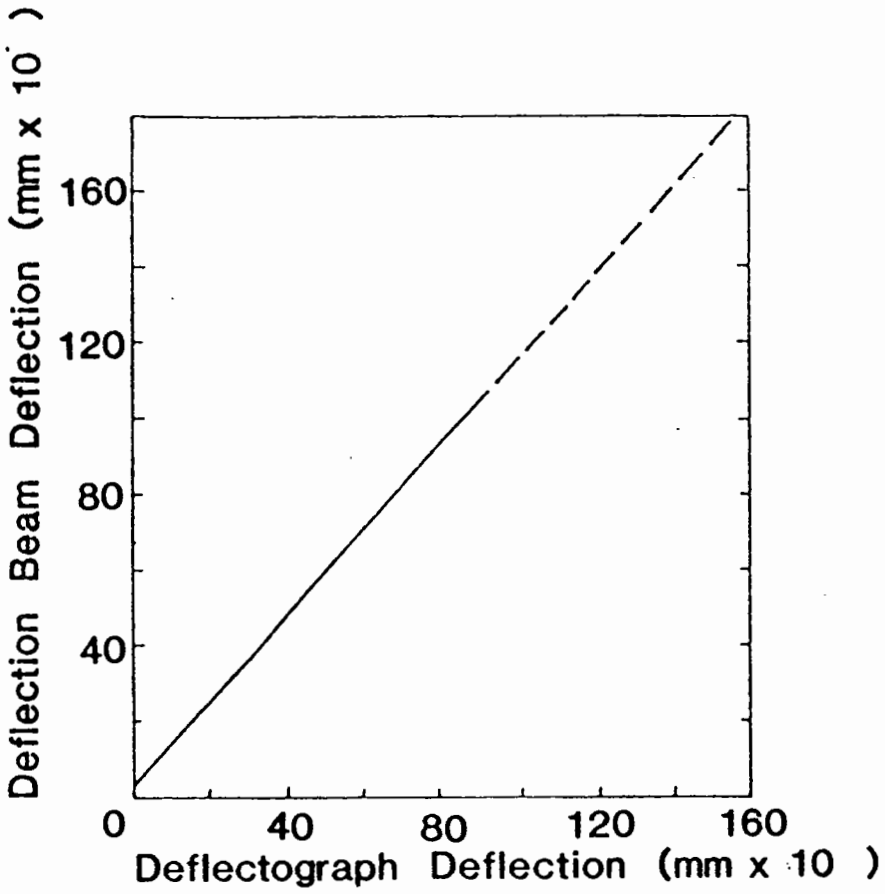

FIG. 8.5 CORRELATION BETWEEN DEFLECTION BEAM AND DEFLECTOGRAPH (AFTER KENNEDY AND LISTER (3))

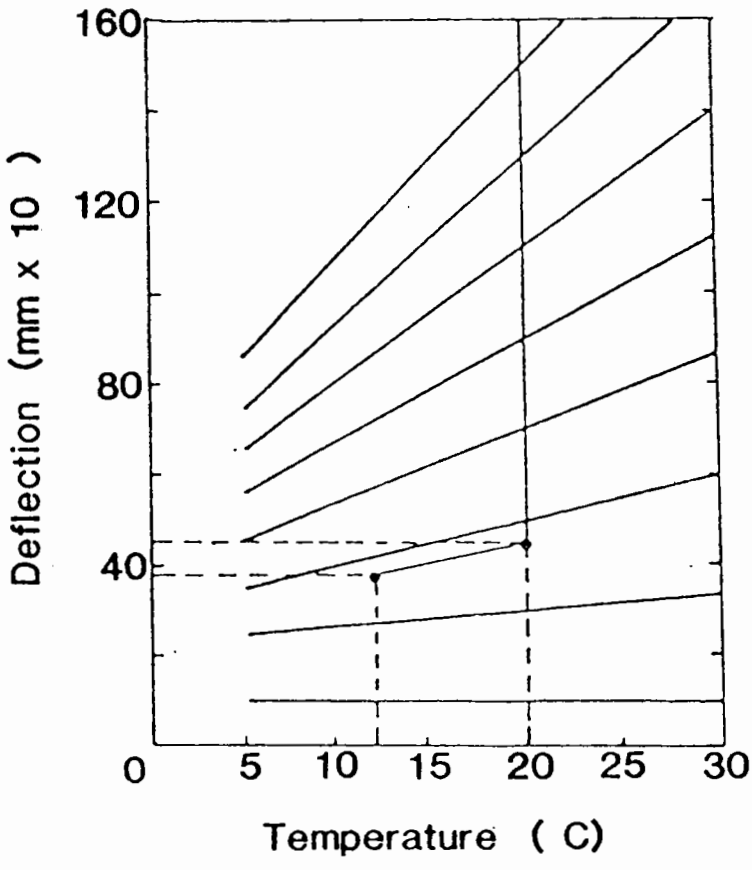

FIG. 8.4 TYPICAL RELATION BETWEEN DEFLECTION AND TEMPERATURE (AFTER KENNEDY AND LISTER (3))

Wheel path cracking	Wheel Path Rutting			
	> 5 mm	5 mm - 10 mm	10 mm - 20 mm	≥ 20 mm
None	SOUND Code 1	SOUND Code 2	CRITICAL Code 3	FAILED Code 6
Less than half width of wheel path or single crack	CRITICAL Code 4	CRITICAL Code 4	CRITICAL Code 4	FAILED Code 7
More than half width or inter-connected multiple cracks	FAILED Code 5	FAILED Code 5	FAILED Code 5	FAILED Code 8

Table 8.2 Classification of Pavement Condition

Material	Thickness factor
Rolled asphalt	1
Dense coated macadam containing 100 pen or B54 binder	1
Dense coated macadam containing 200 pen or B50 binder	1.3
Open-textured macadam	2

Table 8.3 Factors used for Coated Macadam Overlays

condition is reached, when it starts to increase. The critical condition corresponds to the damage visible in the pavement surface shown in Table 8.2. The remaining life of the pavement is computed from the numerical difference between the number of standard axles corresponding to critical condition and the past traffic estimated up to the time of survey.

(5) Overlay design: If the remaining life of the pavement is shorter than the required future life (e.g. estimated from Figure 8.3), overlay is required. Overlay thicknesses may be selected from a set of design charts for probabilities of 0.5 and 0.9 of achieving a specific design life. Figure 8.7 shows a design chart for bituminous roadbases with a probability of 0.5. Other charts have been developed to cover other types of base materials. It is noted that a minimum overlay thickness of 40 mm is recommended. The design charts were developed from field data which have been obtained before and after the application of the hot rolled asphalt only. For coated macadam materials, the overlay thicknesses obtained from the charts are to be converted using factors as shown in Table 8.3. However, a maximum thickness of 100 mm is recommended if coated macadam overlays are used.

The main advantage of the procedure is that it is simple to use.

The main disadvantages of the procedure are:

(a) Restricted use since the procedure is only applicable within a limited range of temperature;

(b) Inability to modify the existing procedure in the light of new design methodology;

(c) Inability to extend the existing procedure to cater for an increase in traffic conditions nor for new and different

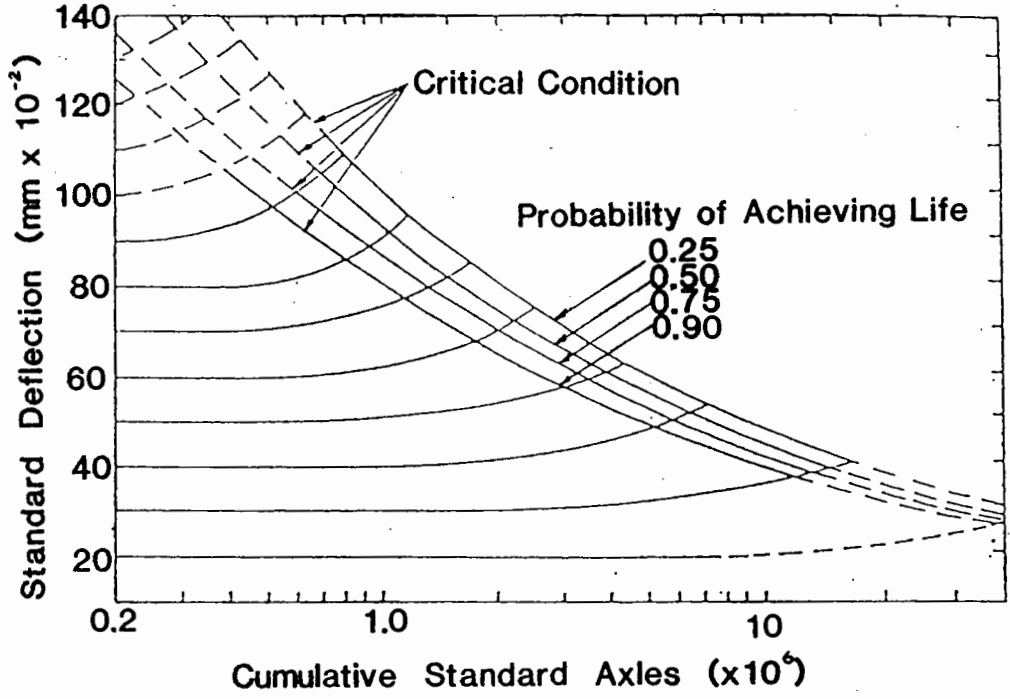

FIG 8.6 RELATION BETWEEN STANDARD DEFLECTION AND LIFE FOR PAVEMENTS WITH BITUMINOUS ROAD BASES (AFTER KENNEDY ET AL(3)

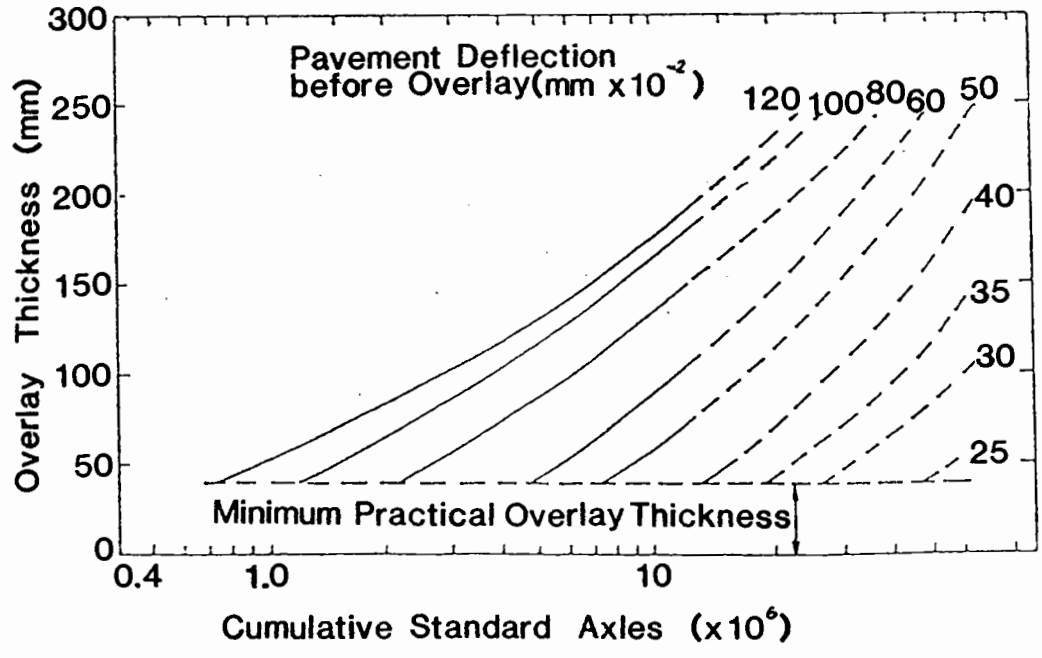

FIG 8.7 OVERLAY DESIGN CHARTS FOR PAVEMENTS WITH BITUMINOUS ROAD BASES (0.50 PROBABILITY) (AFTER KENNEDY ET AL(3))

materials, unless laborious and time-consuming full scale performance surveys have been undertaken.

(C) Analytical overlay design procedures:

During the past decade, numerous new methodologies have been developed, based on analytical procedures, which perform overlay design to an existing pavement using linear elastic theory. The general approach of the procedure is given in Figure 8.8 as extracted from Finn and Monismith (64).

The essential input data for this procedure are deflections from non-destructive testing, condition surveys and traffic requirements. The non-destructive testing devices consist of the FWD, Dynaflect and Road Rater, where deflection bowls are measured. A series of back-analyses is then performed to determine the in-situ pavement conditions by evaluating the stiffnesses of each layer. Remaining life of the existing pavement is computed for the distress modes of fatigue cracking and permanent deformation. In the case of fatigue cracking, Miner's rule has been proposed to estimate the remaining life, viz,

$$\frac{N_r}{N_F} = 1 - \frac{N_p}{N_F} \qquad (8.2)$$

where N_p is the number of load applications to-date (past traffic);

N_F is the allowable pavement life against fatigue cracking;

N_r is the remaining fatigue life of the existing pavement before failure.

Considering the condition of the pavement and future traffic requirements, overlay may be necessary to upgrade the existing pavement. In order to calculate the thickness of overlay to minimize fatigue cracking, the tensile strain is determined at the bottom of the existing bituminous layer using a multi-layered linear elastic

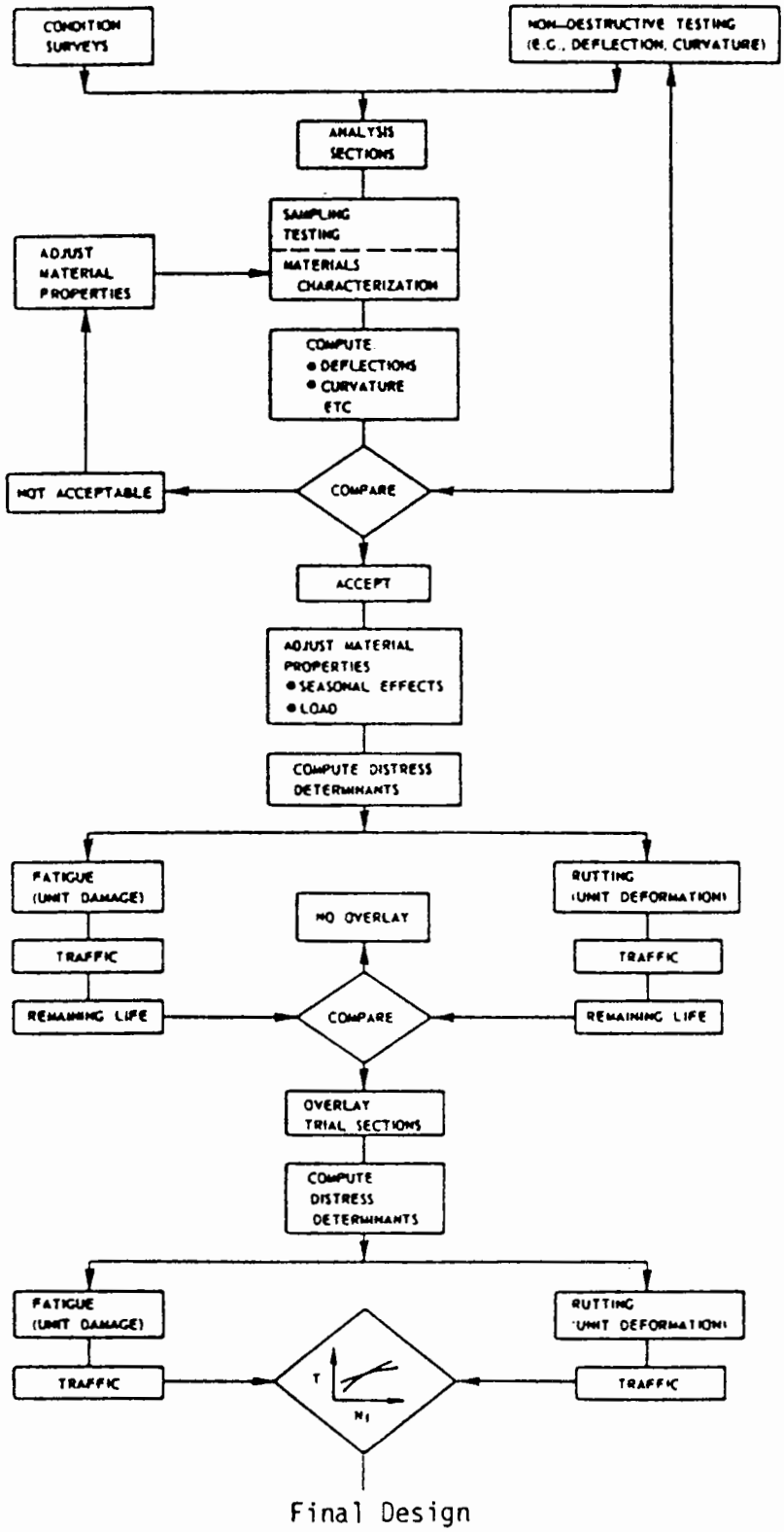

FIG. 8.8 GENERAL PROCEDURE OF ANALYTICAL OVERLAY DESIGN METHOD (64)

program. The required pavement life with overlay is then estimated using Miner's rule,

$$N_{ov} = \frac{N_f}{(1 - N_p/N_F)} \qquad (8.3)$$

where N_{ov} is the pavement life against fatigue cracking for a given overlay thickness;

N_f is the estimated future traffic.

Through a series of analyses for a range of overlay thicknesses, the required thickness corresponding to the additional traffic loading is eventually determined.

To simplify the operation, design and evaluation charts have been developed by Shell (21) as illustrated in Figure 8.9. As seen in Figure 8.9(b), points C and D denote the effective thickness of existing bituminous layers and total thickness including the overlay respectively. The required overlay thickness is then the difference (D - C).

For permanent deformation, it is generally assumed that the overlay will remove the rut on the existing pavement surface. Therefore, the thickness of overlay may be designed as if it were a new pavement structure for the additional traffic loading. As for fatigue cracking, Figure 8.9(a) illustrates a chart developed by Shell (21). As can be seen, the points A and B represent the effective thickness of the existing bituminous layers and the total thickness respectively. The overlay thickness is denoted by h_o, which is the difference of (A - B).

In addition to the above criteria, Shell (21) also propose to calculate overlay thicknesses assuming an existing pavement to be completely cracked using the chart shown in Figure 8.9(c).

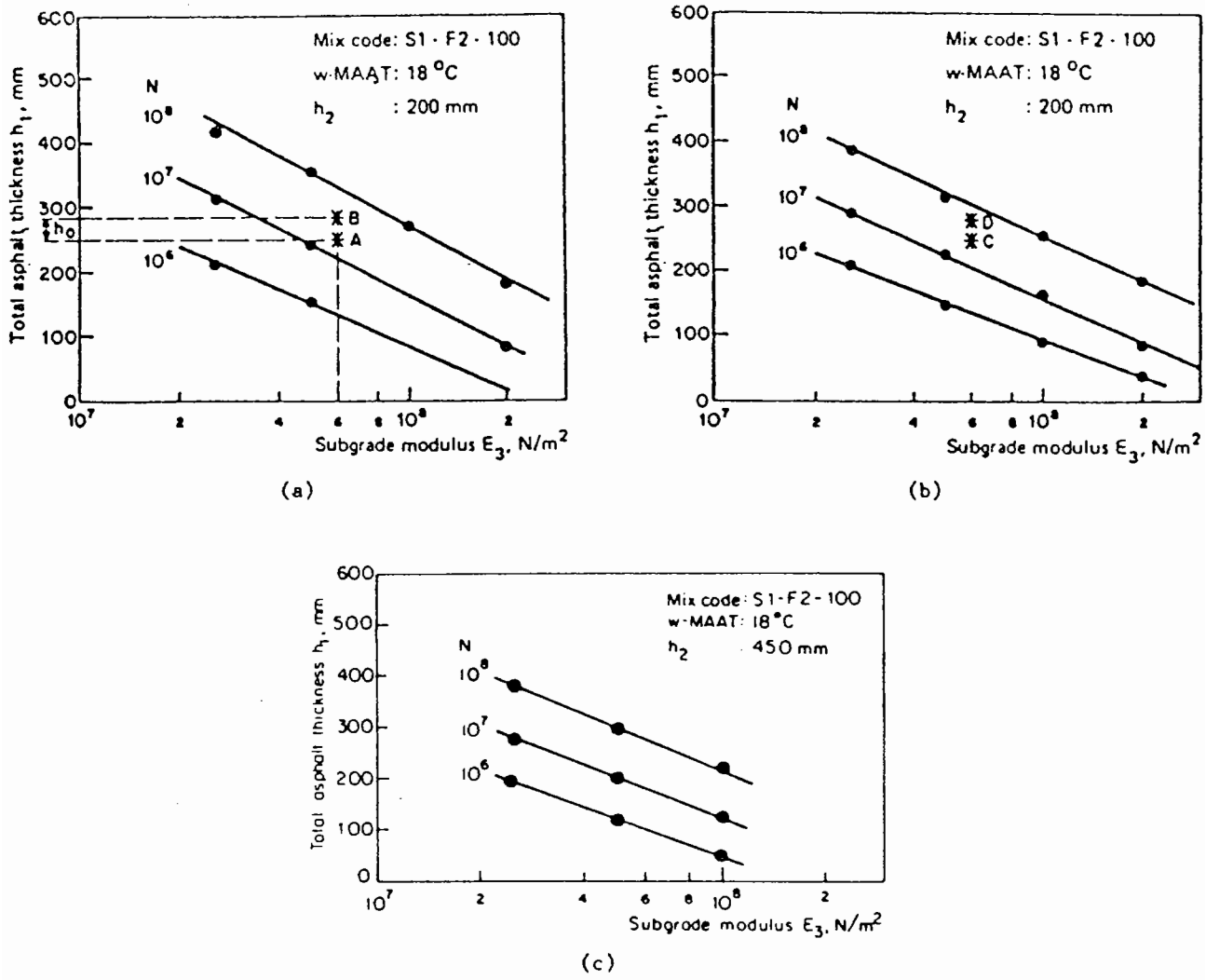

FIG. 8.9 SHELL DESIGN CHARTS : (a) BASED ON SUBGRADE STRAIN CRITERION, (b) BASED ON ASPHALT STRAIN CRITERION, AND (c) BASED ON ASSUMPTION THAT EXISTING BITUMINOUS LAYER BEHAVES AS GRANULAR BASE (21)

Finally, the design overlay thickness will be the largest value, required to satisfy all the criteria.

The main advantages of the procedure are:

(a) It adapts to new methodology if required;

(b) Different distress modes, i.e. fatigue cracking, permanent deformation and so on, can be considered separately;

(c) It is capable of considering varying traffic loadings, new materials, environments, ageing effects on the bituminous material as well as drainage conditions.

The main disadvantages of the procedure are:

(a) A comparatively sophisticated analysis which may involve the use of computer;

(b) It is unfamiliar to most highway engineers;

(c) Limited experience.

In summary, as far as routine evaluation and overlay design is concerned it is considered that the component analysis method is inappropriate because of the slow operation of carrying out laboratory testing. In contrast, the empirical overlay design method based on measured deflections is simple to use. However, the main drawback for this method is inflexibility in application. The basis of the development, i.e. empirical data, makes it very difficult to adapt to increase in traffic conditions or to new and different materials.

The analytical overlay design procedure is considered to be the best overall since it provides the most comprehensive approach to both evaluation of the existing structural capabilities and to the design of pavement overlays. In particular, it can cater for varying traffic conditions and its procedure can be modified quite simply to incorporate new materials, new environments as well as other special considerations like ageing and drainage variations.

8.2.2 Methods of minimizing reflection cracking of overlays

According to Treybig, et al (123), reflection cracks are defined as "fractures in a pavement overlay that are the result of, and reflect, the crack or joint pattern in the underlying layer and may be either environmental or traffic induced". They can be found in bituminous overlays over either concrete or bituminous pavements. The presence of these cracks, as summarised in the Transportation Research Board pavement rehabilitation workshop in 1974 (124), can cause early deterioration in bituminous overlays, thus reducing the useful service life of rehabilitated pavements. Deterioration may take the form of ravelling and spalling occurring at the reflection cracks in overlays on existing bituminous pavements. In addition to these, closely spaced parallel cracks and humps, often occur at reflection cracks in overlays over existing concrete pavements.

The basic mechanism which leads to reflection cracking is the vertical and horizontal movement of the bituminous overlay. Vertical movements are caused by differential movements at a crack or joint in the underlying pavement due to moving loads, whereas horizontal movements are due to expansion and contraction caused by variation of temperature or moisture.

The problem of reflection cracking was first studied in 1932 (125,126). Since then, a number of field trial studies over the years have led to the proposal of a range of solutions as summarised by Sherman (127).

Possible solutions for bituminous overlays on existing bituminous pavements include:

(a) Low viscosity asphalt (200-300 pen) used in the bituminous material either as an overlay or as an interlayer;

(b) Heater-scarifier remix of the existing surface covered with a new bituminous layer;

(c) Stress-absorbing membrane interlayer (SAMI) constructed with asphalt-rubber;

(d) Certain fabric interlayers that retard reflection (128);

(e) Overlays with thickness greater than 50 mm.

Possible solutions for bituminous overlays on existing concrete pavements include:

(a) Overlays with thickness greater than 150 mm;

(b) Prefabricated membrane strips;

(c) Open-graded bituminous basecourse with thickness about 90 mm and about 90 mm thick dense graded wearing course;

(d) Asphalt-rubber interlayer (SAMI) with at least 50 mm thick bituminous layer;

(e) Breaking the existing slabs into small sections (typically 0.9 to 1.5 m) and seating the broken slabs with pneumatic or vibratory rollers before placing the bituminous overlay.

Analytical procedures, e.g. Coetzee and Monismith (129), have recently been proposed for analysis of the reflection cracking problem using the finite element method. However, there are still no analytical procedures that can be used routinely for overlay design that incorporate the range of materials necessary to minimize reflection cracking.

8.2.3 Review of previous development of overlay design technique at Nottingham

Nottingham has engaged in research into the fundamental behaviour of bituminous, as well as unbound granular and clay materials, for about three decades. Over that period, a large number of papers have been published unveilling the complex behaviour of the bituminous (130), granular (131) and clay (75) materials as well as developing novel ideas to explain the interactions of these materials in a composite pavement structure. The papers indicated in brackets summarise the

main findings of the work. This work has led to the development of analytical design procedures and the main-frame computer programs ADEM (Analytical DEsign Method) and ANPAD (ANalytical PAvement Design) as described in Brown et al (132,63). At the same time, simplified design procedures were also developed in Brown and Brunton (133) which allowed the practical engineers flexibility in designing new pavements. Furthermore, the above effort resulted in the Mobil Design Manual (134) being published in 1985. Since then, research has been extended to cover the area of pavement evaluation and overlay design. A fresh attempt was made by Brunton (63), who developed a computer program DEMOD, known as DEflection Modelling for Overlay Design before the writer commenced this research. Continuous research during the past three years has largely superseded the idea proposed in the DEMOD program. The procedure incorporated in the DEMOD program is briefly summarised below and full details of the procedure can be referred to in Brunton (63).

The DEMOD program has incorporated two computer programs as sub-routines, viz the CHEVRON N-layer (61) program for calculation of stresses, strains and deflections, and parts of the PONOS (135) program for determining elastic stiffnesses of the bituminous materials. However, in the present development, CHEVRON N-layer is not selected in favour of the BISTRO computer program (47) for reasons already discussed in Chapter 3. Figure 8.10 shows a simplified flow diagram for DEMOD.

Principle of DEMOD

Two sets of measured deflections are required for overlay design, i.e. one along the wheelpath and the other in the lane centre, as illustrated in Figure 8.11. The reasons for their use are:

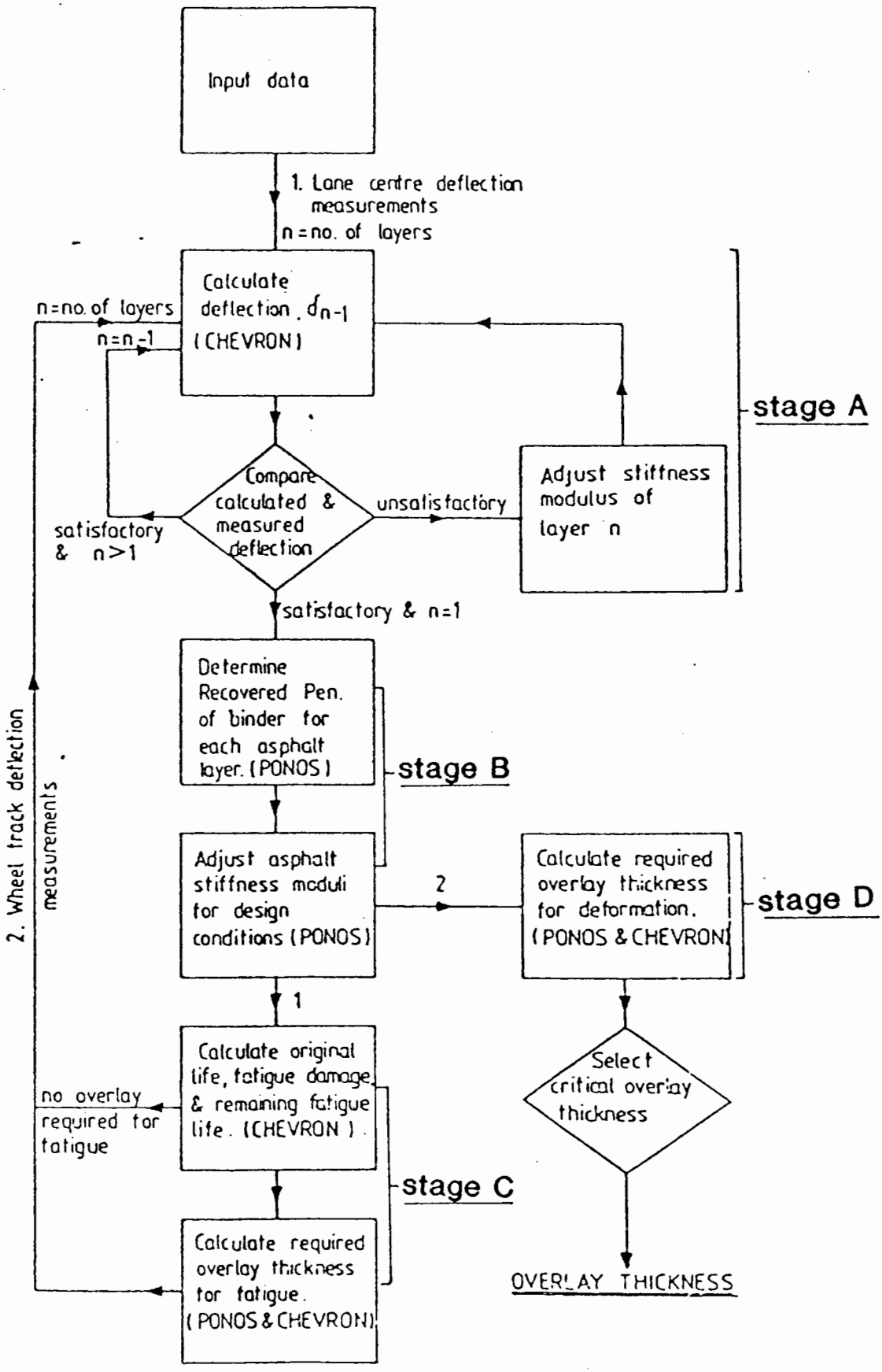

FIG8.10FLOW DIAGRAM FOR DEMOD (AFTER BRUNTON(63))

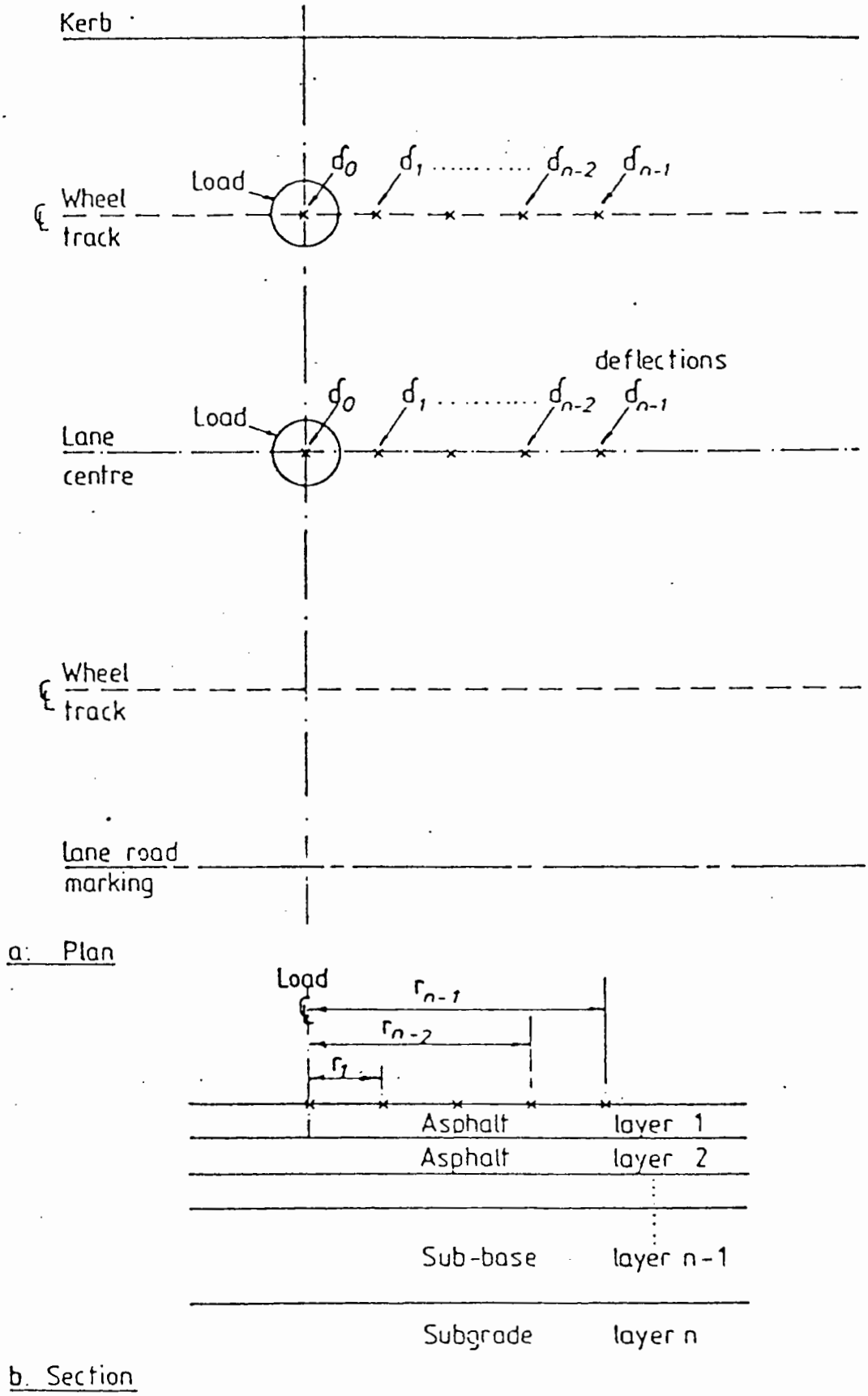

FIG8.11TYPICAL PAVEMENT STRUCTURE AND DEFLECTIONS FOR DEMOD(AFTER BRUNTON(63))

(a) Evaluation of damage against fatigue

The original fatigue life may be assessed using the lane centre deflections. If the past traffic is less than half of the original fatigue life, and the remaining fatigue life (original fatigue life - past traffic) is less than the future traffic, overlay is required. However, if past traffic is more than half of the original fatigue life, reconstruction is required.

(b) Evaluation of damage against permanent deformation

The original pavement life against permanent deformation is determined in the lane centre. The remaining life is then the difference between the original life and the past traffic. Overlay is required if the remaining life is less than the required future life.

(c) Overlay against fatigue damage

Overlay is designed only against damage additional to those which have already taken place at the bottom of the bituminous layers using Miner's rule.

(d) Overlay against permanent deformation damage

Overlay is designed as a 'new' pavement.

Procedure for Analysis

The procedure for overlay design is carried out in four stages, i.e. stages A, B, C, and D as indicated in the flow chart of Figure 8.10. Stages A, B and C involve the overlay design against fatigue damage and permanent deformation using lane centre FWD deflections whereas stages A, B and D utilise deflections on the wheelpath to assist with overlay design against permanent deformation. The essentials of each stage are summarised below. The program assumes a FWD load of 35 kN or contact pressure of 500 kPa with contact area of radius 150 mm.

Stage A

The iteration procedure in this stage is similar to the BASEM

computer program. The program firstly calculates the deflection at radius r_{n-1} where n is the number of layers in the structure (Figure 8.11), using estimated layer stiffnesses and sub-routine CHEVRON. The calculated and measured deflections, d_{n-1}, are compared. If the difference is more than ± 2% of the measured deflection, then the stiffness of layer n is adjusted using the following expression:

$$E_{new} = E_{old} \times \frac{(d_m + d_c)}{2d_c} \qquad (8.4)$$

where E_{new} and E_{old} are the new and old estimate of the stiffness;

d_m and d_c are the measured and calculated deflection values.

The iterative process continues using the new layer n stiffness until the accuracy is achieved. This newly derived stiffness is retained for use in calculation of stiffness of other layers. The same procedure is repeated to calculate and compare deflections one by one at other radii r_{n-2}, r_{n-3} ... until r_o (load centre) each time adjusting the corresponding layer stiffness, E_{n-1}, E_{n-2},... until E_1 (top layer). All the deflections are re-checked using the derived stiffnesses for each layer and further adjustments will be carried out when necessary.

Stage B

This stage is to determine a recovered penetration of the binder for each bituminous layer. The sub-routine PONOS is used for the calculation. The initial estimate for the recovered penetration is 50 pen. The calculated mix stiffness is then compared with that derived from deflection modelling. An iterative procedure follows in which the recovered penetration is adjusted until the calculated mix stiffness differs ±10 MPa from the derived value.

Once the binder properties have been determined, the sub-routine PONOS then calculates the design stiffness of the bituminous layers based on design temperatures of 1.92 and 1.47 times average annual

air temperature for fatigue and permanent deformation respectively and loading times derived from the average speed of the commercial vehicles.

Stage C

This stage assesses the original fatigue and deformation life of the pavement and determines the overlay thickness, if required. The fatigue damage which has already occurred is taken as:

$$\text{Fatigue damage} = \frac{N_p}{N_{of}} \qquad (8.5)$$

where N_p and N_{of} in msa are past traffic and calculated original fatigue life of the existing pavement.

Overlay is required if fatigue damage is less than 0.5 and the remaining fatigue life is less than the future life, otherwise, reconstruction is recommended.

If the remaining fatigue life is less than future traffic, then the design fatigue life of the overlaid pavement, N_{ov} is derived from Miner's rule in which the total damage must be less than or equal to one.

$$\frac{N_p}{N_o} + \frac{N_f}{N_{ov}} = 1 \qquad (8.6)$$

or

$$N_{ov} = \frac{N_f}{(1 - N_p/N_{of})} \qquad (8.7)$$

Using the design fatigue life, N_{ov}, maximum allowable tensile strain (ε_t) at the bituminous layers is determined using equation (8.8) (63).

$$\log \varepsilon_t = \frac{14.39 \log V_B + 24.2 \log SP_i - 46.06 - \log N_{ov}}{5.13 \log V_B + 8.63 \log SP_i - 15.8} \qquad (8.8)$$

where ε_t is the maximum allowable tensile strain ($\mu\varepsilon$)

V_B is the volumetric content of binder (%)

SP_i is the initial softening point of binder (°C)

N_{ov} is the required or design fatigue life of pavement (msa)

With an initial overlay thickness of 100 mm, CHEVRON subroutine then calculates maximum tensile strain at the bottom of bituminous layers which is then compared with the maximum allowable value calculated in equation (8.8). The overlay thickness is adjusted until the criterion is satisfied. The range of overlay thickness allowed in the program is 40 mm - 200 mm.

Using the same back-analysed structure at the lane centre, the original pavement life against permanent deformation is determined by using the vertical strain at the top of the subgrade in the following equation,

$$\varepsilon_z = \frac{451.3}{(N_{op}/f_r)^{0.28}} \qquad (8.9)$$

where ε_z is vertical subgrade strain ($\mu\varepsilon$);

f_r is rut factor ranging from 1.0 to 1.56 depending on types of base material;

N_{op} is original deformation life of the existing pavement(msa).

If the remaining life, which is the difference between the original deformation life and the past traffic, is less than the required future life, overlay will be necessary.

Stage D

This stage, as seen in Figure 8.10, considers overlay thickness design against permanent deformation. Similar to lane centre deflections, deflections in the wheelpath go through stages A and B as described before to backcalculate the layer stiffnesses of the structure using CHEVRON which are then converted to the design

conditions using PONOS. The overlay thickness required for permanent deformation can be determined by comparing the calculated vertical subgrade strain with the allowable subgrade strain for future life, as given in equation (8.9) above, substituting the required future life, N_f, into N_{allow}. Similar to the calculation in Stage C, the overlay thickness is adjusted until the above criterion is satisfied. The resulting design thickness of the overlay is selected to be the larger of the two values.

8.3 DEVELOPMENT OF ANALYTICAL OVERLAY DESIGN PROCEDURE

A detailed description of the new overlay design procedure is given in the following paragraphs, adopting new ideas which have been evolved during the period of the research. As with the majority of analytical procedures already discussed in Section 8.2, the proposed procedure is designed only to strengthen an existing pavement structure suffering conventional distress mechanisms, i.e. fatigue cracking and permanent deformation.

8.3.1 Selection of deflection bowl for analysis

After the FWD deflections have been measured on a test section, they are analysed in detail. Out of the seven deflections measured at each test point, deflection profiles of central deflection, d_1, the seventh deflection, d_7 and deflection difference, d_1-d_4, are plotted along the test section. Figure 8.15(a) shows a typical set of deflection profiles. The above parameters are used to indicate performance responses of the whole pavement structure, subgrade and pavement layers. A deflection bowl, which represents 85 percentile value of the test section based on parameters d_1, d_1-d_4 and d_7, is then selected for detailed analysis using the procedure described in the next section. An 85 percentile value is defined as the value which is greater than 85% of all the measured results.

8.3.2 Stiffness deterioration mechanism of bituminous material under traffic

Under the action of traffic, it is expected that the stiffness of the bituminous layers of a pavement structure will deteriorate from an initial value (E_i), which corresponds to a material in sound condition at the beginning of the pavement life, to a value (E_d) corresponding to complete degradation at the end of its working life. During this period, cracks are progressively developed within the material. The results of this mechanism, where the stiffnesses reduce with increasing numbers of load applications, have been demonstrated in Figure 7.2 of Chapter 7.

When the pavement reaches the end of the working life, it will be highly cracked with its behaviour approaching that of a granular material. In the four-point bending test (refer Chapter 7), it was shown that the residual stiffnesses of the bituminous beams were in the range of 200 to 300 MPa when the crack was completely through the beam section. This range of values is considered to be rather pessimistic but should provide a lower limit of the E_d value for a completely cracked pavement structure. Deflection information on badly cracked pavements is still limited but a structure was evaluated using the BASEM program, for which the bituminous layers were found to have effective stiffnesses of around 500 MPa. Incidentally, Marchionna et al (136) back-analysed a much higher range of E_d values between 1000 to 2000 MPa but suggested that further analysis ought to be carried out to substantiate the above values. Therefore, in the following overlay design procedure, it will be assumed that the value of E_d is 500 MPa. Furthermore, this value is assumed to be independent of temperature variation.

8.3.3 Calculation of pavement remaining life

The following describes the procedures for determining the remaining life of a pavement structure against fatigue cracking and permanent deformation.

(A) Fatigue cracking

As already demonstrated in Chapter 7, the relationship between the reduction in stiffness of a bituminous material and crack growth provides a logical way to determine the remaining life of an in-service pavement. Two procedures have been developed depending on the condition of the pavement, namely, Procedure 's' and Procedure 'c'. Procedure 's' applies to pavements in a sound condition whereas Procedure 'c' applies to partially cracked pavements. When the stiffness ratio between the wheelpath and lane centre is greater than 0.9, the pavement is taken to be in sound condition otherwise it is said to be cracked. The choice of the ratio of 0.9 is arbitrary to allow for variation of compaction effort across the carriageway during construction but further justification will be required to substantiate this value. One possible way is to compare the back-analysed stiffnesses at the lane centre and wheelpath locations on pavements with good condition.

Steps described as follows outline the mechanisms of the two procedures:

(a) Determine the stiffness of each layer at the wheelpath and lane centre locations using the PADAL program.

(b) Adjust the stiffnesses of the bituminous layers to the design conditions for fatigue cracking and permanent deformation (temperature and traffic speed).

(c) Calculate the stiffness ratio (wheelpath/lane centre). If the ratio is greater than 0.9, continue with Procedure 's', otherwise use Procedure 'c'.

Procedure 's':

(i) Taking the structure on the wheelpath, determine the pavement life against fatigue cracking, N_e, of the existing pavement using the horizontal tensile strain calculated at the bottom of the bituminous layer.

(ii) Given the past traffic to-date, N_p, compute the remaining life, N_r of the pavement by taking the difference of (N_e - N_p).

The mechanism of Procedure 's' is illustrated in Figure 8.12.

Procedure 'c':

(i) Calculate the crack length at the bottom of the bituminous layer of the wheelpath structure using the procedure already shown in Figure 7.12 of Chapter 7.

(ii) Split the bituminous layer into two sub-layers, the sound upper sub-layer and the cracked lower sub-layer. Assign the stiffness of the upper sub-layer as that of the lane centre and 500 MPa to the cracked lower sub-layer respectively.

(iii) Compute the failure life based on the horizontal tensile strain at the bottom of the sound upper sub-layer. The computed failure life is the remaining life of the pavement against fatigue cracking.

The advantage of Procedure 'c' is that it does not require the past traffic to compute the remaining life since the damage caused by the traffic loading has been included, by reducing the thickness of the bituminous layer.* However, it is noted that Procedure 'c' is still untried at the time of the writing. But,

* As for permanent deformation, information on past traffic is still required.

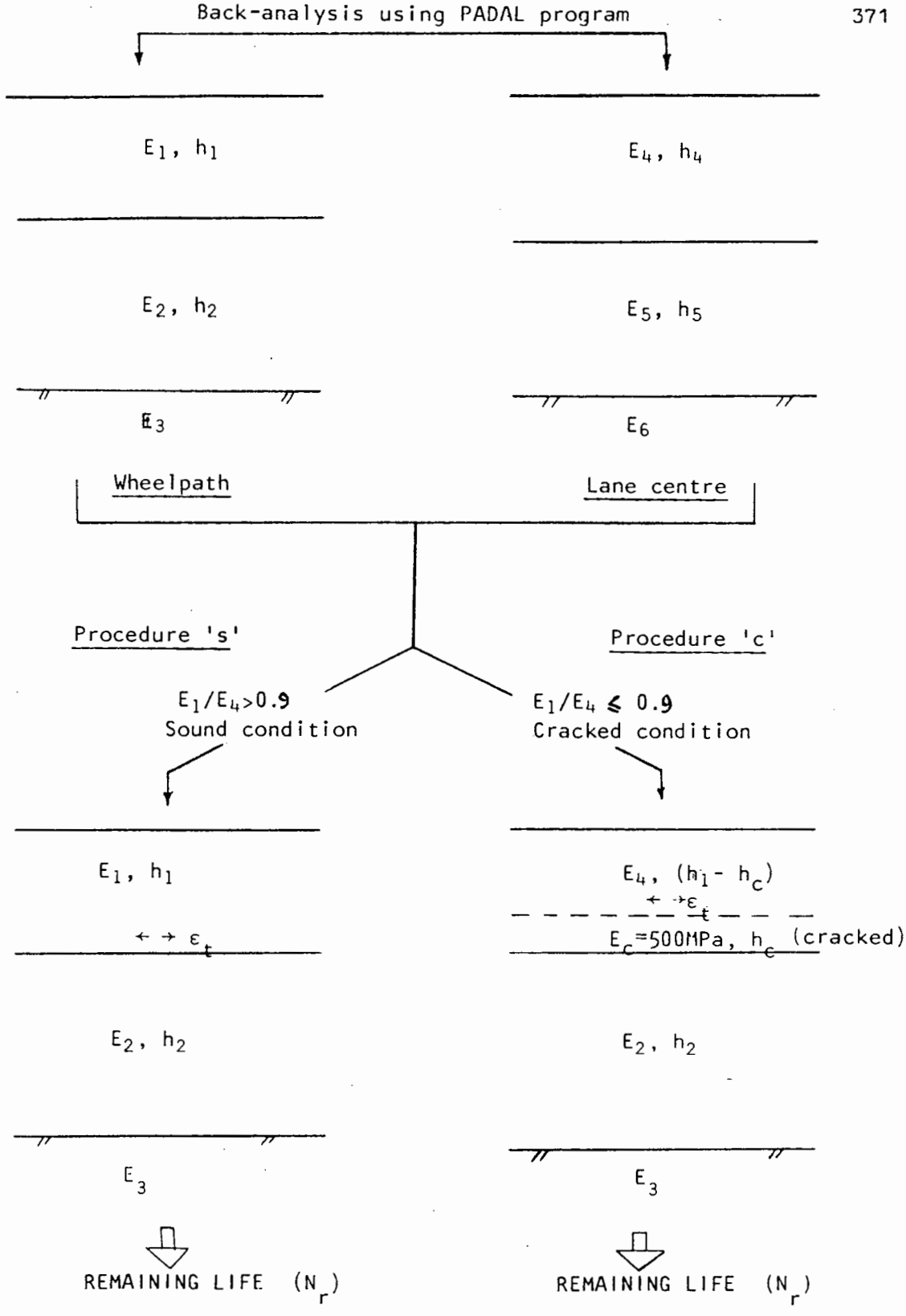

FIG. 8.12 PROCEDURES OF CALCULATING REMAINING LIFE OF PAVEMENTS AGAINST FATIGUE CRACKING

the idea behind its formulation should provide a logical way in determining the remaining life of a pavement against fatigue cracking, It is interesting to observe that similar procedures have also been proposed by Marchionna et al (136). The mechanism of Procedure 'c' is also illustrated in Figure 8.12.

(B) Permanent deformation

The original life of the existing pavement against permanent deformation is evaluated by computing the vertical compressive strain at the top of subgrade layer for the structure in the lane centre (undamaged) location. the remaining life is taken to be the difference between the original life and past traffic. this procedure is mainly based on the proposal in DEMOD (Section 8.2.4).

Finally, the remaining life of the existing pavement is evaluated as the lesser value of the lives for fatigue cracking and permanent deformation.

8.3.4 Calculation of overlay thickness

As with the DEMOD program (refer Section 8.2), the proposed overlay design procedure requires the use of two computer programs, namely, BISTRO which is responsible for the calculation of stresses, strains, and deflections and PONOS which is responsible for determining the elastic stiffnesses of the bituminous materials. Figure 8.13 shows a simplified flow chart of the proposed procedure.

The essential input data include:

(a) Two sets of FWD deflection bowls, measured at wheelpath and lane centre locations;

(b) Layer thicknesses taken from core specimens at wheelpath and lane centre locations;

(c) Past traffic;

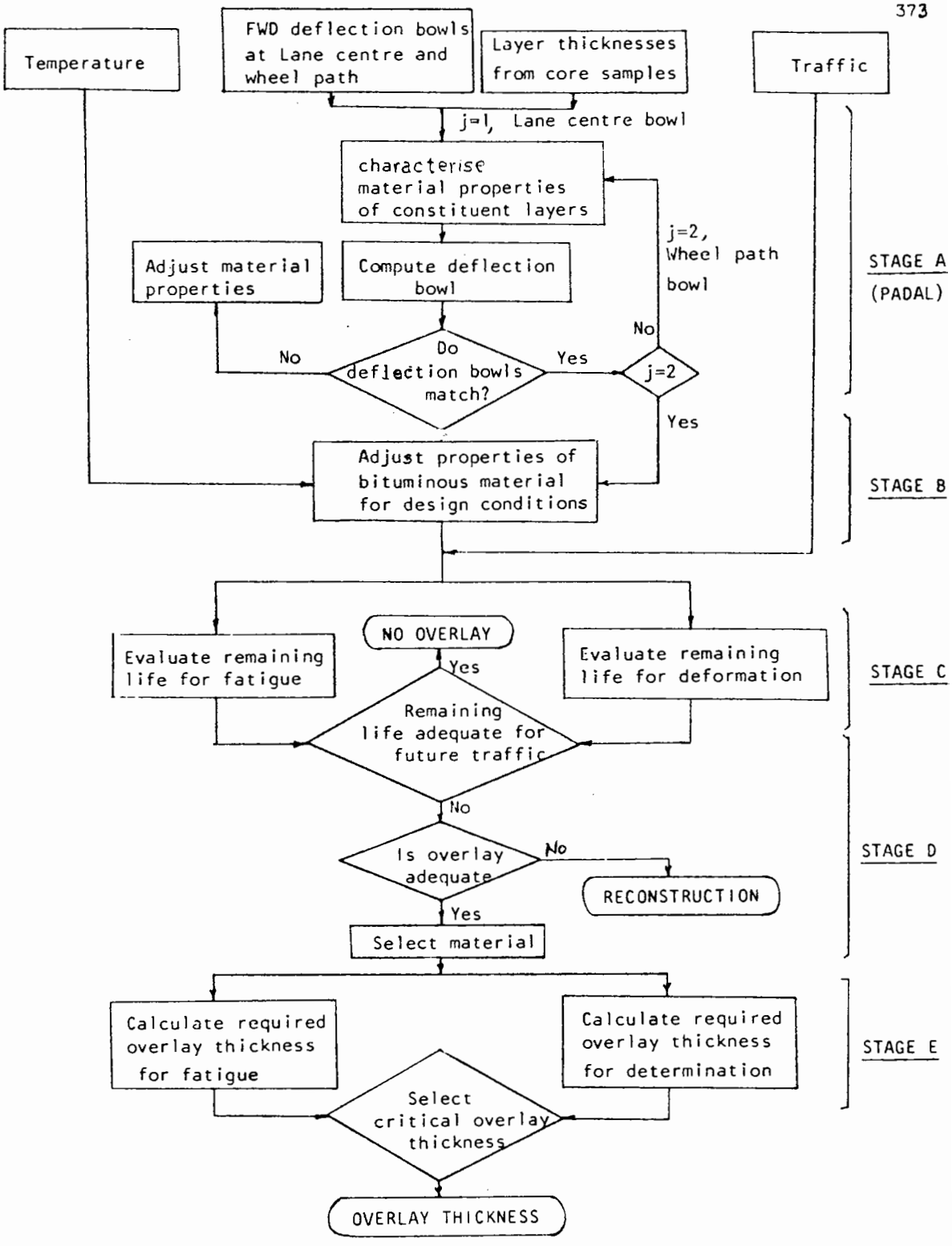

FIG. 8.13 PROCEDURE FOR STRUCTURAL EVALUATION AND OVERLAY DESIGN OF FLEXIBLE PAVEMENTS

(d) Pavement temperature with depth at the time of the deflection survey.

As demonstrated in Figure 8.13, the procedure is carried out in four stages, i.e. Stages A, B, C and D, and each stage is summarised below:

Stage A

This is the back-analysis stage. The stiffnesses of the pavement structure at the wheelpath are back-analysed using the PADAL program (refer Chapter 4 for detailed procedure). A similar calculation is also performed for the lane centre location.

Stage B

This stage adjusts the back-analysed stiffnesses of the bituminous material to allow for differences between site testing temperature and loading time of the FWD and the temperature and loading time for the design condition using PONOS. The loading time of the FWD is taken to be equivalent to a vehicle speed of 30 km/hr. Design temperatures are taken as 1.92 and 1.47 times the annual air temperature for fatigue cracking and permanent deformation respectively. The technique of adjustment is based on Brunton's work (63) on the design of new pavements.

Stage C

This stage estimates the remaining life of the existing pavement. Section 8.3.3 describes full details of the procedure both for fatigue cracking and permanent deformation respectively.

Stage D

After the remaining life of the existing pavement has been evaluated, the next step is to determine the overlay thickness, if required. For the sake of clarity, the calculations of overlay thickness are described separately for fatigue cracking and permanent deformation.

Fatigue cracking:

Table 8.4 shows the criteria which are required for overlay design. As seen in the table, the existing pavement life to the critical condition (or critical life) is determined using the following expression developed by Brunton et al (137). The critical life is defined as the life of the pavement corresponding to a rut depth of 10 mm or first sign of surface cracking (105).

$$\log N_c = 15.8 \log \varepsilon_t - 46.82 - (5.13 \log \varepsilon_t - 14.39) \log V_B - (8.63 \log \varepsilon_t - 24.2) \log SP_i \qquad (8.10)$$

where the parameters have been explained in equation (8.8).

Equation (8.10) has been developed to allow cracks to propagate partially through the bituminous material, either from the top surface downwards or from the bottom of the layer upwards.

Table 8.4 summarises the criteria to decide whether an overlay is necessary. As seen in the table, four points are demonstrated, which are,

(a) No overlay will be required to the existing pavement if the remaining life is greater than the required future traffic.

(b) When the remaining life is less than the critical life but greater than the required future traffic as indicated in case 1 from Table 8.4, nominal thickness (e.g. 40 mm wearing course) of overlay is recommended to protect the existing pavement against further deterioration.

(c) If the remaining life is less than the future traffic requirement, in cases 2 and 3 of Table 8.4, the existing pavement should be overlaid with thicknesses computed using the procedure described below.

(d) Reconstruction on parts or whole of the road section should be considered for reasons of either insufficient clearance for

Table 8.4 Criteria for Overlay Design

Distress type	No Overlay	Overlay	Reconstruction
Fatigue cracking	$N_r > N_c$ and $N_r > N_f$	Case 1: $N_c > N_r \geq N_f$ Case 2: $N_r \leq N_f$ and $(E_e/E_i) < \frac{1}{2}$ Case 3: $N_r \leq N_f$ and $(E_e/E_i) \geq \frac{1}{2}$	Insufficient clearance for normal overlay or Problems in the foundation layers
Permanent deformation	$N_r > N_f$	$N_r \leq N_f$	

where N_p is the past traffic to-date.

N_F is the allowable pavement life to failure condition.

N_c is the allowable pavement life to critical condition.

N_r is the remaining life ($= N_F - N_p$).

N_f is the required future life.

E_e and E_i are effective and initial elastic stiffnesses of bituminous material.

normal overlay (e.g. clearance beneath overhead bridges), or problems in foundation layers.

If overlay is required against fatigue cracking, then the design fatigue life of the overlaid pavement, N_{ov}, is derived from Miner's rule, in which total damage is equal to one.

$$N_f/N_{ov} = 1 - \text{fatigue damage} \quad (8.11)$$

or $$N_{ov} = N_f/(1 - \text{fatigue damage}) \quad (8.12)$$

where, depending on the condition of the existing pavement,

$$\text{fatigue damage} = N_p/N_e \quad \text{(Procedure 's')} \quad (8.13)$$

or $$\text{fatigue damage} = 1 - N_r/N_e \quad \text{(Procedure 'c')} \quad (8.14)$$

where N_f is the required future traffic (msa);

N_p is the past traffic (msa);

N_e is the fatigue life of the existing pavement (msa) determined in Section 8.3.3;

N_r is the remaining life of the existing pavement (msa).

Using the design fatigue life, N_{ov}, a maximum allowable tensile strain (ε_t) of the bituminous layer to the failure condition is determined using equation (8.15) (133),

$$\log \varepsilon_t = \frac{14.39 \log V_B + 24.2 \log SP_i - 46.06 - \log N_{ov}}{5.13 \log V_B + 8.63 \log SP_i - 15.8} \quad (8.15)$$

And to the critical condition,

$$\log \varepsilon_t = \frac{14.39 \log V_B + 24.2 \log SP_i - 46.82 - \log N_{ov}}{5.13 \log V_B + 8.63 \log SP_i - 15.8} \quad (8.16)$$

where the parameters have already been defined in equation (8.8).

The ratio of the effective elastic stiffnesses of the bituminous material in the wheelpath and in the lane centre is next to be calculated. If the ratio is less than 0.5, then, in subsequent calculation of overlay thickness, the effective stiffness of the whole bituminous layer in the wheelpath is downgraded to a value of

500 MPa. This is to allow for further deterioration of the existing bituminous layers under traffic after they have been overlaid. With an initial thickness of overlay, the horizontal tensile strain at the bottom of the overlay is computed, which is then compared with the allowable value calculated either in equation (8.15) or in equation (8.16) depending on whether the design is to failure or critical condition.. The overlay thickness is adjusted until the computed tensile strain is equal to the allowable value. If the stiffness ratio is greater than or equal to 0.5, the bituminous roadbase layer is split up into both sound and cracked portions. the effective stiffness originally determined in the lane centre location is assigned to the sound part of the roadbase whereas the effective stiffness for the cracked portion is taken to be 500 MPa. With an initial thickness of overlay, the horizontal tensile strain is calculated at the bottom of the sound part of the roadbase layer. Again, this computed value of tensile strain is compared with the allowable value determined either in equation (8.15) or in equation (8.16) to failure or critical condition. The overlay thickness is adjusted until the computed and allowable strains are the same.

Permanent deformation:

If the remaining life against permanent deformation is less than the required future traffic, an overlay is required. The overlay thickness corresponding to either failure or critical condition of the overlaid pavement can be determined using back-analysed elastic stiffnesses of the structure at the wheelpath location. This is carried out by comparing the calculated vertical subgrade strain with the allowable subgrade strain as given in equation (8.17) or equation (8.18) (137) either to failure or critical condition, as follows:

$$\varepsilon_z = \frac{451.3}{(N_{ov}/f_r)^{0.28}} \qquad (8.17)$$

$$\varepsilon_z = \frac{250}{(N_{ov}/f_r)^{0.27}} \qquad (8.18)$$

where the parameter f_r has been defined in equation (8.9).

Finally, the resulting design thickness of the overlay is selected to be the larger value of fatigue cracking and permanent deformation.

However, if the existing pavement is to be reconstructed , after the removal of the damaged layers, the design of the reconstruction follows the same principle as for a new pavement, the procedure of which is fully described separately in the Nottingham Design Manual (133).

8.4 EXAMPLE OF PAVEMENT EVALUATION AND STRENGTHENING

The following illustrates an example of the pavement evaluation and overlay design procedure in which the writer has been involved. The exercise was carried out during the early part of the research and, hence, some of the later development discussed above had not been included.

8.4.1 The site

In July 1985, an investigation was carried out by SWK Pavement Engineering for Leicestershire County Council (L.C.C.). The section was a 900 m length single carriageway on the A512, east of junction 23 of the M1 motorway. The existing structure consisted of approximately 120 mm of bituminous material, 240 mm of wet mix base and 160 mm of granular sub-base overlying a clay subgrade. The design is required by L.C.C. to cater for a future traffic of 7.5 msa.

8.4.2 Fieldwork

(a) Site investigation: The visual condition of the existing road surface was generally badly cracked and rutted. An investigation was undertaken by L.C.C. which included the excavation of seven trial pits and five cored specimens between 1983 and 1985. The

records showed that free water was noted in the wet mix layer and that the clay subgrade had an average value of CBR of 6.5%. Layer thicknesses obtained from the investigations are summarised in Figures 8.14 (a) and (b).

(b) F.W.D. survey: The section was tested using the FWD at 30 m intervals along the nearside wheelpaths and at 60 m intervals along the lane centre in both directions. Air and pavement temperatures at different depths of 50, 100, and 150 mm were recorded during the day and are shown in Table 8.5.

The results of the FWD survey are given in Table 8.6. The test location is denoted by the line number followed by the position number. Lines 1 and 3 are the Eastbound and Westbound nearside wheelpaths respectively whilst lines 2 and 4 are Eastbound and Westbound lane centres. Test position 1 is at Ch. 0 m with the following test positions at 30 m intervals to position 31 at Ch. 900 m. The deflection d_1 is measured at the load centre and d_2, d_3, d_4, d_5, d_6, d_7, are measured at offset distances of 300, 600, 900, 1200, 1500, 1800 mm respectively. Figures 8.15 (a) and (b) present the deflection profiles along the length of the section using deflections d_1 and d_7, and the deflection difference (d_1 - d_4). These parameters are indicators of the response of the whole pavement structure, the subgrade and the upper pavement layers respectively and have been normalised to a standard contact pressure of 650 kPa. As can be seen in the figure, the d_7 profile is fairly constant indicating that the stiffness of the subgrade is reasonably uniform. In contrast, (d_1 - d_4) shows substantial variation in the condition of the upper pavement layers including the wet mix.

TABLE 8.5 AIR AND PAVEMENT TEMPERATURES, A512 ASHBY ROAD, LOUGHBOROUGH
8th JULY 1985

Location	Depth in pavement (mm)	Pavement Temperature (°C)				
		Time				
		1000	1200	1300	1400	1500
Chainage 000 m	50	24	29	32	36	-
	100	23	28	30	33	-
	150	-	26	27	29	-
Chainage 450 m	50	27	30	-	36	37
	100	24	26	-	30	31
	150		25	-	29	30
Chainage 900 m	50	28	-	35	-	37
	100	24	-	29	-	31
	135	-	-	28	-	30

Air Temperature am 23°C
pm 24°C

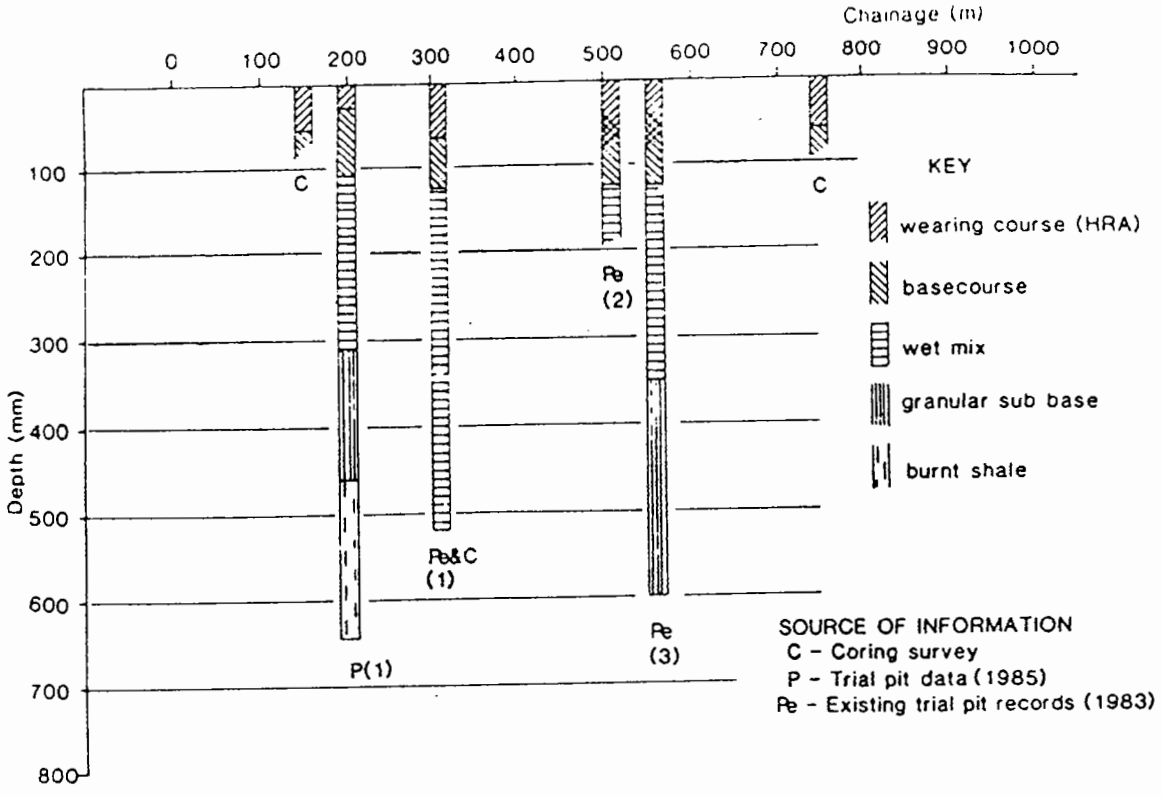

(a) Eastbound carriageway

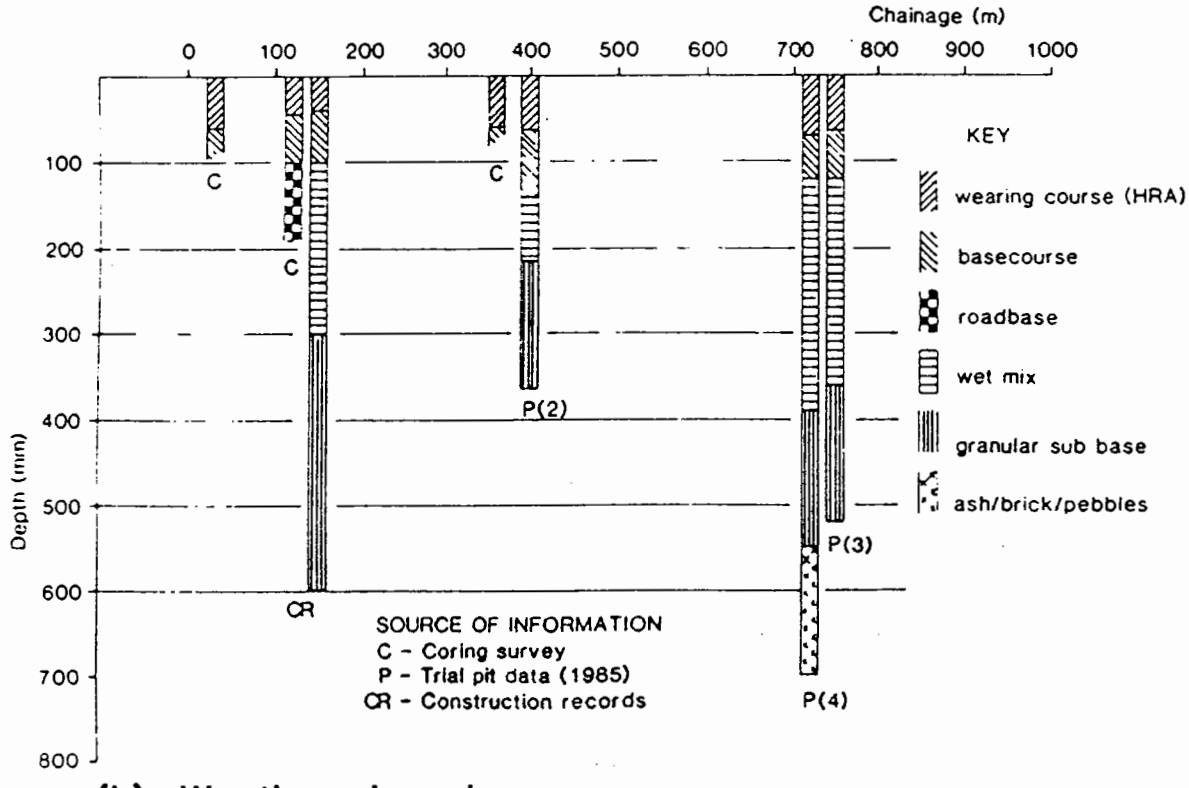

(b) Westbound carriageway

FIG. 8.14 CONSTRUCTION DETAILS OF A512 ASHBY ROAD

TABLE 8.6
A512 ASHBY ROAD LOUGHBOROUGH

FWD pressure=650kN/m^2 Radius of platen=150mm

Test locations	Measured deflections ($m*10^{-6}$)							
	d1	d2	d3	d4	d5	d6	d7	(d1-d4)
1.31	758	459	230	135	86	63	50	622
1.30	795	486	235	133	90	66	56	663
1.29	534	322	155	86	57	44	33	447
1.28	815	493	243	140	92	66	53	675
1.27	1032	705	353	175	103	77	63	857
1.26*	1001	640	331	187	130	97	79	814*
1.25	711	479	270	156	103	80	64	554
1.24	543	399	252	158	102	72	57	385
1.23	1043	698	388	217	145	110	90	825
1.22	1048	689	407	263	182	136	111	785
1.21	1043	689	385	245	168	127	106	798
1.20	394	174	44	15	18	18	16	379
1.19	958	611	299	178	120	91	72	780
1.18	846	503	228	120	74	58	44	725
1.17	841	547	244	117	69	53	46	724
1.16	835	459	193	101	70	52	43	734
1.15	614	386	192	95	55	40	36	520
1.14	523	350	205	120	75	53	42	403
1.13	371	275	182	119	74	49	34	252
1.12	649	512	323	183	95	51	38	466
1.11	1246	808	404	201	97	56	46	1045
1.10	625	407	234	133	77	55	47	492
1.09	375	263	165	100	60	38	30	274
1.08	797	473	225	118	72	53	45	680
1.07	810	491	226	113	70	53	43	698
1.06	881	562	245	111	65	49	40	770
1.05	504	289	152	89	55	37	30	416
1.04	275	182	123	84	57	42	30	191
1.03	359	255	160	100	62	41	31	259
1.02	485	317	186	113	73	53	41	372
1.01	567	350	200	123	79	56	47	444
2.01	389	202	136	94	65	47	43	295
2.03	332	217	136	86	55	38	30	245
2.05	487	263	139	81	51	37	29	406
2.07	625	376	185	99	61	41	35	525
2.09	381	256	151	87	48	34	28	294
2.11	1294	788	404	195	100	60	48	1099
2.13	382	270	178	123	75	52	30	259

Cont'd

TABLE 8.6 (Cont'd)
A512 ASHBY ROAD LOUGHBOROUGH

Tyre pressure=650kN/m^2 Radius of platen 150mm

Test locations	Measured deflections (m*10^{-6})							
	d1	d2	d3	d4	d5	d6	d7	(d1-d4)
2.15	480	302	163	91	50	39	27	389
2.17	564	355	178	97	65	49	40	467
2.19	682	468	232	143	107	84	70	539
2.21	738	523	298	191	137	107	91	547
2.23	958	622	342	214	147	112	87	744
2.25	687	488	266	156	98	73	61	530
2.27	739	466	227	126	85	64	50	613
2.29	450	270	133	76	53	41	31	375
2.31	500	307	152	91	63	48	39	409
3.31	676	417	195	113	78	60	51	563
3.30	662	439	213	117	75	55	44	546
3.29	836	523	230	117	77	56	45	719
3.28	1097	698	290	143	89	68	57	954
3.27	782	516	246	129	85	68	55	653
3.26	995	652	312	180	128	97	81	816
3.25*	910	620	329	182	123	91	74*	728
3.24	604	395	214	128	86	64	51	476
3.23*	1009*	675	386	232	154	111	90	777
3.22	1088	761	410	242	164	121	97	846
3.21	1015	690	379	230	161	123	104	785
3.20	769	507	273	164	114	89	74	604
3.19	963	585	275	146	98	79	68	817
3.18	749	478	227	124	86	66	54	625
3.17	792	456	197	96	62	50	43	696
3.16	731	420	181	91	57	42	37	640
3.15	811	439	181	95	64	48	40	716
3.14	881	498	211	110	68	49	40	772
3.13	1186	745	353	166	91	56	42	1020
3.12	1039	648	321	149	59	24	18	890
3.11	742	497	270	139	65	35	24	603
3.10	1123	698	302	137	73	53	41	986
3.09	915	517	202	92	56	43	35	823
3.08	332	201	141	94	57	36	26	238
3.07	646	399	232	131	75	48	35	515
3.06	397	273	180	112	65	40	28	284
3.05	429	283	182	112	66	42	31	317
3.04	520	295	181	111	67	46	37	409

Cont'd

TABLE 8.6 (Cont'd)
A512 ASHBY ROAD LOUGHBOROUGH

FWD pressure=650kN/m^2 Radius of platen=150mm

Test locations	Measured deflections ($m*10^{-6}$)							
	d1	d2	d3	d4	d5	d6	d7	(d1-d4)
3.03	524	319	190	111	66	45	35	413
3.02	1388	831	381	183	97	66	53	1205
3.01	957	569	285	151	86	48	48	806
4.01	592	250	161	105	71	50	40	488
4.03	664	407	234	130	70	48	39	534
4.05	524	331	199	116	67	44	32	408
4.07	592	392	235	135	73	46	32	456
4.09	465	339	178	97	54	41	33	368
4.11	623	411	243	136	72	36	21	487
4.13	908	593	296	153	81	51	38	756
4.15	599	331	142	72	46	39	32	527
4.17	591	345	174	102	67	49	39	489
4.19	725	441	234	143	93	73	60	582
4.21	717	513	310	202	140	106	88	515
4.23	845	616	400	266	173	118	90	579
4.25	791	521	281	170	113	84	67	620
4.27	890	565	260	133	85	67	55	757
4.29	574	343	171	102	70	51	40	472
4.31	452	293	161	100	68	51	42	352
Statistics summary								
Maximum value	1388						111	1205
Minimum value	275						16	191
50-percentile	725						43	563
85-percentile(*)	1009						74	814

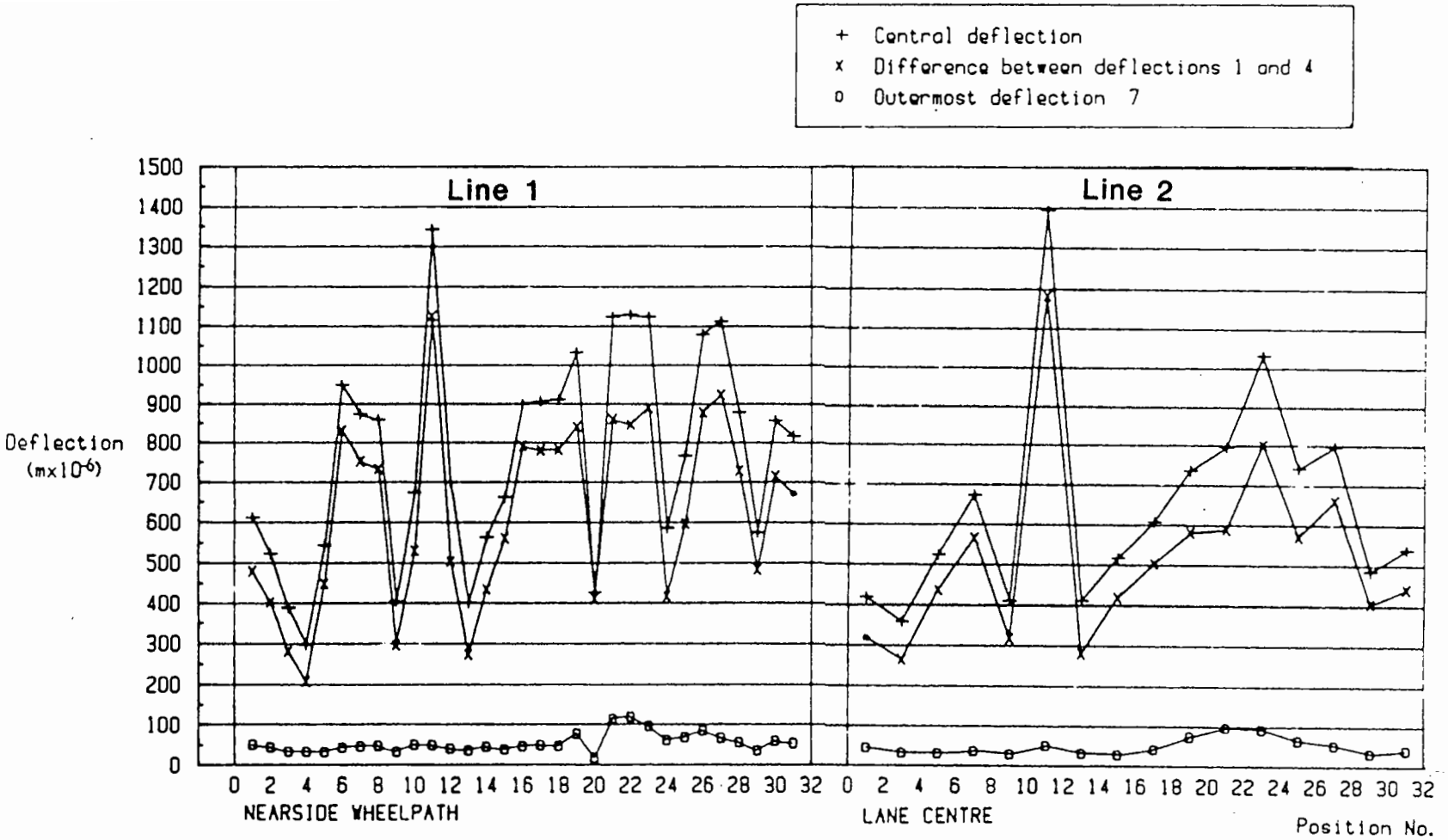

FIG. 8.15 (a) EASTBOUND FWD DEFLECTION PROFILES OF A512 ASHBY ROAD

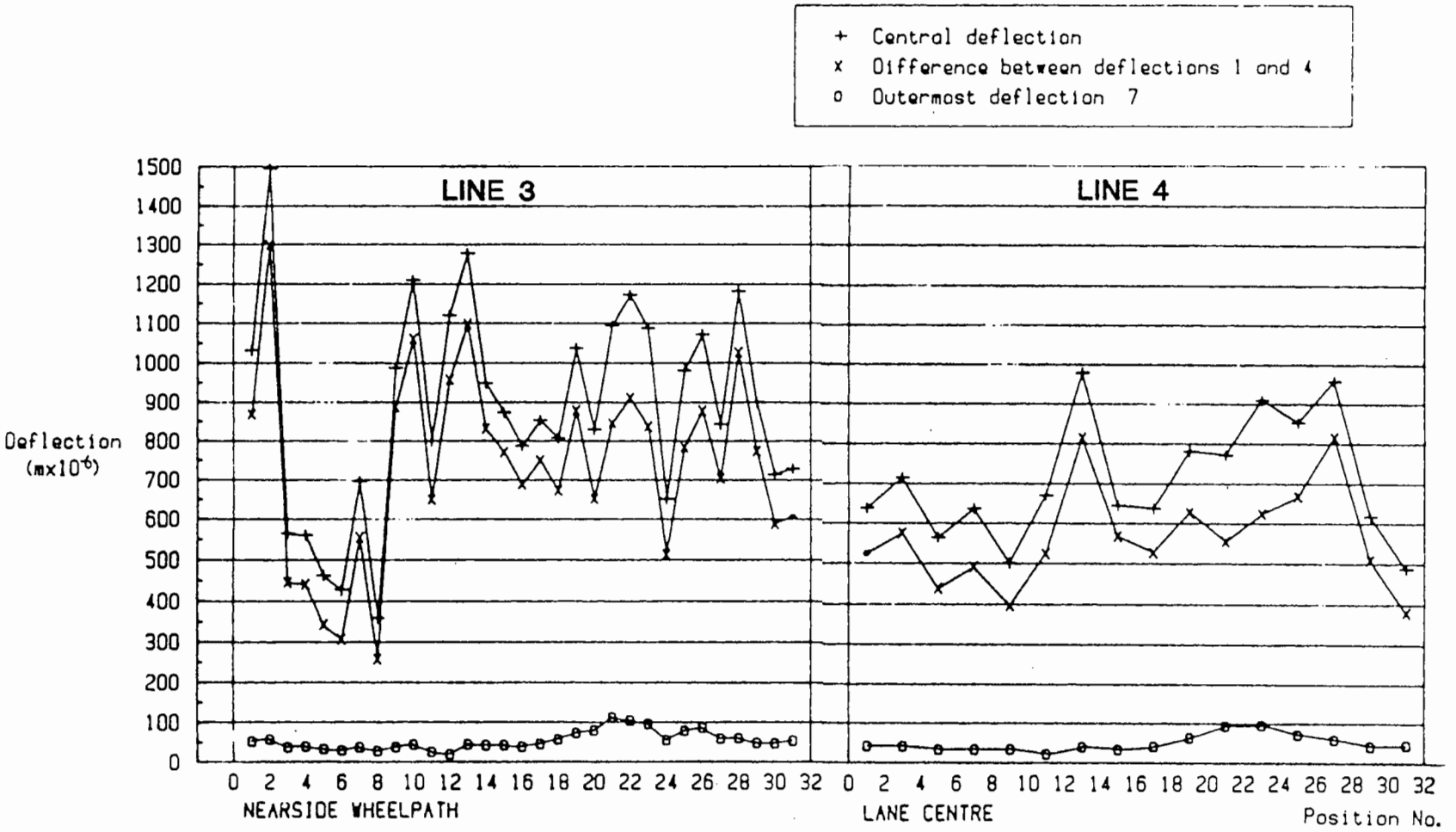

FIG. 8.15(b) WESTBOUND FWD DEFLECTION PROFILES OF A512 ASHBY ROAD

8.4.3 Analysis of deflection data

Five points were analysed using the BASEM program. Details of the points are given in Table 8.7 and they are at the following positions:

Point A - Position 26 at Ch. 750 m of Westbound wheelpath

Point B - Position 26 at Ch. 750 m of Eastbound wheelpath

Point C - Position 25 at Ch. 720 m of Westbound lane centre

Point D - Position 11 at Ch. 300 m of Eastbound wheelpath

Point E - Position 5 at Ch. 120 m of Westbound wheelpath

Points A, B, and C were selected because their measured deflections most closely matched those given by the 85th percentile value for d_1, $(d_1 - d_4)$, and d_7 for the wheelpaths and lane centres of both westbound and eastbound carriageways respectively. Point D was selected as a particularly weak spot, whilst point E was in a good section which had been reconstructed when the road was widened. The thicknesses given in Table 8.7 were taken from the nearest trial pit or core data shown in Figures 8.14 (a) and (b). The analysis of point A found that the elastic stiffness of the wet mix layer was low (E = 35 MPa in Table 8.8). Therefore, the remaining analyses on other points were carried out with the wet mix layer sub-divided into two layers of equal thickness. The results of the calculation are given in Table 8.8.

The analyses confirmed the observations that the bituminous layer was in very poor condition with stiffnesses varying from only 850 to 2250 MPa for points A, B and D. Normally, a stiffness value closer to 5000 MPa would be expected depending on mix details, compaction and temperature. For point C, somewhat less damage had occurred, as expected, as it was in the lane centre. The reconstructed section

TABLE 8.7 DETAILS OF TEST POSITIONS ANALYSED

	A	B	C	D	E
	Position 26 Westbound Wheel path	Position 26 Eastbound Wheel path	Position 25 Westbound Lane centre	Position 11 Eastbound Wheel path	Position 5 Westbound Wheel path
Contact Pressure (kPa)	651	650	660	637	676
Measured deflections (mm x 10^{-6})					
δ_1	997	1001	803	1221	446
δ_2	653	640	529	792	294
δ_3	312	331	285	396	189
δ_4	180	187	173	197	116
δ_5	126	130	115	95	69
δ_6	97	97	85	55	44
δ_7	81	79	68	45	32
layer thicknesses (mm)					
Bituminous layers	120 and 130	120	120	125	100
Wet mix	240	240	240	200	200
Sub-base	160	160	160	160	300

TABLE 8.8 RESULTS OF BACK ANALYSIS USING BASEM COMPUTER PROGRAM

	Calculated Elastic Stiffness E (MPa)						
	A *1	A *1	A *2	B	C	D	E
Bituminous layer	2250	1250	1500	1300	2840	850	3150
Wet mix layer 1	35	60	60	130	75	130	860
layer 2		50	50	40	140	25	250
Granular Sub-base	100	100	100	100	100	100	100
Subgrade layer 1	85	71	70	64	62	36	80
2		77	76	73	76	62	121
3		82	82	81	91	99	168
4		87	87	90	108	160	237
5		95	95	102	135	292	371

Note: *1 130mm bituminous layer assumed
*2 120mm bituminous layer assumed

analysed at point E gave a high stiffness value of 3150 MPa, which was much closer to a typical value.

The wet mix layer was weak with elastic stiffnesses less than 100 MPa. These stiffnesses were generally less than the granular sub-base. However, in the reconstructed section, where drainage had been provided, the elastic stiffnesses mobilised in the wet-mix were much improved at 250 and 860 MPa.

The analysis showed that the subgrade was fairly uniform with a typical value of stiffness at the formation level of between 60 and 70 MPa, which agreed with the averaged CBR value of 6.5% measured in the trial pits. A lower value was found for point D, the weak spot, but in all cases the stiffness increased with depth, as expected, due to the non-linear characteristics of a clay soil.

8.4.4 Design of strengthened pavement

The design life of the strengthened pavement for future traffic was to be 7.5 msa. The following conditions were also assumed in the design:

(a) Average annual air temperature = 9.5°C

(b) Average speed of commercial vehicles = 45 km/hr

(c) Subgrade stiffness = 68 MPa

(d) Thickness of HRA wearing course = 40 mm

Since the condition of the bituminous and wet mix layers was poor, it was recommended that these layers should be removed and the pavement reconstructed. To comply with the recommendations of LR 1132 (105), the thickness of the sub-base layer had to be increased to 225 mm from the original 160 mm. This left a maximum thickness of 255 mm for other layers whilst keeping the overall depth of construction the same.

Two designs were analysed using a conventional HRA roadbase and a modified DBM roadbase material developed at Nottingham (63). Mix details of the bituminous materials are given in Table 8.9. Designs were performed using the BISTRO computer program to calculate the critical strains induced by the design loading for three thicknesses, 180, 220, and 260 mm. The critical strains were the horizontal tensile strain at the bottom of the bituminous roadbase layer, for design against fatigue cracking, and the vertical strain at the top of the subgrade layer, for design against permanent deformation. The maximum allowable strains were calculated using equations (8.4) and (8.10) for critical conditions. The critical strains and the maximum allowable values are shown in Table 8.10. Permanent deformation was found to be critical in both cases. To satisfy the strain criteria, the required thicknesses were interpolated to 215 mm for the HRA roadbase and 180 mm for the modified DBM roadbase. This gave a total thickness of 255 mm for the HRA and 215 mm for the modified DBM roadbase when the 40 mm wearing course was included.

Instead of reconstruction, the possibility of overlaying the existing structure was also considered. In carrying out the design calculation, the effective stiffness of the existing bituminous layers was assigned a low value of 500 MPa. This resulted in an overlay with a total thickness of 215 mm which consists of 40 mm of wearing course and 175 mm of HRA roadbase. The calculation was similar to the above procedure for the reconstructed structure. The critical strains were calculated at the bottom of the overlay and the top of the subgrade layer respectively. However, this solution was not recommended because of the effect on the finished road levels and construction problems. Besides this, the presence of very weak wet mix and the possibility of reflection cracking from the badly cracked existing bituminous material gave cause for concern.

TABLE 8.9 MIX DETAILS USED IN DESIGN

Parameter	HRA wearing course	HRA base	Modified DBM base
Grade of Bitumen	50 pen	50 pen	50 pen
Binder content (%)	7.9	5.7	4.4
Void content (%)	4.0	5.0	6.0
Elastic stiffness for deformation (MPa)	4960	7990	10710
Elastic stiffness for fatigue (MPa)	3540	5900	8080

TABLE 8.10 CALCULATED STRAINS

	Maximum allowable strain (microstrain)		Calculated strain (microstrain)					
	ϵ_z	ϵ_t	ϵ_z			ϵ_t		
			Base thickness (mm)			Base thickness (mm)		
			180	220	260	180	220	260
HRA base	145	99	187	144	114	87	69	57
Modified DBM base	162	78	166	126	99	71	55	44

where ϵ_z is the vertical compressive strain at the top of the subgrade

and ϵ_t is the horizontal tensile strain at the bottom of the asphalt layer

40mm HRA Wearing course	40mm HRA Wearing course
60mm HRA Basecourse	75mm Modified DBM Base Maximum aggregate size 20mm
160mm HRA Base	110mm Modified DBM Base Maximum aggregate size 40mm
225mm Granular Sub-base	225mm Granular Sub-base
Subgrade	Subgrade

FIG.8.16 DESIGN RECOMMENDATIONS
A512 ASHBY ROAD, LOUGHBOROUGH

TABLE 8.11 TARGET AGGREGATE GRADINGS FOR MODIFIED DBM BASE LAYERS

Sieve size	% passing	
	Upper Layer 75 mm Modified DBM base	Lower Layer 110 mm Modified DBM base
37.5 mm		100
28		91 ± 7
20	100	81 ± 7
14	90 ± 7	71 ± 7
6.3	69 ± 6	53 ± 6
3.35	56 ± 5	42 ± 5
1.18	37 ± 4	27 ± 4
.6	27 ± 4	20 ± 4
.3	19 ± 3	14 ± 3
.075	5 ± 2	5 ± 2

8.4.5 Recommendation for the strengthened pavement

The final alternative designs are presented in Figure 8.16. In the HRA design, the top 60 mm of the structural layer can be taken as basecourse. For the modified DBM design, it was recommended that the layer be divided into two, the upper part having 20 mm maximum aggregate size and the lower part 40 mm. The target aggregate gradings are given in Table 8.11. In order to achieve optimum compaction, it is important to meet this grading specification, in particular, the 27% passing 600 micron sieve for the 20 mm maximum aggregate grading and the 27% passing 1.18 mm sieve for the 40 mm maximum aggregate grading (62). It was also recommended that the road drainage be improved during reconstruction.

It is noted that a typical DBM roadbase material has not been considered in the above design since there are problems in achieving good compaction with this type of material and it has poor resistance to fatigue cracking.

8.5 CONCLUSIONS

(1) The review of the literature identifies the majority of overlay design procedures under three main categories, namely, composition analysis, empirical deflection-based and analytical deflection-based procedures. It is concluded that the component analysis method is inappropriate for a routine evaluation and overlay exercise because of the slow operation of carrying out laboratory testing. The empirical overlay design method based on measured deflections is simple to use. However, the main drawback for this method is inflexibility in application. The analytical overlay design procedure is considered to be the best overall since it provides the most comprehensive approach to both evaluation of the existing structural capabilities and the design of pavement overlays. In particular, it can cater for varying

traffic conditions and the procedure can be modified quite simply to incorporate new materials, new environments and other special considerations suca as ageing and drainage variations.

A number of techniques have been observed to minimize the damage to bituminous overlays from reflection cracking but, as yet, no analytical procedure has been proposed for routine overlay design which incorporates a range of material necessary to minimize reflection cracking.

(2) A new method of calculating the remaining life of a bituminous pavement against fatigue cracking has been proposed which includes two procedures, viz, Procedure 's' and Procedure 'c'. Procedure 's' is applicable to sound uncracked pavements whilst Procedure 'c' applies to partially cracked pavements. A stiffness ratio above or below 0.9 between the effective stiffness of the bituminous layer in the wheelpath and the lane centre determines the use of the appropriate procedure. The above procedures thus provide a logical way of determining the remaining life against fatigue cracking.

(3) A new analytical overlay design procedure has been proposed to evaluate the remaining life a bituminous pavement and to design the thickness of a bituminous overlay, which satisfies the criteria of both fatigue cracking and permanent deformation. The criteria for determining whether an overlay is necessary are given in Table 8.4. In the case of reconstructed pavements, the design of reconstruction follows the same procedures as for a new pavement, after removing the damaged layers.

(4) An example demonstrating the use of the principle of pavement evaluation and strengthening of an existing bituminous structure has been given.

CHAPTER 9

CONCLUSIONS

The aim of this research has been to develop analytical procedures for pavement evaluation and overlay design for bituminous pavements, using a computer, which were both realistic and implementable. In this research, the deflection response of the pavement structure has been measured using a FWD which applied an impulse loading to the pavement surface. The device is found to realistically simulate traffic loading conditions in terms of stress level and loading time. The main conclusions of the work are described below.

9.1 ASSESSMENT OF THE FALLING WEIGHT DEFLECTOMETER

In Chapter 2, the capability of the FWD has been assessed in relation to other non-destructive testing devices. The results of the comprehensive literature review demonstrate that the FWD is, on balance, the best device in simulating a moving wheel loading. Other findings of the work are summarised below:

(a) The FWD loading time is found to be in the range of 25 - 40 msec and constant with depth. This is in constrast to the increase of loading time with depth under a the moving wheel. Nonetheless, good correlations of stresses, strains and surface deflections are observed between the FWD and the moving wheel.

(b) The assessment of the Dynatest FWD reveals that the measured deflection is found to be repeatable on stiff pavements but repeatability reduces when used on weaker pavements.

(c) The amplitude of the applied FWD load is influenced by different material properties and compaction levels. Temperature has no noticeable effect on load amplitude. The relationship between the magnitude of contact pressure (or force) and the corresponding surface deflections is not linear but follows a

parabolic shape.

(d) Instrument error of the geophone, unstable support at the tip of the geophone and rocking of slab under the applied load might be the source of error in measured deflections of the FWD. Possible steps to minimize such errors have been proposed.

(e) Increase of temperature affects the FWD deflections between the load and 0.9 m but the deflections from 1.2 m outward are essentially unaffected.

(f) Special investigations on the FWD reveal that it is capable of locating the presence of cracks in a lean concrete roadbase under a bituminous pavement, as well as determining the efficiency of load transfer across the joint of a concrete pavement.

(g) Detailed comparison between the FWD and the Deflectograph has identified a number of significant differences between these two equipments. The FWD, with its more enhanced capabilities and sophistication, is able to obtain more accurate pavement response in order to allow detailed structural evaluation to be carried out using a versatile analytical evaluation procedure. The Deflectograph, however, can be used to monitor a large network of road system in order to identify sections of pavements for further detailed investigation.

9.2 DEVELOPMENT OF ANALYTICAL PAVEMENT EVALUATION PROCEDURES

Chapter 3 describes a careful sensitivity analysis of the influence of material properties on a deflection bowl. In Chapter 4, analytical procedures for pavement evaluation have been developed which incorporate a rational procedure for back-analysing non-linear elastic stiffnesses of the subgrade layer. It can be concluded that:

(a) A comparison between two linear elastic multi-layered computer programs BISTRO and CHEVRON has established that the CHEVRON program produces unrealistic deflections around the loading area,

and hence, the BISTRO program has been selected as an analytical tool for carrying out structural evaluation.

(b) The effect of varying the elastic stiffness of pavement layers modifies the shape of the deflection bowl (from steep gradient to shallow gradient, for instance), while subgrade stiffness variation influences the whole deflection bowl.

(c) The thickness of the roadbase layer, especially if it is lean concrete or bituminous, should be accurately known to avoid serious errors in estimating the elastic stiffness of that layer. On the other hand, accurate thickness of the sub-base layer is not required since it does not influence the deflections significantly.

(d) Analysis of the relationship between layer stiffness and local slope of the deflection bowl indicates a logical pattern. The deflection bowl is found to be influenced progressively from its extremity to the centre by the subgrade through to the total pavement structure.

(e) With the use of influence indices (II), the "best" radial position corresponding to each pavement layer has been identified for both bituminous and concrete structures. These radial positions are found to be sensitive to variations in stiffness and thickness of the pavement layers. The study resulted in a proposal for a rational procedure for determining the position of the FWD geophones in a logical manner.

(f) A rational method of formulating non-linear (or stress-dependent) stiffnesses in the subgrade, the most important layer of a pavement structure, has been developed. The method takes into account the overburden from the pavement layers and the applied stress as well as the position of the water table in the subgrade.

(g) Two computer programs BASEM and BASEMC were first developed to evaluate the in-situ condition of bituminous and concrete structures respectively. After extensive applications, they were found to be sensitive to the initial estimate of layer stiffnesses, which is input into the program at the beginning. As a result of this investigation, these programs were superseded by a new program known as PADAL (PAvement Deflection AnaLysis).

(h) The PADAL program has incorporated the same method of calculating non-linear elastic stiffnesses in the subgrade and the facility to include a rigid layer in the subgrade for back-analysis. Also, it has incorporated improved convergence criteria, limiting the errors in both stiffness and deflection to ensure a unique solution regardless of the initial estimates of layer stiffness. Furthermore, a new algorithm has been proposed to improve the rate of convergence. The program has been formulated to solve both bituminous and concrete pavement structures of up to four layers, including three pavement layers and the subgrade.

(i) The uniqueness of the back-analysed stiffnesses from PADAL has been extensively evaluated using theoretical deflection bowls produced for three- and four-layered bituminous structures. Very good correlations are obtained in all cases except for those structures with thin top layers (e.g. 40 mm). It is observed in the analysis that maximum errors of 2% for all the layer stiffnesses for three-layered structures and 6% for four-layered structures (except the sub-base layer which gave 16%) were obtained. Similar tests were also carried out on four-layered concrete structures and results similar to those for bituminous structures have also been noted.

(j) A set of predictive stiffness equations corresponding to bituminous and concrete structures has been developed using the

multiple regression analysis technique. The R^2 values range from 0.473 to 0.956 for equations corresponding to bituminous structures and, for concrete structures, range from 0.429 to 0.998. However, these equations have not yet been incorporated into the PADAL program for routine analysis, since preliminary checks show that there is no significant improvement in programming efficiency.

(k) The capability of the proposed analytical procedures in practical applications has been evaluated. In the first case, where vertical stresses and strains in the subgrade were measured, it was established that the best agreement with measured values was obtained when non-linear subgrade was considered in the analysis. In the second case, where the elastic stiffnesses were compared, the back-analysed stiffnesses using the PADAL program generally agree well with the laboratory values. The best comparison is observed for the bituminous material where the error of prediction was about 20%. The correlations with the unbound granular sub-base and clay subgrade are less good, with mean ratios of back-analysed to measured stiffness of 0.58 and 1.35 respectively. From the above analysis, it was established that the PADAL program could be used with reasonable confidence for back-analysing elastic stiffnesses in practical situations.

(l) The dynamic loading produced by the FWD is unlikely to cause resonance in pavement structures since it exerts a broad band of frequencies onto the pavement, instead of a single frequency as produced by the Road Rater. The effect of dynamic loading on elastic stiffnesses, back-analysed by a static analysis program like PADAL, has been found to give errors of between 4 and 10%, which is considered to be acceptable for practical applications. The comparison also indicates that the effect of the inertia of a

pavement structure on the deflection response is not significant. Therefore, the findings have led to the conclusion that a static analysis can be used with confidence to back-analyse the elastic stiffnesses of a pavement structure using the deflection bowl measured by a FWD.

9.3 COMPARISON WITH ANOTHER METHOD FOR PAVEMENT EVALUATION

Chapter 5 describes detailed analysis which has been carried out on the computer program ELMOD, to establish its accuracy in predicting elastic stiffnesses. The results of the analysis have led to the following conclusions:

(a) The review of the ELMOD program gives rise to four observations. First, it is not clear how the ELMOD program formulates the iterative procedure, nor what the convergence criteria are, nor how the non-linear subgrade is incorporated in the iterations. Second, the accuracy of back-analysed elastic stiffnesses is uncertain, since no information is given on the degree of goodness of fit with measured deflection bowls. Third, the ELMOD program treats a four-layered structure as three-layered for back-analysis since layer 2 is assumed to vary with the stiffness of layer 3, the granular sub-base layer, according to a certain fixed relationship. Fourth, the ELMOD program cannot analyse structures with a lean concrete roadbase layer.

(b) Evaluation of the ELMOD program reveals that, for linear subgrade, the ELMOD program can predict the elastic stiffness of the subgrade layer with reasonable accuracy, whereas the stiffness prediction for the bituminous layer is less good and is even worse for the sub-base layer. A similar finding is also recorded for a non-linear subgrade formulation. In general, the prediction of layer stiffnesses for structures with non-linear subgrade is worse than with linear. However, no literature is so

far available to determine how exactly the ELMOD program calculates non-linear subgrade stiffnesses. As far as the sub-base layer is concerned, the study has clearly demonstrated that the ELMOD program is unable to accurately predict the stiffness of this layer. The results are extremely variable and grossly over-predict the correct values by as much as 9 times. Even the mean stiffness is consistently around 2 to 3 times the correct value.

(c) The overall finding from the comparison, based on field data, is that there is a general agreement between ELMOD and PADAL in predicting the elastic stiffnesses of the combined bituminous layer, with differences less than 20%. However, it is found that the ELMOD prediction for subgrade stiffness is consistently smaller than the PADAL calculation, by up to 50%. These low predicted stiffnesses in the subgrade layer may then cause over-prediction in the sub-base stiffnesses. In cases where the sub-base is relatively thin, the ELMOD prediction becomes unrealistically large (refer Figure 5.6).

(d) Therefore, it may be concluded that the ELMOD program may only be used for the structural evaluation of existing pavements with two layers(i.e. a bituminous layer overlying the subgrade) with reasonable confidence.

9.4 STRUCTURAL EVALUATION OF A FULL SCALE TRIAL SECTION

The validity of the pavement evaluation procedure is further assessed as part of a detailed structural evaluation of a full scale trial section in Chapter 6. The site investigation includes a deflection survey using the Falling Weight Deflectometer and Benkelman Beam, coring and pitting. Specimens taken from site were carefully tested in the laboratory. Analysis has led to the following conclusions:

(a) All the analysis indicates that the modified bituminous material

which is used in the experimental section is in good condition, demonstrating successful use of the novel mix in a full scale situation.

(b) The pavement lives of the experimental and conventional sections were shown to be similar , both of which are at least 1.5 times greater than the design life of 13 msa. This confirms the basis of the experiment that, given the same pavement life, increasing the stiffness of the bituminous material can bring about reduction in layer thickness. In this experiment, approximately 20% saving in layer thickness has been achieved. The increase in stiffness has been derived from the use of a harder grade bitumen and reduction of air voids.

(c) The subgrade in the test sections is in reasonably stiff condition. The trial pit results show in-situ CBR values of 4% to 8%, which represents a slight reduction since construction and a slight increase in moisture content, which is to be expected as the subgrade approaches its equilibrium condition.

(d) The condition of the granular sub-base layer in the experimental section is found to be poor, with very low elastic stiffnesses being measured. This poor condition is caused by low density, low permeability and high moisture content. Furthermore, analysis reveals that the grading does not comply with the specification for Type 1 material. When combined with ineffective sub-surface drainage, the result is an accumulation of free water on the top surface of the sub-base layer, as observed in trial pits TP1 and TP2. This condition thus resulted in significant permanent deformation of the material and the large rut depths recorded in two areas of the experimental section, namely, at Ch.120 m - Ch.150 m of the eastbound and Ch.100 m - Ch.170 m of the westbound carriageway, are partly the

results of the weak sub-base.

(e) The whole structural evaluation has demonstrated that the PADAL program can be used satisfactorily in evaluating the in-situ stiffnesses of pavement structures. However, further validation is considered necessary.

9.5 LABORATORY INVESTIGATION ON CRACK PROPAGATION

A series of experimental tests, described in Chapter 7, has been performed to investigate the influence of crack growth on the reduction of effective stiffness of bituminous material using a four-point bending apparatus.

It was found that the rate of stiffness reduction was very rapid if the length of the crack were less than 10 to 15% of the total thickness. Thereafter, the rate of change is much reduced. Temperature variation is found to influence the rate of stiffness reduction in its absolute magnitude. The lower the temperature, the greater is the rate of reduction, and vice versa. An analytical procedure relating stiffness reduction to crack growth has been proposed. In general, good agreement is observed, though the prediction for DBM basecourse is not as good as for HRA wearing course.

9.6 DEVELOPMENT OF ANALYTICAL OVERLAY DESIGN PROCEDURE

As shown in Chapter 8, the results of the literature review and the laboratory work carried out on determining the relationship between crack propagation and reduction in elastic stiffness enabled the development of a rational method for calculating the remaining life of a bituminous pavement structure. This has led to the proposal of a new overlay design procedure. The main conclusions of the work include:

(a) A new method of calculating the remaining life of a bituminous pavement against fatigue cracking, which includes two procedures, viz, Procedure 's' and Procedure 'c'. Procedure 's' is

applicable to sound uncracked pavements whilst Procedure 'c' applies to partially cracked pavements. A stiffness ratio of above or below 0.9 between the effective stiffnesses of the bituminous layer in the wheelpath and the lane centre identifies the use of the appropriate procedure. The above procedures thus provide a logical way to determine the remaining life against fatigue cracking.

(b) A new analytical overlay design procedure has been proposed to evaluate the remaining life a bituminous pavement and to design the thickness of a bituminous overlay which satisfies the criteria for both fatigue cracking and permanent deformation. In the case of reconstructed pavements, the design of reconstruction follows the same procedures as for a new pavement, after removing the damaged layers.

CHAPTER 10

RECOMMENDATIONS FOR FURTHER RESEARCH

Through this research, a number of advances have been made in understanding the in-situ condition of pavement structures. This has been achieved by back-analysing the effective stiffnesses of the structures using analytical procedures to match the FWD deflection bowls. It is considered that there is still scope for further improvement and suggestions are discussed below:

1. During the course of the research, there was major concern about the accuracy of the geophones in measuring deflections with time. Hence, the geophones should be calibrated at regular intervals. Using a calibration column, as supplied by the manufacturer, it is possible only to check the relative accuracy of the geophones (refer Chapter 2). However, the necessary equipment has not yet been developed to calibrate the geophones absolutely. Hence, further research should be directed towards the development of such equipment. It is important that the equipment should be able to measure deflections to an accuracy of less than 10 microns.

2. In order to assist with pavement evaluation, a new research project should be initiated to interpret the thickness of the bound layer, e.g. concrete or bituminous material, using the velocity signals received from all the geophones of the FWD.

   The objectives are :

   (a) To reduce the uncertainty in the accuracy of prediction of elastic stiffnesses back-analysed using the PADAL program;

   (b) To be able to monitor the variation in thickness of the bound layer along a test section;

   (c) To reduce greatly the number of core samples taken in the

test section.

The success of this research would greatly enhance the capability of the FWD in evaluating the structural condition of pavements. Other geophysical methods being researched in this area include the electomagnetic method proposed by Berg et al (139).

3. The basis for development of the present analytical procedures for pavement evaluation, being a linear elastic layered system, is both simple and realistic but it has limitations. The procedures can only be applied with success if the measured deflection bowls are near to those expected by linear elastic theory and this assumption has been demonstrated to be reasonably correct for the majority of measured bowls. However, there are some cases such as those deflection bowls presented in Figure 10.1 which cannot be analysed by the present procedure. Therefore, further work should be directed to the understanding of the cause of such deflected shapes. Some of the factors influencing the deflection measurements have been suggested in Chapter 2 (Section 2.6.2). It is considered that a sensitivity analysis using a versatile method, e.g. the finite element method, with cracks assigned at different locations and varying subgrade support, should provide some insight into the origin of some of the special bowl shapes. This work should enable further improvement to the present procedures.

4. Further work should be carried out to develop the new proposed overlay design procedure as described in Chapter 8. The problem of reflection cracking has been the cause of failure for pavements with lean concrete roadbases and for bituminous overlays on concrete pavements. The literature has indicated that, as yet, no overlay design procedure against reflection cracking has been developed for routine computation and,

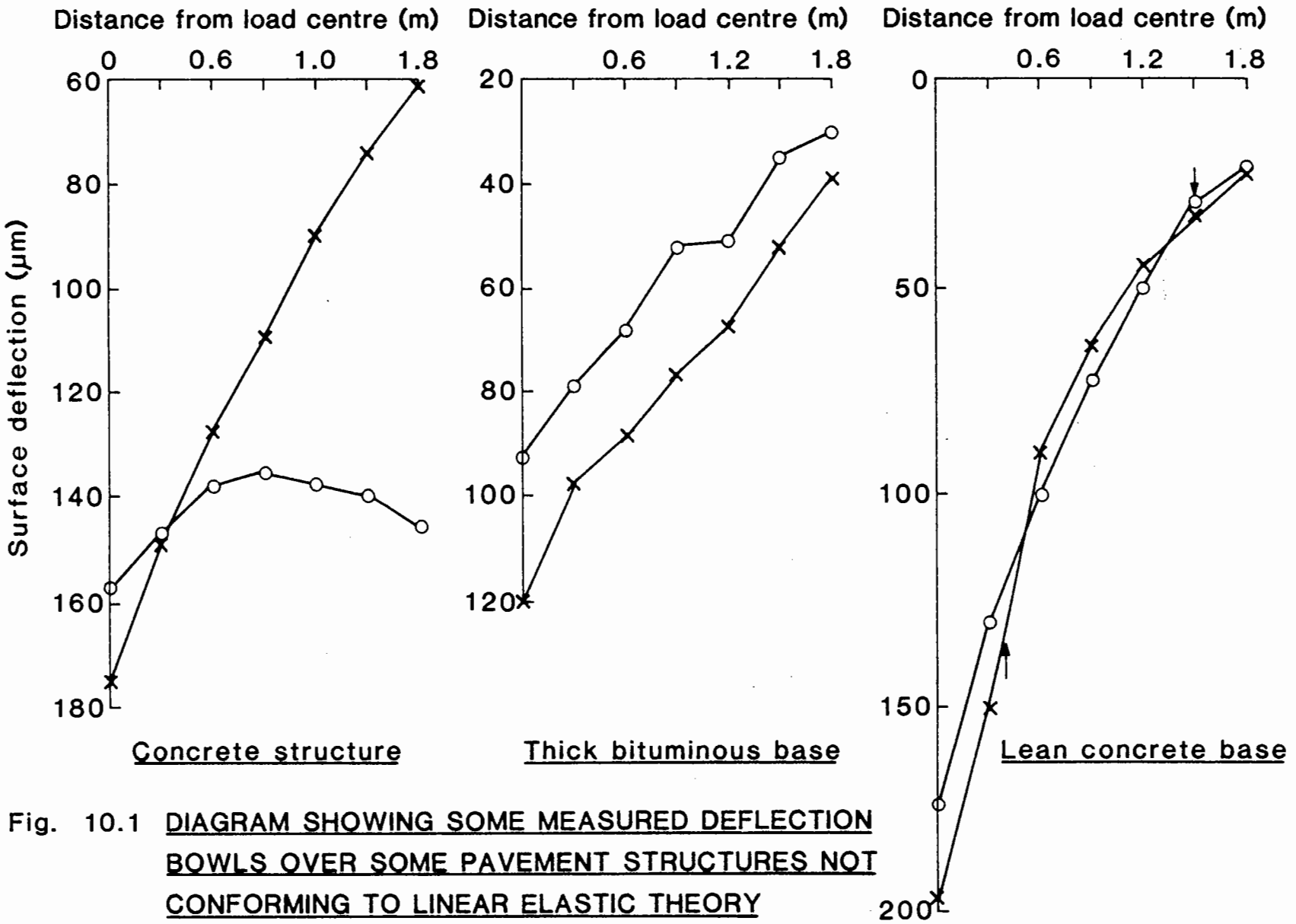

Fig. 10.1 DIAGRAM SHOWING SOME MEASURED DEFLECTION BOWLS OVER SOME PAVEMENT STRUCTURES NOT CONFORMING TO LINEAR ELASTIC THEORY

therefore, such development in the near future would be of great assistance in determining the correct rehabilitation measure in minimizing reflection cracking to bituminous overlays.

REFERENCES

1. Gaffney, J.A., Jacomb, A.W. and Snaith, M.S., "Review of Structural Maintenance of Motorways and All-purpose Trunk Roads", Department of Transport, 1986.
2. Norman, P.J., Snowdon, R.A. and Jacobs, J.C., "Pavement Deflection measurements and their Application to Structural Maintenance and Overlay Design", TRRL Report LR 571, 1973.
3. Kennedy, C.K. and Lister, N.W., "Prediction of Pavement Performance and the Design of Overlays", TRRL Report LR 833, 1978.
4. New Civil Engineer, "Ridley Sets Out New Road Ways", Magazine of the Institution of Civil Engineers, 11 Oct, 1984, pp 20-21.
5. Highway Research Board, "WASHO Road Test", Special Report No. 18, 1954.
6. Highway Research Board, "WASHO Road Test", Special Report No. 22, 1955.
7. "Standard Recommended Practice for Pavement Deflection Measurements", AASHTO Designation T256-77, Standard Specification for Transportation materials and Methods of Sampling and Testing, Part II, AASHTO, Washington, D.C., 1982.
8. Asphalt Institute, "Asphalt Overlays for Highway and Pavement Rehabilitation", Manual Series 17, 2nd edition, 1983.
9. Lister, N.W. and Kennedy, C.K., "A System for the Prediction of Pavement Life and Design of Pavement Strengthening", Proc. 4th Int. Conf. on Struct. Design of Asphalt Pavements, 1977, pp 629-650.
10. Gardiner, J.L., Williams, A. and Kennedy, C.K., "British Equipment for the Evaluation of Highway Pavements and for the Analysis of Collected Measurements", Proc. 2nd Int. Conf. on the Bearing Capacity of Roads and Airfields, Plymouth, England, 16-18th September, 1986, pp 483-494.
11. Hoffman, M.S. and Thompson, M.R., "Mechanistic Interpretation of Non-destructive Pavement Testing Deflections", Report No. UILU-ENG-81-2010, University of Illinois, June 1981.

12. Scrivner, F.H., Swift, G. and Moore, W.M., "A New Research Tool for Measuring Pavement Deflection", Highway Research Record, No. 129, 1966, pp 1-11.

13. Bohn, A., Ullidtz, P.,Stubstad, R. and Sørenson, A., "Danish Experiments with the Falling Weight Deflectometer", Proc. 3rd Int. Conf. on Struct. Design of Asphalt Pavements, Vol. 1, 1972, pp 1119-1128.

14. Bretonniere, S., "Les Deflectometres a Boulet Pour l'etude des Deflections des Chaussees Sous Charges Dynamiques", Bulletin de Liaison nr. 2, July-August 1963.

15. Tholen,O., Sharma, J., Terrel, R.L., "Comparison of Falling Weight Deflectometer with other Deflection Testing Devices", Transportation Research Record No. 1007, 1985, pp 20-25.

16. Larsen, E. and Stubstad, R.N., "The Use of Non-destructive Testing in Flexible Pavement Rehabilitation Design", Proc. Int. Symp. Bearing capacity of Roads and Airfields, Trondheim, Norway, Vol. 1, 1982, pp 31-41.

17. Ullidtz, P., "The Use of Dynamic Plate Loading Tests in Design of Overlays", Conf. on Road Engineering in Asia and Australasia, Kuala Lumpur, 1973.

18. Hoffman, M.S. and Thompson, M.R., "Field Testing Program Summary", Report No. UILU-ENG-81-2003, University of Illinois, 1981.

19. Ullidtz, P., "Overlay and Stage by Stage Design", Proc. 4th Int. Conf. on Struct. Design of Asphalt Pavements, Vol. 1, 1977, pp 722-735.

20. Claessen, A.I.M. and Ditmarsch, R., "Pavement Evaluation and Overlay Design", Proc. 4th Int. Conf. on Struct. Design of Asphalt Pavements, Vol. 1, 1977, pp 649-662.

21. Koole, R.C., "Overlay Design based on Falling Weight Deflectometer Measurements", Transport Research Record, No. 700, 1979, pp 59-71.

22. Way, G.B., Eisenberg, J.F., Delton, J.P. and Lawson, J.E., "Structural Overlay Design Method for Arizona", Proc. AAPT, 1984.

23. Giles, C.G., Sabey, B.E. and Cardew, K.H.F., "Development and Performance of the Portable Skid Resistance Tester", DSIR, Road Research Technical Paper 66, HMSO, 1964.

24. Hosking, J.R. and Woodford, G.C., "Measurement of Skidding Resistance, Part 1, Guide to the Use of SCRIM", TRRL Report LR 737, 1976.

25. Ibid, "Measurement of Skidding Resistance, Part II, Factors Affecting the Slipperiness of a Road Surface", TRRL Report LR 738, 1976.

26. Ibid, "Measurement of Skidding Resistance, Part III, Factors Affecting SCRIM Measurements", TRRL Report LR 739, 1976.

27. Road Note 27, "Instruction for Using the Portable Skid-resistance Tester", HMSO, 1969.

28. Lees, G. and Katekhda, I., "Prediction of Medium and High Speed Skid-resistance Values by Means of a Newly Developed Outflow Meter", Proc. AAPT, Vol. 43, 1974.

29. Potter, J., "Private communication", 2nd Int. Conf. on the Bearing Capacity of Roads and Airfields, Plymouth, England, 16-18th September, 1986.

30. Orr, D.M., Snaith, M.S. and Thompson, A., "A New System for the Recording and Analysis of Bump Integrator Measurements", Highways and Public Works, Vol. 46, No. 1820, London, 1978.

31. Still, P.B. and Jordon, P.G., "Evaluation of the TRRL High Speed Profilometer", TRRL Report LR 922, 1980.

32. Jordon, P.G. and Porter, J., "High-speed Road Monitoring System", Transportation Research Record No. 946, 1983, pp 13-19.

33. Kleyn, E.G., Maree, J.H. and Savage, P.F., "The Application of a Portable Pavement Dynamic Cone Penetrometer to Determine In-situ bearing Properties of Road Pavement Layers and Subgrade in South Africa", Euro. Symp. on Penetration Testing, Amsterdam, Netherlands, May 1982.

34. Clegg, B., "An Impact Soil Test for Low Cost Roads", Proc. Australian Road Research Board, Vol. 8, 1976.

67. Hoyinck, W.Th., Van Den Ben, R. and Gerritsen, W., "Lacroix Overlay Design by Three-layer Analysis", Proc. 5th Int. Conf. on Struct. Design of Asphalt Pavements, Vol. 1, 1982, pp 410-420.

68. Van der Loo, J.M.M., "Simplified Method for Evaluation of Asphalt Pavements", Proc. 5th Int. Conf. on Struct. Design of Asphalt Pavements, Vol. 1, 1982, pp 475-481.

69. Majidzadeh, K., Ilves, G.J. and McComb, R.A., "Overlay Design of Flexible Pavements Using Dynaflect", Proc. Int. Symp. on Bearing Capacity of Roads and Airfields, Vol. 2, 1982, pp 891-902.

70. Sharpe, G.W., Southgate, H.F. and Dean, R.C., "Pavement Evaluation by Using Dynamic Deflections", Transport Research Record No. 700, 1979, pp 34-45.

71. Treybig, H.J., McCullough, B.F., Finn, F.N., McComb, R. and Hudson, W.R., "Design of Asphalt Concrete Overlays using Layer Theory", Proc. 4th Int. Conf. on Struct. Design of Asphalt Pavements, Vol. 1, 1977, pp 589-621.

72. Heukelom, W. and Klomp, A.J.G., "Dynamic Testing as a Means of Controlling Pavements during and after Construction", Proc. 1st Int. Conf. on Struct. Design of Asphalt Pavements, 1962, pp 667-679.

73. Grainger, G.D. and Lister, N.W., "A Laboratory Apparatus for Studying the Behaviour of Soils under Repeated Loading", Geotechnique 12, No. 1, 1962, pp 3-14.

74. Parr, G.B., "Some Aspects of the Behaviour of London Clay under Repeated Loading", PhD Thesis, University of Nottingham, 1972.

75. Brown, S.F., "The Characterisation of Cohesive Soils for Flexible Pavement Design", Proc. 7th Euro. Conf. Soil Mech. and Fdn Engrg, Vol. 2, 1979, pp 15-22.

76. Fredlund, D.G., Bergan, A.T. and Wong, P.K., "Relation between Resilient Modulus and Stress Conditions for Cohesive Subgrade Soils", Transporation Research Board No. 642, 1977, pp 73-81.

77. Loach, S.C., "Repeated Loading of Fine Grain Soils in Pavement Design", PhD Thesis, University of Nottingham, May 1987.

78. Uddin, W., Meyer, A.H., Hudson, W.R. and Stokoe II., K.H., "Project Level Structural Evaluation of Pavements Based on Dynamic Deflections", Transportation Research Record No. 1007, 1985.

79. Tam, W.S., "Design of Overlays for Flexible Pavements", Internal Report No. WST/2, July 1986.

80. Roessett, J.M. and Shao, K.Y., "Dynamic Interpretation of Dynaflect and Falling Weight Deflectometer Tests", Transportation Research Record No. 1022, 1985.

81. Uddin, W., Meyer, A. and Hudson, W., "Evaluation of Structural Capacity and In-situ Moduli of Pavements Based on Dynamic Deflection", Proc. 2nd Int. Conf. on the Bearing Capacity of Roads and Airfields, Plymouth, England, 16-18 September, 1986, pp 309-320.

82. Uddin, W., "A Structural Evaluation Methodology for Pavements Based on Dynamic Deflections", PhD Thesis, University of Taxas at Austin, 1984.

83. "BMDP-Biomedical Computer Programs", UCLA, University of California Press, USA, 1983.

84. Brown, S.F., Cooper, K.E., Brodrick, B.V. and Pell, P.S., "The Hasland Bypass Experiment", Unpublished Report, February 1979.

85. Brodrick, B.V., "The Development and Performance of a Wheel Loading Facility and In-situ Instruments for Pavement Experiments", MPhil. Thesis, University of Nottingham, May 1977.

86. Mamlouk, M.S. and Davies, T.G., "Elastodynamic Analysis of Pavement Deflections", Trans. Engrg Jnl ASCE, Vol. 110, No. 6, November 1984, pp 536-550.

87. Kausel, E. and Peek, R., "Dynamic Loads in the Interior of a Layered Stratum: an Explicit Solution", Bull. of Seismological Soc. of America, Vol. 72, No. 5, October 1982, pp 1459-1481.

88. Davies, T.G. and Mamlouk, M.S., "Theoretical Response of Multi-layered Pavement Systems to Dynamic Non-destructive Testing", Transportation Research Record No. 1022, 1985, pp 1-7.

89. Sebaaly, B., Davies T.G. and Mamlouk, M.S., "Dynamics of Falling Weight Deflectometer", Trans Engrg Jnl, ASCE, No. 6, Nov. 1985, pp 618-632.

90. "Evaluation of Layer Moduli and Overlay Design (ELMOD) user's manual", Dynatest Ltd., Release 3, 1984.

91. Odemark, N., "Undersokning av Elasticitetsegenskaperna hos Olika Jordarter Samt Teori for Berakning av Belagningar Enligt Elasticitetsteorien", Statens Vaginstitut, Meddelande 77, 1949.

92. Ullidtz, P. and Peattie, K.R., "Pavement Analysis by Programmable Calculators", Jnl ASCE, TE5, September 1980, pp 581-597.

93. Dorman, G.M. and Metcalf, C.T., "Design Curves for Flexible Pavements Based on Layered System Theory", Highway Research Record, No. 71, 1965, pp 69-84.

94. Miner, M.A., "Cumulative Damage in Fatigue", Jnl Applied Mechanics, Trans. ASME, Vol 66, A519 - A164, 1954.

95. Tam, W.S., "Design of Overlays for Flexible Pavements", Internal Report No. WST/1, February 1985.

96. Road Research Laboratory, "A Guide to the Structural Design of Pavements for New Roads", Road Note 29 (3rd Ed.), HMSO, London, 1970.

97. Brown, S.F., "Implementation of Analytical Pavement Design: a Case Study", The Highway Engineer, Vol. 27, No. 7, 1980.

98. Tam, W.S., "Structural Evaluation of an experimental road on Hasland Bypass", Unpublished Report submitted to Derbyshire County Council, July,1987.

99. Department of Transport, "Structural Examination of Bituminous Pavements", Advice Note HA 30/85, 1985.

100. Thom, N.H., "Design of Road Foundations", Internal Report No. NHT/2, 1987.

101. Powell, W.D. and Leech, D., "Standards for Compaction of Dense Roadbase Macadam", TRRL SR717, 1982.

102. British Standards Institution, "Specification for Coated Macadam for Roads and Other Paved Areas", BS4987, 1973.

103. British Standards Institution, " Methods of Test for Soil Classification and Compaction", BS1377, 1975

104. British Standards Institution, "Recommendations for Testing of Aggregates, Part 1, Compactibility Test for Graded Aggregates", BS5835: Part 1, 1980.

105. Powell, W.D., Potter, J.F., Mayhew, H.C. and Nunn, M.G., "The Structural Design of Bituminous Roads", TRRL Report LR1132, 1984.

106. Brown, S.F. and Brunton J.M., "The Influence of Bonding between Bituminous Layers", Jnl Institution of Highways and Transportation, May 1984, pp 16-17.

107. Van Dijk, W., "Practical Fatigue Characterisation of Bituminous Mixes", Proc. AAPT, 1975.

108. Majidzadeh, K. and Ramsamooj, D.V., "Mechanistic Approach to the Solution of Cracking in Pavements", Proc. Symp. on Structural Design of Asphalt Concrete Pavements to Prevent Fatigue Cracking, Highway Research Board, 1973, pp 143-153.

109. Paris, P. and Erdogan, F.J., "A Critical Analysis of Crack Propagation Laws", Jnl Basic Engrg, Trans., ASCE, Ser. D, Vol. 85, 1963.

110. Molenaar, A.A.A., "Fatigue and Reflection Cracking due to Traffic Loads", Proc. AAPT, 1984, pp 440-474.

111. Freeme, C. and Marais, C.P., "Thin Bituminous Surfaces: Their Fatigue Behaviour and Prediction", Proc. Symp. on Structural Design of Asphalt Concrete Pavements to Prevent Fatigue Cracking, Highway Research Board, 1973, pp 158-178.

112. Kasianchuk, D.A., "Fatigue Considerations in the Design of Asphalt Concrete Pavements", PhD Thesis, University of California, Berkeley, 1968.

113. "AASHTO Interim Guide for Design of Pavement Structures 1972", revised, Washington, D.C., 1981.

114. U.S. Corps of Engineers, "Engineering and Design - Flexible Airfield Pavement", EM 1110-45-302 or TM 5-824-3.

115. Havens, J.H., "Observations of the Significance of Pavement Deflections", Proc. AAPT, 1962.

116. U.S. Army Engineer Waterways Experimental Station, "Investigations of Pressure and Deflections for Flexible Pavements, Homogeneous Clayey-silt and Sand Test Sections", Tech. Memo Nos. 3-323, Reports 1 and 4 in March 1951 and December 1954.

117. Kingham, R.I., " Development of the Asphalt Institute Method for Designing Asphalt Concrete Overlays for Asphalt Pavement", The Asphalt Institute, RR 69-3, June 1969.

118. Canadian Good Road Association, "Pavement Evaluation Studies in Canada", Proc. 1st Int. Conf. on Struct. Design of Asphalt Pavements, Ann Arbor, Michigan, 1962.

119. Lister, N.W., "Deflection Criteria for Flexible Pavements", TRRL Report LR 375, 1972.

120. Thrower, E.N. and Castledine, L.W.E., "The Design of New Road Pavements and of Overlays: Estimation of Commerical Traffic Flows", TRRL Report LR 844, 1978.

121. Department of Transport, "Road Pavement Design", Tech. Memo H6/78.

122. Currer, E.W.H. and O'Connor, M.G.D., "Commercial Traffic, Its Estimated Damaging Effects, 1945-2005", TRRL Report, LR 910, 1979.

123. Treybig, H.J.,McCullough, B.F., Smith, P and Von Quintus, H., "Overlay Design and Reflection Cracking Analysis for Rigid Pavements", Vols. 1 and 2, Nos. FHWA-RD-77-66 and FHWA-RD-77-67, Fereral Highway Administration, U.S. Department of Transportation, Washington, D.C., August 1977.

124. Schwartz, D.R. and Hughes, C.S., "Reflection Cracking - Group Report", Pavement Rehabilitation: Proceedings of a Workshop. No. FHWA-RD-74-60 Federal Highway Administration, U.S. Department of Transportation, Washington, D.C., June 1974, pp 221-223.

125. Fleming, E.M., "Resurfacing Concrete Pavements with Portland Cement Concrete", Highway Research Board, Vol. 12, 1932, pp 206-226.

126. Gray, B.E. and Martin, G.E., "Resurfacing of Concrete Pavements with Bituminous Types of Surface", Highway Research Board, Vol. 12, 1932, pp 177-192.

127. Sherman, G., "Minimizing Reflection Cracking of Pavement Overlays", NCHRP Synthesis 92, Transportation Research Board, September 1982.

128. Hughes, D.A.B., "Polymer Grid Reinforcement of Asphalt Pavements", PhD Thesis, University of Nottingham, 1986.

129. Coetzee, N.F. and Monsmith, C.L., "Considerations in the Design of Overlay Pavements to Minimize Reflection Cracking", Proc. 3rd Int. Conf. on Asphalt Pavements for South Africa, Durban, South Africa, 1979, pp 290-302.

130. Cooper, K.E. and Pell, P.S., " The Effect of Mix Variables on the Fatigue Strength of Bituminous Materials", TRRL Report LR 633, 1974.

131. Brown, S.F. and Pappin, J.W., "Analysis of Pavement with Granular Bases", Transportation Research Record No. 810, 1981, pp 17-23.

132. Brown, S.F., Pell, P.S.and Stock, A.F., "The Application of Simplified Fundamental Design Procedures for Flexible Pavements", Proc. 4th Int. Conf. on Struct. Design of Asphalt Pavements, Ann Arbor, Michigan, Vol.1, 1977, pp 327-347.

133. Brown, S.F. and Brunton, J.M., "An Introduction to the Analytical Design of Bituminous Pavements", Design Manual, 3rd Edition, 1986.

134. Mobil Oil Ltd., "Asphalt Pavement Design Manual for the U.K.", June, 1985.

135. De Bats, F.Th., "The Computer Program PONOS and POEL: A Computer Simulation of Van der Poel's Nomograph", External Report, Koninklijke/Shell Laboratorium, Amsterdam, 1972.

136. Marchionna, A., Cesarini, M., Fornaci, M. and Malgarani, M., "Evaluation of Pavement Characteristics using the FWD and Remaining Life Prediction in terms of Cracked Areas", Proc. 2nd Int. Conf. on the Bearing Capacity of Road and Airfields, Plymouth, England, 16-18 Sept., 1986, pp 443-452.

137. Brunton J.M., Cooper, K.E., Brown, S.F., and Pell, P.S., "Development of Improved Procedures for Asphalt Pavement Mix Design", Internal Report No. KEC/JMB/5, Feb., 1982.

138. "A512 Ashby Road, Loughborough, Pavement Evaluation and Design", Unpublished report, July,1985.

139. Berg, F., Jansen, J.M. and Ertman Larsen, H.J., "Structural Pavement Analysis based on FWD, Georadar and/or Geosonar Data", Proc. 2nd Int. Conf. on the Bearing Capacity of Road and Airfields, Plymouth, England, 16-18 Sept., 1986, pp 453-461.

Subgrade stiffness parameter

$$\log(A) = a_1 + a_2 d_1 + a_3 d_3 + a_4 d_5 + a_5 d_6 + a_6 h_2^2 + a_7 d_6^2 + a_8 \log(d_5) + a_9 \log(d_6 d_7) + a_{10}(h_1 d_1) + a_{11}(h_1 d_3) + a_{12}(h_2 d_6) + a_{13}(h_3 d_4) + a_{14}(h_3 d_4) + a_{15}(h_3 d_7) + a_{16}(d_4 d_5) + a_{17}(d_4 d_7) + a_{18}(d_6 d_7)$$

($R^2 = 0.915$)

(B.11)

Subgrade stiffness parameter

$$\log(B) = a_1 + a_2 d_4 + a_3 \log(d_6) + a_4 \log(d_7) + a_5 \log(d_5 d_6) + d_6 \log(d_4 d_7) + a_7 \log(d_5 d_7) + a_8 \log(d_6 d_7) + a_9(h_1^2 d_1)$$

($R^2 = 0.805$)

(B.12)

Note : $\log = \log_{10}$

: refer Table B.5 for magnitudes of coefficients a.

Coefficient a with subscript	Predictive stiffness equation for E_1	E_2	E_3	E_f	A	B
1	2.7113	13.5681	14.5093	7.40769	1.41892	-6.48342
2	7.68094	-12.2436	0.04866	0.00087	0.00009	0.00645
3	-13.5962	-2.14223	-0.05176	-0.00674	-0.00403	-8.41145
4	52.1626	14.2140	-2.46837	0.00539	0.04353	3.56863
5	-55.5776	-44.6672	-19.1631	0.60117	-0.05306	-27.8282
6	0.86488	26.7307	-0.07108	-0.04503	0. 75654	4.75654
7	16.4863	29.1664	5.18759	2.41604	-0.00004	28.9913
8	-0.02703	-0.67590	3.14729	0.12458	1.8484	-2.37292
9	24.0437	-28.2252	8.37773	-0.00445	-2.30002	0.00152
10	-0.51992	2.41505	5.96667	0.12121	-0.00202	
11	0.00003	283.531	-14.7514	0.00001	0.00404	
12	0.00327	-3.03378	-10.5237	5.51785	-0.00074	
13		0.00023	-0.01551	6.09279	-0.00005	
14		0.00128	0.00730	-1.12757	0.00208	
15			-0.01800	-7.55242	-0.00462	
16			-0.00001	-3.02536	-0.00004	
17			-0.51452	1.28586	0.00008	
18			-51.459	-4.1444	0.00003	
19			-2.13462	5.52506		
20			49.589	17.7804		
21			31.8622	2.8428		
22			12.9873	-9.58504		
23			0.00003	-14.2164		
24			0.00002	-0.00050		
25			-0.00001	-0.00081		
26			0.00002	0.00594		
27			-0.00004	-0.01140		
28			0.00013	-0.00009		
29			-0.00007	0.00151		
30			0.02976	-0.00613		
31			0.01691	0.01123		
32			-0.1921	-0.01334		
33			0.19756	-0.00001		
34			0.03676	0.00001		
35			-0.08846	-0.00002		
36			0.14107	0.00002		
37			-0.10086			
38			-0.00534			
39			0.00845			
40			0.01422			
41			-0.01494			

Table B.5 Coefficients of Regression Equations for thin bituminous pavement structures (4-layered)

(c) For concrete pavement structures, the predictive stiffness equations are :

Layer 1 ($R^2 = 0.914$)

$$\log(E_1) = a_1 + a_2h_1 + a_3h_3 + a_4(h_3)^2 + a_5(h_1h_3) + a_6\log(h_1) + a_7\log(d_1d_2) + a_8\log(d_1d_3) + a_9\log(d_1d_4) + a_{10}\log(d_3d_7)$$

(B.13)

Layer 2 ($R^2 = 0.857$)

$$\log(E_2) = a_1 + a_2h_1 + a_3h_2 + a_4(h_1)^2 + a_5(h_2)^2 + a_6(h_1h_2) + a_7(h_1d_1) + a_8(h_2d_1) + a_9(h_2d_2) + a_{10}(h_2d_4) + a_{11}(h_3d_5) + a_{12}(h_3d_8) + a_{13}\log(d_1) + a_{14}\log(d_4) + a_{15}(d_1d_7) + a_{16}(d_2d_3) + a_{17}(d_2d_6) + a_{18}(d_3d_4) + a_{19}\log(d_2d_3) + a_{20}\log(d_3d_4) + a_{21}\log(d_1d_5)$$

(B.14)

Layer 3 ($R^2 = 0.429$)

$$\log(E_3) = a_1 + a_2h_3 + a_2(h_2)^2 + a_4d_1 + a_5d_6 + a_6(h_1h_2) + a_7(h_2h_3) + a_8(h_2d_2) + a_9(h_3d_1) + a_{10}(h_3d_8) + a_{11}\log(h_3) + a_{12}\log(d_1) + a_{13}\log(d_2) + a_{14}\log(d_8) + a_{15}\log(d_2d_3) + a_{16}\log(d_2d_4) + a_{17}\log(d_1d_7) + a_{18}\log(d_7d_8) + a_{19}(d_1)^2 + a_{20}(d_2d_3) + a_{21}(d_5d_6) + d_{22}(h_1)^3 + a_{23}(h_2)^3 + a_{24}(h_1h_2)^2 + a_{25}(h_1h_3^2) + a_{26}(h_2h_3^2) + a_{27}(h_3h_1^2) + a_{28}(h_3h_2^2) + a_{29}(h_1d_7^2) + a_{30}(h_1d_8^2) + a_{31}(h_2d_5^2) + a_{32}(h_2d_6^2) + a_{33}(h_3d_3^2)a_{34}(h_3d_7^2) + a_{35}(h_3d_7^2) + a_{35}(h_3d_8^2) + a_{36}(h_2^2d_1) + a_{37}(h_2^2d_2) + a_{38}(h_2^2d_8) + a_{39}(h_3^2d_1) + a_{40}(h_3^2d_2) + a_{41}(h_3^2d_7)$$

(B.15)

Layer 4 ($R^2 = 0.998$)

$$\log(E_4) = a_1 + a_2\log(d_8) + a_3\log(d_4) + a_4\log(d_7d_8)$$

(B.16)

Note: log = $\log_{10}$

: refer Table B.6 for magnitudes of coefficients a.

Coefficient a with subscript	Predictive stiffness equation for E_1	E_2	E_3	E_4
1	5.67452	5.97652	-1.82552	4.92741
2	1.01252	-8.04175	0.01545	-0.82952
3	-0.04008	-7.25834	3.30730	-0.79097
4	-0.00013	3.79971	0.00377	0.59465
5	0.07992	4.48494	-0.01026	
6	-0.59031	7.50184	-2.70432	
7	-9.12227	-0.00078	-0.43330	
8	25.9334	-0.04664	0.00274	
9	-19.8231	0.05982	0.00415	
10	2.03902	-0.01324	-0.01439	
11		0.00015	0.25679	
12		-0.00081	-0.61547	
13		-0.94204	-6.89794	
14		1.62366	8.89415	
15		0.028080	-7.38983	
16		-0.04456	14.7415	
17		-0.07788	-0.27205	
18		0.19146	-7.83152	
19		-0.27926	0.00001	
20		-3.71389	-0.04463	
21		2.25057	0.04089	
22			0.37489	
23			-7.71403	
24			-1.62458	
25			1.82402	
26			1.90050	
27			-1.84112	
28			-1.40173	
29			-0.00011	
30			0.00012	
31			-0.00003	
32			0.00002	
33			-0.00001	
34			-0.00001	
35			0.00015	
36			0.06253	
37			-0.09904	
38			0.04155	
39			-0.01638	
40			0.02100	
41			-0.00820	

Table B.6 **Coefficients of Regression Equations for concrete pavement structures (4-layered)**

35. Garrick, N.W. and Scholer, C.F., "Rapid Determination of Base Course Strength Using the Clegg Impact Tester", Transportation Research Board No. 1022, 1985, pp 115-119.

36. Sørenson, A. and Hayven, M., "The Dynatest 8000 Falling Weight Deflectometer Test System", Proc. Int. Symp. Bearing Capacity of Roads and Airfields, Trondheim, Norway, Vol. 1, 1982, pp 464-470.

37. Pronk, A.C. and Buiter, R., "Aspects of the Interpretation and Evaluation of Falling Weight deflectometer Measurements", Proc. 5th Int. Conf. on Struct. Design of Asphalt Pavements, Vol. 1, Delft, 1982, pp 461-474.

38. Pappin, J.W., "Characteristics of a Granular Material for Pavement Analysis", PhD Thesis, University of Nottingham, 1979.

39. Seed, H.B., Chan, C.K. and Lee, K.L., "Resilience Characteristics of Subgrade Soils and their Relation to Fatigue Failure in Asphalt Pavements", Proc. 1st Int. Conf. on Struct. design of Asphalt Pavements, 1962, pp 611-636.

40. Dehlen, G.L.,"The Effect of Non-linear Material Response on the Behaviour of Pavements Subjected to Traffic Loads", PhD Thesis, University of California, Berkeley, 1969.

41. Lashine, A.K.F., "Some Aspects of the Characteristics of Keuper Marl under Repeated Loading", PhD Thesis, University of Nottingham, 1971.

42. Brown, S.F., Lashine, A.K.F. and Hyde, A.F.L., "Repeated Load Triaxial Testing of a Silty Clay", Geotechnique 25, No. 1, 1975, pp 95-114.

43. Brown, S.F., Tam, W.S. and Brunton, J.M., "Structurdal Evaluation and Overlay Design: Analysis and Implementation", Proc. 6th Int. Conf. on Struct. Design of Asphalt Pavements, Ann Arbor, Michigan, 1987.

44. Teller, L.W. and Sutherland, E.J., "A Study of Structural Action of Several Types of Transverse and Longitudinal Joint Design", Public Roads, Vol. 17, No. 7, September 1936.

45. Gulden, W. and Brown, D., "Establishing Load Transfer in Existing Jointed Concrete Pavements", Transportation Research Board No. 1043, 1985, pp 23-32.

46. Peutz, M.G.F., Van Kempen, H.P.M. and Jones, A., "layered Systems under Normal Surface Loads", Highway Research Record 228, 1968, pp 34-35.

47. Ibid, "Layered Systems under Normal Surface Loads. Computer Program BISTRO", Koninklijke/Shell-Laboratorium, Amsterdam, May 1968.

48. Highway Research Board, "AASHO Road Test", Special Report Nos. 61 and 73, 1962.

49. Vaswani, N.K., "Design of Pavements Using Deflection Equations from AASHO Road Test Results", Highway Research Record No. 239, 1968, pp 76-92.

50. Hveem, F.N., "Pavement Deflections and Fatigue Failures", Highway Research Board Bulletin 114, 1955, pp 43-73.

51. Bisset, J.R. and Ford, M.C.Jr., "A Comparison of Flexible Pavement Deflection Performance with Structure", Proc. AAPT, Vol. 31, 1962, pp 329-342.

52. Rufford, P.G., "A Pavement Analysis and Structural Design Procedure Based on Deflection", Proc. 4th Int. Conf. Struct. Design of Asphalt Pavements, Vol. 1, 1977, pp 710-721.

53. McCullough, B.F. and Taute, A., "Use of deflection Measurements for determining Pavement Material Properties", Transport Research Record, No. 852, 1982, pp 8-25.

54. Majidzadeh, K., "Dynamic Deflection as Pavement Performance Indicators", Proc. Int. Symp. Bearing Capacity of Roads and Airfields, Vol. 1, 1982, pp 97-109.

55. Dehlen, G.L., "Flexure of a Road Surfacing, its Relation to Fatigue Cracking, and Factors determining its Severity", Highway Research Board Bulletin 321, 1962, pp 26-39.

56. Leger, Ph. and Autret, P., "The Use of Deflection Measurements for the Structural Design and Supervision of Pavements", Proc. 3rd Int. Conf. on Struct. Design of Asphalt Pavements, Vol. 1, 1972, pp 1188-1205.

57. Kilareski, W.P. and Anani, B.A., "Evaluation of In-situ Moduli and Pavement Life from Deflection Basins", Proc. 5th Int. Conf. on Struct. Design of Asphalt Pavements, 1982, pp 349-366.

58. Kung, K.Y., "A New Method in Correlation Studies of Pavement Deflection and Cracking", Proc. 2nd Int. Conf. on Struct Design of Asphalt Pavements, Vol. 1, 1967, pp 1037-1046.

59. Stock, A.F. and Yu, J., "Use of Surface Deflection for Pavement Design and Evaluation", Transport Research Record No. 954, 1984, pp 64-69.

60. De Jong, D.L., Peutz, M.G.F. and Korswagen, A.R., "Computer Program BISAR, Layered System under Normal and Tangential Surface Loads", Koninklijke/Shell Laboratorium, Amsterdam, External Report, AMSR. 0006.73, 1973.

61. Warren ,H. and Dieckmann, W.L., "Numerical Computation of Stresses and Strains in a Multi-layered Asphalt Pavement System", Unpublished internal report, Chevron Research Corp., USA, 1963.

62. Brunton, J.M., Cooper, K.E., Brown, S.F. and Pell, P.S., "Development of Improved Procedures for Asphalt Pavement Mix Design", Internal Report No. KEC/JMB/4, May 1984.

63. Brunton, J.M., "Development in the Analytical Design of Asphalt Pavements Using Computers", PhD Thesis, University of Nottingham, May 1983.

64. Finn, F.N. and Monismith, C.L., "Asphalt Overlay and Design Procedures", NCHRP Synthesis 116, Transportation Research Board, December, 1984.

65. Sharma, J. and Stubstad, R.N., "Evaluation of Pavement in Florida by Using the Falling Weight Deflectometer", Transport Research Record No. 755, 1980, pp 42-48.

66. Vaswani, N.K., "Method for Separately Evaluating Structural Performance of Subgrades and Overlying Flexible Pavements", Highway Research Record No. 362, 1971, pp 48-62.